UNIVERSITAT DE BARCELONA

Regulation of ribonucleotide reduction in facultative anaerobic pathogens and its influence in bacterial fitness, virulence and biofilm formation

Lucas Pedraz López

UNIVERSITY OF BARCELONA

FACULTY OF BIOLOGY

Regulation of ribonucleotide reduction in facultative anaerobic pathogens and its influence in bacterial fitness, virulence, and biofilm formation

Lucas Pedraz López

Barcelona, 2019

UNIVERSITY OF BARCELONA

FACULTY OF BIOLOGY

INSTITUTE FOR BIOENGINEERING OF CATALONIA

BACTERIAL INFECTIONS: ANTIMICROBIAL THERAPIES

DOCTORAL PROGRAM IN BIOTECHNOLOGY

Regulation of ribonucleotide reduction in facultative anaerobic pathogens and its influence in bacterial fitness, virulence, and biofilm formation

A thesis submitted for the degree of Doctor from the University of Barcelona

Thesis Director	Doctoral Candidate	Thesis Tutor
Dr. Eduard Torrents Serra	Mr. Lucas Pedraz López	Dr. Antonio Juárez Giménez

To the people whose labors go beyond ideas into the realm of reality

Abstract

The perpetuation of life depends on the ability to reproduce. All known forms of life use DNA as genetic information storage. Ribonucleotide reduction is the process by which ribonucleotides (NTPs) are transformed into deoxyribonucleotides (dNTPs), thereby forming the building blocks for DNA synthesis and repair. This reaction is catalyzed by a family of sophisticated enzymes, the ribonucleotide reductases (RNRs). All RNRs are metalloproteins that use a common, free-radical-based catalytic mechanism. However, depending on the specific mechanisms they use for radical generation, the type of cofactor they require, and differences in the structure of their protein complexes, RNR are divided into three different classes, namely class I, class II and class III. RNR classes also present different relationships with oxygen: class I RNRs are oxygen-dependent, class II RNRs are oxygen-independent, and class III RNRs are oxygen-sensitive. While eukaryotic organisms use only class I RNR, bacteria can encode all RNR classes in any possible combinations, which provides them with a valuable tool for to adapt to different environmental conditions.

Facultative anaerobic bacteria can thrive in the presence or absence of oxygen. Numerous species significant for their clinical relevance are facultative anaerobes, as many environments inside host bodies feature hypoxic or anoxic conditions; microaerobic or anaerobic environments are also found in biofilms in chronic infections. However, a facultative anaerobic lifestyle also implies an increased cost in regulation complexity. This effect extends to the ribonucleotide reductases network, which in facultative anaerobic pathogens must be thoroughly regulated to react to the different challenges imposed by different oxygenation conditions, changing growth speeds, host defense mechanisms, etc.

This study is focused on facultative anaerobic pathogens and the strategies they use to modulate ribonucleotide reduction and balance it under different environmental stimuli, variable oxygenation conditions, and during infection or biofilm formation. We used two very well-studied species: *Pseudomonas aeruginosa* and *Escherichia coli*. First, in *P. aeruginosa*, an opportunistic pathogen well-known for its chronic pulmonary infections, we explore the effects of the AlgZR two-components system, one of the main regulatory elements responsible for biofilm formation and chronification, in the control of the RNR network. We then conducted a comprehensive characterization of the master regulator of ribonucleotide reductases NrdR, from its general role to its specific mechanism of action, in both *E. coli* and *P. aeruginosa*. We also explored the differential roles of RNR classes during biofilm formation and the function that the master regulators of anaerobic metabolism play in their control. Finally, we used a technique developed in this work, a continuous-culture method named *AnaeroTrans*, to characterize in detail the gradual adaptation *E. coli* and *P. aeruginosa* withstand during the aerobic-anaerobic transition and, isolating this effect from all other consequences of biofilm formation, explore the dynamic actions of RNR classes and anaerobic regulators in the microaerobic range.

Overall, this works provides a comprehensive description of the different roles ribonucleotide reductases play in anaerobic facultative pathogens and the regulatory mechanisms that control them.

Resumen

La perpetuación de la vida depende necesariamente de la reproducción. Todas las formas de vida usan ADN para almacenar información genética. La reducción de ribonucleótidos es el proceso por el cual los ribonucleótidos (NTPs) se transforman en desoxirribonucleótidos (dNTP), formando así los precursores básicos necesarios para la síntesis y la reparación del ADN. Esta reacción es catalizada por una familia de enzimas altamente sofisticadas, las ribonucleótido reductasas (RNR). Todas las RNR son metaloproteínas que emplean un mismo mecanismo catalítico basado en radicales libres. No obstante, dependiendo del mecanismo específico que emplean para la generación de dicho radical, el tipo de cofactores que requieren o las diferencias estructurales que presentan, se divide a las RNR en tres clases (clase I, clase II y clase III). Dichas clases también presentan diferentes relaciones con el oxígeno: la clase I es dependiente de oxígeno, la clase II es independiente de oxígeno, y la clase III es sensible a oxígeno. Los organismos eucarióticos utilizan exclusivamente ribonucleótido reductasas de clase I, pero las bacterias pueden codificar todas las clases en cualquier combinación posible, lo que les confiere una importante herramienta para adaptarse a diferentes condiciones ambientales.

Las bacterias anaeróbicas facultativas pueden crecer en presencia o ausencia de oxígeno. Numerosas especies significativas por su importancia clínica son anaeróbicas facultativas, dado que muchos ambientes en el cuerpo presentan condiciones hipóxicas o anóxicas. También se dan ambientes microaeróbicos o anaeróbicos en los biofilms formados en infecciones crónicas. No obstante, la vida anaeróbica facultativa supone también un coste superior en cuanto a la complejidad de su regulación genética. Este efecto se extiende a las ribonucleótido reductasas, que, en patógenos anaeróbicos facultativos, deben ser finamente reguladas para responder a distintas concentraciones de oxígeno, cambios en la velocidad de crecimiento, mecanismos de defensa del anfitrión, etc.

Este trabajo se ha enfocado en los patógenos anaeróbicos facultativos y las estrategias que usan para regular y equilibrar la reducción de ribonucleótidos bajo diversos estímulos ambientales y condiciones variables de oxigenación, así como durante la infección y la formación de biofilm. Para ello, hemos trabajado con dos especies ampliamente conocidas: *Pseudomonas aeruginosa* y *Escherichia coli*. En primer lugar, en *P. aeruginosa*, hemos estudiado los efectos del sistema de dos componentes AlgZR (uno de los más importantes sistemas de regulación responsables de la formación de biofilm y la cronificación) sobre el control de la red de las RNR. Posteriormente realizamos una caracterización completa de NrdR, el regulador principal de las ribonucleótido reductasas, analizando desde su papel general sobre el regulón NrdR hasta su mecanismo molecular, tanto en *E. coli* como en *P. aeruginosa*. También analizamos el papel que desempeñan las distintas clases de RNR durante la formación de biofilm y la función que realizan los reguladores generales del metabolismo anaeróbico en su control. Finalmente, utilizamos una técnica desarrollada específicamente para este trabajo, un método basado en el cultivo en continuo denominado *AnaeroTrans*, para caracterizar en detalle la adaptación gradual que *P. aeruginosa* y *E. coli* sufren durante la transición aerobiosis-anaerobiosis, y, aislando este efecto de otras consecuencias de la formación de biofilm, explorar las acciones dinámicas que ejercen las distintas clases de RNR y los reguladores anaeróbicos durante la microaerobiosis.

Globalmente, este trabajo proporciona una descripción detallada de los diferentes papeles que desempeñan las ribonucleótido reductasas en patógenos anaeróbicos facultativos y los mecanismos regulatorios que las controlan.

Table of contents

List of abbreviations

(d)NDP	(Deoxy)ribonucleotide diphosphate
(d)NMP	(Deoxy)ribonucleotide monophosphate
(d)NTP	(Deoxy)ribonucleotide triphosphate
AdoCbl	5'-Adenosylcobalamin
ALI	Air-Liquid Interface
AFM	Atomic Force Microscopy
Asn	Asparagine
Cm	Chloramphenicol
cAMP	Cyclic adenosine monophosphate
CF	Cystic Fibrosis
CFTR	Cystic Fibrosis Transmembrane conductance Regulator
CFU	Colony-Forming Unit
CLSM	Confocal Laser Scanning Microscopy
CoA	Coenzyme A
COG	Cluster of Orthologous Groups of proteins
COPD	Chronic Obstructive Pulmonary Disease
CRP	Cyclic AMP Receptor Protein
Cys	Cysteine
DMSO	Dimethylsulfoxide
ECO	*Escherichia coli*
EMSA	Electrophoretic Mobility Shift Assay
$FADH_2$	Flavin adenine dinucleotide (reduced)
GFP	Green Fluorescent Protein
Gly	Glycine
Gm	Gentamicin
GRA	Gene Reporter Assay
GRX	Glutaredoxin
HMM	Hidden Markov Model
HU	Hydroxyurea
Km	Kanamycin
LB	Luria Bertani (medium)
LBN	Luria Bertani medium + KNO_3

Lys	Lysine
NADH	Nicotinamide adenine dinucleotide (reduced)
NADPH	Nicotinamide adenine dinucleotide phosphate (reduced)
NAR	Nitrate reductase
NIR	Nitrite reductase
NOR	Nitric oxide reductase
NOS	Nitrous oxide reductase
ORF	Open Reading Frame
PAO	*Pseudomonas aeruginosa*
Phe	Phenylalanine
qRT-PCR	Quantitative Real-Time PCR
RFU	Relative Fluorescent Units
RNA-seq	RNA sequencing
RNR	Ribonucleotide Reductase
ROS	Reactive Oxygen Species
ROS	Reactive Oxygen Species
SAM	S-Adenosylmethionine
Tc	Tetracycline
Thr	Threonine
TRX	Thioredoxin
TSS	Transcription Start Site
Tyr	Tyrosine
UTR	Untranslated Region
Val	Valine

Introduction

1. Model organisms in this study

This study is focused on facultative anaerobic pathogens and the strategies they use to modulate ribonucleotide reduction and balance it under different environmental stimuli, variable oxygenation conditions, as well as during infection or biofilm formation. We used two very well-studied species: *Pseudomonas aeruginosa* and *Escherichia coli*.

1.1 Facultative anaerobic metabolism

Oxygen availability is one of the main factors conditioning life. Most life forms can be defined as aerobic or anaerobic depending on whether they require molecular oxygen for the release and conservation of catabolic energy or they rely on alternative pathways and electron acceptors[11]. Many aerobic organisms cannot survive even for short periods in the absence of oxygen, and, likewise, oxygen is deleterious for most anaerobes. At this level, oxygen availability simple determines which biotopes are accessible for a particular species. However, facultative anaerobes can grow in the presence or absence of oxygen[11, 12], and thus thrive in differently oxygenated environments. Many relevant microorganisms are facultative anaerobes, and the regulatory systems they require to maintain their lifestyle constitutes the main focus of this work.

1.1.1 Aerobic and anaerobic metabolism in bacteria

It is beyond the scope of this work to provide a systematic review of the systems and reactions of aerobic and anaerobic catabolism in bacteria. However, some of the most important elements of these metabolic pathways will be highlighted here, as their regulation will be relevant for this thesis.

Aerobic respiration is the catabolic process by which the energy stored in organic molecules is released and stored in the form of ATP and GTP, generated through substrate-level phosphorylation, and using molecular oxygen as the terminal electron acceptor for the process[13]. It is the most energetically efficient method for pyruvate breakdown after glycolysis[13]. An overview of the pathway as occurs in *Escherichia coli* can be seen in **Figure 1A**. Pyruvate is first oxidized (with coenzyme A) to acetyl-CoA and CO_2 by the pyruvate dehydrogenase complex[14]. The acetyl group in acetyl-CoA is then transferred to oxaloacetate, forming citrate, and thus entering a series of gradual oxidative reactions known as the citric acid cycle or the Krebs cycle[15] meant to release the energy stored in the organic substrate. The cycle regenerates a molecule of oxaloacetate and produces energy (in the form of GTP) and reducing power (in the form of NADH and $FADH_2$[13, 15]). The reducing power is then used (and thus recycled) to produce more energy by the electron transport chain.

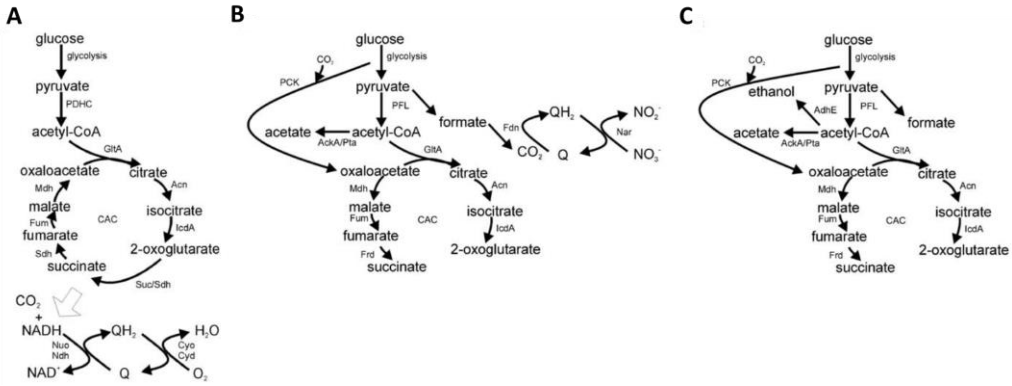

Figure 1. Schematic representation of the three main modes of catabolism in bacteria, as they occur in *E. coli*, represented in order or decreasing energy efficiency. **A**, aerobic respiration; glucose is transformed in pyruvate through glycolysis, and pyruvate is oxidized to acetyl-coA by pyruvate dehydrogenase; a full citric acid cycle occurs, and the reducing power obtained is directed to the electronic transport chain (depicted below the cycle) using oxygen as final electron acceptor. A whole oxidation of organic compounds to CO_2 takes place. **B**, anaerobic respiration; pyruvate is oxidized to acetyl-coA and formate by pyruvate formate lyase. Acetyl-CoA cannot be fully oxidized; it can be either partially oxidized to acetate or reduced to succinate. Formate can be oxidized to CO2. The reducing power obtained is directed to a shorter electronic transport chain using alternative electron acceptors (nitrate in the figure). **C**, fermentation (here mixed-acid fermentation); pyruvate is oxidized to acetyl-coA and formate by pyruvate formate lyase. Formate cannot be further oxidized and is considered a final product. Acetyl-coA can be converted to ethanol via acetaldehyde by alcohol dehydrogenase or be converted to acetate or succinate as previously described.

The electron transport chain[16] is a series of redox reactions conducted by membrane-bound protein complexes where the electrons released by electron donors (in bacteria fundamentally NADH) are transferred through a series of compounds of progressively higher redox potential, and the energy released is coupled to the active transfer of protons across a membrane[13, 16]. The thermodynamically favorable return of the electrons across the membrane is used to store the energy released in the form of ATP[16]. For the electron transport chain to keep working, all the protein complexes and organic compounds that take part must be regenerated, that is, release the electrons they received, transferring them to a new donor. Therefore, a final electron acceptor that is not itself part of the chain is required. The higher the redox potential of this final electron acceptor is, the more redox steps can happen before reaching it (this is usually called the "length" of the chain) and the more energetically effective the process is. Due to its high redox potential, oxygen, the final electron acceptor in aerobic respiration, produces the most effective transfer chain known[13, 16]. Thus, the last step of the aerobic respiration is the reduction of oxygen to water.

Many bacterial species encode redundant elements of the electron transport chain, thus generating multiple and branching chains, as a tool for adaptability[3, 7, 13, 16, 17]. One particularly critical step is the reduction of the final acceptor, as it is ultimately responsible for keeping all the chain working; therefore, this step tends to be especially versatile and subject to differential regulation[16]. This reaction

is controlled by terminal oxidases, membrane-bound enzymes specialized in the catalysis of the four-electron reduction of molecular oxygen to water[18]. Below we will analyze the particularities of the electron transport chain in the facultative anaerobes that are subject to this work, with a special focus in terminal oxidases and their differential regulation (see 1.2.2 and 1.3.2).

In the absence of molecular oxygen, the next most energetically efficient method for pyruvate breakdown is anaerobic respiration, which is illustrated in **Figure 1B**. The pyruvate dehydrogenase complex is no longer active and is replaced by pyruvate formate lyase, which will catalyze its conversion to acetyl-CoA and formate[13, 17, 19]. Acetyl-CoA cannot be oxidized completely as the citric acid cycle is also partly inactive; it can be partially oxidized to acetate (by phosphate acetyltransferase and acetate kinase) or enter a reversed incomplete citric acid cycle to be reduced to succinate, in an energy conservation effort[19]. Formate, on the other hand, can be fully oxidized to CO_2, and the reducing power obtained thereby is recycled in an anaerobic electron transport chain, which uses an alternative final electron donor, such as nitrate, nitrite, sulfate, or fumarate[13, 19]. These present lower redox potentials than oxygen, generating a shortened and less energetically efficient electron transport chain than the aerobic version.

The last option is fermentation. This term englobes all forms of metabolic pathways through which partial oxidation of organic compounds occurs in the absence of molecular oxygen or alternative acceptors for an electron transport chain, and which use an organic molecule as final electron acceptor, forming overflow metabolites such as lactate, acetate or ethanol. An extensive description of fermentation types and fermentative pathways is beyond the scope of this work; mixed-acid fermentation, represented in **Figure 1C**, occurs in *E. coli*[11, 17, 19-21] and will be discussed below (see 1.3).

1.1.2 Biological role of facultative anaerobiosis

Facultative anaerobic organisms can grow in the presence or absence of oxygen, as they can perform aerobic respiration when oxygen is available and switch to an anaerobic alternative (anaerobic respiration, fermentation, phototrophic growth, or a combination thereof) when it is not[11, 12]. Facultatively anaerobic metabolism is wide-spread among all domains of life, and many species significant for their environmental roles, industrial applications, or clinical relevance, are facultative anaerobes: this is the case of bacterial genera such as *Streptococcus, Staphylococcus, Escherichia, Salmonella, Yersinia, Listeria* or *Shewanella*, as well as eukaryotes such as *Saccharomyces cerevisiae*[11, 12]. In the case of pathogenic bacteria, this level of metabolic versatility offers significant advantages, as many environments inside host bodies feature hypoxic or anoxic conditions; microaerobic or anaerobic environments are also found in biofilms in chronic infections (see 1.1.3).

However, a facultatively anaerobic lifestyle is also costly. First, the genetic and enzymatic equipment for at least two redundant metabolic systems must be provided. Catabolism and anabolism are both affected by the switch from aerobic to anaerobic growth[11, 12]: not only energy metabolism exposed is affected, but also all biosynthetic reactions that require oxygen as a cosubstrate, such as oxidations

and hydroxylations, which have to be replaced by alternative reactions[11, 22]. Furthermore, these redundant systems cannot be simultaneously active, so facultative anaerobiosis comes with an increased cost in regulation complexity. It has been estimated that more than 500 genes in the *E. coli* genome are affected by oxygen availability[12, 17]. The transition between aerobic and anaerobic metabolism is mainly effected by transcriptional regulation, and numerous oxygen or redox-responsive transcriptional factors are known[11, 12, 17, 19]. The mechanism of aerobic-anaerobic transition and the regulatory systems responsible of its coordination are detailed below for the two main species that are the object of this work, namely *Pseudomonas aeruginosa* (see 1.2.2) and *Escherichia coli* (see 1.3.2).

1.1.3 Oxygen gradients in biofilms and the aerobic-anaerobic transition

Biofilms are surface-associated bacterial communities where bacteria live encapsulated in an extracellular hydrated polymeric matrix[5, 23]. In biofilms, bacterial cells display different patterns of gene expression and phenotypes than when growing in a planktonic state: they reduce their metabolic rate, increase cell-to-cell communication, change the array of virulence factors they express[23], become less sensitive to chemical and physical stress, and may develop new antibiotic resistances[5, 23, 24]. In some cases, clusters of cells are separated by channels through which fluid can circulate[5].

While planktonic cells in a well-mixed culture are generally considered uniform, biofilms are inherently heterogeneous[5]. Diffusion throughout the biofilm structure, together with the effects of bacterial metabolism, generates concentration gradients[5, 25] for nutrients, bacterial waste compounds, and signaling molecules (see **Figure 2**); in turn, these gradients shape the biofilm[26], generating different phenotypes across its layers. The behavior of these gradients fit the reaction-diffusion theory[25], which studies the distribution of solutes in confined areas, where the solute is being generated or consumed as a result of a reaction, and transported by diffusion. Oxygen is the best-studied and most familiar example[5, 24, 25, 27-29].

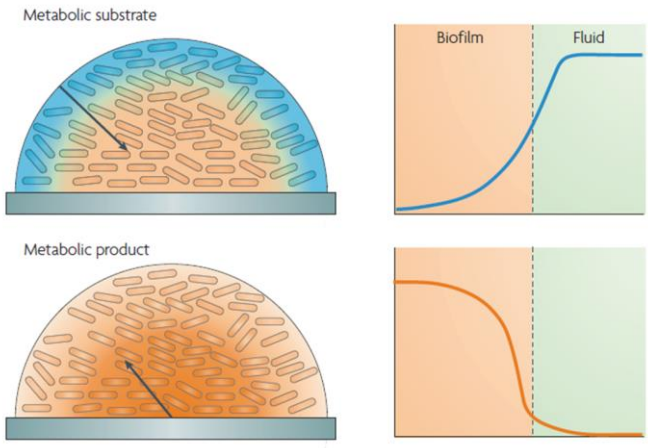

Figure 2. Schematic representation of chemical heterogeneity in biofilms. Different solutes appear in the biofilm as gradients of concentration. Nutrients or other metabolic substrates present a higher concentration in the outer layers and its concentrations decreases gradually in the inside. Conversely, metabolic products are more concentrated inside the biofilm. These concentration gradients are studied by the reaction-diffusion theory. Adapted from (5)

Biofilms composed primarily of facultative anaerobic bacteria exposed to an aerated medium present higher oxygen concentration in the outer layers, but oxygen tension decreases steadily with biofilm depth[5, 25]. The oxic zone can be from tens to a few hundred microns wide. For most bacterial species, a great part of the biofilm structure can be considered microaerobic, and strictly anoxic areas appear in the bottom layers of thick biofilms. Thus, oxygen is one of the most prominent manifestations of biofilm heterogeneity and, simultaneously, one of its leading causes[5, 26]. For this reason, facultative anaerobes display a vast array of different phenotypes across the biofilm structure.

The study of biofilm heterogeneity, therefore, plays a big part in understanding the behavior of facultative anaerobic pathogens. However, most techniques able to capture the different phenotypes present in a biofilm are mostly visual and very limited in their capabilities to quantify gene expression (such is the case of the use of fluorescent reporter genes or FISH coupled to confocal scanning laser microscopy)[5] or are very expensive and disruptive (such as laser capture microdissection)[5]. On the other hand, most common tools of molecular biology, such as qRT-PCR and RNA-seq, are commonly applied to biofilms *en masse*, losing the heterogeneity of individual layers[5, 28, 29]. To date, the study of individual phenotypes in oxygen gradients, such as those present in biofilms, remains one of the greatest challenges in the study of facultative anaerobes.

1.2 *Pseudomonas aeruginosa*

Pseudomonas aeruginosa is a rod-shaped Gram-negative bacterium of the class γ-proteobacteria commonly present as a free-living organism in soil and water environments, but that can also cause disease in plants and animals[30]. In humans, it is mainly an opportunistic pathogen, well-known for chronic lung infections in at-risk groups, such as patients with Cystic Fibrosis (CF) or Chronic Obstructive Pulmonary Disease (COPD), where *P. aeruginosa* grows forming distinctive biofilms[31-33]. *P. aeruginosa* is also a greatly adaptable bacterium: its genome, more than 6.3 million base pairs long[34], encodes more than 690 transcription factors, in a complex regulatory network with more than a thousand described interactions[35]. As another manifestation of adaptability, despite being commonly listed as an aerobe (because no significant growth can be supported by fermentation), *P. aeruginosa* is a facultative anaerobe, able to perform anaerobic respiration[36, 37].

1.2.1 Pseudomonas aeruginosa as a pathogen

In human infections, *P. aeruginosa* is considered a common opportunistic pathogen[30, 38]. It is mostly responsible for acute and chronic respiratory, urinary, and skin infections, especially in hospitalized patients, immunocompromised hosts, and patients with cystic fibrosis or chronic obstructive pulmonary disease[31-33, 39, 40].

As a very adaptable pathogen, *P. aeruginosa* encodes a wide array of virulence factors meant to assist the infection during its different stages[30]. Firstly, we consider the systems required for adhesion and surface colonization: *P. aeruginosa* produces specialized membrane adhesion proteins (adhesins), flagella and pili type IV[30], as well as lipopolysaccharides, which are involved in the interaction with host surface proteins, such as the Cystic Fibrosis Transmembrane conductance Regulator (CFTR)[32, 41]. Secondly, other factors are meant to increase resistance to host defenses and help survivability: *P. aeruginosa* encodes a vast number of two-component systems to respond to different environmental stimuli[42]; furthermore, the type III secretion system allows for the secretion of toxins to inhibit host protein synthesis and cytoskeleton development, to avoid phagocytosis[43]. Finally, other virulence factors assist in the dissemination of the infection: *P. aeruginosa* synthesizes proteases (such as alkaline protease, protease IV, LasA and LasB) to penetrate the extracellular matrix of the host's tissues[30], as well as pore-forming exotoxins to cause cell lysis, and pyocyanin to inhibit ciliary function and produce ROS[30, 44].

P. aeruginosa is naturally resistant to many antibiotics, such as β-lactams, tetracyclines, macrolides, and most fluoroquinolones[45]. Acute infections appear in the respiratory tract, urinary tract, prostheses, or burn wounds and often respond to treatment with select antibiotics[45, 46]. At this stage, alginate levels are usually non-detectable. When the infections persist, however, it can lead to the formation of a biofilm and, eventually, the establishment of a chronic infection. Chronic infections are most commonly seen in the pulmonary tract of at-risk groups, where they are associated with a poor prognosis, leading to severely impaired lung function and an increased risk of respiratory failure, and is the primary cause of morbidity and mortality[31]. Biofilms become more resistant to immune response and physical stress, as well as to antibiotic action[46]. Eventually, alginate-overproducing variants appear (the *mucoid phenotype*), which generate a biofilm much more resistant to antibiotic penetration, desiccation and phagocytosis[47, 48] and is associated with a quick deterioration in pulmonary function[49-51].

Therefore, one of the central elements in the switch to the mucoid phenotype and chronification in lung infections of *P. aeruginosa* is alginate biosynthesis. This process involves a large number of enzymes and substrates. The *algD844KEGXLI* operon is commonly called the alginate biosynthetic operon, as it encodes the main enzymes for alginate production[47, 52]; the *algC* gene from the *algC-argB* operon is also critical, as it encodes a multifunctional enzyme used for different pathways including alginate biosynthesis[47, 53]. The transcription of these genes is controlled by the sigma factor AlgU (sigma E), which is usually sequestered by the anti-sigma factor MucA. The stable mucoid phenotype occurs through the selection of mutations in regulatory genes, usually *mucA*, that cause the release of AlgU[53-

[55]. The pressure exerted by the immune response and antibiotic treatment is responsible for inducing hypermutation and selecting the mucoid variants. This model of the establishment of mucoid biofilms is illustrated in **Figure 3**.

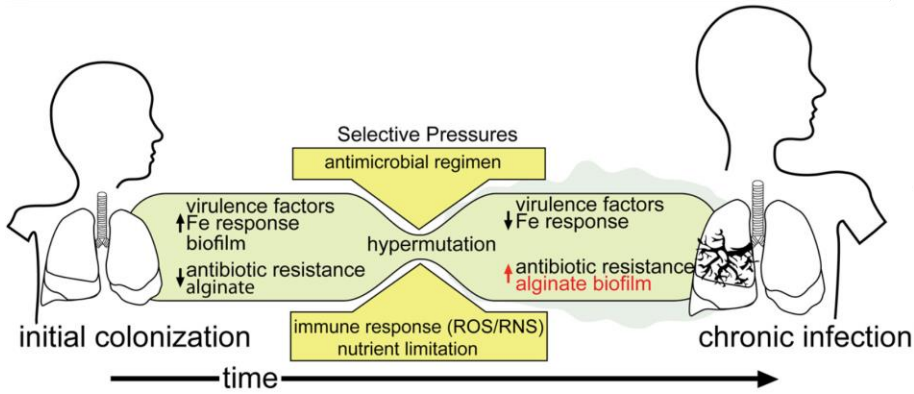

Figure 3. Model of chronification of a pulmonary infection by *P. aeruginosa* in a CF patient. While bacteria in the acute infection display a higher production of virulence factors, negligible production of alginate and significant antibiotic sensibility, the combined pressure exerted by immune response, nutrient limitation and antibiotic treatment stimulates hypermutation and selects mucoid variants, which display slower growth, lower production of virulence factors and highly increased resistance to antimicrobial therapies and other stresses. Adapted from (10)

Besides the *algD* and *algC* operons, the AlgU sigma factor also regulates the transcription of the *algZR* operon, which encodes the AlgZR two-component system[10]. In this system, AlgZ (also known as FimS) is the membrane-bound kinase that, upon binding of an unknown environmental signal, modulates the phosphorylation of AlgR[10, 56]. AlgR, in turn, is the transcription factor that, depending on its phosphorylation state, regulates different aspects of alginate biosynthesis[10, 56] (such as the *algD* and *algC* operons) and other aspects of biofilm formation, surface colonization, and virulence[10, 52, 56, 57].

1.2.2 Pseudomonas aeruginosa as a facultative anaerobe

In the presence of oxygen, *P. aeruginosa* grows using aerobic respiration as its energy-producing system[30]; however, in the absence of oxygen, it can switch to anaerobic respiration of nitrate or nitrite (denitrification)[7, 58, 59]. The different respiratory options in *P. aeruginosa* are illustrated in **Figure 4**. As the ability to grow under different oxygenation conditions is essential to growing as a biofilm, especially in the thick and highly hydrated mucoid biofilms characteristic of *Pseudomonas* chronic infections, the aerobic and anaerobic metabolic mode in *P. aeruginosa* and the mechanisms behind its aerobic-anaerobic transition have been extensively studied.

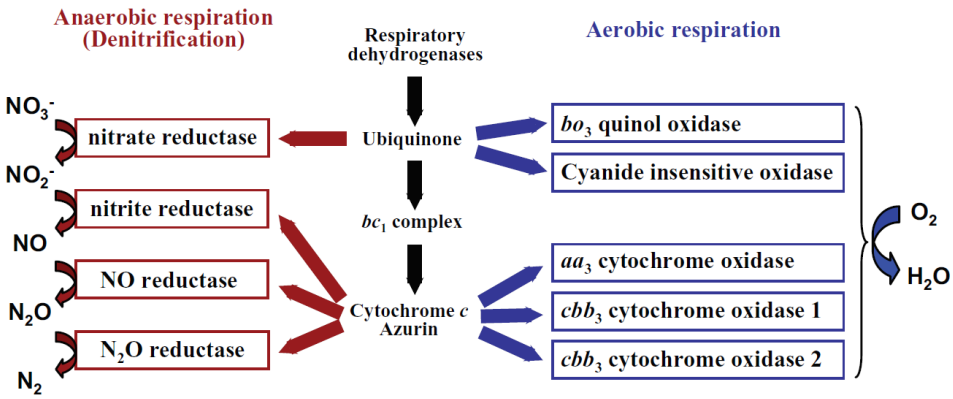

Figure 4. Energy metabolism in *P. aeruginosa*, through aerobic respiration (right) or anaerobic respiration (left). The different denitrification reductases and terminal oxidases are depicted in their corresponding positions in the electron transport chain. Adapted from (3).

The aerobic respiration machinery in this species is surprisingly complex and flexible[3]. *P. aeruginosa* is a species that can grow under high aeration but also thrives in microaerobiosis, adapting its respiration machinery to all the intermediate oxygen concentrations present in a mature biofilm[7], and even secreting substances to reduce the oxygen transfer rate to its surrounding medium, thus using microaerobiosis to obtain a competitive advantage[60]. To date, at least 17 aerobic respiratory dehydrogenases have been described to feed electrons into the quinone pool in the *P. aeruginosa* electron transport chain[61]; likewise, five different terminal oxidases have been identified at the end of the chain[3, 7].

The different terminal oxidases (**Figure 4**, aerobic respiration) reflect different situations to which *P. aeruginosa* may need to adapt. The first three are cytochrome-c oxidases; the constitutively active one is cytochrome cbb_3-1, a high oxygen affinity oxidase adapted to low oxygen levels[3, 7]. The fact that the constitutive oxidase is a high affinity one highlights how important microaerobiosis is for *Pseudomonas.* A second high-affinity oxidase, cytochrome cbb_3-2, exhibits an even lower K_M and is specifically induced under reduced oxygen tensions[3, 7]. The third cytochrome-c oxidase is the aa_3 oxidase, a low oxygen affinity with high proton-pumping activity[3, 7], closely related to the mitochondrial terminal oxidase; its transcription is activated by RpoS, and thus it is only expressed, as a strategy for maximum efficiency, under stationary phase and nutrient starvation. The remaining terminal oxidases are quinol oxidases only activated under particular stress conditions[3, 7].

In the absence of molecular oxygen, *P. aeruginosa* can perform arginine or pyruvate fermentation, but only as a method for anaerobic survival which does not allow for significant growth[62]. Instead, in the presence of nitrate, nitrite or nitric oxide, *Pseudomonas* can perform anaerobic respiration of these substrates, also known as denitrification[63, 64]. In this process (**Figure 4**, anaerobic respiration) nitrate and the products of its reduction can act as final electron acceptors with decreasing redox potential, obtaining nitrite, nitric oxide, nitrous oxide, and finally molecular nitrogen[7, 63]. These consecutive

reactions are conducted by nitrate reductases, nitrite reductases, NO reductases, and N_2O reductases, encoded respectively by the genes *nar*, *nir*, *nor* and *nos.*

The onset of denitrification and the aerobic-anaerobic transition are thoroughly regulated[59]. The direct regulator of denitrification is the two-component system NarXL, in which NarX is the membrane-bound kinase and NarL[36] the transcription factor. The kinase phosphorylates NarL upon detection of nitrate; in turn, NarL acts as a direct activator of nitrate reductase (NAR)[36]. Furthermore, NarL acts indirectly through the anaerobic master regulators, Anr, and Dnr.

Anr is a direct oxygen sensor that is at the highest point of the complex anaerobic regulatory hierarchy in *P. aeruginosa*[36, 65, 66] (**Figure 5**). As a close homolog to *E. coli*'s Fnr, it detects oxygen, or its absence, through a mechanism based on the disruption of Anr-Anr dimers through the oxidation of its 4Fe-4S cluster[59, 67]. Concerning denitrification, Anr acts as a transcriptional activator of nitrate reductase and also increases the transcription of *narXL*. The other genes in the denitrification pathway are activated by Dnr, a transcription factor moderately similar to Anr[68], but that responds to nitrite and nitric oxide[7, 58].

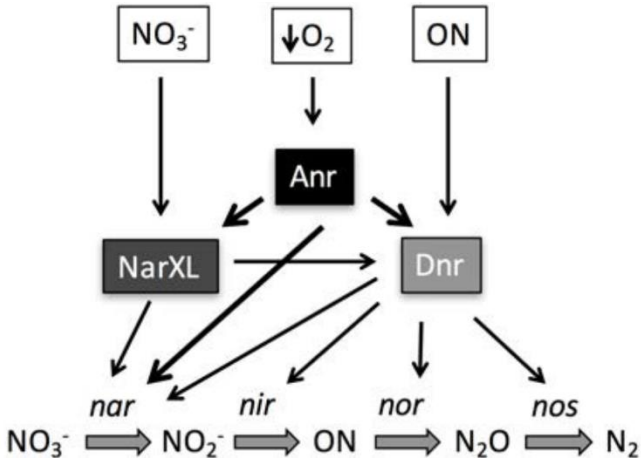

Figure 5. Schematic of the transcriptional regulation of the denitrification pathway in *P. aeruginosa*. The actions of the Anr and Dnr master regulators, together with the NarXL two-component systems, are displayed. The regulated genes are nitrate reductase (*nar*), nitrite reductase (*nir*), nitric oxide reductase (*nor*) and nitrous oxide reductase (*nos*). Adapted from (7).

Most interestingly, the anaerobic regulators also take part in the regulation of aerobic respiration: the most prominent example is the microaerobic activation by Anr of the high oxygen affinity cytochrome cbb_3-2[3]. This activation illustrates the heterogeneity of the aerobic-anaerobic transition, in an excellent example of hybrid metabolism[60].

1.3 *Escherichia coli*

Escherichia coli is a rod-shaped Gram-negative bacterium of the class γ-proteobacteria, commonly found as a commensal in the intestine of most warm-blooded animals[69]. However, some strains of *E. coli* are responsible for severe intraintestinal or extraintestinal infections. It is also a facultative anaerobe, able of growing anaerobically by both fermentation and a very flexible anaerobic respiration[12, 17, 70, 71].

1.3.1 Escherichia coli as a pathogen

Pathogenic *E. coli* strains are characterized depending on the immune response elicited by their main surface antigens[72]. The O antigen is the outer, oligosaccharide part of the lipopolysaccharide in the outer membrane; depending on the immune response elicited, more than 180 types of O antigen have been described[72-74]. Depending on their O antigen, *E. coli* strains are classified into serogroups[72]. The H antigen is a major component of flagella, encoded by *fliC,* of which more than 50 different immune classes have been described[72-74]. Depending on their combination of O and H antigens, *E. coli* strains are divided into serotypes[72].

Three general clinical syndromes can result from infection with different *E. coli* serotypes: intraintestinal infections (enteric/diarrheal disease), urinary tract infections, and sepsis/meningitis[72]. The strains causing these infections are highly adapted *E. coli* clones that possess specific virulence attributes, granting them the capacity to access new niches[74]. Those successful combinations of virulence factors that have survived have become specific pathotypes, depending on the nature of the disease they cause. In human infections, the pathotypes responsible for intraintestinal infections are enteropathogenic (EPEC), enterohaemorrhagic (EHEC), enterotoxigenic (ETEC), enteroaggregative (EAEC), enteroinvasive (EIEC) and diffusely adherent (DAEC)[72-74]. Likewise, urinary tract infections are caused by a different pathotype, the uropathogenic *E. coli* (UPEC). The pathotype associated with sepsis and meningitis is the meningitis-associated *E. coli* (MNEC). All *E. coli* strains responsible for extraintestinal infections are commonly referred to as extraintestinal pathogenic *E. coli* (ExPEC)[75].

1.3.2 Escherichia coli as a facultative anaerobe

In the lower intestine, commensal and pathogenic *E. coli* strains encounter a largely hypoxic environment. Traditionally, the gut has been considered to be anaerobic[76]; however, oxygenized areas exist due to oxygen diffusion from vascularized tissue[77], generating a decreasing gradient of oxygen concentration throughout the gastrointestinal tract and reaching below 0.5 ppm in the colon[78]. *E. coli* is a facultative anaerobe capable of growing with a wide array of different substrates and electron acceptors[17]. Recently, it has been described that both the microaerobic and the anaerobic machinery are required for gut colonization[77, 79].

The preferred mode of growth of *E. coli* is aerobic respiration[80]. This species encodes two main terminal oxidases, which it uses under very different environmental conditions[17]. The constitutively expressed one is cytochrome bo', previously known as bo_3[17, 81]; this is an efficient quinol oxidase with a low affinity for oxygen, thus mainly adapted to highly aerated environments. On the other hand, cytochrome bd-I, another quinol oxidase, presents an extremely high affinity for oxygen and can sustain growth under very low oxygen tensions[17, 81]. There is a third terminal oxidase, cytochrome bd-II, whose function remains mostly unknown[17].

In the absence of molecular oxygen, *E. coli* uses preferentially anaerobic respiration, if other electron acceptors are available. *E. coli* can accept many different molecules as final electron acceptors, such as fumarate, nitrate, nitrite, or dimethylsulfoxide[17], activating different specialized reductases to adapt its electron transport chain. If no other option is available, *E. coli* can grow using mixed-acid fermentation (**Figure 6**). This is a complex, branched pathway that produces a wide variety of final waste products: Pyruvate formate lyase uses the pyruvate obtained from glycolysis to obtain formate and acetyl-CoA. In the absence of redox acceptors, formate cannot be further oxidized and is the waste product detected at the highest concentration[17, 20]. Pyruvate can also be transformed into lactate by lactate dehydrogenase[20]. Acetyl-CoA (or phosphoenolpyruvate, using phosphoenolpyruvate carboxylase) can be converted into succinate via a reversed incomplete citric acid cycle (see 1.1.1). However, most commonly acetyl-CoA is used to produce ethanol (alcohol dehydrogenase) or acetate (phosphate acetyltransferase and acetate kinase)[17, 20]. The production rates of formate, lactate, succinate, ethanol, and acetate are not constant and depend on oxygen concentrations and other environmental factors.

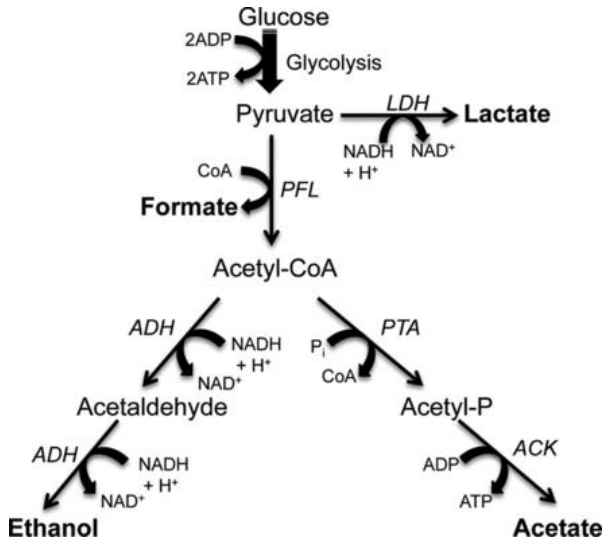

Figure 6. Mixed-acid fermentation. Final products are written in bold. The enzymes indicated are lactate dehydrogenase (LDH), pyruvate formate lyase (PFL), phosphate acetyltransferase (PTA), acetate kinase (ACK) and alcohol dehydrogenase (ADH). Adapted from (2).

As happens in many facultative anaerobes, the aerobic and anaerobic metabolic modes presented above are not necessarily mutually exclusive. Hybrid metabolism has been described, in which anaerobic process occurs in an anoxic cytoplasm while aerobic respiration still occurs in a hypoxic cell membrane[82].

As discussed in 1.1.2, the switch between aerobic respiration, anaerobic respiration, and fermentation, as well the other changes taking place in the aerobic-anaerobic transition, require a full metabolic adaptation in *E. coli*. It is estimated that more than 500 genes, perhaps as many as 1400, are directly or indirectly regulated by oxygen availability[17, 20]. Different oxygen sensors and secondary transcription factors are required for this transition[11, 12], including the oxidative stress-responsive elements (SoxRS, OxyR) and master transcriptional regulators, such as CRP. However, the most important elements in this regulation are the Fnr and ArcBA systems.[11, 12, 17]

Fnr is a direct oxygen sensor, and one of the most well-known oxygen-responsive transcription factors[11, 12, 17]. The structure of the Fnr protein reveals an N-terminal sensor domain and a C-terminal DNA-binding domain[83]. Aerobically, the Fnr protein is isolated as a monomer, which contains low quantities of loosely bound iron[11]. Anaerobically, Fnr acquires an organized [4Fe-4S] cluster in its sensor domain. The binding of the iron-sulfur cluster results in the formation of Fnr-Fnr dimers, which present sequence-specific DNA binding activity[11, 12, 17, 71]; Fnr acts as both a positive and negative regulator. When exposed to oxygen, the [4Fe-4S] cluster is degraded to [2Fe-2S], breaking the dimers and inhibiting site-specific DNA binding activity[11, 12, 17, 71].

In contrast to Fnr, ArcBA is a two-component system[84] that acts as an indirect oxygen sensor[17]. The membrane-bound kinase ArcB can detect oxygen availability reacting to the redox states of quinones in the electron transport chain[11, 12, 17, 84]. ArcB catalyzes its autophosphorylation and the transference of this phosphate group to ArcA when oxygen is not available. ArcA, in turn, is a transcription factor that binds to different promoters depending on its phosphorylation state[11, 12, 17].

The fine coordination of the aerobic-anaerobic transcription depends on the coordinated effort of Fnr and ArcBA, together with other regulatory mechanisms. Both systems control many promoters, and ArcBA or Fnr controlled promoters are also often controlled by CRP, NarL, or other transcription factors[17, 85].

2. Ribonucleotide reduction and biosynthesis of dNTPs

2.1 The enzyme ribonucleotide reductase

2.1.1 Significance of ribonucleotide reduction

The perpetuation of life depends on the ability to reproduce. Reproduction requires a system able to store genetic information stably and replicate it with enough accuracy. All biological functions require a way to express this genetic information and translate it into catalytic molecules. It has been proposed that the primordial genetic storage and catalytic system was RNA-based, in what was termed *the RNA world*. However, large molecules of RNA are inherently fragile, as the presence of a hydroxyl residue in the 2' position of its ribose ring causes it to be more susceptible to hydrolysis[86]. Today, all life forms have transitioned into a DNA-protein world, as described by the central dogma of molecular biology[87].

The transition from an RNA world to a DNA-protein world requires ribosome-based translation, genetic code-based transcription, semi-conservative DNA replication, and the substitution of RNA by DNA as genetic storage system. By the end of the 1950s, most of the basic gears of this central machinery were already discovered[88]. However, the enzyme responsible for the synthesis of the deoxyribonucleotides was not known until 1960, with the discovery of ribonucleotide reductase[89].

2.1.2 Ribonucleotide reductase

Ribonucleotide reductase (RNR) is the only enzyme responsible for reducing all ribonucleotides (NDPs/NTPs) to their corresponding deoxyribonucleotides (dNDPs/dNTPs), thereby forming the building blocks for DNA synthesis and repair[4, 8, 90]. This enzymatic reaction consists in the reduction of the hydroxyl group bound to the 2' ribose carbon of a ribonucleotide diphosphate or triphosphate to a hydrogen residue, thus forming the corresponding deoxyribonucleotide diphosphate or triphosphate (**Figure 7**).

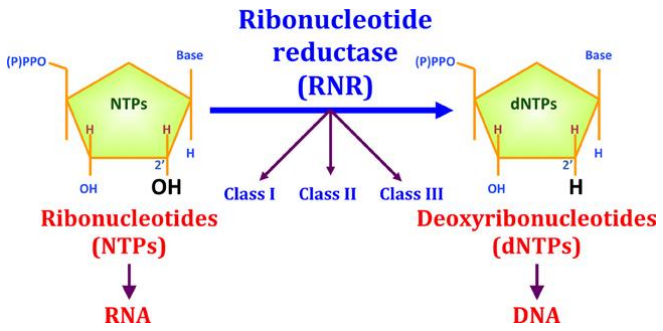

Figure 7. Simplified version of the enzymatic reaction catalyzed by ribonucleotide reductase. Adapted from (8) .

All living cells require dNTPs for DNA synthesis and repair. It is possible to obtain deoxyribonucleotides from intermediates in the degradative pathway for nucleotides through the *salvage* pathway, as has been observed in the mitochondria in eukaryotic cells[91]; however, RNRs remain the only enzyme responsible able to catalyze deoxyribonucleotide synthesis de novo[8].

Ribonucleotide reductases are metalloproteins that use radical chemistry to catalyze the reduction of the substrate and rely on metal cofactors for the initiation of a radical generation system[8, 90, 92]. This radical is then transferred throughout the protein structure through a highly studied radical transfer chain[90, 93], which ends with the formation of a stable organic free radical. Then, adenosine, cytidine, guanosine or thymidine ribonucleotides (diphosphate or triphosphates) are reduced in a single active site using the organic radical as a part of the catalytic mechanism, at the end of which the radical is regenerated[90, 93, 94] (**Figure 8**).

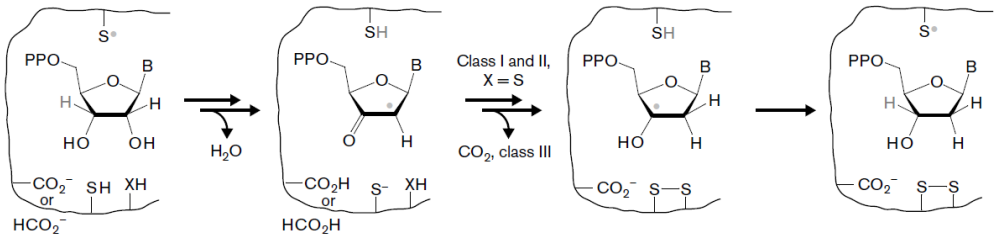

Figure 8. Minimal catalytic mechanism of all ribonucleotide reductases. Adapted from (6) .

The reduction of the ribonucleotide at the active site of RNR is coupled to the oxidation of two conserved cysteine residues, so the mechanism ends with a disulfide bond formed between them[6, 94]. The complete regeneration of the enzyme requires the reduction of this disulfide bond through the RNR electron donors, which are mainly thioredoxins (TRX) and glutaredoxins (GRX)[95, 96]. These are small (9-16 KDa) thiol-dependent reductases, mainly differentiated by the mechanism used for their reduction: TRXs make use of a thioredoxin reductase to couple their reduction to NADPH, while GRXs require the reduction of glutathione as an intermediary, which in turn is catalyzed by a glutathione reductase using NADPH[97].

Apart from the active site and the structures required for radical formation and transfer, RNRs also present dedicated sites for allosteric control of ribonucleotide reduction. The two potential sites (activity and specificity sites) are highly conserved among RNRs and will be discussed in detail below (see 2.2.1).

2.1.3 Classes of ribonucleotide reductase

All ribonucleotide reductases can reduce all four ribonucleotides to deoxyribonucleotides, and they all rely on the aforementioned systems for radical generation, radical transfer, and ribonucleotide reduction. Likewise, RNRs share a conserved tridimensional structure in the catalytic subunit, which

suggest a common ancestor for all the family[8, 98]. Despite all these similarities, evolution has produced remarkably different ribonucleotide reductases, so much that different RNRs encoded in the same genome by different transcriptional units present less than 20% identity in their primary structures[99].

Taking into account the specific mechanisms used for radical generation, the type of cofactor required, the type of electron donor used, differences in the structure of the protein complex, and dependence of oxygen, RNRs can be classified into three classes, namely class I, class II, and class III. Their main differences, explained in detail below, are summarized in **Table 1**.

	Class I			Class II	Class III
	Class Ia	Class Ib	Class Ic		
Genes	*nrdAB*	*nrdHIEF*	*nrdAB*	*nrdJ*	*nrdDG*
Structure	$\alpha_n\beta_n$	$\alpha_2\beta_2$	$\alpha_2\beta_2$	α/α_2	$\alpha_2+\beta_2$
Radical	Tyr -> Cys	Tyr -> Cys	Phe -> Cys	AdoCbl -> Cys	AMet->Gly->Cys
Cofactor	Fe^{III}-O-Fe^{III}	Mn^{III}-O-Mn^{III}	Mn^{IV}-O-Fe^{III}	Co (AdoCbl)	4Fe-4S (SA)
Substrate	NDPs	NDPs	NDPs	NDPs/NTPs	NTPs
Electron donor	TRX/GRX	NrdH/GRX	TRX	TRX/GRX	Formate/TRX
Oxygen dependence	Dependent	Dependent	Dependent	Independent	Sensitive
Specificity site	YES	YES	YES	YES	YES
Activity site	YES	NO	YES	YES / NO	YES

Table 1. Summary of the characteristics used to define RNR classes. Adapted from (8).

The first ribonucleotide reductase that was discovered in 1960 in *Escherichia coli* is now considered the prototype of class I RNR [89]. The existence of different RNRs was first considered in 1964 when the enzyme isolated from *Lactobacillus leichmannii* was demonstrated to present a different catalytic mechanism and require 5'adenosylcobalamin to be active[100]; this enzyme is now the prototype of class II RNR. The last class was discovered in 1989 when RNR activity in *E. coli* was detected under strict anaerobiosis for the first time[101]. The oxygen-sensitive enzyme that was discovered required S-adenosylmethionine (SAM) as a cofactor, and is now considered the class III RNR prototype[102].

2.1.3.1 Class I RNR

Class I RNRs are the most studied ribonucleotide reductases. They are present in all eukaryotic organisms and eukaryotic viruses and are also present in many species of Archaea and Bacteria, as well as some bacteriophages[8]. Class I RNRs take ribonucleotide diphosphate as their substrates.

These enzymes[4, 8, 90] are composed of two different subunits: the larger subunit α (or R1) contains the active site, responsible for the reduction of the ribonucleotides, and up to two different allosteric sites (activity and specificity). The smaller subunit β (or R2) contains the radical generation machinery and harbors the metal cofactor required to initiate the process. The radical is initially formed in a tyrosine

or phenylalanine residue in the β subunit and is transferred to a cysteine residue in the active site, to produce the required tiil radical. Different types of metal cofactors can be found in class I RNR enzymes, but the process requires in all cases the presence of molecular oxygen, so class I RNRs are oxygen-dependent. The active quaternary structure of class I RNRs is an association of several units of the α+β dimer, being the $\alpha_2\beta_2$ form the most commonly found.

In bacteria, this class of RNR has been divided into three subclasses, namely, Ia, Ib, and Ic, differentiated by the presence or absence of the overall activity allosteric site, the exact metal cofactor they use and the amino-acid residue where they generate the radical[4, 8]. The first RNR enzyme that was found in *E. coli* is now considered a class Ia RNR. Class Ib RNR was discovered in *Salmonella typhimurium* in 1994[103]. Class Ic RNR was the last to be discovered in a study with *Chlamydia trachomatis* in 2004[104]. The differences between these subclasses are discussed in detail below. The structure of the first-discovered RNRs class Ia and class Ib is compared in **Figure 9**.

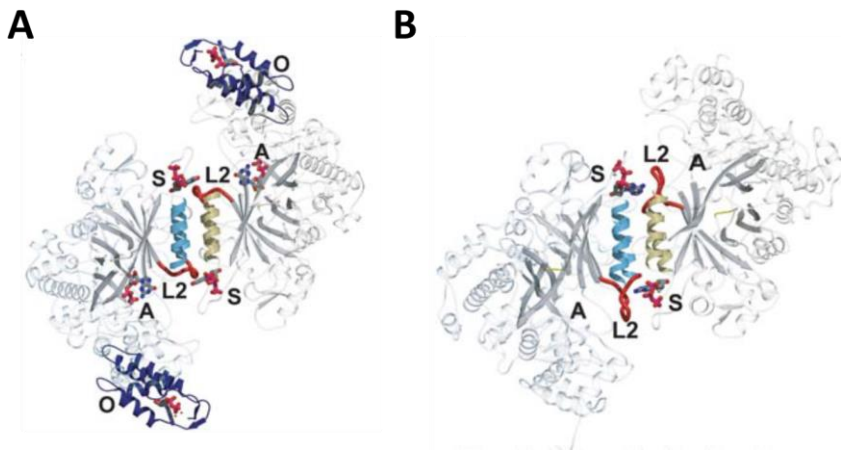

Figure 9. Comparative tridimensional structure of different RNR class I enzymes: *E. coli* RNR class Ia (A) and *S. typhimurium* RNR class Ib (B). The most representative elements of their structures are highlighted and indicated with letters: A, active site; O, overall activity allosteric site; S, specificity allosteric site; L2, loop 2. Adapted from (4).

Class Ia RNRs are the only ribonucleotide reductases expressed by eukaryotic organisms and eukaryotic viruses[4, 8, 90]. In bacteria, they are encoded by genes *nrdA* (subunit α) and *nrdB* (subunit β). These enzymes require a di-iron center (Fe^{III}-O-Fe^{III}) for radical generation, and their catalytic subunit contains two allosteric regulation sites: the overall activity site and the specificity site (see 2.2.1). Taking the class Ia RNR from *E. coli* as a model, we can see that it initially generates the radical in the conserved tyrosine residue Tyr122 of NrdB, which is placed in a highly hydrophobic area, close to the metal center[105]. The radical is transferred to NrdA to form the active radical tiil in Cys439106 finally. The other two conserved cysteine residues of the active site, which are oxidized (forming a disulfide bond) during the catalytic mechanism, are Cys225 (proximal) and Cys462 (distal)[106]. The active center is regenerated

through the action of both glutaredoxins and thioredoxins, which initially interact with two tyrosine residues in NrdA (Tyr370 and Tyr371), transferring the electrons which eventually are responsible for the reduction of Cys225 and Cys462, thus preparing the active site for a new substrate[107]. The typical quaternary structure of class Ia RNR is the homodimer of heterodimers ($\alpha_2\beta_2$), although higher oligomerization structures are possible. In *E. coli*, the formation of an $\alpha_4\beta_4$ structure is related to the allosterically-mediated inactivation of the enzyme[108].

Class Ib RNRs are confined exclusively to bacteria and bacteriophages[8] and are encoded by genes *nrdE* (subunit α) and *nrdF* (subunit β). The class Ib operon *nrdHIEF* also encodes a Ib-specific glutaredoxin-like protein (*nrdH*)[109] and a flavodoxin required for the synthesis and maintenance of the metal center (*nrdI*)[110]. This center is found in nrdF, and *in vivo* it is a very characteristic MnIII-O-MnIII structure[111], although the enzyme remains active *in vitro* when coupled to a Fe^{III}-O-Fe^{III} center[112]. The iron-free metal center explains the use of class Ib RNR in *E. coli* as an alternative aerobically active ribonucleotide reductase to be used under iron deprivation conditions. The catalytic subunit of class Ib RNRs contains the active site and the specificity allosteric site but lacks the overall activity site[8, 90].

Class Ic RNRs were discovered relatively recently in *Chlamydia trachomatis*[104] and are also confined exclusively to bacteria[8]. The α and β subunits in this subclass are codified by genes *nrdA* and *nrdB*, respectively, such as in class Ia RNR. Class Ic RNRs harbor a very particular manganese-iron metal center (MnIV-O-FeIII) in NrdB[113], which is used to produce a radical in a phenylalanine residue instead of a tyrosine (Phe122 in *C. trachomatis*)[104]. The radical is transferred then to the catalytic subunit NrdA, which is considerably larger than its Ia counterpart (286 amino acids longer than the model class Ia RNR in *C. trachomatis)*, due to a duplication in the overall activity catalytic site[114].

2.1.3.2 Class II RNR

Class II RNRs are present exclusively in bacteria, archaea, and some bacteriophages[8]. The members of this class can take ribonucleotide diphosphates or triphosphates as substrates for reduction[8, 90].

These enzymes[4, 8, 90] are formed by a single subunit α, considerably similar to the catalytic subunit of class I RNRs, expressed by the gene *nrdJ.* The active quaternary structure can be a monomer, as in *Lactobacillus leichmannii*[100] (α) or a dimer, as in *Thermotoga maritima*[115] (α_2). These alternative structures are reflected in **Figure 10**.

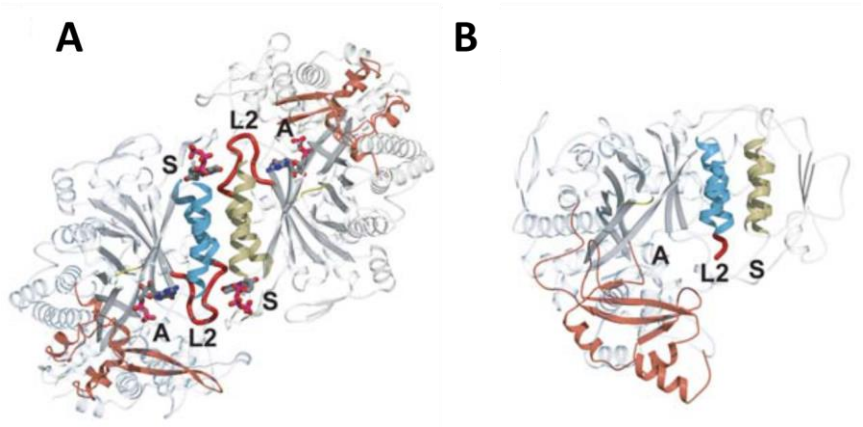

Figure 10. Comparative tridimensional structure of different RNR class II enzymes: The α_2 structure from *T. maritima* (A) and the α structure from *L. leichmannii* (B). The most representative elements of their structures are highlighted and indicated with letters: A, active site; S, specificity allosteric site; L2, loop 2. Adapted from (4).

The NrdJ protein contains the active site[8], where the catalysis of the reaction occurs through a mechanism very similar to the one previously described. A cysteine residue will receive the electrons to form a tiil radical (in the model sequence of *L. leichmannii*, Cys408[115]) and two additional cysteines are involved in the redox reaction, suffering their oxidation (forming a disulfide bond) to catalyze the reduction of the ribonucleotide: in *L. leichmannii*, these are Cys119 (proximal) and Cys419 (distal). The regeneration of the active site occurs through the action of thioredoxins and glutaredoxins interacting with residues Cys731 and Cys736.

In Class II RNRs, the generation of the radical does not occur in a dedicated subunit but occurs through direct interaction of the active site of the enzyme with 5'deoxyadenosylcobalamin, a modification of vitamin B_{12}[4, 8, 90]. The cobalt atom in the vitamin is used as the metal center for the generation of a 5'-deoxyadenosyl radical, which is transferred to Cys408 to form the active tiil radical[116]. This process does not require molecular oxygen to occur, so Class II RNRs are oxygen-independent, although they require a supply of vitamin B_{12} or 5'deoxyadenosylcobalamin to be active.

The NrdJ protein also contains the allosteric sites. Although some particular class II RNRs contain the overall activity site, such as that of *Thermoplasma acidophilum*[117], most NrdJ proteins lack that site and contain only the specificity one[4, 8].

2.1.3.3 Class III RNR

Class III RNRs can be found in bacteria, archaea, and some bacteriophages[8], and take ribonucleotide diphosphates or triphosphates as substrates for reduction[8, 90].

This class is composed by two independent proteins[4, 8, 90], roughly equivalent to the two subunits seen in Class I RNRs: the catalytic protein α, encoded by the gene *nrdD*, and the activase protein β, encoded by *nrdG*. These proteins are found *in vivo* as two independent homodimers (α_2 + β_2). As mentioned above, the first class III RNR to be discovered was that of *E. coli*[118], but, nowadays, the most studied is the one encoded by the bacteriophage T4 (*Escherichia* virus T4)[119]. The structure of the class III RNR T4 α_2 protein is depicted in **Figure 11**.

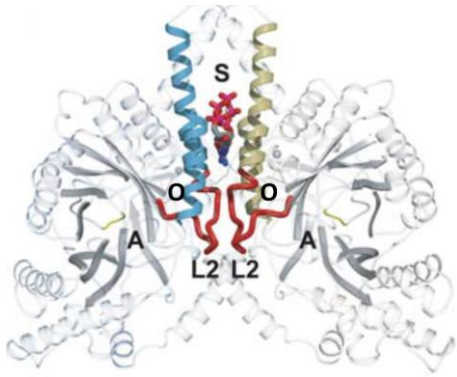

Figure 11. Tridimensional structure of the RNR class III α_2 protein encoded by the bacteriophage T4. The most representative elements of its structure are highlighted and indicated with letters: A, active site; S, specificity allosteric site; O, overall activity site; L2, loop 2. Adapted from (4).

The NrdG activase protein contains the machinery for radical generation in this class of ribonucleotide reductases[8, 105]. Its metallic center is a 4Fe-4S cluster[120, 121], which is reduced by the flavodoxin system (flavodoxin, flavodoxin reductase, and NADPH) and is oxidized and disorganized in the presence of molecular oxygen[122, 123]. The 4Fe-4S cluster is supported by four cysteine residues (in the bacteriophage T4, Cys543, Cys546, Cys562, and Cys564)[124]. The NrdG protein transfers the electrons to an S-adenosylmethionine (SAM), releasing a free methionine and generating a 5'-deoxyadenosyl radical[120]. This radical is then transferred to a glycine residue at the surface of protein NrdD (Gly580 in the bacteriophage T4) forming a highly oxygen-sensitive glycyl radical. Due to the effects that oxygen exerts on the metal center and the glycyl radical, class III RNRs are oxygen-sensitive[4, 98, 122].

The NrdD catalytic protein contains the allosteric sites (both the overall activity site and the specificity site)[8], as well as the active site, which catalyzes the reaction through a mechanism analogous to those described above. The surface oxygen-sensitive glycyl radical is transferred to the active site to form a tiil radical (Cys290 in the bacteriophage T4)[124]. The active site reduces the ribonucleotide through its own oxidation, and it is regenerated through the action of formate as an electron donor, which interacts with an asparagine residue (Asn311)[124].

2.1.4 RNR distribution and its ecological significance

Although there are some very particular cases of simple eukaryotic lifeforms presenting class II and class III RNRs (such as the class II RNR encoded by the microalga *Euglena gracilis*[125] or the class III RNR encoded by the fungus *Giberella zeae*[8, 90]), complex eukaryotic organisms only encode class I RNRs. On the other hand, eubacteria and archaea make use of all known classes of RNR[8], and a single species can encode any potential combination of RNRs.

As described above, RNRs work under a wide range of environmental conditions and present a variety of requirements to work. For example, as class I RNRs are oxygen-dependent, class II RNRs are oxygen-independent, and class III RNRs are oxygen-sensitive, expressing different RNR classes allows bacteria to thrive under differentially oxygenated environments[8]. Additionally, expressing class II RNR or different combinations of classes is especially important for facultative anaerobes, as that facilitates their survival during the aerobic-anaerobic transition. Only class I RNR requires a fully oxygenated environment. This effect is also notable during biofilm formation: distinct chemical gradients are formed throughout the tridimensional structure of the biofilm as compounds are generated or consumed by the cells[5, 25], and this includes oxygen. Thus, as discussed in 1.1.5, gradients are established from a highly oxygenated surface to oxygen-limited or potentially anaerobic bottom layers; encoding class II or class III RNRs is therefore required for the formation of thick biofilms. A simplified schematic depicting how the different RNR classes influence the ability to survive under different oxygenation conditions is shown in **Figure 12**.

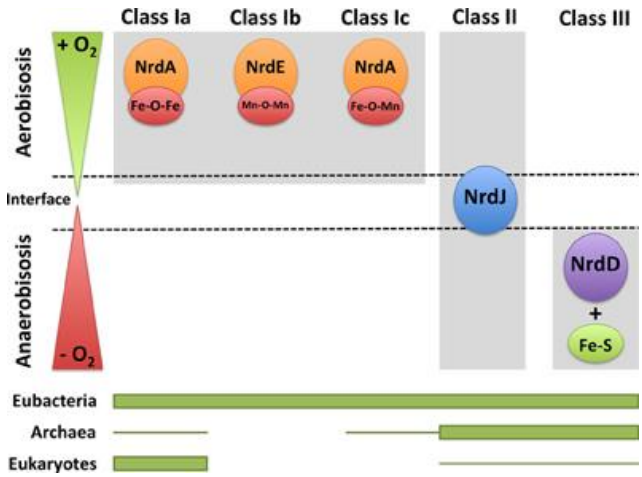

Figure 12. Distribution of RNR classes depending on their activity (grey box) under different oxygenation conditions: aerobic, anaerobic, and interphases. The lines below represent the occurrence of RNR classes among the three domains of life; a thick line represent high occurrence, while a thinner line represents that the corresponding class only appears in a few organisms. Adapted from (8)

Another example of how expressing different ribonucleotide reductase classes allows bacteria to adapt to variable circumstances can be found in the composition of the metal centers. As discussed above (see 2.1.3.1), class Ia RNRs require a di-iron center, while their class Ib counterparts use a di-manganese center. Thus, *E. coli* class Ib RNR has been proved to facilitate survival under iron limitation[126].

For these reasons, the RNR or combination of RNRs encoded by a particular species can reveal significant information about the environments where it can thrive. However, it needs to be stated that RNR occurrence is complex, and there is not always an obvious correlation between the set of RNRs encoded by an organism and its life style and phylogeny[98, 127]. For instance, *Streptomyces coelicolor*, an obligate aerobe, encodes a class II oxygen-independent RNR in addition to its regular class Ia RNR; the meaning of the class II enzyme is not trivial and has been associated to survival after oxygen deprivation periods[128].

2.1.5 RNRs in the model organisms of this study

As a facultative anaerobe and a versatile commensal and pathogenic species, *Escherichia coli* encodes a set of ribonucleotide reductases that allows it to thrive under a variety of environmental conditions. There are three active RNRs encoded in the *E. coli* genome: a class Ia RNR (*nrdAB*), class Ib RNR (*nrdHIEF*), and class III RNR (*nrdDG*)[129, 130].

The class Ia and class III RNRs encoded by *E. coli* were the first enzymes discovered in their respective classes, and are described in detail in 2.1.3.1 and 2.1.3.3, respectively. They are essential and sufficient for aerobic and anaerobic growth, respectively; mutational analysis demonstrates that *E. coli* lacking class Ia RNR cannot grow in the absence of oxygen, while strains lacking class III RNR cannot grow in its presence[131, 132].

The role of class Ib RNR is less evident; although this class appears as the only RNR of some bacterial species[129], in *E. coli* it is apparently redundant with class Ia; and, although functional and responsive to RNR regulation[111, 133], it is not able to sustain aerobic growth on its own[131]. However, since its metal cofactor *in vivo* is a di-manganese center instead of a di-iron, class Ib RNRs are adequate to environments low in iron sources and less susceptible to damage by oxidative stress[134, 135]. Consequently, the class Ib RNR in *E. coli* has been shown to facilitate survival under iron deprivation[126], biofilm formation, and nutrient-limited conditions[136], as well as under high oxidative stress[137].

Pseudomonas aeruginosa, on the other hand, is one of the few organisms known to encode all three ribonucleotide classes: class Ia (*nrdAB*), class II (*nrdJab*) and class III (*nrdDG*) RNRs[34, 129, 138]. This manifestation of metabolic versatility is characteristic of the great adaptability of *Pseudomonas* (see 1.2). The activation and repression of the transcription of these RNRs is further analyzed in 2.2.2 and constitutes one of the main focus points of this work.

The *P. aeruginosa* class Ia RNR exhibits a series of particularities that make it exceptional. Firstly, its sequence is 220-230 amino-acids longer than that of most γ-proteobacteria, due to a duplication in the overall activity allosteric site, the ATP-cone[139] (see 2.1.3.1 and 2.2.1). The N-terminal ATP-cone domain is named ATP-cone 1 and has been described to carry out its regular allosteric function[139, 140]. The additional, internal ATP-cone 2 does not take part in the allosteric regulation of the enzyme but plays a role in the stabilization of its quaternary structure[139, 140]. Additionally, the NrdB protein is also particular in *P. aeruginosa*, as it generates an unusually short-lived radical. Thus, while in the prototypical class Ia RNR oxygen is only required to initiate the process and the enzyme can retain activity for a certain time under anoxic conditions, its *P. aeruginosa* counterpart requires continuous exposure to oxygen[139].

The class II RNR encoded by *P. aeruginosa* is also singular, as it is composed of two ORFs separated by 16 base pairs, namely *nrdJa* and *nrdJb*[34, 141]. These genes produce two independent proteins, NrdJa and NrdJb. NrdJa contains the active site of the enzyme and its allosteric site, while NrdJb is involved in the interaction with 5'hydroxylcobalamin and the electron donors[141, 142]. The enzyme is only active when both proteins are present[142]. As many class II RNRs, the enzyme in *P. aeruginosa* does not include the overall activity catalytic site, and only contains the specificity one[138].

2.2 Regulation of ribonucleotide reduction

Ribonucleotide reduction is an essential activity, as all living cells require a supply of deoxyribonucleotides for DNA synthesis and repair[8]. Furthermore, keeping a balanced supply of all four dNTPs is also critical, as an unbalanced dNTP pool leads to increased mutation rates and the loss of DNA replication fidelity[143, 144]. Therefore, it is critical to maintaining a tight regulation on the expression of the different RNR classes and their enzymatic activity. RNR activity is regulated at the enzymatic activity level through allosteric sites, as previously mentioned, and at the transcriptional level. In this work, we focus on the regulation of bacterial ribonucleotide reductases[90, 145], but the eukaryotic RNR regulation has also been subject to intense study[4, 146, 147].

2.2.1 Allosteric regulation of ribonucleotide reduction

The allosteric regulation of ribonucleotide reduction is responsible for two critical activities: keeping the balance of ribonucleotides and deoxyribonucleotides in the cell (ensuring a sufficient supply of dNTPs) and, likewise, keeping the balance of all four dNTPs[8, 90, 148]. Both levels of regulation are achieved through the binding of nucleotide effectors in allosteric sites.

Any RNR enzyme can reduce all four different NDPs/NTPs to their corresponding dNDPs/dNTPs, using a single active site[4, 149]. All RNRs include a specificity allosteric site responsible for provoking changes in the protein structure to adapt the active center to the specific reduction of a particular substrate[149].

The specificity allosteric site was first studied in the *E. coli* class Ia RNR, but a very similar mechanism has later been described for class II and class III RNRs[148-150]. The allosteric site is placed so that the effector binds in a pocket at the homodimer interface of the catalytic subunits/proteins[149, 150]. A flexible part of the protein structure, the loop 2, corresponding in the class Ia RNR enzyme of *E. coli* to residues 292-301 (see figures 9, 10, 11) bridges the specificity effector site and active sites, forming a different structure for every possible effector-substrate pair, which is in turn responsible for the changes in the specificity of the active site[149, 150]. The changes provoked in specificity are the following: when ATP or dATP are bound as effectors, the enzyme reduces CDP and UDP; when dGTP is bound, the enzyme reduces ADP; finally, when dTTP is bound, the enzyme reduces GDP[8, 149]. A schematic of these effects can be seen in **Figure 13**.

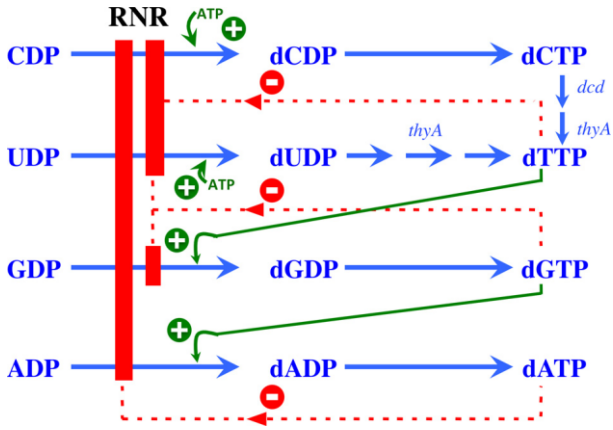

Figure 13. Model of the allosteric regulation of class Ia RNRs. Blue arrows represent the conversion of the 4 NDPs in their corresponding dNDPs/dNTPs. The stimulation of particular reactions through the specificity allosteric site is indicated by green arrows, while the repression of particular reactions is represented by red arrows, affecting the reactions indicated by the rightmost red box. The positive action of the overall activity site is the stimulation of all reactions by ATP (green +ATP) and the repression by dATP (leftmost red box). Adapted from (8).

On the other hand, the overall activity allosteric site is only present in some RNRs and is responsible for up or down-regulating the global activity of the enzyme depending on the binding of ATP or dATP as effectors. To avoid unnecessarily blocking the activity of the enzyme, the affinity of dATP for the overall activity site is ten times lower than for the specificity site[151]. This domain can be found in most class Ia and Ic RNRs, as well as most class III RNRs, and a small subset (around 7%) of class II RNRs[1]. When present, the allosteric site is a distinctive domain in the N-terminal end of the protein sequence, a four-helix bundle covered by a three-stranded beta-sheet[152], forming a characteristic cone-shaped structure, for which it is called the ATP-cone domain[152]. The binding of dATP to the ATP-cone provokes a change in protein structure that affects the overall activity of the enzymes through changes in the quaternary structure of the protein complexk. The exact changes vary between RNRs: in eukaryotic RNRs, the $\alpha_2\beta_2$ and $\alpha_6\beta_6$ structures are both active[4, 153], and the binding of dATP causes an anomalous interaction of the α_6 hexamer to generate an inactive $\alpha_6\beta_2$ complex[153, 154]. On the other hand,

prokaryotic class Ia RNRs exist in their active form as an $\alpha_2\beta_2$ complex (see 2.1.3.1) and the binding of dATP in their ATP-cone increases the oligomerization[118, 151]. These effects are summarized in **Figure 14**.

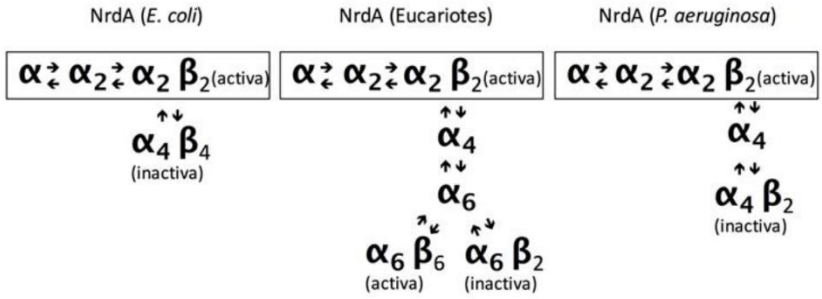

Figure 14. Active and inactive oligomeric states of class Ia RNR in eukaryotic organisms, *P. aeruginosa* and *E. coli*. Adapted from (1).

2.2.2 Transcriptional regulation of ribonucleotide reduction

While the allosteric regulation is in charge of keeping a balanced supply of deoxyribonucleotides, the regulation at a transcriptional level is responsible for two general aspects of the control of ribonucleotide reduction: Firstly, adjusting the expression of the ribonucleotide reductases when a higher production of deoxyribonucleotides is required, that is, during the DNA replication phase in the cell cycle, to maintain a constant DNA / cell mass ratio, and upon DNA damage, to conduct repairs[8, 90, 145]. Secondly, in those species that encode more than one RNR class, the transcriptional regulation of RNRs is also responsible for differential RNR expression, activating or repressing the different classes in response to environmental conditions[8, 90].

In this work, we focus on the transcriptional regulation of bacterial ribonucleotide reductases, but this process has also been extensively studied in eukaryotic organisms, especially in mice[4, 146] and yeasts[4, 155]. The actions of the transcription factor NrdR, a global repressor of all ribonucleotide reductases in bacteria[8, 9, 128] affect all RNR expression and will be analyzed in more detail below (see 2.2.3).

Class Ia RNR transcription in *E. coli* is always active under aerobic conditions, but its expression is also coupled to the cell cycle, increasing during DNA replication[90, 145]; it is also known to be activated by DNA damage, as well as by any alterations in ribonucleotide reduction itself[156]. The class Ia RNR operon *nrdAB* is regulated by the protein DnaA, the main initiator of DNA replication in bacteria. In *E. coli*, DnaA-ATP binds to two boxes in positions -48 and -36 relative to the TSS, acting as a positive regulator of *nrdAB* expression[145, 157, 158]. Another of the proteins involved in coupling *nrdAB* expression to changes in DNA replications is Fis, another nucleoid-associated protein related with the initiation of DNA replication: it acts as an activator of *nrdAB* transcription through binding in up to five different binding sites[159, 160]. The transcription of class Ia RNR is also positively regulated by IciA, an inhibitor of the initiation of DNA replication[161, 162] and the cyclic-AMP Receptor Protein (CRP), which, when coupled to

cAMP, binds in a single box at position -136 relative to the *nrdAB* TSS[163]. Finally, the transcription of this RNR class is negatively regulated by H-NS, a nucleoid-associated protein known as a global transcriptional repressor of environmentally-regulated genes[164]. At a post-transcriptional level, the 5' UTR region of the *nrdABS* messenger in *Streptomyces coelicolor* is known to contain a riboswitch controlled by vitamin B12, to repress class Ia RNR in favor of class II[165].

The transcriptional regulation of class Ib RNR is not as well studied as that of class Ia. As previously suggested, one of the plausible roles for class Ib RNR in those species where it coexists with class Ia is as an alternative aerobically active RNR under iron deprivation conditions (see 2.1.3.1). Consequently, the class Ib RNR operon in *E.coli nrdHIEF* is directly repressed, in the presence of iron, by the binding of the Ferric uptake regulator Fur in a single binding site located at the -61 position relative to the TSS[166].

The transcriptional regulation of class II RNR is mostly unknown. In *P. aeruginosa*, where this class coexists with class Ia and class III RNRs (see 2.1.5), the transcription of class II RNR has been described to increase during stationary phase and under anaerobiosis[167, 168]. No specific transcription factors have been demonstrated to regulate this RNR class, although a putative regulation by the AlgZR system has been suggested[52].

Finally, class III RNRs, as oxygen-sensitive enzymes, are expected to be regulated by the presence or absence of oxygen in facultative anaerobes. In *E. coli*, *nrdDG* transcription increases under anaerobiosis and in the stationary phase[169, 170]. The master regulator of the anaerobic metabolism Fnr (see 1.3.2) is at least partially responsible for that induction through its binding in two boxes in positions -65 and -35, relative to the TSS[170, 171].

As can be seen for all these examples, most of the information known about the transcriptional regulation of ribonucleotide reductases in bacteria are isolated regulation events. However, as a coordinated network responsible for an essential activity, the regulation of ribonucleotide reduction can only be completely understood applying a network perspective in a species-by-species approach, especially in those species encoding more than one RNR class. This perspective will be addressed in this work.

2.2.3 The NrdR transcription factor

The transcription factor NrdR constitutes a distinctive trait of bacterial ribonucleotide reduction, a master regulator of ribonucleotide reductases. NrdR forms a highly conserved family of proteins demonstrated to repress all RNR classes encoded by any bacterial species[8, 9, 129] while being completely absent in archaea and eukaryotes. The data available nowadays suggests that it might be a complex cooperative and allosterically-regulated nucleotide sensor, meant to couple the general coordination and fine-tuning of the RNR network to the overall NTP and dNTP pools in the cell[8, 133, 172]. However, the

exact mechanism through which NrdR carries out its role is mostly unknown and constitutes one of the major focus points of this work.

2.2.3.1 Discovery of NrdR and the nrdR locus

NrdR was first noticed in 2002 as an undescribed ORF located immediately upstream of the *nrdJ* gene in *Streptomyces coelicolor* and *Streptomyces clavuligerus*[173], and its gene was initially named *orfR*. Further study demonstrated *orfR* was co-transcribed with the class II RNR gene, and its name was changed to *nrdR*, forming an *nrdRJ* operon[128]. As *nrdR* was predicted to encode a protein with a DNA-binding domain and an RNR-associated ATP-cone domain (see 2.2.3.3), NrdR was immediately hypothesized to be a transcription regulator of RNR expression[128].

Orthologues of that *nrdR* gene were discovered across the Bacteria domain. The location of these genes varies: in some genera, *nrdR* is clustered with ribonucleotide reductases genes[9, 128] (e.g., with *nrdJ* in *Streptomyces* or with *nrdDG* in *Treponema*), and in many AT-rich gram-positive bacteria (*Bacillus*, *Streptococcus*, *Staphylococcus*, *Lactobacillus*) *nrdR* is located upstream of genes involved in DNA metabolism, such as *dnaB* and *dnaI*[9]. In gamma-proteobacteria, however, *nrdR* appears in the riboflavin biosynthetic operon, upstream of *ribD*, and was previously named *ribX*[9, 128]. **Figure 15** shows some examples of the genetic context of the *nrdR* locus in different bacterial genera.

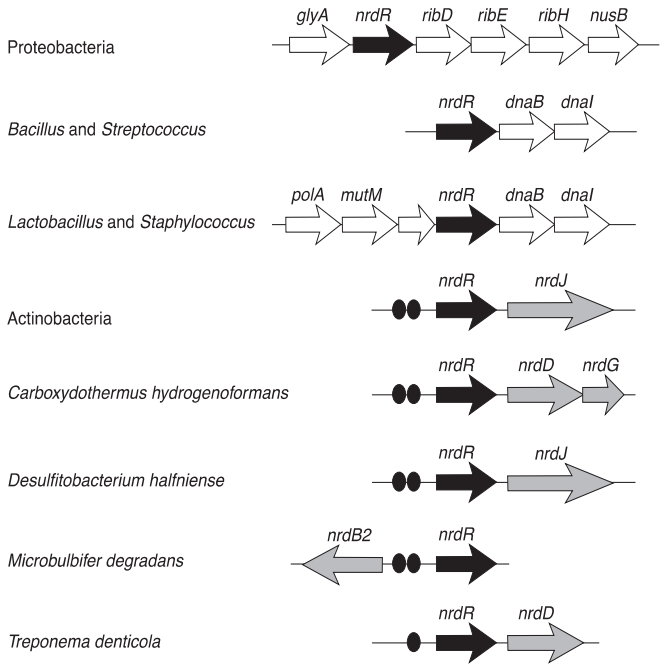

Figure 15. Examples of organization of *nrdR*-containing operons. The *nrdR* gene is represented by a black arrow, and other genes encoding ribonucleotide reductases are painted in grey; non-related genes are represented as white arrows. The black circles indicate predicted NrdR-boxes. Adapted from (9).

In parallel with the discovery of the *nrdR* ORF, an independent group discovered the NrdR transcription factor and its corresponding cis-regulatory elements through a completely different, purely bioinformatical approach. *Rodionov et al.* [9] considered the presence of conserved palindromic consensus sequences that had previously been reported to appear upstream of *nrd* operons[174, 175]. Considering that these sequences were cis-regulatory elements of a transcription factor and in an attempt to identify their corresponding trans-regulatory protein, they gathered genomes that presented and genomes that did not present the mentioned consensus sequences in the *nrd* promoters. Then, they used comparative genomics to correlate the presence or absence of these repeated sequences with the presence or absence of clusters of orthologous groups of proteins (COGs)[176]. Through this approach, *Rodionov et al.* identified a single cluster of orthologous groups of proteins, COG1327, that was present in all species containing the repeated palindromic sequences in their *nrd* operons and absent in all the rest. COG1327 corresponded to the same ORF identified by *Borovok et al.*[128], and it was independently re-named NrdR and its associated cis-elements NrdR-boxes.

This last study confirmed that NrdR is strictly confined to bacteria. Furthermore, it is present in most bacterial species: out of all major taxonomic groups tested it is only completely absent in ε-Proteobacteria, Mycoplasmatales and the *Bacteroidetes/Chlorobi* group. In γ-Proteobacteria, the only known species that do not encode it are obligate intracellular parasites or endosymbionts[9]. Surprisingly, the species that do encode NrdR present NrdR-boxes in all their RNR operons, regardless of the combination of RNRs they encode, with the only known exception of *Rhodobacter capsulatus* (which exhibits NrdR-boxes in only one of the two *nrd* operons it encodes). These findings presented NrdR as a global regulator of all ribonucleotide reductase classes in bacteria.

2.2.3.2 The NrdR-box

The NrdR binding sites were termed NrdR-boxes when they were first discovered by *Rodionov et al.* in 2005[9]. These are 16 base pairs-long palindromic repeats roughly corresponding to the consensus sequence aca**C**w**A**t**AT**a**T**w**G**tgt. The precise consensus sequence of the NrdR-box is slightly different depending on the taxonomic group. Some representative HMM logos for different consensus sequences can be found in **Figure 16**.

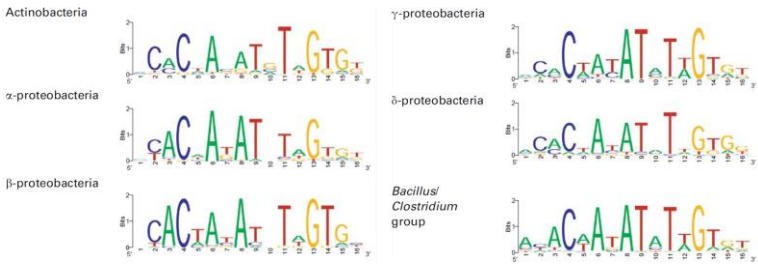

Figure 16. Examples of the NrdR-box consensus sequence in different taxonomic groups. HMM logos for Actinobacteria, α-δ-proteobacteria and the *Bacillus/Clostridium* group. Adapted from (9),

NrdR-boxes are almost always encountered in tandem. Single NrdR-boxes were found in only 27 out of the original 243 NrdR-regulated operons studied[9]. The distance between the boxes is itself significant, as they are placed so that the difference between the center of the sequences equals an integer number of turns in the B-DNA helix (21 bp, 31-32 bp, or 41-42 bp, for 2, 3, or 4 turns respectively). This spacing suggests protein-protein interactions between the NrdR molecules bound to both boxes[8, 172]. Finally, the location of the NrdR-boxes in the *nrd* promoters is also significant, as they always overlap with the consensus sequences of the basal promoter, suggesting that NrdR may be acting as a repressor[9, 128, 133, 172].

2.2.3.3 NrdR structure and function

The tridimensional structure of the NrdR protein has never been determined. According to domain predictions, the protein is formed by two domains: an N-terminal Zn-finger domain and a central ATP-cone domain, with a smaller C-terminal acidic tail[8, 128, 177]. The best characterized NrdR protein is that of *S. coelicolor*[128, 172, 178] and will be used as a reference here.

The N-terminal domain is a DNA-binding, zinc-binding domain that has been described as a type of Zn-finger, an atypical rubredoxin-like Zn-ribbon module[128, 172]. This domain is characterized by the presence of the four cysteine residues that bind the zinc atom; in *S. coelicolor* these are Cys3, Cys6, Cys31, and Cys34, and they are highly conserved among all known NrdR sequences. This domain also exhibits a unique R4 arginine motif, which also plays an important role in DNA-protein binding[179].

The central domain is a nucleotide-binding ATP-cone, very similar to the overall activity allosteric domain found in Class I and Class III RNRs (see 2.2.1)[128, 180]. This domain is structured as a four-helix bundle covered by a three-stranded mixed beta-sheet[180], so that the nucleotide is coordinated by six conserved amino-acids, corresponding in *S. coelicolor* to Val48, Val63, Lys50, Arg51, Lys62, and Thr95[172]. The nucleotide-binding properties of the NrdR ATP-cone domain have been extensively studied[133, 172, 177, 178]. The general structure of the domain is predicted to be very similar to that found in ribonucleotide reductases, although the cleft that contains the nucleotide is narrower, and there are two new tyrosine residues (Tyr121 and Tyr128 in *S. coelicolor*) which are predicted to interact with the 3'OH group of the ribose ring of the nucleotide[178].

Concerning the quaternary structure, the NrdR protein is known to exist as different oligomeric forms[128, 133, 172, 177]. The mechanism of oligomerization and its implications are mostly unknown, although it has been described that the degree of oligomerization is defined by the nucleotide bound to the ATP-cone domain[8, 177]. The parts of the NrdR structure involved in protein-protein interactions are not known either, although the ATP-cone domain alone can only form dimers[178]. That finding suggests a model in which this domain is responsible for one level of interaction forming stable dimers, while the nucleotide bound to it provokes a change of conformation in other parts of the structure that are responsible for further protein-protein contacts[177, 178].

Globally, the presence of a DNA-binding domain and a nucleotide-binding domain suggests a hypothetical mechanism of action for NrdR: this protein would act as a nucleotide sensor, repressing the ribonucleotide reductases depending on changes in the NTP/dNTP pool[8]. More specifically, several authors have suggested that the levels of ATP and dATP bound to NrdR may provoke differences in the NrdR oligomerization state that would be in turn responsible for increasing the degree of repression when the amount of dATP in the cell rises[133, 172, 178]. A simple schematic illustrating this hypothetical mechanism is shown in **Figure 17**. However, this mechanism has never been proved, and a recent study, which introduces the differences provoked by nucleotide monophosphates and triphosphates and the possibility of NrdR-bound-nucleotide hydrolysis[177], suggests that the real mechanism of action of NrdR might be more complex than was initially suspected.

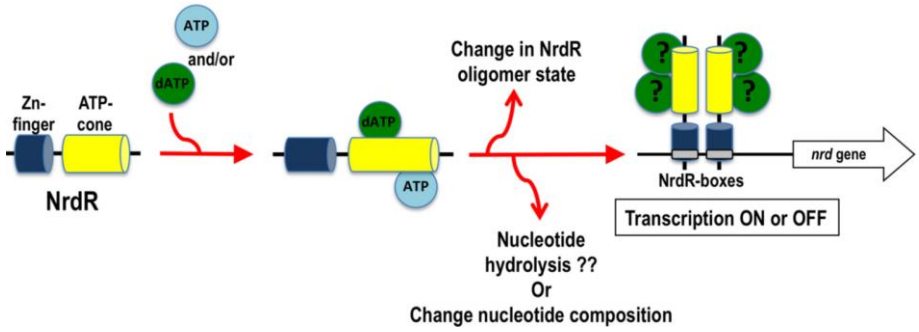

Figure 17. Simplified schematic for the hypothetical mechanism of action of NrdR. Depending on the cellular levels of dNTPs and NTPs, ATP or dATP may bind to the ATP-cone domain, causing an alteration in the oligomerization state of NrdR that affects the ability of its Zn-finger domain to bind *nrd* promoters, thus affecting the degree of repression on ribonucleotide reductase transcription. Adapted from (8).

2.2.3.4 Known actions of NrdR

When NrdR was first discovered it was demonstrated to act as a transcriptional repressor of both RNR operons in *S. coelicolor*: the class Ia RNR (*nrdABS*) and class II RNR (*nrdRJ*) operons[128]. As the *nrdR* gene is located in the class II RNR operon, NrdR represses its own transcription, in a negative feedback loop. NrdR has also been proved (by EMSA) to bind *in vitro* the promoter region of the *nrdABS* and *nrdRJ* operons[172].

Later studies in *E. coli* using mutational analysis and GFP-based Gene Reporter Assays (GRAs) demonstrated a similar effect: NrdR acts as a repressor of all three RNR classes encoded in the *E. coli* genome (class Ia, Ib, and III RNRs)[133]. The predicted NrdR-boxes are required for the binding of RNR to the *nrd* promoters *in vitro*[133, 177]. Since these early studies, the NrdR repression on all ribonucleotide reductases has been studied in many other bacterial species, such as *Salmonella typhimurium*[181], *Chlamydia trachomatis*[182], *Streptococcus pyogenes*[183], and *Bacillus subtilis*[184].

A well-known property of ribonucleotide reductase regulation is its adaptability and network behavior: the expression of the different RNR classes reacts to perturbations in other RNRs, keeping the deoxyribonucleotide synthesis stable[90, 145]. Using hydroxyurea (HU), a radical scavenger compound that acts as a specific inhibitor of class I RNR activity[156], causes all RNR expression to increase[90, 145]. However, it has been described that the increase in RNR transcription caused by HU treatment is not additive with that observed when inactivating the *nrdR* gene[181]. This finding suggests that derepression by NrdR may be behind the capacity of the RNR network to react against alterations in ribonucleotide reduction.

Putative NrdR-boxes have been found upstream of other, non-related genes, such as the replication initiator gene *dnaA* in *Shewanella* spp. or the DNA topoisomerase III gene *topA* in *Pseudomonas* spp.[9] However, no studies are available that explore if these genes are regulated by NrdR, and it is still unclear if the NrdR regulon extends beyond RNRs.

Objectives

This work is focused on the comparative regulation of ribonucleotide reductases in two species of facultative anaerobic pathogens, namely *Pseudomonas aeruginosa* and *Escherichia coli.* More specifically, it explores the action of the master regulator of ribonucleotide reduction NrdR (from its basic function to the specifics of its mechanism of action), the alginate regulator AlgR, and the master anaerobic regulators on the expression of all classes of ribonucleotide reductases, especially in the context of the aerobic/anaerobic transition, biofilm formation, and the oxygen gradients formed thereby, and during infection. The main objectives of this work can be outlined as follows:

1. Explore the action of the AlgZR two-component system on the expression of ribonucleotide reductases in *P. aeruginosa*.
2. Establish the relationship between AlgZR and the oxidative stress-mediated induction of ribonucleotide reduction in *P. aeruginosa*.
3. Study the general role of the master regulator of the RNR network, NrdR in *P. aeruginosa*
4. Identify the mechanism of action of NrdR in *P. aeruginosa* and *E. coli* and its effects as a nucleotide sensor.
5. Estimate the extent of the NrdR regulon.
6. Establish a new an *in vitro* transcription-based technique to study the action of transcription factors and apply it to the study of NrdR.
7. Identify the role of the different RNR classes during biofilm formation in *P. aeruginosa* and the function of the anaerobic master regulators under these conditions.
8. Identify the role of the different RNR classes during the aerobic-anaerobic transition in *P. aeruginosa* and *E. coli* and the function of the anaerobic master regulators under these conditions.
9. Establish a new technique for the study of gene expression during the aerobic-anaerobic transition.

Results

Summary of the results presented

Ribonucleotide reduction is a thoroughly regulated activity in bacteria. As discussed in 2.2, the regulatory systems controlling the ribonucleotide reductases achieve two main goals: first, keeping a continuous and balanced supply of dNTPs, to be able to replicate and repair chromosomal DNA, and maintaining the fidelity of DNA replication. Second, allowing the adaptation of the ribonucleotide reductase network to different conditions and environmental stimuli. This last effect is of particular importance in those species that encode multiple RNR classes.

As a highly adaptable opportunistic pathogen, *P. aeruginosa* encodes all three RNR classes: an oxygen-dependent class Ia enzyme (NrdAB), an oxygen-independent class II enzyme that requires 5'deoxyadenosylcobalamin (NrdJab), and an oxygen-sensitive class III enzyme only functional under anaerobic growth (NrdDG). Both as a free-living organism and during infection, *P. aeruginosa* encounters diverse environmental conditions and oxygen concentrations, and the differential regulation of its RNRs is thought to be essential to thrive under these growing conditions.

Of special interest is the regulation that occurs in the biofilm. *P. aeruginosa* forms thick, highly hydrated biofilms, resulting in the establishment of oxygen concentration gradients from an aerated surface to hypoxic or strictly anaerobic layers in the bottom. During chronic pulmonary infections, such as in cystic fibrosis or chronic obstructive pulmonary disease patients, alginate-overproducing *mucoid* biofilms appear. The process is coordinated by the two-component system AlgZR, which is not only responsible for the regulation of alginate production, but also controls other aspects of surface colonization, biofilm formation, and virulence (see 1.2.1). Using bioinformatic predictions and high throughput transcriptomics, other authors have suggested a possible implication of the AlgZR system in the regulation of ribonucleotide reduction[52, 57]. In **Objective 1**, we aim to confirm this regulation and establish a model of RNR regulation by the AlgZR system in *P. aeruginosa*. This objective is addressed in **Article 1**: *Regulation of ribonucleotide synthesis by the Pseudomonas aeruginosa AlgR two-component system*[185].

In this article, we confirmed that the AlgZR system regulates class Ia RNR and class II RNR. We used a carefully optimized bioinformatic search to predict AlgR binding sites, that were later confirmed by Electrophoretic Mobility Shift Assay (EMSA): we described one AlgR-box in the class Ia RNR promoter and two additional AlgR boxes in the class II RNR promoter. As the location of these binding sites relative to the base promoter indicated a mechanism involving DNA bending, we analyzed the structure of the AlgR-DNA complex by Atomic Force Microscopy (AFM) imaging, confirming the bending activity.

Later, using GFP-based gene reporter assays in different models (planktonic growth, surface colonization and biofilm formation, with both mucoid and non-mucoid strains) we determined the

nature of the AlgZR regulation on ribonucleotide reduction: both classes Ia and II RNR are specifically activated by phosphorylated AlgR, and class II, additionally, is repressed by high levels of unphosphorylated AlgR, which is responsible for the downregulation of class II RNR in mucoid isolates.

The nature of the signal recognized by AlgZ (and thus responsible for the phosphorylation of AlgR) remains unknown. Given the different pathways induced or repressed by phosphorylated or non-phosphorylated AlgR in non-mucoid *P. aeruginosa*, we hypothesized that the signal might be related to oxidative stress. Ribonucleotide reductase transcription has been described to be activated by oxidative stress signals through unknown mechanisms[137, 186]. Addressing **Objective 2**, we were able to establish that, under the conditions studied, the activation of class Ia and class II RNR by oxidative stress in *P. aeruginosa* occurs via AlgZR.

> **Article 1 highlights**. This article is a comprehensive study of the regulation of the RNR network in *P. aeruginosa* by the AlgZR two-component system. *In vitro*, we characterize the AlgR binding sites in the *nrd* promoters and analyze nature of its binding through EMSA and AFM. *In vivo*, we explore the effects of AlgZR-mediated regulation on RNR expression in three different models: liquid culture, surface colonization and biofilm formation. Finally, we explore the relationship between the AlgZR system and the well-known activation of RNR transcription through oxidative stress.

Another key system in the regulation of ribonucleotide reduction is the NrdR transcription factor, the master regulator of ribonucleotide reductases (see 2.2.3). This regulator has been described to be encoded by most bacterial species while being completely absent in Archaea and Eukarya; when present, it acts as a repressor of all RNR classes. Despite having been studied in detail in many bacterial species (*Escherichia coli, Streptomyces coelicolor, Salmonella typhimurium, Chlamydia trachomatis, Streptococcus pyogenes, Bacillus subtilis*) the mechanism of action and the biological role of NrdR have thus far remain elusive.

First, in **Objective 3**, we aimed to study the general role of NrdR in P. aeruginosa, which is addressed in **Article 2**: *Function of the Pseudomonas aeruginosa NrdR transcription factor: global transcriptomic analysis and its role on ribonucleotide reductase gene expression*[187]. We demonstrated that, as expected, NrdR acts as a repressor of all RNRs in P. aeruginosa. However, we also observed that the degree of repression on the different classes varied significantly depending on the environmental conditions: most significantly, the anaerobically-active class II and class III RNRs were strongly repressed by NrdR under aerobic conditions, but the effects of its repression were unnoticeable under anaerobiosis, when these classes are specifically induced by other factors. The transcription of *nrdR* was also demonstrated to be induced under anaerobiosis. We showed that this effect was caused by the NarXL system via binding of NarL on two NarL-boxes in the nrdR promoter (PnrdR).

The effects of NrdR on ribonucleotide reduction were also assayed functionally, demonstrating that the intracellular dNTP levels are higher in the *nrdR* mutant strain.

Furthermore, in this article, we also explored the regulation NrdR exerts on the transcription of *topA*, the DNA topoisomerase I, which has been suggested as a particularity of NrdR in *Pseudomonas* since the discovery of this transcription factor[9]. We demonstrated that NrdR acts as an activator of *topA* transcription through its binding on a single NrdR-box in the corresponding promoter (P*topA*). As with ribonucleotide reductases, the functional effect of this regulation was also tested, demonstrating that during the exponential phase there is a higher amount of negative supercoiled DNA in an *nrdR* mutant strain, compared to wild-type *P. aeruginosa*.

In this article, we also explored the possible effects of an *nrdR* mutation in the virulence of *P. aeruginosa*, although it did not increase survival rates in a *Drosophila* model. Finally, we did a first analysis of the global effects of NrdR, to determine the extent of the NrdR regulon (**Objective 5**); a comparative transcriptomics study using a microarray platform revealed a moderate subset of genes whose transcription is affected by an *nrdR* mutation.

> **Article 2 highlights**. This article is focused on the characterization of NrdR in *P. aeruginosa* (operon structure, transcription, effect on bacterial fitness), the regulation of its transcription by the NarXL two-component system, and its regulatory effects on the RNR network and the DNA topoisomerase I *topA*. Concerning the ribonucleotide reductases, we demonstrated the existence of variable repression levels on the different RNR classes: the transcription of all RNRs is repressed by NrdR, but the downregulation in class II and class III RNRs disappears under anaerobiosis. We also explored other possible effects of NrdR by gene profiling using a microarray platform and analyzed the possible effects of an *nrdR* mutation in the virulence of *P. aeruginosa* using a *Drosophila* model.

The findings presented in Article 2 extended the knowledge of NrdR to a new species, *P. aeruginosa*, and demonstrated the particularities of NrdR regulation in that organism. However, they still did not reveal the mechanism of action and the biological role of this transcription factor. Since its first description, it has been proposed that NrdR may act as a nucleotide sensor, detecting the comparative levels of dNTPs and NTPs and regulating the RNR transcription accordingly. Elucidating this mechanism constitutes **Objective 4** of this thesis, which was addressed in **Article 3**: *Mechanism of action of NrdR, a global regulator of ribonucleotide reduction* (unpublished manuscript).

In this article, we conducted a thorough examination of the mechanism of action of NrdR, comparing the system we analyzed before in *P. aeruginosa* with that of *E. coli,* another facultative anaerobic pathogen encoding a different set of ribonucleotide reductase classes. To conduct *in vitro* studies, we optimized a process for producing and purifying recombinant NrdR, obtained as a fusion protein with different stabilization domains. With the recombinant NrdR from *E. coli* and *P. aeruginosa*, we then conducted different studies aimed at understanding the role of the different nucleotide co-factors when bound to NrdR. We explored the differences in NrdR binding at the RNR promoters by EMSA, the functional differences in NrdR-mediated RNR repression using *in vitro* transcription, and the differences in NrdR oligomerization using size exclusion chromatography and SEC-MALS.

Furthermore, as an excess of NrdR may be more detrimental for the cell than its absence, we explored the effect of extra copies of *nrdR*, as well as the *nrdR* deletion, in growth speed (as an indicator of bacterial fitness) and in the virulence of *P. aeruginosa* strains in a *Galleria mellonella* infection model.

Addressing again **Objective 5**, in this article, we conducted a detailed examination of the NrdR regulon. Different high-throughput studies suggest that more operons beyond RNRs may be regulated by NrdR, but in most cases there are no putative NrdR-boxes predicted to justify this potential regulation. We obtained compared transcriptomics data using RNA-seq of *nrdR* mutant strains and wild-type strains of *P. aeruginosa* and combined this data with previous microarray data in *P. aeruginosa* and *E. coli* to obtain a comprehensive list of potential differentially expressed genes. Next, we conducted a whole-genome search for NrdR-boxes with an optimized bioinformatical search in both species and correlated the transcriptomics data with the presence or absence of potential binding sites.

The results suggest that most putative NrdR-regulated genes identified by high-throughput techniques are the result of indirect effects of false negatives, as a complete correlation of functional effect and presence of NrdR-boxes occurs only for RNR operons.

The *in vitro* transcription technique used studying the functional effect of different nucleotide cofactors in the NrdR-mediated repression of RNR transcription is a novel technique we designed specifically for this purpose; however, it can be applied to the study of other transcription factors. With that in mind, the technique is presented under the name ReViTA (Regulated *in Vitro* Transcription Assay). The development and optimization of this technique constitute **Objective 6**.

The technique is based on the quantification of *in vitro* transcription products obtained using a series of specifically designed plasmids. These plasmids include a non-functional *cat* gene whose transcription is controlled by a promoter including the desired transcription factor binding sites The levels of the gene controlled by the transcription factor are quantified by qRT-PCR (TEST sequence) and compared with the transcription of a constitutive gene in the same plasmid (CTRL sequence), which will be used as an internal control for normalization. The normalized expression values of the TEST sequence can be used to study the effect of different transcription factors or their quantities. In the pReViTA plasmids, the genes used for TEST and CTRL quantification are isolated using strong synthetic terminators, to ensure that their transcriptions remain independent.

Article 3 highlights. This article is a comprehensive analysis of the role and mechanism of action of NrdR, using two bacterial species to identify differences (*E. coli* and *P. aeruginosa*). We explore the extent of the NrdR regulon identifying NrdR-boxes bioinformatically and correlate them with differentially expressed genes in a comparative transcriptomics study by RNA-seq. Using pure recombinant NrdR obtained via an optimized procedure, we study the effect of different nucleotide co-factors *in vitro*, and how they affect NrdR-binding to RNR promoters (EMSA), NrdR oligomerization (size exclusion chromatography and SEC-MALS) and functional repression of RNR transcription (*in vitro* transcription). We also studied the effect of the *nrdR* mutation on the virulence of *P. aeruginosa* using a *Galleria mellonella* infection model.

Concerning the regulation of the RNR network in *P. aeruginosa*, to this point we have explored the actions of two regulatory systems: First, we established the role of the NrdR master regulator in the repression or derepression of all RNR classes depending on alterations in the dNTP pool (this system is also extended to other species). Second, we described the regulation of RNR expression by the biofilm-related AlgZR two-component system in the activation of class Ia and class II RNR upon stress and the early steps of biofilm formation, and the repression of class II RNR under mature, mucoid biofilms (this system is specific from *P. aeruginosa*).

However, additional systems have to be involved in RNR regulation in this species, that responsible of adapting RNR expression to different oxygenation conditions. In the biofilm structure, all substrates and waste products appear as gradients (see 1.1.3). Oxygen is the paramount example of this gradient generation: biofilms in aerated environments present aerobic surfaces and microaerobic to anaerobic conditions in the deeper layers. Therefore, this next part is focused on identifying the role of the different RNR classes at different depths throughout the structure of the biofilm and exploring the role of the anaerobic master regulators in controlling RNR expression in the corresponding oxygen gradient (**Objective 7**). This objective is addressed in **Article 4**: *Pseudomonas aeruginosa exhibits deficient biofilm formation in the absence of class II and class III ribonucleotide reductases due to hindered anaerobic growth*[188].

Using a simple planktonic culture model as comparison and the mutant strains for RNR class II (Δ*nrdJ*), RNR class III (Δ*nrdD*) and both RNR classes ((Δ*nrdJ* Δ*nrdD*) we demonstrated that class II RNR alone is unable to sustain anaerobic growth of *P. aeruginosa*. However, it can support the same level of growth as class III if the culture is supplemented with vitamin B_{12}. This consideration is of particular significance, as *P. aeruginosa* does not produce vitamin B_{12} anaerobically, but in a thick biofilm the vitamin can be produced at the surface and diffuse toward deeper layers, reaching anaerobic areas. This finding suggests a possible prominent role for RNR class II in the intermediate layers of thick biofilms (featuring hypoxic or anoxic conditions but within reach of vitamin B_{12} diffusion).

To test this hypothesis, we first used the same RNR mutant strains in two different biofilm formation systems: a static biofilm model (quantified using crystal violet staining) and a continuous-flow biofilm

model (quantified using Confocal Laser Scanning Microscopy – CLSM). We demonstrated that mutating any of the anaerobically active RNRs caused a reduction in biofilm biomass and thickness, and these reductions are additive, suggesting that both RNR classes play a role in biofilm growth, even without the next of an external supply of vitamin B_{12}. Furthermore, analyzing cell structure in the different layers of the continuous flow biofilm with CLSM revealed filamented bacteria in the bottom layers when either class II RNR or class III RNR were inactivated, suggesting a deficit in dNTPs causing alterations in DNA replication.

Given the importance of ribonucleotide reductase classes II and III, we studied the transcription levels of *nrdJab* and *nrdDG* in anaerobic cultures and during biofilm formation. We demonstrated that both RNR classes are induced during anaerobiosis and in the biofilm. Then, using mutant strains for the core regulators of anaerobic metabolism, bioinformatic predictions to search for potential binding sites, and site-directed mutagenesis to confirm them, we determined that class II RNR is regulated by the anaerobic master regulator Dnr. This transcription factor binds to a single box in the class II RNR promoter (P*nrdJ*). Another putative box was found in the class III promoter (P*nrdD*); however, this box showed no evidence of functionality (see Discussion).

Article 4 highlights. This article is focused on the study of the role different RNR classes play throughout the biofilm structure in *P. aeruginosa*. We first determined that, in liquid cultures, class II or class III RNR mutants are unable to grow anaerobically; however, class II can sustain anaerobic growth when supplemented with vitamin B_{12}. We then studied this effect in static and continuous-flow biofilm models, measured using crystal violet staining and Confocal Laser Scanning Microscopy (CLSM), respectively. We then studied RNR expression in planktonic and biofilm cultures using qRT-PCR, determining that class II and class III RNRs are induced anaerobically, and used a combination of bioinformatical prediction and site-directed mutagenesis to determine that the induction of class II RNR is conducted by the anaerobic regulator Dnr.

In other species, such as *E. coli*, the basic elements of the anaerobic regulation of ribonucleotide reduction are already known (see 2.2.2). However, as exemplified by the previous studies in the *P. aeruginosa* biofilm, facultative anaerobes often encounter variations in oxygenation as concentration gradients, be them over space (as in the biofilm structure or the interior of the gut) or over time (in a gradually evolving environment). Studying this aerobic-anaerobic transition is complicated, as there are no efficient models for quantifying oxygen availability in the cells. Biofilms studies are rarely efficient to analyze gene expression and studying the biofilm as a whole implies the loss of all information about individual layers. To study the role and regulation of the different RNR classes in *E. coli* and *P. aeruginosa* during all intermediate stages of the aerobic-anaerobic transition, isolating this effect from any other changes (**Objective 8**) we developed a new chemostat-based technique, that can also be applied to other species and systems (**Objective 9**). This is addressed in **Article 5**: *Gradual*

adaptation of facultative anaerobic pathogens to microaerobic and anaerobic conditions (pending publication).

The method we developed was named AnaeroTrans. Briefly, it is based on using a customized chemostat layout to grow a culture of the desired species under aerobic conditions (using air bubbling) until it reaches a certain growth phase, and then stabilize biomass concentration increasing the culture flow-rate to reach a steady-state, and stop air bubbling. The bacterial culture then starts to consume all available oxygen gradually, and the state of the system will be characterized using gas-phase oxygen concentration (which is continuously monitored with an oxygen microoptode) as the state variable. Samples for RNA extraction are taken throughout the process and used to obtain gene expression data from different oxygenation conditions characterized by a reliable state variable.

The results we present in Article 6 are focused on the development and optimization of the AnaeroTrans method. We demonstrated that using dissolved oxygen (DO) as a state variable was not adequate for describing oxygen availability in the cells, as it can fall to zero while bacteria are still performing aerobic respiration. On the other hand, the oxygen concentration in the gas phase (under self-consumption conditions) was demonstrated to be a reliable variable to define different oxygenation states in the microaerobic range.

We also applied the same setup we used for measuring gas-phase and dissolved oxygen concentration to the characterization of the dynamic oxygen concentration profiles in a model of biofilm co-culture of *Pseudomonas aeruginosa* and *Staphylococcus aureus*; although this is not strictly related to the central message of this thesis, the resulting article is provided as an Annex (Annex 3: Article 6).

The application of the AnaeroTrans method to *P. aeruginosa* and *E. coli* highlighted key differences in the evolution of their oxygen consumption rate under different oxygen concentrations. We also characterized the fitness of the cultures by two independent methods: a LIVE/DEAD viability fluorescent stain, and the estimation of the culture doubling speed using the chemostat parameters. The same studies were conducted in two strains of *P. aeruginosa* (a lab strain, PAO1; and a cystic fibrosis isolate, PAET1) and two strains of *E. coli* (a lab, commensal strain, K-12; and an enterohaemorrhagic strain O157:H7).

The expression of the different RNR classes was characterized through all the aerobic-anaerobic transition. In *P. aeruginosa* there occurred a gradual induction of the anaerobically active class II and class III RNRs, while the expression of class I RNR remained constant. The anaerobic induction occurred as two independent reproducible events. Furthermore, the lab strain PAO1 showed a very characteristic delayed activation of class III RNR, compared to the natural, pathogenic strain PAET1. On the other hand, *E. coli* exhibited no anaerobic induction of class III RNR, while its two aerobic RNRs (class Ia and class Ib RNRs) were gradually repressed throughout the transition.

The role of the anaerobic master regulators Anr/Dnr (*P. aeruginosa*) and Fnr (*E. coli*) was also addressed, identifying not only the role they played in the different regulatory events observed on the RNR network, but also their general role throughout the transition and the influence they have on bacterial fitness under different oxygenation conditions.

Article 5 highlights. This article is focused on the development and application of a method to study bacterial cultures and bacterial gene expression under gradients of oxygen concentration during the aerobic-anaerobic transition. The method we described (AnaeroTrans) is based on chemostat growth, taking advantage of the oxygen consumption by the culture, and characterizing the state of the system through the gas-phase oxygen concentration. We studied the differences in oxygen consumption rate, growth speed, and bacterial fitness in two species (*P. aeruginosa* and *E. coli*), comparing a lab strain and a pathogenic strain for each species. In the different stages we defined during the aerobic-anaerobic transition we explored the evolution of RNR expression and the actions of the anaerobic master regulators Anr/Dnr (*P. aeruginosa*) and Fnr (*E. coli*).

In subsequent chapters, we include the full content of the articles mentioned above. Regardless of their status of publication, we have reproduced the text and figures of the articles in the format of this thesis, for the convenience of the reader. All figures in the articles have been relabeled including the number of the article they belong to in their names (e.g., Figure 1 in Article 3 would be labeled as Figure A1:3), to prevent any confusion regarding the figures in the different articles and the main text. The information in each article is presented in the order requested by the journal it was published in.

Article 1

Regulation of ribonucleotide synthesis by the *Pseudomonas aeruginosa* AlgR two-component system

Published in *Scientific Reports* (Q1, IF_{2017} = 4.122)

doi: 10.1038/s41598-017-17917-7 (185)

December 2017

Anna Crespo[1¶], Lucas Pedraz[1¶], Marc Van Der Hofstadt[2], Gabriel Gomila[2], Eduard Torrents[1*]

¶: AC and LP contributed equally to this work.

[1] Bacterial Infections: Antimicrobial Therapies, Institute for Bioengineering of Catalonia (IBEC), The Barcelona Institute of Science and Technology, Barcelona, Spain.

[2] Nanoscale Bioelectrical Characterization, Institute for Bioengineering of Catalonia (IBEC), The Barcelona Institute of Science and Technology, Barcelona, Spain.

*: Corresponding author: Eduard Torrents (etorrents@ibecbarcelona.eu)

Abstract

Ribonucleotide reductases (RNR) catalyze the last step of deoxyribonucleotide synthesis, and are therefore essential to DNA-based life. Three forms of RNR exist: classes I, II, and III. While eukaryotic cells use only class Ia RNR, bacteria can harbor any combination of classes, granting them adaptability. The opportunistic pathogen *Pseudomonas aeruginosa* surprisingly encodes all three classes, allowing it to thrive in different environments.

Here we study an aspect of the complex RNR regulation whose molecular mechanism has never been elucidated, the well-described induction through oxidative stress, and link it to the AlgZR two-component system, the primary regulator of the mucoid phenotype.

Through bioinformatics, we identify AlgR binding locations in RNR promoters, which we characterize functionally through EMSA and physically through AFM imaging. Gene reporter assays in different growth models are used to study the AlgZR-mediated control on the RNR network under various environmental conditions and physiological states.

Thereby, we show that the two-component system AlgZR, which is crucial for bacterial conversion to the mucoid phenotype associated with chronic disease, controls the RNR network and directs how the DNA synthesis pathway is modulated in mucoid and non-mucoid biofilms, allowing it to respond to oxidative stress.

Introduction

Pseudomonas aeruginosa is a ubiquitous environmental Gram-negative bacterium, but it can also be a dangerous and adaptable opportunistic pathogen. In particular, it is known to cause severe chronic lung infections in immunocompromised patients and other at-risk groups. In cystic fibrosis (CF) patients, this infection is associated with a poor prognosis, leading to severely impaired lung function and an increased risk of respiratory failure, and is the primary cause of morbidity and mortality [1]. *P. aeruginosa* initially colonizes the CF lung in a non-mucoid form (characterized by non-detectable alginate production and causing an asymptomatic infection). However, at later stages of lung colonization, *P. aeruginosa* switches its phenotype to a mucoid alginate-overproducer variant, leading to rapid pulmonary deterioration [2,3].

Alginate production protects *P. aeruginosa* from phagocytosis, antibiotic penetration, and desiccation [4,5], but it is also an energy-intensive process and is therefore closely regulated and activated only when a chronic infection reaches a critical point. It involves a large number of enzymes and precursor substrates. Of particular relevance is the *algD* (and consecutive genes) operon, encoding the main enzymes for alginate production, and the *algC* gene from the *algC-argB* operon, a multifunctional enzyme required for several pathways including alginate biosynthesis and LPS production [6]. These genes are controlled by products of the *algU/mucABCD* operon; their transcription is directed by the alternative sigma factor AlgU (sigma E), which is commonly sequestered by the anti-sigma factor MucA. It has been reported that several types of cellular stress can induce proteolytic degradation of MucA, releasing AlgU and transiently activating alginate synthesis [7], but the stable mucoid phenotype is generated through the selection of mutations in the regulatory genes, usually in *mucA* [8,9].

Apart from the *algD* and *algC* operons, the AlgU sigma factor regulates the transcription of the *fimS*(*algZ*)-*algR* operon, which encodes the AlgZR two-component system [10,11]. In this system, FimS is the membrane kinase that can detect an unknown environmental signal and accordingly modulate the phosphorylation of AlgR. In turn, AlgR is the transcriptional factor that, depending on its phosphorylation state, regulates all aspects of alginate biosynthesis (controlling the *algD* and *algC* operons), as well as several aspects of anaerobic metabolism, type IV pili formation, rhamnolipid biosynthesis, type III secretion, and cyanide and nucleotide synthesis [12,13]. Furthermore, it has recently been reported to bind with high affinity to 157 loci in the *P. aeruginosa* genome [12]. Many of the functions regulated by the AlgZR system are important for biofilm formation and chronic infection [14]. When AlgR is phosphorylated, it controls functions related to cell attachment and initial biofilm formation, while a high excess of non-phosphorylated AlgR induces late biofilm and chronic infection traits, including alginate biosynthesis and the mucoid phenotype [12]. Several observations have also linked this system with the *P. aeruginosa* ribonucleotide reductases (RNR) network [6,12].

Ribonucleotide reductases are the enzymes responsible for reducing the ribonucleotides (NTP) to the corresponding deoxyribonucleotides (dNTP), thereby forming the building blocks for DNA synthesis and

repair [15]. There are three known RNR classes (I, II and III), and all use a free-radical-based catalysis; however, they rely on different metallo-cofactors for the initiation of the radical reduction step, and each one exhibits a different behavior towards oxygen. Class I RNR can be enzymatically active only under aerobic conditions, class II RNR is oxygen-independent and requires vitamin B_{12} for enzyme activation, and class III RNR requires strict anaerobic conditions to be active. While almost all eukaryotic organisms encode exclusively class Ia RNR, prokaryotes are known to encode more than one, in all possible combinations [16]. *P. aeruginosa* encodes all three RNR classes: class Ia (*nrdAB*), class II (*nrdJab*) and class III (*nrdDG*) [17]. Their different requirements and relationships with oxygen give them different roles throughout the *Pseudomonas* life cycle and in the biofilm structure [15,18,19].

The RNR activity is known to be extensively regulated at both the transcriptional and post-translational levels; it is delicately modulated to keep a balanced nucleotide pool and globally regulated according to the life cycle, stress situations, and environmental conditions. However, much remains unknown about which factors allow bacteria to activate the different classes under different circumstances.

Several years ago, one of the genes found in a transcriptomics experiment to be regulated by AlgR in *P. aeruginosa* was the *nrdJ* gene (PA5497) [6], which encodes a class II ribonucleotide reductase that plays a crucial role during biofilm formation and infection. In addition, a recent study that aimed to identify AlgZR-regulated genes using ChIP-seq showed a particular region for AlgR binding (AlgR-box) in a short DNA fragment within the intergenic region between the class I RNR operon first gene (P*nrdA*; PA1156) and the PA1157 gene [12]. All of these observations point to the existence of a relationship between the AlgZR system and the RNR network.

In this study, we aimed to uncover this relationship. We demonstrate that AlgR regulates both RNR classes I and II in a differential way, depending on its phosphorylation state. We explore how this differential regulation allows bacteria to adapt to different situations when living in a free form, during colonization of surfaces and in mucoid or non-mucoid biofilms. Finally, we unravel for the first time the molecular mechanisms behind the well-known activation of ribonucleotide reductase activity that occurs under oxidative stress.

Results

Ribonucleotide reduction is regulated by AlgR in P. aeruginosa.

Previous studies have suggested a regulation by the two-component system AlgZR on class II RNR [6]. Furthermore, AlgR has been reported to bind upstream to the class Ia RNR operon [12], facing the neighboring gene PA1157. We aimed to explore a possible regulation by AlgZR on the RNR network, and clarify if the already detected binding site regulates the RNR class Ia operon *nrdAB* or the PA1157.

We initially used plasmids carrying a transcriptional fusion of the *nrdA* (pETS134), *nrdJ* (pETS180), *nrdD* (pETS136) or PA1157 (pETS206) promoters to the green fluorescent protein (GFP). The promoter of the *algD* (and consecutive genes) operon, main responsible for alginate biosynthesis, was used here as a positive control, as it is well-known to be regulated by non-phosphorylated AlgR (pETS205) [3,14,20,21].

As shown in **Fig. A1:1**, comparing the expression of the wild-type *P. aeruginosa* PAO1 strain with its isogenic *algR* mutant strain (Δ*algR*; PW9855), the regulation of the P*algD* promoter expression by AlgR is consistent with what has been extensively reported. AlgR acts as an activator of its transcription, although it is typically almost fully inactive in the non-mucoid phenotype [3,14].

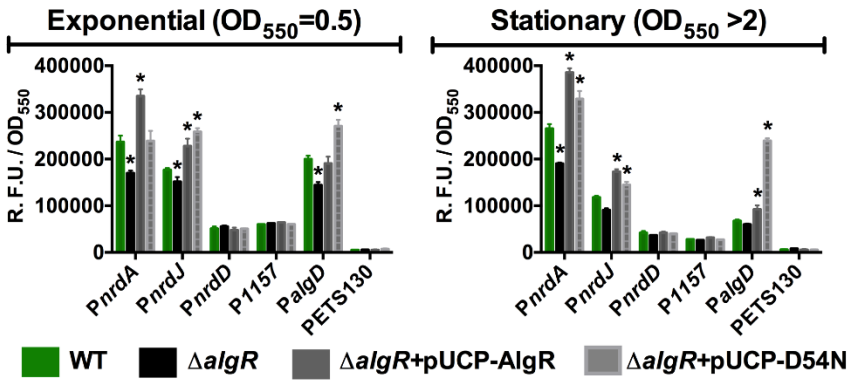

Figure A1:1. *In vivo* AlgR regulation of RNR promoters and related genes. Gene reporter assays for P*nrdA* (pETS134), P*nrdJ* (pETS180), P*nrdD* (pETS136), P_{PA1157} (pETS206) and P*algD* (pETS205) fused to GFP at exponential and stationary growth phases. Values are averages from at least three independent experiments, and error bars show positive standard deviation. The promoterless pETS130-GFP plasmid values are provided for comparison. Asterisks (*) indicate a statistically significant difference from the wild-type strain (*p*-value less than 0.05 in pairwise *t*-tests). Shortened names are used (see Supplementary Table A1:S1).

Studying the control on the RNR operons, we detect similar positive regulation by AlgR on the class I operon (*nrdAB*) and class II operon (*nrdJab*). Complementation with a *fimS-algR* overexpression construct (pETS203, pUCP-AlgR) increased the expression of both promoters beyond the levels of the wild-type. The PA1157 promoter was not affected by either the absence or overexpression of the AlgR regulator. Thus, there is no evidence of the AlgR binding in the PA1156-PA1157 intergenic region

regulating the PA1157 gene as previously reported [12]. Instead, it controls the adjacent *nrdAB* genes. No change was found in P*nrdD* promoter expression (pETS136), so class III RNR is not regulated by AlgZR under the studied conditions.

The AlgZR phosphorylation switch modulates RNR regulation.

As a two-component system, the biological function of the AlgR regulation is conditioned by its phosphorylation state [14]. We aimed to explore the effect of AlgR phosphorylation on the RNR genes regulation. To do so, we took advantage of the AlgR D54N mutant: it has been shown that a conserved substitution of the D54 residue of AlgR to an asparagine (AlgR D54N) abolishes its *in vitro* and *in vivo* phosphorylation by the FimS(AlgZ) kinase in response to environmental signals, while keeps protein structure apparently intact [11,20]. Hence, we used the wild-type AlgR (pUCP-AlgR) and its variant AlgRD54N (pUCP-D54N) overexpression plasmids to determine the influence of phosphorylation in regulating *nrdA* and *nrdJ* transcription (**Fig. A1:1**).

Validating our approach, AlgR D54N increases *algD* expression much more than wild-type AlgR complementation does, as AlgR needs to be non-phosphorylated to regulate positively *algD* transcription [14,22].

Studying the RNR genes, both pUCP-AlgR and pUCP-D54N were able to increase *nrdJ* transcription levels beyond the wild-type values in a similar way, both in the exponential and stationary growth phases. Therefore, no apparent global effect of AlgR phosphorylation on RNR class II regulation could be identified under these conditions. However, the transcription of class Ia RNR (*nrdA*) showed evidence of dependence on the phosphorylation state of AlgR, presenting a higher increase in expression with phosphorylatable AlgR. Further results in other growth models demonstrated this effect (see below). The transcription of *nrdD* and PA1157 were, as expected, unresponsive to either pUCP-AlgR or pUCP-D54N overexpression.

AlgR binds to the nrdA and nrdJ promoter regions through specific AlgR-binding boxes.

To localize the AlgR binding sites in the class Ia and II RNR promoter regions, a thorough bioinformatics search was conducted. First, to characterize the AlgR-box consensus sequence, we used MEME (MEME suite), starting from three different sources of information (see Materials and Methods), to obtain three count matrices characteristic of the AlgR binding site (**Supplementary Fig. A1:S1**). A FIMO search (MEME suite) was later conducted with all three matrices. Using positive and negative control probes (see Material and Methods), we concluded that a 1e-4 p-value threshold showed no false positives and identified strong AlgR binding sites in all situations. On the other hand, a 1e-3 p-value threshold recognized all boxes with all sets but also showed up to 5 non-specific hits in the negative control. Using the three count matrices on a FIMO search of promoters P*nrdA*, P*nrdJ* and P*nrdD*, applying the 1e-4 p-value threshold, a single binding site was identified on P*nrdA* and P*nrdJ*, while no hits were retrieved from P*nrdD*. As further results showed that P*nrdJ* included more than one binding site (see below), a

less stringent search was conducted for this probe, in which all hits obtained from applying a 1e-3 p-value threshold was considered. All the identified boxes are represented in **Fig. A1:2**.

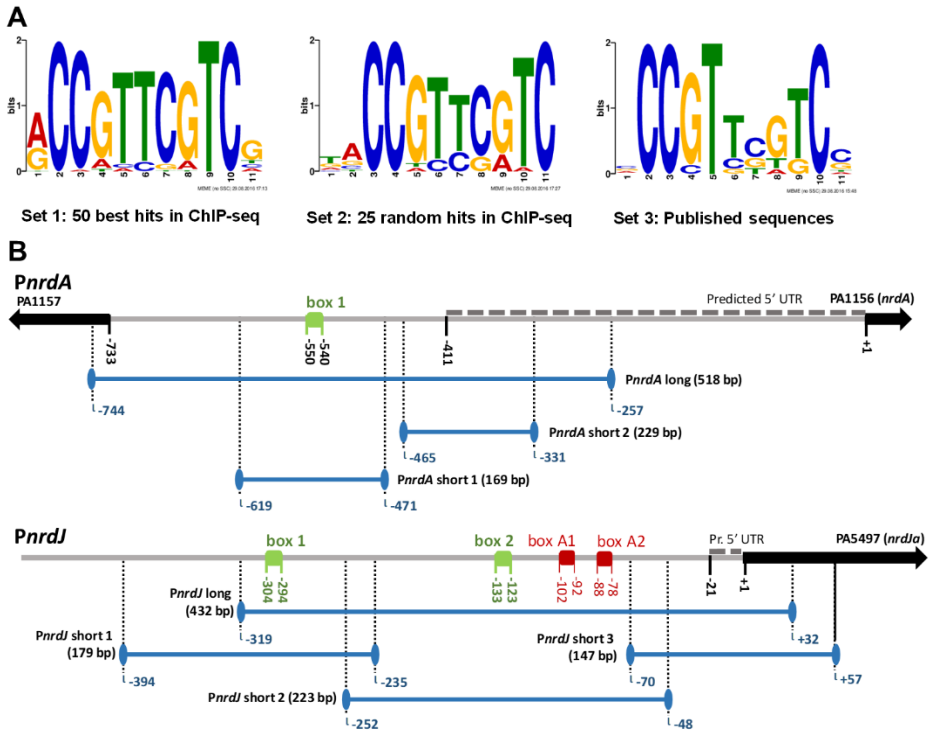

Figure A1:2. AlgR boxes in the RNR promoters. **A**, Sequence logos for the AlgR binding box. HMM logos are generated from count matrices (see Supplementary Fig. A1:S1) produced by FIMO using three different sets of sequences containing AlgR binding sites (see Materials and Methods). **B**, Schematics for promoters P*nrdA* (RNR class I promoter) and P*nrdJ* (RNR class II promoter). Identified boxes are represented in green, artifact boxes identified as false positives in the bioinformatics search are represented in red. Genes are represented by arrows; gene *znuA* has been eliminated from the P*nrdJ* schematic for improved readability. An approximated prediction of the 5'UTR for the studied operons (BPROM) is shown as dashed lines. Locations are indicated in base pairs relative to the ATG translation start codon of the first gene of the corresponding operon. DNA probes used for EMSA studies are indicated by solid blue lines.

To characterize the AlgR-DNA binding activity and experimentally demonstrate AlgR binding to the identified putative boxes, we performed Electrophoretic Mobility Shift Assays (EMSA). Initially, long DNA probes spanning all the predicted promoter regions for class I (P*nrdA*), class II (P*nrdJ*) and class III (P*nrdD*) were analyzed, with the corresponding positive control (a band of the P*algD* promoter including its two strong binding sites) and a negative control. The P*algD* band showed, as expected, evidence of two strong binding events. We also identified one binding activity in the P*nrdA* promoter and two binding events in the P*nrdJ* promoter, while no evidence of an AlgR-DNA interaction was found for P*nrdD* (**Fig. A1:3A**).

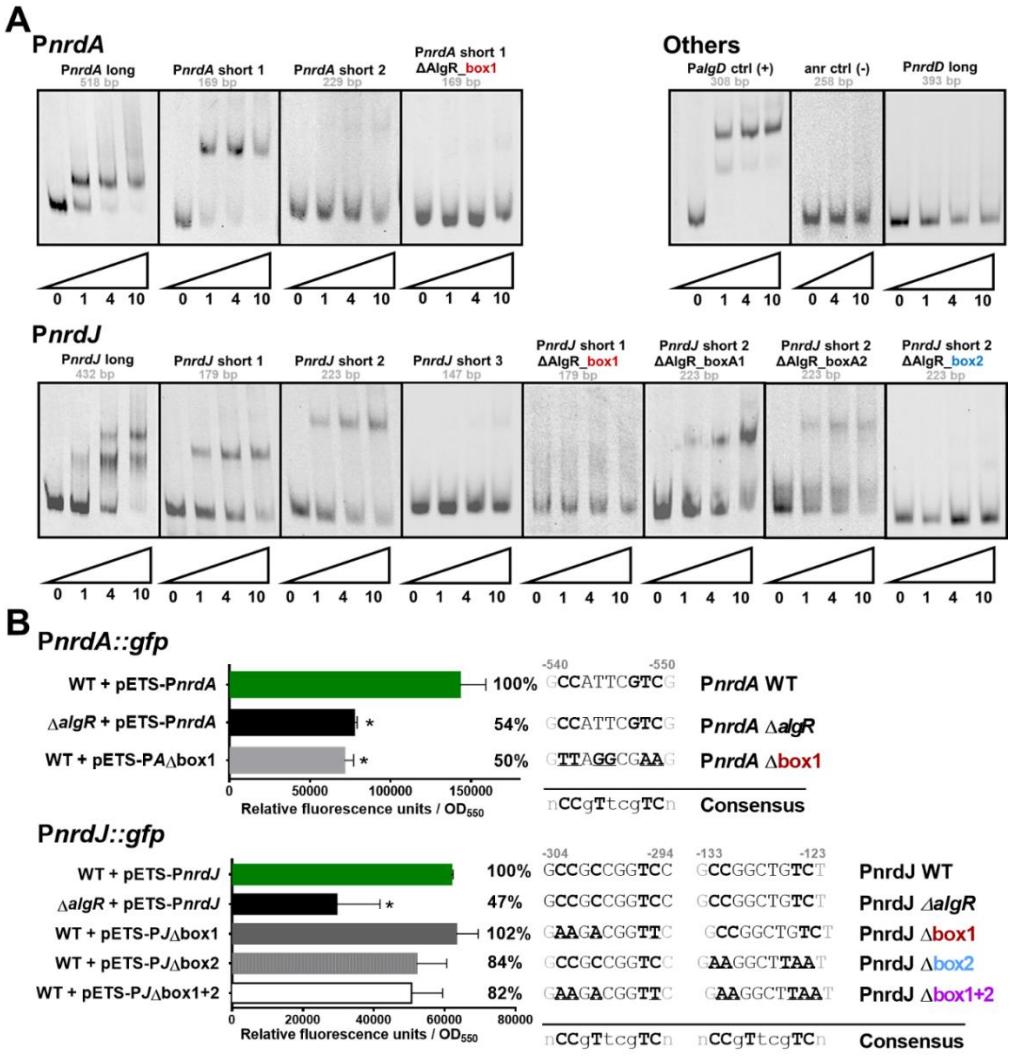

Figure A1:3. Functional study of the AlgR boxes in RNR promoters. **A**, EMSA experiments promoters P*nrdA,* P*nrdJ,* and P*nrdD*, together with positive control (P*algD*) and negative control probes. Probe sizes are indicated below their names; numbers below the triangles represent pmol of AlgR. **B**, Gene reporter assay for P*nrdA* and P*nrdJ*, during the early stationary phase (OD_{550} = 2.0) and under aerobic conditions. Error bars represent positive standard deviations; the asterisk indicates a statistically significant difference from the wild-type strain (*p*-value less than 0.05 in pairwise *t*-tests). The exact mutations introduced are detailed at the right of the graphic, and a simplified consensus sequence of the AlgR box is provided for comparison. The position of each box is indicated in bp (to the ATG of the first gene in the operon). Shortened names are used (see Supplementary Table A1:S1). The images in A was cropped for clarity from the originals in Supplementary Fig. A1:2.

To localize more precisely the AlgR binding locations, we segmented them into smaller DNA probes (**Fig. A1:2**). As seen in **Fig. A1:3A**, we established that binding activity was localized to one location in

probe P*nrdA* short 1, as well as in one location in P*nrdJ* short 1 and another in P*nrdJ* short 2. We then proceeded with putative AlgR box mutagenesis, determining as final binding sites the ones now labeled as P*nrdA* box 1, P*nrdJ* box 1 and P*nrdJ* box 2, whose mutagenesis abolished DNA shifts. The other boxes we proposed in P*nrdJ* short 2 are considered artifacts of the bioinformatic search. P*nrdA* box 1 colocalizes with the DNA fragment enriched by AlgR-precipitation in ChIP-seq [12]. Therefore, the identified boxes confirmed the presence of the previously described AlgR binding site in the intragenic region between the *nrdA* and PA1157 genes [12] and also included previously unreported putative binding sites in the class II RNR promoter region.

The *in vivo* effect of the described boxes was first assessed under liquid culture conditions by using promoter-GFP fusions in gene reporter assays (**Fig. A1:3B**). In P*nrdA* class I RNR, we determined that the identified AlgR box is fully responsible for the AlgR regulation of this promoter, as mutation of this box resembles the effect of mutating the *algR* gene. The effect of the boxes identified in P*nrdJ* class II RNR is complex; even though it was demonstrated that mutating box 1 abolished AlgR binding in the immediate region, this mutation had no significant effect on P*nrdJ* expression in liquid cultures. Mutating box 2 or both boxes reduced the P*nrdJ* expression, but not to the levels seen in a Δ*algR* mutant strain. The effect of P*nrdJ* AlgR boxes is further studied below, under different conditions.

Finally, when comparing the identified AlgR boxes with those previously known, we realized that P*nrdA* box 1 is more similar to those described as "strong binders," while P*nrdJ* boxes resemble the so-called "weak-binders" (**Supplementary Fig. A1:S3**) [14]. Specifically, there is one cytosine in position 7 present in all strong binders that is absent in all weak binders. A comparative EMSA with a wide array of protein concentrations shows that, as expected, binding in P*nrdA* and P*algD* requires smaller quantities of protein and results in sharper, more stable bands. Binding in P*nrdJ* requires higher protein levels for full occupation of both boxes and forms blurrier bands, indicative of a more unstable complex.

AlgR binding on RNR promoters alters the DNA structure.

It has been reported that AlgR control, usually performed through binding hundreds of base pairs upstream of the basal promoter, often implies DNA bending [14]. In the regulation of the promoter of the *algD* operon, the best-known AlgR regulatory process, a wide DNA loop is formed integrating the actions of AlgR on its three binding locations (strong sites RB1 / RB2, weak site RB3) and other proteins [14,21]. However, there is no published visual evidence of this process, and no studies have demonstrated if AlgR can alter the DNA structure by itself, in the absence of other factors.

To explore the physical effect of AlgR binding on RNR promoters, we observed previously formed DNA-AlgR complexes, compared to free DNA probes, using Atomic Force Microscopy (AFM) (**Fig. A1:4**). AlgR binding can be observed on both P*nrdA* and P*nrdJ* probes (yellow/red spot), although several series of images showed that the P*nrdA* complex was easier to obtain and more stable. One single binding site is observed in the P*nrdA* promoter, while the P*nrdJ*-AlgR complexes show bindings in two locations.

There is also a binding event on two sites in the P*algD* probe, containing its two strong boxes RB1 / RB2.

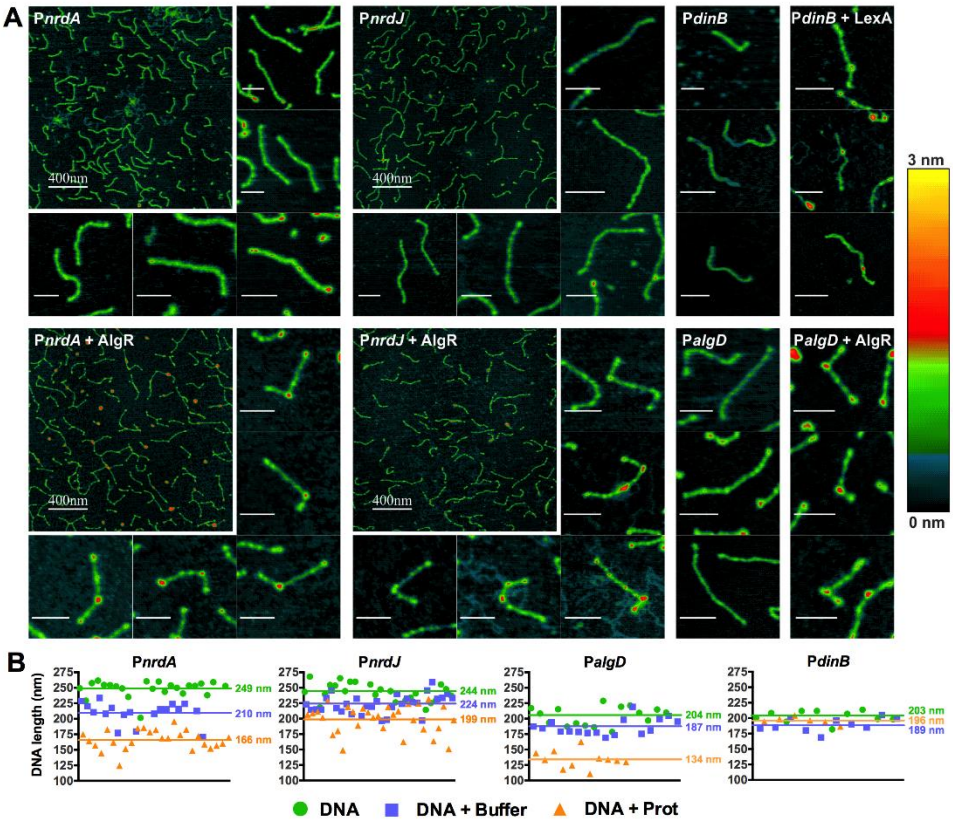

Figure A1:4. Atomic force microscopy images of DNA and DNA-protein complexes. **A**, AFM images of DNA molecules or DNA-protein complexes, taken on mica under ambient conditions, are shown for P*nrdA*, P*nrdJ*, P*algD* and P*dinB* promoters. Small images depict single DNA probes; scale bars without numbers above represent 80 nm. For the *PnrdA* and P*nrdJ* promoters, a general image at a higher scale is also shown. Colors represent the height of the structures, according to the scale at the right. **B**, comparison of the apparent length of randomly selected units of all DNA probes when, before drying, they were in water (images not shown) or in binding buffer, as well as when complexed with AlgR.

Despite the possible artifact introduced by the natural positioning of the DNA probes on the mica surface, we can observe that AlgR binding colocalizes with a remarkable DNA bending event. To explore the nature of these bindings, they were compared to the very well-known binding of the LexA repressor to the damage-inducible DNA polymerase IV (*dinB)* promoter region [23]. No bending is observed due to LexA binding on P*dinB* (**Fig. A1:4A**).

Moreover, we determined the apparent length of the DNA fragments in the AFM images (**Fig. A1:4B**), observing that although it was already reduced when the DNA was in the protein binding buffer rather

than in water prior to drying, it got reduced to a greater extent when AlgR protein was bound. This effect is quite apparent in P*nrdA* and P*algD* probes and is also detectable in P*nrdJ*, whereas no evidence of it is found due to LexA-P*dinB* binding.

AlgR regulation during surface colonization reveals a complex mechanism behind RNR transcription fine tuning.

The AlgZR system is required for fimbrial biogenesis [11] and rhamnolipid formation [24], both activities of the utmost importance for surface colonization and colony and biofilm formation [25,26]. We, therefore, considered it necessary to explore the AlgR regulation of *nrd* genes during surface growth. In our surface colonization experiments, different strains harboring promoter::*gfp* fusion plasmids were grown on agar plates for 36 h, and fluorescence was determined at 3-h intervals during all growth. This model is also useful for exploring the AlgR action on *nrd* genes in the mucoid phenotype, using the *P. aeruginosa* PAOMA (Δ*mucA*) strain, which forms very characteristic mucoid colonies.

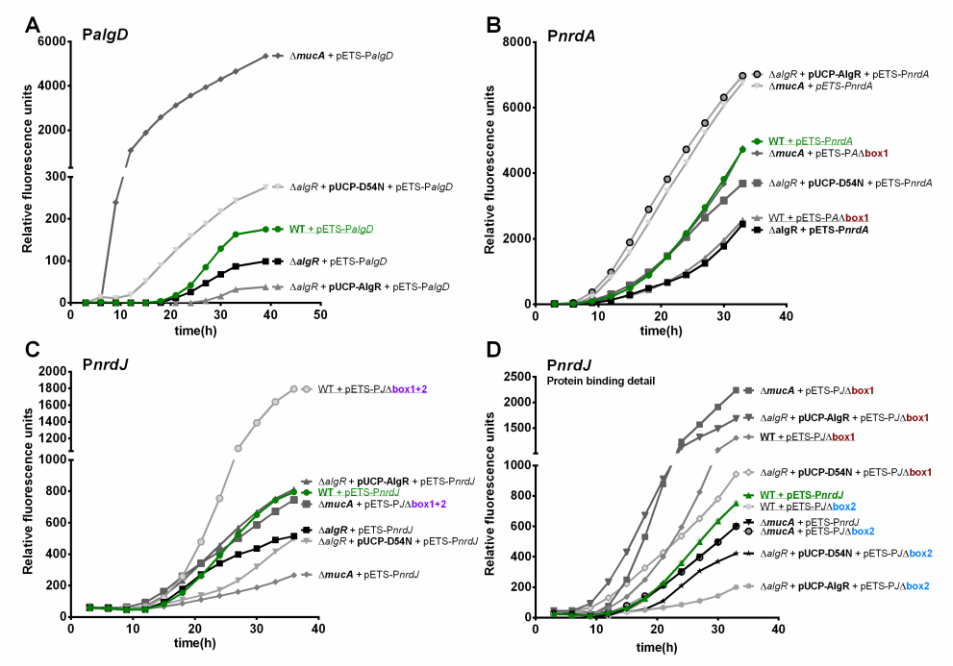

Figure A1:5. AlgR regulation of RNR promoters during surface colonization. GFP-based gene reporter assays for P*algD* (pETS205, **A**), P*nrdA* (pETS134, **B**) and P*nrdJ* (pETS180, **C**) promoters fused to GFP, during surface colonization. GFP fluorescence is measured at different times of incubation during colony formation and presented as relative fluorescence units. Mucoid strains (PAOMA, PAO Δ*mucA*) are included. A fourth panel (**D**) shows further experiments with P*nrdJ* AlgR boxes to study the fine regulation performed at this level. For improved readability, shortened names are used (see Supplementary Table A1:S1), the key features of each strain are highlighted in bold, wild-type strains are underlined and mutant boxes are color-coded.

We first analyzed the regulation of the P*algD* promoter (**Fig. A1:5A**). The basal level of P*algD* expression in a non-mucoid phenotype is very low, although it can be seen that the Δ*algR* deletion reduces its expression and that it can be complemented by the non-phosphorylatable AlgR D54N protein, whereas the wild-type protein does not complement (or even slightly inhibits) P*algD* transcription. In the Δ*mucA* strain, the great increase in non-phosphorylated AlgR levels causes a very significant increase in P*algD* transcription (>6000 RFU). All results agree with our previous observations and published data [3,14,27], serving as a control for this technique.

For the class I RNR P*nrdA* promoter (**Fig. A1:5B**), the results confirm what was observed in the liquid cultures, although they are more evident under these conditions: mutating the *algR* gene causes a clear reduction in *nrdAB* transcription, and mutating the AlgR-box in the promoter mimics this effect. Complementation with AlgR wild-type protein over-activates the promoter whereas D54N is not able to fully complement the mutation, demonstrating that AlgR phosphorylation is required for the induction of class I RNR.

The results are more complex for the class II RNR P*nrdJ* promoter (**Fig. A1:5C**). As previously described (**Fig. A1:1**), mutating the *algR* gene causes a reduction in P*nrdJ* transcription, much evident than in liquid cultures, which can be complemented by introducing additional copies of *algR* (pUCP-AlgR). The overexpression of wild-type AlgR protein complements the mutation, while, in this model, AlgR D54N overexpression causes a reduction of the operon transcription. This first evidence that accumulation of AlgR can inhibit P*nrdJ* transcription is supported by the fact that, unlike for P*nrdA*, the activity of the promoter is severely reduced in the mucoid phenotype (Δ*mucA*). Additionally, mutation of both AlgR boxes in the P*nrdJ* promoter causes not a reduction, but a significant increase in the transcription of the promoter, indicating a more complicated underlying mechanism.

To explore the independent action of the AlgR boxes, we performed several colony formation experiments with single-box mutants (**Fig. A1:5D**). Both boxes display very different behaviors. Mutating box 1 increases the expression of the promoter, therefore suggesting that AlgR is inhibiting P*nrdJ* transcription by binding to box 1. Eliminating box 1 can switch the effect of the Δ*mucA* background from a significant reduction to a large increase in transcription, suggesting that the previously observed inhibition of class II RNR transcription in the mucoid phenotype happens through AlgR binding in the AlgR box 1. The effect of mutating box 2 is not detectable in a wild-type background, but its mutation switches the effect of the AlgR-overexpression strain from an increase (even higher with phosphorylatable AlgR) to a dramatic decrease in P*nrdJ* transcription. Box 2 is therefore proposed to be implicated in P*nrdJ* activation in response to AlgR phosphorylation, in competition with the action of box 1, which would be involved in P*nrdJ* inhibition in the mucoid phenotype. The implications of this dual mechanism on stress conditions and the mucoid phenotype are further discussed below (see Discussion).

The AlgR regulation mechanism is reproduced in mucoid and non-mucoid biofilms.

Our group recently demonstrated the importance of class II RNR (*nrdJab*) during *P. aeruginosa* biofilm formation and its transcriptional activation by anaerobic regulators under this condition [19]. However, the regulators involved in modulating RNR transcription in the biofilm are still unknown. The AlgZR system has been extensively associated with different aspects of biofilm formation, and here we have demonstrated that it controls the *nrd* genes, which are also differentially regulated in the mucoid phenotype. Therefore, we decided to explore the modulation of class I and II RNR expression by AlgZR in mucoid and non-mucoid biofilms. In **Fig. A1:6**, we determined the *nrdA* and *nrdJ* expression, together with the *algD* expression as a control, during biofilm formation. Measurements were taken at different time intervals during growth (from 3h to 72h). The un-complemented PW9855 (Δ*algR* mutant) strain could not be used, as it presents severely impaired biofilm formation capabilities.

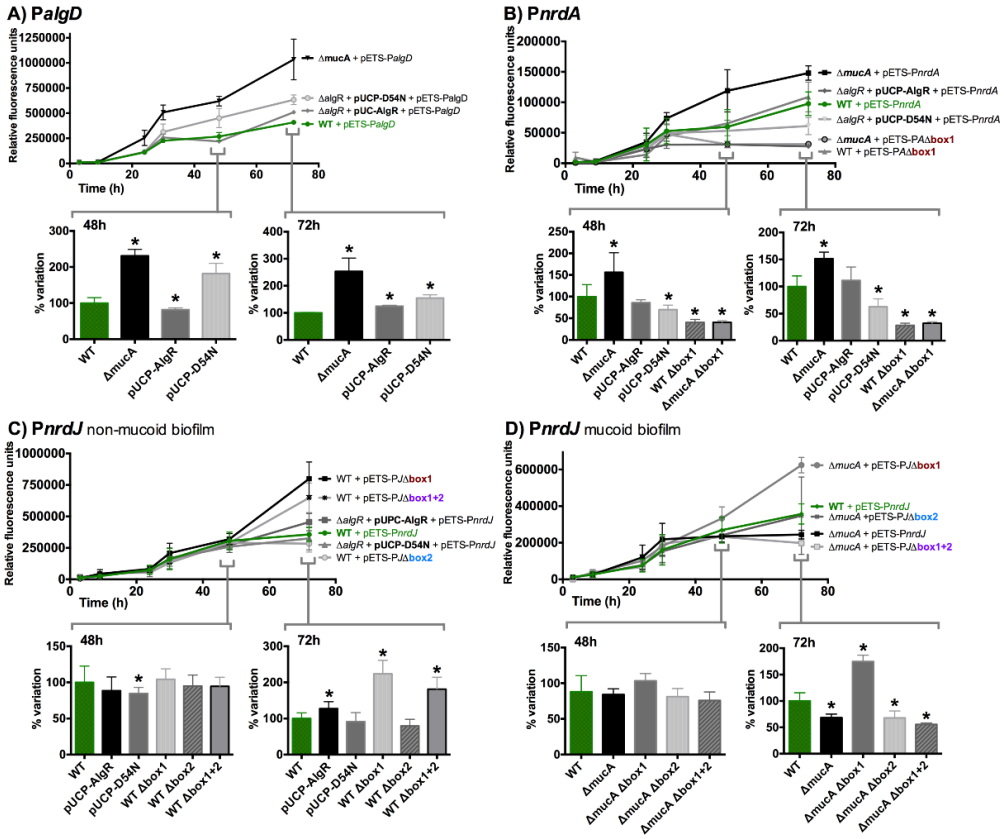

Figure A1:6. AlgR regulation of RNR promoters in mucoid and non-mucoid biofilms. Gene reporter assay at different time points during static biofilm formation for P*algD* (pETS205, **A**), P*nrdA* (pETS134, **B**) and P*nrdJ* (pETS180, **C** and **D**). The values shown are the means of three independent experiments in 8 wells; error bars indicate positive and negative standard deviation. Shortened names are used (see Supplementary Table A1:S1). For 48 h and 72 h, results are depicted as bar graphs; error bars show positive standard deviation, and the asterisk indicates a statistically significant difference from the wild-type strain (*p*-value less than 0.05 in pairwise *t*-tests).

As in our previous experiments in colonies, AlgR functions in the biofilm as an activator of P*algD* transcription, where it is more responsive to non-phosphorylatable AlgR D54N than to wild-type AlgR, and shows a high induction in the mucoid *P. aeruginosa* PAOMA (Δ*mucA*) strain (**Fig. A1:6A**).

Class I RNR transcription (**Fig. A1:6B**) is induced in the mucoid biofilm at a very early stage in its formation. P*nrdA* induction occurs only due to phosphorylated AlgR overexpression and not with its non-phosphorylatable counterpart AlgR D54N (although the effect of AlgR overexpression does not go beyond complementing the mutation). The AlgZR regulation appears to be responsible for the effect in the mucoid biofilm, as mutating AlgR box 1 eliminates this induction, as well as in the non-mucoid variant.

Finally, the complex regulation of class II RNR is also reproduced in biofilm formation conditions (**Fig. A1:6C** and **A1:6D**). The changes in transcription can be more easily detected in mature biofilms (72h), while younger biofilms show almost no evidence of regulation. In a mature mucoid biofilm, there is a clear reduction in P*nrdJ* expression, which can be restored with the mutation of AlgR box 1. Mutating this box causes a general increase in class II transcription while mutating box 2 causes a reduction. The double mutation causes an opposite effect in both the regular mature biofilm and in the mucoid biofilm. The differential action of AlgR box 1 and AlgR box 2 is therefore demonstrated, and it is related to both AlgR-mediated induction of class II RNR in non-mucoid biofilms and AlgR-mediated repression of class II RNR in the mucoid biofilm.

Ribonucleotide reductase induction under oxidative stress acts through AlgR regulation.

There are several reports which describe that RNR activity is strongly activated under oxidative stress conditions by increasing *nrd* gene transcription through an unknown molecular mechanism [15,28,29]. Here, we explore the ability of AlgR to sense oxidative stress and accordingly regulate RNR gene expression.

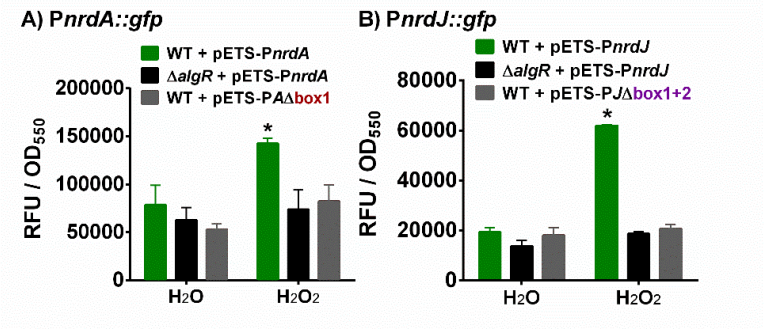

Figure A1:7. AlgR regulation of RNR during oxidative stress. Gene reporter assays for the P*nrdA* and P*nrdJ* promoters fused to GFP. All strains were grown to OD_{550} = 0.5 and then subjected to 30 minutes of incubation with a stressing agent (1.0 mM H_2O_2) or control (equivalent volume of water). Values are averages from three independent experiments, and error bars show positive standard deviation. Asterisks (*) indicate statistically significant difference from the untreated wild-type strain (*p*-value less than 0.05 in pairwise *t*-tests).

As hypothesized, class I (*nrdA*) and II (*nrdJ*) RNR respond to oxidative stress (induced by hydrogen peroxide treatment) by significantly increasing their transcription (**Fig. A1:7**). Surprisingly, this response to oxidative stress is entirely abolished if the *algR* gene is inactivated (Δ*algR* mutant strain). Introducing mutations in the identified AlgR binding regions of the *nrdA* and *nrdJ* promoter regions mimics the effect of the *algR* isogenic mutant, rendering them unable to respond to oxidative stress.

These results indicate, for the first time, that the well-described activation of the *nrd* genes by oxidative stress occurs through the action of the AlgZR two-component system.

Discussion

As an essential activity for the life of any cell, ribonucleotide reduction is always thoroughly regulated. In bacteria, where different RNR classes could be present and required for changing situations, the activation and inactivation of the several classes add another layer of complexity.

Several pieces of this regulatory puzzle are already known. In *P. aeruginosa*, apart from class Ia (whose transcription has been mainly studied in *E. coli*), class II is known to be especially important in biofilms and positively regulated by the anaerobic system Anr/Dnr, although we proposed the action of other biofilm-related factors [19]. Class III is highly activated under strictly anaerobic conditions by still unknown regulators. Moreover, the global regulator NrdR, which negatively regulates all RNR expression in almost all bacterial species [15], is also present in the *P. aeruginosa* network [30]. However, despite all known information, there are yet many missing pieces. RNR activity is modulated under oxidative stress conditions [28,29] and specific environmental conditions through unknown factors. The data linking the AlgZR two-component system to the RNR network [6,12] could reveal another piece of this complex regulation.

For our bioinformatics analysis, we took advantage of published information regarding DNA sequences that bind AlgR [12], but we realized that these data accounted only for high-affinity binders. Therefore, we also used several published sequences [14], including weak binders, to produce a more relaxed search pattern (**Supplementary Fig. A1:S1**). We identified putative binding sites in the P*nrdA* and P*nrdJ* promoters (**Fig. A1:2**) that were experimentally demonstrated (**Fig. A1:3A**); the absence of boxes in P*nrdD* suggests that class III RNR is not regulated by AlgZR. Contrary to the well-known *algD* promoter, which contains 3 AlgR-boxes (RB1, RB2, and RB3) [3,31], one unique AlgR-box was identified in the P*nrdA* promoter, and two were identified in the P*nrdJ* promoter. Although members of the AgrA family such as AlgR usually bind to direct repeats of their binding sequence [14], it is known that other genes regulated by AlgR contain different numbers of boxes in their promoters (*algD*, 3 boxes; fimU, 2 boxes; *hcnA*, 1 box; *rhlA,* 1 box; *rhlI*, 1 box). The distance from these boxes to their predicted transcription start sites (from 100 bp to 300 bp; **Fig. A1:2**) suggests that DNA bending will be necessary to interact with the transcription machinery. A deeper analysis of their sequences also reveals that the box in the P*nrdA* promoter is that of a strong binder, while P*nrdJ* boxes resemble that of known weak binders (**Supplementary Fig. A1:S3B**). The cytosine (C) in position 7 is present only in strong binding sequences; this difference can be used to conduct new bioinformatics searches specifically geared towards AlgR weak-binding sequences.

Consequently, the results of the AFM imaging (**Fig. A1:4**) of the DNA-protein complexes confirmed that binding of AlgR to the RNR promoters causes bending of the DNA; this explains how binding sites that are so far away from the transcription start site can interfere with transcription. Although AlgR-mediated bending has been proposed many times, to our knowledge, this is the first time that it has

been experimentally demonstrated. The so-formed loops suggest interactions with other factors, such as the Anr/Dnr system, which also regulates class II RNR.

In studying the AlgR *in vivo* regulation of the RNR network, we used different models of growth to analyze its effects under different metabolic conditions: liquid cultures (**Fig. A1:1** and **Fig. A1:3B**), a model for surface colonization (**Fig. A1:5**), and a model for biofilm formation (**Fig. A1:6**). Wild-type, Δ*algR* and AlgR / AlgR D54N complementation strains were used on all models; these strains grow at comparable rates, although the complementation strains present a slight growth reduction in early exponential phase (data not shown). The P*algD* promoter was used as a control, demonstrating that all methods are suitable for studying the effects of the AlgZR system; in all models, it acts as an activator of P*algD*, whose transcription is activated by non-phosphorylated AlgR. As expected, under some circumstances its basal expression is not sufficient to observe an effect when mutating the gene, and regulation becomes apparent only when over-activating it. Using these methods, we identified a clear control by the AlgZR system of class I and class II RNR, while class III RNR demonstrated no evidence of regulation. This was also assayed under anaerobic conditions (in liquid cultures and surface colonization models; the biofilm forms its own anaerobic areas) but no differences worth highlighting appear (data not shown). The bioinformatics search identified binding sites only where regulation was later demonstrated.

For class I RNR regulation, we determined that AlgR is activating P*nrdA* transcription (**Fig. A1:1**). The identified box, which correlates with the DNA fragment recovered in prior ChIP-seq experiments [12], despite facing PA1157, is regulating the *nrdAB* operon (**Fig. A1:1**, **Fig. A1:3**). Other boxes with the same orientation have been described, such as the RB3 site on *algD* [10]. The functionality of the box can be demonstrated *in vivo* (**Fig. A1:3B**), and the effects of mutating the box or the gene are reproducible and even more evident during surface colonization (**Fig. A1:5B**) or biofilm formation (**Fig. A1:6B**). We used the AlgR D54N mutant to determine the involvement of AlgR phosphorylation in *nrd* regulation [11,14], determining that phosphorylatable AlgR is a better inducer of class I RNR expression in all models. It is known that several stress conditions, such as oxidative stress, induce *nrd* transcription [28,29] and can also activate the two-component AlgZR system, inducing genes for cell attachment and biofilm formation [6,32]. We hypothesized that the kinase FimS could respond to stress or stress-derived signals to activate the phosphorylation of AlgR. This would give significance to P*nrdA* control by AlgR, which would be activating it in response to stress conditions. Additionally, our surface colonization and static biofilm models (**Fig. A1:5B** and **Fig. A1:6B**) determined that class I RNR is induced in the mucoid phenotype and that this happens, at least partially, through AlgZR control. As non-phosphorylated AlgR, the form that is mostly predominant on the mucoid phenotype, has demonstrated less capacity to induce P*nrdA*, but is still capable to complement at least partially the Δ*algR* mutation, it is possible that this induction happens as a collateral effect of the great increase in AlgR levels.

Concerning class II RNR regulation, initial experiments suggested that it was also activated by AlgZR (**Fig. A1:1**); however, the mutation of the identified boxes quickly suggested a more complex

mechanism (**Fig. A1:3B**). Surprisingly, although mutating the gene causes a reduction in P*nrdJ* expression, mutating both boxes in a wild-type background caused an increase in biofilm and colony formation models (**Fig. A1:5C**, **Fig. A1:6C**); this suggests that AlgR could be acting both directly and indirectly on class II RNR expression. A more detailed mutagenesis of the boxes (**Fig. A1:5D**, **Fig. A1:6C-D**) revealed that mutating box 2 causes a slight reduction of class II expression while mutating box 1 causes a clear induction in biofilms or colonies, an effect that was not seen in liquid cultures. The simplest explanation is that the positive regulation by AlgZR occurs through binding to AlgR box 2, whereas box 1 is responsible for inhibition under some circumstances. By overexpressing AlgR and AlgR D54N, we realized that the wild-type AlgR protein can complement the mutation, while AlgR D54N causes a clear inhibition in colonies and biofilms (**Fig. A1:5C-D**, **Fig. A1:6C**). However, mutating AlgR box 2 can immediately switch the effect of AlgR overexpression from an induction to a strong repression (**Fig. A1:5D**). We, therefore, deduce that under some circumstances the AlgR protein can bind to box 1 to inhibit class II RNR. In the mucoid phenotype, we can see a surprisingly strong reduction of class II expression in both colonies and biofilms, but this changes to an even higher induction when mutating box 1 (**Fig. A1:5C**, **Fig. A1:6D**). We propose that box 2 could be responsible for increasing P*nrdJ* expression under some stress conditions. Meanwhile, box 1 could be inhibiting class II RNR expression in the mucoid phenotype (likely in favor of class III RNR activity, but further experiments will be needed to determine this).

In light of the differences observed with AlgR phosphorylation, which must be dependent on an external signal, we tested the effect of oxidative stress; this condition is reported to dramatically induce RNR transcription through unknown mechanisms [28,29]. Surprisingly, we demonstrated that despite being in the exponential phase, where AlgR regulation is not normally very prominent, eliminating the AlgR system caused the RNR network to be insensitive to stress (**Fig. A1:7**). This is, to our knowledge, the first description of a molecular link between oxidative stress conditions and RNR expression.

Based on these results, we suggest a model for *nrd* regulation by the AlgZR system (**Fig. A1:8**). In this model, on the one hand, class I and class II RNR are being activated by AlgR under planktonic or early colonies/biofilms, responding to AlgR phosphorylation under stress. On the other hand, in the mucoid biofilm, the high accumulation of non-phosphorylated AlgR would cause an inhibition of class II RNR through binding on box 1.

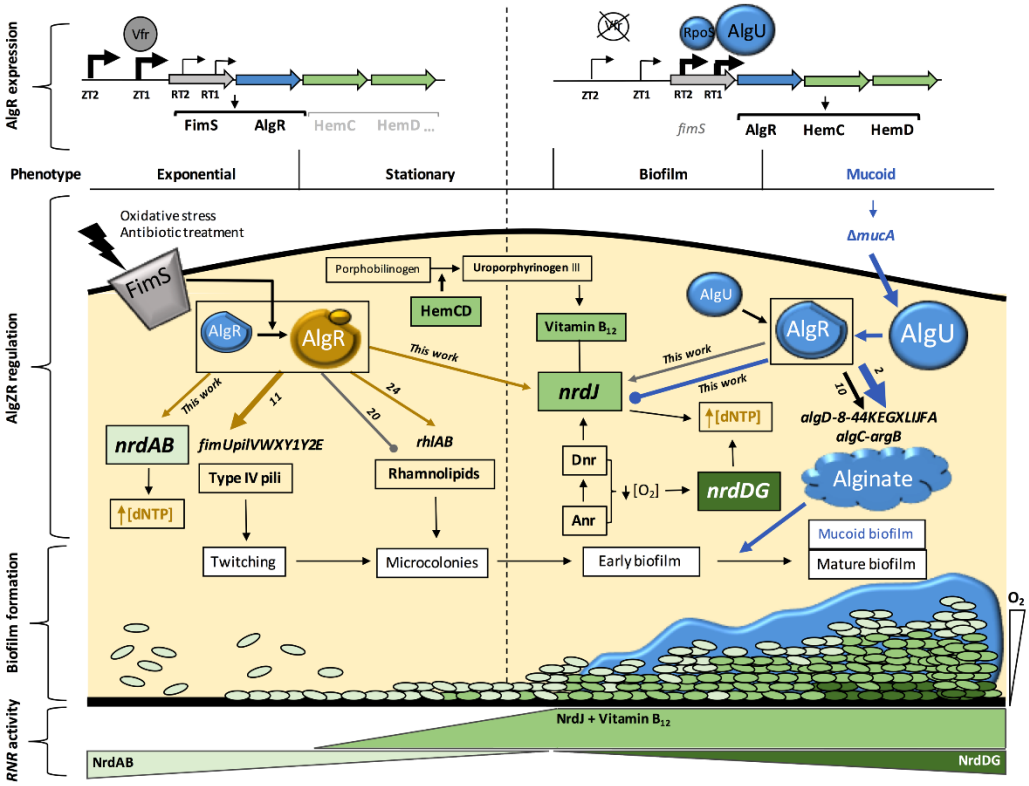

Figure A1:8. Model of AlgZR regulation of ribonucleotide reduction. Schematic representation of the AlgZR regulation of ribonucleotide reduction, in the context of other AlgZR-mediated regulation events. Arrows represent positive regulation, while lines with a bullet point represent negative regulation. Events characteristic of phosphorylated AlgR are highlighted in yellow, and events happening mostly in the mucoid phenotype are highlighted in blue. The representation is not exhaustive, and some events are eliminated for the sake of clarity. The source of information for any AlgR regulative event is indicated beside the corresponding line.

Examining this throughout all biofilm life cycle, when planktonic cells suffer the presence of a stress condition (oxidative stress, antibiotic treatment, etc.) it activates AlgR [13,14,33]. Under these conditions, the *algR* gene is expressed from promoters ZT1 (further activated by Vfr) and ZT2 (constitutive) as *fimS-algR* [33], a combination that favors phosphorylation. AlgR will induce the *nrdAB* and *nrdJ* genes, the operon of *fimUpilVWXY1Y2E* (Type IV pili) for the adhesion to surfaces [34], and the *rhlAB* for quorum sensing cell communication and microcolony formation [24]. In the absence of these genes, a biofilm is not formed, and cells are more sensitive to stress conditions or antibiotic treatment [13,25]. When *P. aeruginosa* is attached to the surface, cells grow as microcolonies, which can slowly evolve to a biofilm phenotype. In biofilm conditions, a further induction of the RT1 and RT2 promoters in the *algR* operon starts to appear, controlled by AlgU and RpoS, and *algR* is therefore also expressed as *algR-hemCD* (avoiding the *fimS* gene and so being non-phosphorylated). Then, AlgR favors the induction of genes such as the *algD* and *algC* operons for the synthesis of alginate [33] and *hemC* and *hemD* for the synthesis of the heme group (as well as allowing the formation of uroporphyrinogen III, a precursor of vitamin

B_{12} [35] which is the essential cofactor for NrdJ activity). NrdJ is also induced by the Dnr transcriptional factor [19]. When biofilm becomes mature, fully anaerobic conditions appear [36,37], inducing both *nrdJab* and *nrdDG* [19]. It has been reported that many genes regulated by AlgR are also controlled by anaerobic transcriptional factors such as Anr or Dnr *(arcDABC, ccoP2, hcnB, oprG, hemN or nrdJ)* [6,14,19,38-42]. We observed a significant decrease when inhibiting AlgR and Dnr binding and a gradual reduction of P*nrdJ* expression when mutating both systems (**Supplementary Fig. A1:S4**). If selected mutations degenerate the biofilm into a mucoid phenotype, the full release of AlgU from MucA causes a dramatic induction of RT1 and RT2 promoters in P*algR*, highly increasing the cellular levels of non-phosphorylated AlgR, and in turn decreasing the expression of NrdJ by binding to P*nrdJ* AlgR-box 1. This favors class III RNR, which is better-suited for full anaerobiosis and does not require vitamin B_{12}.

Several pieces of information remain unknown. The fact that mutating the *algR* gene has a different effect than mutating both AlgR-boxes on P*nrdJ* shows us that there could be more regulation events that have not yet been described. Besides, the differences observed between surface colonization and biofilm formation conditions suggest interactions with other factors. However, we believe that these new results bring us closer to understanding the regulation of complex RNR networks such as that of *P. aeruginosa*, as well as how it adapts to environmental conditions and evolves throughout the biofilm life cycle. The link between oxidative stress, the AlgZR system, and RNR regulation provides, for the first time, a molecular explanation for this effect. In most bacterial species, there are no described analogs of the AlgZR system, but there are AgrA family two-component systems which could be candidates; further experiments will be conducted to evaluate whether these results extend to other bacterial species.

Methods

Bacterial strains, plasmids and growth conditions.

Different *Pseudomonas aeruginosa* and *Escherichia coli* strains were used, as listed in **Supplementary Table A1:S1**. Bacteria were routinely grown in LB medium (Scharlab, Spain) at 37˚C; when needed, antibiotics were added at the following concentrations: 100 μg ml^{-1} gentamicin, 40 μg ml^{-1} tetracycline, or 500 μg ml^{-1} carbenicillin for *P. aeruginosa* and 30 μg ml^{-1} chloramphenicol, 10 μg ml^{-1} gentamicin, 50 μg ml^{-1} ampicillin and 50 μg ml^{-1} kanamycin for *E. coli*. Anaerobic growth was performed in LB medium containing 10 g/l KNO_3 in screw-cap tubes (Hungate Tubes) that were filled to the top with N2.

DNA manipulation and plasmid construction.

Molecular biology enzymes and kits were purchased from Fermentas (ThermoFisher) and used according to the manufacturer's instructions. DNA amplification was performed by PCR using DreamTaq MasterMix (2X) or High-Fidelity PCR Enzyme Mix (Fermentas, ThermoFisher) following the manufacturer's instructions, with the primers listed in Supplementary Table S2. All other manipulations were performed using standard procedures [43]. DNA was transferred into *P. aeruginosa* cells via electroporation using a Gene Pulser XCell™ electroporator (Bio-Rad) as previously described [30]. The absence of mutations introduced during cloning was verified via DNA sequencing.

An AlgR transcriptional factor overproducer was built by cloning the *algR* gene (PA5261) into the pET28a overexpression system (Novagen) downstream of the T7 RNA polymerase promoter. The *algR* gene was amplified from *P. aeruginosa* PAO1 by PCR using the primers AlgR-up and AlgR-low and High-Fidelity PCR Enzyme Mix. The fragment amplified (747 bp) was cloned into the pGEM-T easy vector and transformed into *E. coli* DH5α. After plasmid isolation using GeneJET Plasmid Miniprep Kit, the plasmid was digested with *Nde*I and *Not*I restriction enzymes and ligated with T4 DNA ligase into the pET28a vector, obtaining plasmid pETS201. Finally, pETS201 was transformed into the Rosetta(DE3) strain for AlgR overproduction and purification.

To produce the AlgRD54N mutant overproducer, the *alg*R gene was specifically mutated by PCR-based site-directed mutagenesis as previously described [19] using primer pair 1 (see Supplementary Table S3). The mutant gene obtained was cloned into the pGEM-T easy vector, transformed into *E. coli* DH5α cells and verified by DNA sequencing. The *fimS* gene was not included in the cloned fragment to ensure the maximum possible difference in the AlgR phosphorylation state. NdeI and *Not*I restriction enzymes were used for fragment digestion and cloning into the pET28a vector using T4 DNA ligase. Finally, pETS202 was transferred into the Rosetta(DE3) strain for AlgRD54N overproduction and purification.

Complementation vectors for providing extra copies of AlgR and AlgRD54N were constructed by cloning the corresponding genes under the control of their own promoter regions into the pUCP20T vector. First, a band containing the *algR* gene, the neighboring gene *fimS,* and their promoter region was amplified (2286 bp) using primer pair 2 and cloned into pUCP20T, generating pETS203. The *algR* was site-specifically mutagenized as previously described [19] to produce *algR*D54N using mutagenic primer pair 1 and outer primer pair 2 and cloned into pUCP20T to generate pETS204.

To construct the *algD, algR* and PA1157 transcriptional GFP fusions, 900 bp, 483 bp and 769 bp long fragments encompassing the *algD, algR,* and PA1157 promoter regions were amplified by PCR using primer pairs 3-5; the obtained DNA fragments were cloned into pGEM-T easy and transformed into *E. coli* DH5α cells. *BamHI* and *SmaI* restriction enzymes were used for fragment digestion and for cloning into pETS130-GFP, to generate pETS205, pETS206 and pETS207 plasmids for *algD*, *PA1157* and *algR* promoter regions, respectively.

For AlgR-box mutagenesis in the studied promoters, PCR-based site-directed mutagenesis was used as previously described [19], using outer primer pairs 6 and 7 for the *nrdAB* and *nrdJab* promoter regions, respectively; mutagenic internal primer pairs 8-10 were used. Two regions of the P*nrdJ* promoter mistakenly identified as AlgR-boxes as artifacts in the bioinformatic search were also mutated using mutagenic primer pairs 11 and 12. For all the positively identified AlgR boxes, the mutant DNA fragments were later cloned into the pGEM-T easy vector and transformed into *E. coli* DH5α cells. BamHI and SmaI restriction enzymes were used for fragment digestion and cloning into pETS130-GFP, to generate pETS208 (for P*nrdA* box1), pETS209 (for P*nrdJ* box1) and pETS210 (for P*nrdJ* box2). For the exact sequence of the mutations introduced, see **Fig. A1:3B**.

Green fluorescent protein-based gene reporter assay.

The different *P. aeruginosa* strains were grown in separate Erlenmeyer flasks containing 20 ml LB broth and the specified antibiotic. Flasks were incubated at 37˚C and agitated at 200 rpm. Bacterial growth was monitored by measuring optical density at 550 nm (OD_{550}). Upon reaching the desired OD_{550}, three independent 1 ml samples were taken from each analyzed strain and centrifuged for 10 minutes at 13.000 rpm; the supernatant was removed, and the pellet was washed with PBS 1x containing 2% formaldehyde. Suspensions were left on ice for ten minutes before being centrifuged again, the supernatant removed and PBS 1x added. The fluorescence was then measured after diluting the sample 8 times in PBS 1x, using 96-well plates (Costar® 96-Well Black Polystyrene plate, Corning) on an Infinite 200 Pro Fluorescence Microplate Reader (Tecan).

To determine gene expression during biofilm formation, an aerobic static biofilm was grown on 96-well plates (Nunclon Delta Surface, Thermo Scientific) in LB containing 0.2 % glucose. At the desired time, the planktonic cells on the supernatant were removed, and the biofilm was washed three times with PBS 1x and then fixed with 2 % formaldehyde. GFP was measured using Infinite 200 Pro Fluorescence Microplate Reader (Tecan). Fluorescence obtained at each time point was compared with fluorescence at 3h of biofilm formation to calculate the induction factor of the gene expression.

For gene expression measurement during colony formation, 5 µl inocula at an OD_{550} of 0.05 of the corresponding *P. aeruginosa* strains were grown on 6-well plates (Nunclon Delta Surface, Thermo Scientific) containing LB with 1.5 % agar and the corresponding antibiotics. Plates were incubated at 37ºC, and GFP expression was measured at different phases of colony formation; fluorescence measurements were performed by using an Infinite 200 Pro Fluorescence Microplate Reader (Tecan).

Bioinformatic prediction of AlgR binding boxes.

To identify putative AlgR binding sites on RNR promoters, a thorough bioinformatics search was conducted. As a first step, we used MEME (MEME suite, [44,45]) to generate count matrices characteristic of the AlgR binding box. As the binding sequence is small and somehow flexible [14], different sources were considered to obtain the AlgR box motif. Three sets of sequences were therefore used: set 1, to obtain a motif characteristic of strong binders, formed by the 50 most enriched sequences in ChIP-seq after AlgR precipitation [12]; set 2, to form a more flexible motif sequence, 25 randomly selected sequences from the enriched group in the same ChIP-seq experiments; and set 3, to capture the variation observed in some experimentally demonstrated boxes, confirmed by a previously published cluster of representative binding sites [14]. Assuming one occurrence of the AlgR box on every sequence, a single 11-bp long motif was obtained from each set (see **Supplementary Fig. A1:S1**), each one defined by a count matrix.

Using the generated count matrices, we used FIMO (MEME suite, [44,46]) to search for AlgR binding sites. We calibrated the search from each count matrix by using a negative control (a 1050 bp-long probe of random DNA with a 67% GC content, to match genomic *P. aeruginosa* DNA) and a positive control (a 1050 bp probe

of *algD* promoter spanning all three identified AlgR binding sites [3], from -900 to +150 bp, counted from the *algD* start codon). For the final search, DNA probes used were 900 bp long for P*nrdJ* and P*nrdD* (from -750 bp to +150 bp, counted from the corresponding start codons) and 1050 bp long for P*nrdA*, given the predicted long 5' UTR present (from -900 bp to +150 bp, counted from the *nrdA* start codon).

AlgR overexpression and purification.

AlgR and AlgRD54N proteins were overexpressed in a Rosetta (DE3) *E. coli* strain transformed with pETS201 or pETS202, respectively (**Supplementary Table A1:S1**). Cells were grown in LB medium with 30 µg ml^{-1} kanamycin and 17 µg ml^{-1} chloramphenicol and incubated at 37ºC with vigorous shaking (250 rpm). When cultures reached an $OD_{550} \approx 0.5$, protein overexpression was induced by adding IPTG to a concentration of 1.0 mM (Isopropyl β-D-1-thiogalactopyranoside; Fermentas, Thermo Scientific); cells were cultured at 37ºC for 6 hours and later pelleted by centrifugation.

For preparing the protein extract, the pellet was suspended in 15 ml of AlgR lysis buffer per liter of original culture (50 mM Tris, pH 7.8 at 25ºC; 300 mM NaCl; 20 mM imidazole; 2 mM DTT; 10% glycerol), supplemented with 1 mM PMSF as a protease inhibitor. The resulting suspension was sonicated on ice using a 6 mm conical microtip, until clear, to generate the crude extract (CE). It was centrifuged at 15000 g for 30 minutes at 4ºC, keeping the supernatant as the soluble fraction (SF), which was frozen at -80ºC for long term storage.

AlgR and AlgRD54N were purified from their corresponding SF by Immobilized Metal Affinity Chromatography (IMAC) using a 5 ml His-Trap™ HP column (GE Healthcare) in an FPLC system (BioLogic DuoFlow System, Bio-Rad). First, the column was equilibrated with 5 column volumes (CV) of Buffer A (50 mM Tris-HCl pH 7.8 at 25ºC; 300 mM NaCl; 20 mM imidazole). Protein samples were diluted with buffer A to a concentration of less than 1 mg/ml of total protein content and then injected into the column. A washing step was then carried out with 5 CV of Buffer A, and contaminant proteins were removed with a non-specific elution step using 5 CV of Buffer A with 50 mM imidazole. Finally, the protein was recovered in a specific elution step using 5 CV of Buffer A with 400 mM imidazole. The resulting fractions were analyzed by SDS-PAGE protein electrophoresis and dialyzed against AlgR Binding buffer (20mM Tris-HCl, pH 7.8 at 25ºC; 120 mM KCl; 2 mM MgCl2; 10% glycerol) and stored at -80ºC (see **Supplementary Fig. A1:S5**). Protein concentrations were determined by the Bradford assay (Bio-Rad) with crystalline bovine serum albumin as a standard.

Electrophoretic mobility shift assays (EMSA).

DNA probes for EMSA were produced for analyzing full promoter regions of the *nrdAB* and *nrdJab* operons (P*nrdA* long and P*nrdJ* long bands) or fragments of these promoters (P*nrdA* short 1 and P*nrdA* short 2, as well as P*nrdJ* short 1, P*nrdJ* short 2 and P*nrdJ* short 3; see Fig. 2). DNA probes were also generated for the *nrdDG* operon promoter region (P*nrdD* long band) and the negative control (inner region of non-related *anr* gene) and positive control, using the *algD* operon promoter region (P*algD* band). All probes were generated by amplifying the corresponding region in a first PCR reaction that uses the reverse primer to also add the arbitrary sequence 5'-CTGGGCGTCGTTTTAC-3' at the 3' end of every probe (a sequence that we call the M13 complementarity tail) and later applying a second PCR reaction using primer WellRed-M13 to label the probes; WellRed-M13 is a WellRED dye-labeled oligo (Sigma-ALDRICH) coupled to the near-infrared fluorophore D3-phosphoramidite (D3-PA). Resultant probes are hence double-stranded DNA fragments labeled with a single molecule of D3-PA. Primer pairs 13-21 were used for EMSA band generation (see **Supplementary Table A1:S3**). All wild-type probes were copied from *P. aeruginosa* PAO1 genomic DNA. All probes harboring mutations in putative AlgR-boxes were copied from the corresponding plasmids including mutant promoters (see the DNA manipulation and plasmid construction section).

Purified AlgR or AlgRD54N proteins were used in binding reactions for a total amount of 0, 1, 4 or 10 pmol per reaction. A fixed amount of 100 fmol of DNA was used for all bands. Binding reactions also contained BSA (0.25 µg / reaction) and salmon sperm DNA (1 µg / reaction), as well as 2x-AlgR-binding buffer, added to a final 1x concentration of 20 mM Tris-HCl (pH 7.8 at 25ºC), 100 mM KCl, 2 mM $MgCl_2$, 2 mM dithiothreitol, and 10% glycerol. Water was added to every reaction for a final volume of 20 µl. Reactions were incubated at room temperature for 20 minutes before gel electrophoresis.

Electrophoresis was performed in 5% acrylamide gels, prepared with a 37.5:1 proportion of acrylamide:bis-acrylamide and using 5% triethylene glycol as an additive for increased DNA-protein complex stability. Final images were obtained by scanning the gels using the Odyssey Imaging System (LI-COR Biosciences) working in the 700-nm channel.

Atomic force microscopy (AFM).

DNA probes for AFM studies were generated by PCR from *P. aeruginosa* PAO1 genomic DNA and designed so that binding sites were closer to one of the ends, to easily distinguish binding events. Primer pairs 22-25 were used for generating the DNA probes (see **Supplementary Table A1:S3**). The length of this probes is higher than 700 bp, to ensure enough DNA for a proper binding to the surface even in the presence of protein. This length is much higher than the expected persistence length of the *P.* aeruginosa DNA, yielding probes that are assumed to bind in stochastic shapes, and will, therefore, be analyzed in large groups to provide statistically significant information. To avoid agarose contamination, when PCR conditions were proved to result in one single amplification band, DNA probes were purified directly from PCR reactions using a GeneJET PCR Purification Kit (Fermentas, ThermoFisher). Purified DNA probes were diluted to 2-4 nM with DNA AFM buffer (10 mM HEPES, pH 7.8 at 25ºC; 5 mM $MgCl_2$; 50 mM NaCl). Ten milliliters of DNA solution were pipetted onto a freshly cleaved mica and allowed to deposit for 1 min. The mica surface was then rinsed with 200 ml of MilliQ water and dried under a nitrogen stream. For the DNA-protein complex images, protein (AlgR / LexA) was previously mixed with the DNA fragments to a molar ratio of 3:1; the complex was incubated for 20 minutes at room temperature, and 10 ml of the solution was deposited on freshly cleaved mica and allowed to deposit for 4 minutes before rinsing and drying. Topographic images were obtained with a commercial AFM system (CypherTM, Asylum Research) in conventional dynamic mode. A PPP-CONTR (Nanosensors) tip was used, with a nominal spring constant of ~ 0.3 N / m and tip radius of ~ 7 nm, scanning in ambient conditions using small oscillation amplitudes (~20 nm). Image resolution was not lower than 6 nm / pixel since this is close to the tip radius curvature. AFM image processing and determination of DNA length were carried out using WSxM 5.0 develop 7.0 (WSxM solutions).

References

1 Govan, J. R. & Deretic, V. Microbial pathogenesis in cystic fibrosis: mucoid *Pseudomonas aeruginosa* and *Burkholderia cepacia*. *Microbiol Rev* **60**, 539-574 (1996).

2 Deretic, V., Dikshit, R., Konyecsni, W. M., Chakrabarty, A. M. & Misra, T. K. The algR gene, which regulates mucoidy in *Pseudomonas aeruginosa*, belongs to a class of environmentally responsive genes. *J Bacteriol* **171**, 1278-1283 (1989).

3 Mohr, C. D., Hibler, N. S. & Deretic, V. AlgR, a response regulator controlling mucoidy in *Pseudomonas aeruginosa,* binds to the FUS sites of the algD promoter located unusually far upstream from the mRNA start site. *J Bacteriol* **173**, 5136-5143 (1991).

4 Leid, J. G. *et al.* The exopolysaccharide alginate protects *Pseudomonas aeruginosa* biofilm bacteria from IFN-gamma-mediated macrophage killing. *J Immunol* **175**, 7512-7518 (2005).

5 Hentzer, M. *et al.* Alginate overproduction affects *Pseudomonas aeruginosa* biofilm structure and function. *J Bacteriol* **183**, 5395-5401 (2001).

6 Lizewski, S. E. *et al.* Identification of AlgR-regulated genes in *Pseudomonas aeruginosa* by use of microarray analysis. *J Bacteriol* **186**, 5672-5684, doi:10.1128/JB.186.17.5672-5684.2004 (2004).

7 Damron, F. H. & Goldberg, J. B. Proteolytic regulation of alginate overproduction in *Pseudomonas aeruginosa*. *Mol Microbiol* **84**, 595-607, doi:10.1111/j.1365-2958.2012.08049.x (2012).

8 Mena, A. *et al.* Genetic adaptation of *Pseudomonas aeruginosa* to the airways of cystic fibrosis patients is catalyzed by hypermutation. *J Bacteriol* **190**, 7910-7917, doi:10.1128/JB.01147-08 (2008).

9 Hogardt, M. *et al.* Stage-specific adaptation of hypermutable *Pseudomonas aeruginosa* isolates during chronic pulmonary infection in patients with cystic fibrosis. *J Infect Dis* **195**, 70-80, doi:10.1086/509821 (2007).

10 Darzins, A. & Chakrabarty, A. M. Cloning of genes controlling alginate biosynthesis from a mucoid cystic fibrosis isolate of *Pseudomonas aeruginosa*. *J Bacteriol* **159**, 9-18 (1984).

11 Whitchurch, C. B. *et al.* Phosphorylation of the *Pseudomonas aeruginosa* response regulator AlgR is essential for type IV fimbria-mediated twitching motility. *J Bacteriol* **184**, 4544-4554 (2002).

12 Kong, W. *et al.* ChIP-seq reveals the global regulator AlgR mediating cyclic di-GMP synthesis in *Pseudomonas aeruginosa*. *Nucleic Acids Res* **43**, 8268-8282, doi:10.1093/nar/gkv747 (2015).

13 Lizewski, S. E., Lundberg, D. S. & Schurr, M. J. The transcriptional regulator AlgR is essential for *Pseudomonas aeruginosa* pathogenesis. *Infect Immun* **70**, 6083-6093 (2002).

14 Okkotsu, Y., Little, A. S. & Schurr, M. J. The *Pseudomonas aeruginosa* AlgZR two-component system coordinates multiple phenotypes. *Front Cell Infect Microbiol* **4**, 82, doi:10.3389/fcimb.2014.00082 (2014).

15 Torrents, E. Ribonucleotide reductases: Essential Enzymes for bacterial life. *Front. Cell. Infect. Microbiol.* **4**, 52, doi:10.3389/fcimb.2014.00052 (2014).

16 Lundin, D., Torrents, E., Poole, A. M. & Sjöberg, B. M. RNRdb, a curated database of the universal enzyme family ribonucleotide reductase, reveals a high level of misannotation in sequences deposited to Genbank. *BMC Genomics* **10**, 589, doi:10.1186/1471-2164-10-589 (2009).

17 Torrents, E., Poplawski, A. & Sjöberg, B. M. Two proteins mediate class II ribonucleotide reductase activity in *Pseudomonas aeruginosa*: expression and transcriptional analysis of the aerobic enzymes. *J Biol Chem* **280**, 16571-16578, doi:10.1074/jbc.M501322200 (2005).

18 Sjöberg, B. M. & Torrents, E. Shift in ribonucleotide reductase gene expression in *Pseudomonas aeruginosa* during infection. *Infect Immun* **79**, 2663-2669, doi:10.1128/IAI.01212-10 (2011).

19 Crespo, A., Pedraz, L., Astola, J. & Torrents, E. *Pseudomonas aeruginosa* Exhibits Deficient Biofilm Formation in the Absence of Class II and III Ribonucleotide Reductases Due to Hindered Anaerobic Growth. *Frontiers in microbiology* **7**, 688, doi:10.3389/fmicb.2016.00688 (2016).

20 Okkotsu, Y., Tieku, P., Fitzsimmons, L. F., Churchill, M. E. & Schurr, M. J. *Pseudomonas aeruginosa* AlgR phosphorylation modulates rhamnolipid production and motility. *J Bacteriol* **195**, 5499-5515, doi:10.1128/JB.00726-13 (2013).

21 Mohr, C. D. & Deretic, V. In vitro interactions of the histone-like protein IHF with the *alg*D promoter, a critical site for control of mucoidy in *Pseudomonas aeruginosa*. *Biochem Biophys Res Commun* **189**, 837-844 (1992).

22 Yu, H., Mudd, M., Boucher, J. C., Schurr, M. J. & Deretic, V. Identification of the *algZ* gene upstream of the response regulator *algR* and its participation in control of alginate production in *Pseudomonas aeruginosa*. *J Bacteriol* **179**, 187-193 (1997).

23 Sanders, L. H., Rockel, A., Lu, H., Wozniak, D. J. & Sutton, M. D. Role of *Pseudomonas aeruginosa dinB*-encoded DNA polymerase IV in mutagenesis. *J Bacteriol* **188**, 8573-8585, doi:10.1128/JB.01481-06 (2006).

24 Morici, L. A. *et al. Pseudomonas aeruginosa* AlgR represses the Rhl quorum-sensing system in a biofilm-specific manner. *J Bacteriol* **189**, 7752-7764, doi:10.1128/JB.01797-06 (2007).

25 O'Toole, G. A. & Kolter, R. Flagellar and twitching motility are necessary for *Pseudomonas aeruginosa* biofilm development. *Mol Microbiol* **30**, 295-304 (1998).

26 Stapper, A. P. *et al.* Alginate production affects *Pseudomonas aeruginosa* biofilm development and architecture, but is not essential for biofilm formation. *Journal of medical microbiology* **53**, 679-690, doi:10.1099/jmm.0.45539-0 (2004).

27 Xu, B., Soukup, R. J., Jones, C. J., Fishel, R. & Wozniak, D. J. *Pseudomonas aeruginosa* AmrZ Binds to Four Sites in the *algD* Promoter, Inducing DNA-AmrZ Complex Formation and Transcriptional Activation. *J Bacteriol* **198**, 2673-2681, doi:10.1128/JB.00259-16 (2016).

28 Gon, S. & Beckwith, J. Ribonucleotide reductases: influence of environment on synthesis and activity. *Antioxid Redox Signal* **8**, 773-780, doi:10.1089/ars.2006.8.773 (2006).

29 Monje-Casas, F., Jurado, J., Prieto-Alamo, M. J., Holmgren, A. & Pueyo, C. Expression analysis of the *nrdHIEF* operon from *Escherichia coli*. Conditions that trigger the transcript level in vivo. *J Biol Chem* **276**, 18031-18037, doi:10.1074/jbc.M011728200 (2001).

30 Crespo, A., Pedraz, L. & Torrents, E. Function of the *Pseudomonas aeruginosa* NrdR Transcription Factor: Global Transcriptomic Analysis and Its Role on Ribonucleotide Reductase Gene Expression. *PloS one* **10**, e0123571, doi:10.1371/journal.pone.0123571 (2015).

31 Kato, J. & Chakrabarty, A. M. Purification of the regulatory protein AlgR1 and its binding in the far upstream region of the algD promoter in *Pseudomonas aeruginosa*. *Proc Natl Acad Sci U S A* **88**, 1760-1764 (1991).

32 Martin, D. W., Schurr, M. J., Yu, H. & Deretic, V. Analysis of promoters controlled by the putative sigma factor AlgU regulating conversion to mucoidy in *Pseudomonas aeruginosa*: relationship to sigma E and stress response. *J Bacteriol* **176**, 6688-6696 (1994).

33 Pritchett, C. L. *et al.* Expression analysis of the *Pseudomonas aeruginosa* AlgZR two-component regulatory system. *J Bacteriol* **197**, 736-748, doi:10.1128/JB.02290-14 (2015).

34 Belete, B., Lu, H. & Wozniak, D. J. *Pseudomonas aeruginosa* AlgR regulates type IV pilus biosynthesis by activating transcription of the fimU-pilVWXY1Y2E operon. *J Bacteriol* **190**, 2023-2030, doi:10.1128/JB.01623-07 (2008).

35 Warren, M. J., Raux, E., Schubert, H. L. & Escalante-Semerena, J. C. The biosynthesis of adenosylcobalamin (vitamin B12). *Nat Prod Rep* **19**, 390-412 (2002).

36 Stewart, P. S. & Franklin, M. J. Physiological heterogeneity in biofilms. *Nature reviews. Microbiology* **6**, 199-210, doi:10.1038/nrmicro1838 (2008).

37 Hassett, D. J. *et al.* Anaerobic metabolism and quorum sensing by *Pseudomonas aeruginosa* biofilms in chronically infected cystic fibrosis airways: rethinking antibiotic treatment strategies and drug targets. *Advanced drug delivery reviews* **54**, 1425-1443 (2002).

38 McPhee, J. B. *et al.* The major outer membrane protein OprG of *Pseudomonas aeruginosa* contributes to cytotoxicity and forms an anaerobically regulated, cation-selective channel. *FEMS Microbiol Lett* **296**, 241-247, doi:10.1111/j.1574-6968.2009.01651.x (2009).

39 Filiatrault, M. J., Picardo, K. F., Ngai, H., Passador, L. & Iglewski, B. H. Identification of *Pseudomonas aeruginosa* genes involved in virulence and anaerobic growth. *Infect Immun* **74**, 4237-4245, doi:74/7/4237 [pii]10.1128/IAI.02014-05 (2006).

40 Pessi, G. & Haas, D. Transcriptional control of the hydrogen cyanide biosynthetic genes hcnABC by the anaerobic regulator ANR and the quorum-sensing regulators LasR and RhlR in *Pseudomonas aeruginosa*. *J Bacteriol* **182**, 6940-6949 (2000).

41 Cody, W. L. *et al. Pseudomonas aeruginosa* AlgR controls cyanide production in an AlgZ-dependent manner. *J Bacteriol* **191**, 2993-3002, doi:10.1128/JB.01156-08 (2009).

42 Zimmermann, A., Reimmann, C., Galimand, M. & Haas, D. Anaerobic growth and cyanide synthesis of *Pseudomonas aeruginosa* depend on *anr*, a regulatory gene homologous with fnr of *Escherichia coli*. *Mol Microbiol* **5**, 1483-1490 (1991).

43 Sambrook, J., Fritsch, E. F. & Maniatis, T. *Molecular Cloning: A Laboratory Manual*. 2nd edn, (Cold Spring Harbor Laboratory Press, 1989).

44 Bailey, T. L. *et al.* MEME SUITE: tools for motif discovery and searching. *Nucleic Acids Res* **37**, W202-208, doi:10.1093/nar/gkp335 (2009).

45 Bailey, T. L. & Elkan, C. Fitting a mixture model by expectation maximization to discover motifs in biopolymers. *Proc Int Conf Intell Syst Mol Biol* **2**, 28-36 (1994).

46 Grant, C. E., Bailey, T. L. & Noble, W. S. FIMO: scanning for occurrences of a given motif. *Bioinformatics* **27**, 1017-1018, doi:10.1093/bioinformatics/btr064 (2011).

Acknowledgements

We are grateful to Michael Brennan and Ana Jareño for their excellent technical assistance. This work was supported in part by grants to ET from the Spanish Ministerio de Economia y Competitividad (MINECO / FEDER) (BFU2011-24066 and BIO2015-63557-R), Generalitat de Catalunya (2014 SGR01260 and CERCA programme), the Catalan and Spanish Cystic Fibrosis foundations and La Caixa Foundation. ET was also supported by the Ramón y Cajal I3 program from the Ministerio de Economia y Competitividad. LP is thankful to the Generalitat de Catalunya for its financial support through the FI program (2015-FI-B-00817).

Authors contributions

AC, LP and ET designed the experiments. AC, LP, MvdH performed the experiments. AC, LP, MvdH, ET and GG analyzed the data. AC, LP and ET wrote the manuscript. ET supervised the whole work.

Additional information

Supplementary information

Accompanies this paper.

Competing interests

The author(s) declare(s) that they have no competing interests

Availability of Data and Materials

All data generated or analyzed during this study are included in this manuscript and it supplementary information files, or is available upon request.

A1 Supporting information

Regulation of ribonucleotide synthesis by the *Pseudomonas aeruginosa* AlgR two-component system

Supplementary Fig. A1:S1. Count matrices for AlgR-box identification.

Count matrices were generated by FIMO search using three different sets of sequences containing AlgR binding spots (see Materials and Methods). Matrices are adjusted for a box size of 11 bp, represented in rows, and the bases are expressed in columns in the order A–C–G–T; each matrix is accompanied by its corresponding HMM logo.

Set 1: 50 best hits in ChIP-seq

30	0	19	1
0	50	0	0
1	49	0	0
6	0	42	2
2	2	0	46
0	5	0	45
0	46	3	1
5	0	44	1
0	0	0	50
0	50	0	0
6	6	32	6

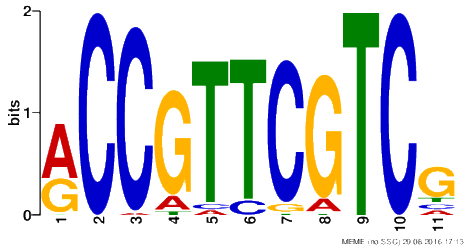

Set 2: 25 random hits in ChIP-seq

4	2	6	11
14	3	4	2
0	23	0	0
0	23	0	0
1	0	21	1
0	3	0	20
0	6	0	17
0	19	4	0
5	0	18	0
1	0	0	22
0	23	0	0

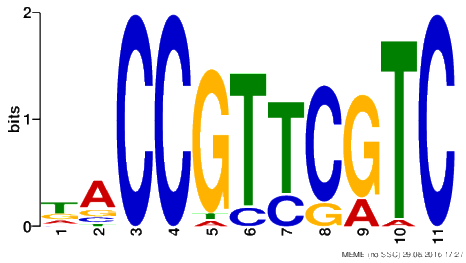

Set 3: Published sequences

3	4	3	1
0	11	0	0
0	11	0	0
0	1	10	0
0	0	0	11
0	2	1	8
0	6	3	2
1	0	8	2
0	0	2	9
0	11	0	0
1	6	3	1

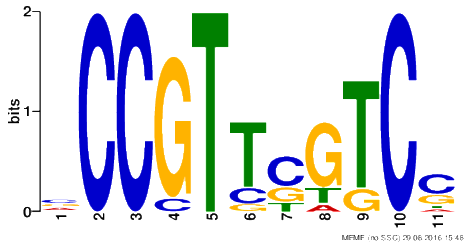

Supplementary Fig. A1:S2. Original EMSA images used to generate Figure A1:3A.

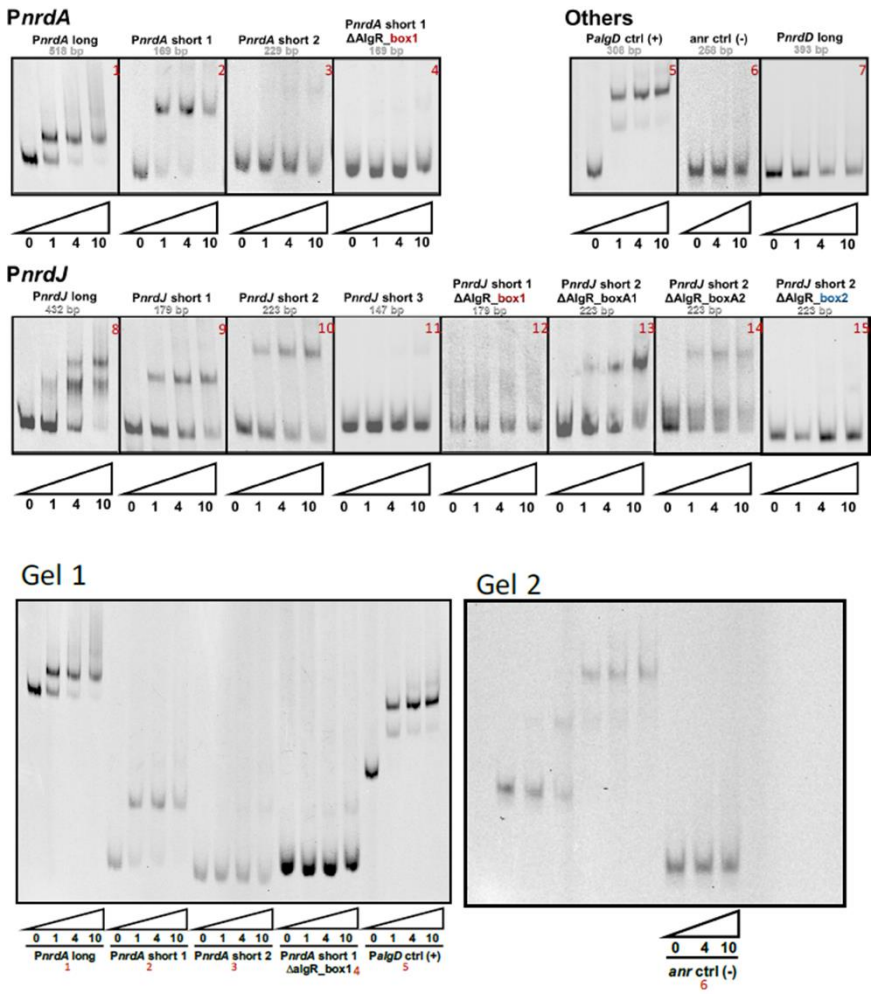

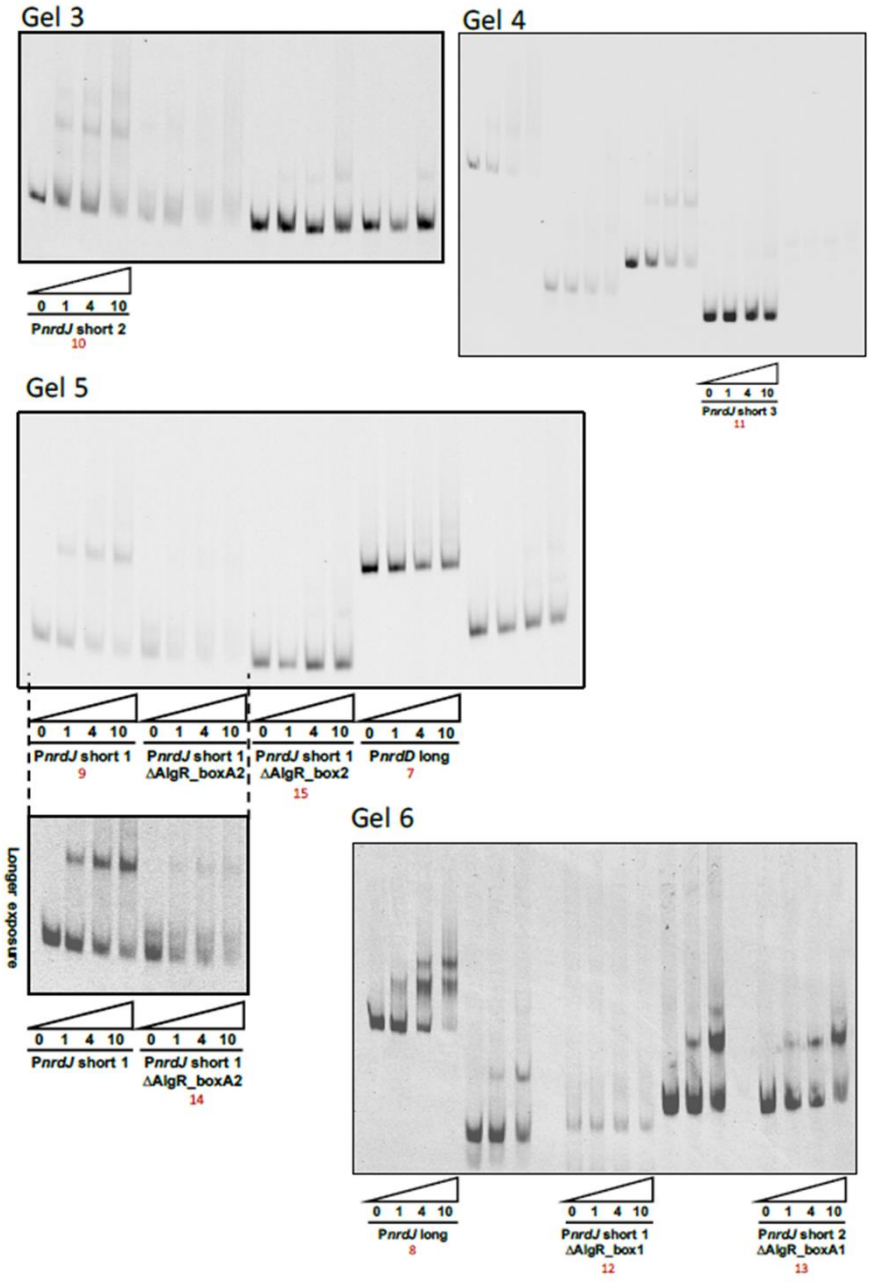
Gel 3
0 1 4 10
PnrdJ short 2
10
Gel 4
0 1 4 10
PnrdJ short 3
11
Gel 5
0 1 4 10
PnrdJ short 1
9
0 1 4 10
PnrdJ short 1
ΔAlgR_boxA2
0 1 4 10
PnrdJ short 1
ΔAlgR_box2
15
0 1 4 10
PnrdD long
7
Longer exposure
0 1 4 10
PnrdJ short 1
0 1 4 10
PnrdJ short 1
ΔAlgR_boxA2
14
Gel 6
0 1 4 10
PnrdJ long
8
0 1 4 10
PnrdJ short 1
ΔAlgR_box1
12
0 1 4 10
PnrdJ short 2
ΔAlgR_boxA1
13

Supplementary Fig. A1:S3. AlgR – DNA binding affinities.

EMSA assays for P*nrdA*, P*nrdJ,* and *PalgD* promoter long bands. (**A**), A wide array of concentrations was used to illustrate different binding affinities (shown below the figures; numbers represent protein amount in pmol). Different boxes involved in bindings are shown in the table below, (**B**). Most conserved base pairs are underlined, and cytosine in position 7, which is described to distinguish weak and strong binding sites, is marked in gray.

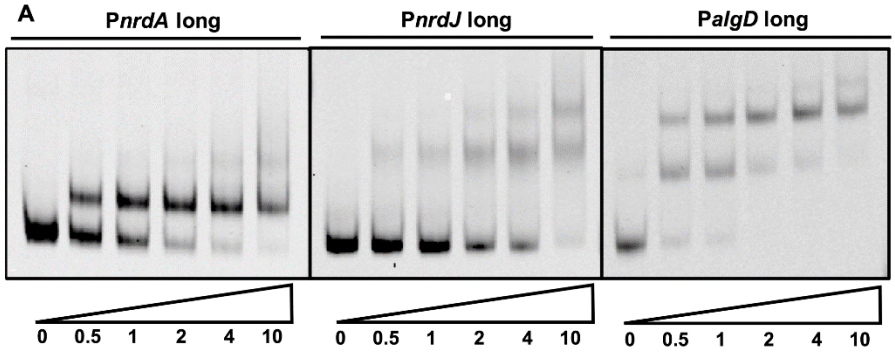

B

Binding site	Sequence	Orientation	Strength	Source
P*nrdA* box 1	G**CCATTCGTC**G	3'-5' ←	Strong	This work
P*nrdJ* box 1	G**CCGCCGGTC**C	5'-3' →	Weak	This work
P*nrdJ* box 2	G**CCGGCTGTC**T	5'-3' →	Weak	This work
P*algD* RB1	A**CCGTTCGTC**C	5'-3' →	Strong	1, 2
P*algD* RB2	A**CCGTTCGTC**T	5'-3' →	Strong	1, 2
P*algD* RB3	G**CCGTTTGTC**C	3'-5' ←	Weak	1, 2
P*algC* ABS1	C**CCGTTCGTC**G	5'-3' →	Strong	3
P*algC* ABS2	T**CCGTTGTTC**C	5'-3' →	Weak	3
P*algC* ABS3	A**CCGTGCGTC**G	5'-3' →	Strong	3

(1) Kato, J. and A. M. Chakrabarty (1991). "Purification of the regulatory protein AlgR1 and its binding in the far upstream region of the algD promoter in Pseudomonas aeruginosa." Proc Natl Acad Sci U S A 88(5): 1760-1764.

(2) Mohr, C. D., et al. (1991). "AlgR, a response regulator controlling mucoidy in Pseudomonas aeruginosa, binds to the FUS sites of the algD promoter located unusually far upstream from the mRNA start site." J Bacteriol 173(16): 5136-5143.

(3) Zielinski, N. A., et al. (1991). "Characterization and regulation of the Pseudomonas aeruginosa algC gene encoding phosphomannomutase." J Biol Chem 266(15): 9754-9763.

Supplementary Fig. A1:S4. Cooperative regulation of AlgZR and Anr/Dnr systems on RNR class II.

Gene reporter assay for the P*nrdJ* promoter fused to GFP, during anaerobic liquid cultures, grown to OD_{550} = 2.0. The cooperative action of these two systems is explored by combining a Δ*algR* background with the mutation of the Anr/Dnr box on P*nrdJ*. Values are averages from at least three independent experiments; error bars show positive standard deviation. Asterisks (*) indicate statistically significant differences from the wild-type strain harboring P*nrdJ* wild-type promoter (*p*-value less than 0.05 in pairwise T-tests). Shortened names are used (see Table A1:S1).

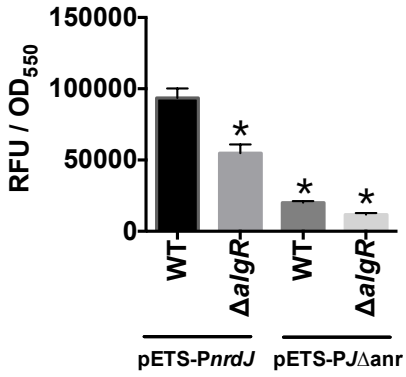

Supplementary Fig. A1:S5. Protein overexpression and purification.

Coomassie blue-stained gel showing SDS-PAGE analysis of AlgR wild type and AlgRD54N overexpression. MW, molecular weight marker; CE, crude extract; FT, flow through; UN, nonspecific elution step; P, protein recovered after specific elution step. Molecular weights of the standards are indicated.

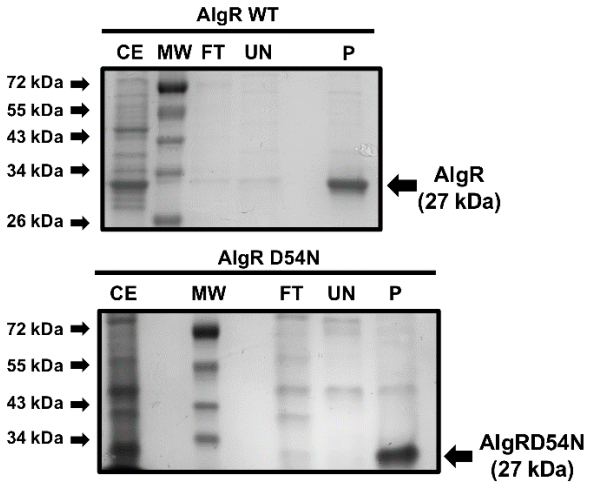

Supplementary Table A1:S1. Bacterial strains and plasmids used in this study.

For each element, a general description is provided, together with an alternative self-explanatory name which will be commonly used in figures to make interpretation of the data easier for the reader. Throughout all the paper, a P before the name of a gene indicates the promoter controlling this gene (e.g., P*nrdA* for *nrdAB* operon promoter).

Name	Referred as…	Description	Source
Plasmids			
pGEM-T easy	pGEM-T easy	A/T cloning vector; Amp^R	Promega
pUCP20T	pUCP20T	Broad-host-range vector; Amp^R	(1)
pET28a	*pETS28a*	*Vector for His_6-tagged protein overexpression; Kn^R*	Laboratory
pETS130-GFP	pETS130	Broad host range, promoterless GFP; Gm^R	(2)
pETS134	pETS-P*nrdA*	pETS130 derivative carrying *nrdA* promoter; Gm^R	(2)
pETS136	pETS-P*nrdD*	pETS130 derivative carrying *nrdD* promoter; Gm^R	(2)
pETS180	pETS-P*nrdJ*	pETS130 derivative carrying *nrdJ* promoter; Gm^R	(3)
pETS191	pETS-PJΔdnr	pETS130 derivative carrying Anr/Dnr box mutating in P*nrdJ*; Gm^R	(4)
pETS201	pETS201	pET28a derivative carrying *algR*, AlgR overproducer, Kn^R	This work
pETS202	pETS202	pET28a derivative carrying algRD54N, AlgRD54N overproducer, Kn^R	This work
pETS203	pUCP-AlgR	pUCP20T derivative carrying the *algR* gene; Cb^R	This work
pETS204	pUCP-D54N	pUCP20T derivative carrying the *algRD54N* gene; Cb^R	This work
pETS205	pETS-P*algD*	pETS130 derivative carrying *algD* promoter; Gm^R	This work
pETS206	pETS-P1157	pETS130 derivative carrying *PA1157* promoter; Gm^R	This work
pETS207	pETS-P*algR*	pETS130 derivative carrying *algR* promoter; Gm^R	This work
pETS208	pETS-PAΔbox1	pETS130 derivative carrying AlgR-box1 mutation in P*nrdA*, Gm^R	This work
pETS209	pETS-PJΔbox1	pETS130 derivative carrying AlgR-box1 mutation in P*nrdJ*, Gm^R	This work
pETS210	pETS-PJΔbox2	pETS130 derivative carrying AlgR-box2 mutation in P*nrdJ*, Gm^R	This work
pETS211	pETS-PJΔbox1+2	pETS130 derivative carrying AlgR-box1 and AlgR-box2 mutation in P*nrdJ*, Gm^R	This work
Strains			
E. coli			
DH5α	DH5α	*recA1 endA1 hsdR17 supE44 thi-1 relA1 Δ(lacZYA-argF)U169 deoR Φ80dlacZM15*	Laboratory
Rossetta(DE3)	Rosetta	*F^- ompT $hsdS_B$ (r_B^- m_B^-) gal dcm (DE3) pRARE (CamR)*	Merck
P. aeruginosa			

1. **West SE, Schweizer HP, Dall C, Sample AK, Runyen-Janecky LJ.** 1994. Construction of improved *Escherichia-Pseudomonas* shuttle vectors derived from pUC18/19 and sequence of the region required for their replication in *Pseudomonas aeruginosa*. Gene **148:**81-86.
2. **Sjöberg BM, Torrents E.** 2011. Shift in ribonucleotide reductase gene expression in *Pseudomonas aeruginosa* during infection. Infect Immun **79:**2663-2669.
3. **Crespo A, Pedraz L, Torrents E.** 2015. Function of the *Pseudomonas aeruginosa* NrdR Transcription Factor: Global Transcriptomic Analysis and Its Role on Ribonucleotide Reductase Gene Expression. PLoS One **10:**e0123571.
4. **Crespo A, Pedraz L, Astola J, Torrents E.** 2016. *Pseudomonas aeruginosa* Exhibits Deficient Biofilm Formation in the Absence of Class II and III Ribonucleotide Reductases Due to Hindered Anaerobic Growth. Front Microbiol **7:**688.
5. Jacobs MA, Alwood A, Thaipisuttikul I, Spencer D, Haugen E, Ernst S, Will O, Kaul R, Raymond C, Levy R, Chun-Rong L, Guenthner D, Bovee D, Olson MV, Manoil C. 2003. Comprehensive transposon mutant library of *Pseudomonas aeruginosa*. Proc Natl Acad Sci U S A 100:14339-14344.

Supplementary Table A1:S2. Primers and probes used in this study.

Name	Sequence (5'→3')	Application
M13-dir	GTTTTCCCAGTCACGAC	Check-Cloning
M13-rev	CAGGAAACAGCTATGACC	Check-Cloning
pUCP20T-up	CCTCTTCGCTATTACGCCAG	Cloning
pUCP20T-low	TCCGGCTCGTATGTTGTGTG	Cloning
pBBR1-up	CATCGCAGTCGGCCTATTGG	Cloning
pBBR1-low	CACTTTATGCTTCCGGCTCG	Cloning
AlgR-up	ACATATGAATGTCCTGATTGTCGATG	AlgR overproducer
AlgR-low	ATCAGAGCTGATGCATCAGAC	AlgR overproducer
AlgRD54N-up	GCGGATGTTCAGCAGGAC	AlgRD54N overproducer
AlgRD54N-low	GTCCTGCTGAACATCCGC	AlgRD54N overproducer
PfimSalgR-up	GGATCCTGTCTTCCTGGTTGTCCTTGTT	P*fimSalgR* cloning / AlgR complementation
PalgR-SmaI-GFP-low	TTCCCGGGCTTGAATCGGAT	P*fimSalgR* cloning
PA1157-up	AAGGATCCGGTATGCATGGGTGGGTATC	*PA1157* promoter cloning
PA1157-low	AACCCGGGTTCTTGCTCCACACAGCCTC	*PA1157* promoter cloning
PnrdA-BamHI-EcoRI-GFP-up	AGGATCCGAATTCTTGCTCCACACAGCCTC	P*nrdAB* cloning / EMSA P*nrdA* long / AFM
PnrdA-SmaI-GFP-low	ACCCGGGTTCTCGCGTGTGGTGTCG	P*nrdAB* cloning / AFM
PnrdA-EXT-low-M13	CTGGGCGTCGTTTTACGGCTCCTTGCGATGAG	EMSA P*nrdA* long
PnrdA-AlgR-EMSA-up	TACATATTGTGGGTAGGGTG	EMSA P*nrdA* short 1
PnrdA-AlgR-EMSA-low-M13	CTGGGCGTCGTTTTACGGATAAAGTGTGGGTCTTCT	EMSA P*nrdA* short 1
PnrdA-EMSA-up	TTTCCCCCAGACTGTCAC	EMSA P*nrdA* short 2
PnrdA-EMSA-low-M13	CTGGGCGTCGTTTTACTCAGAGTGGTCCGTGCG	EMSA P*nrdA* short 2
PnrdJ-AlgR-BamHI-EMSA-up	GGATCCTACGGGTTGCGCCATA	P*nrdJ* promoter cloning
PnrdJ-SmaI-GFP-low	AACCCGGGGACTGCGTTGCGTCTGTC	P*nrdJ* promoter cloning / AFM
PnrdJ-BamHI-GFP-up	GGATCCCGCGCCCAGCTGAAGGCC	EMSA P*nrdJ* long
PnrdJ-EXT-low-M13	CTGGGCGTCGTTTTACGGCCACCGTACGCAAC	EMSA P*nrdJ* long
PnrdJ-AlgR-EMSA-up	TACGGGTTGCGCCATA	EMSA P*nrdJ* short 1
PnrdJ-AlgR-EMSA-low-M13	CTGGGCGTCGTTTTACTTCGCTGAGGGTGTCG	EMSA P*nrdJ* short 1
PnrdJ-mid-up	CCGACACCCTCAGCGAAG	EMSA P*nrdJ* short 2
PnrdJ-mid-low-M13	CTGGGCGTCGTTTTACAGACAACCTTAGTCATCGG	EMSA P*nrdJ* short 2
PnrdJ-EMSA-up	TCCCGATGACTAAGGTTGTC	EMSA P*nrdJ* short 3
PnrdJ-EMSA-low-M13	CTGGGCGTCGTTTTACCTGATTAACCTCCCGATGG	EMSA P*nrdJ* short 3
PnrdJ-AFM-up	GCGCAAGTTCGTCAATTTCG	AFM
PnrdD-BamHI-GFP-up	AGGATCCCGCGACGCCCATTTC	EMSA P*nrdD* long
PnrdD-EMSA-low-M13	CTGGGCGTCGTTTTACCTTGAGCAGGGTGGCC	EMSA P*nrdD* long
PalgD-BamHI-GFP-up	GGATCCCTCCTCTTTCGGCAC	P*algD* cloning / EMSA positive control
PalgD-low-M13	CTGGGCGTCGTTTTACTTCCTTAATCTTCGACCCA	EMSA positive control / AFM
PalgD-SmaI-GFP-low	CCCGGGAGATGCTGATTCGCATC	P*algD* cloning
PalgD-BamHI-AFM-up	TGGATCCCCCTATCGACTGGAAATGG	AFM
Anr-EcoRI-up	GAATTCATGGCCGAAACCATCAAG	EMSA negative control
Anr-low-M13	CTGGGCGTCGTTTTACGCATCGGTGATGCTGAAG	EMSA negative control
DinB-AFM-up	CTGGTGATGCTGGTCGTG	AFM
DinB-low-M13	CTGGGCGTCGTTTTACCAGCTCCCGCAACCAC	AFM
PnrdA-mutAlgR1-up	GCTTCGCCTAACATTCTCCAGCGCTG	Mutagenesis P*nrdA* box1
PnrdA-mutAlgR1-low	TGTTAGGCGAAGCCCTCGGAAAGC	Mutagenesis P*nrdA* box1
PnrdJ-mutAlgR1-up	GGTTGCCGTAACGGTCTGCA	Mutagenesis P*nrdJ* box1
PnrdJ-mutAlgR1-low	CAGACCGTTACGGCAACCT	Mutagenesis P*nrdJ* box1
PnrdJ-mutAlgR2-up	GCTCTGAAAACTAGTTCCTGATATCCGC	Mutagenesis P*nrdJ* boxA1
PnrdJ-mutAlgR2-low	GCGCGGATATCAGGAACTAGTTT	Mutagenesis P*nrdJ* boxA1
PnrdJ-mutAlgR3-up	ATGGCCGCGAACGCTTGAGCG	Mutagenesis P*nrdJ* boxA2
PnrdJ-mutAlgR3-low	CGCTCAAGCGTTCGCGGCCAT	Mutagenesis P*nrdJ* boxA2
PnrdJ-mutAlgR4-up	CGAATTTGAAGGCTTAATGGAAAAGC	Mutagenesis P*nrdJ* box2
PnrdJ-mutAlgR4-low	TTCCATTAAGCCTTCAAATTCGC	Mutagenesis P*nrdJ* box2
WellRed-M13	[D3-PA]GTCACTGGGCGTCGTTTTAC	EMSA band infrared labelling

Supplementary Table S3. PCR reactions and primer pairs used.

Primer pair	Forward primer	Reverse primer	Application
1	AlgR-D54N-up	AlgR-D54N-low	AlgR D54N directed mutagenesis
2	PfimSalgR-up	AlgR-low	AlgR complementation plasmids
3	PalgD-BamHI-GFP-up	PalgD-SmaI-GFP-low	P*algD*::*gfp* transcriptional fusion
4	PfimSalgR-up	PalgR-SmaI-GFP-low	P*algR*::*gfp* transcriptional fusion
5	PA1157-up	PA1157-low	P_{PA1157}::gfp transcriptional fusion
6	PnrdA-BamHI-EcoRI-GFP-up	PnrdA-SmaI-GFP-low	Outer primers in P*nrdA* promoter
7	PnrdJ-AlgR-BamHI-GFP-up	PnrdJ-SmaI-GFP-low	Outer primers in P*nrdJ* promoter
8	PnrdA-mutAlgR1-up	PnrdA-mutAlgR1-low	P*nrdA* AlgR box 1 mutagenesis
9	PnrdJ-mutAlgR1-up	PnrdJ-mutAlgR1-low	P*nrdJ* AlgR box 1 mutagenesis
10	PnrdJ-mutAlgR4-up	PnrdJ-mutAlgR4-low	P*nrdJ* AlgR box 2 mutagenesis
11	PnrdJ-mutAlgR2-up	PnrdJ-mutAlgR2-low	P*nrdJ* AlgR box A1 mutagenesis
12	PnrdJ-mutAlgR3-up	PnrdJ-mutAlgR3-low	P*nrdJ* AlgR box A2 mutagenesis
13	PnrdA-BamHI-EcoRI-GFP-up	PnrdA-EXT-low-M13	EMSA P*nrdA* long band
14	PnrdA-AlgR-EMSA-up	PnrdA-AlgR-EMSA-low-M13	EMSA P*nrdA* short 1 band
15	PnrdA-EMSA-up	PnrdA-EMSA-low-M13	EMSA P*nrdA* short 2 band
16	PnrdJ-BamHI-GFP-up	PnrdJ-EXT-low-M13	EMSA P*nrdJ* long band
17	PnrdJ-AlgR-EMSA-up	PnrdJ-AlgR-EMSA-low-M13	EMSA P*nrdJ* short 1 band
18	PnrdJ-mid-up	PnrdJ-mid-low-M13	EMSA P*nrdJ* short 2 band
19	PnrdJ-EMSA-up	PnrdJ-EMSA-low-M13	EMSA P*nrdJ* short 3 band
20	PalgD-BamHI-GFP-up	PalgD-low-M13	EMSA P*algD* positive control band
21	Anr-EcoRI-up	Anr-low-M13	EMSA *anr* negative control band
22	PnrdA-BamHI-EcoRI-GFP-up	PnrdA-SmaI-GFP-low	AFM P*nrdA* probe
23	PnrdJ-AFM-up	PnrdJ-SmaI-GFP-low	AFM P*nrdJ* probe
24	PalgD-BamHI-AFM-up	PalgD-low-M13	AFM P*algD* probe
25	PdinB-AFM-up	PdinB-low-M13	AFM P*dinB* probe

Article 2

Function of the *Pseudomonas aeruginosa* NrdR transcription factor: global transcriptomic analysis and its role on ribonucleotide reductase gene expression

Published in *PLoS ONE* (Q1, IF_{2015} = 3.057)

doi: 10.1371/journal.pone.0123571 (187)

April 2015

Anna Crespo[1], Lucas Pedraz[1] and Eduard Torrents[1*]

[1] Bacterial Infections: Antimicrobial Therapies, Institute for Bioengineering of Catalonia (IBEC), The Barcelona Institute of Science and Technology, Barcelona, Spain.

*: Corresponding author: Eduard Torrents (etorrents@ibecbarcelona.eu)

Abstract

Ribonucleotide reductases (RNRs) are a family of sophisticated enzymes responsible for the synthesis of the deoxyribonucleotides (dNTPs), the building blocks for DNA synthesis and repair. Although any living cell must contain one RNR activity to continue living, bacteria have the capacity to encode different RNR classes in the same genome, allowing them to adapt to different environments and growing conditions. *Pseudomonas aeruginosa* is well known for its adaptability and surprisingly encodes all three known RNR classes (Ia, II and III). There must be a complex transcriptional regulation network behind this RNR activity, dictating which RNR class will be expressed according to specific growing conditions.

In this work, we aim to uncover the role of the transcriptional regulator NrdR in *P. aeruginosa*. We demonstrate that NrdR regulates all three RNR classes, being involved in differential control depending on whether the growth conditions are aerobic or anaerobic. Moreover, we also identify for the first time that NrdR is not only involved in controlling RNR expression but also regulates topoisomerase I (*topA*) transcription. Finally, to obtain the entire picture of NrdR regulon, we performed a global transcriptomic analysis comparing the transcription profile of wild-type and *nrdR* mutant strains.

The results provide many new data about the regulatory network that controls *P. aeruginosa* RNR transcription, bringing us a step closer to the understanding of this complex system.

Introduction

The opportunistic pathogen *Pseudomonas aeruginosa* has the ability to grow under a variety of environmental conditions; it can be free-living in soil and water, as well as growing in human and plant host-associated environments. It is responsible for severe nosocomial infections in immunocompromised patients and, in particular, causes chronic lung infections in patients suffering from the inherited disease cystic fibrosis [1]. The genome of *P. aeruginosa* is relatively large (6.3 Mb), and contains a large number of genes to perform different metabolic activities, which might contribute to the environmental adaptability of this bacterium [2].

One such example is the enzyme ribonucleotide reductase (RNR), a key enzyme that catalyzes the reduction of all four ribonucleotides to their corresponding deoxyribonucleotides, providing the necessary precursors for DNA synthesis and repair in all organisms. All known RNRs can be divided into three classes (I, II and III) based on their structural differences, metallocofactor requirements, and mechanisms used for radical generation [3-6]. Class I RNRs require oxygen to produce a tyrosyl radical using a diferric iron or dimanganese iron center, and thereby functions only under aerobic conditions. Based on sequence identity, the metal cofactor center and allosteric properties, class I RNRs are subdivided into classes Ia, Ib and Ic, encoded, respectively, by *nrdAB, nrdHIEF* and the *nrdAB* genes. Class II enzymes require S-adenosylcobalamine (AdoCob) for radical generation and do not depend on oxygen. Members of class III RNR carry a stable but oxygen-sensitive glycyl residue plus an iron-sulfur center that catalyzes the reduction of S-adenosylmethionine to generate this radical. This class can only function under anaerobic conditions.

P. aeruginosa is one of the few microorganisms that encodes the three-different RNR classes (Class Ia, II and III) in its genome, which are apparently redundant, but reflect its need to adapt its metabolism to grow under specific conditions or during infection [7,8].

Relatively little is known about how bacteria control RNR activity at the gene level, and particularly in *P. aeruginosa*, in which it is totally unknown which transcriptional factors regulate the expression of the three RNR classes. The original study conducted by an Israeli group identified a novel transcriptional regulator in *Streptomyces coelicolor* termed NrdR, which controlled the expression of both class I and II RNR gene clusters. It was shown for the first time that in streptomycetes *nrdR* gene is linked to and co-transcribed with *nrdJ*. In *S. coelicolor*, a deletion of this gene produces a transcriptional derepression of the *nrd* genes [9,10]. Later, Rodionov and Gelfand described a bacterial regulatory system through a bioinformatics approach, with the identification of a highly conserved 16 bp palindromic signal, named NrdR-box, upstream of most operons encoding the ribonucleotide reductases [11]. Subsequently, our group described an analogous situation in *Escherichia coli,* with an NrdR homolog that was shown to regulate all three *nrd* systems (class Ia, Ib and III) and binding to the predicted NrdR binding sites. Remarkably, class Ib was highly derepressed (more than 150 times) in the *nrdR* mutant compared with the wild-type strain [12].

NrdR proteins are composed of 140-200 amino-acids, and present two differentiated domains: a zinc ribbon DNA-binding domain and an ATP-cone domain similar to that present in the N-terminal part (the allosteric activity site) of many RNRs. It seems that when the NrdR ATP-domain binds dATP instead of ATP, it changes its conformation and binds to its cognate DNA recognition sequences to repress RNR gene expression [10,13]. A recent study has unveiled a more complex control behind the NrdR nucleotide binding activity [14].

In this study, we uncovered the role of NrdR on the transcriptional regulation of the different ribonucleotide reductase and *topA* genes in *P. aeruginosa*. This is the first report in which the role of NrdR was analyzed in *P. aeruginosa* whose genome encodes all three different RNR classes. We also studied the global expression profile of *P. aeruginosa* when the *nrdR* gene was mutated, and the role of this transcription factor as a global regulator.

Materials and Methods

Bacterial strains, plasmids and growth conditions

Bacterial strains and plasmids are listed in **Table A2:1**. *Escherichia coli* and *Pseudomonas aeruginosa* cells were routinely grown in Luria-Bertani broth (LB) at 37ºC. When necessary, antibiotics were added at the following concentrations: for *E. coli*, 10 µg/ml gentamicin and 50 µg/ml ampicillin; for *P. aeruginosa*, 150 µg/ml gentamicin, 300 µg/ml carbenicillin and 50 µg/ml tetracycline. Liquid cultures were shaken on a horizontal shaker at 200 rpm. Anaerobic growth was performed in LB medium containing 10 g/l KNO_3 in screw-cap tubes (Hungate Tubes) that were filled to the top with N_2.

Strain or plasmids	Description	Source
Plasmids		
pGEM-T easy	A/T cloning vector, Amp^R	Promega
pUCP20T	Broad-host-range vector, Amp^R	[32]
pBBR1MCS-5	High-copy number cloning vector, Gm^R	[33]
pETS130-GFP	Broad host range, promoterless GFP, Gm^R	[7]
pETS134	pETS130 derivative carrying *nrdA* promoter, Gm^R	[7]
pETS136	pETS130 derivative carrying *nrdD* promoter, Gm^R	[7]
pETS161	pETS130 derivative carrying *nrdR* promoter, Gm^R	This work
pETS176	pUCP20T derivative carrying *nrdR* gene, Amp^R	This work
pETS177	pETS130 derivative carrying *topA* promoter, Gm^R	This work
pETS178	pETS130 derivative carrying NrdR box mutated in *topA* promoter, Gm^R	This work
pETS180	pETS130 derivative carrying *nrdJ* promoter, Gm^R	This work
pETS181	pETS130 derivative carrying NarL box1.1 mutation (box NarL1) in *nrdR* promoter, Gm^R	This work
pETS182	pETS130 derivative carrying NarL box1.2 mutation (box NarL1) in *nrdR* promoter, Gm^R	This work
pETS183	pETS130 derivative carrying NarL box1.3 mutation (box NarL1) in *nrdR* promoter, Gm^R	This work
pETS184	pETS130 derivative carrying NarL box2.1 mutation (box NarL2) in *nrdR* promoter, Gm^R	This work
pETS185	pETS130 derivative carrying NarL box2.2 mutation (box NarL2) in *nrdR* promoter, Gm^R	This work
pETS186	pETS130 derivative carrying NarL box2.3 mutation (box NarL2) in *nrdR* promoter, Gm^R	This work
pETS187	pETS130 derivative carrying NarL box1 and box2 mutation in *nrdR* promoter, Gm^R	This work
pETS188	pETS130 derivative carrying NrdR box2 mutated in *nrdA* promoter, Gm^R	This work
pETS189	pETS130 derivative carrying NrdR box2 mutated in *nrdJ* promoter, Gm^R	This work
pETS190	pETS130 derivative carrying NrdR box2 mutated in *nrdD* promoter, Gm^R	This work
Strains		
E. coli		
DH5α	*recA1 endA1 hsdR17 supE44 thi-1 relA1 Δ(lacZYA-argF)U169 deoR Φ80dlacZM15*	Laboratory stock
P. aeruginosa		
PAO1	Wild-type (ATCC 15692 / CECT 4122)- Spanish Type Culture Collection	Lab strain
PW7549	*P. aeruginosa* PAO1 *narL::ISlacZ*/hah, Tc^R	[20]
PW7855	*P. aeruginosa* PAO1 *nrdR::ISlacZ*/hah, Tc^R	[20]

Table A2:1. Bacterial strains and plasmids used in this study.

Strains and plasmids construction

Recombinant DNA manipulations were carried out according to published protocols [15]. Plasmid DNA was prepared using the QIAprep miniprep kit (Qiagen) and was transformed into *P. aeruginosa* cells by electroporation as previously described [16] using a Gene Pulser Xcell™ electroporator (Bio-Rad). Digestions with restriction enzymes were performed according to the manufacturer's instructions (Fermentas). Ligations were performed with T4 DNA ligase (Fermentas, Thermo Scientific), except as otherwise stated. DNA fragments were amplified by PCR using High-Fidelity PCR enzyme mix (Fermentas) using chromosomal DNA as a template.

When necessary, specific restriction site sequences were incorporated at the 5' ends of the primers to facilitate the cloning of the fragments in the appropriate vector. Plasmids pETS161, pETS177 and pETS180 were constructed as follows: First, the *nrdR* (277 bp), *topA* (348 bp) and *nrdJ* (419 bp) promoter regions were

amplified from *P. aeruginosa* PAO1 genomic DNA using the primer pair P*nrdRBHI*-up/P*nrdRClaI*-lw; PtopA-BamHI-up/PtopA-ClaI-low; and PnrdJ-BamHI new-up/PnrdJSmaI-new-low, respectively (**A2:S1 Table**). The resulting DNA fragment and the pETS130-GFP plasmid were both digested with the corresponding restriction enzymes, and ligation was performed. Complementation plasmid (pETS176) was constructed by cloning the *nrdR* gene, under the control of its native promoter, into plasmid pUCP20T using the primer pair P*nrdRBamHI*-up/NrdRHindIII-low.

Site-directed mutagenesis of the putative NarL and NrdR binding sites

The two NarL binding boxes (NarL1 and NarL2) in the nrdR promoter region were mutated using PCR-based site-directed mutagenesis using the following primer pairs: mutNarL1up/mutNarL1low; mutNarL1.2 up/mutNarL1.2 low; mutNarL1.3 up/mutNarL1.3 low; mutNarL R-dir/mutNarL-rev; mutNarL2.2 up/mutNarL2.2 low; and mutNarL2.3 up/mutNarL2.3 low, to generate pETS181, pETS182, pETS183, pETS184, pETS185, pETS186 and pETS187, respectively.

The putative NrdR box2 in the promoter regions of *nrdAB*, *nrdJ*, *nrdDG* and *topA* was mutagenized using the following primer pairs: AmR2-up/AmR2-low; JmR2-up/JmR2-low; DmR2-up/DmR2-low; and TmR-up/TmpR-low, to generate pETS188, pETS189, pETS190 and pETS178, respectively. The resulting amplicons were cloned into the pGEM-T easy vector, according to the manufacturer's instructions, and then, after digestion with the corresponding restriction enzymes, to pETS130-GFP. Each mutation was verified by DNA sequencing.

Green fluorescent protein gene reporter assay

Bacterial cultures were grown to the corresponding A_{550}, and three independent 1-ml samples of each culture were collected. Cells were pelleted, and fixed with 1 ml of freshly prepared phosphate buffered saline (PBS) solution containing 2% formaldehyde and stored in the dark at 4ºC. Fluorescence was measured in 96-well plates on an Infinite 200 Pro fluorescence microplate reader (Tecan). Three measurements were performed for each independent sample.

DPA assay

For total cellular dNTP quantification we used the diphenylamine assay (DPA) following the described procedures [17,18]. Briefly, DPA reagent (Sigma-Aldrich) was dissolved in a 2:1 acetic acid–sulfuric acid mixture. The solution was incubated at 37ºC for 4 h, and all measurements were performed at 595 nm. Bacterial cell extracts from *P. aeruginosa* wild-type cells grown to an A_{550} of 0.5 and normalized by equal protein content were analyzed using the DPA assay. Three independent experiments were performed.

Supercoiling assay

pUCP20T plasmid was transformed into PAO1 wild-type and *nrdR* mutant strains by electroporation, to corroborate differences in supercoiling activity. Strains were grown aerobically at 37ºC to mid-logarithmic and stationary phases (A_{600} of 0.5 and 2, respectively) in LB containing 300 μg/ml of carbenicillin. Plasmid DNA was purified via a previously described protocol [19]. Briefly, a 16 h gel electrophoresis at 50 V was performed in 1.2% agarose gels containing 5 mg/L of chloroquine, to separate 0.5 μg of plasmid. After washing for 3 h in water, to remove chloroquine, the gels were stained with ethidium bromide and visualized on an ultraviolet transilluminator.

RNA extraction, reverse transcription and real-time PCR

Total RNA from *P. aeruginosa* PAO1 was isolated with an RNeasy Mini Kit (Qiagen) and RNAprotect Bacteria Reagent (Qiagen), according the manufacturer's instructions. DNase I (Turbo DNA-free, Applied Biosystems) was used to remove DNA contamination. Reverse transcription PCR (RT-PCR) was performed with 1 μg of

RNA in a total 20-µl reaction volume, using the SuperScript III First-Strand Synthesis System for RT-PCR (Applied Biosystems), and PCR amplification of the cDNA was performed with High-Fidelity PCR enzyme mix (Fermentas). Primers used in this study are listed in **A2:S1 Table**. The first-strand cDNA synthesis step was conducted at 55ºC for 1 h, and the cycling conditions for PCR were performed as follows: 3-min denaturation period at 94ºC; 20 cycles for 1 min at 94ºC, 45 s at 51ºC, and 1 min per kb of DNA template at 72ºC; and final 7-min extension at 72ºC.

Real-Time PCR measurements were carried out using TaqMan primers and probes (S1 Table), and detection was performed using and ABI Step One Plus detection system from Applied Biosystems as described previously [12]. The *gapA* sequence was used as an internal standard since their expression is constitutive during *P. aeruginosa* growth.

Microarray analysis

The *P. aeruginosa* strains were grown aerobically and anaerobically until the mid-logarithmic growth phase. Total bacterial RNA was isolated as previously stated from each of three independent cultures. Eight micrograms of purified RNA were used for a GeneChip® genome array analysis. The GeneChip® probes (Affymetrix) were prepared according to Affymetrix's instructions. RNA integrity, target hybridization, washing, staining and scanning steps were performed by the Functional Genomics Core facility at the Institute for Research in Biomedicine (Barcelona, Spain). Data analysis was initially performed with the Microarray suite software and then imported into Microsoft Excel for further statistical analysis. Only those genes that had a mean signal $\log_2$-ratio of >1.5 (up-regulated transcripts) and <1.5 (down-regulated transcripts) were kept in the final list of genes. Microarray data are available in the Array express database (www.ebi.ac.uk/arrayexpress) under accession number E-MTAB-3006.

Fly infection assays

All experiments used healthy 3-4 days old adult *Drosophila melanogaster* Oregon^R flies, maintained at 25ºC in vials with standard corn-meal agar medium. A suspension of *P. aeruginosa* cells in PBS, adjusted at $A_{550}\approx0.1$, was injected using a capillary glass with a microinjector (TriTEch Research, CA) as previously described [7]. Survival curves were plotted using Kaplan-Meier analysis and differences of survival rates were analyzed by the log-rank test (GraphPad Prism 6.0, GraphPad Software, La Jolla California USA).

Results

NrdR expression pattern in P. aeruginosa

The *P. aeruginosa* transcriptional regulator homolog of the *E. coli nrdR* gene is the PA4057 gene (**Fig. A2:1A**). The translation of the PA4057 gene, here denoted as *nrdR*, is expected to produce a 154 amino-acid protein, with a predicted molecular weight of 17.9 kDa. A search in the Conserved Domain Database revealed two major domains: a zinc-finger (3-34 aa) and an ATP-cone domain (49-139 aa), at the N-terminus and C-terminus, respectively, showing a structure similar to all NrdR proteins [13]. In a 149 amino-acid overlap, *P. aeruginosa* NrdR showed 70% identity and 82% similarity with *E. coli* NrdR (see alignment in **Fig. A2:1B**).

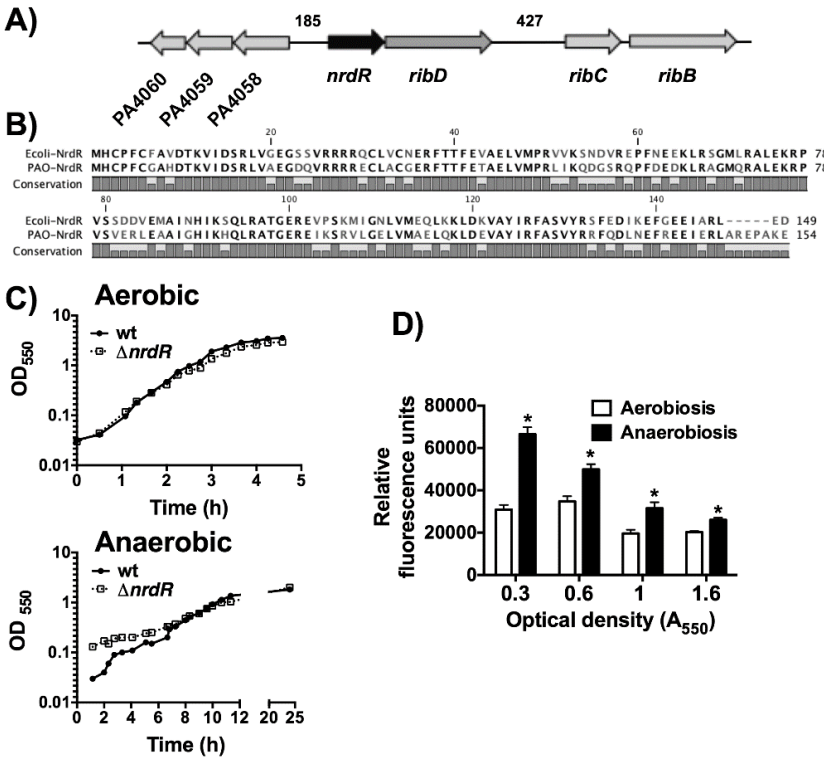

Figure A2:1. *nrdR* operon organization and expression. **A)** Gene organization scheme of the *nrdR-rib*D operon. **B)** Sequence alignment (Clustal W) of *P. aeruginosa* (PAO-NrdR; Uniprot Q9HWX1) and *Escherichia coli* (Ecoli-NrdR; Uniprot P0A8D0) NrdR proteins. **C)** Aerobic and anaerobic growth curve of *P. aeruginosa* strains PAO1 (wild-type) and PW7855 (Δ*nrdR*). **D)** Fluorescence (GFP) was measured in both strains harboring pETS161 (P*nrdR*-GFP) at different points of growth, at 37ºC in LB medium. The fluorescence was normalized dividing by the optical density (A_{550}), and it is given in relative fluorescence units. Each experiment was repeated three times, and the results are the mean ± standard deviation. *: Significantly different compared with wild-type strain in an unpaired *t*-test ($P<0.05$).

Contrary to the observation in the initial IS insertion *nrdR* mutant in *E. coli* [12], a *P. aeruginosa nrdR* mutant showed a similar growth curve to that of the wild-type strain, under both aerobic and anaerobic conditions (**Fig. A2:1C**). The insertion sequence element disrupting the *nrdR* gene (strain PW7855, from now on Δ*nrdR*) contains an internal promoter that allows the expression of downstream genes, as indicated by the authors [20].

As shown in **Fig. A2:1D**, the transcriptional fusion of the *nrdR* promoter to the green fluorescent protein (GFP) (see materials and methods) revealed an increased *nrdR* expression in exponential phase and a decrease in stationary phase, under both aerobic and anaerobic growing conditions. Clearly, the NrdR protein is expressed at higher levels during the exponential growth phase, particularly under anaerobic conditions.

NarL is responsible for the anaerobic expression of the nrdR gene

We investigated the molecular mechanism that carries out the transcriptional activation of the *nrdR* gene under anaerobic conditions. An initial examination of the *nrdR* promoter region, using the Virtual Footprint tool from the PRODORIC database [21], revealed two heptameric NarL-binding sites located at 18 and 40 bp upstream of the translation start codon, denoted here as NarL1 (CTACCAT) and NarL2 (TACGCCT) boxes (**Fig. A2:2**). To confirm the bioinformatical prediction, the two putative heptameric NarL-binding sites (NarL1 and NarL2 boxes) were mutated.

Constructions	Sequence	Strains	RFU ±SD	Ratio
	NarL box1 **NarL box2**			
pETS161	cgcggatgcg**ctaccat**gcggcttccttcagc**tacgcct**gtatcagcacc**ATG**	wt	495664 ±15181	100%
pETS161	cgcggatgcg**ctaccat**gcggcttccttcagc**tacgcct**gtatcagcacc**ATG**	Δ*narL*	354540 ±8914*	71%
	NarL box1 mutations			
pETS181	cgcggatgcg**cCCAATt**gcggcttccttcagc**tacgcct**gtatcagcacc**ATG**	wt	327658 ±6400*	66%
pETS182	cgcggatgcg**ctGGcat**gcggcttccttcagc**tacgcct**gtatcagcacc**ATG**	wt	243025 ±3033*	49%
pETS183	cgcggatgcg**ctGccat**gcggcttccttcagc**tacgcct**gtatcagcacc**ATG**	wt	309904 ±4057*	62%
	NarL box2 mutations			
pETS184	cgcggatgcg**ctaccat**gcggcttccttcagc**ATAATTA**gtatcagcacc**ATG**	wt	279610 ±6003*	56%
pETS185	cgcggatgcg**ctaccat**gcggcttccttcagc**tGGgcct**gtatcagcacc**ATG**	wt	306321 ±2615*	61%
pETS186	cgcggatgcg**ctaccat**gcggcttccttcagc**tGcgcct**gtatcagcacc**ATG**	wt	317780 ±7775*	64%
	NarL box1 and box2 mutations			
pETS187	cgcggatgcg**cCCAATt**gcggcttccttcagc**ATAATTA**gtatcagcacc**ATG**	wt	336341 ±2008*	67%

Figure A2:2. NarL-dependent expression of *nrdR*. **A)** Representation of the *P. aeruginosa* PAO1 *nrdR* promoter region sequence, indicating the different mutated NarL binding sites. Black boxes indicate the putative NarL recognition sites, and mutated sequences are shown in upper case and in bold letters. The transcription start site is indicated in bold. The RFU column shows the relative fluorescence intensity presented by the *P. aeruginosa* wild-type *nrdR* promoter fusion (pETS161), compared with their mutated NarL boxes (pETS181, pETS182 and pETS183 for NarL box1, pETS184, pETS185 and pETS186 for NarL box2, and pEST187 harboring the double mutation). The expression of wild-type *nrdR* promoter under a Δ*narL* mutant background is also stated. The ratio column shows a comparison of all the conditions with the expression of a wild-type promoter under a wild-type background. Strains were grown anaerobically until the mid-logarithmic phase. Values represent the mean of three independent experiments. Transcriptional start codon is shown in bold. Three independent experiments were performed and the mean plus/minus standard deviation is shown). *: Significantly different compared with wild-type promoter region (pETS161) in an unpaired *t*-test ($P<0.05$).

Three mutations were performed in each box, focusing on the most important nucleotides according to the published *P. aeruginosa* NarL consensus binding sequence ($TAC^{C}/_{T}N^{A}/_{C}T$) [22]. Therefore, plasmids harboring the different mutations in NarL1 and NarL2 boxes were made (pETS181 to pETS187, see Table A2:1). A decrease of the promoter expression under anaerobic conditions was observed, compared with the wild-type promoter (pETS161) (**Fig. A2:2**, **A2:S1 Fig.**). The activities obtained when mutating NarL1 and NarL2 boxes were similar to those obtained for the wild-type promoter region (pETS161) in the *narL* knockout strain (PW7549; from now on Δ*narL*) (**Fig. A2:2**). These results confirm a direct activation of the *nrdR* expression via binding of NarL.

NrdR regulates the expression of the three different ribonucleotide reductase classes

To study whether the NrdR protein regulates the expression of the different *nrd* genes, we measured the expression of the different *nrd* promoters in *P. aeruginosa* wild-type and a Δ*nrdR* mutant strain (PW7855), using plasmids carrying a transcriptional fusion of each RNR promoter region and the *gfp* reporter gene (see materials and methods, and [7]).

Under aerobic conditions (**Fig. A2:3A-C**), all three *nrd* genes (*nrdA*, *nrdJa* and *nrdD*) showed an evident increase in their expression (from 3 to 6-fold) in the *nrdR* mutant, compared with the wild-type strain, indicating that NrdR acts as its repressor. The maximal difference appeared in the transcription of the class II RNR (*nrdJa*). Note that the aerobic transcription of the *nrdJa* and *nrdD* genes was approximately 8-10 times lower compared with the *nrdA* gene and highly expressed under anaerobic conditions in the wild-type strain, compared to aerobic conditions.

A completely different expression pattern was observed under anaerobic conditions (**Fig. A2:3D-F**). Expression of the *nrdA* gene slightly increased in the *nrdR* mutant (1.3-fold, **Fig. A2:3D**). Expression of *nrdJa* is down-regulated in the *nrdR* mutant, and no change in *nrdD* expression was observed compared with the wild-type strain (**Fig. A2:3E-F**). Under all conditions, complementation with the *nrdR* gene cloned into plasmid pUCP20T (pETS176) returned the expression to the wild-type level.

One of the two putative NrdR boxes that were identified in all RNRs promoters (**A2:S3 Fig.**) was mutated by PCR-based site-directed mutagenesis. Plasmids harboring the mutant promoter confirmed our previous results, hence indicating the functionality of the NrdR boxes (**A2:S2** and **A2:S3 Figs.**).

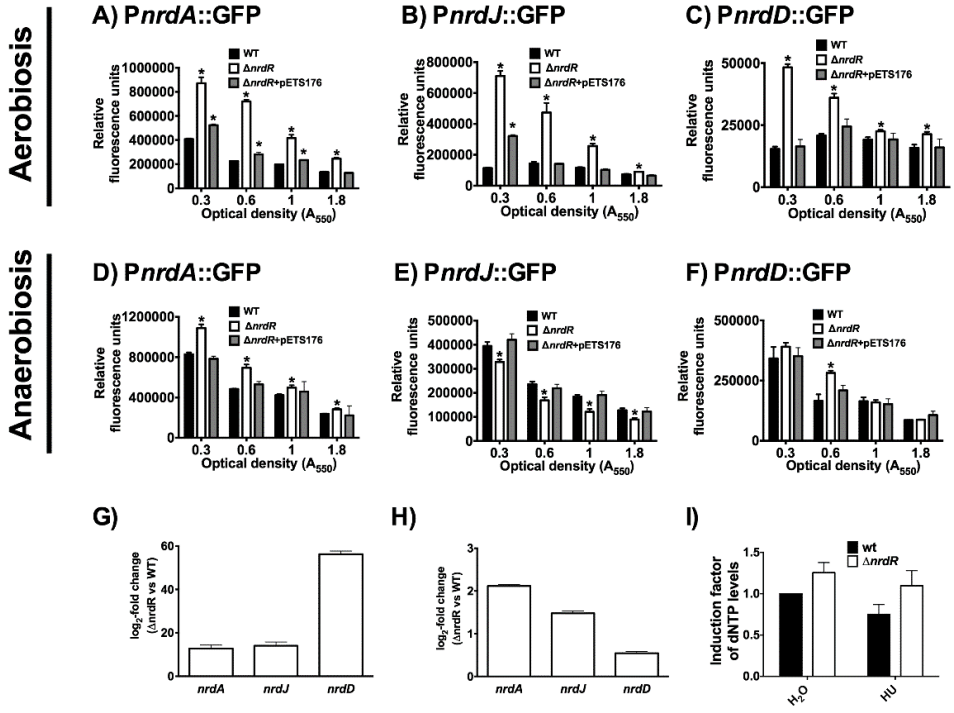

Figure A2:3. NrdR differentially regulates ribonucleotide reductase genes in aerobiosis or anaerobiosis. Aerobic expression studies are shown in **A-C** and **G**, and anaerobic expression studies in **D-F** and **H**. *P. aeruginosa* wild-type strain (black bars), Δ*nrdR* mutant strain (white bars) and the deficiency-complemented *nrdR* strain (Δ*nrdR*+pETS176) (gray bars) bearing the promoter fusions P*nrdA-gfp* (panel **A** and **D**), P*nrdJ-gfp* (panel **B** and **E**) and P*nrdD-gfp* (panel **C** and **F**), were grown as indicated in the material and methods. GFP fluorescence is expressed as arbitrary units subtracting the reads of the control plasmid pETS130. **G**) and **H**) Quantitative RT-PCR analysis of genes encoding three different classes of RNR. qRT-PCR was conducted on cDNA synthesized from wild-type, compared with Δ*nrdR* cells, both grown aerobically (A_{550}=0.6) (**G**) and anaerobically (A_{550}=0.6) (**H**). The means of three independent experiments are displayed, and the error bars represent the positive standard deviation **I)** dNTPs pool level of aerobic *P. aeruginosa* wild-type and *nrdR* mutant cells treated with 10 mM hydroxyurea (HU), measured by DPA assay. DNA contents were normalized with those of wild-type strain. Three independent experiments were performed and the mean ± standard deviation is shown. *, Significantly different compared with the wild-type strain in an unpaired *t*-test (*P*<0.05).

To correlate the transcriptional data with mRNA quantity, we measured the levels of mRNA for each RNR class in wild-type cells and Δ*nrdR* mutant strain by real-time PCR (**Fig. A2:3G-H**) at mid-logarithmic phase (A_{550}=0.6). Aerobically, (**Fig. A2:3G**) all RNR genes were highly expressed (from 13 to 56 times) in the *nrdR* mutant compared with the wild-type. By contrast, anaerobically (**Fig. A2:3H**), the *nrdA* gene slightly increased its expression (2.1 times), and no effect was observed on the transcription of the

nrdJa and *nrdD* genes in the *nrdR* mutant compared with the wild-type strain, corroborating our transcriptional fusion expression results.

As expected, when we inactivated the *nrdR* gene, the dNTP pool levels observed were 25% higher compared with the wild-type strain (**Fig. A2:3I**), suggesting that we eliminated the NrdR repressor, and, therefore, increased global RNR activity under all conditions.

Finally, we aimed to address the effect of the NrdR regulation at a physiological level by changing the levels of dNTPs as seen by other authors [23,24]. Hydroxyurea is a known radical scavenger that inhibits class Ia RNR catalytic activity, thus reducing the amounts of dNTPs. When 10 mM hydroxyurea were added to the medium during aerobic growth, the dNTP amounts were 25% lower. This reduction could be restored in an *nrdR* mutant strain (enhancing class II RNR activity) which returns to wild-type dNTPs levels (**Fig. A2:3I**).

NrdR activates topA expression

All genes that have been described as transcriptionally regulated by NrdR were ribonucleotide reductase encoding genes. Rodionov and Gelfand [11] and recent databases (RegPrecise; http://regprecise.lbl.gov/RegPrecise/index.jsp) highlighted the possible implication of NrdR in the regulation of the *P. aeruginosa* DNA topoisomerase I gene *topA* (PA3011), identifying a single putative NrdR box in its promoter region (see **A2:S3 Fig.**).

Expression of the *topA* gene during exponential growth under aerobic or anaerobic conditions was repressed in the *nrdR* mutant (2-3 times) compared with the wild-type strain, suggesting that NrdR acts as a *topA* activator during the exponential growth phase (**Fig. A2:4**).

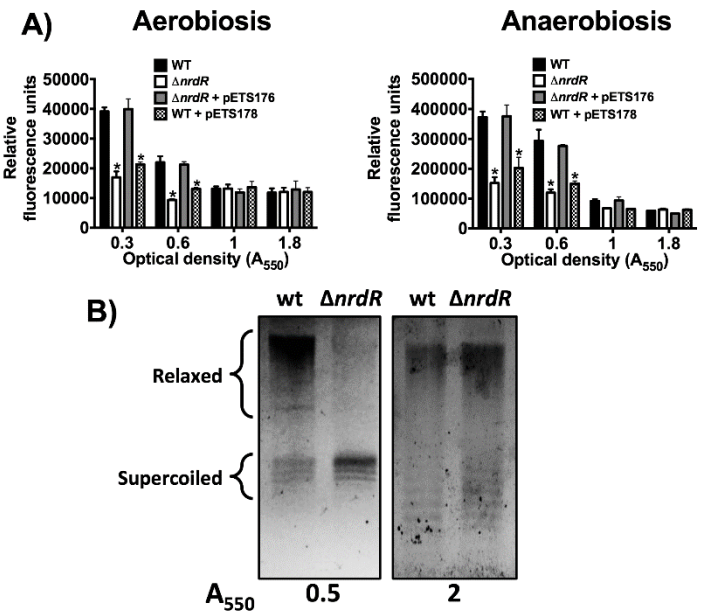

Figure A2:4. *topA* expression is activated aerobically and anaerobically by NrdR. **A)** GFP fluorescence was measured in *P. aeruginosa* strains PAO1 (wild-type) and PW7855 (Δ*nrdR*) harboring plasmid pETS177 (P*topA*::GFP). The *nrdR* cloned into plasmid pUCP20T (pETS176) was used to complement *nrdR* deficiency in strain PW7855. Plasmid pETS178 harbors a *topA* promoter with a mutation in the NrdR box. The fluorescence was normalized with the absorbance at 550 nm (A_{550}) and it is given in relative fluorescent units. The bars represent the mean of three independent experiments ± standard deviation. **B)** A gel electrophoresis assay, in an agarose gel containing chloroquine, of plasmid DNA isolated from *P. aeruginosa* wild-type and Δ*nrdR* strains, at mid-logarithmic and stationary phases. The direction of migration was from top to bottom. *, Significantly different compared with the wild-type strain in an unpaired *t*-test ($P<0.05$).

Complementation with an extra *nrdR* gene (pETS176) returned the *topA* expression level to the wild-type levels. When the NrdR binding box was mutated in the promoter *topA* region (pETS178) the expression levels were similar to the levels found in the *ΔnrdR* strain, therefore corroborating the functionality of the unique NrdR-binding region on the *topA* promoter region (**Fig. A2:**4, **A2:S3 Fig.**).

The degree of supercoiling in bacterial DNA is determined by the balance between DNA-relaxing activity and DNA-supercoiling activity, regulated by the opposing actions of topoisomerase I encoded by the *topA* gene and DNA gyrase, respectively [19]. The prokaryotic topoisomerase I is only capable of relaxing negatively supercoiled DNA. To phenotypically corroborate the *topA* down-regulation in the *P. aeruginosa* Δ*nrdR* strain, we analyzed the DNA topology of pUCP20T in an electrophoresis assay in an agarose gel with chloroquine. pUCP20T plasmid extracted from the Δ*nrdR* mutant strain showed more negative supercoiled DNA compared with the wild-type strain (**Fig. A2:4B**) when measured during exponential growing phase. According to the gene reporter assay, no difference in supercoiled DNA levels appears during stationary growing phase. This result reflects a possible change in DNA topology in the *P. aeruginosa* Δ*nrdR* strain, compared with the wild-type strain.

Global gene expression profiling of the P. aeruginosa nrdR mutant strain compared with the wild-type strain

We previously showed that NrdR directly regulates the three *P. aeruginosa* RNR classes and topoisomerase I (*topA*), all of which are involved in bacterial DNA replication. To determine the global transcriptional changes produced by a mutation in *nrdR*, we initiated a gene profiling experiment using the Affymetrix *P. aeruginosa* GeneChip microarray platform.

RNA was isolated from a *P. aeruginosa* PAO1 wild-type strain and a Δ*nrdR* mutant strain, both grown aerobically and anaerobically in LB medium to mid-logarithmic growth phase. Labeled RNA was hybridized to Affymetrix *P. aeruginosa* GeneChips and gene expression levels between Δ*nrdR* mutant and wild-type strains were compared.

Results showed altered transcription levels in only a few genes, comparing the Δ*nrdR* mutant strain to the wild-type strain. Aerobically only 47 genes (0.8%) were significantly deregulated, with 31 genes up-regulated (0.5%) and 16 genes down-regulated (0.3%). Anaerobically, 111 genes were differentially

regulated, with 26 genes up-regulated (0.45%) and 85 genes down-regulated (1.45%). Only few genes were expressed or repressed more than 3 log_2 fold change (**Fig. A2:5B**). To corroborate our array a selection of some deregulated genes was measured by quantitative PCR (**A2:S5 Fig.**).

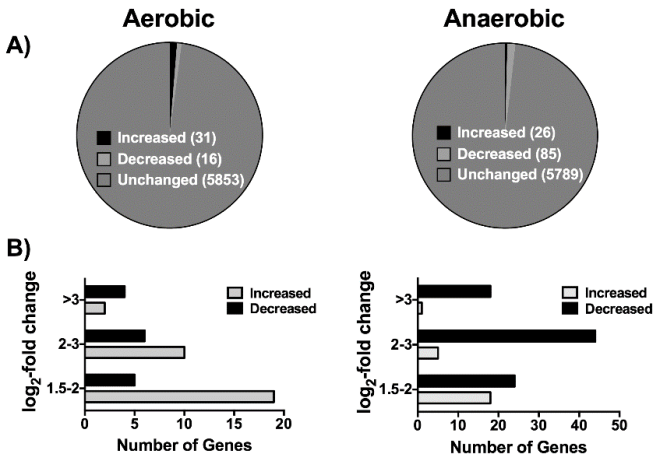

Figure A2:5. Summary of the effects of the *nrdR* mutation on *P. aeruginosa* gene expression under aerobic and anaerobic conditions**. A)** Distribution of the different genes (up-regulated, down-regulated and unchanged) in gene expression (>1.5 Log_2 fold change). The number of gens in each category is indicated. **B)** Distribution of genes whose expression was either increased or decreased in a Δ*nrdR* mutant strain, grouped according to fold-changes in expression levels.

Under aerobic conditions, among the most up-regulated genes we found the fimbrial subunit *cupA1* (log_2-fold change of 4.13), several hypothetical proteins (PA4139, PA1383 and PA2223 with log_2-fold changes of 3.78, 2.42 and 2.37, respectively) and antibiotic resistance related genes, such as the entire *mexAB-orpM* operon (log_2-fold change from 2.13 to 1.43) (**Table A2:2** and **A2:S2 Table**). In addition, the RNR genes were found to be up-regulated, as expected (log_2-fold changes from 2.41 and 1.96). The highest repression under this condition was found in several hypothetical proteins (PA3283, PA3281, PA0565 with log_2-fold changes of -4.57, -3.73, -3.06) and also several genes involved in antibiotic resistance, such as the entire *mexEF-oprN* operon (log_2-fold change from -3.19 to -1.13).

Under anaerobic conditions, despite the hypothetical proteins (PA5507 and PA5509, with log_2-fold changes of 3.21 and 2.99), *mexS* and *pyoS5* were the more strongly repressed genes (log_2-fold changes of -4.69 and -3.9) (**Table A2:2** and **A2:S3 Table**).

ID	Gene	Operon arrangement	Log2 Fold-Change	Gene Product
Aerobic				
PA2128	*cupA1*	*cupA12345*	4.13	Fimbrial subunit CupA1
PA1383			2.42	Hypothetical protein
PA4139			3.78	Hypothetical protein
PA5497	*nrdJa*	*nrdJab*	2.41	Class II (cobalamin-dependent) ribonucleotide-diphosphate reductase subunit, NrdJa
PA1718	*pscE*	*pscBCDEFGHIJKL*	2.32	Type III export protein PscE
PA1156	*nrdA*	*nrdAB*	2.24	Ribonucleoside reductase, large chain
PA0992	*cupC1*	*cupC123*	2.19	Fimbrial subunit CupC1
PA0425	*mexA*	*mexAB-oprM*	2.13	Resistance-Nodulation-Cell Division (RND) multidrug efflux membrane fusion protein
PA0424	*mexR*		2.06	Multidrug resistance operon repressor MexR
PA1693	*pscR*	*PA1697-pscOPQRSTU*	2.00	Translocation protein in type III secretion
PA1155	*nrdB*	*nrdAB*	1.96	Ribonucleoside reductase, small chain
PA0426	*mexB*	*mexAB-oprM*	1.93	Resistance-Nodulation-Cell Division (RND) multidrug efflux transporter MexB
PA4086	*cupB1*	*cupB123456*	1.89	Probable fimbrial subunit CupB1
PA1723	*pscJ*	*pscBCDEFGHIJKL*	1.63	Type III export protein PscJ
PA0958	*oprD*		1.61	Basic amino acid, basic peptide and imipenem outer membrane porin OprD precursor
PA0427	*oprM*	*mexAB-oprM*	1.43	Major intrinsic multiple antibiotic resistance efflux outer membrane protein Opr
PA2491	*mexS*		-2.17	Hypothetical protein (MexEF-OprN regulator)
PA0998	*pqsC*	*pqsABCDE*	-2.83	Homologous to beta-keto-acyl-acyl-carrier protein synthase
Anaerobic				
PA1718	*pscE*	*pscBCDEFGHIJKL*	2.23	Type III export protein PscE
PA0958	*oprD*		1.76	Basic amino acid, basic peptide and imipenem outer membrane porin OprD precursor
PA3616		*recA-PA3616*	-1.61	Hypothetical protein
PA3008		*lexA-PA3008*	-1.81	Hypothetical protein
PA3007	*lexA*	*lexA-PA3008*	-1.88	Repressor protein LexA
PA3617	*recA*	*recA-PA3616*	-1.96	RecA protein
PA0807	*ampDh3*		-2.44	Beta-lactamase expression regulator AmpD
PA2485		*PA2485-PA2486*	-2.66	Hypothetical protein
PA4763	*recN*		-2.71	DNA repair protein RecN
PA2486	*ptrC*	*PA2485-PA2486*	-2.94	Hypothetical protein (T3SS regulator)
PA2494	*mexF*	*mexEF-oprN*	-3.01	Resistance-Nodulation-Cell Division (RND) multidrug efflux transporter MexF
PA2484			-3.55	Hypothetical protein

Table A2:2. Global transcriptomic analysis of a Δ*nrdR* mutant strain compared with the *P. aeruginosa* PAO1 wild-type strain**.** Selected differentially regulated genes, under both aerobic and anaerobic conditions. Complete list of all the genes (>1.5-fold) is available in A2:S2 and A2:S3 Table.

Classifying the transcriptionally altered genes in metabolic categories [2] (**A2:S4 Fig.**), the categories in which more genes were included were antibiotic resistance, antibiotic susceptibility and small molecules transportation. By contrast, under anaerobic conditions, the main metabolic category with altered transcription was small molecules transportation.

NrdR is not essential during P. aeruginosa infection

We have previously shown that the *nrdJ* and the *nrdD* genes of *P. aeruginosa* are important during infection of *Drosophila melanogaster* [7]. As the NrdR regulates the expression of the different *nrd* genes, both aerobically and anaerobically, we wondered whether a mutant for this transcriptional regulatory protein is important during bacterial infections.

Injections of the same number of cells of a wild-type strain and a *ΔnrdR* mutant strain showed exactly the same killing behavior in flies (**Fig. A2:6**), showing a 50% death rate 25 h post-infection. Therefore,

this situation does not alter the virulence capacity of PAO to infect flies despite presenting an up-regulation of all *nrd* genes in the Δ*nrdR* mutant strain.

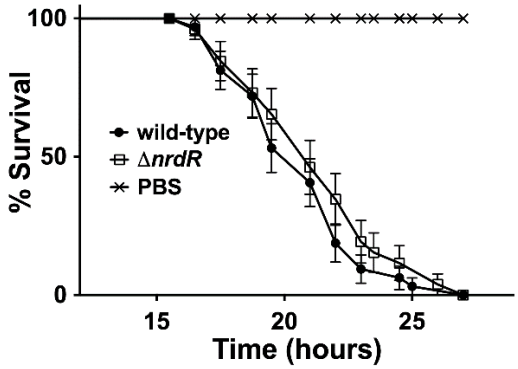

Figure A2:6. The *nrdR* mutant of *P. aeruginosa* does not alter the kinetics of D. melanogaster killing**.** Control flies were injected with PBS. Fly survival was monitored for 48 h. Approximately 100 flies were used for each experiment.

Discussion

Ribonucleotide reductases are key enzymes for all living cells, as they are responsible for the dNTP supply that is essential for DNA synthesis and repair. Eukaryotic cells encode only one type of RNR, class Ia, which is responsible for providing the different dNTPs under all conditions. Surprisingly, prokaryotic cells, which can be considered *a priori* as less complex organisms, have the capacity to encode different RNR classes in the same genome [25,26]. The presence of different paralogous genes performing the same enzymatic activity is astonishing, leading us to question why prokaryotes encode different RNR classes. Addressing this question is crucial for the understanding of the transcriptional regulation of each RNR class.

The NrdR factor was first identified in *S. coelicolor* [10], and proposed, by phylogenetic profiling, as a potential transcriptional regulator of different RNR genes [11], which was later confirmed in *E. coli* [12,13] and mycobacteria [27]. In our study, we aimed to gain insight into the role of this transcriptional factor in *P. aeruginosa*; this is the first attempt to study NrdR-related regulation in an organism in which all three RNR classes are encoded [7,28]. The *nrdR* gene also presents a unique genomic context in this bacterium: a polycistronic transcript encoding for *nrdR* and *ribD* genes can be detected (unpublished data), as an evidence of a *nrdR-ribD* operon (**Fig. A2:1A**), instead of the longer operon that is present in other γ-Proteobacteria (*nrdR-ribD-ribH-nusB*) [11,12].

We showed that NrdR is transcribed under both aerobic and anaerobic conditions, but increases substantially during anaerobic growth, and especially in the exponential growth phase (**Fig. A2:1**). This increase can be explained through the transcriptional activation by NarL, a transcription factor that is strongly related to anaerobic growth [29], and according to the presented results (**Fig. A2:1**, **A2:2**, **A2:S1 Fig.**) activates *nrdR* transcription by binding and interacting with two NarL boxes located at the *nrdR* promoter region.

As expected, NrdR regulates all three RNR classes, but surprisingly, it acts differently during aerobic or anaerobic growth. Aerobically, NrdR acts as a repressor of all RNR genes (**Fig. A2:3**), although maximum repression is exerted on class II and class III RNRs, while class Ia repression is less strict, conforming fully with the hypothesis that class Ia supports aerobic growth in this bacterium [3,7,8,28,30]. By contrast, NrdR does not repress class II and class III expression under anaerobic conditions, showing only a slight repression of class Ia RNR: as class II and III RNRs support the *P. aeruginosa* anaerobic growth [7]; this also fits with our model (**Fig. A2:7**). The results of the gene reporter assay were confirmed by qRT-PCR (**Fig. A2:3**), therefore providing strong evidence supporting our model.

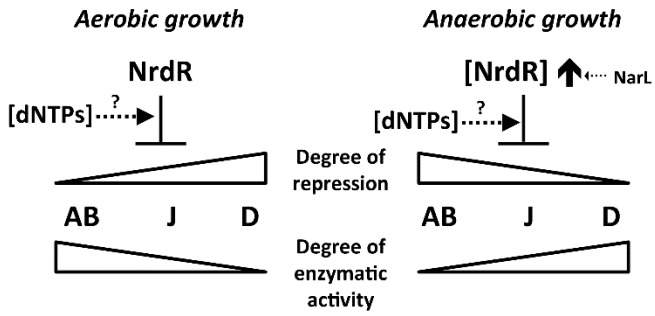

Figure A2:7. Model of NrdR-related control on RNR gene expression**.** The degree of repression on each RNR class expression, under aerobic or anaerobic conditions, is opposite to the enzymatic activity of these classes under each condition. Considering the presence of an ATP-cone domain in NrdR, dNTPs level alterations could also be affecting the results.

Two NrdR boxes have been identified in each RNR gene promoter (**A2:S2** and **A2:S3 Fig.**). Although we could not obtain pure soluble NrdR to perform DNA gel shift assays (all attempts to overproduce this protein lead to the formation of inclusion bodies), the results of the gene reporter assay with a mutation in the identified NrdR boxes agree with our previous results [12]; in all cases we have mutated the NrdR-box2 (because NrdR-box1 overlaps with the -10 promoter sequence), and we have obtained similar expression levels compared with the Δ*nrdR* mutant strain demonstrating the physiological role of these DNA regions to bind a functional NrdR.

To this point we can assume that we have strong evidence to support our working model (**Fig. A2:7**); RNR activity in *P. aeruginosa* is controlled by the NrdR factor, which acts by binding in the NrdR boxes in all RNR gene promoters (it is believed that it can act by forming a dimer to bind the two characteristic boxes), and repressing RNR activity according to the needs of the bacterium: high repression of class II and III RNRs under aerobic conditions, and repression of class I only under anaerobic conditions.

As the NrdR protein harbors an ATP-cone domain that is able to bind nucleotides, it seems logical to assume that NrdR activity is modulated by differential nucleotide binding [13,14] so that high dNTP levels (indicating high RNR activity) might activate NrdR-related repression. To do so, its ATP-cone is likely to be fully occupied (to its allosterically controlled limit) with ATP in usual situations, but competent to bind dATP and act as a dNTP pool sensor [14]; the binding of the nucleotide should control the oligomeric state of NrdR by a conformational change in the zinc-finger domain, and thereby modulate its interaction with the NrdR boxes. To evaluate this control we compared RNR transcription in wild-type and Δ*nrdR* mutant strains while treating with hydroxyurea (decreasing dATP levels, and hence modulating the bound nucleotide) but we did not obtain significant results (data not shown), most likely because treatment with hydroxyurea only affected class Ia RNR activity (and not class II and class III RNRs), and therefore the dNTP pool slightly decreased (**Fig. A2:3**) and class II was fully active [7]. In other studies in *S. typhimurium* and *Chlamydia sp* [23,24], hydroxyurea treatment completely abolished the dNTP supply, making this type of study far easier. In our model the role of the alteration

of the dNTP pool in the fine-tuning transcriptional regulation of the different RNR genes by NrdR is still inconclusive. Despite the lack of data in our working model, which was still not completely set, we hypothesized that NrdR could be responding to alteration of the dNTP pool, inhibiting RNR gene transcription when necessary. In contrast to anaerobic conditions when only class Ia RNR is affected by NrdR, during aerobic growth NrdR is able to down-regulate all RNR gene transcription, so this response to increased dNTPs may be its main role under this condition. This model is summarized in **Fig. A2:7**.

Moreover, we also identified for the first time that NrdR is not only involved in RNR activity regulation but also regulates *topA* expression, a gene encoding for *P. aeruginosa* topoisomerase I. The *topA* promoter region presents only a single NrdR putative binding site (**Fig. A2:S2**), suggesting different NrdR binding and regulation on this gene compared to RNR genes. In agreement with this hypothesis, we have shown that NrdR up-regulates *topA* transcription, instead of repressing it (**Fig. A2:4**). As with RNR activity, we confirmed this effect at a physiological level: as TopA relaxes negative supercoiled DNA, a high level of negative supercoiled DNA appears in a *ΔnrdR* mutant strain, during exponential growing phase, without NrdR-related topA activation (**Fig. A2:4B**).

There were no more promoters harboring putative NrdR boxes, but, according to our global transcriptomic analysis results, in a Δ*nrdR* mutant strain, a small but significant group of 47 genes (log_2-fold change > 1.5) was deregulated during aerobic conditions, and 111 genes (log_2-fold change > 1.5) presented similar behavior during anaerobic conditions (**Fig. A2:6**, **A2:S2** and **A2:S3 Table**). Among those genes we can identify some related to the SOS system, antibiotic resistance, transport of small molecules, etc. (**A2:S4 Fig.**) This deregulation does not lead to a loss of infectivity (**Fig. A2:6**). Given the absence of putative NrdR-boxes on the promoter regions of the deregulated genes detected in the array, we believe the change in the expression of these genes to be due to indirect effects. We propose that TopA down-regulation in the absence of NrdR may alter gene transcription by changing DNA topology and causing the accumulation of cleavage complexes. For instance, it has been described that SOS system can be deregulated by TopA depletion during antibiotic treatment [31]. In addition, some of the deregulated genes appear to also show altered transcription in a Δ*topA* mutant strain, according to a previous transcriptomic assay by the Lawrence G. Rahme group (unpublished data, Gene Expression Omnibus GSE24038).

The difference observed between the two groups of deregulated genes under aerobic and anaerobic conditions provides further evidence of the differential behavior of NrdR in *P. aeruginosa* as we have proposed, although the NarL-related activation and the dNTP-binding modulation may not be the only systems acting on this regulation.

In summary, this study has provided evidence of control of the three RNR operons and the *topA* gene by NrdR in *P. aeruginosa*, which is a differential control sensitive to oxygenation conditions and the growth phase. This control clearly plays an important role in the coordination of the expression of the different RNRs, dictating which RNR is expressed under certain growing conditions. By studying this and other factors controlling RNR activity we will be nearer to an explanation of the apparent

redundancy among the three RNR classes, and to an understanding of how this bacterium uses all three classes to survive under different environmental conditions.

Acknowledgments

This work was supported in part through grants from the Ministerio de Economia y Competitividad (BFU2011-24066), Generalitat de Catalunya (2014 SGR01260) and Associació Catalana de Fibrosis Quísica. E.T. was supported through funding from the Ramón y Cajal and I3 program from the Ministerio de Ciencia e Innovación.

References

1. Davies JC, Alton EW, Bush A (2007) Cystic fibrosis. BMJ 335: 1255-1259.
2. Stover CK, Pham XQ, Erwin AL, Mizoguchi SD, Warrener P, et al. (2000) Complete genome sequence of *Pseudomonas aeruginosa* PA01, an opportunistic pathogen. Nature 406: 959-964.
3. Torrents E, Sahlin M, Sjöberg B-M (2008) The Ribonucleotide Reductase Family- Genetics and Genomics. In: Ribonucleotide Reductases (ed KK Andersson) Nova Science Publishers: pp. 17-77.
4. Nordlund P, Reichard P (2006) Ribonucleotide reductases. Annu Rev Biochem 75: 681-706.
5. Torrents E (2014) Ribonucleotide reductases: Essential Enzymes for bacterial life. Front Cell Infect Microbiol 4: 52.
6. Hofer A, Crona M, Logan DT, Sjoberg BM (2012) DNA building blocks: keeping control of manufacture. Crit Rev Biochem Mol Biol 47: 50-63.
7. Sjoberg BM, Torrents E (2011) Shift in ribonucleotide reductase gene expression in *Pseudomonas aeruginosa* during infection. Infect Immun 79: 2663-2669.
8. Torrents E, Poplawski A, Sjöberg B-M (2005) Two proteins mediate class II ribonucleotide reductase activity in *Pseudomonas aeruginosa*: expression and transcriptional analysis of the aerobic enzymes. J Biol Chem 280: 16571-16578.
9. Borovok I, Gorovitz B, Yanku M, Schreiber R, Gust B, et al. (2004) Alternative oxygen-dependent and oxygen-independent ribonucleotide reductases in *Streptomyces*: cross-regulation and physiological role in response to oxygen limitation. Mol Microbiol 54: 1022-1035.
10. Grinberg I, Shteinberg T, Gorovitz B, Aharonowitz Y, Cohen G, et al. (2006) The *Streptomyces* NrdR transcriptional regulator is a Zn ribbon/ATP cone protein that binds to the promoter regions of class Ia and class II ribonucleotide reductase operons. J Bacteriol 188: 7635-7644.
11. Rodionov DA, Gelfand MS (2005) Identification of a bacterial regulatory system for ribonucleotide reductases by phylogenetic profiling. Trends Genet 21: 385-389.
12. Torrents E, Grinberg I, Gorovitz-Harris B, Lundstrom H, Borovok I, et al. (2007) NrdR controls differential expression of the *Escherichia coli* ribonucleotide reductase genes. J Bacteriol 189: 5012-5021.
13. Grinberg I, Shteinberg T, Hassan AQ, Aharonowitz Y, Borovok I, et al. (2009) Functional analysis of the *Streptomyces coelicolor* NrdR ATP-cone domain: role in nucleotide binding, oligomerization, and DNA interactions. J Bacteriol 191: 1169-1179.
14. McKethan BL, Spiro S (2013) Cooperative and allosterically controlled nucleotide binding regulates the DNA binding activity of NrdR. Mol Microbiol 90: 278-289.
15. Sambrook J, Fritsch EF, Maniatis T (1989) Molecular Cloning: A Laboratory Manual: Cold Spring Harbor Laboratory Press.
16. Chuanchuen R, Narasaki CT, Schweizer HP (2002) Benchtop and microcentrifuge preparation of *Pseudomonas aeruginosa* competent cells. Biotechniques 33: 760, 762-763.
17. Lee KM, Go J, Yoon MY, Park Y, Kim SC, et al. (2012) Vitamin B12-mediated restoration of defective anaerobic growth leads to reduced biofilm formation in *Pseudomonas aeruginosa*. Infect Immun 80: 1639-1649.
18. Blakley RL (1966) Cobamides and ribonucleotide reduction. II. Estimation of the enzymic formation of purine and pyrimidine deoxyribonucleotides by the use of the diphenylamine reagent. J Biol Chem 241: 176-179.
19. Zechiedrich EL, Khodursky AB, Bachellier S, Schneider R, Chen D, et al. (2000) Roles of topoisomerases in maintaining steady-state DNA supercoiling in *Escherichia coli*. J Biol Chem 275: 8103-8113.
20. Jacobs MA, Alwood A, Thaipisuttikul I, Spencer D, Haugen E, et al. (2003) Comprehensive transposon mutant library of *Pseudomonas aeruginosa*. Proc Natl Acad Sci U S A 100: 14339-14344.

21. Munch R, Hiller K, Grote A, Scheer M, Klein J, et al. (2005) Virtual Footprint and PRODORIC: an integrative framework for regulon prediction in prokaryotes. Bioinformatics 21: 4187-4189.

22. Van Alst NE, Picardo KF, Iglewski BH, Haidaris CG (2007) Nitrate sensing and metabolism modulate motility, biofilm formation, and virulence in *Pseudomonas aeruginosa*. Infect Immun 75: 3780-3790.

23. Panosa A, Roca I, Gibert I (2010) Ribonucleotide reductases of *Salmonella typhimurium*: transcriptional regulation and differential role in pathogenesis. PLoS One 5: e11328.

24. Case ED, Akers JC, Tan M (2011) CT406 encodes a chlamydial ortholog of NrdR, a repressor of ribonucleotide reductase. J Bacteriol 193: 4396-4404.

25. Lundin D, Gribaldo S, Torrents E, Sjoberg BM, Poole AM (2010) Ribonucleotide reduction - horizontal transfer of a required function spans all three domains. BMC Evol Biol 10: 383.

26. Lundin D, Torrents E, Poole AM, Sjoberg BM (2009) RNRdb, a curated database of the universal enzyme family ribonucleotide reductase, reveals a high level of misannotation in sequences deposited to Genbank. BMC Genomics 10: 589.

27. Mowa MB, Warner DF, Kaplan G, Kana BD, Mizrahi V (2009) Function and regulation of class I ribonucleotide reductase-encoding genes in mycobacteria. J Bacteriol 191: 985-995.

28. Jordan A, Torrents E, Sala I, Hellman U, Gibert I, et al. (1999) Ribonucleotide reduction in *Pseudomonas* species: simultaneous presence of active enzymes from different classes. J Bacteriol 181: 3974-3980.

29. Schobert M, Tielen P (2010) Contribution of oxygen-limiting conditions to persistent infection of *Pseudomonas aeruginosa*. Future Microbiol 5: 603-621.

30. Torrents E, Westman M, Sahlin M, Sjöberg B-M (2006) Ribonucleotide reductase modularity: Atypical duplication of the ATP-cone domain in Pseudomonas aeruginosa. J Biol Chem 281: 25287-25296.

31. Cirz RT, O'Neill BM, Hammond JA, Head SR, Romesberg FE (2006) Defining the Pseudomonas aeruginosa SOS response and its role in the global response to the antibiotic ciprofloxacin. J Bacteriol 188: 7101-7110.

32. West SE, Schweizer HP, Dall C, Sample AK, Runyen-Janecky LJ (1994) Construction of improved *Escherichia-Pseudomonas* shuttle vectors derived from pUC18/19 and sequence of the region required for their replication in *Pseudomonas aeruginosa*. Gene 148: 81-86.

33. Kovach ME, Elzer PH, Hill DS, Robertson GT, Farris MA, et al. (1995) Four new derivatives of the broad-host-range cloning vector pBBR1MCS, carrying different antibiotic-resistance cassettes. Gene 166: 175-176.

A2 Supporting information

Regulation of ribonucleotide synthesis by the *Pseudomonas aeruginosa* AlgR two-component system

Figure A2:S1: NarL-dependent expression of *nrdR.*

Fluorescence intensity measurements of *P. aeruginosa nrdR* promoter fusions compared with their mutagenized NarL boxes (box1 and box2, three different mutations in each one), expressed in relative fluorescence units. The experiment was performed in a wild-type *P. aeruginosa* background (pETS161 (wt), pETS181 (box1), pETS182 (box1.2), pETS183 (box1.3), pETS184 (box2), pETS185 (box2.2), pETS186 (box2.3) and pEST187 (box1 and 2)) and in a Δ*narL* background (only wt promoter, pETS161). Strains were grown anaerobically until the mid-logarithmic phase. Values represent the mean of three independent experiments.

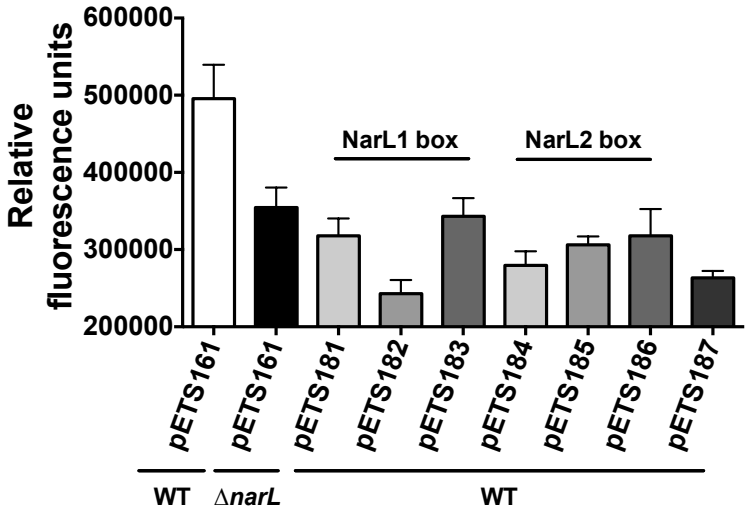

Figure A2:S2: NrdR binding sites in the three *P. aeruginosa* PAO1 RNRs and *topA* promoter regions.

An overview of the entire operon is shown, with open rectangular frames indicating the two NrdR boxes in RNR promoters and the one in the *topA* promoter. The detailed sequence of the area surrounding the boxes is displayed below; the predicted NrdR binding sites are indicated by the nucleotides in bold and black boxes. The position of the NrdR boxes is given relative to the translation start codon of the first gene of the *nrd* operon, as previously described (Rodionov DA and Gelfand MS (2005) Identification of a bacterial regulatory system for ribonucleotide reductases by phylogenetic profiling. Trends in Genetics 21:385-389).

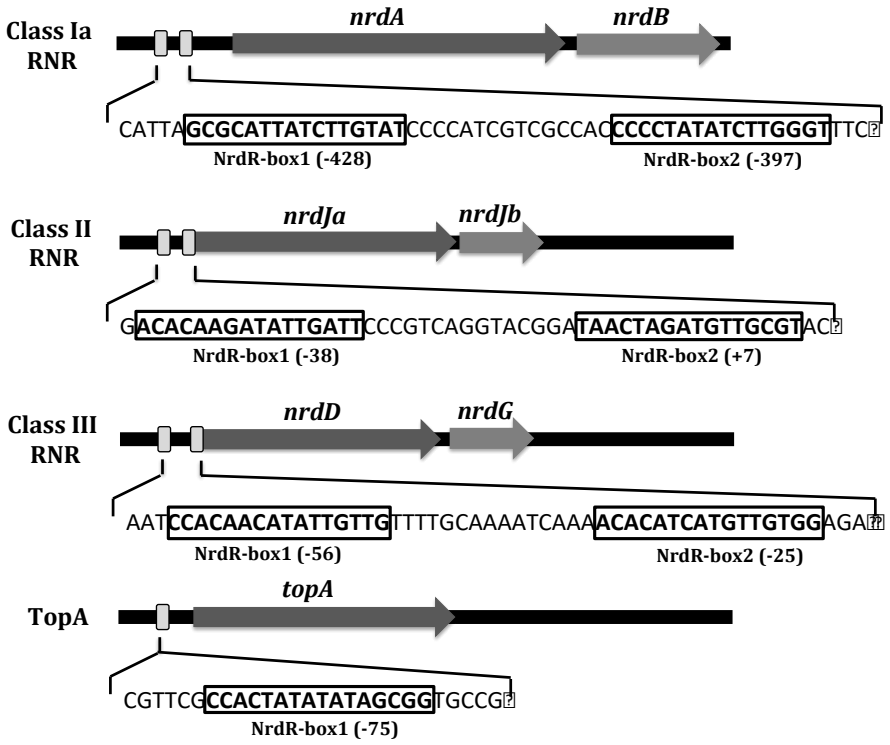

Figure A2:S3: Site-directed mutagenesis of the predicted NrdR box in RNR promoters and *topA* promoter.

Representation of RNR and *topA* promoters' region sequence of *P. aeruginosa* strain PAO1 indicating the NrdR binding sites. Black boxes indicate NrdR recognition sites, and the NrdR box2 mutated residues are shown in upper case and in bold letters. Fluorescence measurements of *P. aeruginosa* RNR promoter fusions (pETS134, pETS180 and pETS136) and P*topA* (pETS177) compared with their mutagenized NrdR mutated box2 (pETS188, pETS189, pETS190 and pETS178, respectively) were measured in relative fluorescence units (RFUs) in a wild-type *P. aeruginosa* background and in a Δ*nrdR* background. Strains were grown aerobically and anaerobically until the mid-logarithmic phase. Values represent the mean of three independent experiments.

Constructions	Sequence	Strains	Aerobic RFU	Aerobic Ratio	Anaerobic RFU	Anaerobic Ratio
	NrdR box1 ********** NrdR box2					
	P*nrdA*					
pETS134	attaGCGCATTATCTTGTATcccatcgtcgccacCCCCTATATCTTGGGTttc	wt	408141.2	100%	113428.8	100%
pETS134	attaGCGCATTATCTTGTATcccatcgtcgccacCCCCTATATCTTGGGTttc	Δ*nrdR*	871571.3	213.5%	710367	626.2%
pETS188	attaGCGCATTATCTTGTATcccatcgtcgccacGAccTatGCcCCAggttc	wt	603210.4	147.8%	521431.1	459.7%
	P*nrdJ*					
pETS180	cctgACACAAGATATTGATTcccgtcaggtacggaTAACTAGATGTTGCGTac	wt	146666.7	100%	398534.6	100%
pETS180	cctgACACAAGATATTGATTcccgtcaggtacggaTAACTAGATGTTGCGTac	Δ*nrdR*	530250	361.5%	430670	108%
pETS189	cctgACACAAGATATTGATTcccgtcaggtacggaTAGAGGgatgGCTcgtac	wt	257274.3	175.4%	378124	94.8%
	P*nrdD*					
pETS136	aatCCACAACATATTGTTGttttgcaaaatcaaaACACATCATGTTGTGGaga	wt	15385.3	100%	359914.2	100%
pETS136	aatCCACAACATATTGTTGttttgcaaaatcaaaACACATCATGTTGTGGaga	Δ*nrdR*	48245	313.5%	280989.6	78%
pETS190	aatCCACAACATATTGTTGttttgcaaaatcaaaACAtGGcCGgCtgtggaga	wt	40334.17	262.1%	276954.7	76.9%
	P*topA*					
pETS177	cgttcgCCACTATATATAGCGGtgccgcgctagtcgctccctccttatattc	wt	39156.4	100%	372360.9	100%
pETS177	cgttcgCCACTATATATAGCGGtgccgcgctagtcgctccctccttatattc	Δ*nrdR*	17022.5	43.5%	152059.7	40.8%
pETS178	cgttcgCAGTtatGGaCaTcggtgccgcgctagtcgctccctccttatattc	wt	21336.3	54.5%	202601.3	54.4%

Figure A2:S4: Distribution of deregulated genes in the global transcriptional analysis according to assigned metabolic classes.

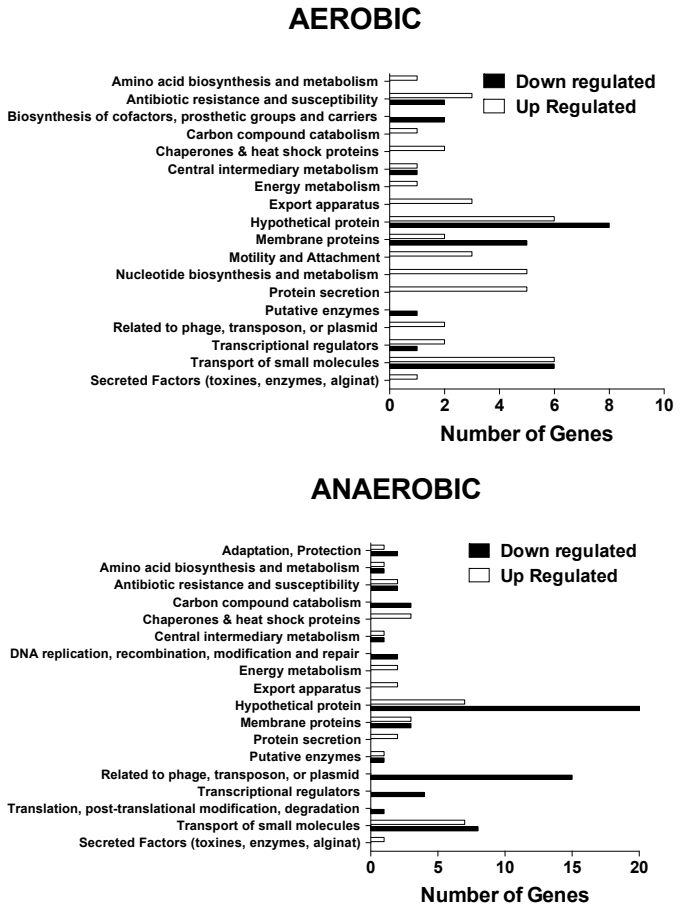

Figure A2:S5: Transcriptional analysis of deregulated genes on global transcriptional analysis of a Δ*nrdR* mutant strain.

Total RNA was reverse transcribed with gene-specific primers as described in Materials and Methods. The analysis demonstrates the specificity of global transcriptional analysis in the absence of *nrdR*.

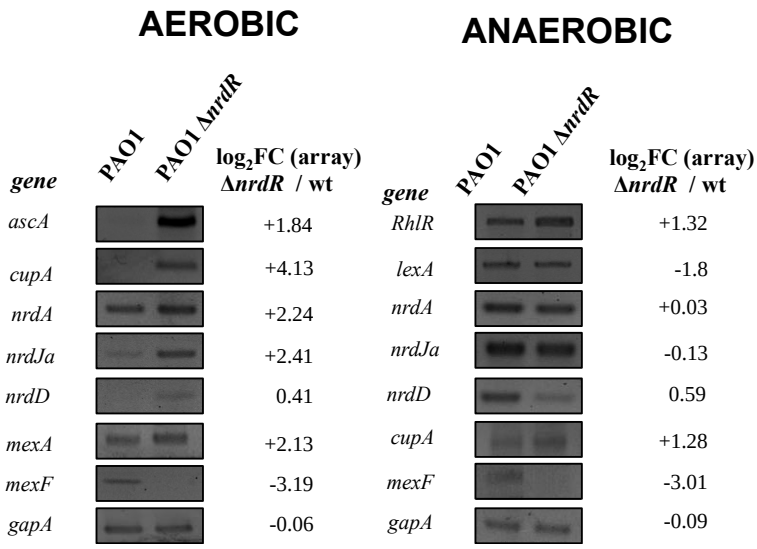

Table A2:S1. Primers and probes used in this study.

Name	Sequence (5'→3')	Application
PnrdRBHI-up	AGGATCCAGGAGAAGGACGGCCAGCAG	Promoter-probe cloning
PnrdRClaI-lw	AAAATCGATATGGTGTCATGGGCACCGCAG	Promoter-probe cloning
NrdRHindIII-low	AAGCTTCATGTACAGCGGGT	Cloning
pBBR1-up	CATCGCAGTCGGCCTATTGG	Check-Cloning
pBBR1-lw	CACTTTATGCTTCCGGCTCG	Check-Cloning
M13-dir	GTTTTCCCAGTCACGAC	Check-Cloning
M13-rev	CAGGAAACAGCTATGAC	Check-Cloning
pUCP20T-up	CCTCTTCGCTATTACGCCAG	Cloning
pUCP20T-low	TCCGGCTCGTATGTTGTGTG	Cloning
PtopA BamHI-up	GGATCCGAAGAGGCGCTGGTGATCTA	Cloning
PtopA ClaI-low	ATCGATGTACTGGCTGCCCAGGTACT	Cloning
PnrdA-up	AGGATCCGAATTCTTGCTCCACACAGCCTC	Cloning/RT-PCR
PnrdA-low	ACCCGGGTTCTCGCGTGTGGTGTCG	Cloning/RT-PCR
PnrdJ BamHI new-up	GGATCCCGCGCCCAGCTGAAGGCC	Cloning/RT-PCR
PnrdJ SmaI new-low	AACCCGGGGACTGCGTTGCGTCTGTC	Cloning/RT-PCR
PnrdD-up	AGGATCCGAATTCGCCCGCCTCGCCCAGG	Cloning/RT-PCR
PnrdD new-low	AATCGATCAGGGTGGCCGGCCAGGTAG	Cloning/RT-PCR
AmR2-up	CAACGACCTATGCCCCAGGTT	Mutation of NrdRbox2 in P*nrdA*
AmR2-low	AACCTGGGGCATAGGTCGTTG	Mutation of NrdRbox2 in P*nrdA*
JmR2-up	GGATAGAGGGATGGCTCGTAC	Mutation of NrdRbox2 in P*nrdJ*
JmR2-low	GTACGAGCCATCCCTCTATCC	Mutation of NrdRbox2 in P*nrdJ*
DmR2-up	AAACATGGCCGGCTGTGGAG	Mutation of NrdRbox2 in P*nrdD*
DmR2-low	CTCCACAGCCGGCCATGTTT	Mutation of NrdRbox2 in P*nrdD*
TmR up	CAGTTATGGACATCGGTGCC	Mutation of NrdRbox2 in P*topA*
TmR low	GGCACCGATGTCCATAACTG	Mutation of NrdRbox2 in P*topA*
nrdATaqM-up	CCCTTCCTGAAAGTGGTCAA	qRT-PCR
nrdATaqM2-low	TGTTCATGTCGTGGGTACG	qRT-PCR
nrdJTaqM-up	CGGGTCAACGAACTGAACA	qRT-PCR
nrdJTaqM2-low	GTAAACACCCGCACCACTTC	qRT-PCR
nrdDTaqM-up	CCGAGATGGACCTGATCAAC	qRT-PCR
nrdDTaqM2-low	CCGAGTTGAGGAAGTTCTGG	qRT-PCR
nrdRTaqM-up	GTTCGACGAGGACAAGCTG	RT-PCR
nrdRTaqM2-low	ATGTAGGCGACTTCGTCGAG	RT-PCR
gapTaqM-up	GAGTGCACGGGGCTCTTC	qRT-PCR
gapTaqM-low	GAGGTTCTGGTCGTTGGT	qRT-PCR
mexA-up	GCCATGCGTGTACTGGTTCC	RT-PCR
mexA-low	GCTCTGGTAGTCGGCCTCGT	RT-PCR
mexF-up	CGAACTACGCGGTGCTCAAC	RT-PCR
mexF-low	GCGCGGATGATGATGTTCTC	RT-PCR
cupA-up	GTGATCCTCGACAGCGTACC	RT-PCR
cupA-low	GTCGTGCTGGTGCTGGTG	RT-PCR
RhlRNdeI-up	ACATATGAGGAATGACGGAGGCT	RT-PCR
RhlR-low	ATCAGATGAGACCCAGCGC	RT-PCR
acsAa up	TGGTACGACGACCTGATGAA	RT-PCR
acsAa low	CCTCGAACAGAATGGTGGTG	RT-PCR
PAlexA- up	ACATATGCAGAAGCTGACGCC	RT-PCR
PAlexA-lw	ACTCGAGTCAGCGCCGGATCACG	RT-PCR
nrdA-FAM	CTGGCACCTGGACATC	qRT-PCR probe
nrdJ-FAM	TCGGCTCGGTCAACCT	qRT-PCR probe
nrdD-FAM	CCCGACCTACAACATC	qRT-PCR probe
gap-FAM	CCTGCACCACCAACTG	qRT-PCR probe
mutNarL1 up	CGCGGATGCGCCCAATTGCGGCTTCCTTCA	Mutation of NarLbox1 in P*nrdR*
mut NarL1 low	TGAAGGAAGCCGCAATTGGGCGCATCCGCG	Mutation of NarLbox1 in P*nrdR*
mutNarL1.2 up	CGCGGATGCGCTGGCATGCGGCTTCCTTCA	Mutation of NarLbox1 in P*nrdR*
mutNarL1.2 low	TGAAGGAAGCCGCATGCCAGCGCATCCGCG	Mutation of NarLbox1 in P*nrdR*
mutNarL1.3 up	CGCGGATGCGCTGCCATGCGGCTTCCTTCA	Mutation of NarLbox1 in P*nrdR*
mutNarL1.3 low	TGAAGGAAGCCGCATGGCAGCGCATCCGCG	Mutation of NarLbox2 in P*nrdR*
mutNarL R dir	TTCCTTCAGCATAATTAGTATCAGCACCA	Mutation of NarLbox2 in P*nrdR*
mutNarL R rev	TGGTGCTGATACTAATTATGCTGAAGGAA	Mutation of NarLbox2 in P*nrdR*
mut NarL2.2 up	TTCCTTCAGCTGGGCCTGTATCAGCACCA	Mutation of NarLbox2 in P*nrdR*
mut NarL2.2 low	TGGTGCTGATACAGGCCCAGCTGAAGGAA	Mutation of NarLbox2 in P*nrdR*
mut Narl2.3 up	TTCCTTCAGCTGCGCCTGTATCAGCACCA	Mutation of NarLbox2 in P*nrdR*
mutNarL 2.3 low	TGGTGCTGATACAGGCGCAGCTGAAGGAA	Mutation of NarLbox2 in P*nrdR*

Table A2:S2: Global transcriptomic analysis of a Δ*nrdR* mutant strain compared with *P. aeruginosa* PAO1 wild-type strain grown aerobically.

List of all differentially regulated genes identified (more than 1.5-fold change in expression).

ID	*Gene*	*Operon arrangement*	Log2 Fold Change	*Gene Product*
PA2128	*cupA1*	*cupA12345*	4.13	Fimbrial subunit CupA1
PA4139			3.78	Hypothetical protein
PA1383			2.42	Hypothetical protein
PA5497	*nrdJa*	*nrdJab*	2.41	Class II (cobalamin-dependent) ribonucleotide-diphosphate reductase subunit, NrdJa
PA2223			2.37	Hypothetical protein
PA1718	*pscE*	*pscBCDEFGHIJKL*	2.32	Type III export protein PscE
PA1156	*nrdA*	*nrdAB*	2.24	Ribonucleoside reductase, large chain
PA0992	*cupC1*	*cupC123*	2.19	Fimbrial subunit CupC1
PA0425	*mexA*	*mexAB-oprM*	2.13	Resistance-Nodulation-Cell Division (RND) multidrug efflux membrane fusion protein
PA3188			2.11	Hypothetical protein
PA0424	*mexR*		2.06	Multidrug resistance operon repressor MexR
PA1693	*pscR*	*PA1697-pscOPQRSTU*	2.00	Translocation protein in type III secretion
PA3144			1.99	Hypothetical protein
PA2322			1.98	Hypothetical protein
PA3842			1.96	Hypothetical protein
PA1155	*nrdB*	*nrdAB*	1.96	Ribonucleoside reductase, small chain
PA0865	*hpd*		1.94	4-hydroxyphenylpyruvate dioxygenase
PA0426	*mexB*	*mexAB-oprM*	1.93	Resistance-Nodulation-Cell Division (RND) multidrug efflux transporter MexB
PA4086	*cupB1*	*cupB123456*	1.89	Probable fimbrial subunit CupB1
PA0887	*acsA*		1.84	Acetyl-coenzyme A synthetase
PA0978			1.78	Hypothetical protein
PA5169			1.77	Hypothetical protein
PA1333			1.65	Hypothetical protein
PA1723	*pscJ*	*pscBCDEFGHIJKL*	1.63	Type III export protein PscJ
PA0958	*oprD*		1.61	Basic amino acid, basic peptide and imipenem outer membrane porin OprD precursor
PA3720			1.61	Hypothetical protein
PA1386			1.54	Hypothetical protein
PA5491			1.53	Hypothetical protein
PA0717			1.51	Hypothetical protein
PA0427	*oprM*	*mexAB-oprM*	1.43	Major intrinsic multiple antibiotic resistance efflux outer membrane protein Opr
PA2813			-1.58	Hypothetical protein
PA4881			-1.59	Hypothetical protein
PA0567			-1.64	Hypothetical protein
PA2812			-1.68	Hypothetical protein
PA2811			-1.75	Hypothetical protein

PA0281	*cysW*		-2.05	Sulfate transport protein CysW
PA2491	*mexS*		-2.18	Hypothetical protein
PA3931			-2.21	Hypothetical protein
PA3229			-2.37	Hypothetical protein
PA4691			-2.55	Hypothetical protein
PA0998	*pqsC*	*pqsABCDE*	-2.83	Homologous to beta-keto-acyl-acyl-carrier protein synthase
PA0565			-3.06	Hypothetical protein
PA2494	*mexF*		-3.19	Resistance-Nodulation-Cell Division (RND) multidrug efflux transporter MexF
PA3281			-3.73	Hypothetical protein
PA3283			-4.57	Hypothetical protein

Table A2:S3: Global transcriptomic analysis of a Δ*nrdR* mutant strain compared with *P. aeruginosa* PAO1 wild-type strain grown anaerobically.

List of all differentially regulated genes identified (more than 1.5-fold change in expression).

ID	*Gene*	*Operon arrangement*	Log2 Fold Change	*Gene Product*
PA5507		*PA5506-PA5507-pauA7-PA5509*	3.2	Hypothetical protein
PA5509		*PA5506-PA5507-pauA7-PA5509*	2.98	Hypothetical protein
PA4058		*PA4058-PA4059-PA4060*	2.23	Hypothetical protein
PA1718	*pscE*	*exsD-pscBCDEFGHIJKL*	2.23	Type III export protein PscE
PA1984	*exaC*	*exaB-exaC*	2.13	Hypothetical protein
PA0713			2.03	Hypothetical protein
PA1556	*ccoO2*	*ccoN2-ccoO2*	1.90	Hypothetical protein
PA1073	*braD*	*braD-braE-braF-braG*	1.79	Branched-chain amino acid transport protein BraD
PA1337	*ansB*	*ansB-PA1336-PA1335*	1.77	Glutaminase-asparaginase
PA1340			1.76	Hypothetical protein
PA1555	*ccoP2*		1.75	Hypothetical protein
PA0958	*oprD*		1.7	Basic amino acid, basic peptide and imipenem outer membrane porin OprD precursor
PA1072	*braE*	*braD-braE-braF-braG*	1.69	Branched-chain amino acid transport protein BraE
PA1070	*braG*	*braD-braE-braF-braG*	1.68	Branched-chain amino acid transport protein BraG
PA5506		*PA5506-PA5507-pauA7-PA5509*	1.67	Hypothetical protein
PA1341		*PA1341-PA1340-PA1339*	1.63	Hypothetical protein
PA2436		*PA2436-PA2435-PA2434*	1.62	Hypothetical protein
PA1596	*htpG*	*htpG-PA1597*	1.57	Heat shock protein HtpG
PA3842	*spcS*	*spcS-PA3843*	1.56	Hypothetical protein
PA1339		*PA1341-PA1340-PA1339*	1.54	Hypothetical protein
PA4587	*ccpR*		1.54	Cytochrome c551 peroxidase precursor
PA1338	*ggt*		1.53	Gamma-glutamyltranspeptidase precursor
PA1571			1.53	Hypothetical protein
PA0026	*plcB*	*plcB-PA0027-PA0028*	-1.50	Phospholipase C, PlcB
PA5107	*blc*	*fbp-PA5109-PA5108-blc*	-1.50	Outer membrane lipoprotein Blc
PA0612	*ptrB*	*ptrB-PA0613*	-1.54	Transcriptional regulators
PA0909		*PA0908-PA0909*	-1.54	Membrane proteins

PA0462		*PA0462-creB-creC*	-1.55	Hypothetical, unclassified, unknown
PA3720		*PA3720-armR*	-1.55	Hypothetical, unclassified, unknow
PA5526			-1.55	Hypothetical, unclassified, unknown
PA4817		*PA4816-PA4817*	-1.56	Hypothetical, unclassified, unknown
PA5217		*PA5218-PA5217-PA5216*	-1.58	Transport of small molecules
PA0490		*PA0491-PA0490*	-1.59	Hypothetical, unclassified, unknown
PA5212			-1.60	Hypothetical, unclassified, unknown
PA3616		*recA-PA3616*	-1.61	Hypothetical, unclassified, unknown
PA0284			-1.68	Hypothetical, unclassified, unknown
PA0327			-1.69	Hypothetical, unclassified, unknown
PA4515		*PA4515-PA4516*	-1.72	Hypothetical, unclassified, unknown
PA3413		*PA3413-PA3414*	-1.73	Hypothetical, unclassified, unknown
PA0529			-1.79	Hypothetical, unclassified, unknown
PA3008		*lexA-PA3008*	-1.81	Hypothetical, unclassified, unknown
PA0130	*bauC*	*bauA-bauB-bauC*	-1.83	Carbon compound catabolism
PA3007	*lexA*	*lexA-PA3008*	-1.88	Repressor protein LexA
PA0922			-1.89	Hypothetical, unclassified, unknown
PA3268			-1.91	Membrane proteins
PA0132	*bauA*	*bauA-bauB-bauC*	-1.92	Amino acid biosynthesis and metabolism
PA0132	*recA*	*recA-PA3616*	-1.96	RecA protein
PA0131	*bauB*	*bauA-bauB-bauC*	-2.01	Carbon compound catabolism
PA0283	*sbp*		-2.01	Sulfate-binding protein precursor
PA0204		*PA0206-PA0205-PA0204-PA0203*	-2.17	Membrane proteins/Transport of small molecules
PA0622		*PA0622-PA0623-PA0624*	-2.18	Related to phage, transposon, or plasmid
PA2813		*PA2813-PA2812-PA2811*	-2.24	Central intermediary metabolism
PA0911			-2.32	Hypothetical, unclassified, unknown
PA4195		*PA4195-PA4194-PA4193-PA4192-PA4191*	-2.33	Transport of small molecules
PA3445			-2.34	Hypothetical, unclassified, unknown
PA0621		*PA0617-PA0618-PA0619-PA0620-PA0621*	-2.4	Related to phage, transposon, or plasmid
PA5525		*PA5524-PA5525*	-2.42	Transcriptional regulators
PA0641			-2.44	Related to phage, transposon, or plasmid
PA0807	*ampDh3*		-2.44	Antibiotic resistance and susceptibility
PA3866			-2.45	Secreted Factors (toxins, enzymes, alginate)
PA0646		*PA0646-PA0647-PA0648*	-2.48	Hypothetical, unclassified, unknown
PA3931			-2.48	Hypothetical, unclassified, unknown
PA0610	*prtN*		-2.49	Transcriptional regulator PrtN
PA0633		*PA0633-PA0634-PA0635*	-2.52	Related to phage, transposon, or plasmid
PA0203		*PA0206-PA0205-PA0204-PA0203*	-2.59	Transport of small molecules
PA1150	*pys2*		-2.62	Pyocin S2
PA0642			-2.63	Related to phage, transposon, or plasmid
PA0648		*PA0646-PA0647-PA0648*	-2.63	Related to phage, transposon, or plasmid
PA0615		*PA0614-PA0615-PA0616*	-2.67	Hypothetical, unclassified, unknown
PA0647		*PA0646-PA0647-PA0648*	-2.68	Related to phage, transposon, or plasmid
PA0623		*PA0622-PA0623-PA0624*	-2.71	Related to phage, transposon, or plasmid
PA4763	*recN*		-2.71	DNA repair protein RecN
PA0644		*PA0643-PA0644-PA0645*	-2.72	Related to phage, transposon, or plasmid
PA0910			-2.72	Hypothetical, unclassified, unknown
PA0616		*PA0614-PA0615-PA0616*	-2.73	Related to phage, transposon, or plasmid

PA0619		*PA0617-PA0618-PA0619-PA0620-PA0621*	-2.74	Related to phage, transposon, or plasmid
PA2485		*PA2485-PA2486*	-2.77	Hypothetical, unclassified, unknown
PA0626		*PA0625-PA0626-PA0627*	-2.78	Related to phage, transposon, or plasmid
PA0620		*PA0617-PA0618-PA0619-PA0620-PA0621*	-2.79	Related to phage, transposon, or plasmid
PA0625		*PA0625-PA0626-PA0627*	-2.84	Related to phage, transposon, or plasmid
PA0320		*PA0319-PA0320*	-2.85	Hypothetical, unclassified, unknown
PA0613		*ptrB-PA0613*	-2.87	Hypothetical, unclassified, unknown
PA0629		*PA0628-PA0629-PA0630-PA0631-PA0632*	-2.87	Related to phage, transposon, or plasmid
PA0639		*PA0636-PA0637-PA0638-PA0639-PA0640*	-2.93	Related to phage, transposon, or plasmid
PA2486		*PA2485-PA2486*	-2.94	Hypothetical, unclassified, unknown
PA3446			-2.95	Hypothetical, unclassified, unknown
PA0624		*PA0622-PA0623-PA0624*	-2.96	Related to phage, transposon, or plasmid
PA0637		*PA0636-PA0637-PA0638-PA0639-PA0640*	-2.96	Related to phage, transposon, or plasmid
PA3938		*PA3938-PA3937-PA3936*	-2.97	Transport of small molecules
PA2494	*mexF*	*mexE-mexF-oprN*	-3.01	Resistance-Nodulation-Cell Division (RND) multidrug efflux transporter MexF
PA0632		*PA0628-PA0629-PA0630-PA0631-PA0632*	-3.06	Related to phage, transposon, or plasmid
PA0635		*PA0633-PA0634-PA0635*	-3.13	Related to phage, transposon, or plasmid
PA0645		*PA0643-PA0644-PA0645*	-3.13	Related to phage, transposon, or plasmid
PA0627		*PA0625-PA0626-PA0627*	-3.15	Related to phage, transposon, or plasmid
PA0638		*PA0636-PA0637-PA0638-PA0639-PA0640*	-3.16	Related to phage, transposon, or plasmid
PA0640		*PA0636-PA0637-PA0638-PA0639-PA0640*	-3.17	Related to phage, transposon, or plasmid
PA0628		*PA0628-PA0629-PA0630-PA0631-PA0632*	-3.21	Related to phage, transposon, or plasmid
PA0634		*PA0633-PA0634-PA0635*	-3.21	Related to phage, transposon, or plasmid
PA0643		*PA0643-PA0644-PA0645*	-3.21	Related to phage, transposon, or plasmid
PA0617		*PA0617-PA0618-PA0619-PA0620-PA0621*	-3.33	Related to phage, transposon, or plasmid
PA0636		*PA0636-PA0637-PA0638-PA0639-PA0640*	-3.41	Related to phage, transposon, or plasmid
PA0618		*PA0617-PA0618-PA0619-PA0620-PA0621*	-3.46	Related to phage, transposon, or plasmid
PA3229			-3.51	Hypothetical, unclassified, unknown
PA2484			-3.55	Hypothetical, unclassified, unknown
PA4881			-3.77	Hypothetical, unclassified, unknown
PA0985	*pyoS5*		-3.9	Membrane proteins/Secreted Factors (toxins, enzymes, alginate)
PA2491	*mexS*		-4.69	Negative regulation of secondary metabolite biosynthetic process

Article 3

Mechanism of action of NrdR, a global regulator of ribonucleotide reduction

Lucas Pedraz[1], Arkadiusz Szura[2], María Solà[2], Eduard Torrents[1].

[1] Bacterial Infections: Antimicrobial Therapies, Institute for Bioengineering of Catalonia (IBEC), The Barcelona Institute of Science and Technology, Barcelona, Spain.

[2] Structural Biology of Mitochondrial Macromolecules, Structural Biology Unit (SBU), Molecular Biology Institute of Barcelona (IBMB), Consejo Superior de Investigaciones Científicas (CSIC).

*Corresponding authors: Eduard Torrents (etorrents@ibecbarcelona.eu) and Lucas Pedraz (lpedraz@ibecbarcelona.eu).

Abstract

All living cells require a supply of deoxyribonucleotides (dNTPs) for DNA synthesis and repair. The only *de novo* pathway for dNTP synthesis is ribonucleotide reduction, catalyzed by a sophisticated family of enzymes, the ribonucleotide reductases (RNRs). Numerous studies have explored the effect of specific transcription factors in the different RNR classes. However, the RNR network is also controlled by its own specific master regulator, NrdR.

NrdR is a nucleotide-binding, oligomeric, global repressor of all RNRs, which is encoded by almost all bacterial species, but completely absent in *Eukarya* and *Archae*a. It has been proposed by many authors as a potential candidate for antimicrobial therapies. However, its mechanism of action and biological role remain fundamentally unknown, due to, among other reasons, the challenge it supposes to obtain this transcription factor in a pure and stable form for *in vitro* studies.

In this work, we conducted a thorough study of NrdR and the NrdR regulon. First, we performed whole-genome searches for NrdR-boxes in *Escherichia coli* and *Pseudomonas aeruginosa* and correlate the data with transcriptomics results from RNA-seq and DNA microarray studies, to draw a global picture of the NrdR regulon. We then designed and purified a series of NrdR fusion proteins to improve the stability of the recombinant protein and facilitate its purification. Using these proteins, we conducted a series of tests aimed toward two purposes: first, analyzing the oligomerization of NrdR depending on the different nucleotide co-factors it binds, using size-exclusion chromatography and SEC-MALS; second, understanding the functional meaning of these oligomeric states, using EMSAs and *in vitro* transcription. The latter evolved into a new molecular biology technique developed for this work, which we named Regulated *in Vitro* Transcription Assay (ReViTA). We also performed test infections in the moth *Galleria mellonella* to determine the effect that alterations in *nrdR* suppose for bacterial fitness and virulence.

Overall, the results reported in this work offer the first demonstration of a mechanism of action for NrdR, in which this transcription factor acts as a nucleotide-sensor, modulating its oligomerization state and its repression on RNR operons depending on the nucleotide co-factor bound to its ATP-cone domain.

Introduction

Ribonucleotide reductases (RNRs) are the enzymes responsible for the reduction of ribonucleotides (NDPs or NTPs) to deoxyribonucleotides (dNDPs or dNTPs), thereby forming the building blocks needed for DNA synthesis and repair[3, 4].

Three different RNR classes have been described, namely class I (subclassified into Ia, Ib, and Ic), class II and class III. All ribonucleotide reductases can reduce all four ribonucleotides, and they all share a common, free-radical-based mechanism[4, 8]. The different RNR classes, however, rely on different mechanisms for the generation of the radical, use different electron donors and present different 3D structures[2-4]. As a consequence of these differences, RNRs also display different behaviors toward oxygen: class I RNRs are oxygen-dependent, class II RNRs are oxygen-independent (but require 5'hydroxylcobalamin as a cofactor, which in some species can only be synthesized aerobically[2, 6, 7]), and class III RNRs are oxygen-sensitive, and thus only active under strict anaerobic conditions[2, 3]. While complex eukaryotic organisms only encode class Ia RNR, eubacteria and archaea make use of all RNR classes in any possible combination[2, 3].

As all living cells require a supply of deoxyribonucleotides, and a balanced supply of all four dNTPs is critical to avoid increased mutation rates during DNA replication[9, 10], ribonucleotide reductase activity needs to be tightly regulated. This occurs at the allosteric level and at the transcriptional level[3, 4, 11, 12].

The allosteric regulation of ribonucleotide reductases is responsible for two different aspects of nucleotide homeostasis: keeping the balance of ribonucleotide and deoxyribonucleotides, and, likewise, keeping the balance of all four different dNTPs[2, 12-14]. The latter action is addressed by a specificity allosteric site present in all RNRs[3, 12, 15, 16]: nucleotide co-factors bound to the specificity site introduce changes at the protein structure to shift the specificity of the active site toward other nucleotides. On the other hand, to keep the overall deoxyribonucleotide levels balanced, most class I and class III RNRs (and a small subset of class II RNRs) include a second allosteric site, the overall activity site[17, 18]. This allosteric element appears as a distinctive domain in the N-terminal end of the protein sequence, a four-helix bundle covered by a three-stranded beta-sheet[19], forming a cone-shaped structure, for which it is called the ATP-cone domain[3, 19]. The binding of ATP or dATP to the ATP-cone activates or inactivates the overall activity of the ribonucleotide reductase through changes in the quaternary structure of the RNR protein complex[3, 19].

The transcriptional regulation of RNRs is responsible for controlling the overall expression of RNR genes (increasing it in certain points in the cell cycle or upon DNA damage)[3, 11], and, in those species encoding more than one ribonucleotide reductase class, controlling differential RNR expression, activating or repressing the different classes in response to changing environmental conditions[3, 11]. Ribonucleotide reductase transcription is thus controlled by known, general regulators, in a class-specific manner. In *E. coli*, for instance, class Ia RNR expression is controlled by DnaA, Fis, IciA and H-NS to couple its

transcription to the cell cycle, class Ib RNR expression is controlled by Fur, to activate it under iron deprivation, and class III RNR is controlled by the anaerobic master regulator Fnr, to induce its expression under anaerobic conditions[2, 3]. However, specifically in bacteria, all RNR classes are also controlled by a regulator exclusive to this pathway, the master regulator NrdR[1, 3, 20].

NrdR was first discovered in *Streptomyces coelicolor* as an undescribed ORF in the same operon as the class II RNR gene *nrdJ*[21]. Structural analysis revealed that NrdR contained an N-terminal Zn-finger DNA binding domain (an atypical rubredoxin-like Zn-ribbon module)[20, 22] and a central ATP-cone domain, very similar to the overall activity allosteric site of ribonucleotide reductases[20, 22]. NrdR was immediately hypothesized to be a transcriptional regulator of RNR expression controlled by nucleotide binding[20], although this has never been completely demonstrated.

A global bioinformatic search identified orthologs of NrdR across the Bacteria domain, as well as linked it to a consensus 16 bp palindromic sequence that appears in all ribonucleotide reductase operons in species encoding NrdR[1]. These repeats (NrdR-boxes) roughly correspond the consensus sequence aca**C**w**A**t**AT**a**T**w**G**tgt, and in RNR operons are always found in pairs where the centers of the sequences are separated by an integer number of turns in the DNA helix (21 bp, 31-32 bp, or 41-42 bp, for two, three, or four turns, respectively) and overlapping with the base promoter sequences[1]. These findings suggest that NrdR is a transcriptional repressor[1, 20, 22, 23] and that it relies on protein-protein interactions between NrdR molecules bound to both boxes[3, 22], which is further supported by the fact that the ATP-cone is known to regulate protein activity through changes in the quaternary structure depending on which nucleotide is bound. The distribution of *nrdR* genes and NrdR-boxes suggests that NrdR is present in most bacterial species while being completely absent in *Eukarya* and *Archaea*, and that, when present, it controls all RNR classes[1].

The functionality of NrdR was first studied in *S. coelicolor* and *E. coli*[23, 24]. It was demonstrated that it contained zinc[24], that it was able to bind nucleotides, and that it was an oligomeric protein[20, 22-25]. Further studies concerning the nucleotide binding capabilities of NrdR show that it uses a negative-cooperative mechanism to bind both dATP and ATP *in vivo*[25], despite being present at very different concentration ranges, which allows its function as a sensor of the dATP-ATP balance. NrdR affinity for nucleotide monophosphates is very low, but it Is found *in vivo* bound to a mixture of mono, di and triphosphate ribo- and deoxyribonucleotides[25]. As expected, the oligomeric state of the protein is influenced by nucleotide binding[25], although no particular stoichiometry or mechanism has been described, and, thus, its biological role remains unknown.

One of the major challenges in the study of this transcription factor is the difficulty to express and purify it in a recombinant form: NrdR is reportedly unstable and tends to precipitate even after purification[24-26]. The functional effect of NrdR has also been studied through *in vitro* transcription, although the instability of the protein made impossible to conduct experiments to differentiate the effects of nucleotide co-factors[26].

Here, we report a study aimed toward a better understanding of the mechanism of action and the biological role of NrdR. We first explored the extent of the NrdR regulon in *Escherichia coli* and *Pseudomonas aeruginosa* using global transcriptomics data (RNA-seq and DNA microarrays) and correlating it to a new bioinformatic identification of NrdR-boxes. To conduct *in vitro* studies, we then developed a series of NrdR protein fusions (using NrdR from *E. coli* and *P. aeruginosa*) designed to increase the stability of the protein and facilitate its purification. These proteins were used for a series of SEC and SEC-MALS experiments to explore the effect of the binding of different nucleotide cofactors on its quaternary structure. Then, we also analyzed the meaning of these nucleotide-NrdR pairs for NrdR activity, both at a DNA-binding level (using EMSA) and at a functional level (using a novel, *in vitro* transcription-based technique named *Regulated in Vitro* Transcription Assay, ReViTA, developed in this work). Finally, as the presence of a bacteria-exclusive protein able to repress all enzymes of an essential pathway has often been regarded as an opportunity for antimicrobial therapies, we explored the effects that impaired *nrdR* expression presents on bacterial virulence and fitness. Globally, these results offer insight into the meaning of NrdR as a nucleotide sensor and provide a first mechanism for the NrdR regulation on ribonucleotide reduction.

Results

The established NrdR repression mechanism is limited to ribonucleotide reductases.

Previous studies have tried to define the extent of the NrdR regulon and explored the possibility of it extending beyond ribonucleotide reductases. The first identification of NrdR-boxes conducted by *Rodionov et al.*[1] considered the possibility of non-RNR genes regulated by NrdR, such as *dnaA* in *Shewanella* or *topA* in *Pseudomonas*. In the promoter regions controlling these genes, however, one single NrdR-box can be found, instead of the pattern observed for all RNR promoters, which always present two NrdR-boxes separated by an integer number of turns in the DNA helix.

In this study, we explored the extent of the NrdR regulon using different techniques. First, we conducted a global search of NrdR-boxes in the *P. aeruginosa* genome. To do so, we gathered the published sequences of NrdR binding sites for *P. aeruginosa* and all the class γ-proteobacteria[1] and produced two consensus sequences using MEME[27] (MEME suite[28]) (**Figure A3:1A**). We obtained a whole-genome query enriched in promoter sequences using the annotated *P. aeruginosa* genome[29] and extracting 470 bp sequences including 450 bp upstream and 20 bp downstream of the translation start codon of each known gene using SAMTools[30] (see Materials and Methods). We then searched for NrdR-boxes in the promoter-enriched whole-genome query using the MEME consensus sequences using FIMO[31] (MEME suite[28]). Here we present the results obtained with the global γ-proteobacteria consensus, as it proved better suited for identifying slightly different NrdR-boxes (see Discussion).

In the *P. aeruginosa* genome, we identified a total of 33 putative NrdR-boxes with a *p*-value lower than $1 \cdot 10^{-4}$ (**Supplementary table A3:S2**). These hits include all known sites in the RNR promoters: two NrdR-boxes in the *nrdDG* promoter (class III RNR), two more in the *nrdJab* promoter (class II RNR), and three (including an isolated one already identified by *Rodionov et al.*[1]) in the *nrdAB* promoter (class Ia RNR). We also identified a fourth box close to the *nrdAB* genes (inside the 5' untranslated region) and the *topA* binding site. All other hits were associated with highly diverse genes, such as the quorum-sensing regulator *lasR* and the starvation and stationary-phase sigma factor *rpoS*, although no other operon includes more than one box.

The second step was identifying NrdR-regulated genes. We previously used global gene expression profiling with a DNA microarray to explore the effect of an *nrdR* mutation in *P. aeruginosa*, identifying 47 differentially expressed genes[32]. However, it remained unclear if any of those genes were directly regulated by NrdR or if they were the result of indirect effects. In this study, we conducted a thorough search of potential NrdR-regulated genes using RNA-seq. We compared the transcriptome of three independent clones of *P. aeruginosa* PAO1 (wild type) and three clones of its isogenic Δ*nrdR* mutant strain (see **Supplementary table A3:S1**), grown in LB, at 37 ºC, and sampled during exponential phase. We identified a total of 97 upregulated genes in the Δ*nrdR* strain with a fold-change higher than 2 (**Supplementary table A3:S4**), as well as 50 downregulated genes (**Supplementary table A3:S5**). Among

the upregulated genes we found, as expected, all the ribonucleotide reductase operons: *nrdA* showed a fold-change of 2.96, *nrdJa* a 13.25, and *nrdD* a 13.65. The *nrdR-ribD* operon was also upregulated, most likely as an effect of the transposon interrupting the *nrdR gene*. Other upregulated genes included the whole PQS operon (*pqsABCDE*), responsible for one of the quorum-sensing systems in *P. aeruginosa,* several stress-related genes, such as the heat-shock genes *grpEi* and *hslU*, and a total of 14 genes related to the type III secretion system. A Gene Ontology Enrichment Analysis (GO Gene Ontology[33, 34]) showed hits for biological processes such as type III secretion system, interaction with host, cellular response to heat, and protein folding (data not shown). On the other hand, the downregulated genes were very disparate, including the arginine deiminase and the pyoverdine biosynthetic operon. Most significantly, *topA* was not downregulated in the *nrdR* strain.

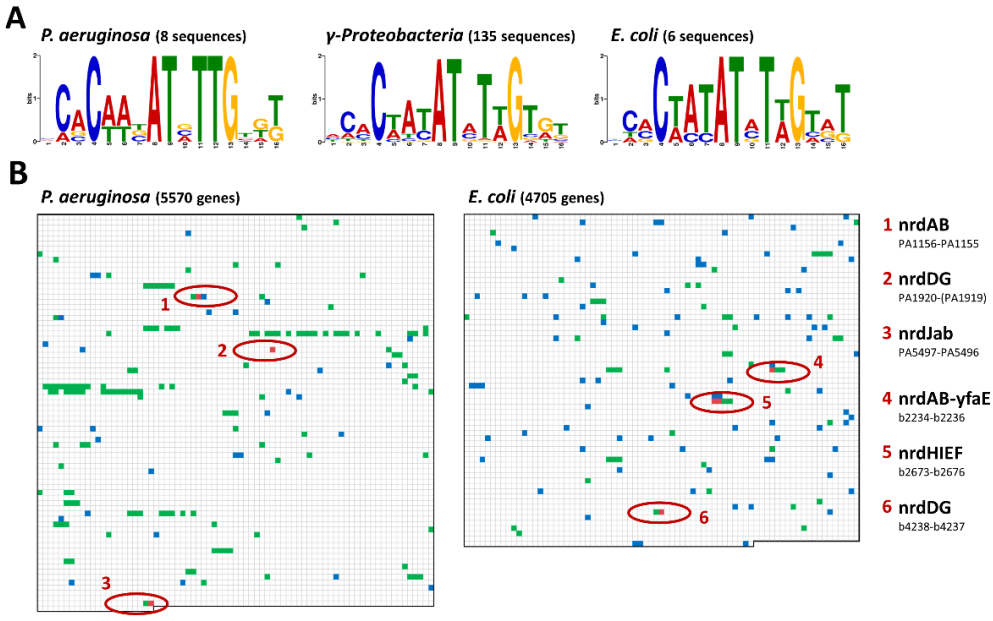

Figure A3:1. Whole-genome analysis of the NrdR regulon. **A**, HMM logos used in the whole-genome search for NrdR-boxes, obtained using sequences from *P. aeruginosa* (left), *E. coli* (right) or all the class γ-proteobacteria (middle) as described by *Rodionov et al.*[1, 2]. **B**, representation of the colocalization of differentially expressed genes obtained in high throughput transcriptomics experiments (RNA-seq or DNA microarrays) and the presence of NrdR-boxes in the 450 base pairs upstream of the translation start codon. Data from *P. aeruginosa* (left) or *E. coli* (right). Each square represents a gene in the genome, from top left (PA0001 *dnaA* in *P. aeruginosa*, b0001 *thrL* in *E. coli*) to bottom right (PA5570 *rpmH* in *P. aeruginosa*, b4705 *mntS* in *E.coli*). Green squares represent genes found to be differentially expressed in an *nrdR* mutant strain compared to its isogenic wild-type strain (RNA-seq data in *P. aeruginosa* PAO1, DNA microarray experiment in *E. coli* K-12 *substr*. MG1655[2, 5-7]). Blue squares represent genes for which at least one NrdR-box was found within the 450 bp prior to its translation start codon. Red squares represent genes for which both previous conditions are true; operons including these genes are circled in red, and its names are detailed at the right of the plots.

To analyze if any of the genes identified in the RNA-seq experiment are directly regulated by NrdR, we did a colocalization experiment with the previous search for NrdR-boxes (**Figure A3:1B**, *P. aeruginosa*). A direct correlation between genes containing putative NrdR-boxes in the 450 bp prior to its ATG (blue squares) and genes found to be differentially expressed in a Δ*nrdR* mutant strain (green squares) shows that the only genes belonging to both categories (red squares) are in the RNR operons.

To see if this was extensible to other species, we then repeated the experiment in *E. coli*, the only other species for which transcriptomics data of an *nrdR* mutant are available, in the form of a DNA microarray comparing *E. coli* K-12 *substr*. MG1655 (wild type) and a *nrdR*ΔATP-cone strain encoding a non-functional NrdR[5]. A summary of differentially expressed genes identified in this microarray experiment can be found in **Supplementary Table A3:S6** (upregulated) and **Supplementary table A3:S7** (downregulated).

A global search for NrdR-boxes using the same $1 \cdot 10^{-4}$ *p*-value threshold as in *P. aeruginosa* showed 113 hits (**Supplementary table A3:S3)**, including all known NrdR-boxes in the RNR promoters (2 boxes in the *nrdAB* promoter, class Ia RNR, 2 more in the *nrdHIEF* promoter, class Ib RNR, and 2 more in *nrdDG,* class III RNR). The other potentially NrdR-regulated genes are highly diverse, and a Gene Ontology Enrichment Analysis shows no statistically significant results (data not shown), suggesting that they may be mostly false positives. Consequently, the higher number of results compared to *P. aeruginosa* probably can be attributed to a higher A-T percentage in the *E: coli* genome, causing a higher percentage of false positives. Only one gene other than the ribonucleotide reductases showed two NrdR-boxes (the transcriptional regulator *slyA*), although these are separated by an unusually large distance.

The correlation between genes containing putative NrdR-boxes in their immediate upstream region and differentially expressed genes in the DNA microarray experiment boxes (**Figure A3:1B**, *E. coli*) showed that the only genes belonging to both categories are in the RNR operons, as shown for *P. aeruginosa*. Therefore, we proposed that the established mechanism of NrdR repression, via binding to pairs of NrdR-boxes overlapping with the base promoter, is limited to ribonucleotide reductase operons. No evidence of other genes regulated by NrdR through a similar mechanism was found in either *E. coli* or *P. aeruginosa*.

NrdR can be produced as a fusion protein with solubilization tags to obtain a pure and stable recombinant protein.

To gain further insight into the mechanism used by NrdR in the repression of RNR expression, we aimed to express and purify NrdR protein from both *E. coli* and *P. aeruginosa* to conduct different *in vitro* studies. NrdR is, however, a protein known to be highly unstable when overexpressed[20, 23, 25, 26]. The optimization process yielded different NrdR fusion proteins that we used in different experiments (**Figure A3:2B**).

The simplest protein we purified was a His_6-tagged version of the NrdR protein from *P. aeruginosa* (**Figure A3:2B**, NrdR-H6*)*. However, as previously reported[25, 26], this protein is mainly recovered as inclusion bodies, and its soluble fraction is highly unstable during the purification process, as it tends to precipitate during the whole procedure, as well as during freeze-thaw steps (data not shown).

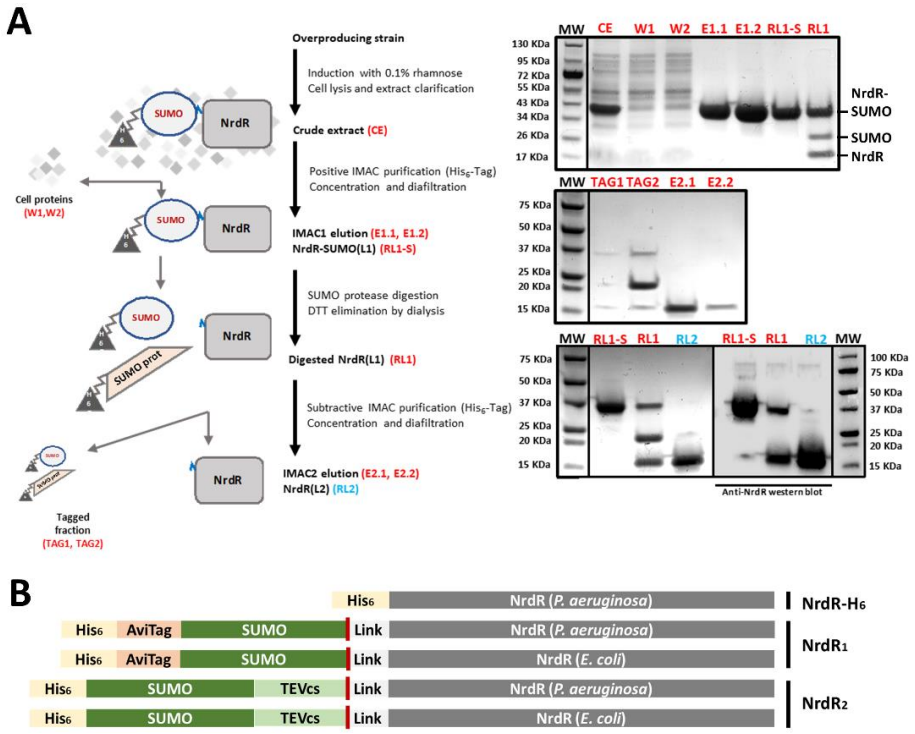

Figure A3:2. Expression and purification of recombinant NrdR fusion proteins. **A**, detailed purification procedure for protein $NrdR_1$ (P. *aeruginosa*); the different intermediate steps indicated in red, and the final protein indicated in blue, are shown in the Coomassie-blue-stained gels at the right. The protein is first produced as an NrdR-SUMO-AviTag-His_6 fusion protein and purified in an immobilized ion chromatography step (IMAC1). The concentrated elution peak of IMAC1 suffers a SUMO digestion, using a His_6-tagged SUMO protease. After a DTT elimination step, the digested mixture is purified through a second, *negative* immobilized ion chromatography (IMAC2), where the flow-through contains the desired protein and both the tagged-SUMO protein and the SUMO protease are retained by the column. A concentration / buffer exchange step (diafiltration) is required after each chromatography. An anti-NrdR western blot image of the digestion step and the final product is provided. **B**, schematic of the NrdR fusion proteins used in this study. The red line indicates the exact digestion site of SUMO protease ($NrdR_1$) or TEV protease ($NrdR_2$). The diagram is not to scale. Coomasie-blue-stained SDS-PAGE gels illustrating the key parts in the purification of other proteins can be found in Supplementary Image A3:S1.

Next, we introduced the Small Ubiquitin-like Modifier (SUMO), a small protein known for its solubilization and stabilization effects in fusion proteins, and which can be seamlessly digested by the SUMO protease[35, 36]. We thereby obtained the $NrdR_1$ fusion proteins, which include (from N-terminus

to C-terminus): a His_6-tag, an AviTag (Avidity Biosciences, CA USA), the SUMO tag, and the NrdR protein, separated from the SUMO by a small peptide linker to enhance protease accessibility (**Figure A3:2B**, $NrdR_1$). The expression and purification procedure of the $NrdR_1$ is detailed in the Materials and Method section, but a simplified schematic can be found in **Figure A3:2A**, left. Briefly, the expression of the protein is induced using rhamnose by a *Rha-Pbad* promoter present a low copy-number plasmid. The fusion protein is first purified in a regular immobilized metal ion chromatography (IMAC) and concentrated through diafiltration prior to the digestion. The preparation is then digested by the SUMO-protease (also His_6-tagged) in the presence of DTT. After a DTT elimination step, the digestion mixture suffers a second, negative IMAC step (IMAC2), where the digested SUMO fraction and the SUMO-protease are retained by the column. The different steps of this method for the NrdR1 protein from *P. aeruginosa* are documented in Coomasie blue-stained SDS-PAGE gels (**Figure A3:2A**, right), and a Western blot was used to identify the NrdR-containing and non-NrdR-containing bands in the digestion mixture. Representative steps of the purification for *E.* coli can be found in **Supplementary figure A3:S1**. Using this method, we obtained a high yield of $NrdR_1$-SUMO fusion protein, which can be stored and subjected to freeze-thaw cycles without significant losses. The final yield of $NrdR_1$ monomer is still small, and the process is not cost-effective, as the efficiency of the SUMO digestion is relatively low (see RL1 in **Figure A3:2A**).

To increase the total yield and improve the cost-effectiveness of the process we then designed a second generation of NrdR fusion proteins ($NrdR_2$), which include (From N-terminus to C-terminus): a His6-tag, the SUMO-tag, the cutting site of the TEV protease from Tobacco Etch Virus[37] (TEVcs), and the NrdR protein, separated from the TEVcs by a small peptide linker (**Figure A3:2B**, $NrdR_2$). When purifying this protein, the SUMO tag is only used for stabilization purposes, while the protein digestion is done with TEV protease. Representative steps of the NrdR2 purification for *E. coli* can be found in **Supplementary figure A3:S1**. The protein from *P. aeruginosa* still presented precipitation issues, however. Changes in the protocol are being tested to overcome this problem, but, to date, the *P. aeruginosa* NrdR protein has only been purified with a significant yield and in a stable form when adding AMP as a cofactor during the purification procedure, which significantly compromises the interpretation of the experiments performed with it (see below). Therefore, $NrdR_2$ from *E. coli* was used as the standard protein for the following experiments, while the other protein forms were used in initial tests or to identify differences.

Using PCA precipitation and ion-pair reverse phase HPLC chromatography, we determined that, when no co-factor is added, as-prepared NrdR proteins contain no detectable amounts of nucleotide (**Supplementary figure A3:S2**).

NrdR exists as a dynamic population of nucleotide-dependent oligomeric forms

In class Ia, Ic and III ribonucleotide reductases, the ATP-cone domain controls the overall enzyme activity by inducing alterations in the quaternary structure of the complexes depending on the

nucleotide bound to it[12, 19]. A similar mechanism is expected to occur in NrdR, as has been hypothesized since its early discovery[20, 24].

To verify this hypothesis, we first conducted Size-Exclusion Chromatography (SEC) experiments using the NrdR-H_6 protein (*P. aeruginosa*) and the $NrdR_1$ proteins (*P. aeruginosa* and *E. coli*). A full chromatogram of a representative experiment can be found in **Supplementary figure A3:S3A**, and a detail of the results for *P. aeruginosa* $NrdR_1$ is in **Figure A3:3A**.

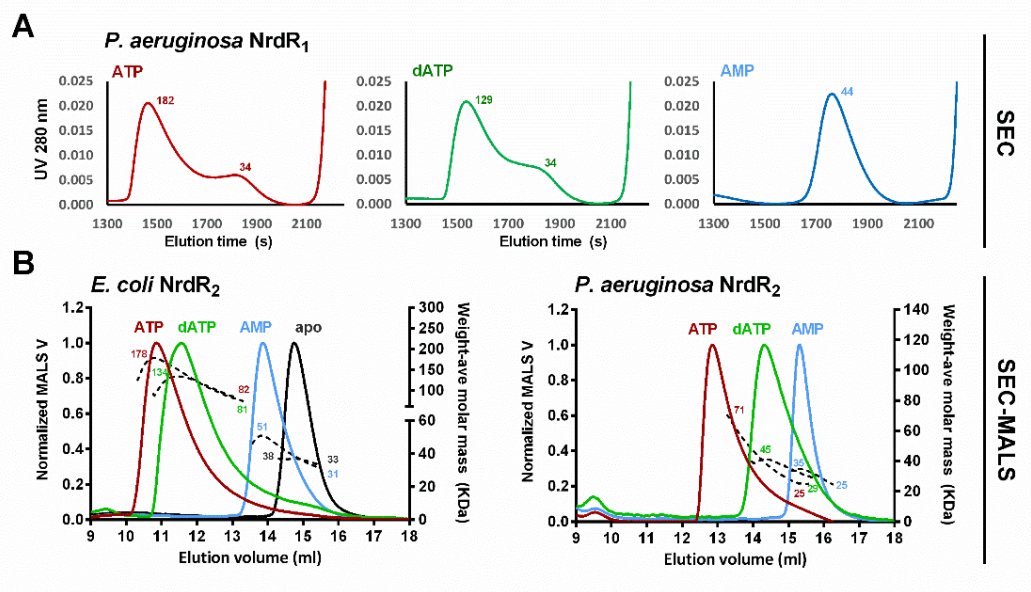

Figure A3:3. Nucleotide-dependent quaternary structure of NrdR. **A**, size-exclusion chromatography results of $NrdR_1$ from *P. aeruginosa*, pre-incubated with a 20:1 nucleotide:protein molar ratio and exposed to a 1:1 nucleotide:protein ratio in the running buffer. Full chromatogram and control data available in Supplementary figure A3:S3. The numbers near the peaks indicate the average estimated molecular weight for the corresponding protein structure. The results are representative of three independent experiments. **B**, SEC-MALS results of $NrdR_2$ from *E. coli* (left) or *P. aeruginosa* (right) exposed to 0.025 mM nucleotide in the running buffer. Left OY axis (solid lines) represents MALS detection data normalized to a maximum signal of 1.0 in each sample. Right OY axis (dashed lines) represents weight-average molar mass (KDa). The numbers near the peaks indicate the maximum and minimum weight-average molar mass of the corresponding peaks. The results are representative of two independent experiments.

In these experiments, NrdR was pre-incubated with a 20:1 molar excess of different nucleotide cofactors and then run on a Superdex 200 column with a concentration of nucleotide in the buffer enough for a 1:1 molar ratio. NrdR elutes between peaks corresponding to oxidized DTT and excess nucleotide, but only the intermediate peaks contain protein (**Supplementary figure A3:S3B**), which was demonstrated to be active (**Supplementary figure A3:S3C**). The $NrdR_1$ protein from *P. aeruginosa*

produced a very stable pattern: in the presence of AMP (Figure A3:3A, right) or dAMP (data not shown) it run as a single, highly stable peak with an average apparent molar mass of 44 KDa, an intermediate value between the expected for a dimer and a trimer of NrdR. On the other hand, when bound to nucleotide triphosphates, it appeared simultaneously as a dimer (34 KDa) and higher oligomeric forms. These forms were reproducibly higher for ATP (182 KDa, 10-mer or higher) (**Figure A3:3A**, left) than for dATP (129 KDa, 6-mer to 8-mer). A mechanism of action based on the difference between ribonucleotides and deoxyribonucleotides would make the most sense for a regulator of ribonucleotide reduction; therefore, the shift between the NrdR-ATP heavier peak and the NrdR-dATP hexamer/octamer peak might be significant. The effect of the AMP was considered difficult to interpret without absolute molecular weight information, as the intermediate structure could be caused by an intermediate state between dimer and tetramer, but also by a "bloated" dimer with a significant change in the structure of each monomer. Most significantly, all peaks are wide, spanning several possible conformations, and their average apparent molar masses depending on protein concentration and nucleotide-protein incubation time, especially in the case of NrdR-ATP (data not shown). This is interpreted as NrdR forming labile complexes with dynamic protein-protein associations and non-defined stoichiometry.

The $NrdR_1$ proteins barely offered enough yield to conduct these SEC experiments. Moving to the $NrdR_2$ proteins, we then performed SEC-MALS experiments (Size-Exclusion Chromatography coupled to Multi-Angle Light Scattering) to get a clear interpretation of the meaning of the NrdR complexes we had observed. The same experiments were conducted with protein from *E. coli* (**Figure A3:3B**, left) and *P. aeruginosa* (**Figure A3:3B**, right), although, as the latter had to be co-purified with AMP, the differences caused by the nucleotides will be affected by this fact.

In the SEC-MALS experiments presented here, the proteins were not pre-incubated with nucleotides, but just exposed to a fixed concentration of 0.025 mM nucleotide in the running buffer, as this demonstrated to produce the most reproducible results (see chromatograms in **Figure A3:3B** and molecular weight values in **Table A3:1**, nucleotide in buffer). In the absence of a nucleotide co-factor, NrdR ran as a clear dimer, with a weight-average molar mass (Mw) of 35.98 KDa. When bound to AMP, the peak presents an average Mw of 44.56 KDa, but with absolute molar mass determination ranging between 51 KDa and 31 KDa, strongly suggesting a dimer/trimer mixture. The nucleotide triphosphates, as seen before, produced higher-order oligomers: NrdR-ATP appeared with an average Mw of 140.17 KDa (octamer), while NrdR-dATP showed an average Mw of 113.36 (hexamer).

These peaks showed a high range of molar masses (see black, dashed lines in **Figure A3:3B**), as well as a higher polydispersity (**Table A3:1**), suggesting unstable complexes with dynamic interactions again. The results for *P. aeruginosa* show much lower weight-average molar masses, most likely due to the presence of AMP in all preparations, but the relative order of the peaks is the same, suggesting the same mechanism, which also coincides with what was seen for *P. aeruginosa* with the $NrdR_1$ protein (**Figure A3:3A**). Further experiments with apo-$NrdR_2$ in *P. aeruginosa* will be needed to confirm it.

Nucleotide in buffer				
Nucleotide	**Mn (KDa)**	**Mw (KDa)**	**Polydispersity**	**Composition**
+ ATP	131.52 ± 0.32	140.17 ± 0.30	1.07 ± 0.00	R_8 **(octamer)**
+ dATP	110.83 ± 0.21	113.36 ± 0.21	1.02 ± 0.00	R_6 **(hexamer)**
+ AMP	43.81 ± 0.09	44.56 ± 0.08	1.02 ± 0.00	$R_2 \leftrightarrow R_3$
Apo	35.95 ± 0.08	35.98 ± 0.08	1.00 ± 0.00	R_2 **(dimer)**
Nucleotide in pre-incubation and buffer				
Nucleotide	**Mn (KDa)**	**Mw (KDa)**	**Polydispersity**	**Composition**
+ ATP	179.75 ± 0.76	200.31 ± 0.53	1.11 ± 0.01	$R_{10} \leftrightarrow R_{12}$
+ dATP	118.52 ± 0.22	121.83 ± 0.21	1.02 ± 0.00	R_6 **(hexamer)**
+ AMP	44.02 ± 0.10	44.75 ± 0.09	1.02 ± 0.00	$R_2 \leftrightarrow R_3$

Table A3:1. Molecular weight of NrdR-nucleotide complexes. Values for SEC-MALS experiments with nucleotide only present in the running buffer (top) or pre-incubated with the protein as well (bottom). Mn, number-average molar mass; Mw, weight-average molar mass. The polydispersity index is defined as Mw/Mn. All values listed as average ± standard deviation. The composition column lists the proposed quaternary structure of the major component in each mixture of NrdR-nucleotide complexes rounded to the closest integer. When multiple forms are present in significant number (as indicated by an intermediate average molecular weight) they are separated by double arrows (←→). Using protein conjugate analysis, we can separate the fractions of the molecular weight of the complex belonging to protein and co-factors (see Supplementary table A3:S7).

When proteins were incubated with nucleotide prior to the SEC-MALS experiment, further differentiation of the protein-nucleotide complexes occurred (**Table A3:1**, nucleotide in pre-incubation and buffer; **Supplementary figure A3:S4**). The NrdR-AMP peak did not vary, with a weight-average molar mass of 44.75 KDa, and the NrdR-dATP suffered only a small increase at 121.83 KDa (suggesting that the main form is still octamer); however, the NrdR-ATP complex suffered a major shift, reaching an Mw of 200.31 KDa (10-mer to 12-mer).

The activity of NrdR is modulated by its nucleotide co-factor

The next step was to explore at a function level the meaning of the oligomerization differences we had seen. The first experiment to be conducted to characterize the differences in the activity of a transcription factor is an Electrophoretic Mobility Shift Assay (EMSA). The most reproducible EMSA experiments were obtained using the $NrdR_2$ protein from *E. coli*.

The EMSA results of an NrdR-sensitive probe (the whole *nrdAB* promoter from *E. coli*, P*nrdA* 519 bp) clearly show the effect of the different nucleotide co-factors bound to the protein (**Figure A3:4**). The $NrdR_2$ protein was incubated with a 20:1 molar excess of the desired nucleotide for 1 hour at room temperature. Without nucleotide (+0) or with AMP, NrdR produced only a small shift with an unstable, smeary complex band. NrdR-ATP caused no significant shift, appearing as an inactive protein. However, NrdR-dATP produced a clear and intensive shift, consistent with the binding of a hexamer. An NrdR-

insensitive probe was used as a negative control, showing only faint binding bands under the same EMSA conditions used for the P*nrdA* band (which include high concentration of unmarked competition DNA). The NrdR-dATP presented a slight increase in its unspecific binding. The full, unedited images of the EMSA gels, including more nucleotides and controls, can be consulted in **Supplementary figure A3:S5**.

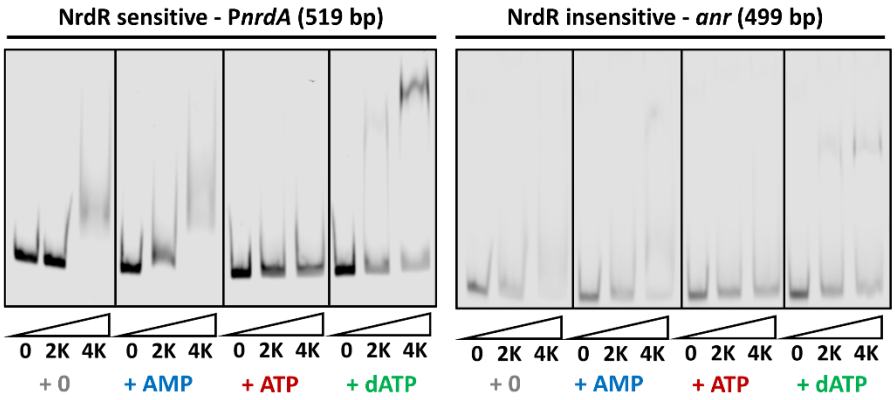

Figure A3:4. Nucleotide-dependent DNA-binding activity in NrdR. EMSA gels obtained using the $NrdR_2$ protein from *E. coli*. Two DNA probes were used: P*nrdA* promoter from *E. coli* (left, 519 bp, probe including two known NrdR-boxes) and *anr* (right, 499 bp, negative control probe without NrdR binding sites). Numbers below the triangles indicate the molar ratio of protein and marked DNA (0:1, 1000:1 or 4000:1). When required, nucleotide was pre-incubated with NrdR at a fixed 20:1 nucleotide:protein ratio.

However, the EMSA experiments cannot discern if a DNA-protein complex results in transcriptional repression or not. To address this problem, we used a novel technique, developed in this work, based on *in vitro* transcription.

This technique was named ReViTA (Regulated *in Vitro* Transcription Assay) and is further detailed in the Materials and Methods section. Briefly, it is based on conducting the *in vitro* transcription of two genes in a single reaction: one whose transcription is sensitive to the transcription factor under study (TEST) and another with a completely constitutive transcription (CTRL). Both genes are present in a synthetic plasmid (pReViTA) and separated by strong transcription terminators, to keep their mRNAs independent. The number of mRNA copies produced for both genes is measured using absolute-quantification qRT-PCR. The copies of the CTRL gene are used as an internal control to normalize the TEST copies, as the technique is very sensitive to small changes. The normalized TEST copies can be compared between reactions to evaluate the positive or negative effect of transcription factors. Schematics of the pReViTA plasmid and the synthetic DNA cassette used to generate it can be found in the **Supplementary figure A3:S6**.

The first results obtained using ReViTA demonstrate that the NrdR repression on RNR gene transcription can be detected with this technique: In **Figure A3:5A**, we can see that the normalized transcription of a TEST sequence controlled by the *nrdAB* promoter region (P*nrdA*) from *E. coli* is reduced to close to a 25% when adding $NrdR_2$-dATP (*E. coli*) in a 1000:1 protein:DNA proportion, while the normalized transcription of the control sequence remains unaltered. To use this technique to discern the effects of each nucleotide co-factor in the functionality of NrdR, the $NrdR_2$ protein was pre-incubated for 1 hour at room temperature with a 20:1 excess of the desired nucleotides and then added to the *in vitro* transcription reactions. In these experiments (**Figure A3:5B**) we can see that the NrdR-dATP complex, here added at a 2000:1 protein:DNA proportion, caused almost complete inhibition of P*nrdA* transcription, while the addition of NrdR-ATP complex caused no significant effect. The complex with AMP produced a significant inhibition, although not so pronounced, reaching close to 65% of the control transcription rate. Two identical control reactions without NrdR were included to illustrate the low variability of the technique after data normalization.

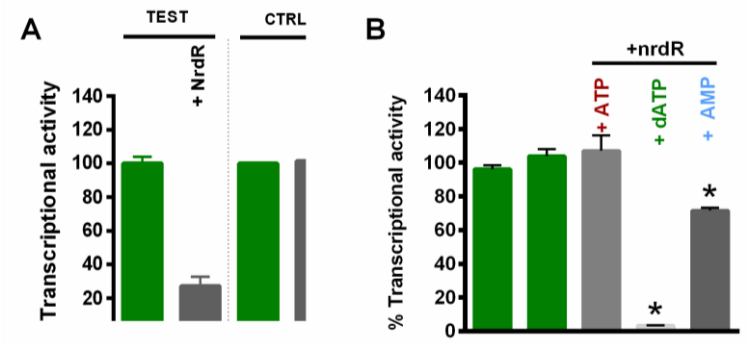

Figure A3:5. Nucleotide-dependent NrdR repression of RNR transcription. Regulated *in Vitro* Transcription Assay (ReViTA) results, using pReViTA-PA (*nrdAB* promoter from *E. coli*) as template, and repressing its transcription with $NrdR_2$ (*E. coli*). The percentage of transcriptional activity is defined as the ratio of normalized copies generated in a reaction compared to the normalized copies generated of a reference reaction (here, *ctrl* reactions without NrdR). Both the problem and the control reactions include TEST and CTRL expression, to convert copy numbers into normalized copies, thus eliminating the effect of unspecific repression (see Materials and Methods). **A**, specific repression of RNR transcription by NrdR. The transcription of the TEST sequence, controlled by P*nrdA*, is specifically repressed by $NrdR_2$-dATP (molar proportion 1000:1 protein:DNA), while the CTRL sequence (controlled by an unrelated Pc promoter) suffers no specific repression. **B**, functional effects of the nucleotide co-factor in NrdR. Nucleotides were pre-incubated (1 hour at room temperature) with $NrdR_2$ (*E. coli*) before adding the protein to the *in vitro* transcription reaction (molar proportion 2000:1 protein:DNA. All values correspond to the TEST sequence. Error bars represent positive standard deviation. *: p-value less than 0.05 in a two-tailed t-test.

Positive or negative alterations in NrdR affect bacterial fitness and virulence

One of the main driving forces between the study of NrdR is its suitability as a potential target for antimicrobial therapies, as a general regulator of an essential pathway that is additionally confined only to bacteria. As a first approach to discern if there is a potential application of NrdR as an antibacterial

target we conducted test infections and growth curves using *P. aeruginosa* strains with altered *nrdR* expression.

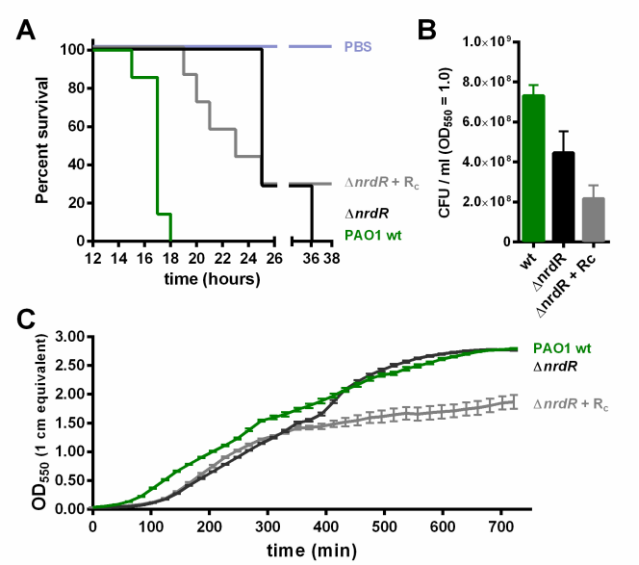

Figure A3:6. Effect of alterations in NrdR on bacterial virulence and fitness. **A**, Kaplan-Meier survival curve, infection assay in a *Galleria mellonella* model using *P. aeruginosa* PAO1 wild-type (wt), an isogenic *nrdR* mutant strain (Δ*nrdR*) and a complementation strain bearing additional plasmidic copies of pUCP20T::*nrdR* (Δ*nrdR* + Rc). 10 larva per condition were infected with a $2 \cdot 10^{-6}$ dilution of a PBS suspension (OD_{550} = 1.0) of the corresponding strains. The result is representative of two individual experiments. **B**, viable counting of the PBS suspensions of the previous strains, as used for *Galleria* infection or growth curve experiments. Error bars represent positive standard deviation. The result is representative of four individual experiments. **C**, growth curve of the previous strains, grown for 12 hours in LB in 96-well plates, at 37 ºC, and with continuous humidity. OD_{550} values were obtained for an optical path length of 5.4 mm and converted to equivalent OD_{550} in 1 cm path length for the convenience of the reader. Error bars represent standard deviation. The result is representative of two individual experiments.

First, to evaluate the effect of altered *nrdR* expression in the virulence of *P. aeruginosa*, we conducted a series of test infections in *Galleria mellonella* using a wild type PAO1 strain, a deletion Δ*nrdR* strain, and the previous strain complemented with a pUCP20T::*nrdR* plasmid adding additional *nrdR* copies per cell (Δ*nrdR* + Rc). We performed two individual experiments, in each one injecting ten larvae per condition (with a PBS group as negative control), with an average infection of 12 CFU/larva. The results (**Figure A3:6A**) show a surprising effect of the *nrdR* alteration: in the experiment shown, while the wild type strain killed its first larva 15 hours after infection, and had killed the whole group after 18 hours, all larvae infected with the Δ*nrdR* mutant and the complementation strain were alive at this time point. These strains required more than 24 hours to eliminate half the larva, and the NrdR complementation strain was unable to kill the remaining individuals even 36 hours after infection.

As NrdR does not directly regulate genes involved in virulence factors or other infection-related traits, the differences shown in the infection model are most likely due to its effect in bacterial fitness and growth speed. Viable cell counts of suspensions prepared like that for *Galleria* infections showed a reproducible reaction of CFUs to half in the Δ*nrdR* strain and almost to one fourth in the Δ*nrdR* + Rc strain (**Figure A3:6B**). Likewise, growth curves showed that the strains with altered *nrdR* expression displayed a longer lag phase and, most significantly, that the NrdR complementation strains presented a much lower growth speed after five hours of culture (**Figure A3:6C**).

Discussion

Since its first description, NrdR has been proposed to be a nucleotide-modulated transcriptional regulator of ribonucleotide reduction[1, 20], as it was described as a protein formed by two different domains: a DNA-binding domain and an RNR-related nucleotide-binding ATP-cone domain. The location of its cis elements, the NrdR-boxes, also offered significant insight on the NrdR mechanism of action: In RNR promoters, NrdR-boxes always appear in pairs, separated by an integer number of turns in the DNA helix, and overlapping the basal promoter elements[1]. These findings suggested that NrdR acts as a repressor, and that It may rely on protein-protein interactions. It is known that, when present in ribonucleotide reductases, the ATP-cone domain controls overall enzymatic activity by introducing changes in the protein structure that affect protein-protein interactions, changing the quaternary structure of the complex[3, 19], so a similar mechanism was proposed for the transcriptional regulator NrdR.

The fact that NrdR is encoded by almost all bacterial species, and that, when present, it controls all RNR classes[1, 3] suggests that its biological role is an universal one, not related to the specific needs of a particular species or to the differential expression of a single RNR class. These findings led to a first hypothesis for the mechanism of action of NrdR, expressed by different authors[20, 22, 23, 25, 26, 32, 38], in which this protein would act as a global regulator of RNR activity, repressing all RNR classes when dNTP was bound to its ATP-cone domain, meaning that the cellular deoxyribonucleotide levels were high, as it would happen after a period where RNR activity had been high.

However, this hypothesis presented significant problems. Although it was experimentally demonstrated that NrdR acts as an RNR repressor[22, 23], binds nucleotides[22, 39], and forms oligomers in a manner dependent of its nucleotide co-factor[39], other findings suggested a more complex mechanism of action. First, all different nucleotides were detected bound to NrdR, including monophosphates and diphosphates[22]. Moreover, the first experiments trying to associate different oligomeric states to nucleotide co-factors did not differentiate between ATP and dATP[39], only describing that the ATP-cone domain alone is able to form dimers, and that the full protein adopts higher oligomeric forms when bound to nucleotide triphosphates. No *in vitro* studies addressing the effect of the different nucleotides were conducted, as NrdR was reported to be highly unstable during purification and storage[20, 22, 23, 25, 26], which still represents the main challenge in studying this regulator.

Finally, when the first study about the effect of nucleotide binding on NrdR was published by *McKethan et al.* in 2013[25], it did not fit the original hypothesis: their study, performed using a NrdR-His_6 fusion protein from *E. coli,* describes the formation of high oligomeric forms (up to 20-mer) with no fixed stoichiometry, only differentiating that oligomerization levels were higher with ATP than with dATP, and much lower with monophosphates. They only detected DNA binding activity with NrdR bound to monophosphates and very high NrdR-DNA proportions, up to 28000:1. All these findings highlighted the need for *in vitro* studies using stable proteins to revisit the proposed mechanism of action of NrdR.

In this work, we presented new strategies to obtain stable and pure recombinant NrdR. The simple NrdR-His_6 protein from *P. aeruginosa* was, as described for other species, highly unstable. Although it was possible to conduct some experiments with it (**Supplementary Figure A3:S3**) new strategies were required to obtain a reliable source of protein for more advanced studies. We developed two generations of fusion proteins to purify NrdR from *E. coli* and *P. aeruginosa* (**Figure A3:2B**). The purification protocol (**Figure A3:2A**, Materials and Methods) was gradually optimized to keep the protein stable. To maintain NrdR soluble in the absence of nucleotides, a high salt concentration (up to 1 M NaCl in the crude extract) and a continuous presence of DTT were required, the latter most likely to prevent the exposed cysteines in the Zn-finger domain from forming inter-protein disulfide bonds[20]. The introduction of the SUMO tag was required to stabilize the protein during the initial overexpression step, and an additional cutting site for TEV protease was added in the $NrdR_2$ proteins to avoid using SUMO protease. This strategy proved remarkably effective for the *E. coli* protein, although the *P. aeruginosa* one remained unstable and could only be purified in high quantities as an NrdR-AMP complex. When no nucleotides were added during overexpression or purification, our fusion proteins were proved to contain no co-factor bound **(Supplementary Figure A3:S2)**, probably due to the repeated diafiltration steps. The fact that NrdR is much more stable when coupled to a nucleotide monophosphate than without co-factor is highly significative. We are, however, exploring new conditions to purify this protein in its apo- form, as this would help the interpretation of some *in vitro* experiments and demonstrate if the NrdR proteins from distinct species behave differently.

Concerning the effect of ATP / dATP, which was initially expected to be the main aspect in the regulation of NrdR activity, we demonstrated for the first time a differential effect caused by these co-factors. The Size Exclusion Chromatography (SEC) results of the $NrdR_1$ proteins (**Figure A3:3A**, **Supplementary Figure A3:S3**) suggested that, while NrdR stayed as a dimer/trimer when coupled to monophosphates, but formed high-order oligomers when coupled to triphosphates, and even higher with ATP (10-mer or more) than with dATP (6-mer to 8-mer). This was confirmed using the $NrdR_2$ protein from *E. coli* in SEC-MALS (Size Exclusion Chromatography – Multi Angle Light Scattering) experiments (**Figure A3:3B**): when the apo-protein was exposed to nucleotides in the running buffer, it reproducibly ran as a octamer or higher with ATP, as a hexamer with dATP, and as a dimer/trimer with AMP. When the protein was incubated for a long time with nucleotides prior to the SEC-MALS run, NrdR-ATP shifted towards even higher oligomerization, while NrdR-dATP suffered a smaller change, and NrdR-AMP remained unchanged (**Supplementary Figure A3:S4**). These findings are consistent with the previously published SEC experiments[25], but also offer the first clear distinction between NrdR-ATP and NrdR-dATP. Although the $NrdR_2$ protein from *P. aeruginosa*, previously exposed to AMP during the purification, ran at lower molecular weights, the fact that the relative order or the peaks remained the same, together with the consistent results of $NrdR_1$ in SEC experiments, strongly suggests that NrdR is this species suffers the same oligomerization changes when coupled to these nucleotide co-factors.

The functional effect of the previous differences in oligomerization were studied by EMSA and *in vitro* transcription. The NrdR-dATP complex produced a clear shift in EMSA experiments conducted with high

concentration of unmarked competition DNA, while NrdR-ATP appeared inactive (**Figure A3:4**). In the ReViTA experiments, a 2000:1 NrdR-dATP:DNA complex displayed a severe reduction in transcription, while NrdR-ATP caused no significant effect (**Figure A3:5B**). These findings support the hypothesis that NrdR may act as a sensor of the NTPs-dNTPs balance and repress ribonucleotide reduction when bound to dATP. Although NrdR was reported to have less affinity for dATP than for ATP, and the cellular levels of the former are significantly lower[25], the negative-cooperative mechanism proposed by *McKethan et al*, in which the binding of a nucleotide stimulates the affinity for the other[25], explains how NrdR may act as an efficient ribonucleotide-deoxyribonucleotide sensor.

The meaning of the NrdR-AMP (or NrdR-dAMP) complex is harder to ascertain. While apo-NrdR runs as a dimer (**Figure A3:3B**), as does the ATP-cone domain alone[39], the protein takes a different form when coupled to nucleotide monophosphates. The results obtained for both species in SEC and SEC-MALS (**Figure A3:3**) suggest an intermediate dynamic structure or a mixture of forms between dimer and trimer. NrdR-AMP caused a short but clear shift in the EMSA experiments (**Figure A3:4**), although it also presented significant unspecific binding activity (**Figure A3:4** and **Supplementary Figure A3:S5**, notice the disappearance of the base level band). In ReViTA experiments, it caused a repression of P*nrdA* transcription, but considerably less significant that that caused by NrdR-dATP. In all experiments, dAMP displayed identical behavior. It has been reported that NrdR has a very low affinity for nucleotide monophosphates[25], but also that NrdR is naturally bound to a mixture of different nucleotides, including monophosphates[39]. These observations suggest that, *in vivo*, the complexes of NrdR and nucleotide monophosphates occur not as a result of a direct interaction, but rather to the loss of phosphates from ATP or dATP already bound to NrdR. This effect might occur through unspecific events, or be controlled by a specific phosphatase, as has been proposed[25]. At the light of the behavior displayed by NrdR-AMP complexes, and given the fact that NrdR was proven to be much more stable when coupled with nucleotide monophosphates than without co-factor, we hypothesize that NrdR-AMP and NrdR-dAMP may exist in the cell as non-active or low activity storage forms, used to keep the protein from eventually form large aggregates (NrdR-ATP behavior) when dNTPs levels are not high enough to require RNR repression.

Considering all these facts, we propose a working model for the NrdR mechanism of action (**Figure A3:7**). In this model, NrdR is only found without co-factor as a transitory state, as it is much more stable when coupled to nucleotides. Using a negative-cooperative mechanism, it binds ATP or dATP depending on the cellular levels of ribonucleotides and deoxyribonucleotides. NrdR always exists as a dynamic population of different protein-nucleotide complexes and oligomeric forms. The hexamer form, which is favored upon binding of dATP, is active (or more active) for RNR repression, while higher-order oligomers are inactive, and appear when NrdR repression is released after a reduction in dNTP levels (during DNA replication, DNA repair, or when ribonucleotide reduction is compromised), which agrees with the published observations suggesting that NrdR derepression may be the cause for the observed general increase in RNR expression when class Ia RNR activity is blocked by hydroxyurea treatment[26, 38].

The identification of the hexameric form of NrdR as the active one in *E. coli* is consistent with the fact that NrdR-boxes appear as pairs separated by an integer number of turns in the DNA-helix. It would be of utmost interest to study if in other species with a wider separation of NrdR-boxes in their RNR promoters (up to 42 bp have been reported) a higher-order oligomer is required for NrdR to be active. All other genes that have been proposed to be candidate members to the NrdR regulon, such as *topA* in *Pseudomonas* and *dnaA* in *Shewanella*, display one single NrdR box in its promoter region. Our search for NrdR boxes (**Figure A3:1**, **Supplementary Tables A3:S2** and **A3:S3**) did not identify any other gene with two NrdR-boxes in tandem: a single gene from *E. coli*, the transcription regulator *slyA*, shows two putative NrdR boxes, but the distance between them is much wider than any reported for RNR promoters. Likewise, the colocalization experiment did not yield any other gene simultaneously reported as differentially expressed in transcriptomics experiments and containing a putative NrdR-box in its promoter region (**Figure A3:1B**). This, however, should not be necessarily understood as that no other genes are regulated by NrdR: in fact, NrdR has already been demonstrated to act as an activator of *topA* in *P. aeruginosa* via its binding to a single NrdR box[32]. On the contrary, the results shown in **Figure A3:1B** should be interpreted as a demonstration that the mechanism we know, NrdR-mediated repression via its binding to pairs of NrdR-boxes detectable under any physiological conditions, is limited to ribonucleotide reductases, and if other genes are controlled by NrdR we can expect a different mechanism of action.

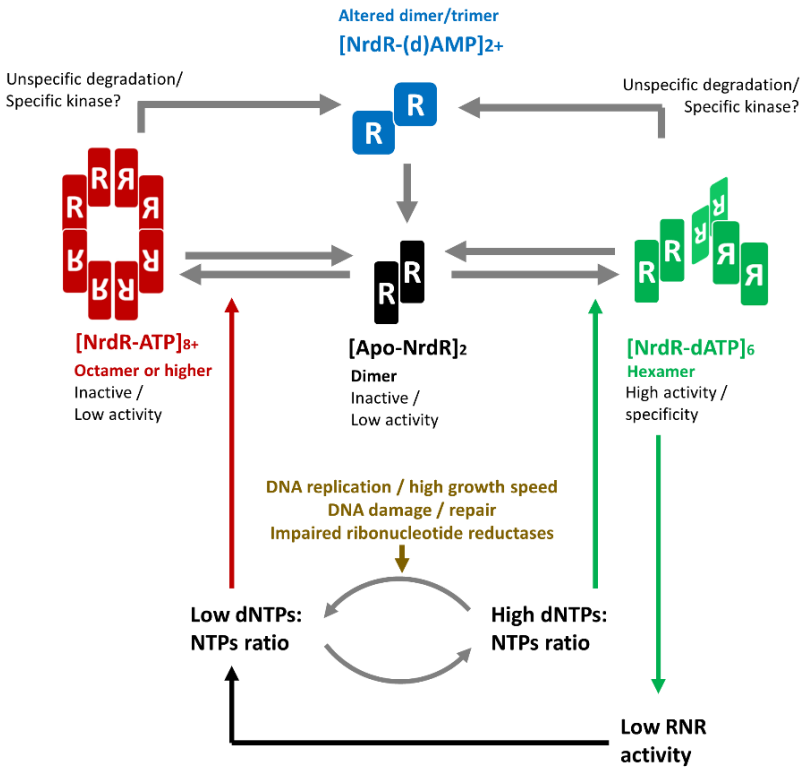

Figure A3:7. Working model of the NrdR mechanism of action. Apo-NrdR (NrdR bound to no nucleotide co-factor) is dimeric. When bound to dATP it forms hexamers, while, when bound to ATP, it forms higher oligomeric associations. The hexamer structure is the active or more-active form, which is responsible for lowering general ribonucleotide reductase activity. A high accumulation of dNTPs results in more NrdR being in its hexamer form. The dNTPs:NTPs ratio decreases during DNA replication or high DNA repair periods, as well as upon environmental alterations on ribonucleotide reduction. NrdR can also be found coupled to AMP or dAMP; evidences suggest that it does not bind nucleotide monophosphates *in vivo*, but that this form appears as an specific or unspecific degradation of NrdR-ATP or NrdR-dATP complexes. When coupled to nucleotide monophosphates, NrdR adopts a dimer-trimer form with an intermediate molecular weight.

The NrdR boxes in the known RNR promoters are also worth of mention. In *P. aeruginosa*, the main NrdR-box pair of each operon was correctly were identified (**Supplementary Table A3:S2**), but we also identified NrdR-box 3, already described by *Rodionov et al*[1], as well as an additional NrdR-box 4, located in the area identified as the 5' untranslated region (starting position -194). The function of these additional boxes is unknown, but they might uncover new levels of NrdR-mediated RNR regulation. Furthermore, concerning the main NrdR-box pair in *E. coli* (**Supplementary Table A3:S3**), it is highly significant that the NrdR-box 2 of each pair always present much higher scores than the NrdR-box 1 (less-conserved). It was described that point-mutations in NrdR box 1 caused no significant reduction in NrdR-binding, while mutations in NrdR-box 2 completely disrupted this activity[23]. Given that NrdR repression of RNR transcription has been proved to require protein oligomerization, a plausible interpretation of this fact would be that NrdR-box 2 is highly conserved to serve as a central anchor for the NrdR complex, while NrdR-box 1 would serve to position the oligomer, and could be less conserved. Additional experiments are required to verify this hypothesis.

Finally, as a bacteria-exclusive global repressor of an essential activity, NrdR has been proposed as a potential target for antimicrobial therapies[3, 22, 23, 39]. However, previous experiments showed that a *P. aeruginosa nrdR* mutant strain displayed no reduction of virulence in a *Drosophila* infection model. Our results (**Figure A3:6**) showed that the *nrdR* deletion, or, most significantly, NrdR overexpression, caused a significant decrease in viable counts and growth speed, as well as reduced virulence in *Galleria mellonella* infection. These effects agree with the observations of *Naveen et al*[40]*.,* who already proposed that antimicrobial therapies based on NrdR should be focused on its overactivation, not its repression.

Overall, the results reported in this work offer the first demonstration of the ATP/dATP-based NrdR mechanism that was proposed since the first description of this protein, as well as a reconciliation of this model with the work of *McKethan et al*[25]. The next experiments will be focused on the purification and characterization of the $NrdR_2$ protein from *P. aeruginosa*, to identify potential differences in the mechanism between species, as well as on exploring the importance of NrdR in the adaptation of the RNR network to different causes of variation of the dNTP pool, such as hydroxyurea treatment, changes in growth speed, oxidative stress, etc.

Materials and methods

Bacterial strains, plasmids and growth conditions

Bacterial strains and plasmids are listed in **Supplementary Table A3:S1**. *Escherichia coli* and *Pseudomonas aeruginosa* cells were routinely grown in Luria-Bertani broth (LB) at 37 ºC. When necessary, antibiotics were added at the following concentrations: for *E: coli*, 10 μg/ml gentamicin (Gm^R), 50 μg/ml ampicillin (Amp^R), 30 μg/ml kanamycin (Kn^R); for *P. aeruginosa*, 150 μg/ml gentamicin (Gm^R), 300 μg/ml carbenicillin (Amp^R). Liquid cultures were shaken on a horizontal shaker at 200 rpm.

Growth curves were conducted in 96-well plates. Overnight cultures (in LB medium, with the required antibiotics) of the desired strains were prepared. Cells were pelleted by centrifugation (5000 g, 10 minutes) and resuspended in sterile PBS, calculated for an OD_{550} of 1.0. The cultures for the growth curves were prepared with LB medium, the required antibiotics, and cell suspension to a final OD_{550} of 0.05. Plates were incubated at 37 ºC with orbital shaking and constant humidity in the SPARK Multimode Microplate Reader (TECAN, Switzerland) using the SPARK Small Humidity Cassette (TECAN, Switzerland). OD_{550} was monitored every 20 minutes.

DNA manipulation and plasmid construction

Recombinant DNA manipulations were carried out according to published protocols[42]. Plasmid DNA was prepared using the GeneJET Plasmid MiniPrep Kit (Thermo Scientific, ThermoFisher, MA USA), according to the manufacturer's instructions. Plasmid transformation into *P. aeruginosa* cells was done by electroporation, as previously described[43], using a Gene Pulser Xcell electroporator (Bio-Rad, CA USA). Digestion reactions with restriction enzymes were performed according to the manufacturer's instructions (Fermentas, ThermoFisher, MA USA). Ligations were performed with the T4 DNA ligase (Fermentas, ThermoFisher, MA USA). DNA fragments for cloning were obtained by PCR using Phusion High-Fidelity DNA Polymerase (Thermo Scientific, ThermoFisher, MA USA). During all plasmid construction procedures, fragments synthesized by PCR and digested with restriction enzymes were first cloned via blunt-end cloning to pJET1.2b (CloneJET PCR Cloning Kit, ThermoFisher, MA USA), according to the manufacturer's instructions, and then digested from the resulting carrier plasmid. Colony PCR reactions to test plasmid incorporation was carried out using DreamTaq Green PCR Master Mix (Thermo Scientific, ThermoFisher, MA USA). All PCR primers used in this study are listed in **Supplementary Table A3:S9**. PCR primers will be referred by their numbers, as listed on the table.

To construct the overexpression plasmid for NrdR-His_6, plasmid pET-NrdR(PAO), the *nrdR* gene from *P. aeruginosa* PAO1 was copied by PCR, obtained between restriction sites *Nde*I and *Xho*I, using primers 1 and 2. The resulting fragment and plasmid pET22b+ were digested with *Nde*I and *Xho*I and ligation was performed. The incorporation of the insert was tested by colony PCR using primers 3 and 4.

To construct plasmid pSUMO-NrdR(PAO), used for overexpression of the $NrdR_1$(PAO) protein, the *nrdR* gene from *P. aeruginosa* PAO1 was copied by PCR, obtained between long 5' and 3' tails for homologous recombination-based cloning, using primers 5 and 6. The resulting fragment was inserted into plasmid pAviTag-NN-His-SUMO-Kan (pSUMO) using a recombineering procedure according to the manufacturer's instructions (Expresso Biotin SUMO Cloning and Expression System, Lucigen, WI USA). The incorporation of the insert was tested by colony PCR using primers 9 and 10.

To construct plasmid pSUMO-NrdR(ECO), used for overexpression of the $NrdR_1$(ECO) protein, the *nrdR* gene from *E. coli* K-12 *substr*. MG1655 was copied by PCR, obtained between long 5' and 3' tails for homologous recombination-based cloning, using primers 7 and 8. The resulting fragment was inserted into plasmid pAviTag-NN-His-SUMO-Kan (pSUMO) as described above. The incorporation of the insert was tested by

colony PCR using primers 9+ and 0. The resulting fragments and plasmid pCri11a were digested and ligation was performed.

To construct plasmids pCri-NrdR(PAO) and pCri-NrdR(ECO), used for the overexpression of the $NrdR_2$ proteins, a new insert including the cutting site of the TEV protease was included by PCR amplification of the previous pSUMO-NrdR plasmids: for *P. aeruginosa*, pSUMO-NrdR(PAO) was used as a template, and PCR was performed using primers 11 and 12; for *E. coli*, pSUMO-NrdR(ECO) was used as a template, and PCR was performed using primers 13 and 14. Inserts were ligated to pCri11a as previously described[44]. The incorporation of the insert was tested by colony PCR using primers 3 and 4.

To construct plasmid pReViTA, used as a general template for ReViTA experiments, the backbone from plasmid pETS130[45] was copied by PCR and obtained between restriction sites *Xba*I and *Aat*II using primers 15 and 16. The ReViTA cassette was synthesized *de novo* using the sequence of a non-functional truncated *cat* gene[45], constitutive promoter J23119 (BBA_J23119, Registry of Standard Biological Parts), and transcription terminator B0015 (BBA_B0015, Registry of Standard Biological Part). A schematic of the ReViTA cassette can be found in **Supplementary Figure A3:S6**; its full sequence is available upon request. The ReViTA cassette and the pETS130 backbone fragment were digested with *Aat*II and *Xba*I and ligation was performed. To obtain the derivative plasmid pReViTA-PA, the promoter of the *nrdAB* operon in *E. coli* K-12 *substr*. MG1655 was copied by PCR and obtained between sites *Bam*HI and *Spe*I using primers 17 and 18. The resulting fragment and plasmid pReViTA were digested with *Bam*HI and *Spe*I and ligation was performed. The incorporation of the insert was tested by colony PCR using primers 17 and 23.

NrdR overexpression and purification

The different NrdR proteins used in this study are described in **Figure A3:2**.

The NrdR-H_6 protein from *P. aeruginosa* was overexpressed in BL21(DE3) transformed with plasmid pET-NrdR(PAO). Cells were grown in LB medium with 50 µg/ml ampicillin and 100 µM $ZnSO_4$ and incubated at 37 ºC with vigorous shaking. When cultures reached and OD_{550} of 0.5, protein overexpression was induced by adding IPTG to a concentration of 0.1 mM. Cells were then cultured at 18 ºC over-night (14-16 hours).

To obtain the crude extracts, cells were pelleted by centrifugation (6000 g, 20 min, 4 ºC) and resuspended in 25 ml (per liter of original culture) of NrdR-lysis buffer: 50 mM Tris-HCl (pH 8.5 at 25 ºC), 1 M NaCl, 20 mM imidazole, 1 mM phenylmethylsulphonyl fluoride (PMSF), 100 µM $ZnSO_4$, and 10% glycerol. The suspension was then sonicated until clear (20 pulses of 20 s, with 50 s cooldown between pulses, using a 1/2'' tip in a Branson 450 Digital Sonifier, Marshal Scientific, NH USA) and centrifuged at high speed (15000 g, 20 min, 4 ºC), keeping the supernatant containing the soluble fraction, which was frozen at -80 ºC for long term storage. To obtain the crude extracts, cells were pelleted, resuspended, sonicated and centrifuged as described above for NrdR-H_6. The crude extracts then suffered a first step of purification by Immobilized Metal Affinity Chromatography (IMAC1) using a 5 ml Mini-Nuvia IMAC Cartridge (Bio-Rad, CA USA) in an FPLC system (Biologic DuoFlow System, Bio-Rad, CA USA). Protein samples suffered a DNA precipitation step (30 minutes incubation with streptomycin sulfate 1%, at 4ºC) and were diluted with buffer A1 to a concentration of less than 1 mg/ml of total protein before being injected into the column. The column was equilibrated with 5 column volumes (CV) of Buffer A1 (50 mM Tris-HCl pH 8.5, 1 M NaCl, 20 mM imidazole). A washing step was carried out using 5 CV of Buffer A1. Mixtures with buffer B1 was then introduced to start the elution (50 mM Tris-HCl pH 8.5, 1 M NaCl, 500 mM imidazole). First, contaminant proteins were removed with a non-specific elution step using 5 CV of buffer with 50 mM imidazole. Then, the protein was recovered in a specific elution step using 5 CV of buffer with 200 mM imidazole. The resulting fractions were analyzed by SDS-PAGE. Fractions containing the protein of interest were concentrated and diafiltrated against buffer 5x NrdR: 100 mM Tris-HCl (pH 9.0 at 25 ºC), 400 mM KCl, 5 mM MgC_{l2}, 5 mM DTT, 250 µM $ZnSO_4$, and 25% glycerol, using VivaSpin 20 10000 MWCO Ultrafiltration units (Sartorius AG, Germany).

The $NrdR_1$ proteins from *E. coli* and *P. aeruginosa* were overexpressed in XCell F' Chemically Competent Cells (Expresso Biotin SUMO Cloning and Protein Expression System, Lucigen, WI USA) transformed with plasmids pSUMO-NrdR(ECO) and pSUMO-NrdR(PAO), respectively. Cells were grown in 1-liter cultures of LB medium supplemented with 30 µg/ml kanamycin and 50 µM $ZnSO_4$ and incubated at 37 ºC with vigorous shaking. When cultures reached and OD_{550} of 1.0, protein overexpression was induced by adding 0.1% rhamnose. Cells were then cultured at 18 ºC over-night (14-16 hours).

To obtain the crude extracts, cells were pelleted, resuspended, sonicated and centrifuged as described above for NrdR-H_6. The crude extracts then suffered a first step of purification (IMAC1) using the same procedure described above for NrdR-H_6. The resulting fractions were analyzed by SDS-PAGE. Fractions containing the protein of interest were concentrated and diafiltrated against buffer 4x NrdR-PROT: 100 mM Tris-HCl (pH 8.5 at 25 ºC), 600 mM NaCl, 4 mM DTT, 40 µM $ZnSO_4$ using VivaSpin 20 10000 MWCO Ultrafiltration units (Sartorius AG, Germany).

Before SUMO protease digestion, the protein was diluted with water to a final concentration of 1x NrdR-PROT buffer, and + 2 mM fresh DTT was added. SUMO protease (Lucigen, WI USA) was added (1 unit for each 300 µg of protein) and the reaction mixture was incubated for 3 hours at 30 ºC with gentle mixing. The extra DTT was removed from the digested protein mixture (but not completely, to avoid protein precipitation) by dialysis against 50 mM Tris-HCl (pH 9.0 at 25 ºC), 1 M NaCl, 0.5 mM DTT, using Slide-a-Lyzer Dialysis Cassettes (ThermoFisher, MA USA).

The digested protein then suffered a second step of purification by a negative IMAC (IMAC2) in the same column and system mentioned above. First, the column was equilibrated with 5 CV of Buffer A2 (50 mM Tris-HCl pH 9.0, 1 M NaCl, 20 mM imidazole). Protein samples were then injected into the column. The protein was recovered from the flow-through, as the SUMO-tag and SUMO-protease are retained. The resulting fractions were analyzed by SDS-PAGE. Fractions containing the protein of interest were concentrated and diafiltrated as described above, against buffer 5x NrdR: 100 mM Tris-HCl (pH 9.0 at 25 ºC), 400 mM KCl, 5 mM MgC_{l2}, 5 mM DTT, 250 µM $ZnSO_4$, 25% glycerol.

The $NrdR_2$ proteins from *E. coli* and *P. aeruginosa* were purified using the same protocol as the $NrdR_1$ presented above, with the following changes: The first difference is the protein expression step. $NrdR_2$ proteins were overexpressed in BL21(DE3) transformed with plasmids pCri-NrdR(PAO) or pCri-NrdR(ECO). Cells were grown in LB medium with 30 µg / ml kanamycin and 200 µM $ZnSO_4$ and incubated at 37 ºC with vigorous shaking. After 3 hours of incubation, protein overexpression was induced by adding IPTG to a concentration of 0.2 mM. Cells were then cultured at 18 ºC over-night (16 hours). The second difference is the fusion-protein digestion step. Instead of SUMO protease, recombinant TEV protease produced as previously described[44] was added to the concentrated fusion protein obtained from IMAC-1 at an NrdR:protease molar ratio of 25:1, and digestion occurred for 16 hours at 4 ºC.

All proteins were quantified after every purification step using BIO-RAD Protein Assay (Bio-Rad, CA USA), according to the manufacturer's instructions. If necessary, the concentrated protein was frozen at -80 ºC for long term storage.

Protein techniques

Proteins were routinely examined in pre-cast SDS-PAGE gels (4–20% Mini-PROTEAN TGX Precast Protein Gels, Bio-Rad, CA USA), and stained with a Coomasie-blue-based stain (PageBlue Protein Staining Solution, Thermo Scientific, ThermoFisher, MA USA), according to the manufacturer's instructions.

Anti-NrdR western blotting was carried out as previously described[45]. A TransBlot-Turbo device and TransBlot-Turbo Mini PVDF Transfer packs (Bio-Rad, CA USA) were used for transferring the proteins to the membranes, according to the manufacturer's instructions. As primary antibody, we used a rabbit polyclonal anti-NrdR serum (ThermoFisher, MA USA), applying 2 hours of incubation at 4 ºC with a 1:500 dilution of the

serum. The detection of primary antibodies was carried out using a goat anti-rabbit horseradish peroxidase (HRP) conjugate (Bio-Rad, CA USA), applying 1 hour of incubation at 4 ºC with a 1:5000 dilution of the antibody. The antibody-antigen complex was detected using the Amersham ECL Primer Western Blotting Reagent (GE Healthcare, IL USA) according to the manufacturer's instructions. Proteins were visualized in an ImageQuant LAS4000 Mini device (GE Healthcare, IL USA).

Electrophoretic mobility shift assay

Two DNA probes were used for EMSA: an NrdR-sensitive probe containing the full promoter region of *nrdAB* from *E. coli* K-12 *substr*. MG1655 (P*nrdA* ECO) and a negative-control, NrdR-insensitive probe containing an unrelated internal sequence of the *anr* gene from *P. aeruginosa* PAO1 (*anr*). Probes were generated by a two PCRs method, as described before[46]. Briefly, a first PCR is conducted to obtain the corresponding fragments with an arbitrary sequence added at the 3' end of every fragment (M13 complementarity tail); primers 17 and 25 were used for *PnrdA* ECO, and primers 26 and 27 for *anr*. Then, a second PCR uses a WellRED oligo (Millipore Sigma, MA USA) coupled to the near-infrared fluorophore D3-phosphoramidite (D3-PA); primers 17 and 28 were used for *PnrdA* ECO, and primers 26 and 28 for *anr*. Probes were purified from agarose gels using the GeneJET Gel Extraction Kit (Thermo Scientific, ThermoFisher, MA USA) and used in EMSA experiments at a fixed quantity of 100 fmol.

Purified NrdR-H_6, $NrdR_1$, or $NrdR_2$ proteins were used in DNA-protein binding reactions in total amounts of 0, 200 or 400 pmol per reaction, corresponding to 0, 2000 or 4000 protein:DNA molar ratios. Binding reactions (20 µl) also contained BSA (0.2 µg / reaction) and salmon sperm DNA (2 µg / reaction), as well as 4x NrdR-binding buffer, added to a final 1x concentration of 20 mM Tris-HCl (pH 9.0 at 25 ºC), 80 mM KCl, 1 mM $MgCl_2$, 1 mM dithiothreitol, 50 µM $ZnSO_4$, and 5% glycerol. Reactions were incubated at room temperature for 60 minutes before gel electrophoresis.

Electrophoresis was performed in 4% acrylamide gels, prepared with a 37.5:1 proportion acrylamide:bis-acrylamide and using 5% triethylene glycol as an additive for increase DNA-protein complex stability. Gels were casted and run using the PROTEAN II xi system (Bio-Rad, CA USA), according to the manufacturer's instructions. Gels were run with 25 mA constant current, at 4 ºC, for 4 hours. Final images were obtained by scanning the gels in an Odyssey Imaging System device (LI-COR Biosciences, NE USA) working in the 700 nm channel.

Study of the NrdR quaternary structure

For SEC (Size-Exclusion Chromatography) experiments, purified NrdR-H_6 protein from *P. aeruginosa*, as well as $NrdR_1$ proteins from *E. coli* and *P. aeruginosa*, were used. Protein was pre-incubated with nucleotides, added as 10 mM solutions directly to the concentrated protein to a final molar ratio of 20:1 nucleotide:protein, and incubated for 1 hour at room temperature. We used a Superdex 200 10/300 GL column (20 ml bed volume) (GE Healthcare, IL USA) in a BioLogic DuoFlow FPLC System (Bio-Rad, CA USA). All the process occurred at a fixed flow rate of 0.5 ml/min with the following elution buffer: 50 mM Tris-HCl (pH 9.0 at 25 ºC), 250 mM NaCl, 5 mM DTT. When required, nucleotide was added to the column, calculated for a 1:1 molar ratio of nucleotide:protein (taking the samples as reference). The column was equilibrated with 2 column volumes (CV) of elution buffer before injecting the samples, and when protein-nucleotide complexes were to be run it was re-equilibrated with 0.5 CV of elution buffer containing the corresponding nucleotide before their injections. Sample concentrations were normalized at 0.5 mg / ml, and a fixed injection volume of 220 µl was used. Data was analyzed using BioLogic DuoFlow Software (Bio-Rad, CA USA).

For SEC-MALS (Size-Exclusion Chromatography – Multi Angle Light Scattering) experiments, purified $NrdR_2$ proteins from *E. coli* or *P. aeruginosa* were used. When required, protein was pre-incubated with nucleotides, added as 10 mM solution directly to the concentrated protein to a final molar ratio of 20:1

nucleotide:protein, and incubated for 3 hours at room temperature. We used a Superdex 200 10/300 GL column (20 ml bed volume) (GE Healthcare, IL USA) in an ÄKTA Pure Protein Purification System (GE Healtchare, IL USA). All the process occurred at a fixed flow rate of 0.5 ml/min with the following elution buffer: 50 mM Tris-HCl (pH 9.0 at 25 ºC), 250 mM NaCl, 1 mM DTT. When necessary, fresh nucleotides were added to the elution buffer at a final concentration of 0.025 mM.

For *E. coli*, sample concentrations were normalized at 1 mg / ml before injection. Injection volumes were limited by sample availability, and were as follows: 80 µl $NrdR_2$, 85 µl $NrdR_2$ + AMP, 60 µl $NrdR_2$ + ATP, 60 µl $NrdR_2$ + dATP. For *P. aeruginosa*, sample concentrations were normalized at 2 mg / ml, and injection volumes were as follows: 60 µl $NrdR_2$ + AMP, 40 µl $NrdR_2$ + ATP, 40 µl $NrdR_2$ + dATP. SEC data was analyzed using UNICORN 7 (GE Healthcare, IL USA). MALS data was obtained with a MiniDawn MALS Detector (Wyatt Technology, CA USA), and analyzed using ASTRA 7 (Wyatt Technology, CA USA).

Bioinformatic prediction of NrdR-boxes

The DNA queries used for the global search for NrdR-boxes were composed of sequences containing 450 bp and 20 bp downstream of each gene in the genomes of *E. coli* K-12 *substr.* MG1655 and *P. aeruginosa* PAO1. To obtain these sequences, we started from the FASTA files containing their genomes and the GFF3 files containing the features lists for their genomes: MG1655 (NCBI Reference Sequence NC_000913.3) and PAO1 (NCBI Reference Sequence NC_002516.2). Each GFF3 file was then modified to contain only the features corresponding to genes, and deduplicated so that each gene will only be included one; this was carried out using an R function written as a part of this work, gff.to.genes.R (**File A3:1.R**). We indexed the FASTA files using SAMtools[30] function *faidx* and limited the index file (FAI) to the first two columns. Then, we modified the genes list GFF3 using BEDtools[47] using functions *bedtools flank* and *bedtools slop* to point not at the genes, but at the sequences from 450 bp before their ATG to 20 bp after it. Finally, we obtained the DNA sequence of these features using function *bedtools getfasta*. A comprehensive UNIX Shell Script for the whole process is available upon request.

Weight matrices for the NrdR-box consensus sequence in *E. coli*, *P. aeruginosa* or all the class γ-proteobacteria were generated using the data published by *Rodionov et al.*[1] in a MEME[27] (MEME Suite[28]) run, searching for a 16 bp motif with one occurrence per sequence, only on the given strand. The weight matrices generated in the previous step were then used in a FIMO[31] (MEME Suite[28]) search on the promoter-enriched FASTA file generated for both genomes, with a *p*-value threshold of $1 \cdot 10^{-4}$.

RNA-seq and RNA-seq data treatment

To extract samples for RNA-seq, we used three independent cultures of *P. aeruginosa* PAO1 in 25 ml LB medium and three of its isogenic mutant strain PAO1 Δ*nrdR* in 25 ml LB medium supplemented with 40 µg/ml tetracycline. Cultures were grown to an OD_{550} of 0.5, and then stopped and fixed using RNAprotect Bacteria Reagent (QIAGEN, Germany), according to the manufacturer's instructions. Then, RNA was extracted using RNeasy Mini RNA Isolation Kit (QIAGEN, Germany), according to the manufacturer's instructions. Reverse transcription, library generation, and RNA sequencing were performed by Beckman Coulter Genomics (CA USA), according to the protocol "Illumina TruSeq Stranded Total RNA with Ribo-Zero rRNA Removal (Bacteria)". The platform used was Illumina 1.9, with library TruSeq3-PE-2. A total of 6 samples were analyzed, and a total of 362 million paired-end reads were generated (2 x 100 bp each).

RNA-seq data were received as untreated sequence+quality data (FASTQ). To remove adapter sequences and low quality bases, a first FASTQ trimming step was introduced using Trimmomatic[48] version 0.36 (LEADING:5, TRAILING:5, SLIDINGWINDOW 4:15, MINLEN:25, LLUMINACLIP:/RNA/REF/TruSeq3-PE-2.fa:2:30:10:2:true). Data was then mapped using end-to-end alignment with bowtie[49] version 1.5, allowing multiple binding. Mapping parameters were: *-S -t --fr -n 2 -l 28 -e 70 -k 5 --best --strata --allow-contain --no-*

unal –nomaqround. The *P. aeruginosa* PAO1 genome was used as reference (NCBI Reference Sequence NC_002516.2). The output SAM file generated by bowtie was converted to BAM and sorted using SAMtools[30] functions *view* and *sort*, with default parameters. The quality of the mapped data was assessed using Qualimap[50] 2.2.1. Differentially expressed genes were then obtained using DESeq2[51] version 3.9 (R, Bioconductor[52]) according to the general pipeline[53]. Only genes with an absolute fold-change over 2.0 were considered.

Regulated in Vitro Transcription Assay (ReViTA)

The ReViTA experiments in this work were made with the pReViTA-PA plasmid, a derivative of pReViTA containing the P*nrdA* promoter from *E. coli* K-12 *substr*. MG1655. 100 fmol of this plasmid were used as a template for all reactions.

The first step was the protein-nucleotide incubation reaction. The required amount of NrdR was mix with its corresponding nucleotide, added as 10 mM solution directly to the concentrated protein, and incubated for 1 hour at room temperature.

The second step was the DNA-protein binding reaction. Protein-nucleotide complex calculated for 0 pmol, 100 pmol or 200 pmol of total protein (corresponding to 0, 1000 or 2000 protein:DNA molar ratio) were added to a reaction containing 100 fmol of pReViTA-PA, 2 µg of poly(d[I-C]) as competition DNA, as well as 5x-IVT buffer, added to a final 1x concentration of: 40 mM Tris-HCl (pH 8.0 at 25 ºC), 150 mM KCl, 10 mM MgCl2, 1 mM DTT, 5% glycerol. Water was added to each reaction to a final volume of 15 µl. Reaction were incubated at room temperature for 1 hour.

The third step was *in vitro* transcription. To the previous DNA-protein binding reaction, we added: 0.5 units of *E. coli* RNA polymerase saturated with Sigma70 factor (New England Biolabs, MA USA), 20 units of Ribolock RNase inhibitor (Thermo Scientific, ThermoFisher, MA USA), 0.05 units of yeast inorganic pyrophosphatase (Millipore Sigma, MA USA), spermidine to a final concentration of 1 mM, and extra 5x IVT-buffer to a final concentration of 1x. These components were added as a total volume of 5 µl, so that the *in vitro* transcription reactions had a final volume of 20 µl. Reactions were then incubated at 37 ºC for 4 hours, after which they were stopped by removing the DNA template using TURBO DNase (Invitrogen, ThermoFisher, MA USA), according to the manufacturer's instructions.

The fourth step was RNA quantification by qRT-PCR. RNA was reverse transcribed using Maxima Reverse Transcriptase (Thermo Scientific, ThermoFisher, MA USA), according to the manufacturer's instructions, and using a mixture of two gene-specific primers for the TEST and CTRL sequences (primers 21 and 24, respectively). The resulting cDNAs were diluted 1:100 with water and quantified in a qPCR reaction with PowerUP SYBR Green Master Mix (Applied Biosystems, CA USA) in a StepOne Plus Real-Time PCR System (Applied Biosystems, CA USA). Two independent qPCR reactions were used for the TEST (primers 19+20) and CTRL sequences (primers 22+23). For absolute quantitation, the same qPCR amplicons were obtained from chromosomic DNA and diluted to a 1 ng/µl concentration. Then, decimal serial dilutions of the amplicons were prepared, and dilutions 10^{-4}, 10^{-6}, 10^{-7}, and 10^{-9} were used for the standard curve.

The fifth and final step was data treatment. All qRT-PCR data was converted into copies using the standard curves. Then, for each sample, TEST copies were divided by its corresponding CTRL copies to capture all unspecific inhibition. Normalized copies of problem reactions (with NrdR) were then divided by the normalized copies of control reactions (without NrdR) to obtain the relative percentage of transcriptional activity.

Galleria mellonella model of infection

Galleria mellonella larvae were routinely grown at 35 ºC and 100% humidity. 3 weeks-old larvae were separated for infection and placed in Petri dishes (5 larvae per dish).

To prepare bacterial cultures for infection, overnight cultures (in LB medium, with the required antibiotics) of the desired strains were first prepared. Cells were pelleted by centrifugation (5000 g, 10 minutes) and resuspended in sterile PBS, calculated for an OD_{550} of 1.0. The centrifugation-resuspension step was repeated three additional times. Sterile PBS was added to the final suspension to obtain an OD_{550} of 1.0. Decimal serial dilutions of these suspensions in PBS were prepared from 10^{-1} to 10^{-5}, and then a 1:5 dilution to $2 \cdot 10^{-6}$. 10 µl of the $2 \cdot 10^{-6}$ dilutions per larva were injected using Hamilton syringes (Hamilton, NE USA).

10 larvae (2 Petri dishes) per condition were infected, and a control group of 10 larvae injected with sterile PBS was included. Larvae were then incubated at 37 ºC and monitored from 12 h to 24 h after injection every 30 minutes, and a final time 36 h after infection. Kaplan-Meier survival curves were drawn and analyzed using PRISM 6 (GraphPad Software, CA USA).

References

1. Rodionov DA, Gelfand MS. Identification of a bacterial regulatory system for ribonucleotide reductases by phylogenetic profiling. Trends Genet. 2005;21(7):385-9.
2. Torrents E, Shanin M, Sjöberg B-M. The ribonucleotide reductase family - genetics and genomics. Ribonucleotide reductases. Hauppauge, NY: Nova Science Publishers; 2008. p. 17-77.
3. Torrents E. Ribonucleotide reductases: essential enzymes for bacterial life. Frontiers in cellular and infection microbiology. 2014;4:52.
4. Nordlund P, Reichard P. Ribonucleotide reductases. Annu Rev Biochem. 2006;75:681-706.
5. Cendra MdM. Estudi de l'expressió i funció de les Ribonucleotidil Reductases d'Escherichia coli. 2013.
6. Blakley RL, Barker HA. Cobamide stimulation of the reduction of ribotides to deoxyribotides in Lactobacillus leichmannii. Biochemical and biophysical research communications. 1964;16(5):391-7.
7. Crespo A, Blanco-Cabra N, Torrents E. Aerobic Vitamin B12 Biosynthesis Is Essential for Pseudomonas aeruginosa Class II Ribonucleotide Reductase Activity During Planktonic and Biofilm Growth. Frontiers in microbiology. 2018;9:986.
8. Reichard P, Ehrenberg A. Ribonucleotide Reductase-- a Radical Enzyme. Science. 1983;221(4610):514-9.
9. Mathews CK. DNA precursor metabolism and genomic stability. Faseb j. 2006;20(9):1300-14.
10. Wheeler LJ, Rajagopal I, Mathews CK. Stimulation of mutagenesis by proportional deoxyribonucleoside triphosphate accumulation in Escherichia coli. DNA repair. 2005;4(12):1450-6.
11. Herrick J, Sclavi B. Ribonucleotide reductase and the regulation of DNA replication: an old story and an ancient heritage. Molecular microbiology. 2007;63(1):22-34.
12. Reichard P. Ribonucleotide reductases: the evolution of allosteric regulation. Arch Biochem Biophys. 2002;397(2):149-55.
13. Brown NC, Reichard P. Role of effector binding in allosteric control of ribonucleoside diphosphate reductase. Journal of molecular biology. 1969;46(1):39-55.
14. Hofer A, Crona M, Logan DT, Sjoberg BM. DNA building blocks: keeping control of manufacture. Crit Rev Biochem Mol Biol. 2012;47(1):50-63.
15. Larsson KM, Andersson J, Sjoberg BM, Nordlund P, Logan DT. Structural basis for allosteric substrate specificity regulation in anaerobic ribonucleotide reductases. Structure. 2001;9(8):739-50.
16. Larsson KM, Jordan A, Eliasson R, Reichard P, Logan DT, Nordlund P. Structural mechanism of allosteric substrate specificity regulation in a ribonucleotide reductase. Nature structural & molecular biology. 2004;11(11):1142-9.
17. Johansson R, Jonna VR, Kumar R, Nayeri N, Lundin D, Sjoberg BM, et al. Structural Mechanism of Allosteric Activity Regulation in a Ribonucleotide Reductase with Double ATP Cones. Structure. 2016;24(6):906-17.
18. Jonna VR, Crona M, Rofougaran R, Lundin D, Johansson S, Brannstrom K, et al. Diversity in Overall Activity Regulation of Ribonucleotide Reductase. The Journal of biological chemistry. 2015;290(28):17339-48.
19. Eriksson M, Uhlin U, Ramaswamy S, Ekberg M, Regnstrom K, Sjoberg BM, et al. Binding of allosteric effectors to ribonucleotide reductase protein R1: reduction of active-site cysteines promotes substrate binding. Structure. 1997;5(8):1077-92.
20. Borovok I, Gorovitz B, Yanku M, Schreiber R, Gust B, Chater K, et al. Alternative oxygen-dependent and oxygen-independent ribonucleotide reductases in Streptomyces: cross-regulation and physiological role in response to oxygen limitation. Molecular microbiology. 2004;54(4):1022-35.
21. Borovok I, Kreisberg-Zakarin R, Yanko M, Schreiber R, Myslovati M, Aslund F, et al. Streptomyces spp. contain class Ia and class II ribonucleotide reductases: expression analysis of the genes in vegetative growth. Microbiology. 2002;148(Pt 2):391-404.

22. Grinberg I, Shteinberg T, Gorovitz B, Aharonowitz Y, Cohen G, Borovok I. The Streptomyces NrdR transcriptional regulator is a Zn ribbon/ATP cone protein that binds to the promoter regions of class Ia and class II ribonucleotide reductase operons. Journal of bacteriology. 2006;188(21):7635-44.
23. Torrents E, Grinberg I, Gorovitz-Harris B, Lundstrom H, Borovok I, Aharonowitz Y, et al. NrdR controls differential expression of the Escherichia coli ribonucleotide reductase genes. Journal of bacteriology. 2007;189(14):5012-21.
24. Borovok I, Gorovitz B, Schreiber R, Aharonowitz Y, Cohen G. Coenzyme B12 controls transcription of the Streptomyces class Ia ribonucleotide reductase nrdABS operon via a riboswitch mechanism. Journal of bacteriology. 2006;188(7):2512-20.
25. McKethan BL, Spiro S. Cooperative and allosterically controlled nucleotide binding regulates the DNA binding activity of NrdR. Molecular microbiology. 2013;90(2):278-89.
26. Case ED, Akers JC, Tan M. CT406 encodes a chlamydial ortholog of NrdR, a repressor of ribonucleotide reductase. Journal of bacteriology. 2011;193(17):4396-404.
27. Grant CE, Bailey TL, Noble WS. FIMO: scanning for occurrences of a given motif. Bioinformatics (Oxford, England). 2011;27(7):1017-8.
28. Bailey TL, Boden M, Buske FA, Frith M, Grant CE, Clementi L, et al. MEME SUITE: tools for motif discovery and searching. Nucleic acids research. 2009;37(Web Server issue):W202-8.
29. Stover CK, Pham XQ, Erwin AL, Mizoguchi SD, Warrener P, Hickey MJ, et al. Complete genome sequence of *Pseudomonas aeruginosa* PAO1, an opportunistic pathogen. Nature. 2000;406(6799):959-64.
30. Li H, Handsaker B, Wysoker A, Fennell T, Ruan J, Homer N, et al. The Sequence Alignment/Map format and SAMtools. Bioinformatics (Oxford, England). 2009;25(16):2078-9.
31. Bailey TL, Elkan C. Fitting a mixture model by expectation maximization to discover motifs in biopolymers. Proceedings International Conference on Intelligent Systems for Molecular Biology. 1994;2:28-36.
32. Crespo A, Pedraz L, Torrents E. Function of the *Pseudomonas aeruginosa* NrdR Transcription Factor: Global Transcriptomic Analysis and Its Role on Ribonucleotide Reductase Gene Expression. PloS one. 2015;10(4):e0123571.
33. The Gene Ontology Resource: 20 years and still GOing strong. Nucleic acids research. 2019;47(D1):D330-d8.
34. Ashburner M, Ball CA, Blake JA, Botstein D, Butler H, Cherry JM, et al. Gene Ontology: tool for the unification of biology. Nature genetics. 2000;25(1):25-9.
35. Hay RT. SUMO: A History of Modification. Molecular cell. 2005;18(1):1-12.
36. Kuo D, Nie M, Courey AJ. SUMO as a solubility tag and in vivo cleavage of SUMO fusion proteins with Ulp1. Methods in molecular biology (Clifton, NJ). 2014;1177:71-80.
37. Tropea JE, Cherry S, Waugh DS. Expression and purification of soluble His 6-tagged TEV protease. High throughput protein expression and purification: Springer; 2009. p. 297-307.
38. Panosa A, Roca I, Gibert I. Ribonucleotide reductases of Salmonella typhimurium: transcriptional regulation and differential role in pathogenesis. PloS one. 2010;5(6):e11328.
39. Grinberg I, Shteinberg T, Hassan AQ, Aharonowitz Y, Borovok I, Cohen G. Functional analysis of the Streptomyces coelicolor NrdR ATP-cone domain: role in nucleotide binding, oligomerization, and DNA interactions. Journal of bacteriology. 2009;191(4):1169-79.
40. Naveen V, Hsiao CD. NrdR Transcription Regulation: Global Proteome Analysis and Its Role in Escherichia coli Viability and Virulence. PloS one. 2016;11(6):e0157165.
41. Mao X, Ma Q, Zhou C, Chen X, Zhang H, Yang J, et al. DOOR 2.0: presenting operons and their functions through dynamic and integrated views. Nucleic acids research. 2014;42(Database issue):D654-9.
42. Russell J, David W. Sambrook, Molecular cloning: a laboratory manual. Cold; 2001.

43. Chuanchuen R, Narasaki CT, Schweizer HP. Benchtop and microcentrifuge preparation of *Pseudomonas aeruginosa* competent cells. BioTechniques. 2002;33(4):760, 2-3.
44. Goulas T, Cuppari A, Garcia-Castellanos R, Snipas S, Glockshuber R, Arolas JL, et al. The pCri System: a vector collection for recombinant protein expression and purification. PloS one. 2014;9(11):e112643.
45. Sjoberg BM, Torrents E. Shift in ribonucleotide reductase gene expression in *Pseudomonas aeruginosa* during infection. Infection and immunity. 2011;79(7):2663-9.
46. Crespo A, Pedraz L, Van Der Hofstadt M, Gomila G, Torrents E. Regulation of ribonucleotide synthesis by the *Pseudomonas aeruginosa* two-component system AlgR in response to oxidative stress. Scientific reports. 2017;7(1):17892.
47. Quinlan AR, Hall IM. BEDTools: a flexible suite of utilities for comparing genomic features. Bioinformatics (Oxford, England). 2010;26(6):841-2.
48. Bolger AM, Lohse M, Usadel B. Trimmomatic: a flexible trimmer for Illumina sequence data. Bioinformatics (Oxford, England). 2014;30(15):2114-20.
49. Langmead B, Trapnell C, Pop M, Salzberg SL. Ultrafast and memory-efficient alignment of short DNA sequences to the human genome. Genome biology. 2009;10(3):R25.
50. Okonechnikov K, Conesa A, Garcia-Alcalde F. Qualimap 2: advanced multi-sample quality control for high-throughput sequencing data. Bioinformatics (Oxford, England). 2016;32(2):292-4.
51. Love MI, Huber W, Anders S. Moderated estimation of fold change and dispersion for RNA-seq data with DESeq2. Genome biology. 2014;15(12):550.
52. Huber W, Carey VJ, Gentleman R, Anders S, Carlson M, Carvalho BS, et al. Orchestrating high-throughput genomic analysis with Bioconductor. Nat Methods. 2015;12(2):115-21.
53. Love M, Anders S, Huber W. Beginner's guide to using the DESeq2 package. Genome biology. 2014;15:550.

A3 Supporting information

Mechanism of action of NrdR, a global regulator of ribonucleotide reduction

Supplementary figure A3:S1. Additional SDS-PAGE gel images of the NrdR fusion-proteins.

Coomasie-blue-stained SDS-PAGE gels of the critical steps of the expression and purification of NrdR fusion proteins $NrdR_1$ (*E. coli*) and $NrdR_2$ (*P. aeruginosa* and *E. coli*). A step-by-step purification procedure of $NrdR_1$ (*P. aeruginosa*) can be found in Figure A3:2. Samples are labeled as follows: **CE**, overexpression crude extract; **NI**, non-induced protein extract; **E1**, elution of the chromatographic step IMAC1; **TAG1**, first elution peak of tagged proteins in chromatographic step IMAC2; **TAG2**, second elution peak of tagged proteins in chromatographic step IMAC2; **WM**, weight marker. The numbers at the left of the weight number indicate molecular weight in KDa. The bands in RL1 corresponding to the undigested fusion protein, digested tagged fraction, and digested NrdR monomer, are labeled at their approximated heights at the right of the images.

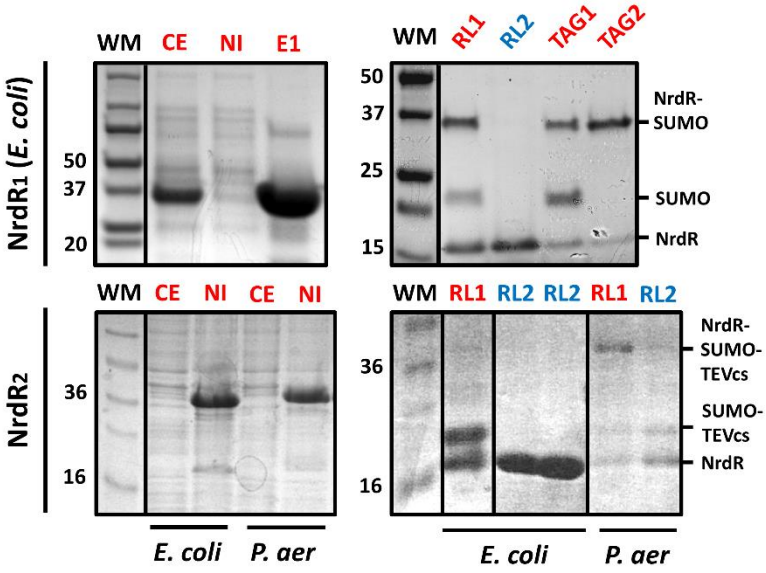

Supplementary figure A3:S2. Control of nucleotide absence in as-prepared $NrdR_1$

Ion-pair reverse-phase HPLC chromatograms of nucleotide and protein-nucleotide preparations. **A, B**, standard nucleotide mixtures, 20 µmol each, in the same buffer as the NrdR samples: ribonucleotides (A), and deoxyribonucleotides (B). dADP was not included in the experiment. **C, D,** supernatant of a PCA precipitation of $NrdR_1$ protein from *P. aeruginosa*: after pre-incubation for 1 hour at room temperature with a 20:1 molar excess of AMP and removal of non-bound nucleotide through size-exclusion desalting (Zeba Spin Desalting Columns, ThermoFisher, MA USA) (C), and without nucleotide pre-incubation (D). An equivalent experiment was conducted using $NrdR_2$ protein from *E. coli*, with a similar result (data not shown).

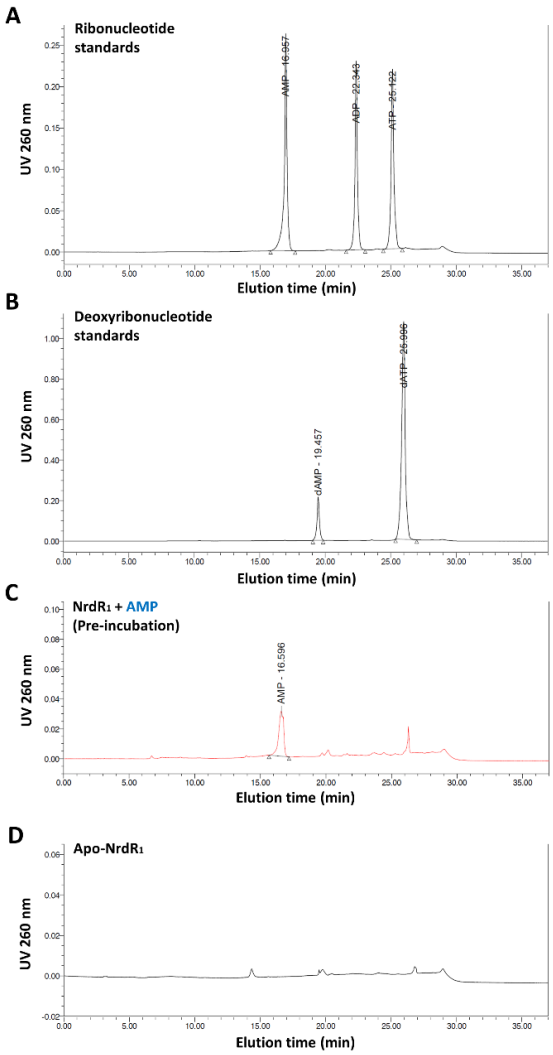

Supplementary figure A3:S3. NrdR-nucleotide size exclusion chromatography.

A, size-exclusion chromatogram. All peaks were analyzed by SDS-PAGE electrophoresis to evaluate the presence or absence of protein. Protein-containing peaks are labeled indicating its injection and peak numbers. Other peaks are caused by the free nucleotide in the samples (labeled as N) or by the oxidized DTT in the column wash buffer or samples (labeled as D). Equilibration and washing steps between nucleotide series are omitted. **B**, SDS-PAGE analysis of representative peaks. The numbers in the weight marker lanes indicate the molecular weight in KDa of the band above. **C**, EMSA of the proteins used for the size exclusion chromatography experiments. The DNA band used is P*nrdA* ECO (see materials and methods). Numbers indicate the amount of protein in pmol.

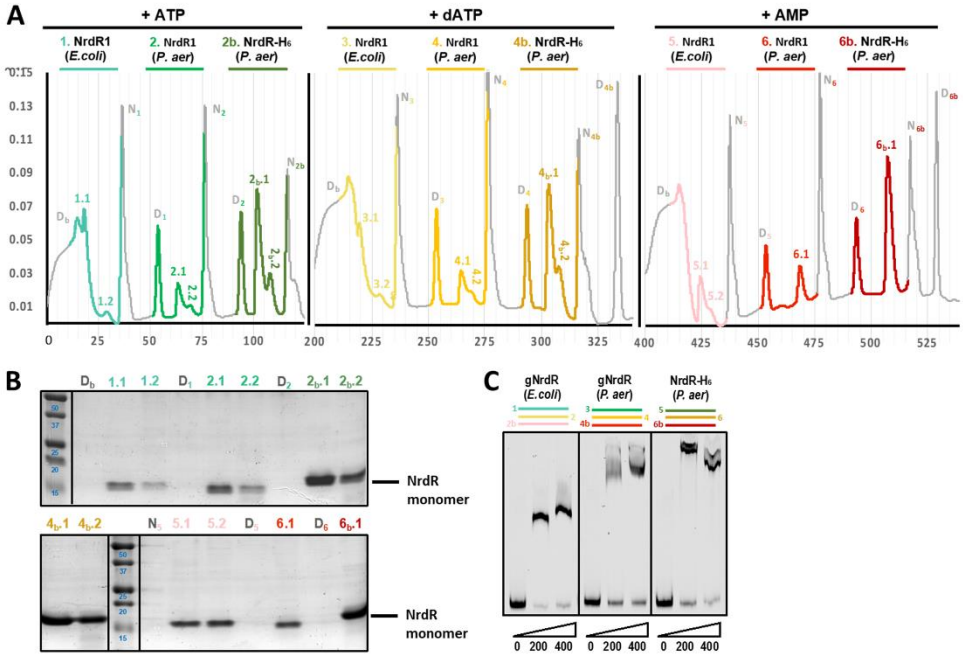

Supplementary figure A3:S4. Effect of long protein-nucleotide incubation on NrdR quaternary structure

SEC-MALS experiment comparing NrdR quaternary structure when exposed to different nucleotides in the running buffer (light colors) and when pre-incubated with different nucleotides for 3 hours and then exposed to the same nucleotide in the running buffer (right colors). Only the elution volumes corresponding to protein peaks are shown. MALS detection data is normalized to a maximum signal of 1.0 in each sample. The shift in the protein peak caused by additional pre-incubation step is indicated on top of the peaks, together with the difference it represents in molecular weight.

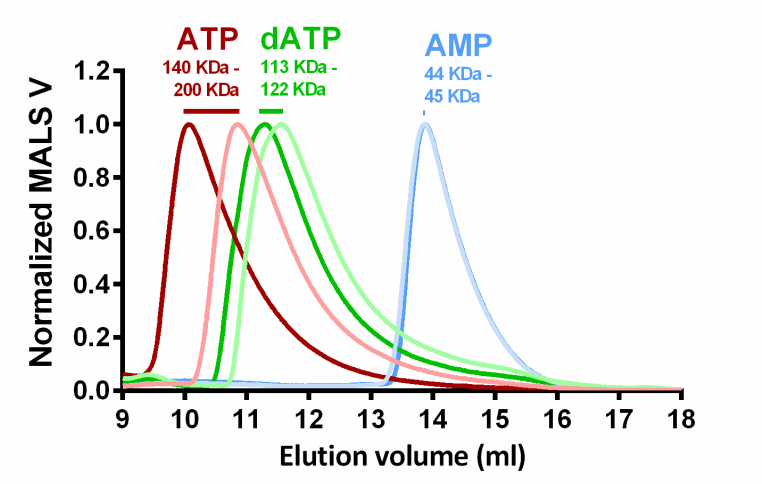

Supplementary figure A3:S5. Full images of EMSA gels.

Full unedited version of the EMSA gels used for Figure A3:4. The DNA probes used were the P*nrdA* promoter from *E. coli* (519 bp), labeled as PnrdA (ECO), and a negative control *anr* band (499 bp), labeled as Ctrl (-). Numbers below the triangles indicate the molar ratio of NrdR protein and marked DNA (0:1, 2000:1, or 4000:1). When indicated, NrdR was preincubated with nucleotides at a 20:1 nucleotide : protein proportion. The P*nrdA* (ECO) data was repeated in the second gel to confirm the results of the first.

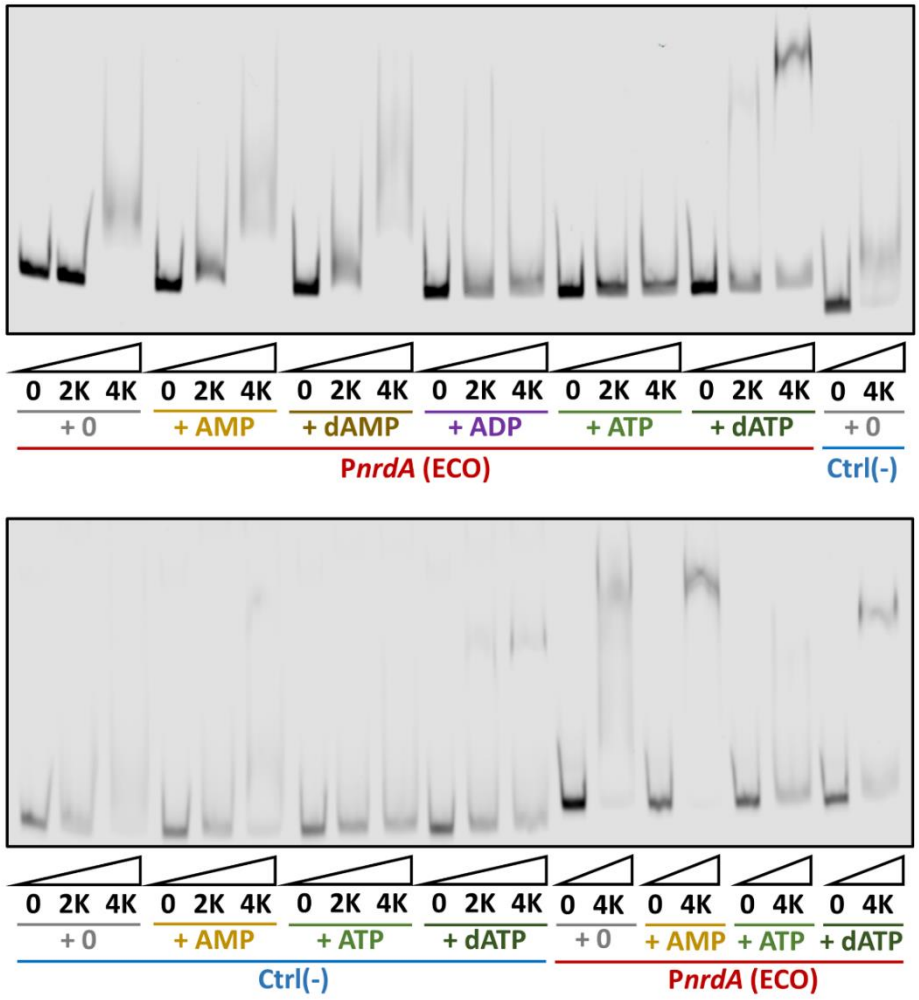

Supplementary figure A3:S6. Schematic of the sequences used for ReViTA

DNA sequence of elements used in the Regulated in Vitro Transcription Assays (ReViTA). **A**, ReViTA synthetic cassette. The cassette is surrounded by transcription terminators (BBA_B0015 terminator, Registry of Standard Biological Parts). From 5' (left) to 3' (right), after the terminator, we find the space for cloning the desired promoter (in the example, the constitutive promoter BBA_J23119, Registry of Standard Biological Parts) between the restriction sites BamHI and SpeI. After the promoter there is a truncated, non-functional version of the *cat* gene (Chloramphenicol Acetyltransferase). The TEST sequence that will be quantified in ReViTA experiment can be found inside this gene. **B**, pReViTA plasmid, obtained inserting the ReViTA cassette in the backbone of plasmid pETS130; the CTRL sequence that will be quantified in ReViTA experiments can be found inside the gentamicin resistance *aacC1* (GmR) gene.

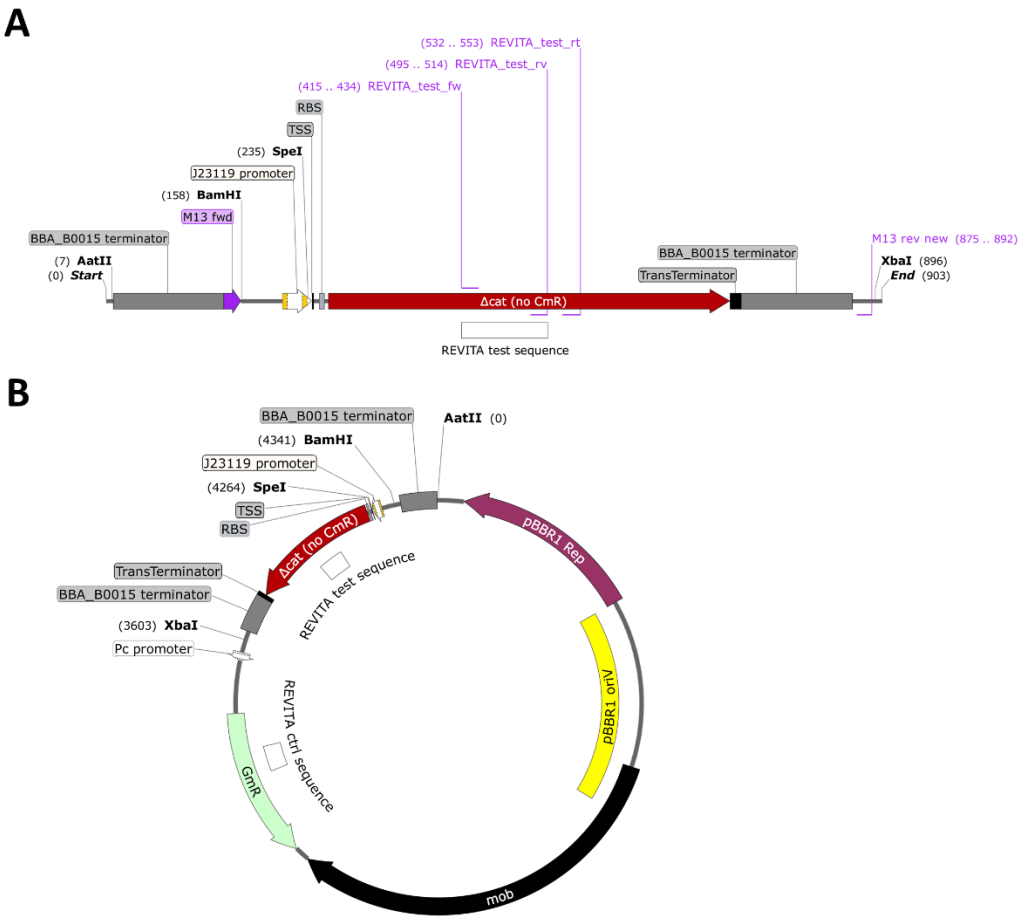

Supplementary table A3:S1. Strains and plasmids used in this study

Strains and plasmids are listed with simplified, self-explanatory names (Referred to as…), which are commonly used in the text. For strains, a detailed genotype is also provided. In the plasmids used for NrdR overexpression, the origin species of each *nrdR* gene is specified: *P. aeruginosa* (*P. aer*) or *E. coli.*

Item	Referred to as	(Strain) Genotype	Description	Source
Strains				
PAO1	PAO1 (WT)	Wild-type (ATCC 15692 / CECT 4122)	Wild-type *P. aeruginosa* lab strain	ATCC
PW7855	PAO1 Δ*nrdR*	PAO1 *nrdR*::IS*lacZ/hah*, **Tc^R**	PAO1 derivative with a transposon interrupting *nrdR*	*Jacobs et al.* [1]
K-12	K12 MG1655	F$^-$ *λ* $^-$ *ilvG*$^-$ *rfb*-50 *rph*-1 (ATCC 700926)	Wild-type *E. coli* lab strain	Laboratory stock
BL21(DE3)	BL21	F$^-$ *ompT gal dcm lon hsdSB*(r_B^- m_B^-) λ(DE3 [*lacI lacUV5-T7p07 ind1 sam7 nin5*]) [malB$^+$]$_{K\text{-}12}$(λ^S)	*E. coli* strain for IPTG-induced T7 protein overexpression	Lucigen, WI USA
DH5α	DH5α	*recA1 endA1 hdsR17 supE44 thi-1 relA1 Δ(lacZYA-argF)U169 deoR Φ80dlacZM15*	*E.* coli strain for cloning procedures	Lucigen, WI USA
Plasmids				
pJET1.2-blunt	pJET1.2		General carrier vector for cloning procedures, **Amp^R**	ThermoFisher, MA USA
pET22b$^+$	pET22b+		Vector for IPTG-induced T7 protein overexpression of His_6-fusion proteins, **Amp^R**	Millipore Sigma, MA USA
pET22b$^+$::*nrdR*(*P.aer)*	pET-NrdR(PAO)		pET22b+ derivative producing an NrdR-His6 (*P. aer)* fusion protein, **Amp^R**	This work
pAviTag-NN-His SUMO Kan	pSUMO		Vector for Rhamnose-induced overexpression of SUMO-fusion proteins, **Kn^R**	Lucigen, WI USA
pAviTag-NN-His SUMO Kan::*nrdR*(*P. aer*)	pSUMO-NrdR(PAO)		pSUMO derivative producing a His_6-AviTag-SUMO-NrdR (*P. aer*) fusion protein, **Kn^R**	This work
pAviTag-NN-His SUMO Kan::*nrdR*(*E. coli*)	pSUMO-NrdR(ECO)		pSUMO derivative producing a His_6-AviTag-SUMO-NrdR (*E. coli*) fusion protein, **Kn^R**	This work
pCri11a	pCri11a		Vector for IPTG-induced overexpression of His_6-SUMO-HIs_6 fusion proteins, **Kn^R**	*Goulas et al.* [2]
pCri11a::*nrdR*(*P. aer*)	pCri-NrdR(PAO)		pCri derivative producing a His_6-SUMO-TEVcs-NrdR (*P. aer*) fusion protein, **Kn^R**	This work
pCri11a::*nrdR*(*E. coli*)	pCri-NrdR(ECO)		pCri derivative producing a His_6-SUMO-TEVcs-NrdR (*E. coli*) fusion protein, **Kn^R**	Work
pETS130-GFP	pETS130		Broad-host range, promoterless GFP, Gm^R, **Gm^R**	*Sjoberg et al.* [3]
pReViTA	pReViTA		pETS130 derivative, *in vitro* transcription template plasmid for ReViTA, **Gm^R**	This work
pReViTA-P*nrdA* (*E. coli*)	pReViTA-PA		pReViTA derivative, carrying the promoter region of *nrdAB* in *E. coli*, **Gm^R**	This work
pETS176	pUCP20T::nrdR		pUC2P0T derivative, complementation plasmid for *nrdR*, **Amp^R**	*Crespo et al.* [4]

1. Jacobs MA, Alwood A, Thaipisuttikul I, Spencer D, Haugen E, Ernst S, et al. Comprehensive transposon mutant library of Pseudomonas aeruginosa. Proceedings of the National Academy of Sciences of the United States of America. 2003;100(24):14339-44.
2. Goulas T, Cuppari A, Garcia-Castellanos R, Snipas S, Glockshuber R, Arolas JL, et al. The pCri System: a vector collection for recombinant protein expression and purification. PloS one. 2014;9(11):e112643.
3. Sjoberg BM, Torrents E. Shift in ribonucleotide reductase gene expression in *Pseudomonas aeruginosa* during infection. Infection and immunity. 2011;79(7):2663-9.
4. Crespo A, Pedraz L, Torrents E. Function of the *Pseudomonas aeruginosa* NrdR Transcription Factor: Global Transcriptomic Analysis and Its Role on Ribonucleotide Reductase Gene Expression. PloS one. 2015;10(4):e0123571.

Supplementary table A3:S2. Putative NrdR-boxes in *P. aeruginosa*

Putative NrdR-boxes identified in a FIMO[27] (MEME Suite[28]) search using the general γ-proteobacteria weight matrix (see Figure A3:1) on a whole-genome search including 450 bp upstream and 20 bp downstream of the translation start codon for each gene in the *P. aeruginosa* PAO1 genome. Only hits with a p-value lower than $1 \cdot 10^{-4}$ are included. Each hit is listed with its FIMO score and P-value. The sequence of the putative box is provided, as well as its start and stop positions relative to the translation start codon of the corresponding gene.

NrdR boxes						
Gene code	Gene name	Score	P-value	Start	Stop	Sequence
PA1157	nrdA	20.197	4.86E-08	-125	-110	CCACAATATGTAGTGT
PA1156	nrdA	18.513	2.88E-07	-398	-383	CCCCTATATCTTGGGT
PA3011	topA	18.237	3.72E-07	-76	-61	CCACTATATATAGCGG
PA1920	nrdD	16.895	1.15E-06	-57	-42	CCACAACATATTGTTG
PA1383		16.000	2.25E-06	-181	-166	CCACTTCATGTAGTGG
PA1920	nrdD	15.421	3.37E-06	-26	-11	ACACATCATGTTGTGG
PA5325	sphA	13.618	1.04E-05	-156	-141	TCCCATCATATAGCGT
PA1156	nrdA	12.737	1.70E-05	-194	-179	CCACTAGGTATTGTGT
PA1802	clpX	12.487	1.94E-05	-42	-27	TGCCTTCATCTTGTGT
PA5497	nrdJa	12.197	2.25E-05	-7	8	TAACTAGATGTTGCGT
PA2523	czcR	12.118	2.35E-05	-21	-6	ATACTTTATATAGGGG
PA5497	nrdJa	12.066	2.41E-05	-38	-23	ACACAAGATATTGATT
PA1156	nrdA	11.842	2.70E-05	-429	-414	GCGCATTATCTTGTAT
PA4523	PA4523	11.553	3.11E-05	-152	-137	ACCCTCTATCTAGATT
PA0254	hudA	11.553	3.11E-05	-23	-8	CCTCTATATGATGCGT
PA2229	PA2229	11.382	3.39E-05	-53	-38	GGACTCTATATTGTAT
PA4280	birA	11.290	3.54E-05	-38	-23	CCTCTATATGATGCGT
PA4210	phzA1	11.105	3.86E-05	-388	-373	CTACCAGATCTTGTAG
PA2167	PA2167	10.737	4.60E-05	-250	-235	CCCCTCCATCTAGAAG
PA3162	rpsA	10.540	5.03E-05	-219	-204	AGACCTTATGTTGTGG
PA1430	lasR	10.540	5.03E-05	-167	-152	CAACTCTATAGAGTGG
PA2668	PA2668	9.908	6.67E-05	-413	-398	GAACAATATGTTGTCG
PA0837	slyD	9.855	6.83E-05	-330	-315	CACCAGTATGTTGCGT
PA5203	gshA	9.658	7.44E-05	-52	-37	CACCCTCATATTGGGG
PA1244	PA1244	9.500	7.95E-05	-424	-409	TCACAAAATATTGAAT
PA3133	PA3133	9.461	8.09E-05	-290	-275	CCCCTTCGTCTAGTGG
PA3622	rpoS	9.434	8.18E-05	-88	-73	CCACATCATGTAGGTG
PA3414	PA3414	9.395	8.32E-05	-368	-353	ACGCCATATACTGTAT
PA5157	PA5157	9.395	8.32E-05	-264	-249	AAACAATATCTTGATA
PA3001	PA3001	9.329	8.55E-05	-88	-73	CCCCTACATGTGGAAG
PA5182	PA5182	9.303	8.65E-05	-109	-94	ACTCTCTATGAAGTAT
PA2600	PA2600	9.224	8.94E-05	-135	-120	TTCCATCATGTAGTTT
PA1796	folD	8.961	9.98E-05	-439	-424	CTCCTTTATATAGCTG

Supplementary table A3:S3. Putative NrdR-boxes in *E. coli*

Putative NrdR-boxes identified in a FIMO[27] (MEME Suite[28]) search using the general γ-proteobacteria weight matrix (see Figure A3:1) on a whole-genome search including 450 bp upstream and 20 bp downstream of the translation start codon for each gene in the *E. coli* K-12 *substr.* MG1655 genome. Only hits with a p-value lower than $1 \cdot 10^{-4}$ are included. Each hit is listed with its FIMO score and P-value. The sequence of the putative box is provided, as well as its start and stop positions relative to the translation start codon of the corresponding gene.

NrdR boxes						
Gene code	Gene name	Score	P-value	Start	Stop	Sequence
b2234	nrdA	21.724	5.42E-09	-92	-77	CCCCTATATATAGTGT
b4238	nrdD	18.395	3.18E-07	-176	-161	ACCCAATATGTTGTAT
b2674	nrdI	17.263	8.63E-07	-330	-315	CAACTACATCTAGTAT
b2673	nrdH	17.263	8.63E-07	-88	-73	CAACTACATCTAGTAT
b3052	hldE	16.711	1.33E-06	-313	-298	ACCCAATATCTGGTGT
b1491	yddW	15.737	2.73E-06	-165	-150	CCACACTATATTGTGA
b2674	nrdI	15.724	2.75E-06	-361	-346	TTGCTATATATTGTGT
b2673	nrdH	15.724	2.75E-06	-119	-104	TTGCTATATATTGTGT
b0055	djlA	15.671	2.85E-06	-54	-39	CACCTTTATATTGTGG
b0720	gltA	15.658	2.88E-06	-448	-433	AACCTACATATAGTTT
b4684	yqfG	15.276	3.71E-06	-276	-261	AACCTCTATATTGTGG
b1128	roxA	13.882	8.90E-06	-314	-299	CATCTCTATATTGTGG
b4270	leuX	13.855	9.03E-06	-291	-276	CTTCAACATCTTGTGG
b1000	cbpA	13.776	9.48E-06	-266	-251	TACCCATATATAGCGT
b0645	ybeR	13.737	9.71E-06	-256	-241	CAACAATATATTGAGC
b1298	puuD	13.658	1.02E-05	-334	-319	CATCAACATATTGCGT
b2159	nfo(	13.592	1.06E-05	-71	-56	CCACTACATCTTGCTC
b1114	mfd(	13.513	1.11E-05	-44	-29	CCCCCATATGTTGAGG
b2593	yfiH	13.421	1.16E-05	-73	-58	CCACAAGATATGGTGG
b1487	ddpA	13.342	1.22E-05	-339	-324	CCGCAATATGTTGTTG
b0382	iraP	12.895	1.56E-05	-172	-157	AGCCTATATTTTGTGT
b0721	sdhC	12.882	1.57E-05	-274	-259	AAACTATATGTAGGTT
b0213	yafS	12.855	1.59E-05	-285	-270	TTCCCTTATCTTGTGT
b0014	dnaK	12.447	1.98E-05	-25	-10	ACCGAATATATAGTGG
b1642	slyA	12.368	2.06E-05	-248	-233	ACACCAGATCTTGTAA
b4177	purA	12.171	2.28E-05	-133	-118	CTACTACATGTTGAGG
b0113	pdhR	12.158	2.30E-05	-311	-296	TCTCAATATGTAGAAT
b3186	rplU	12.105	2.36E-05	-303	-288	CCGCCATATCTTGCGC
b2234	nrdA	12.040	2.45E-05	-124	-109	TCACACTATCTTGCAG
b2351	gtrB	12.000	2.49E-05	-157	-142	ATGCTATATGTTGGGT
b0815	opgE	11.737	2.84E-05	-334	-319	GCTCTCTATGTTGTGC
b4238	nrdD	11.632	2.99E-05	-207	-192	GCACTATATATAGACT
b3155	yhbQ	11.487	3.22E-05	-101	-86	TGACAACATGTTGTTT
b1466	narW	11.474	3.24E-05	-374	-359	CGCCAATATGTTGAGT
b3745	viaA	11.461	3.26E-05	-241	-226	GCCCAACATCTTGTCG
b1089	rpmF	11.395	3.36E-05	-319	-304	ACACAACGTATTGTTT
b2348	argW	11.342	3.45E-05	-296	-281	ATCCTCTATCTGGTGT
b1443	ydcV	11.329	3.48E-05	-358	-343	TCTCTATATCTGGTTG
b3647	ligB	11.303	3.52E-05	-284	-269	AAACAATATAAAGCGT
b3454	livF	11.290	3.54E-05	-157	-142	CACCACTATCTTGTTG
b3180	yhbY	11.276	3.56E-05	-335	-320	TGACCACATATTGTGA
b1642	slyA	11.237	3.63E-05	-181	-166	ACCGAATATATTGCGT
b1791	yeaN	11.171	3.75E-05	-300	-285	AAACCGCATATTGTGG
b0583	entD	11.026	4.01E-05	-87	-72	ATTCAATATATTGCAG

b4180	rlmB	11.026	4.01E-05	-75	-60	ATTCAATATATTGCAG
b2025	hisF	10.895	4.27E-05	-397	-382	TCACAAGATATGGTGA
b0098	secA	10.803	4.45E-05	-237	-222	GCGCAACATCTTGCAT
b0460	hha(	10.790	4.48E-05	-154	-139	CACCTTTATGTTGTTC
b3210	arcB	10.711	4.65E-05	-382	-367	CCGCTGCATATTGTGA
b2543	yphA	10.579	4.94E-05	-26	-11	TCACATTATCTTGCAA
b2724	hycB	10.513	5.09E-05	-364	-349	CCACACCATCGAGTAT
b0674	asnB	10.513	5.09E-05	-308	-293	CTGCAATATATTGAAT
b2924	mscS	10.513	5.09E-05	-256	-241	CTGCAATATATTGAAT
b3944	yijF	10.513	5.09E-05	-192	-177	CTGCAATATATTGAAT
b2404	lysV	10.461	5.22E-05	-244	-229	CTACTTTATGTAGTCT
b2403	valY	10.461	5.22E-05	-164	-149	CTACTTTATGTAGTCT
b2402	valX	10.461	5.22E-05	-42	-27	CTACTTTATGTAGTCT
b1644	ydhJ	10.355	5.47E-05	-205	-190	TTACAAGATCTGGTGT
b2998	yghW	10.303	5.60E-05	-27	-12	TGACAATATATAGCGA
b3087	ygjR	10.303	5.60E-05	-24	-9	TCCCTTTATGGAGTAT
b1112	bhsA	10.276	5.66E-05	-98	-83	AAAAAATATCTTGTAT
b0622	pagP	10.224	5.80E-05	-87	-72	ATTCTTTATGTTGGGT
b3342	rpsL	10.224	5.80E-05	-69	-54	CGTCCTCATATTGTGT
b2984	yghR	10.145	6.01E-05	-421	-406	TCGCAAAATGTTGTGT
b2599	pheA	10.092	6.15E-05	-249	-234	GTCCTTTATATTGAGT
b2598	pheL	10.092	6.15E-05	-103	-88	GTCCTTTATATTGAGT
b3974	coaA	10.066	6.22E-05	-109	-94	CCTCCCCATCTGGTGT
b0073	leuB	10.013	6.37E-05	-83	-68	GAACAATATCTGGCGT
b3508	yhiD	9.974	6.48E-05	-415	-400	AATCTCTATATTGAAT
b3371	frlB	9.974	6.48E-05	-248	-233	CTCCATCATCTGGTGT
b3068	mug(	9.974	6.48E-05	-209	-194	TTGCTATATCTGGTGG
b3509	hdeB	9.974	6.48E-05	-25	-10	AATCTCTATATTGAAT
b1481	bdm(	9.934	6.60E-05	-194	-179	CCAAAAGATATTGTAT
b2376	ypdI	9.921	6.63E-05	-260	-245	CGCCATCATATTGGGT
b1527	yneK	9.921	6.63E-05	-48	-33	ATGCTCTATATAGTGA
b1689	ydiL	9.908	6.67E-05	-233	-218	AATCAACATATTGATT
b0275	insA	9.842	6.87E-05	-437	-422	ACACAACAAATGGTGT
b4704	arrS	9.842	6.87E-05	-146	-131	ACTCCATATATTGATC
b2848	yqeJ	9.829	6.91E-05	-51	-36	AACCAACATGAAGTGG
b3020	ygiS	9.697	7.31E-05	-430	-415	ACGGTTTATATTGTGT
b1743	spy(	9.684	7.36E-05	-415	-400	ACCCATGATGTAGAGT
b4683	yqeL	9.684	7.36E-05	-51	-36	GCACCAGATGTTGTTG
b0447	ybaO	9.658	7.44E-05	-382	-367	ACCCAACATTTAGGTT
b3915	fieF	9.645	7.48E-05	-107	-92	CCCCCACATGCTGTGG
b1608	rstA	9.618	7.56E-05	-266	-251	CAACAATATAATGCGC
b4299	yjhI	9.592	7.65E-05	-414	-399	CAACACTATCATGTAT
b0558	ybcV	9.579	7.69E-05	-265	-250	GCTCTTCATCTAGCGG
b1141	xisE	9.579	7.69E-05	-231	-216	CAACTTTATGCTGTGT
b2440	eutC	9.566	7.73E-05	-218	-203	CAACTACATCATGGGG
b3630	waaP	9.566	7.73E-05	-201	-186	GCGCATTATATTGCGG
b0112	aroP	9.553	7.78E-05	-243	-228	ATTCTACATATTGAGA
b1137	ymfD	9.539	7.82E-05	-284	-269	AAACATTATATTGAAC
b3323	gspA	9.539	7.82E-05	-247	-232	AATCAATATATTGATG
b0707	ybgA	9.539	7.82E-05	-203	-188	CGTCTTCATATTGTTT
b0264	insB	9.474	8.04E-05	-333	-318	CAACCAGATCTAGTTC
b0265	insA	9.474	8.04E-05	-139	-124	CAACCAGATCTAGTTC
b0054	lptD	9.461	8.09E-05	-214	-199	CCACAATATAAAGGTG
b4178	nsrR	9.382	8.36E-05	-312	-297	GAACTATATCAAGCGT
b0597	entH	9.382	8.36E-05	-46	-31	CTACAGGATATTGTGG
b4536	yobH	9.368	8.41E-05	-241	-226	GCACATCATGTTGAAT
b1004	wrbA	9.316	8.60E-05	-350	-335	AGACATCATATTGCAT
b1168	ycgG	9.289	8.70E-05	-241	-226	CCGCAATATCAGGTGT
b2426	ucpA	9.263	8.80E-05	-75	-60	CAGCAATATTTTGTTT
b4218	ytfL	9.250	8.84E-05	-228	-213	ATTCAATATATTGCAA
b2050	wcaI	9.224	8.94E-05	-178	-163	ACTCACTATGTGGTGC
b3102	yqjG	9.211	8.99E-05	-359	-344	CAACAATATATGGAAG
b3789	rffH	9.184	9.09E-05	-311	-296	AATCTCGATGTTGTGG
b4565	sgcB	9.171	9.14E-05	-411	-396	TCACTCCATCGTGTGA
b0763	modA	9.158	9.19E-05	-336	-321	TGACTATATCTGGAGT
b0762	acrZ	9.158	9.19E-05	-20	-5	TGACTATATCTGGAGT
b3806	cyaA	9.053	9.61E-05	4	19	TACCTCTATATTGAGA
b2400	gltX	9.039	9.66E-05	-350	-335	AGACTACATAAAGTAG
b0050	apaG	8.974	9.92E-05	-416	-401	GCACTTTATGTTGCAA

Supplementary table A3:S4. RNA-seq study in *P. aeruginosa*; upregulated genes.

Differentially expressed genes (DEGs) showing upregulation in a ΔnrdR mutant strain in *P. aeruginosa*, compared to a wild-type isogenic PAO1 strain. Only genes with a fold-change higher than 2.0 are included. A positive fold-change indicates higher expression in the mutant strain compared to the wild-type. Genes are listed by its gene code; when available, a gene name is also included. The operon context for each gene is provided[41], as well as a short description of its function. The genes in the *nrd* operons are indicated in black.

UPREGULATED GENES

Gene code	Fold change	Operon and environment	Gene name	Function
PA0050	3.27	PA0550 (1)		Hypothetical protein
PA0201	2.39	PA0201 (1)		Hypothetical protein
PA0526	2.40	PA0526-PA0527 (2)		Hypothetical protein
PA0604	2.05	PA0601-PA0604 (5)	*agtB*	AgtB protein
PA0721	4.56	PA0720-PA0723 (4)		Hypothetical protein of bacteriophage Pf1
PA0779	2.61	PA0777-PA0779 (4)	*asrA*	Peptidase, antibiotic responsive
PA0839	8.52	PA0837-PA0841 (5)		Prob. transcriptional regulator
PA0996	5.55	PA0996-PA1000 (5)	*pqsA*	Quorum sensing, PQS signal synthesis
PA0997	5.35	PA0996-PA1000 (5)	*pqsB*	Quorum sensing, PQS signal synthesis
PA0998	4.52	PA0996-PA1000 (5)	*pqsC*	Quorum sensing, PQS signal synthesis
PA0999	3.95	PA0996-PA1000 (5)	*pqsD*	Quorum sensing, PQS signal synthesis
PA1000	3.53	PA0996-PA1000 (5)	*pqsE*	Quorum sensing, PQS signal synthesis
PA1001	3.42	PA1001-PA1002 (2)	*phnA*	Anthranilate synthase component I
PA1155	**3.30**	**PA1155-PA1156 (2)**	***nrdB***	**Ribonucleotide reductase class I**
PA1156	**2.96**	**PA1155-PA1156 (2)**	***nrdA***	**Ribonucleotide reductase class I**
PA1168	2.32	PA1168 (1)		Hypothetical protein
PA1331	2.54	PA1331-PA1333 (3)		Cons. Hypothetical protein
PA1429	2.11	PA1428-PA1429 (2)		Prob. cation-transporting P-type ATPase
PA1596	2.45	PA1596-PA1597 (2)	*htpG*	Heat shock protein, protein folding
PA1597	3.92	PA1596-PA1597 (2)		Prob. Hydrolase
PA1598	3.06	PA1598 (1)		Cons. hypothetical protein
PA1600	2.83	PA1600-PA1602 (3)		Prob. cytochrome c
PA1601	3.43	PA1600-PA1602 (3)		Prob. aldehyde dehydrogenase
PA1602	3.44	PA1600-PA1602 (3)		Prob. oxidoreductase
PA1649	2.38	PA1649-PA1650 (2)		Prob. short-chain dehydrogenase
PA1691	2.07	PA1690-PA1697 (8)	*pscT*	Type III secretion system related
PA1692	2.17	PA1690-PA1697 (8)	*pscQ*	Prob. type III secretion system related
PA1694	2.22	PA1690-PA1697 (8)	*pscQ*	Type III secretion system related
PA1695	2.41	PA1690-PA1697 (8)	*pscP*	Type III secretion system related
PA1696	2.15	PA1690-PA1697 (8)	*pscO*	Type III secretion system related
PA1698	2.02	PA1698-PA1709 (12)	*popN*	Type III secretion system related, regulator
PA1700	2.39	PA1698-PA1709 (12)	*pcr2*	Type III secretion system related
PA1701	2.56	PA1698-PA1709 (12)	*pcr3*	Type III secretion system related
PA1702	2.36	PA1698-PA1709 (12)	*pcr4*	Type III secretion system related
PA1703	2.08	PA1698-PA1709 (12)	*pcrD*	Type III secretion system related
PA1705	2.05	PA1698-PA1709 (12)	*pcrG*	Type III secretion system related, regulator
PA1707	2.57	PA1698-PA1709 (12)	*pcrH*	Type III secretion system related
PA1708	2.10	PA1698-PA1709 (12)	*popB*	Type III secretion system related, translocator
PA1709	2.10	PA1698-PA1709 (12)	*popD*	Type III secretion system related, translocator
PA1711	2.16	PA1710-PA1712 (3)	*exsE*	Exoenzyme S synthesis
PA1715	2.12	PA1713-PA1725	*pscB*	Type III secretion system related
PA1721	2.12	PA1713-PA1725	*pscH*	Type III secretion system related
PA1722	2.24	PA1713-PA1725	*pscI*	Type III secretion system related
PA1724	2.05	PA1713-PA1725	*pscK*	Type III secretion system related
PA1796.1	2.01	PA1796.1 (1)		tRNA-Arg
PA1920	**13.65**	**PA1919-PA1920 (2)**	***nrdD***	**Ribonucleotide reductase class III**
PA2018	2.48	PA2018-PA2019 (2)	*mexY*	Resistance-Nodulation-Cell Division, multidrug efflux transporter
PA2019	2.96	PA2018-PA2019 (2)	*mexX*	Resistance-Nodulation-Cell Division, multidrug efflux membrane protein
PA2170	2.32	PA2169-PA2170 (2)		Hypothetical protein

PA2193	2.53	PA2193-PA2195 (3)	*hcnA*	Hydrogen cyanide synthesis
PA2194	2.12	PA2193-PA2195 (3)	*hcnB*	Hydrogen cyanide synthesis
PA2321	2.09	PA2321-PA2322 (2)		Gluconokinase
PA2322	2.05	PA2321-PA2322 (2)		gluconate permease
PA2403	2.51	PA2403-PA2406 (4)		Hypothetical protein
PA2404	2.64	PA2403-PA2406 (4)		Hypothetical protein
PA2405	2.51	PA2403-PA2406 (4)		Hypothetical protein
PA2406	2.72	PA2403-PA2406 (4)		Hypothetical protein
PA2407	2.97	PA2407-PA2410 (4)		Prob. adhesion protein
PA2408	3.02	PA2407-PA2410 (4)		Prob. ATP-binding component of ABC transporter
PA2409	2.67	PA2407-PA2410 (4)		Prob. permease of ABC transporter
PA2410	2.24	PA2407-PA2410 (4)		Hypothetical protein
PA2550	5.50	PA2550 (1)		Prob. acyl-CoA dehydrogenase
PA2570	2.88	PA2570 (1)	*lecA*	Pred. in movement and adhesion
PA2593	2.07	PA2593 (1)	*qteE*	Quorum sensing related
PA2852.2	7.92	PA2852.2 (1)	PA14	ncRNA
PA3126	2.19	PA3126 (1)	*ibpA*	Heat shock protein
PA3427	2.26	PA3426-PA3427 (2)		Prob. short-chain dehydrogenases
PA3449	2.09	PA3447-PA3449 (3)		Cons. Hypothetical protein
PA3906	2.02	PA3904-PA3908 (5)		Hypothetical protein
PA3907	2.07	PA3904-PA3908 (5)		Hypothetical protein
PA4056	**2.98**	**PA4056-PA4057**	***ribD***	**Riboflavin-specific deaminase/reductase**
PA4057	**2.81**	**PA4056-PA4057**	***nrdR***	**NrdR regulator (MUTANT ASSIG.)**
PA4058	2.11	PA4058-PA4061 (4)		Hypothetical protein, consecutive to nrdR
PA4218	3.31	PA4218-PA4219 (2)	*ampP*	Antibiotic resistance, beta-lactamase activity
PA4219	3.22	PA4218-PA4219 (2)	*ampO*	Antibiotic resistance, beta-lactamase activity
PA4220	2.37	PA4220-PA4221 (2)		Hypothetical protein
PA4224	3.29	PA4222-PA4226 (5)	*pchG*	Pyochelin biosynthesis
PA4225	2.84	PA4222-PA4226 (5)	*pchF*	Pyochelin biosynthesis
PA4226	2.68	PA4222-PA4226 (5)	*pchE*	Pyochelin biosynthesis
PA4228	2.12	PA4228-PA4231 (4)	*pchD*	Salicylate biosynthesis
PA4230	2.78	PA4228-PA4231 (4)	*pchB*	Salicylate biosynthesis
PA4277.1	2.01	PA4277.1 (1)		tRNA-Thr
PA4384	2.73	PA4384 (1)		Hypothetical protein
PA4542	2.14	PA4542-PA4544	*clpB*	ClpB protein
PA4673.1	3.86	PA4673-1 (1)		tRNA-Met
PA4758.1	3.03	PA4758.1 (1)	P32	ncRNA
PA4759	2.51	PA4759-PA4762 (4)	*dapB*	Dihydrodipicolinate reductase
PA4760	2.46	PA4759-PA4762 (4)	*dnaJ*	DnaJ protein
PA4761	2.41	PA4759-PA4762 (4)	*dnaK*	DnaK protein
PA4762	2.07	PA4759-PA4762 (4)	*grpE*	Heat shock protein
PA5020	2.71	PA5020 (1)		Prob. acyl-CoA dehydrogenase
PA5054	2.48	PA5053-PA5055 (3)	*hslU*	Heat shock protein
PA5055	2.17	PA5053-PA5055 (3)		Hypothetical protein
PA5144	2.02	PA5144-PA5149 (6)		Hypothetical protein
PA5207	2.18	PA5207-PA5208 (2)		Prob. phosphate transporter
PA5496	**8.96**	**PA5496-PA5498 (3)**	***nrdJb***	**Ribonucleotide reductase class II**
PA5497	**13.25**	**PA5496-PA5498 (3)**	***nrdJa***	**Ribonucleotide reductase class II**

Supplementary table A3:S5. RNA-seq study in *P. aeruginosa*; downregulated genes.

Differentially expressed genes showing downregulation in a ΔnrdR mutant strain in *P. aeruginosa*, compared to a wild-type isogenic PAO1 strain. Only genes with a fold-change higher than 2.0 are included. A positive fold-change indicates higher expression in the mutant strain compared to the wild-type. Genes are listed by its gene code; when available, a gene name is also included. The operon context for each gene is provided[41], as well as a short description of its function. Genes in the *nrd* operons are indicated in bold.

DOWNREGULATED GENES				
Gene code	Fold change	Operon and environment	Gene name	Function
PA0132	-2.25	PA0129-PA0132 (4)	*bauA*	bauA ,Beta-alanine:pyruvate transaminase
PA0713	-2.06	PA0713 (1)		Hypothetical protein
PA0887	-2.14	PA0887 (1)	*acSA*	Acetyl-coenzyme A synthetase
PA1664	-2.23	PA1664-PA1671 (8)	*orfX*	Type VI secretion system related
PA1942	-2.99	PA1942 (1)		Hypothetical protein
PA2140	-2.52	PA2140-PA2412 (3)		Prob. metallothionein
PA2395	-2.01	PA2393-PA2395 (3)	*pvdO*	Pyoverdine biosynthesis
PA2402	-2.07	PA2399-PA2402		Prob. non-ribosomal peptide synthetase
PA2413	-2.08	PA2411-PA2413	*pvdH*	Pyoverdine biosynthesis
PA2424	-2.16	PA2424-PA2425	*pvdL*	Pyoverdine biosynthesis
PA2426	-2.65	PA2426 (1)	*pvdS*	Sigma factor PvdS
PA2472	-2.33	PA2472-PA2474 (3)		Prob. major facilitator superfamily (MFS) transporter
PA2478	-32.04	PA2475-PA2478 (4)		Prob. thiol:disulfide interchange protein
PA2479	-73.92	PA2479-PA2480 (2)		Prob. two-component response regulator
PA2481	-376.48	PA2481-PA2484 (4)		Hypothetical protein
PA2482	-266.62	PA2481-PA2484 (4)		Prob. cytochrome c
PA2483	-316.20	PA2481-PA2484 (4)		Cons. hypothetical protein
PA2484	-110.89	PA2481-PA2484 (4)		Cons. hypothetical protein
PA2488	-42.83	PA2488-PA2490 (3)		Prob. transcriptional regulator
PA2489	-89.57	PA2488-PA2490 (3)		Prob. transcriptional regulator
PA2490	-105.84	PA2488-PA2490 (3)		Cons. hypothetical protein
PA2491	-2228.67	PA2491 (1)	*mexS*	MexS protein, regulator
PA2492	-114.79	PA2492-PA2495 (4)	*mexT*	Multidrug efflux system
PA2493	-40.67	PA2492-PA2495 (4)	*mexE*	Multidrug efflux system
PA2494	-13.90	PA2492-PA2495 (4)	*mexF*	Multidrug efflux system
PA2495	-7.88	PA2492-PA2495 (4)	*oprN*	Multidrug efflux system
PA2570.1	-3.91	PA2570.1 (1)		tRNA-Leu
PA2581.1	-2.59	PA2581.1 (1)		tRNA-Cys
PA2811	-2.88	PA2811-PA2813 (3)		Prob. permease of ABC-2 transporter
PA2812	-3.37	PA2811-PA2813 (3)		Prob. ATP-binding component of ABC transporter
PA2813	-8.11	PA2811-PA2813 (3)		Prob. glutathione S-transferase
PA3038	-2.13	PA3038 (1)		Prob. porin
PA3229	-6.75	PA3229 (1)		Hypothetical protein
PA3234	-2.44	PA3230-PA3235 (6)		Prob. sodium:solute symporter
PA3235	-2.47	PA3230-PA3235 (6)		Cons. hypothetical protein
PA3268	-2.22	PA3267-PA3270 (4)		Prob. TonB-dependent receptor
PA3496	-2.34	PA3486-PA3496 (11)		Hypothetical protein
PA3530	-2.52	PA3530-PA3531 (2)	*bfd*	Bacterioferritin-associated ferredoxin Bfd
PA3901	-3.30	PA3898-PA3901 (4)	*fecA*	Fe(III) dicitrate transport protein FecA
PA4354	-5.28	PA4354-PA4356 (3)		Cons. hypothetical protein
PA4355	-3.04	PA4354-PA4356 (3)	*pyeM*	Transmembrane protein
PA4356	-2.93	PA4354-PA4356 (3)	*xenB*	Xenobiotic reductase
PA4500	-2.03	PA4499-PA4506 (8)		Prob. binding protein component of ABC transporter
PA4514	-3.31	PA4513-PA4514 (2)		Prob. outer membrane receptor for iron transport
PA4881	-8.04	PA4881 (1)		Hypothetical protein
PA4882	-2.02	PA4882-PA4884 (3)		Hypothetical protein
PA5149.1	-8.60	PA5149.1 (1)		tRNA-Phe
PA5171	-3.31	PA5170-PA5173 (4)	*arcA*	Arginine deiminase
PA5172	-5.64	PA5170-PA5173 (4)	*arcB*	Ornithine carbamoyltransferase, catabolic
PA5173	-5.38	PA5170-PA5173 (4)	*arcC*	Carbamate kinase

Supplementary table A3:S6. DNA microarray assay in *E. coli*; upregulated genes.

Differentially expressed genes showing upregulation in an *nrdR*-ATPcone mutant strain in *E. coli*, compared to a wild-type isogenic K-12 *substr*. MG1655. Only genes with a p-value lower than $1 \cdot 10^{-5}$ and a log(fold-change) higher than 1.0 are included. A positive log(fold-change) indicates higher expression in the mutant strain compared to the wild-type. Genes are listed by its gene code; when available, a gene name is also included. When available, a short description of the function of the gene is provided. Genes in the *nrd* operons are indicated in bold.

UPREGULATED GENES				
Gene code	Gene name	log (Fold-change)	P-value	Function
b0150	fhuA	1.499	1.171E-09	outer membrane protein receptor for ferrichrome
b0592	fepB	1.057	5.458E-06	ferric enterobactin (enterochelin) binding protein
b0593	entC	1.573	2.899E-08	isochorismate hydroxymutase 2, enterochelin biosynthesis
b0594	entE	1.388	1.421E-09	2,3-dihydroxybenzoate-AMP ligase
b0595	entB	1.200	7.026E-07	2,3-dihydro-2,3-dihydroxybenzoate synthetase, isochroismatase
b1018	efeO	1.210	4.795E-08	orf, hypothetical protein
b1020	phoH	1.174	4.298E-06	PhoH protein
b1321	ycjX	1.039	4.887E-06	putative EC 2.1 enzymes
b1452	yncE	1.222	3.039E-08	putative receptor
b1495	yddB	1.218	2.091E-07	orf, hypothetical protein
b1627	rsxA	1.012	2.167E-07	hypothetical protein
b1747	astA	1.030	2.258E-07	Arginine N-succinyltransferase
b1796	yoaG	2.215	6.599E-08	orf, hypothetical protein
b1797	yeaR	2.483	3.130E-09	orf, hypothetical protein
b2000	flu	1.100	1.420E-06	putative outer membrane receptor for iron transport
b2155	cirA	1.363	1.856E-08	outer membrane receptor for iron-regulated colicin I receptor; porin
b2214	yojI	1.266	7.676E-07	putative ATP-binding component of a transport system
b2234	**nrdA**	**1.664**	**3.742E-10**	**ribonucleoside diphosphate reductase 1, alpha subunit, B1**
b2235	**nrdB**	**1.476**	**2.983E-09**	**ribonucleoside-diphosphate reductase 1, beta subunit, B2**
b2236	yfaE	1.637	8.346E-09	orf, hypothetical protein
b2537	hcaR	1.001	3.139E-07	transcriptional activator of hca cluster
b2673	**nrdH**	**6.494**	**3.387E-13**	**glutaredoxin-like protein; hydrogen donor**
b2674	**nrdI**	**6.193**	**1.891E-12**	**orf, hypothetical protein**
b2675	**nrdE**	**4.763**	**3.460E-11**	**ribonucleoside-diphosphate reductase 2, alpha subunit**
b2676	**nrdF**	**5.549**	**1.006E-11**	**ribonucleoside-diphosphate reductase 2, beta chain, frag**
b3359	argD	1.168	1.955E-06	acetylornithine delta-aminotransferase
b4237	nrdG	1.153	3.492E-07	anaerobic ribonucleotide reductase activating protein
b4238	**nrdD**	**1.244**	**3.784E-09**	**anaerobic ribonucleoside-triphosphate reductase**
b4490	**efeU**	**1.017**	**3.495E-07**	**orf, hypothetical protein**
b4490	efeU	1.167	7.498E-07	high-affinity iron permease
b4511	ybdZ	1.666	1.097E-07	orf; Unknown function

Supplementary table A3:S7. DNA microarray assay in *E. coli*; downregulated genes.

Differentially expressed genes showing downregulation in a *nrdR*-ATPcone mutant strain in *E. coli*, compared to a wild-type isogenic K-12 *substr*. MG1655. Only genes with a p-value lower than $1 \cdot 10^{-5}$ and a log(fold-change) higher than 1.0 are included. A positive log(fold-change) indicates higher expression in the mutant strain compared to the wild-type. Genes are listed by its gene code; when available, a gene name is also included. When available, a short description of the function of the gene is provided. Genes in the *nrd* operons are indicated in bold.

DOWNREGULATED GENES				
Gene code	Gene name	log (Fold-change)	P-value	Function
b0034	caiF	-1.128	7.724E-07	transcriptional regulator of cai operon
b0231	dinB	-1.168	4.107E-08	DNA-damage-inducible protein
b0798	ybiA	-1.302	1.292E-07	orf, hypothetical protein
b0919	ycbJ	-1.136	1.181E-06	orf, hypothetical protein
b1225	narH	-1.659	1.612E-07	nitrate reductase 1, beta subunit
b1226	narJ	-1.739	4.872E-07	nitrate reductase 1, delta subunit, assembly function
b1227	narI	-1.939	1.863E-07	nitrate reductase 1, cytochrome b(NR), gamma subunit
b1426	ydcH	-1.649	8.993E-07	orf, hypothetical protein
b1475	fdnH	-1.565	2.187E-08	formate dehydrogenase-N, nitrate-inducible, iron-sulfur beta subunit
b1476	fdnI	-1.432	5.215E-08	formate dehydrogenase-N, cytochrome B556(Fdn) gamma subunit
b2000	flu	-2.370	6.738E-11	antigen 43, phase-variable bipartite outer membrane fluffing protein
b2001	yeeR	-2.362	3.735E-10	orf, hypothetical protein
b2203	napB	-1.081	2.080E-07	cytochrome c-type protein
b2204	napH	-1.086	4.001E-07	ferredoxin-type protein: electron transfer
b2205	napG	-1.289	2.649E-07	ferredoxin-type protein: electron transfer
b2995	hybB	-1.031	8.525E-06	probable cytochrome NiFe component of hydrogenase-2
b3115	tdcD	-1.384	5.522E-06	putative kinase
b3478	nikC	-1.491	1.165E-07	transport of nickel, membrane protein
b3479	nikD	-1.563	1.524E-07	ATP-binding protein of nickel transport system
b3480	nikE	-1.552	4.076E-09	ATP-binding protein of nickel transport system
b3571	malS	-1.366	1.055E-06	alpha-amylase
b3774	ilvC	-1.237	6.069E-07	ketol-acid reductoisomerase
b3947	ptsA	-1.003	1.306E-06	PEP-protein phosphotransferase system enzyme I
b4118	melR	-1.199	5.160E-06	regulator of melibiose operon
b4188	yjfN	-1.350	5.584E-08	orf, hypothetical protein
b4435	isrC	-2.854	6.690E-12	

Supplementary table A3:S8. Protein-conjugate analysis of NrdR-nucleotide complexes

Protein conjugate analysis (ASTRA 7, Wyatt Technology, CA USA) applied to NrdR-nucleotide complexes (see Table A3:1). Molecular weight (weight-average molar mass) of the complex (total), the NrdR fraction (protein) and nucleotide fraction (co-factor). All values listed as average ± standard deviation. The composition column lists the number of NrdR and nucleotide units corresponding to the listed molecular weights, rounded to the closest integer. For ATP and dATP we considered a molecular weight of 507.18 Da and 491.18 Da, respectively. Given that the associations formed in the NrdR quaternary structure are dynamic (peaks display a range of molar masses), all data from the protein-conjugate analysis should be considered an approximation.

Nucleotide in buffer				
Nucleotide	Mw (total)	Mw (protein)	Mw (co-factor)	Composition
+ ATP	140.17 ± 0.30	135.59 ± 0.29	4.98 ± 0.30	R_8 + ATP_{9-10}
+ dATP	113.36 ± 0.21	109.36 ± 0.21	4.36 ± 0.22	R_6 + $dATP_{8-9}$

Nucleotide in pre-incubation and buffer				
Nucleotide	Mw (total)	Mw (protein)	Mw (co-factor)	Composition
+ ATP	200.31 ± 0.53	193.80 ± 0.51	7.09 ± 0.53	R_{10}+ATP_{13-15}
+ dATP	121.83 ± 0.21	117.49 ± 0.22	4.73 ± 0.22	R_6 + $dATP_{9-10}$

Supplementary table A3:S9. Sequence and application of the primers used in this study

Primers are commonly referred to in the text by their numbers as listed here. [D3-PA] in 28 indicates D3-phosphoramidite

Number	Name	Sequence	Application
1	NrdR_NdeI_fw	CATATGCATTGTCCCTTCTGCGGTG	Cloning, pET-NrdR(PAO)
2	NrdR_XhoI_rv	CTCGAGTTCCTTGGCCGGCTCGCG	Cloning, pET-NrdR(PAO)
3	T7-promoter_fw	TAATACGACTCACTATAGGG	PCR test, pET-NrdR / pCri-NrdR
4	T7-terminator_rv	CTAGTTATTGCTCAGCGGTG	PCR test, pET-NrdR / pCri-NrdR
5	NrdR-PAO_SUMO_fw	CGCGAACAGATTGGAGGTGGCAGCATGCATTGTCCCTTCTGCGGT	Cloning, pSUMO-NrdR(PAO)
6	NrdR-PAO_SUMO_rv	GTGGCGGCCGCTCTATTACGTTCATTCCTTGGCCGGCTC	Cloning, pSUMO-NrdR(PAO)
7	NrdR-ECO_SUMO_fw	CGCGAACAGATTGGAGGTGGATCCATGCATTGCCCATTCTGTTTCG	Cloning, pSUMO-NrdR(ECO)
8	NrdR-ECO_SUMO_rv	GTGGCGGCCGCTCTATTAGGCTTAGTCCTCCAGGCGC	Cloning, pSUMO-NRdR(ECO)
9	SUMO_fw	ATTCAAGCTGATCAGACCCCTGAA	PCR test, pSUMO-NrdR
10	pETite_rv	CTCAAGACCCGTTTAGAGGC	PCR test, pSUMO-NrdR
11	NrdR-PAO_TEV_fw	ATTACCATGGGCGAGAACCTTTACTTTCAAGGCAGCGGCAGCGGCAGCATGCATTGTCCCTTCTGC	Cloning, pCri-NrdR(PAO)
12	NrdR-PAO_TEV_rv	TATATACTCGAGTCATTCCTTGGCCGGCTCGCG	Cloning, pCri-NrdR(PAO)
13	NrdR-ECO_TEV_fw	TATACCATGGGCGAGAACCTTTACTTTCAAGGATCCGGATCCGGATCCATGCATTGCCCATTCTGTTTCGC	Cloning, pCri-NrdR(ECO)
14	NrdR-ECO_TEV_rv	TATATACTCGAGTTAGTCCTCCAGGCGCGCGATCT	Cloning, pCri-NrdR(ECO)
15	pETS130-backB_fw	AATCTAGATGCCCATGGACGCACAC	Cloning, pReViTA
16	pETS130-backB_rv	AAGACGTCCGGGGAGGCAGACAAGGTATA	Cloning, pReViTA
17	PnrdA-ECO_BamHI_fw	AAAGGATCCATCATTTTCTATAAGACGG	Cloning, pReViTA-PA / EMSA probes
18	PnrdA-ECO_SpeI_rv	AACTAGTAGCAGATTCTGATTCATG	Cloning, pReViTA-PA
19	ReViTA_TEST_fw	AGCACAAGTTTTATCCGGCC	ReViTA, qPCR
20	ReViTA_TEST_rv	CATATCACCAGCTCACCGTC	ReViTA, qPCR
21	ReViTA_TEST_rt	TGCTCATGGAAAACGGTGTAAC	ReViTA, rev. transcription
22	ReViTA_CTRL_fw	TTTCGGTCGTGAGTTCGGAG	ReViTA, qPCR
23	ReViTA_CTRL_rv	GCAAGCGCGATGAATGTCTT	ReViTA, qPCR
24	ReViTA_CTRL_rt	CGCCAACAACCGCTTCTTG	ReViTA, rev. transcription
25	PnrdA-ECO_m13_rv	CTGGGCGTCGTTTTACAAACTGAATGTGGGAGCG	EMSA probes
26	Anr-ctrlNEG_fw	GAATTCATGGCCGAAACCATCAAG	EMSA probes
27	Anr-ctrlNEG_m13_rv	CTGGGCGTCGTTTTACCTTCTTCGACAGCAGCAG	EMSA probes
28	WellRed M13	[D3-PA]GTCACTGGGCGTCGTTTTAC	EMSA probes, infrared dye

Supplementary table A3:1.R. Code of the gff.to.genes R function

```
function(gff.path,outfolder,prefix="parsedgff") {

      all.gff.data <- read.table(gff.path,sep="\t",stringsAsFactors=FALSE,quote="")
      is.gene <- rep(FALSE,nrow(all.gff.data))
      is.cds <- rep(FALSE,nrow(all.gff.data))

      for (i in 1:nrow(all.gff.data)) {
            if (all.gff.data[i,3]=="gene") {
                  is.gene[i] <- TRUE
            } else if (all.gff.data[i,3]=="CDS") {
                  is.cds[i] <- TRUE
            }
      }

      gene.gff.data <- all.gff.data[is.gene,]
      cds.gff.data <- all.gff.data[is.cds,]

      gene.message <- paste(c("The provided genome has ",nrow(gene.gff.data)," gene features"),collapse="")
      cds.message <- paste(c("The provided genome has ",nrow(cds.gff.data), "CDS features"),collapse="")

      geneIDtable <- vector()
      geneNAMEtable <- vector()
      locusTAGtable <- vector()

      PARENTtable <- vector()
      cdsNAMEtable <- vector()
      cdsTAGtable <- vector()

      outgff.col3 <- vector()
      outgff.col9 <- vector()

      outgffCDS.col3 <- vector()
      outgffCDS.col9 <- vector()

      for (i in 1:nrow(gene.gff.data)) {

            ind.annotations.gene <- unlist(strsplit(gene.gff.data[i,9],";"))

            is.geneID <- grepl("ID=",ind.annotations.gene)
            is.geneNAME <- grepl("Name=",ind.annotations.gene)
            is.locusTAG <- grepl("locus_tag=",ind.annotations.gene)

            geneIDtable[i] <- sub("ID=", "",ind.annotations.gene[is.geneID])
            geneNAMEtable[i] <- sub("Name=","",ind.annotations.gene[is.geneNAME])
            locusTAGtable[i] <- sub ("locus_tag=","",ind.annotations.gene[is.locusTAG])

            outgff.col3[i] <- paste(c("Locus=",locusTAGtable[i],"_Gene=",geneNAMEtable[i]),collapse="")
            outgff.col9[i] <- paste(c(geneIDtable[i],"_",locusTAGtable[i],"_",geneNAMEtable[i]),collapse="")

      }

      message(paste(c("Gene table created for ",nrow(gene.gff.data)," genes"),collapse=""))

      for (j in 1:nrow(cds.gff.data)) {

            this.gene.flag <- FALSE
            ind.annotations.cds <- unlist(strsplit(cds.gff.data[j,9],";"))

            is.PARENT <- grepl("Parent=",ind.annotations.cds)
            is.cdsNAME <- grepl("gene=",ind.annotations.cds)
```

```
        PARENTtable[j] <- sub("Parent=","",ind.annotations.cds[is.PARENT])

        if(sum(is.cdsNAME)==1){
              cdsNAMEtable[j] <- sub("gene=","",ind.annotations.cds[is.cdsNAME])
        } else {
              this.gene.flag <- TRUE
        }

        for (k in 1:nrow(gene.gff.data)) {
              if (geneIDtable[k]==PARENTtable[j]){
                    cdsTAGtable[j] <- locusTAGtable[k]
              }
              if (this.gene.flag) {
                    cdsNAMEtable[j] <- geneNAMEtable[k]
              }
        }

        outgffCDS.col3[j] <- paste(c("Locus",cdsTAGtable[j],"_Gene=",cdsNAMEtable[j]),collapse="")
        outgffCDS.col9[j] <- paste(c(PARENTtable[j],"_",cdsTAGtable[j],"_",cdsNAMEtable[j]),collapse="")

  }

  message(paste(c("CDS table created for ",nrow(cds.gff.data)," CDS"),collapse=""))

  out.gff.genes <- cbind.data.frame(gene.gff.data[,1:2],outgff.col3,gene.gff.data[,4:8],outgff.col9)
  out.gff.cds <- cbind.data.frame(cds.gff.data[,1:2],outgffCDS.col3,cds.gff.data[,4:8],outgffCDS.col9)

  geneID.file.out <- paste(c(outfolder,"/Auxiliar/",prefix,"_geneIDlist.txt"),collapse="")
  geneNAME.file.out <- paste(c(outfolder,"/Auxiliar/",prefix,"_geneNAMElist.txt"),collapse="")
  locusTAG.file.out <- paste(c(outfolder,"/Auxiliar/",prefix,"_locusTAGlist.txt"),collapse="")
  GFFgfile.out <- paste(c(outfolder,"/",prefix,"_OUTgenes.gff"),collapse="")

  cdsID.file.out <- paste(c(outfolder,"/Auxiliar/",prefix,"_cdsIDlist.txt"),collapse="")
  cdsNAME.file.out <- paste(c(outfolder,"/Auxiliar/",prefix,"_cdsNAMElist.txt"),collapse="")
  cdsTAG.file.out <- paste(c(outfolder,"/Auxiliar/",prefix,"_cdsTAGlist.txt"),collapse="")
  GFFcfile.out <- paste(c(outfolder,"/",prefix,"_OUTcds.gff"),collapse="")

  dir.create(paste(c(outfolder,"/Auxiliar"),collapse=""),showWarnings=FALSE)

  write(geneIDtable,geneID.file.out)
  write(geneNAMEtable,geneNAME.file.out)
  write(locusTAGtable,locusTAG.file.out)
  write.table(out.gff.genes,GFFgfile.out,sep="\t",quote=FALSE,col.names=FALSE,row.names=FALSE)

  message("Gene table stored in the following path")
  message(GFFgfile.out)

  write(PARENTtable,cdsID.file.out)
  write(cdsNAMEtable,cdsNAME.file.out)
  write(cdsTAGtable,cdsTAG.file.out)
  write.table(out.gff.cds,GFFcfile.out,sep="\t",quote=FALSE,col.names=FALSE,row.names=FALSE)

  message("CDS table stored in the following path")
  message(GFFcfile.out)

  message("All supplementary data stored in the following path")
  message(paste(c(outfolder,"/Auxiliar"),collapse=""))

}
```

Article 4

Pseudomonas aeruginosa exhibits deficient biofilm formation in the absence of class II and class III ribonucleotide reductases due to hindered anaerobic growth

Published in *Frontiers in Microbiology* (Q1, IF_{2016} = 4.165)

doi: 10.3389/fmicb.2016.00688 (188)

May 2016

Anna Crespo[1], Lucas Pedraz[1], Josep Astola[1], and Eduard Torrents[1*]

[1] Bacterial Infections: Antimicrobial Therapies, Institute for Bioengineering of Catalonia (IBEC), The Barcelona Institute of Science and Technology, Barcelona, Spain.

*: Corresponding author: Eduard Torrents (etorrents@ibecbarcelona.eu)

Abstract

Chronic lung infections by the ubiquitous and extremely adaptable opportunistic pathogen *Pseudomonas aeruginosa* correlate with the formation of a biofilm, where bacteria grow in association with an extracellular matrix and display a wide range of changes in gene expression and metabolism. This leads to increased resistance to physical stress and antibiotic therapies, while enhancing cell-to-cell communication. Oxygen diffusion through the complex biofilm structure generates an oxygen concentration gradient, leading to the appearance of anaerobic microenvironments.

Ribonucleotide reductases (RNRs) are a family of highly sophisticated enzymes responsible for the synthesis of the deoxyribonucleotides, and they constitute the only *de novo* pathway for the formation of the building blocks needed for DNA synthesis and repair. *P. aeruginosa* is one of the few bacteria encoding all three known RNR classes (Ia, II and III). Class Ia RNRs are oxygen dependent, class II are oxygen independent, and class III are oxygen sensitive. A tight control of RNR activity is essential for anaerobic growth and therefore for biofilm development.

In this work we explored the role of the different RNR classes in biofilm formation under aerobic and anaerobic initial conditions and using static and continuous-flow biofilm models. We demonstrated the importance of class II and III RNR for proper cell division in biofilm development and maturation. We also determined that these classes are transcriptionally induced during biofilm formation and under anaerobic conditions. The molecular mechanism of their anaerobic regulation was also studied, finding that the Anr/Dnr system is responsible for class II RNR induction. These data can be integrated with previous knowledge about biofilms in a model where these structures are understood as a set of layers determined by oxygen concentration and contain cells with different RNR expression profiles, bringing us a step closer to the understanding of this complex growth pattern, essential for *P. aeruginosa* chronic infections.

Introduction

Pseudomonas aeruginosa is a common Gram-negative bacterium that is recognized for its ubiquity and its advanced antibiotic resistance mechanisms. It is also relevant for its great adaptability, being able to inhabit many different environments; it can live free in soil and water and can growing in human and plant host-associated environments. This bacterium is related to clinically relevant human infections in immunocompromised patients and other risk groups. In particular, it causes severe chronic lung infections in patients suffering from cystic fibrosis (CF) or chronic obstructive pulmonary disease (COPD) (Lyczak et al., 2002;Davies et al., 2007;Ito and Barnes, 2009).

The establishment of chronic *P. aeruginosa* infections correlates with the formation of biofilm, a structure with clusters of cells encapsulated in a complex extracellular polymeric matrix. Bacteria in biofilms display different patterns of gene expression and phenotypes, reducing their metabolic rate and increasing cell-to-cell communication (Costerton et al., 1999) while becoming less sensitive to chemical and physical stresses, and they show increased chances of developing new antibiotic resistances (Xu et al., 1998;Stewart and Franklin, 2008). Oxygen does not diffuse freely through the biofilm structure, leading to the formation of an oxygen concentration gradient, which generates anaerobic microenvironments (Xu et al., 1998;Werner et al., 2004;Stewart and Franklin, 2008). The oxygen (and other chemical compounds) gradients are major driving forces for regulating the morphogenesis of the biofilm (Dietrich et al., 2013;Kempes et al., 2014;Okegbe et al., 2014).

While usually listed as an obligate aerobe, *P. aeruginosa* is able to grow in the absence of oxygen via anaerobic respiration using nitrates or other oxidized forms of nitrogen (NO_2, NO) as electron acceptors in a chain of reductions ending in molecular nitrogen (N_2) (Schobert and Jahn, 2010;Arat et al., 2015). The Anr, Dnr and NarL transcriptional factors are essential for regulating the expression of genes that encode the enzymes needed for denitrification, as well as regulating other genes related to anaerobic metabolism (Schreiber et al., 2007;Arai, 2011). Anr acts as a global oxygen-sensing regulator, controlling essential enzymes such as arginine deiminase and nitrate reductase and controlling *dnr* and *narL* gene expression. Dnr is a NO sensor and is able to modulate the expression of several genes under anaerobic conditions, including the enzymes thought to be involved in dissimilatory nitrogen reduction. NarL is a member of the NarLX two-component system, also thought to be involved in the regulation of nitrate reduction (Benkert et al., 2008). Bioinformatic studies have failed to identify differences between the Anr and Dnr binding sites (Trunk et al., 2010).

Anaerobic growth in *P. aeruginosa* biofilms is thought to be essential for full biofilm establishment (Stewart and Franklin, 2008) and has proven to be clinically relevant. In chronic CF lung infections, it has been shown that *P. aeruginosa* grows in low-oxygen environments within mucus plugs or biofilms (Schobert and Jahn, 2010). Furthermore, it has been shown that microaerophilic and anaerobic conditions are predominant in the sputum of patients with CF (Yoon et al., 2002;Alvarez-Ortega and Harwood, 2007;Hassett et al., 2009).

As another manifestation of its metabolic versatility, *P. aeruginosa* is one of the few microorganisms that encodes the three different ribonucleotide reductase classes in its genome. ribonucleotide reductases (RNRs) are key enzymes that catalyze the reduction of all four ribonucleotides to their corresponding deoxyribonucleotides, providing the necessary precursor molecules for DNA synthesis and repair in all organisms (Cotruvo and Stubbe, 2011;Sjoberg and Torrents, 2011;Hofer et al., 2012;Torrents, 2014;Lundin et al., 2015). RNRs are divided into three classes (I, II and III) based on their structural differences, metallocofactor requirements, and the mechanisms used for radical generation. Class I RNRs require oxygen to produce a tyrosyl radical using a diferric iron or a dimanganese iron centre and, thereby, function only under aerobic conditions. Class II RNRs require adenosylcobalamin (AdoCob) for radical generation and do not depend on oxygen (Torrents et al., 2005;Sjoberg and Torrents, 2011). Class III RNR belongs to the family of glycyl radical enzymes. The radical is generated by an activating enzyme with a [4Fe-4S] cluster that catalyses the reduction of S-adenosylmethionine (SAM). This class can only function under anaerobic conditions. Genes for active representatives of all three classes are present in *P. aeruginosa* metabolism: class I, subclass Ia (*nrdAB*), class II (*nrdJab*) and class III (*nrdDG*). Exceptionally the *P. aeruginosa* class II RNR is splitted and expressed in two different polypeptides (denoted as *nrdJa* and *nrdJb*) (Torrents et al., 2005;Crona et al., 2015). The presence and coordinated activity of the three classes is essential to ensure a supply of precursor molecules for DNA synthesis under both aerobic and anaerobic conditions (Sjoberg and Torrents, 2011). However, specifically in *P. aeruginosa* the synthesis of vitamin B_{12} only occurs in aerobic conditions (Lee et al., 2012) and its availability determines the class II RNR activity. Unfortunately, the exact role of each class and how they are genetically regulated is not yet fully understood.

In this work we aimed to study the importance of the different *P. aeruginosa* RNR classes for biofilm formation. We assessed the effect of class II and class III RNR deletion on static and continuous-flow biofilm formation and examined the phenotypic effects of this inactivation to establish the essential roles of RNRs in proper biofilm development. We also studied the genetic regulation responsible for modulating class II and class III RNR gene expression in biofilms, and we incorporated our data into a model where the *P. aeruginosa* biofilm is considered a set of layers determined by oxygen concentration gradients, vitamin-B_{12} and cells with different RNR expression profiles.

Materials and methods

Bacterial strains, plasmids and growth conditions

All bacterial strains and plasmids are listed in **Table A4:S1**. *Escherichia coli* and *Pseudomonas aeruginosa* cells were routinely grown in Luria-Bertani broth (LB) at 37ºC. Anaerobic growth occurred in LB medium containing KNO_3 (10 g/l) (LBN medium) or 1 mM S-nitrosoglutathione (GSNO) in screw-cap tubes (Hungate Tubes) that were purged with N_2 (Garriga et al., 1996;Arai, 2003). For the anaerobic culture of *P. aeruginosa anr, dnr* and *narL* isogenic mutant strains, which are not able to grow anaerobically, cells were first grown under aerobic conditions in LB medium to a mid-exponential phase (OD_{550}=0.5) and then the cultures were pelleted, resuspended in the same volume of LBN medium, and inoculated into screw-cap tubes containing anaerobic LBN medium. Finally, they were incubated for 3 hours to induce anaerobic metabolism.

When necessary, antibiotics were added at the following concentrations: for *E. coli*, 10 μg/ml gentamicin and 50 μg/ml ampicillin and for *P. aeruginosa*, 150 μg/ml gentamicin, 300 μg/ml carbenicillin and 50 μg/ml tetracycline. Vitamin B_{12} was added when necessary at a concentration of 1 μg/mL.

DNA manipulations and construction of plasmids and strains

Recombinant DNA techniques were performed using standard procedures (Sambrook et al., 1989). DNA fragments were amplified via PCR using High-Fidelity PCR Enzyme Mix (Fermentas, Thermo Scientific). All primers used in this study are listed in **Table A4:S2**. DNA fragments were digested by the corresponding restriction enzymes (Fermentas, Thermo Scientific) and ligated with T4 DNA ligase (Fermentas, Thermo Scientific) according to the manufacturer's instructions. Plasmid DNA was isolated using the GeneJET Plasmid Miniprep Kit (Fermentas, Thermo Scientific). DNA was transferred into *P. aeruginosa* cells either via electroporation using a Gene Pulser Xcell™ electroporator (Bio-Rad) or via conjugation, as previously described (Crespo et al., 2015).

pETS191 and pETS192 plasmids were generated by applying PCR-based site-directed mutagenesis at the putative Anr/Dnr binding boxes of the P*nrdJ* and P*nrdD* promoter regions ($TTGA^{T}/_{C}NNNN^{A}/_{G}TCAA$, from the PRODORIC database, http://www.prodoric.de/vfp/) and then cloning the resultant mutant promoters into pETS130-GFP plasmids. Anr/Dnr box mutagenesis was performed according to previously published procedures (Urban et al., 1997) using the following primers: for the P*nrdJ* promoter region, mutanrJ-up / mutanrJ-low as the inner primers and PnrdJ BamHI new-up / PnrdJ SmaI new-low as the outer primers; for the P*nrdD* promoter region, mutanrD-up / mutanrD-low as the inner primers and PnrdD-up / PnrdD new-low as the outer primers. The mutant fragments obtained from this process were cloned into pGEM-T Easy vectors, and the Anr/Dnr box mutation was verified via DNA sequencing. Finally, the fragments were digested with the corresponding restriction enzymes (BamHI/SmaI for P*nrdJ* and BamHI/ClaI for P*nrdD*) and cloned into pETS130-GFP plasmids.

For pETS193 generation, the *oprF* promoter region was amplified from *P. aeruginosa* PAO1 genomic DNA using the following primer pair: PoprFBHI-up / PoprFClaI-low. The amplicon (460 bp) was cloned into pGEM-T Easy vectors, verified via DNA sequencing, digested with BamHI/ClaI and cloned into pETS130-GFP plasmids.

For pETS195 generation, an amplicon containing the *dnr* promoter region and the full ORF (1128 bp) was amplified from *P. aeruginosa* PAO1 genomic DNA using the following primer pair: Pdnr-BHI up / Dnr-low. The amplicon was cloned into pGEM-T Easy vectors, verified via DNA sequencing, digested with BamHI/SalI and cloned into pUCP20T plasmids.

A *P. aeruginosa* Δ*nrdJ*Δ*nrdD* double mutant strain (ETS125) was constructed from the *P. aeruginosa* PAO1 *nrdD*::ΩTc; Tc^R (ETS103) strain (Sjoberg and Torrents, 2011) through the insertion of the gentamicin-resistance gene (*aacC1*) into the *nrdJ* gene using homologous recombination with the pETX100-Tlink vector, as previously described (Quenee et al., 2005). Briefly, two 400 bp areas surrounding the *nrdJ* gene were amplified via PCR with the following primer pairs: Jmut1HIIIup / Jmut2BIIw and Jmut3BIup / Jmut4SIIw. The two amplicons obtained were then cloned separately into pGEM-T Easy vectors. A plasmid containing both fragments was generated by BamHI/SacI digestion. The gentamicin resistance gene *aacC1* was obtained using *BamHI* digestion of pUCGmlox, and the corresponding cassette was ligated inside the two previous fragments. Next, the construct was cloned into the pEX100Tlink vector. The obtained plasmid pET100Tlink-*nrdJ*::ΩGm was transferred into the S17.1λ*pir* strain and conjugated to the *P. aeruginosa* ETS103 strain. Transformants were selected by plating them with tetracycline and gentamicin; 5% sucrose was added for *sacB*-mediated counterselection of the plasmids. The insertion of *aacC1* was screened via PCR with the primer pair Jmut1HIIIup / Jint-2-3lw and later confirmed via DNA sequencing.

Quantitative reverse transcription PCR (qRT-PCR)

RNA from *P. aeruginosa* PAO1 cells (either planktonic or from a biofilm) was isolated with RNAprotect Bacterial Reagent (Qiagen), according the manufacturer's instructions. RNA purification steps were carried out using the RNeasy Mini Kit (Qiagen), according the manufacturer's instructions. DNase I (Turbo DNA-free, Applied Biosystems) was used to remove the remaining DNA, and RNA samples were subjected to PCR to verify the absence of DNA. For cDNA synthesis, RNA was quantified using a NanoDrop 1000 spectrophotometer (Thermo Scientific), and 0.5 µg of RNA was reverse transcribed with SuperScript® III Reverse Transcriptase (Applied Biosystems) using the following primers for each gene: nrdATaqM2-low for *nrdA*, nrdJTaqM2-low for *nrdJa*, nrdDTaqM2-low for *nrdD* and gapTaqM-low for *gapA*. qRT-PCR quantification used nrdA-FAM, nrdJ-FAM, nrdD-FAM and gap-FAM qRT-PCR probes (Crespo et al., 2015).

Western immunoblot analysis

Western blotting was carried out as previously described (Sjoberg and Torrents, 2011), using anti-NrdJ (Agrisera, Sweden; and Thermo Fisher, USA) at a 1:1000 dilution. The detection of primary antibodies was performed using donkey anti-rabbit (Bio-Rad) horseradish peroxidase-conjugated secondary antibodies at a 1/50,000 dilution. The antibody-antigen complex was detected using the Amersham™ ECL™ Prime western blotting reagent (GE Healthcare), according the manufacturer's protocol. Proteins were visualized and analysed using an ImageQuant™ LAS4000 mini system (GE Healthcare).

Static and continuous-flow biofilm formation

To determine the biomass of static biofilms grown under aerobic conditions, cells were grown on 96-well plates (Nunclon Delta Surface, Thermo Scientific) in LB containing 0.2% glucose for 3 days at 37ºC. Fully anaerobic static biofilms were grown in the same plates using LBN medium containing 0.2% glucose, and they were incubated inside GENbag ANAER (Biomerieux) devices. After the incubation period, the culture supernatant was removed, and both kinds of biofilms plates were washed three times with 1x phosphate buffered saline (PBS) to eliminate any remaining planktonic cells. Cells attached to the wells were then fixed with methanol and stained with 1% crystal violet (Cendra Mdel et al., 2012). After staining, excess crystal violet was eliminated with water, and 33% acetic acid was used to dissolve the remaining dye. Biofilm mass was finally determined as a function of the concentration of this dye based on the absorbance at 570 nm ($A4_{70}$).

Continuous-flow biofilms were cultured as previously described (Christensen et al., 1999;Baelo et al., 2015) with the following modifications. Biofilms were grown into three-channel flow cells made of Perspex (poly[methyl methacrylate], channel size 40x4x1 mm) (DTU Systems Biology, Technical University of

Denmark) covered with a nº1 24x50 mm glass coverslip (Deltalab, ref. D102450) which served as the biofilm substratum. Flow cells were supplied with LB broth supplemented with 0.2% glucose, pumped by a high precision multichannel peristaltic pump (Ismatec ISM 943, Idex). Flow cells were inoculated using a 1-ml syringe with a 26 G needle and kept static for 1 h. After this point, flow was initiated at a rate of 3 ml/channel/hour. After 5-6 days of growth, biofilms were analysed through staining the formed biofilm with the LIVE/DEAD BacLight Bacterial Viability Kit (Molecular Probes, Life Science), according to the manufacturer's instructions, and the biofilms were visualized with a Leica TCS SP5 confocal scanning laser microscope (CSLM) (Leica Microsystems, Wetzlar, Germany). The excitation wavelength was 488 nm and the emission wavelength was 500 nm. Images were obtained using a 20X/0.70 air objective. Simulated fluorescence projections and sections were generated using ImageJ software, and COMSTAT 2 software was used to quantify the biomass and thickness of the biofilms (Weiss Nielsen et al., 2011).

Green fluorescent protein gene reporter assay

Promoters of the different RNR genes fused to GFP in pETS130-GFP plasmids were used to determine RNR gene expression (pETS134 (P*nrdA*::GFP), pETS180 (P*nrdJa*::GFP) and pETS136 (P*nrdD*::GFP)). pETS191 (P*nrdJ Δ*Anr/Dnr-box::GFP) and pETS192 (P*nrdD Δ*Anr/Dnr-box::GFP) plasmids were used to evaluate the effect of an Anr/Dnr box mutation on *nrdJ* and *nrdD* expression, respectively. pETS193 (P*oprF*::GFP) plasmids were used as a control.

For liquid culture experiments, GFP fluorescence was measured in 96-well plates (Costar® 96-Well Black Polystyrene Plate, Corning) on an Infinite 200 Pro Fluorescence Microplate Reader (Tecan), as previously described (Crespo et al., 2015). Briefly, three independent 1-ml samples of cells harbouring the corresponding gene reporter assay plasmids grown to the mid-logarithmic phase (OD_{550}) were collected and pelleted. Cells were fixed with 1 ml of a freshly prepared 1x PBS solution containing 2% formaldehyde and stored in the dark at 4ºC. Three measurements were performed for each independent sample.

To determine gene expression during biofilm formation, experiments were performed on static biofilms formed in 96-well plates (Nunclon Delta Surface, Thermo Scientific) after the incubation of a liquid culture of the corresponding strain in LB containing 0.2% glucose at 37ºC. After incubating the plate for a specific time (from 3 h to 72 h), the culture supernatant was removed, and each well was washed three times with PBS to eliminate and remaining planktonic cells. The biofilm cells attached to the wells were then fixed with PBS containing 2% formaldehyde. Finally, fluorescence measurements were performed on an Infinite 200 Pro Fluorescence Microplate Reader (Tecan).

Results

Anaerobic RNR classes play an important role in P. aeruginosa biofilm formation

The *P. aeruginosa* genome encodes genes for three different ribonucleotide reductase (RNR) genes, two of them (class II and III) are able to function enzymatically under anaerobic conditions, as previously described (Sjoberg and Torrents, 2011). The individual Δ*nrdJ* and Δ*nrdD* mutant strains showed a strong reduction in their anaerobic growth capacity (**Table A4:S3**). The Δ*nrdD* strain was able to grow under anaerobic conditions when supplemented with adenosylcobalamin or vitamin B_{12} to enhance class II RNR activity, agreeing with our previous report (Torrents et al., 2005;Sjoberg and Torrents, 2011). In this work, we generated a double class II (Δ*nrdJ*) and class III (Δ*nrdD*) RNR mutant (ETS125) that was unable to grow anaerobically (only growing to OD_{550} = 0.05 after a standard overnight anaerobic culture) and only was capable to grow under aerobic conditions (OD_{550}=3.8). These growth patterns indicate the simultaneous need for class II and III RNRs in *P. aeruginosa* for anaerobic metabolism (**Table A4:S3**).

As anaerobic growth is needed to support full biofilm establishment (Stewart and Franklin, 2008), we explored the role of the different RNR classes in *P. aeruginosa* biofilm formation. The *P. aeruginosa* PAO1 wild-type strain, single Δ*nrdJ* (class II RNR) and Δ*nrdD* (class III RNR) isogenic mutant strains and double Δ*nrdJ*Δ*nrdD* mutant strain were assayed for their ability to form static biofilms under aerobic and anaerobic conditions (**Figure A4:1A**). The class I RNR mutation (Δ*nrdA*) strain is not viable and was not used in the current study (Sjoberg and Torrents, 2011). The results show that deficiencies in class II RNR activity (in ETS102 Δ*nrdJ* strain) and in class III RNR activity (in ETS103 Δ*nrdD* strain) resulted in decreased static biofilm formation under both aerobic and anaerobic initial conditions. Complementation of the mutation with a copy of the corresponding wild-type RNR gene (*nrdJ* or *nrdD* cloned into plasmids pEST159 and pETS160, respectively) returned biofilm formation to a level similar to that of the wild-type strain. The double Δ*nrdJ*Δ*nrdD* RNR mutant (ETS125) showed almost no biofilm formation, and the decrease was even stronger in anaerobic biofilm formation experiments, demonstrating the key role of anaerobic RNR activity in *P. aeruginosa* biofilm formation. However, our results suggest that anaerobic RNR activity is needed for biofilm formation even when the experiment is performed under aerobic conditions. A *P. aeruginosa* Δ*dnr* mutant strain (PW1965), unable to grow anaerobically, was used to compare the results from the RNR mutant with those from a strain unable to perform general anaerobic metabolism. Dnr is a transcriptional factor that regulates the expression of essential genes during *P. aeruginosa* anaerobic growth (Trunk et al., 2010). As expected, the PW1965 strain showed strong differences in biofilm formation when compared with the wild-type strain, even when the initial culture conditions were aerobic, and its ability to form biofilms resembled the ability shown by the ETS125 double RNR mutant strain.

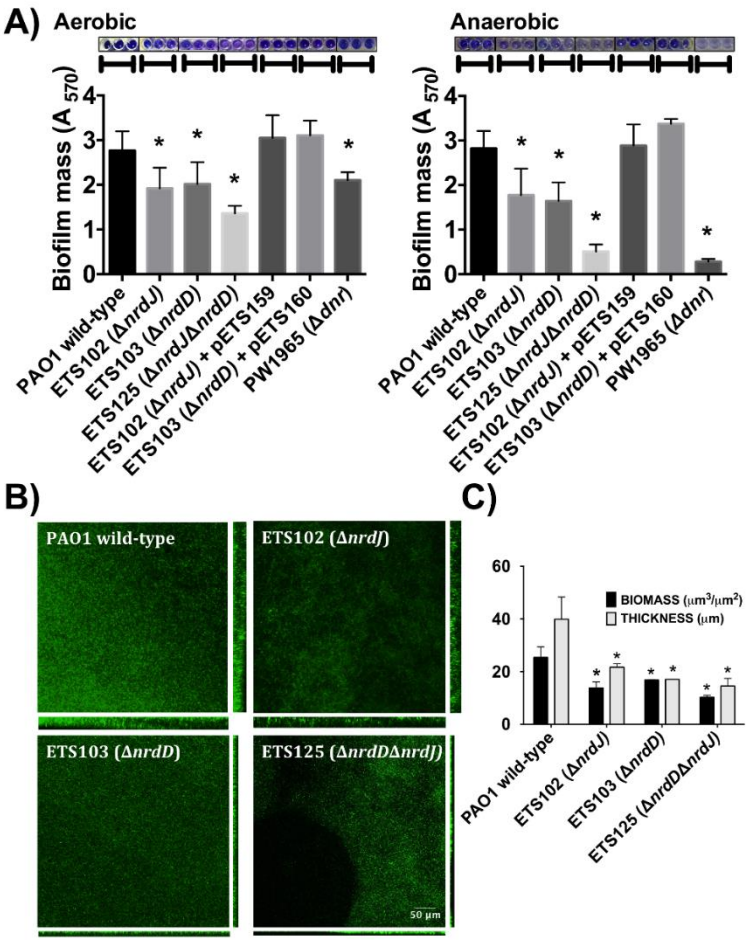

Figure A4:1. Biofilm formation in *P. aeruginosa* PAO1 wild-type and RNR mutant strains. **A)** Initially aerobic and fully anaerobic static biofilm biomass quantification after growing at 37ºC for 4 days. Each value is accompanied by the corresponding crystal violet-stained biofilm image. More than 20 replicates were performed in three independent experiments. The *nrdJab* and *nrdDG* genes cloned into pETS159 and pETS160 plasmids were used to complement *nrdJ* and *nrdD* deficiencies in ETS102 and ETS103 strains. The Δ*dnr* strain was included to compare RNR mutant strains with a strain defective in anaerobic metabolism. **B)** Confocal laser scanning microscopy images of continuous-flow biofilms (sum of stack images) and their corresponding orthogonal views for *P. aeruginosa* PAO1 wild-type, ETS102 Δ*nrdJ*, ETS103 Δ*nrdD* and ETS125 Δ*nrdD*Δ*nrdJ* strains. **C)** Quantification of total biomass ($\mu m^3/\mu m^2$) and average thickness (µm) for the biofilms from the previous continuous-flow experiments. Data are the average of three independent experiments. *: Significantly different from the wild-type strain in an unpaired *t*-test (P<0.05).

To further corroborate our previous static biofilm formation experiments, we explored the importance of the different RNR classes in continuous-flow biofilm formation performed in flow cells. This technique better mimics the biofilms found in nature and specifically in the mucus plaques within the lungs of CF patients (Weiss Nielsen et al., 2011;Lebeaux et al., 2013). Biofilm cultures of different strains were cultivated under a continuous flow of LB medium over 6 days to obtain a robust and mature

biofilm. The formed biofilms were then stained and visualized using confocal laser scanning microscopy (CLSM), as described in the Materials and Methods section.

Figure A4:1B shows the images obtained for the biofilms formed by the different strains that were evaluated and their corresponding orthogonal views. The thickness and total biomass values for each biofilm, estimated by COMSTAT software, are presented in **Figure A4:1C**. The biomass ($\mu m^3/\mu m^2$) and average thickness (µm) of the biofilms formed by all RNR mutant strains were decreased; biomass of the wild-type strain biofilm was 2.2, 1.8 and 2.7 times higher than the corresponding biomass of the anaerobic RNR mutant strains (ETS102 Δ*nrdJ*, ETS103 Δ*nrdD* and ETS125 Δ*nrdD*Δ*nrdJ*, respectively). The greatest thickness observed was in the *P. aeruginosa* wild-type strain biofilm (49.40 µm), while the different class II and III RNR mutant strains formed significantly thinner biofilms, with an average thickness of 24.84, 15.5 and 14.53 µm for ETS102 Δ*nrdJ*, ETS103 Δ*nrdD* and ETS125 Δ*nrdD*Δ*nrdJ*, respectively. It is important to note that the *P. aeruginosa* double RNR class mutant (ETS125 Δ*nrdD*Δ*nrdJ*) grew in a discontinuous pattern and showed difficulties in attaching to the glass surface. These results confirm our previous observations in static biofilms, highlighting the importance of anaerobic RNRs in biofilm formation even when culture conditions are initially aerobic.

RNR enzymes contribute to proper cell division in a biofilm.

Figure A4:2 shows the CLSM analysis of the longitudinal cell morphology in a structured biofilm formed by the different *P. aeruginosa* strains (PAO1 wild-type, ETS102 Δ*nrdJ*, ETS103 Δ*nrdD* and ETS125 Δ*nrdD*Δ*nrdJ*). As described previously, the different RNR mutant strains showed elongated morphologies during anaerobiosis (Lee et al., 2012). The *P. aeruginosa* wild-type cells showed a normal rod-shape cell morphology throughout the biofilm in both the aerobic and anaerobic regions (top and bottom segments of the biofilm, respectively). However, the *P. aeruginosa* ETS102 Δ*nrdJ* mutant strain showed significant cell elongation in both the top and the bottom parts of the biofilm structure, indicating some disturbances in cell growth and division, as was clearly demonstrated in previous planktonic anaerobic cultures (Yoon et al., 2011;Lee et al., 2012). Some *P. aeruginosa* ETS103 Δ*nrdD* cells also showed cell elongation but only in the bottom layer of the biofilm (anaerobic region), while rod-shaped cells were found in the upper region that were similar to the shapes of the wild-type strain. Finally, the *P. aeruginosa* double mutant (ETS125 Δ*nrdJ*Δ*nrdD*) exhibited cell elongated along the entire span of the biofilm, similar to the results seen in the II RNR mutant (ETS102 Δ*nrdJ*).

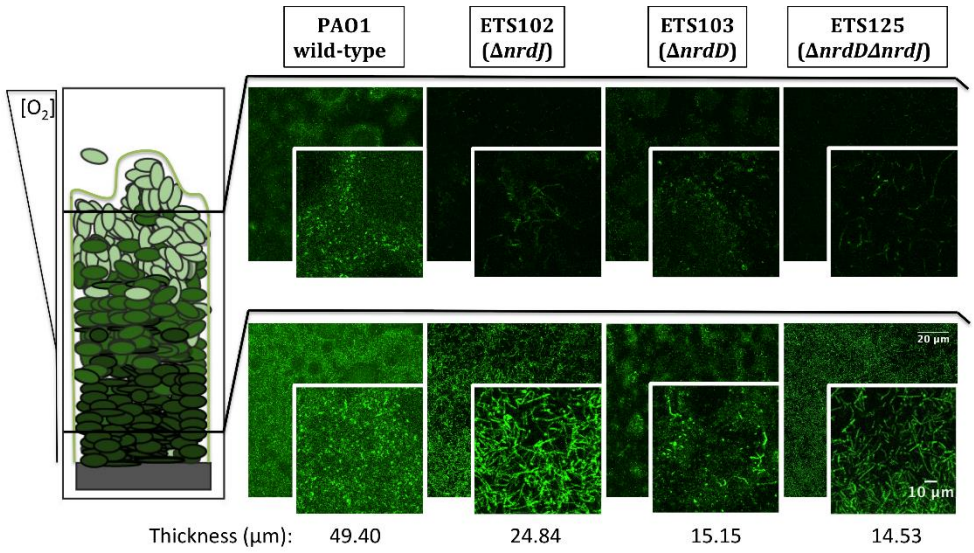

Figure A4:2. Detailed microscopy observations of structured biofilms from *P. aeruginosa* PAO1 wild-type, ETS102, ETS103 and ETS125 strains. On the left side, a scheme of the longitudinal structure of *P. aeruginosa* biofilm is represented, labelled with indications of the oxygen concentration along the biofilm (Stewart and Franklin, 2008). On the right side, CLSM images are shown, which were taken from the aerobic region of the biofilm (top part, superficial biofilm) and from the anaerobic region (bottom part, deeper in the biofilm structure). An internal panel with a magnification of a local area is shown for each image. The corresponding average thickness of each strain is representative of three independent experiments.

During biofilm formation, expression of the nrdJ and nrdD genes is increased.

Our previous results demonstrate the importance of class II and class III RNRs for anaerobic growth and biofilm formation in *P. aeruginosa* and show that these two processes are related as biofilm growth is characterized by a decrease oxygen tension that results in anaerobic conditions in the bottom regions of the structure (Werner et al., 2004;Stewart and Franklin, 2008). We hypothesized that the expression of class II and class III RNRs could be induced under these growing conditions. To explore this, we studied the induction of the different RNR genes using RT-PCR.

	Differential expression (fold-change)		
	nrdA	***nrdJa***	***nrdD***
Planktonic anaerobic vs. Planktonic aerobic	2.1 ± 0.4	85.2 ± 5.0	110.6 ± 19.2
Biofilm aerobic vs. Planktonic aerobic	13.1 ± 6.2	1500 ± 150	128.2 ± 5.1
Biofilm aerobic vs. Planktonic anaerobic	2.4 ± 1.0	51.6 ± 7.3	−12.3 ± 1.6

Table A4:1. Relative expression of RNR genes based on real-time PCR. Fold change in *P. aeruginosa* PAO1 *nrdA, nrdJa* and *nrdD* transcription determined using real time PCR from 16-hour-old planktonic cells grown aerobically or anaerobically and 4-day-old cells growing in biofilms. "Biofilm aerobic" refers to biofilms grown under initially aerobic conditions. The *gap* gene was used as an internal standard. The results shown represent the average of three independent experiments ± standard deviation.

First, we explored the induction of RNR genes by comparing anaerobic growth with aerobic growth in liquid cultures at the stationary phase (**Table A4:1**). The results showed a strong increase in *nrdJa* and *nrdD* expression (85.2 and 110.6), while *nrdA* expression (2.1 times) was only slightly increased under anaerobic conditions.

We also explored the effect of biofilm growth itself on RNR expression. To do this, we analysed the RNA expression of each RNR class in aerobic planktonic cells (at the stationary phase) relative to the RNR expression in cells growing in aerobically made biofilms (a 4-day-old biofilm) (**Table A4:1**) using RT-PCR. The results obtained in the *P. aeruginosa* wild-type strain showed significant differences in RNR expression between the two conditions: expression levels of *nrdA* showed a slight increase, but the expression of *nrdJa* and *nrdD* were both highly induced in the cells forming a robust biofilm relative to expression in the planktonic culture.

The induction of *nrdJa* and *nrdD* gene expression shown in biofilm formation and under anaerobic conditions could be due to control by factors related to anaerobic metabolism (i.e., factors acting in anaerobic cultures and in the anaerobic areas of biofilms) or/and due to specific biofilm-related factors. As a first approach to exploring this control, we examined the patterns of our previous RT-PCR results (**Table A4:1**). When comparing the results in the initially-aerobic biofilm conditions with those of the anaerobic planktonic conditions, it is clear that *nrdJa* expression was highly increased during biofilm formation (1500 fold-change vs 85), while *nrdD* expression was increased to a higher rate by factors related to anaerobic metabolism (almost same fold-change levels 110 vs 128).

Class II RNRs are transcriptionally activated by a dnr transcription factor.

To this point, we have demonstrated that class II and class III RNRs are of great importance for biofilm formation and that biofilm growth and an anaerobic environment strongly induce their expression. Therefore, the key transcriptional factors involved in *P. aeruginosa* anaerobic metabolism (Anr, Dnr and NarL) were studied as putative transcriptional regulators for inducing RNR anaerobic expression (Arai, 2011;Arat et al., 2015).

The different transcription factors (Anr, Dnr and NarL) are responsible for the regulation of different parts of the reduction chain in anaerobic respiration in *P. aeruginosa* (from NO_3 to N_2, through NO_2 and NO (Trunk et al., 2010)). Therefore, in the anaerobic transcriptional regulation study, *P. aeruginosa* was grown using KNO_3 and GSNO (a NO donor) as final electron acceptors to obtain more information about

which transcriptional regulator might be involved in the RNR transcriptional regulation under anaerobic conditions.

Transcriptional fusions of the *nrdJ* and *nrdD* promoter regions to GFP (present in the pETS180 and pETS136 plasmids, respectively) were transformed in different *P. aeruginosa* strains (PAO1, PW3784 Δ*anr*, PW1965 Δ*dnr* and PW7549 Δ*narL*) and used for gene reporter assays (see Materials and Methods). As seen in **Figure A4:3A**, the results show an increased expression of both *nrdJ* and *nrdD* under anaerobic growth in the presence of both NO_3^- (321 and 188, respectively) and GSNO (351 and 163, respectively) compared to the expression during aerobic growth (146 and 101, respectively).

A)

	Strains	Relative fluorescence units (kRfu)		
		O_2	NO_3	GSNO
pETS180 (P*nrdJ*)	PAO1 wild-type	146 ± 8	321 ± 34	351 ± 13
	PW3784 (Δ*anr*)	132 ± 18	181 ± 18*	248 ± 16*
	PW1965 (Δ*dnr*)	136 ± 10	204 ± 34*	242 ± 25*
	PW7549 (Δ*narL*)	123 ± 24	315 ± 27	344 ± 21
pETS136 (P*nrdD*)	PAO1 wild-type	101 ± 3	188 ± 22	163 ± 6
	PW3784 (Δ*anr*)	106 ± 18	217 ± 26	101 ± 9
	PW1965 (Δ*dnr*)	96 ± 18	221 ± 17	102 ± 11
	PW7549 (Δ*narL*)	100 ± 7	188 ± 12	244 ± 12

B)

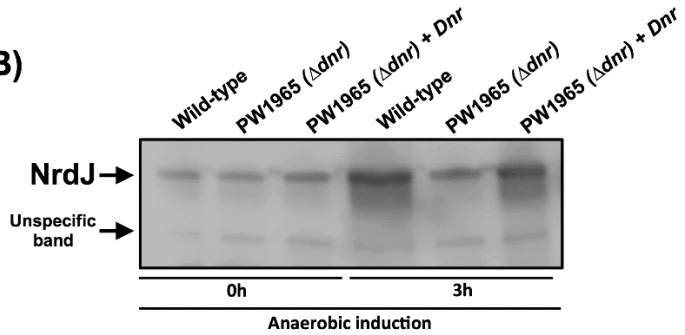

Figure A4:3. Transcriptional regulation of *nrdJ* and *nrdD* during anaerobic growth. **A)** Transcriptional expression of *nrdJ* (pETS180) and *nrdD* (pETS136) promoters in *P. aeruginosa* wild-type, PW3785 Δanr, PW1965 Δ*dnr* and PW7549 Δ*narL* strains. Cells were grown aerobically to a mid-logarithmic phase (A_{550}=0.5) and then were grown anaerobically (with NO_3 or GSNO as electron acceptors) for 3 hours to induce anaerobic metabolism. Values are the means ±SD from more than three independent experiments. *: Significantly different from the *P. aeruginosa* wild-type strain in an unpaired t-test (p-value <0.05). kRfu = 1000 relative fluorescence units. **B)** NrdJ protein expression analysis in PAO1 wild-type, PW1965 Δ*dnr* and PW1965 Δ*dnr* + pETS195 (*dnr* complementation plasmid) via western blot analysis performed at a mid-logarithmic phase after 0 h or 3 h of anaerobic induction. A representative blot of three independent western blot analyses is shown. An unknown, unspecific band that is present at an almost constant intensity in all samples is shown in the blot and served as a loading control.

Comparing *nrdJ* expression between the *P. aeruginosa anr*, *dnr*, and *narL* knockout mutant strains and the wild-type strain (**Figure A4:3A**), we identified a reduced anaerobic induction of *nrdJ* expression in

the Δ*anr* (PW3784) and Δ*dnr* (PW1965) mutant strains compared with the values of the wild-type strain. No effect was observed on *nrdJ* transcription when the *narL* gene was mutated. Our results show the dependence of the anaerobic induction of *nrdJ* gene expression on Anr and Dnr transcriptional regulators. As the effect is shown when any of these two genes are mutated and Dnr is controlled by Anr (which acts early in the regulatory chain of anaerobic metabolism), Dnr was considered the most likely candidate for being responsible for regulating *nrdJ.*

This control of *nrdJ* expression by Dnr was later verified at the protein level using a western blotting assay (**Figure A4:3B**). Although no differences were found in the amount of NrdJ protein between *P. aeruginosa* wild-type and PW1965 Δ*dnr* mutant strains when measured during aerobic growth, 3 hours of anaerobic metabolism induced a strong reduction in NrdJ levels in the Δ*dnr* strain relative to expression in the wild-type cells. This effect was reverted back to near wild-type levels by Dnr complementation using the pETS195 complementation plasmid.

We failed to identify any regulation on *nrdD* expression by anaerobiosis-related Anr, Dnr or NarL factors, as demonstrated in our results (**Figure A4:3A**).

To determine if the anaerobiosis-related transcriptional factors bind specifically on the RNR promoters, a bioinformatic search of putative Anr-Dnr binding sites was performed on the P*nrdJ* and P*nrdD* promoter regions. One Anr/Dnr-box was identified on both P*nrdJ* and P*nrdD* promoters (see Materials and Methods) according to the $TTGA^{T}/_{C}NNNN^{A}/_{G}TCAA$ consensus present in PRODORIC database. The putative Anr/Dnr boxes identified are shown in **Figure A4:4**.

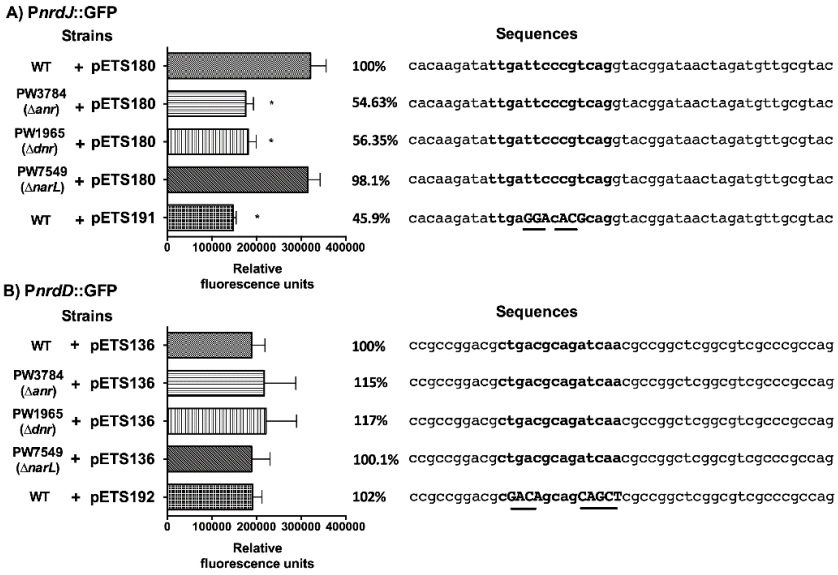

Figure A4:4. *nrdJ* and *nrdD* expression in *P. aeruginosa* wild-type, PW3784 Δ*anr*, PW1965 Δ*dnr* and PW7549 Δ*narL* strains. GFP fluorescence of **A)** P*nrdJ* and P*nrdJ* ΔAnr/Dnr-box and **B)** of P*nrdD* and P*nrdD* ΔAnr/Dnr-box measured in the wild-type, PW3784 Δ*anr*, PW1965 Δ*dnr* and PW7549 Δ*narL* strains at a mid-logarithmic phase after 3 h of anaerobic induction. A fragment of the sequence of the corresponding promoter regions surrounding the putative Anr/Dnr-box is added at the right, and the sequence of the box is indicated in bold letters. In the mutant Anr/Dnr-boxes, mutated nucleotides are indicated in capital letters and underlined. The Anr/Dnr box is centred at –84 and at –98 bp from the translation start site of the *nrdJ* and *nrdD* genes, respectively. *: Significantly different from the wild-type strain in an unpaired *t*-test (P<0.05). Error bars represent the standard deviation for three independent experiments.

To confirm the binding of Anr/Dnr to the promoters, we specifically mutated the essential nucleotides of the putative Anr/Dnr-boxes identified, fused the mutant promoters to GFP and constructed plasmids for gene reporter assays (pETS191 for the *nrdJ* promoter and pETS192 for the *nrdD* promoter). In the corresponding assay, P*nrdJ* expression decreased when the Anr/Dnr-box was mutated. Moreover, the ΔAnr/Dnr-box P*nrdJ* (pETS191) expression was similar to that found in Δ*anr* and Δ*dnr* mutant strains (**Figure A4:4A**). However, no significant results were obtained when mutating the P*nrdD* Anr/Dnr-box (**Figure A4:4B**).

The presence of anaerobic environments in the biofilm increases nrdJ expression through dnr activation.

Our previous results demonstrate that class II and class III RNRs are of great importance for biofilm formation and anaerobic growth in *P. aeruginosa* and that their expression is specifically induced under these conditions. As the induction of anaerobic metabolism increases as biofilm growth advances, we expected to detect a progressive induction of the expression of both RNRs during biofilm establishment and maturation.

To determine this, a GFP-based gene reporter assay was performed on a static biofilm culture over time. The expression of wild-type P*nrdA*, *PnrdJ* and P*nrdD* was determined together with that of the mutant versions of P*nrdJ* and P*nrdD* (carrying mutant Anr/Dnr-boxes); a promoterless GFP plasmid (pETS130) was used as a negative control, and the *oprF* promoter (P*oprF*) was used as a positive control for anaerobic induction. OprF is a membrane protein that has its highest expression under anaerobic conditions, and it can be used as a marker of infection in a CF patient's lung or sputum (Yoon et al., 2002;Eichner et al., 2014).

As expected (**Figure A4:5A**), P*oprF* expression increased greatly during mature biofilm development, demonstrating the progressive establishment of anaerobic conditions in the deep layers of the biofilm structure. Simultaneously, the P*nrdJ* and P*nrdD* promoter expression increased, although P*nrdD* expression increased only in the later stages when a mature and robust biofilm was formed. Mutating the Anr/Dnr-box severely reduced P*nrdJ* expression, while the anaerobic induction of P*nrdD* remained unaffected.

As a *P. aeruginosa* Dnr deficient strain is still able to grow as a biofilm, we further explored how Dnr controls RNR expression during biofilm formation by comparing *nrdA*, *nrdJ* and *nrdD* transcription in planktonic cells with that in biofilm-forming cells using the PW1965 Δ*dnr* mutant strain. Comparing the results obtained (**Figure A4:5B**) with those from a P. *aeruginosa* wild-type biofilm vs. planktonic comparison (**Table A4:1**), we can see that when mutating the Dnr gene, the induction of *nrdJ* expression in biofilms becomes severely reduced but not completely abolished. Surprisingly, we also noticed that the induction of *nrdD* expression was also strongly reduced in the PW1965 Δ*dnr* strain, which is in contrast with what was observed in the gene reporter assays (**Figure A4:3A** and **Figure A4:4B**).

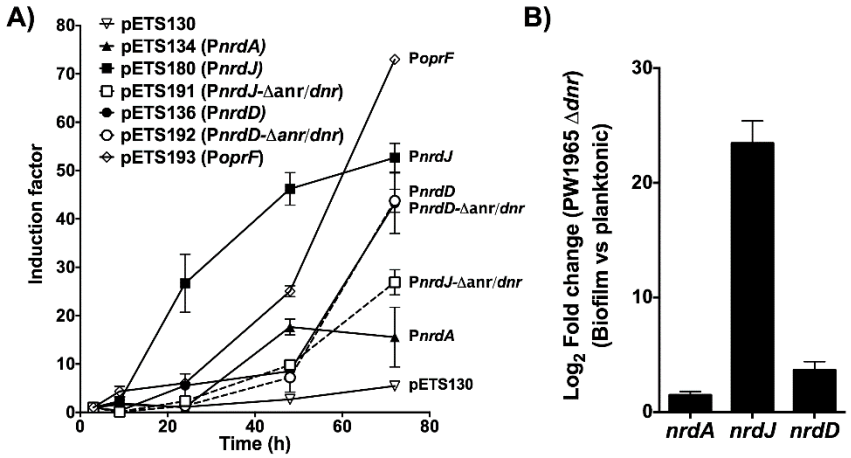

Figure A4:5. Regulation of RNR expression during biofilm formation. **A)** GFP-based gene reporter assay of *P. aeruginosa* cells growing as a static biofilm. The induction factor is expressed as the quotient of the fluorescence units measured from one strain at one point in time relative to the corresponding value measured at the first time point (3 hours of culture). Each strain was monitored between 3 h and 72 h of biofilm growth. Wild-type RNR promoters (P*nrdA*, P*nrdJ*, and P*nrdD*) are represented in continuous lines, and mutant RNR promoters (P*nrdJ* and P*nrdD* carrying a mutant version of the putative Anr/Dnr-box identified) are plotted in dotted lines. A promoterless GFP in pETS130 plasmids was used as a negative control, and the P*oprF* promoter in pETS193 plasmids was used as a positive control for anaerobic induction of gene expression. **B)** Fold change in *P. aeruginosa* PW1965 Δ*dnr* P*nrdA*, P*nrdJ* and P*nrdD* promoter transcription was determined through real time PCR in 4-day-old cells grown as a static biofilm and compared with transcription in 16-hour-old planktonic cells, both of which were cultured under aerobic conditions. The *gap* gene was used as an internal standard. The results shown represent the mean of three independent experiments ± standard deviation.

Discussion

Pseudomonas aeruginosa is well known for its genetic diversity. It has a relatively large genome (6.3 Mb) for a bacterium, and contains a large number of genes involved in different metabolic activities, which might contribute to the environmental adaptability of this bacterium. Its ability to grow in the absence of oxygen using nitrates or other forms of oxidized nitrogen as electron acceptors is an important example of *P. aeruginosa's* anaerobic growth capacity (Trunk et al., 2010;Arat et al., 2015), which opens up a wide range of environments in which *P. aeruginosa* can grow.

Such anaerobic environments are present in a mature biofilm, in which different nutrient gradients and differential physical properties appear. Previous reports have highlighted the oxygen concentration heterogeneity in biofilms using microelectrodes, and have described the oxygen diffusion profiles in continuous biofilms (Werner et al., 2004). The oxygen concentration throughout the biofilm is thus a crucial parameter for bacterial growth in a mature biofilm (Stewart and Franklin, 2008) and strongly defines its morphogenesis and final structure (Dietrich et al., 2013;Kempes et al., 2014;Okegbe et al., 2014). Metabolites and oxygen easily diffuse in the outer layers of the biofilm; however, the free oxygen concentration becomes reduced in lower layers, resulting in strict anaerobic conditions in the depths of the mature biofilm. The three ribonucleotide reductase classes encoded by *P. aeruginosa* (class Ia, encoded in *nrdA* and *nrdB*; class II, encoded in *nrdJa* and *nrdJb*; and class III, encoded in *nrdD* and *nrdG*) are likely to increase the capacity of this bacterium to grow in the different environments generated throughout biofilms (Torrents et al., 2005;Sjoberg and Torrents, 2011).

Class Ia activity is strictly oxygen dependent, while class III is oxygen sensitive and can only function under strict anaerobic conditions. Class II is oxygen independent but needs vitamin B_{12} (S-adenosylcobalamin) for the completion of its catalytic cycle (Torrents et al., 2005). In accordance of these different levels of oxygen dependence, we hypothesized that all three RNR classes would have a predominant role in the progressively deeper layers of the biofilm structure, with class II and class III RNRs essential for anaerobic growth and therefore for the establishment of fully mature biofilms.

The most basic study was performed to analyse the differential ability of Δ*nrdJ* and Δ*nrdD* mutant strains and a Δ*nrdJ* Δ*nrdD* double mutant strain to grow in aerobic and anaerobic liquid cultures. The large reduction in anaerobic growth found after altering class II or class III RNRs highlights the importance of both RNR classes for anaerobic growth (**Table A4:S3**). In addition, the ability of class II RNRs alone to sustain anaerobic growth when the culture was supplemented with exogenous S-adenosylcobalamin suggests that class II RNRs can theoretically synthesize enough dNTPs to maintain normal growth rates, with S-adenosylcobalamin levels under anaerobic conditions being the limiting step.

The next step was to study how these same effects act on the natural formation of the anaerobic environments that appear during biofilm formation. Static biofilm formation was severely diminished

when class II or class III RNRs were mutated (**Figure A4:1A**). This effect was higher when biofilms were built directly under anaerobic conditions but was also present under aerobic conditions. We associated this effect to the formation of anaerobic microenvironments in the biofilm depths that will undoubtedly occur if biofilms grow thick enough, and this was demonstrated by the analogous effect observed when mutating the *dnr* gene, which is one of the main transcriptional regulators of anaerobic metabolism (Schreiber et al., 2007). In this case, the impaired anaerobic metabolism implies that biofilm biomass will be reduced even when conditions are initially aerobic.

As static biofilm formation in microplates can be considered an artificial lab condition, we also studied the effect of class II and class III RNR alterations on continuous-flow biofilm formation, a technique that is thought to better the mimic biofilms present in nature and in clinically relevant cases, such as lung infections in cystic fibrosis patients (Weiss Nielsen et al., 2011;Lebeaux et al., 2013). Agreeing with our previous results, both biofilm biomass and thickness were considerably reduced when mutating the class II and/or class III RNRs (**Figure A4:1B** and **A4:1C**). The structure of the so-formed biofilm also changed compared with that of the wild-type biofilm. It is particularly important that in the Δ*nrdJ* Δ*nrdD* double mutant strain, a growth pattern of discontinuous patches appeared, showing the dependence on aeration of this strain.

All these data can be incorporated into a model in which the biofilm is considered a set of layers where the free oxygen concentration is progressively reduced with depth (**Figure 6**). Interestingly, vitamin B_{12} can only be synthesized under aerobic conditions (Lee et al., 2012); to our knowledge the diffusion properties of vitamin B_{12} in the biofilm have never been formally determined, but we can expect it to be gradually diffused throughout the biofilm layers and actively consumed when crossing them, therefore the deeper layers would not only be anaerobic but also limited in adenosylcobalamin. Therefore, at the top of the biofilm, class I RNRs would be the main enzyme responsible for dNTP synthesis, while class II RNRs would gain more importance in the middle layers (characterized by reduced oxygen levels but within the range of vitamin B_{12} diffusion) and class III RNRs would support growth in the lower layers as it does not depend on oxygen or metabolite diffusion from the outer regions.

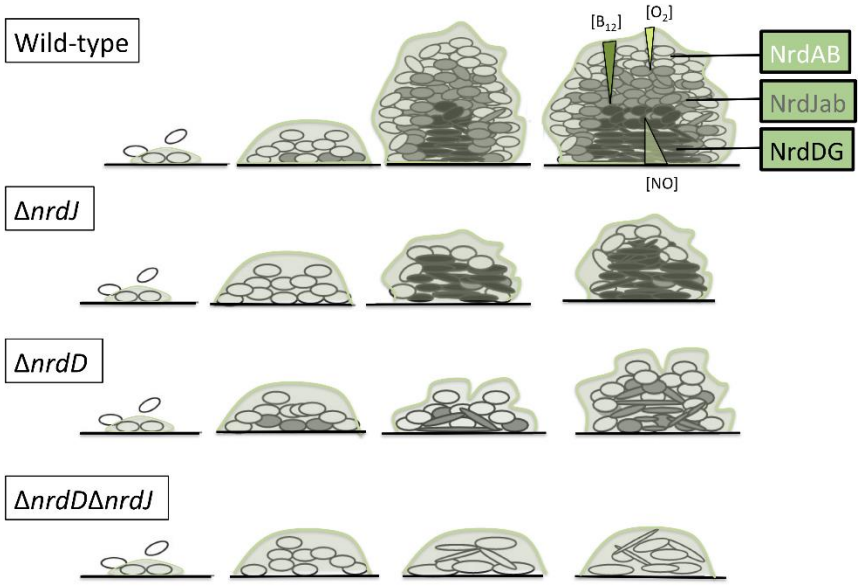

Figure A4:6 Model of ribonucleotide reductases expression during *P. aeruginosa* biofilm formation. Oxygen concentration is progressively reduced throughout the biofilm structure in a well-established gradient (Xu et al., 1998; Stewart and Franklin, 2008). Vitamin B_{12} and NO gradient concentrations also presented here are hypothetical (see the discussion section).

Additionally, we studied the cell morphology in the different layers of the biofilm. A cell elongation phenotype is associated with impaired cell division, which can be triggered by depletion of the dNTP pool when RNR metabolism is affected. According to our model, the Δ*nrdJ* mutant strain and the Δ*nrdJ* Δ*nrdD* double mutant strain showed elongated cells throughout almost the entire biofilm depth, while the Δ*nrdD* strain only presented elongation in the lower layers (**Figure A4:2**). These results must be interpreted by also taking into account the fact that reductions in biofilm biomass and thickness were also happening, so the thin layer in which class the III RNR mutation seems to affect cell morphology means only that strictly anaerobic areas were unable to form.

Given the importance of class II and class III RNRs for anaerobic growth and biofilm formation, we expected an up-regulation of these enzymes under these conditions. It is known that as much as half of the *P. aeruginosa* genome is differentially expressed during biofilm development, including many genes involved in anaerobic metabolism, which are up-regulated in mature biofilms (Waite et al., 2006). Some studies have highlighted that the differential gene expression of class II RNRs depends on levels of oxygenation and have shown a 3.2-fold up-regulation under anaerobic conditions compared with expression during aerobiosis (Filiatrault et al., 2005). *nrdJ* up-regulation has also been noticed in anaerobic sputum (Palmer et al., 2007), and NrdJ and NrdD proteins were also identified to have an increased concentration under anaerobic conditions (Wu et al., 2005).

In agreement with these observations, we observed a large increase in *nrdJ* and *nrdD* mRNA levels under anaerobic conditions (compared with aerobiosis) and in biofilm-forming cells (compared with planktonic cells) (**Table A4:1**). These results imply the existence of a direct or indirect mechanism to activate *nrdJ* and *nrdD* transcription as a result of anaerobic metabolism and/or due to specific biofilm-related factors. The comparison between the expression in initially aerobic biofilm cells and in anaerobic planktonic cells shows that *nrdD* transcription was mainly activated by anaerobiosis, while *nrdJ* expression levels appeared to also be regulated by specific biofilm factors, as *nrdJ* induction in the biofilm (where only some anaerobic and microaerophilic areas are present) is higher than in fully anaerobic planktonic cultures.

To sustain anaerobic metabolism, *P. aeruginosa* uses NO_3 or other more oxidized forms of nitrogen (NO_2, NO) as final electron acceptors for anaerobic respiration: the final product of the full chain of reductions is molecular nitrogen (N_2) (Schreiber et al., 2007). Anr acts as a general regulator of all anaerobic metabolism, activating the transcription of all metabolic enzymes thought to be involved in the pathway and that of the more specific regulators *dnr* and *narL*. NarL and Dnr transcription factors are in turn responsible for the control of the enzymes acting in the first reduction (from NO_3 to NO_2) and in the whole pathway, respectively. When analysing the effects of mutations of these transcription factors on the RNR expression levels measured in a gene reporter assay, we observed a strong reduction in the anaerobic induction of *nrdJ* expression in the Δ*dnr* and Δ*anr* mutant strains, while no effect was observed when mutating the *narL* gene, and *nrdD* expression was not altered (**Figure A4:3**).

Therefore, we suggest that regulation by Anr/Dnr is partially responsible for class II RNR anaerobic induction. If Anr is active in the upper part of the regulation cascade, a simple transcriptional activation by Dnr would be the easiest explanation for the results obtained. Furthermore, as *nrdJ* expression was increased when GSNO, as an NO donor, was used as an electron acceptor, and NO levels affect the denitrification process by modulating Dnr regulation (Van Alst et al., 2007;Castiglione et al., 2009), these findings support the hypothesis of transcriptional control of *nrdJ* expression by Dnr. According to the biofilm reaction-diffusion theory (Stewart, 2003) we hypothesize that NO, described to be the main metabolite accumulated as a consequence of anaerobic metabolisms (Ye et al., 1994), should see its concentration increased in the lower layers, enhancing the effect of Dnr regulation (see **Figure A4:6**).

The genes belonging to the Anr/Dnr regulons are associated with Anr and Dnr binding boxes (Trunk et al., 2010), although the binding sites are still not well determined and more studies are needed to distinguish between them. Surprisingly, we identified a putative Anr/Dnr binding box in both class II and class III RNR promoters (P*nrdJ* and P*nrdD*) (Figure 4). In our gene reporter assays, we determined that the mutation of the putative Anr/Dnr box in P*nrdJ* dramatically reduced the anaerobic induction of class II RNR expression (resembling the effect of *dnr* or *anr* gene mutation), while mutating the putative Anr/Dnr box in P*nrdD* had no significant effect.

According to these results, we can assume that under anaerobic conditions or in the anaerobic and microaerophilic environments generated during biofilm formation, NrdJ activity is essential for proper

growth and that it is activated under these conditions by Dnr or Anr/Dnr via direct binding with its promoter. However, further studies are needed to determine if there are other specific biofilm-related factors activating NrdJ transcription and to define the mechanism for class III RNR anaerobic induction. This could be due to other factors that have not yet been studied, or it could even be related to Anr/Dnr pathways (as suggested the putative box found in the promoter) that may only be detectable under specific conditions that have not yet been tested.

Integrating our experiments on the effects of RNR mutation on biofilm formation and on RNR regulation in biofilm growth and under anaerobic conditions, we performed a gene reporter assay during biofilm formation, which supported our model: as the *P. aeruginosa* PAO1 wild-type biofilm structure matured, anaerobic areas were generated (as defined by the induction of the control promoter P*oprF*) and P*nrdJ* and P*nrdD* were consequently induced (**Figure A4:5A**). Again, mutating the putative Anr/Dnr boxes reduced class II RNR induction and had no effect on class III RNRs. However, analysing the difference in expression in a PAO1 Δ*dnr* mutant strain between biofilm forming cells and planktonic cells, we not only observed a reduced anaerobic induction of class II RNRs but also, surprisingly, a considerably reduced induction of class III RNRs (**Figure A4:5B**), reinforcing the hypothesis that there could be an as-yet-undefined direct or indirect mechanisms by which Anr/Dnr controls *PnrdD* expression.

The model of a *P. aeruginosa* biofilm as a set of layers with different RNR expression profiles that are determined by oxygen concentration and B_{12} diffusion gradients and by cells with specific genetic regulation to support the differential RNR activities is of great importance for our understanding of this particular growth pattern. These results could play an important role in understanding the virulence of bacterial biofilms as it has been shown that the growth conditions in the lungs of CF patients include oxygen-limited growth and anaerobic environments (Schobert and Jahn, 2010) and that susceptibility to antibiotics in biofilms is modulated by limited oxygen availability (Borriello et al., 2006).

Author contributions

AC, LP and ET designed the study. AC, LP and JA performed the experiments. All authors analysed the data, wrote the paper, read and approved the final version.

Funding

This work was supported in part through grants to ET from the Ministerio de Economia y Competitividad (BFU2011-24066 and BIO2015-63557-R), Generalitat de Catalunya (2014 SGR01260) and Catalan and Spanish Cystic Fibrosis foundations. ET was also supported by the Ramón y Cajal I3 program from the Ministerio de Economia y Competitividad.

References

Alvarez-Ortega, C., and Harwood, C.S. (2007). Responses of *Pseudomonas aeruginosa* to low oxygen indicate that growth in the cystic fibrosis lung is by aerobic respiration. *Mol Microbiol* 65**,** 153-165. doi: 10.1111/j.1365-2958.2007.05772.x.

Arai, H. (2003). Transcriptional regulation of the nos genes for nitrous oxide reductase in *Pseudomonas aeruginosa*. *Microbiology* 149**,** 29-36. doi: 10.1099/mic.0.25936-0.

Arai, H. (2011). Regulation and Function of Versatile Aerobic and Anaerobic Respiratory Metabolism in *Pseudomonas aeruginosa*. *Front Microbiol* 2**,** 103. doi: 10.3389/fmicb.2011.00103.

Arat, S., Bullerjahn, G.S., and Laubenbacher, R. (2015). A network biology approach to denitrification in *Pseudomonas aeruginosa*. *PLoS One* 10**,** e0118235. doi: 10.1371/journal.pone.0118235.

Baelo, A., Levato, R., Julian, E., Crespo, A., Astola, J., Gavalda, J., Engel, E., Mateos-Timoneda, M.A., and Torrents, E. (2015). Disassembling bacterial extracellular matrix with DNase-coated nanoparticles to enhance antibiotic delivery in biofilm infections. *J Control Release* 209**,** 150-158. doi: 10.1016/j.jconrel.2015.04.028.

Benkert, B., Quack, N., Schreiber, K., Jaensch, L., Jahn, D., and Schobert, M. (2008). Nitrate-responsive NarX-NarL represses arginine-mediated induction of the *Pseudomonas aeruginosa* arginine fermentation *arcDABC* operon. *Microbiology* 154**,** 3053-3060. doi: 10.1099/mic.0.2008/018929-0.

Borriello, G., Richards, L., Ehrlich, G.D., and Stewart, P.S. (2006). Arginine or nitrate enhances antibiotic susceptibility of *Pseudomonas aeruginosa* in biofilms. *Antimicrob Agents Chemother* 50**,** 382-384. doi: 10.1128/AAC.50.1.382-384.2006.

Castiglione, N., Rinaldo, S., Giardina, G., and Cutruzzola, F. (2009). The transcription factor DNR from *Pseudomonas aeruginosa* specifically requires nitric oxide and *haem* for the activation of a target promoter in *Escherichia coli*. *Microbiology* 155**,** 2838-2844. doi: 10.1099/mic.0.028027-0.

Cendra Mdel, M., Juarez, A., and Torrents, E. (2012). Biofilm modifies expression of ribonucleotide reductase genes in *Escherichia coli*. *PLoS One* 7**,** e46350. doi: 10.1371/journal.pone.0046350.

Christensen, B.B., Sternberg, C., Andersen, J.B., Palmer, R.J., Jr., Nielsen, A.T., Givskov, M., and Molin, S. (1999). Molecular tools for study of biofilm physiology. *Methods Enzymol* 310**,** 20-42.

Costerton, J.W., Stewart, P.S., and Greenberg, E.P. (1999). Bacterial biofilms: a common cause of persistent infections. *Science* 284**,** 1318-1322.

Cotruvo, J.A., and Stubbe, J. (2011). Class I ribonucleotide reductases: metallocofactor assembly and repair in vitro and in vivo. *Annu Rev Biochem* 80**,** 733-767. doi: 10.1146/annurev-biochem-061408-095817.

Crespo, A., Pedraz, L., and Torrents, E. (2015). Function of the *Pseudomonas aeruginosa* NrdR Transcription Factor: Global Transcriptomic Analysis and Its Role on Ribonucleotide Reductase Gene Expression. *PLoS One* 10**,** e0123571. doi: 10.1371/journal.pone.0123571.

Crona, M., Hofer, A., Astorga-Wells, J., Sjoberg, B.M., and Tholander, F. (2015). Biochemical Characterization of the Split Class II Ribonucleotide Reductase from *Pseudomonas aeruginosa*. *PLoS One* 10**,** e0134293. doi: 10.1371/journal.pone.0134293.

Davies, J.C., Alton, E.W., and Bush, A. (2007). Cystic fibrosis. *BMJ* 335**,** 1255-1259. doi: 10.1136/bmj.39391.713229.AD.

Dietrich, L.E., Okegbe, C., Price-Whelan, A., Sakhtah, H., Hunter, R.C., and Newman, D.K. (2013). Bacterial community morphogenesis is intimately linked to the intracellular redox state. *J Bacteriol* 195**,** 1371-1380. doi: 10.1128/JB.02273-12.

Eichner, A., Gunther, N., Arnold, M., Schobert, M., Heesemann, J., and Hogardt, M. (2014). Marker genes for the metabolic adaptation of *Pseudomonas aeruginosa* to the hypoxic cystic fibrosis lung environment. *Int J Med Microbiol* 304**,** 1050-1061. doi: 10.1016/j.ijmm.2014.07.014.

Filiatrault, M.J., Wagner, V.E., Bushnell, D., Haidaris, C.G., Iglewski, B.H., and Passador, L. (2005). Effect of anaerobiosis and nitrate on gene expression in *Pseudomonas aeruginosa*. *Infect Immun* 73**,** 3764-3772. doi: 10.1128/IAI.73.6.3764-3772.2005.

Garriga, X., Eliasson, R., Torrents, E., Jordan, A., Barbe, J., Gibert, I., and Reichard, P. (1996). *nrdD* and *nrdG* genes are essential for strict anaerobic growth of *Escherichia coli*. *Biochem Biophys Res Commun* 229**,** 189-192. doi: 10.1006/bbrc.1996.1778.

Hassett, D.J., Sutton, M.D., Schurr, M.J., Herr, A.B., Caldwell, C.C., and Matu, J.O. (2009). *Pseudomonas aeruginosa* hypoxic or anaerobic biofilm infections within cystic fibrosis airways. *Trends Microbiol* 17**,** 130-138. doi: 10.1016/j.tim.2008.12.003.

Hofer, A., Crona, M., Logan, D.T., and Sjoberg, B.M. (2012). DNA building blocks: keeping control of manufacture. *Crit Rev Biochem Mol Biol* 47**,** 50-63. doi: 10.3109/10409238.2011.630372.

Ito, K., and Barnes, P.J. (2009). COPD as a disease of accelerated lung aging. *Chest* 135**,** 173-180. doi: 10.1378/chest.08-1419.

Kempes, C.P., Okegbe, C., Mears-Clarke, Z., Follows, M.J., and Dietrich, L.E. (2014). Morphological optimization for access to dual oxidants in biofilms. *Proc Natl Acad Sci U S A* 111**,** 208-213. doi: 10.1073/pnas.1315521110.

Lebeaux, D., Chauhan, A., Rendueles, O., and Beloin, C. (2013). From in vitro to in vivo Models of Bacterial Biofilm-Related Infections. *Pathogens* 2**,** 288-356. doi: 10.3390/pathogens2020288.

Lee, K.M., Go, J., Yoon, M.Y., Park, Y., Kim, S.C., Yong, D.E., and Yoon, S.S. (2012). Vitamin B12-mediated restoration of defective anaerobic growth leads to reduced biofilm formation in *Pseudomonas aeruginosa*. *Infect Immun* 80**,** 1639-1649. doi: 10.1128/IAI.06161-11.

Lundin, D., Berggren, G., Logan, D.T., and Sjoberg, B.M. (2015). The origin and evolution of ribonucleotide reduction. *Life (Basel)* 5**,** 604-636. doi: 10.3390/life5010604.

Lyczak, J.B., Cannon, C.L., and Pier, G.B. (2002). Lung infections associated with cystic fibrosis. *Clin Microbiol Rev* 15**,** 194-222.

Okegbe, C., Price-Whelan, A., and Dietrich, L.E. (2014). Redox-driven regulation of microbial community morphogenesis. *Curr Opin Microbiol* 18**,** 39-45. doi: 10.1016/j.mib.2014.01.006.

Palmer, K.L., Brown, S.A., and Whiteley, M. (2007). Membrane-bound nitrate reductase is required for anaerobic growth in cystic fibrosis sputum. *J Bacteriol* 189**,** 4449-4455. doi: 10.1128/JB.00162-07.

Quenee, L., Lamotte, D., and Polack, B. (2005). Combined *sacB*-based negative selection and cre-lox antibiotic marker recycling for efficient gene deletion in *Pseudomonas aeruginosa*. *Biotechniques* 38**,** 63-67.

Sambrook, J., Fritsch, E.F., and Maniatis, T. (1989). *Molecular Cloning: A Laboratory Manual.* Cold Spring Harbor Laboratory Press.

Schobert, M., and Jahn, D. (2010). Anaerobic physiology of *Pseudomonas aeruginosa* in the cystic fibrosis lung. *Int J Med Microbiol* 300**,** 549-556. doi: 10.1016/j.ijmm.2010.08.007.

Schreiber, K., Krieger, R., Benkert, B., Eschbach, M., Arai, H., Schobert, M., and Jahn, D. (2007). The anaerobic regulatory network required for *Pseudomonas aeruginosa* nitrate respiration. *J Bacteriol* 189**,** 4310-4314. doi: 10.1128/JB.00240-07.

Sjoberg, B.M., and Torrents, E. (2011). Shift in ribonucleotide reductase gene expression in *Pseudomonas aeruginosa* during infection. *Infect Immun* 79**,** 2663-2669. doi: 10.1128/IAI.01212-10.

Stewart, P.S. (2003). Diffusion in biofilms. *J Bacteriol* 185**,** 1485-1491.

Stewart, P.S., and Franklin, M.J. (2008). Physiological heterogeneity in biofilms. *Nat Rev Microbiol* 6**,** 199-210. doi: 10.1038/nrmicro1838.

Torrents, E. (2014). Ribonucleotide reductases: Essential Enzymes for bacterial life. *Front. Cell. Infect. Microbiol.* 4**,** 52. doi: 10.3389/fcimb.2014.00052.

Torrents, E., Poplawski, A., and Sjoberg, B.M. (2005). Two proteins mediate class II ribonucleotide reductase activity in *Pseudomonas aeruginosa*: expression and transcriptional analysis of the aerobic enzymes. *J Biol Chem* 280**,** 16571-16578. doi: 10.1074/jbc.M501322200.

Trunk, K., Benkert, B., Quack, N., Munch, R., Scheer, M., Garbe, J., Jansch, L., Trost, M., Wehland, J., Buer, J., Jahn, M., Schobert, M., and Jahn, D. (2010). Anaerobic adaptation in *Pseudomonas aeruginosa*: definition of the Anr and Dnr regulons. *Environ Microbiol* 12**,** 1719-1733. doi: 10.1111/j.1462-2920.2010.02252.x.

Urban, A., Neukirchen, S., and Jaeger, K.E. (1997). A rapid and efficient method for site-directed mutagenesis using one-step overlap extension PCR. *Nucleic Acids Res* 25**,** 2227-2228.

Van Alst, N.E., Picardo, K.F., Iglewski, B.H., and Haidaris, C.G. (2007). Nitrate sensing and metabolism modulate motility, biofilm formation, and virulence in *Pseudomonas aeruginosa*. *Infect Immun* 75**,** 3780-3790. doi: 10.1128/IAI.00201-07.

Waite, R.D., Paccanaro, A., Papakonstantinopoulou, A., Hurst, J.M., Saqi, M., Littler, E., and Curtis, M.A. (2006). Clustering of *Pseudomonas aeruginosa* transcriptomes from planktonic cultures, developing and mature biofilms reveals distinct expression profiles. *BMC Genomics* 7**,** 162. doi: 10.1186/1471-2164-7-162.

Weiss Nielsen, M., Sternberg, C., Molin, S., and Regenberg, B. (2011). *Pseudomonas aeruginosa* and *Saccharomyces cerevisiae* biofilm in flow cells. *J Vis Exp*. doi: 10.3791/2383.

Werner, E., Roe, F., Bugnicourt, A., Franklin, M.J., Heydorn, A., Molin, S., Pitts, B., and Stewart, P.S. (2004). Stratified growth in *Pseudomonas aeruginosa* biofilms. *Appl Environ Microbiol* 70**,** 6188-6196. doi: 10.1128/AEM.70.10.6188-6196.2004.

Wu, M., Guina, T., Brittnacher, M., Nguyen, H., Eng, J., and Miller, S.I. (2005). The *Pseudomonas aeruginosa* proteome during anaerobic growth. *J Bacteriol* 187**,** 8185-8190. doi: 10.1128/JB.187.23.8185-8190.2005.

Xu, K.D., Stewart, P.S., Xia, F., Huang, C.T., and Mcfeters, G.A. (1998). Spatial physiological heterogeneity in *Pseudomonas aeruginosa* biofilm is determined by oxygen availability. *Appl Environ Microbiol* 64**,** 4035-4039.

Ye, R.W., Averill, B.A., and Tiedje, J.M. (1994). Denitrification: production and consumption of nitric oxide. *Appl Environ Microbiol* 60**,** 1053-1058.

Yoon, M.Y., Lee, K.M., Park, Y., and Yoon, S.S. (2011). Contribution of cell elongation to the biofilm formation of *Pseudomonas aeruginosa* during anaerobic respiration. *PLoS One* 6**,** e16105. doi: 10.1371/journal.pone.0016105.

Yoon, S.S., Hennigan, R.F., Hilliard, G.M., Ochsner, U.A., Parvatiyar, K., Kamani, M.C., Allen, H.L., Dekievit, T.R., Gardner, P.R., Schwab, U., Rowe, J.J., Iglewski, B.H., Mcdermott, T.R., Mason, R.P., Wozniak, D.J., Hancock, R.E., Parsek, M.R., Noah, T.L., Boucher, R.C., and Hassett, D.J. (2002). *Pseudomonas aeruginosa* anaerobic respiration in biofilms: relationships to cystic fibrosis pathogenesis. *Dev Cell* 3**,** 593-603.

A4 Supporting information

Pseudomonas aeruginosa exhibits deficient biofilm formation in the absence of class II and class III ribonucleotide reductases due to hindered anaerobic growth

Supplementary Table A4:S1. Bacterial strains and plasmids used in this study.

Strain or plasmid	Description	Source
Plasmids		
pGEM-T easy	A/T cloning vecto;, Amp^R	Promega
pUCP20T	Broad-host-range vector; Amp^R	(West et al., 1994)
pUCGmlox	pUC18-based vector containing the lox flanked aacC1 gene; Amp^R, Gm^R	(Quenee et al., 2005)
pEX100Tlink	*Pseudomonas* suicide vector pEX100T with a MCS, *sacB*, *oriT;* Amp^R	(Quenee et al., 2005)
pETS130-GFP	Broad host range, promoterless GFP; Gm^R	(Sjoberg and Torrents, 2011)
pETS134	pETS130 derivative carrying *nrdA* promoter; Gm^R	(Sjoberg and Torrents, 2011)
pETS136	pETS130 derivative carrying *nrdD* promoter; Gm^R	(Sjoberg and Torrents, 2011)
pETS159	pBBR1 derivative carrying *nrdJab* operon; Gm^R	(Sjoberg and Torrents, 2011)
pETS160	pBBR1 derivative carrying *nrdDG* operon; Gm^R	(Sjoberg and Torrents, 2011)
pETS180	pETS130 derivative carrying *nrdJ* promoter; Gm^R	(Crespo et al., 2015)
pETS191	pETS130 derivative carrying mutant Anr/Dnr box in *nrdJ* promoter; Gm^R	This work
pETS192	pETS130 derivative carrying mutant Anr/Dnr box in *nrdD* promoter; Gm^R	This work
pETS193	pETS130 derivative carrying *oprF* promoter; Gm^R	This work
pETS195	pUCP20T derivative carrying *dnr* gene; Amp^R	This work
pETS196	pET100Tlink-*nrdJ* ::ΩGm	This work
Strains		
E. coli		
DH5α	*recA1 endA1 hsdR17 supE44 thi-1 relA1 Δ(lacZYA-argF)U169 deoR Φ80dlacZM15*	Laboratory stock
S17.1λ*pir*	*recA thi pro hsdR- M+RP4::2-Tc::Mu::Km Tn7 Tpr Smr Xpir*	(de Lorenzo et al., 1993)
P. aeruginosa		
PAO1	Wild-type (ATCC 15692 / CECT 4122)- Spanish Type Culture Collection	Lab strain
PW3784	*P. aeruginosa* PAO1 *anr*::*IS*l*acZ* /hah; Tc^R	(Jacobs et al., 2003)
PW1965	*P. aeruginosa* PAO1 *dnr*::*IS*l*acZ* /hah; Tc^R	(Jacobs et al., 2003)
PW7549	*P. aeruginosa* PAO1 *narL*::*IS*l*acZ* /hah; Tc^R	(Jacobs et al., 2003)
ETS102	*P. aeruginosa* PAO1 *nrdJ*:: ΩTc; Tc^R	(Sjoberg and Torrents, 2011)
ETS103	*P. aeruginosa* PAO1 *nrdD* ::ΩTc; Tc^R	(Sjoberg and Torrents, 2011)
ETS125	*P. aeruginosa* PAO1 *nrdD* ::ΩTc; Tc^R, *nrdJ* ::ΩGm; Gm^R	This work

Supplementary Table A4:S2. Primers and probes used in this study.

Name	Sequence (5'→3')	Application
M13-dir	GTTTTCCCAGTCACGAC	Check-Cloning
M13-rev	CAGGAAACAGCTATGACC	Check-Cloning
pUCP20T-up	CCTCTTCGCTATTACGCCAG	Cloning
pUCP20T-low	TCCGGCTCGTATGTTGTGTG	Cloning
pBBR1-up	CATCGCAGTCGGCCTATTGG	Cloning
pBBR1-low	CACTTTATGCTTCCGGCTCG	Cloning
PnrdA-up	AGGATCCGAATTCTTGCTCCACACAGCCTC	Cloning
PnrdA-low	ACCCGGGTTCTCGCGTGTGGTGTCG	Cloning
PnrdJ BamHI new-up	GGATCCCGCGCCCAGCTGAAGGCC	*PnrdJ* promoter cloning
PnrdJ SmaI new-low	AACCCGGGGACTGCGTTGCGTCTGTC	*PnrdJ* promoter cloning
PnrdD-up	AGGATCCGAATTCGCCCGCCTCGCCCAGG	*PnrdD* promoter cloning
PnrdD new-low	AATCGATCAGGGTGGCCGGCCAGGTAG	*PnrdD* promoter cloning
nrdATaqM2-low	TGTTCATGTCGTGGGTACG	qRT-PCR
nrdJTaqM2-low	GTAAACACCCGCACCACTTC	qRT-PCR
nrdDTaqM2-low	CCGAGTTGAGGAAGTTCTGG	qRT-PCR
gapTaqM-low	GAGGTTCTGGTCGTTGGT	qRT-PCR
nrdA-FAM	CTGGCACCTGGACATC	qRT-PCR probe
nrdJ-FAM	TCGGCTCGGTCAACCT	qRT-PCR probe
nrdD-FAM	CCCGACCTACAACATC	qRT-PCR probe
gap-FAM	CCTGCACCACCAACTG	qRT-PCR probe
mutanrJ-up	TATTGAGGACACGCAGGTACGGA	Mutation of Anr box in P*nrdJ*
mutanrJ-low	TCCGTACCTGCGTGTCCTCAATA	Mutation of Anr box in P*nrdJ*
mutanrD-up	GACGCGACAGCAGCAGCTCGCCGGC	Mutation of Anr box in P*nrdD*
mutanrD-low	GCCGGCGAGCTGCTGCTGTCGCGTC	Mutation of Anr box in P*nrdD*
Jmut1HIIIup	AAAGCTTCCCGTCAGGTACGGATAAC	*nrdJ* gene mutation
Jmut2BIIw	AAAAGGATCCATGGAGTCCTGGATGGTCC	*nrdJ* gene mutation
Jmut3BIup	AAAAGGATCCTATTACGGCAAGTACTGAGG	*nrdJ* gene mutation
Jmut4SIIw	AGAGCTCGACAAGGAAGGTGCAGTC	*nrdJ* gene mutation
Jint-2-3Iw	TAGATGTCCATGAACGACAGC	checking *nrdJ* gene mutation
PoprFBHI-up	GGATCCCAACGAGTGCATCACG	P*oprF* promoter cloning
PoprFClaI-low	ATCGATGGTGTTCTTCAGTTTCAT	*PoprF* promoter cloning
Pdnr-BHI-up	GGATCCACGGCAGATGCACT	*dnr* cloning for
Dnr-low	ATCACTCGAAGCACTCCAGGC	*dnr* cloning for

Supplementary Table A4:S3. Growth of *P. aeruginosa* wild-type and mutant strains under aerobic and anaerobic conditions. Δ*nrdJ*, Δ*nrdD*, Δ*nrdD*Δ*nrdJ* and wild-type PAO1 strains were grown for 16 h under aerobic and anaerobic conditions in LB and LBN, respectively. Bacterial growth was measured by reading the optical density at 550 (OD_{550}). Vitamin B_{12} was added when necessary at a concentration of 1 µg/mL. Final OD_{550} values are listed in the table.

		OD_{550}			
	B_{12}	**PAO1 wild-type**	**ETS102 Δ*nrdJ***	**ETS103 Δ*nrdD***	**ETS125 Δ*nrdD*Δ*nrdJ***
Aerobic	-	4.00	3.70	3.90	3.80
	+	3.90	3.80	3.87	3.76
Anaerobic	-	1.58	0.13	0.17	0.05
	+	1.91	0.13	2.00	0.07

Article 5

Gradual adaptation of facultative anaerobic pathogens to microaerobic and anaerobic conditions

Sent for publication to *Environmental microbiology* (Q1, IF_{2018} = 5.147)

August 2019

Lucas Pedraz[1,*], Núria Blanco-Cabra[1], Eduard Torrents[1,*]

[1]: "Bacterial Infections: Antimicrobial Therapies" group, Institute for Bioengineering of Catalonia (IBEC), The Barcelona Institute of Science and Technology (BIST), Barcelona, Spain.

*Corresponding authors: Eduard Torrents (etorrents@ibecbarcelona.eu) and Lucas Pedraz (lpedraz@ibecbarcelona.eu).

Summary

Many notable human pathogens are facultative anaerobes. These pathogens exhibit redundant metabolic pathways and a whole array of regulatory systems to adapt to changing oxygen levels. However, our knowledge of facultative anaerobic pathogens is mostly based on fully aerobic or anaerobic cultures, while the microaerobic range remains understudied. Here, we examine the behavior of *Escherichia coli* and *Pseudomonas aeruginosa* during the aerobic-anaerobic transition. To do so, our work introduces a technique that we named *AnaeroTrans*, in which we allow self-consumption of oxygen by steady-state cultures and monitor the system by measuring the gas-phase oxygen concentration. We explore the different behavior of the studied species toward oxygen, by analyzing oxygen consumption, bacterial fitness, and growth speed under different oxygen availability levels. As a model, we characterize the adaptation profile of the ribonucleotide reductase network, a complex oxygen-dependent system responsible for the generation of deoxyribonucleotides. We also explore the actions of the most important anaerobic regulators and how these regulators influence bacterial fitness. Our results allow us to classify the different elements that compose the aerobic-anaerobic transition into reproducible stages defined by oxygen availability values, thus showing a significantly different adaptation mechanism for the studied species.

Significance

Studying the aerobic-anaerobic transition is critical to understand the behavior of facultative anaerobes in both natural environments and infection conditions. However, most studies are conducted under fully aerobic or anaerobic conditions, and the lack of a system to define oxygen availability in the cell have so far made impossible to describe reproducible events in the microaerobic range. In this study, we introduce a new, simple method to do so. Furthermore, in the application of the method that we present we not only show how a particular oxygen-regulated system behaves under reproducible stages in the microaerobic range, but we also relate these findings to other important components of the anaerobic metabolism, venturing to include our results in a global model of the aerobic-anaerobic transition.

Introduction

Oxygen is one of the main factors affecting the growth of microorganisms. For obligate aerobes or anaerobes, oxygen availability determines whether a biotope is suitable. Facultative anaerobes can thrive in differently oxygenated environments; however, these organisms must undergo extensive metabolic adaptation to do so (Unden et al., 1994; Unden et al., 1995). Oxygen availability determines possible sites of infection, as many environments inside host bodies feature hypoxic or anoxic conditions. In chronic infections, where bacteria grow as biofilms, the oxygen concentration declines gradually throughout the biofilm structure, reaching zero dissolved oxygen (DO) at a depth of a few microns (de Beer et al., 1994; Xu et al., 1998; Stewart, 2003). This gradient has been described as one of the main factors driving biofilm morphogenesis (Dietrich et al., 2013).

Despite it being such a crucial factor, there remain significant gaps in our understanding of the bacterial response to oxygen availability. One reason for this gap in knowledge is that microaerobiosis is understudied. Bacteria almost always encounter oxygen variations as continuous gradients; however, most of our knowledge is based on fully aerobic or anaerobic cultures, while the intermediate states, often referred to as the *microaerobic range*, are significantly less well characterized (Bettenbrock et al., 2014).

Another reason is the lack of a system to quantify oxygen availability in the cell. DO is routinely controlled in bioreactor cultures, and there exist many examples of DO profiles in biofilms (de Beer et al., 1994; Xu et al., 1998; Rani et al., 2007; Stewart and Franklin, 2008). It has been reported, however, that detection of a DO of zero may not imply anaerobiosis but rather that all the oxygen transferred to the liquid phase was used for respiration (Alexeeva et al., 2002). For instance, the oxygen supply required for detection of a DO above zero in an *Escherichia coli* steady-state culture exceeds the amount required to support fully aerobic respiratory growth (Rolfe et al., 2012). Therefore, DO is not a valid measure of oxygen availability. Other strategies use the oxygen supply rate in a chemostat culture or the redox potential, but these approaches are associated with similar problems (Alexeeva et al., 2002). One successful approach, the AU scale, uses a perceived aerobiosis metric based on the production of acetate by *E. coli* under anaerobic and microaerobic conditions (Alexeeva et al., 2002), which can reproducibly describe events in the microaerobic range (Bettenbrock et al., 2014). However, this approach can be applied to only *E. coli* and only when the cells are grown under particular conditions and in certain media. In this study, we will explore a system to describe changes in gene expression depending on oxygen availability in this understudied microaerobic range. We will apply this method to two facultative anaerobic pathogens: *Escherichia coli* and *Pseudomonas aeruginosa*.

E. coli is a facultative anaerobe that is usually found as a commensal in the lower intestine. However, this microbe can also cause both intraintestinal and extraintestinal infections (Tenaillon et al., 2010). The gut has traditionally been described as an anaerobic environment (Backhed et al., 2005), although it is now known that there is significant microaerobiosis in the gut due to diffusion from vascularized

tissue (Jones et al., 2007). The preferred mode of growth of *E. coli* is aerobic respiration (Partridge et al., 2007), presenting two main alternative terminal oxidases: cytochrome bo' (used mainly for highly aerated environments) and cytochrome bd-I (with extremely high affinity for oxygen, it can sustain growth under very low oxygen tensions) (Bettenbrock et al., 2014); there is a third, less studied oxidase, cytochrome bd-II (Bettenbrock et al., 2014). In the absence of oxygen, *E. coli* can grow via anaerobic respiration or mixed-acid fermentation. Hybrid metabolism has been described, in which anaerobic processes occur in the cytoplasm while aerobic respiration occurs in the cell membrane (Rolfe et al., 2012). Two regulators control the relationship between *E. coli* and oxygen: the fumarate-nitrate reduction regulator (Fnr) and the ArcBA two-component system (Unden et al., 1994; Unden et al., 1995). Fnr is a direct regulator that senses oxygen via oxidation of a [4Fe-4S] cluster, and is involved in the activation or repression of a large set of operons (Unden et al., 1994; Unden et al., 1995; Becker et al., 1996). ArcBA is a two-component system that acts as an indirect oxygen regulator, sensing the redox states of membrane-bound quinones (Georgellis et al., 2001; Malpica et al., 2004; Bettenbrock et al., 2014).

Although *P. aeruginosa* can also grow in the presence or absence of oxygen, this species exhibits a very different relationship with oxygen limitation. *P. aeruginosa* can grow as a free-living organism in the environment but also infects a wide variety of hosts. As an opportunistic pathogen, it is mainly associated with chronic lung infections in at-risk groups, such as patients with cystic fibrosis (Govan and Deretic, 1996; Lyczak et al., 2002) (CF) or chronic obstructive pulmonary disease(Murphy et al., 2008) (COPD), where *P. aeruginosa* forms distinctive biofilms. In CF, mucoid biofilms are particularly depleted of oxygen (Worlitzsch et al., 2002). Furthermore, *P. aeruginosa* has been described to secrete substances that reduce the oxygen transfer rate (Sabra et al., 2002). This organism encodes at least five terminal oxidases (Arai, 2011), and the constitutively expressed oxidase (cytochrome cbb_3-1) is a high-oxygen-affinity oxidase, adapted to low oxygen levels (Arai, 2011; Arai et al., 2014). Cytochrome cbb_3-2 is induced under very low oxygenation, and the low-affinity oxidases are mostly activated under nutrient deprivation or some form of stress (Arai, 2011; Arai et al., 2014). In *P. aeruginosa,* the preferred option in the absence of oxygen is anaerobic respiration of nitrate or nitrite (denitrification) (Zumft, 1997), which can also occur under microaerobiosis, in hybrid metabolism (Chen et al., 2006). The relationship of *P. aeruginosa* with oxygen is mainly driven by the Fnr-type transcription factor Anr, a direct oxygen sensor that is at the highest position in a complex regulatory hierarchy (Galimand et al., 1991; Sawers, 1991; Trunk et al., 2010; Arai, 2011). Another Fnr-like regulator, Dnr, is known to control the denitrification process, as well as a small subset of other anaerobically activated genes (Arai et al., 1997; Trunk et al., 2010; Arai, 2011), while being itself controlled by Anr.

In addition to studying the behavior of these two species during the aerobic-anaerobic transition, we will also characterize in detail the global regulation of a gene network during this process. The model system that we will use as is the ribonucleotide reductase (RNR) network. RNRs are the enzymes responsible for reducing ribonucleotides (NTPs) to deoxyribonucleotides (dNTPs), the building blocks for DNA synthesis and repair (Hofer et al., 2012; Torrents, 2014). As this process is essential for life,

RNRs have been proposed as promising targets for cancer treatment and antimicrobial therapies (Torrents, 2014). RNRs share a common radical-based mechanism but are divided into three classes (class I, which is subdivided into Ia, Ib and Ic, class II and class III) based on structure, metallocofactor requirement, and the mechanism used for radical generation (Torrents, 2014). Due to these differences, each RNR class exhibits a different behavior toward oxygen: class I RNRs are oxygen dependent, class II RNRs are oxygen independent, and class III RNRs are oxygen sensitive. Complex eukaryotic organisms only encode class Ia RNRs, but bacteria can encode any RNR combination in a manner that reflects the ecological niches available to each organism (Torrents, 2014).

The species in this study encode different sets of RNRs. *E. coli* grows aerobically using a class Ia RNR (Tuggle and Fuchs, 1986), although this species also encodes a class Ib RNR that is proposed to have roles in infection and iron deprivation (Monje-Casas et al., 2001; Martin and Imlay, 2011; Cendra Mdel et al., 2012). In the absence of oxygen, this organism uses a class III enzyme (Garriga et al., 1996), the transcription of which is activated by Fnr (Boston and Atlung, 2003; Roca et al., 2008). Class Ia and Ib RNRs are repressed anaerobically via unknown mechanisms (Boston and Atlung, 2003; Baughn and Malamy, 2004). On the other hand, *P. aeruginosa* encodes class Ia, II, and III RNRs (Sjoberg and Torrents, 2011). Class I RNR is constitutively expressed, as Anr/Dnr do not repress aerobic metabolism (Trunk et al., 2010). Class II and III RNRs are induced under reduced oxygen tension by Dnr (Crespo et al., 2016) and Anr (Crespo et al., 2017), respectively.

In this study, we will compare the gradual adaptation of two facultative anaerobic pathogens over entire oxygen gradients. As a model, we comprehensively examine the mechanism by which RNR operons are modulated and the association of this regulation with the ecology and pathogenesis of each species. We will also characterize the modulation of anaerobiosis regulators and how the actions of these regulators influence bacterial fitness. This study will help us look beyond aerobic and anaerobic *in vitro* cultures and further understand how facultative anaerobic pathogens adapt to changing oxygen availability in real infections.

Results

The dynamics of gene regulation can be expressed as a function of oxygen concentration in the gas phase

Continuous-culture techniques offer the possibility of studying the effect of one or more parameters while keeping the remaining conditions constant. Among other applications, these techniques have been used to explore the adaptation of bacterial metabolism to aerobic, microaerobic and anaerobic conditions (Alexeeva et al., 2002; Partridge et al., 2007; Rolfe et al., 2012; Bettenbrock et al., 2014). In this work, we used the setup illustrated in **Fig. A5:1A, B** in a method that we named *AnaeroTrans*. In a standard AnaeroTrans experiment, the culture initially grows with a dilution rate lower than the specific growth rate to reach the desired OD_{600} while the oxygen concentration is kept constant. At the desired biomass concentration, the dilution rate is increased to establish a steady state, the airflow is stopped, and the oxygen levels decrease naturally via bacterial respiration. Samples for RNA extraction are obtained at the desired oxygen concentrations, and gene expression is evaluated by qRT-PCR.

Initially, we tried to characterize the state of system via the DO in the liquid phase. However, it became evident that the DO was not the correct parameter to describe changes in oxygen availability in cells. As an example, we used *Pseudomonas aeruginosa* PAO1 to study the expression of *nrdD*, a gene that is strongly induced under anaerobiosis (Crespo et al., 2016). The DO could not be maintained at near-saturation levels but was stabilized at different values depending on the air flow rate (**Fig. A5:1C**; liquid phase, blue line). Although it was possible to characterize these states to determine differences in gene expression, the DO level decreased to zero quickly after the bubbling of air was stopped. After this point, the samples did not show the expected levels of anaerobic induction of *nrdD* expression, despite being oxygen free in terms of DO (**Fig. A5:1D**; liquid phase), demonstrating that there were indistinguishable states of adaptation beyond the zero-DO level.

On the other hand, characterization of the cell state based on the gas-phase oxygen concentration solved these problems. The oxygen tension was maintained before the culture reached the desired OD_{600}. When the airflow stopped, the gas-phase oxygen concentration decreased slowly (**Fig. A5:1C**; gas phase, blue line). Different samples exhibited surprisingly clear, gradual induction of *nrdD* (>250-fold) (**Fig. A5:1D**; gas phase). The DO level decreased to zero before sampling began (Supporting Information **Fig. A5:S1A**), but the culture remained functionally aerobic (see expression results below).

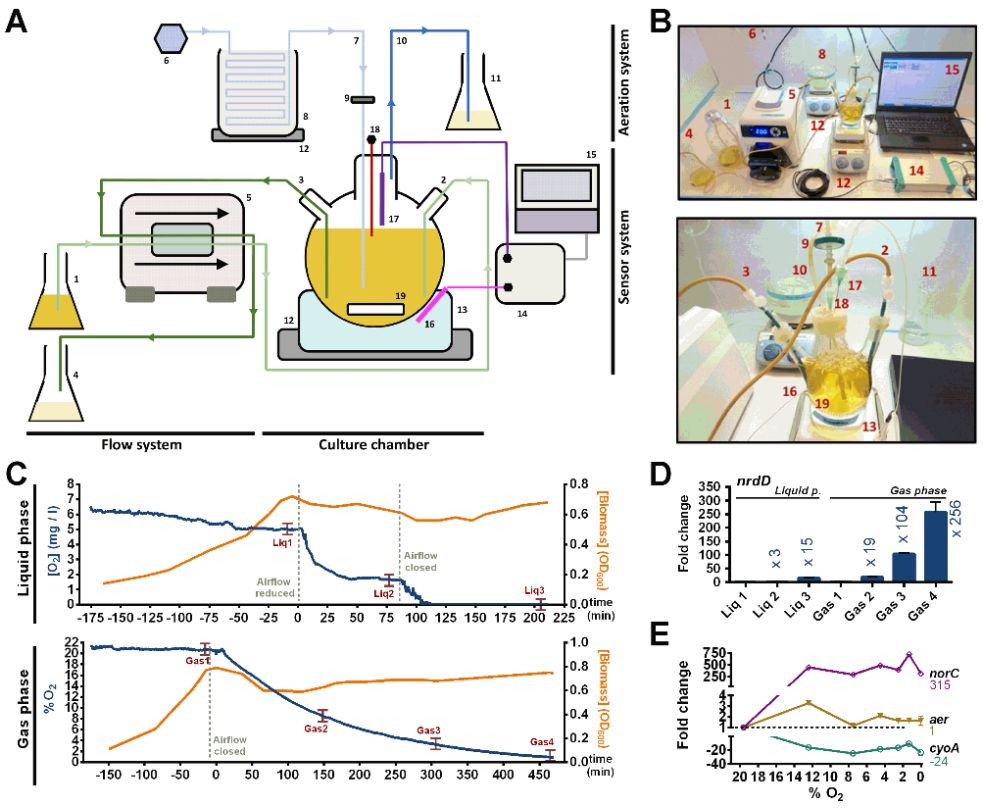

Figure A5:1. Bioreactor setup for the AnaeroTrans system. **A**, schematic representation of the system in the standard setup. Other dispositions are described in the Methods section. Each component is labeled with numbers as follows: fresh medium, **1**; inflow tube, **2**; outflow tube, **3**; waste container, **4**; peristaltic pump, **5**; compressed-air/nitrogen connection, **6**; in-gas tube, **7**; heater, **8**; filter, **9**; out-gas tube, **10**; out-gas collection solution, **11**; stirrer hotplates, **12**; water bath, **13**; OxyMicro sensor system, **14**; computer, **15**; temperature probe, **16**; oxygen micro-optode, **17**; inoculum needle, **18**; stir bar, **19**. **B**, general photo of the system (top) and details of the culture chamber connections (bottom). **C**, example control charts of AnaeroTrans experiments measuring dissolved oxygen (DO) in the culture (top) or oxygen concentration in the gas phase (bottom). The changes in the air flow rate are indicated in the main text. Biomass (OD_{600}) is represented in orange and oxygen concentration (O_2% v/v) in blue; sampling points are indicated by red bars. **D**, fold-change (each sample compared to the first aerobic measurement) of *nrdD* expression levels in the previous experiments. **E**, fold-change (each sample compared to an independent aerobic control culture) of *norC* and *cyoA* gene expression levels. Samples were obtained from AnaeroTrans experiments (control charts not shown). Error bars represent standard deviation.

As controls, we used genes with different, known regulation patterns in *P. aeruginosa*. For aerobic induction, we used *norC,* which encodes a nitric oxide reductase and is strongly induced by Dnr (Alvarez-Ortega and Harwood, 2007; Trunk et al., 2010). As an example of anaerobic repression, the chosen gene was *cyoA*, encoding a low-oxygen-affinity terminal oxidase (Filiatrault et al., 2005; Alvarez-Ortega and Harwood, 2007). Finally, as a model with a distinctive pattern under intermediate oxygen concentrations, we chose the *aer* gene, encoding aerotaxis receptor I. *aer* is activated by Anr under anaerobiosis (Hong et al., 2004); however, this gene has exhibited both anaerobic activation and

repression in different studies (Filiatrault et al., 2005; Trunk et al., 2010; Tata et al., 2016), and given the function of the aerotaxis receptor, peak expression in microaerobiosis can be expected. In the AnaeroTrans experiments (**Fig. A5:1E**), *norC* showed sharp induction with reducing oxygen availability, reaching maximum expression levels at approximately 2% O_2. *cyoA* presented near 20-fold repression throughout the oxygen gradient. Finally, *aer* expression did not exhibit high variability but was induced up to three-fold in early microaerobiosis and decreased to almost the initial value under anaerobiosis. These results demonstrate the capacity of our system to detect different variations in microaerobic and anaerobic gene expression.

The behavior of each species in the aerobic-anaerobic transition reflects different relationships with oxygen.

We applied the AnaeroTrans system to two facultative anaerobic pathogens: *E. coli* and *P. aeruginosa*. We used the model strain *P. aeruginosa* PAO1; however, this strain is deficient in anaerobic growth and may not be a good model for anaerobic culture and infection (Sjoberg and Torrents, 2011; Yoon et al., 2011; Crespo et al., 2017). Therefore, we also included a clinical isolate, *P. aeruginosa* PAET1, obtained from a cystic fibrosis patient (Crespo et al., 2017). Consequently, for *E.* coli, we used the model commensal strain K-12 *substr.* MG1655 and compared this strain to the enterohemorrhagic strain O157:H7 (Supporting Information **Table A5:S1**).

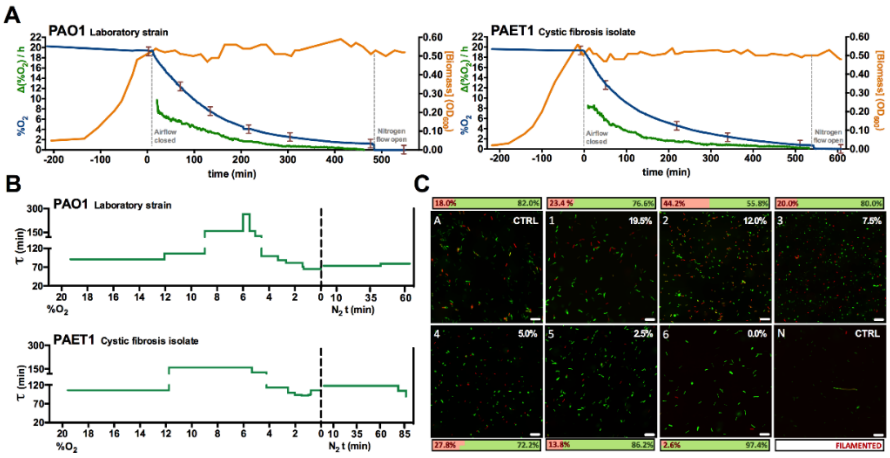

Figure A5:2. Growth and behavior of *P. aeruginosa* in oxygen gradients. **A**, control charts of AnaeroTrans experiments with *P. aeruginosa* strains PAO1 and PAET1, representative of three replicates per strain. Biomass (OD_{600}) is represented in orange, oxygen concentration (O_2% v/v) in blue, and oxygen consumption rate ($\Delta O_2\ h^{-1}$) in green. Sampling points are indicated by red bars. **B,** estimated doubling time of the previous strains (in minutes, Y-axis) depending on the oxygen concentration in the gas phase (in % v/v, X-axis) and the time after start of nitrogen flow (in minutes, X-axis). **C**, Fluorescence microscopy images of LIVE/DEAD viability staining of PAO1. The concentration of oxygen at which each sample was obtained is indicated in the corresponding photograph, and the average percentage of green/red cells is presented next to it. The scale bar represents 10 µM. Images of *in vitro* aerobic (A) and anaerobic (N) control cultures are provided as a reference. Additional images and controls are shown in Supporting Information Fig. A5:S2.

Pseudomonas strains were routinely grown with KNO_3 for denitrification (Zumft, 1997). The oxygen consumption rate of these strains started high, but decreased gradually as oxygen availability declined, and eventually the oxygen concentration reached an asymptotical value that was impossible to eliminate via respiration (**Fig. A5:2A**; blue lines). *E. coli* strains were cultured without substrates for anaerobic respiration and relied on mixed-acid fermentation for anaerobic growth (Guest, 1992; Tseng et al., 1996). The oxygen consumption profile of these strains was highly representative: at high oxygen tensions, they presented a strong oxygen consumption rate. Below approximately 15% O_2, the rate decreased to a stable value that was maintained throughout the remainder of the process (**Fig. A5:3A**; green line), leading to an almost linear oxygen decay (blue line). These results show that fermentative metabolism in *E. coli* only replaces respiration under strict anaerobiosis and that aerobic respiration can continue to occur under very low oxygen tensions.

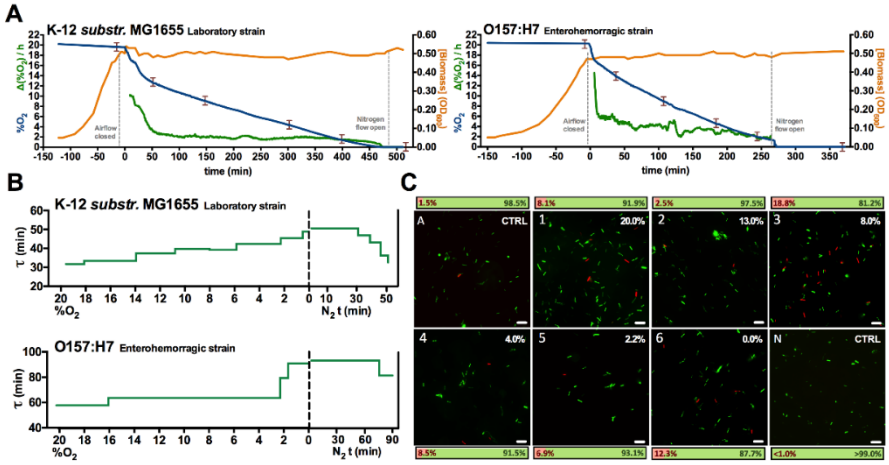

Figure A5:3. Growth and behavior of *E. coli* in oxygen gradients. **A**, control charts of AnaeroTrans experiments with *E. coli* strains K-12 *substr.* MG1655 and O157:H7, representative of three replicates per strain. Biomass (OD_{600}) is represented in orange, oxygen concentration (O_2% v/v) in blue, and oxygen consumption rate (ΔO_2 h^{-1}) in green. Sampling points are indicated by red bars. **B,** estimated doubling time of the previous strains (in minutes, Y-axis) depending on the oxygen concentration in the gas phase (in % v/v, X-axis) and the time after start of nitrogen flow (in minutes, X-axis). **C**, Fluorescence microscopy images of LIVE/DEAD viability staining of K-12. The concentration of oxygen at which each sample was obtained is indicated in the corresponding photograph, and the percentage of green/red cells is presented next to it. The scale bar represents 10 µM. Images of *in vitro* aerobic (A) and anaerobic (N) control cultures are provided as a reference. Additional images and controls are shown in Supporting Information Fig. A5:S2.

We used two approaches to detect differences in bacterial fitness during adaptation. First, we estimated doubling times (τ). In *P. aeruginosa* (PAO1 and PAET1), the doubling time was constant at oxygen concentrations greater than 12% (**Fig. A5:2B**), as the microaerobic respiration machinery is constitutively expressed in this species (Arai, 2011; Arai et al., 2014). After 12% O_2, the doubling time increased significantly, and was recovered at approximately 5% O_2. This effect was more prominent in PAO1, which presented a peak in doubling time just before 5% O_2. On the other hand, the doubling

time of the *E. coli* strains increased as soon as the oxygen availability decreased (**Fig. A5:3B**), showing that even though the oxygen consumption remained high, this species could not grow as fast microaerobically as they could under full aerobiosis. The doubling time of the *E. coli* strains gradually increased during the gradient and did not recover to the initial value until the strains were exposed for some time to strict anaerobic conditions, presumably to induce fermentative metabolism.

For the model strains, we used a second approach to estimate bacterial fitness: a LIVE/DEAD viability stain. For aerobic *P. aeruginosa*, the red ("dead") percentage started at more than 20% (**Fig. A5:2C**). The control samples demonstrated that this effect was due to the toxicity of KNO_3 under aerobiosis (Supporting Information **Fig. A5:S2A**; see Aero. LBN vs. Aero. LB), but the results did not suggest a significant difference in the aerobic expression of the studied genes (data not shown). The percentage of dead cells decreased gradually throughout the gradient, although reproducible peaks were observed at approximately 12% and 5% O_2, suggesting two thresholds for adaptation. In *E. coli*, on the other hand, the percentage of dead cells started low, exhibited a mid-microaerobic peak at 8% O_2, and then increased towards anaerobiosis, only returning to zero after an adaptation period (**Fig. A5:3C**, Supporting Information **Fig. A5:S2B**). This finding is correlated with the pattern observed in the doubling time and highlights how *E. coli* grows better under full aerobiosis or anaerobiosis than in the microaerobic range.

The morphology of *E. coli* cells remained mostly unchanged. The *P. aeruginosa* PAO1 cells were shorter between 12% and 5% O_2 and recovered their average proportions after the final adaptation threshold. The fully anaerobic sample showed elongated cells, most likely exhibiting initial signs of filamentation (**Fig. A5:2C**). Control anaerobic cultures showed filamentous cells as previously described (Yoon et al., 2011) (Supporting Information **Fig. A5:S2A**) due to a defect in the oxygen control of the ribonucleotide reduction network (Crespo et al., 2017).

To ascertain whether the changes in *P. aeruginosa* during the aerobic-anaerobic transition were related to denitrification, we grew PAO1 without KNO_3. This culture grew without alteration at more than 15% O_2 (Supporting Information **Fig. A5:S3A, B**). Below that level, PAO1 started to exhibit increased doubling time, reaching a very slow growth speed at less than 12% O_2. Therefore, we concluded that denitrification started as early as in the 15-12% O_2 range, and became essential below 12%. The culture exhibited no evidence of adaptation to microaerobiosis: the oxygen consumption rate remained constant (Supporting Information **Fig. A5:S3A**), and there were no variations in the percentage of dead cells (Supporting Information **Fig. A5:S2C**).

The RNR network reacts to differences in oxygen availability with a coordinated response

We used the previous AnaeroTrans samples to study the response of the ribonucleotide reductases (RNR) network (Hofer et al., 2012; Torrents, 2014) to changing oxygenation conditions. As RNR activity is essential, and RNR deficient strains are known to present altered growth profiles or be unable to grow under specific oxygen levels (Garriga et al., 1996; Torrents, 2014; Crespo et al., 2016). The

different RNR classes exhibit distinct behaviors toward oxygen, defining available ecological niches (Poole et al., 2002; Torrents, 2014).

P. aeruginosa encodes all three RNR classes: Ia (*nrdAB*), II (*nrdJab*) and III RNR (*nrdDG*). In the AnaeroTrans data, the CF isolate PAET1 exhibited the expected profile (**Fig. A5:4A**; PAET1): after the oxygen concentration decreased, the class III RNR (*nrdD*, blue line) level started to increase relatively early, as activation of this class is Anr dependent (Crespo et al., 2017), while the class II RNR, which is Dnr dependent (*nrdJa*, green line), was induced at a relatively low oxygen concentration. The class I RNR (*nrdA*, red line) was not repressed anaerobically (Crespo et al., 2017). The lab strain PAO1 exhibited a significantly different profile (**Fig. A5:4A**; PAO1): the mutational disruption of the Anr-dependent activation of the class III RNR (Crespo et al., 2017) that this strain presents caused delayed induction at less than 5% O_2 (*nrdD,* blue line). This effect provoked a surprisingly clear reaction of class II (*nrdJa*, green line), the expression of which started much earlier, presumably to compensate for the absence of class III activity. A cross-strain comparison (**Fig. A5:4C**) revealed that the class III RNR level was consistently high in PAET1 and highlighted the microaerobic overexpression of class II in PAO1. When grown without KNO_3, the anaerobic regulation was completely absent (**Fig. A5:4E**), demonstrating that nitrate is not only required for anaerobic survival, but also for the regulation changes responsible for other aspects of microaerobic and anaerobic adaptation.

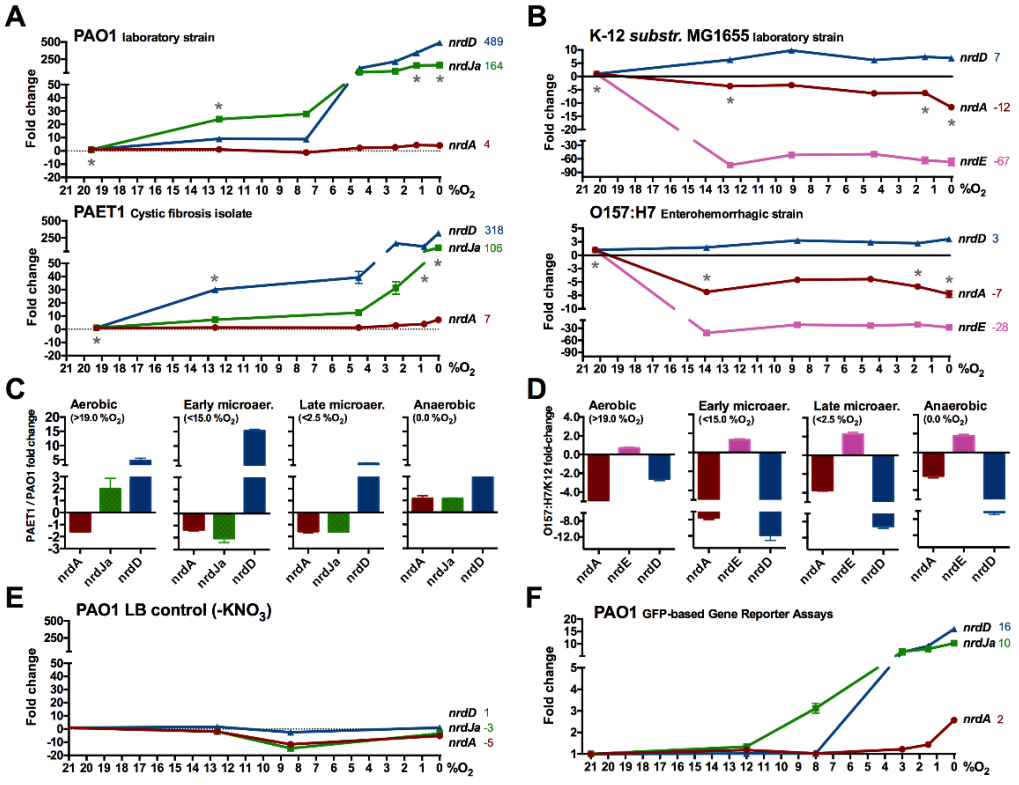

Figure A5:4. Global expression of the RNR network throughout the oxygen gradients. **A, B**, fold-change (each sample compared to the first aerobic measurement) of *nrd* genes in *P. aeruginosa* strains PAO1/PAET1 (**A**) and *E. coli* strains K-12/O157:H7 (**B**). The asterisks (*) indicate samples that were used for C-D. **C, D,** fold-change in a cross-strain comparison between the indicated samples of *P. aeruginosa* (**C**) and *E. coli* (**D**). **E**, Repetition of the experiment in A with *P. aeruginosa* PAO1 using LB medium without KNO_3; the control chart can be found in Supporting Information Fig. A5:S3A. **F**, fold-change (each sample compared to the aerobic experiment) in individual GFP-based gene reporter assays of *P. aeruginosa* PAO1 conducted under different oxygenation conditions. Error bars represent standard deviation.

E. coli only encodes classes Ia (*nrdAB*), Ib (*nrdHIEF*) and III RNR (*nrdDG*). In contrast to our observations for *Pseudomonas*, *E. coli* K-12 and O157:H7 repressed their aerobically active RNRs under reduced oxygen availability (**Fig. A5:4B**; red and pink lines). Class Ib was poorly expressed during the entire process and exhibited a reproducible minimum of approximately 12-14% O_2. The class III RNR (*nrdD*, blue line) had a relatively high basal expression and was only slightly induced under microaerobic and anaerobic conditions. The adaptation of the RNR network occurred almost entirely as a single event as soon as the oxygen availability decreased, in contrast with the gradual adaptation observed in *Pseudomonas*. The cross-strain comparison showed that any differences in RNR expression remained unchanged throughout the oxygen gradient (**Fig. A5:4D**).

As a technical control, we determined the RNR profile for *P. aeruginosa* PAO1 using GFP-based gene reporter assays under controlled atmospheres. Despite this technique being significantly less sensitive than qRT-PCR, the profile that we obtained was remarkably similar to that of the AnaeroTrans system (**Fig. A5:4F**) (same delayed class III RNR activation (*nrdD*, blue line) and early, compensatory induction of class II (*nrdJa*, green line)). At 8% O_2, the system exhibits activation of class II but not class III, even after a long incubation time, thus validating the AnaeroTrans results.

To evaluate whether the previous experiments represented complete adaptation to anaerobiosis, we performed an in-place nitrogen purge of the culture media and used longer anaerobic incubation periods (Supporting Information **Fig. A5:S4**). No new regulatory events were observed, and we concluded that the standard experiments captured the whole aerobic-anaerobic transition. The AnaeroTrans data showed markedly low variation between replicates (Supporting Information Fig. **A5:S5**). As the base expression levels of the studied genes are considerably different, we provide the base aerobic expression of each studied gene in the reference strains, to put the fold-change data in context (Supporting Information **Fig. A5:S6**).

The master regulator NrdR is required for native RNR adaptation to oxygen deprivation

NrdR is the master regulator of the RNR network. In bacteria, NrdR represses all RNR classes; this protein is absent in Archaea and Eukarya (Grinberg et al., 2006; Torrents et al., 2007; Torrents, 2014). Although several studies have explored the mechanism of action of NrdR in different bacterial species (Grinberg et al., 2006; Torrents et al., 2007; McKethan and Spiro, 2013; Crespo et al., 2015), the biological purpose of this protein remains unknown.

The AnaeroTrans profile of PAO1 Δ*nrdR* demonstrated the effects of the absence of NrdR on the regulation of the RNR network. Beyond the expected derepression of all RNRs, the elimination of NrdR provoked a severe alteration in the RNR profile in the aerobic-anaerobic transition (**Fig. A5:5A**). The class III RNR was activated first (*nrdD*, blue line), and the class II RNR (*nrdJa,* green line) did not show the early compensatory induction observed in PAO1. Both classes reached near-maximum levels of expression after a single regulatory event: the gradual pattern of induction disappeared. This finding demonstrates how the native anaerobic regulation of the RNR network requires the presence of NrdR. Due to the altered profile, the effect of NrdR repression was stronger in the microaerobic range than in fully aerobic or anaerobic states (**Fig. A5:5B**).

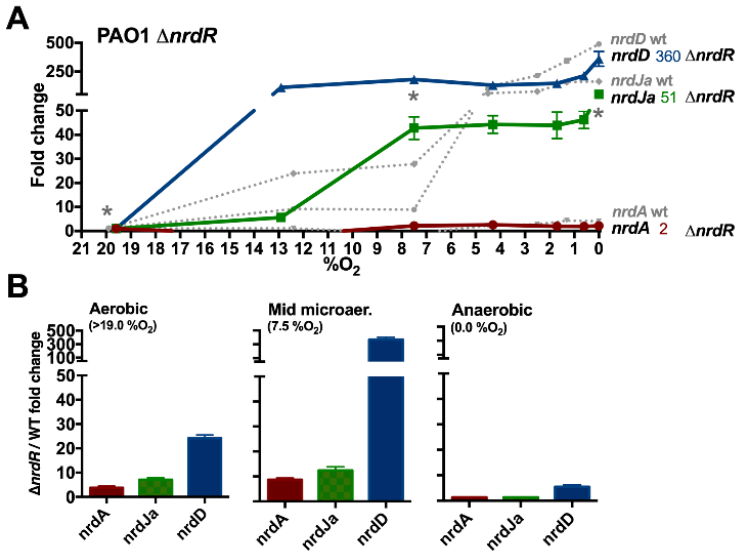

Figure A5:5 Effect of the global regulator NrdR on RNR expression throughout the oxygen gradients. **A**, fold-change (each sample compared to the first aerobic measurement) of *nrd* genes in the *P. aeruginosa* PAO1 Δ*nrdR* mutant strain (see Supporting Information Table S1). The corresponding values of the wild-type strain are provided (in gray) for comparison. The asterisks (*) indicate samples that were used for B. The control chart can be found in Supporting Information Fig. A5:S3C. **B,** fold-change in a cross-strain comparison between PAO1 Δ*nrdR* and wild-type strains. Error bars represent standard deviation.

The regulators of anaerobic metabolism play specific roles throughout the microaerobic range

All the genetic and metabolic changes that we described in the aerobic-anaerobic transition are orchestrated by an intricate network of regulatory systems. We evaluated the action of the Fnr oxygen sensor in *E. coli* and the analogs in *P. aeruginosa*, namely, Anr and Dnr.

In *P. aeruginosa* (**Fig. A5:6A**), the Δ*anr* strain (gray line) first showed an increase in doubling time as soon as the oxygen availability decreased, reaching a very slow growth speed at less than 15% O_2. The Δ*dnr* mutant strain (black line) started showing reduced fitness at approximately 12% O_2 and reached

a maximum doubling time near 8%. The oxygen consumption rate of these strains was almost constant for the remainder of the growth period, as activation of the denitrification machinery was impossible (Supporting Information **Fig. A5:S3C**; green lines). In *E. coli* (**Fig. A5:6B**), the Δ*Fnr* mutant started to show slightly increased doubling times early in the gradient and a more prominent increase after 8% O_2. Under microaerobic conditions, Fnr activates the high-oxygen-affinity terminal oxidase bd-I (Bettenbrock et al., 2014); this activation is correlated with the gradually decreasing oxygen consumption rate (Supporting Information **Fig. A5:S3D**; green line). Nonetheless, the most significant effect of the Fnr system was observed at less than 2% O_2 (**Fig. A5:6A**), most likely corresponding to the activation of fermentative pathways.

The expression of the anaerobic regulators varied throughout the gradient (Supporting Information **Fig. A5:S7**). Both *anr* and *Fnr* were repressed under low oxygen tension, as they negatively regulate their own expression (Mettert and Kiley, 2007; Trunk et al., 2010). On the other hand, *dnr* was induced early in the microaerobic range, as observed for other Anr-activated genes (Trunk et al., 2010). The related two-component systems *narXL* in *P. aeruginosa* and *arcBA* in *E. coli* are also controlled by Anr and Fnr, respectively, and the expression of these systems is induced when the activities of Anr and Fnr increase significantly.

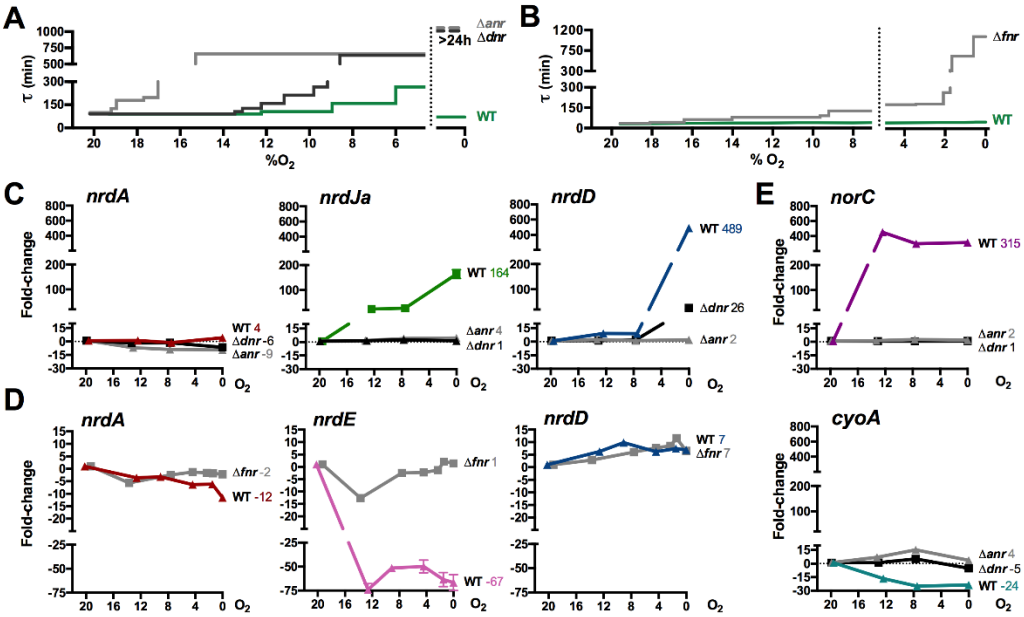

Figure A5:6 Role of the master anaerobic regulators throughout the oxygen gradients. **A,B**, estimated doubling time of *P. aeruginosa* PAO1 (A), *E. coli* K-12 *substr*. MG1655 (B), and their isogenic mutants, Δ*anr, Δdnr,* and Δ*fnr*. Doubling time is represented in minutes, depending on the oxygen concentration in the gas phase (% O_2 v/v). Wild-type values are provided as a reference (in green). **C, D, E**, fold-change (each sample compared to the first aerobic measurement) of *nrd* genes in the previous mutant strains of *P. aeruginosa* (C) and *E. coli* (D), as well as fold-change of *norC* and *cyoA* in *P. aeruginosa* (E). Wild-type values at the same oxygen tensions are provided as a reference. Error bars represent standard deviation.

Regarding the RNR network, in *P. aeruginosa* (**Fig. A5:6C**), induction of the class II RNR (*nrdJa*, green line) was absent in both the Δ*anr* and Δ*dnr* strains, as expected for a Dnr-regulated gene (Trunk et al., 2010; Crespo et al., 2016). The class III RNR (*nrdD*, blue line) showed no induction in the Δ*anr* mutant, as this protein is described to be controlled by Anr (Crespo et al., 2017). However, anaerobic induction of this protein was also significantly reduced in the Δ*dnr* mutant strain. Finally, the class I RNR (*nrdA*, red line) exhibited slight anaerobic repression in the mutant strains via an as-yet-unknown mechanism. We also studied the genes *norC* and *cyoA*, which we had previously used as controls. *norC* exhibited the expected profile of a Dnr-dependent gene (**Fig. A5:6E**; top). The repression of *cyoA* was absent in the mutant strains (**Fig. A5:6E**; bottom).

In *E. coli* (**Fig. A5:6D**), the repression of the aerobically active class Ia (*nrdA*, red line) and class Ib (*nrdE*, pink line) RNRs was Fnr dependent. No Fnr boxes have been identified in the promoters of these genes (Boston and Atlung, 2003), so the repression might be the result of indirect mechanisms of regulation. The minimum in early microaerobiosis remained present in the Δ*Fnr* mutant. The slight anaerobic induction of the class III RNR (*nrdD*, blue line) was not affected by the Δ*Fnr* mutation: we did not detect Fnr-dependent regulation of *nrdDG* (Boston and Atlung, 2003; Roca et al., 2008).

Discussion

The AnaeroTrans system is based on the exposure of an isolated steady-state culture to a small oxygenated gas phase, allowing the culture to consume oxygen via aerobic respiration and characterizing the aerobic-anaerobic transition using the remaining oxygen concentration as the state variable. The intermediate stages between aerobiosis and anaerobiosis show a surprising degree of granularity.

Despite the common misconception that facultative anaerobes cleanly switch between aerobic and anaerobic metabolism, hybrid states are possible and have been described in many species. In *E. coli*, it has been reported that the cytoplasm can be oxygen free while respiration continues to occur in the membrane (Rolfe et al., 2012). In *P. aeruginosa*, aerobic and anaerobic respiration can occur simultaneously (Chen et al., 2006). In this study, we clearly observed hybrid metabolism: in *P. aeruginosa*, for example, during most of the microaerobic range, the denitrification machinery was already induced (**Fig. A5:1E**), the Anr/Dnr regulators were already essential (**Fig. A5:6B**), and the culture could not grow in the absence of nitrate (Supporting Information **Fig. A5:S3B**) while oxygen continued to be consumed (**Fig. A5:2A**).

Application of the AnaeroTrans system to two facultative anaerobic pathogens, namely, *E. coli* and *P. aeruginosa*, provided an entirely different picture of the relationships of these species with oxygen. In *P. aeruginosa,* we can divide the microaerobic regulation into three phases (**Fig. A5:7A**). The first phase occurs in the *early microaerobic range*, corresponding to approximately 21-12% gas-phase O_2 in our system. The DO levels exhibit a sharp decrease, as this species actively restricts oxygen transfer to its cultures (Sabra et al., 2002) until all diffused oxygen is captured and used for respiration. Both *P. aeruginosa* strains show a high oxygen consumption rate (**Fig. A5:2A**) and no increase in doubling time compared to that under aerobiosis (**Fig. A5:2B**), demonstrating high fitness under these oxygenation conditions. Anr starts to be required at this stage (**Fig. A5:6B**). Among the expected actions of Anr in this range is the activation of cytochrome cbb_3-2 (Arai, 2011), which has an even higher affinity for oxygen than the constitutively expressed cbb_3-1 (Arai et al., 2014), and presents up to ten-fold anaerobic induction from this moment on (data not shown). Anr activates *aer* transcription (**Fig. A5:1E**) and is also responsible for the first start of denitrification at the end of this stage (Supporting Information **Fig. A5:S3B**). Dnr-dependent pathways are not yet essential at this stage (**Fig. A5:6B**), although in the presence of nitrate, some Dnr regulation is already noticeable, as, for example, in the induction of *norC* (**Fig. A5:1E**). Regarding the RNR network, initial activation of the class III RNR in PAET1 was observed (**Fig. A5:4A**; PAET1, blue line). The laboratory strain PAO1, in which Anr-dependent activation of *nrdD* is impaired (Crespo et al., 2017), exhibits compensatory induction of the class II RNR (**Fig. A5:4A**; PAO1, green line), clearly demonstrating the reactive nature of the network and implying that at least one anaerobically active RNR is required even in the early microaerobic range.

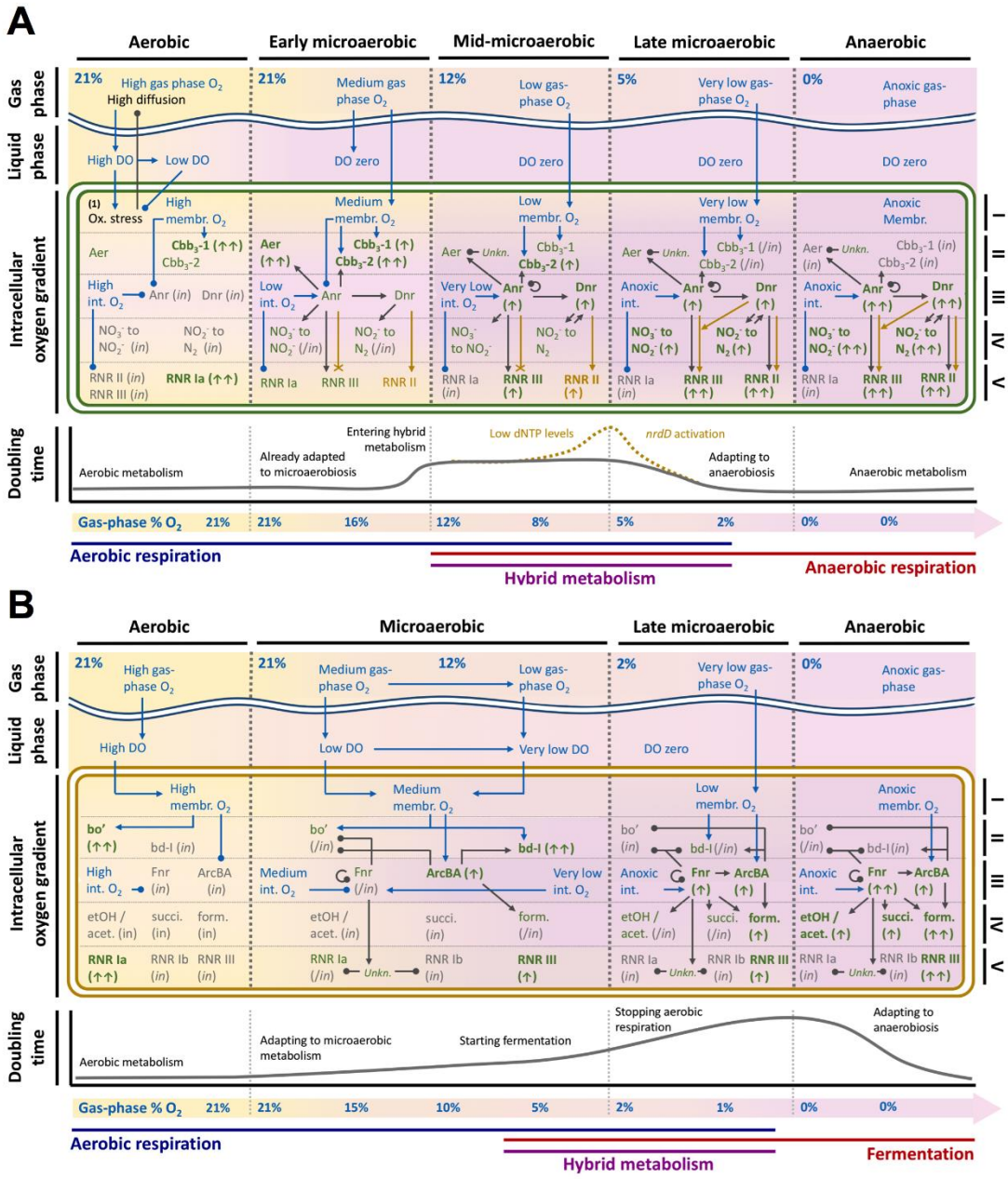
A
Aerobic
Early microaerobic
Mid-microaerobic
Late microaerobic
Anaerobic
Gas phase
Liquid phase
Intracellular oxygen gradient
21%
High gas phase O2
High diffusion
21%
Medium gas phase O2
12%
Low gas-phase O2
5%
Very low gas-phase O2
0%
Anoxic gas-phase
High DO
Low DO
DO zero
DO zero
DO zero
DO zero
(1) Ox. stress
High membr. O2
Medium membr. O2
Low membr. O2
Very low membr. O2
Anoxic Membr.
Aer
Cbb3-1 (↑↑)
Cbb3-2
Aer (↑↑)
Cbb3-1 (↑)
Cbb3-2 (↑↑)
Aer
Unkn.
Cbb3-1
Cbb3-2 (↑)
Aer
Unkn.
Cbb3-1 (/in)
Cbb3-2 (/in)
Aer
Unkn.
(in)
Cbb3-1 (in)
Cbb3-2 (in)
High int. O2
Anr (in)
Dnr (in)
Low int. O2
Anr
Dnr
Very Low int. O2
Anr (↑)
Dnr (↑)
Anoxic int.
Anr (↑)
Dnr (↑)
Anoxic int.
Anr (↑↑)
Dnr (↑↑)
NO3- to NO2- (in)
NO2- to N2 (in)
NO3- to NO2- (/in)
NO2- to N2 (/in)
NO3- to NO2-
NO2- to N2
NO3- to NO2- (↑)
NO2- to N2 (↑)
NO3- to NO2- (↑↑)
NO2- to N2 (↑↑)
RNR II (in)
RNR III (in)
RNR Ia (↑↑)
RNR Ia
RNR III
RNR II
RNR Ia (in)
RNR III (↑)
RNR II (↑)
RNR Ia (in)
RNR III (↑↑)
RNR II (↑↑)
RNR Ia (in)
RNR III (↑↑)
RNR II (↑↑)
I
II
III
IV
V
Doubling time
Aerobic metabolism
Already adapted to microaerobiosis
Entering hybrid metabolism
Low dNTP levels
nrdD activation
Adapting to anaerobiosis
Anaerobic metabolism
Gas-phase % O2
21%
21%
16%
12%
8%
5%
2%
0%
0%
Aerobic respiration
Hybrid metabolism
Anaerobic respiration
B
Aerobic
Microaerobic
Late microaerobic
Anaerobic
Gas phase
Liquid phase
Intracellular oxygen gradient
21%
High gas-phase O2
21%
Medium gas-phase O2
12%
Low gas-phase O2
2%
Very low gas-phase O2
0%
Anoxic gas-phase
High DO
Low DO
Very low DO
DO zero
High membr. O2
Medium membr. O2
Low membr. O2
Anoxic membr. O2
bo' (↑↑)
bd-I (in)
bo' (/in)
bd-I (↑↑)
bo' (in)
bd-I (/in)
bo' (/in)
bd-I (in)
High int. O2
Fnr (in)
ArcBA (in)
Medium int. O2
Fnr (/in)
ArcBA (↑)
Very low int. O2
Anoxic int.
Fnr (↑)
ArcBA (↑)
Anoxic int.
Fnr (↑↑)
ArcBA (↑)
etOH / acet. (in)
succi. (in)
form. (in)
etOH / acet. (in)
succi. (in)
form. (/in)
etOH / acet. (/in)
succi. (/in)
form. (↑)
etOH / acet. (↑)
succi. (↑)
form. (↑↑)
RNR Ia (↑↑)
RNR Ib (in)
RNR III (in)
RNR Ia (/in)
Unkn.
RNR Ib (in)
RNR III (↑)
RNR Ia (in)
Unkn.
RNR Ib (in)
RNR III (↑)
RNR Ia (in)
Unkn.
(in)
RNR Ib (in)
RNR III (↑↑)
I
II
III
IV
V
Doubling time
Aerobic metabolism
Adapting to microaerobic metabolism
Starting fermentation
Stopping aerobic respiration
Adapting to anaerobiosis
Gas-phase % O2
21%
21%
15%
10%
5%
2%
1%
0%
0%
Aerobic respiration
Hybrid metabolism
Fermentation

Figure A5:7 Interpretation and model of the data. Adaptation of *P. aeruginosa* **(A)** and *E. coli* **(B)** to microaerobic and anaerobic conditions. The information is divided into different stages (from aerobic to anaerobic). For each stage, the oxygen concentration is depicted in the gas and liquid phases, as well as inside a cell, and represented by the background colors from yellow (aerobic) to pink (anaerobic). Intracellular oxygen forms a gradient, as it is consumed near the membrane (membr.) and less oxygen reaches the inner parts of the cytoplasm (int.). The most relevant changes discussed in the main text are grouped as follows: oxygen capture **(I)**, aerobic respiration and aerotaxis **(II)**, anaerobic regulation **(III)**, anaerobic metabolism **(IV)** and ribonucleotide reduction **(V)**. In the anaerobic metabolism area (IV), for *P. aeruginosa,* denitrification is divided into two steps: from nitrate to nitrite (NO_3^- to NO_2^-) and from nitrite to nitrogen (NO_2^- to N_2). Likewise, for *E. coli,* mixed-acid fermentation is divided into three pathways, named according to their final products: ethanol and acetate pathway (etOH/acet.), succinate pathway (succ.), and formate pathway (form.). The position of the different elements inside the cell is not related to their real subcellular location. Inactive elements are gray and indicated as (*in.*); when one element is activated or inactivated during one stage, it is represented as (*/in.*). Active elements are green, and higher activation is represented with arrows (↑). Oxygen concentration and its direct effects are drawn in blue. Positive relationships are represented by regular arrows, while arrows with round heads represent negative relationships. Crossed-out arrows represent inactive or impeded relations. Below the cell, an interpretation is drawn of the variations in doubling time. In *P. aeruginosa*, events only occurring in the PAO1 strain are represented in brown. The lines at the bottom of the figure represent the approximate moments during the transition where aerobic respiration (dark blue) or anaerobic respiration/fermentation (red) are active, and the overlapping area indicates hybrid metabolism (purple). This schematic does not constitute a full review of the aerobic-anaerobic transition, and only those elements related to the discussion in the main text are represented.

The next phase occurs in the *mid-microaerobic range*, approximately between 12% and 5% O_2, when Dnr-dependent pathways start to be required (**Fig. A5:6B**), and *anr* is controlled via a negative feedback loop (Supporting Information **Fig. A5:S7**). Most of the changes that occur in this phase are related to the gradually increasing activation of the Anr/Dnr system, as the cytoplasm becomes increasingly hypoxic. During this intermediate adaptation period, both *P. aeruginosa* strains showed a significant reduction in oxygen consumption rate (**Fig. A5:2A**), as well as a marked decrease in fitness, with increased doubling times (Fig. 2B) and peaks in the percentage of dead cells (**Fig. A5:2C**, Supporting Information **Fig. A5:S2C**). In the CF strain PAET1, the adaptation appears as a single event, but in PAO1, there is a second threshold at approximately 6% O_2 (**Fig. A5:2B**). RNR may be at least partially responsible for this last stress period, as fitness is not restored until late activation of the class III RNR occurs (**Fig. A5:4A**), via a mechanism that is partly dependent on Dnr (**Fig. A5:6D**). Notably, these intermediate stages are reproducible under this range of oxygen concentrations, as a prolonged incubation time does not change the result (**Fig. A5:4F**). This phase presents clear hybrid metabolism, and denitrification is already essential (Supporting Information **Fig. A5:S3B**).

Finally, at less than 5% O_2, a third phase occurs in the *late microaerobic range*. Oxygen consumption occurs at a very low rate or stops altogether (**Fig. A5:2A**), as the oxygen affinity of the microaerobic terminal oxidases in *P. aeruginosa* is not as high as that of the *E. coli* counterparts (Bettenbrock et al., 2014). Anr and Dnr become essential at this stage (**Fig. A5:6B**), and via anaerobic respiration, the original growth rate is fully recovered (**Fig. A5:2B**). The class II and III RNRs show a new induction event (**Fig. A5:4A**), preparing the cell for strict anaerobic growth.

To provide an ecological context for our results, it is worth discussing where *P. aeruginosa* encounters different states of oxygenation. In some of the potential habitats in which *P. aeruginosa* resides as a free-living organism, as well as in the early stages of some acute infections, *P. aeruginosa* encounters high oxygen concentrations. However, due to its capacity to restrict oxygen diffusion (Sabra et al., 2002), this organism probably often lives in what we called the early microaerobic range, which can give this species a competitive advantage. In other infections, oxygen availability is reduced further: in the CF lung, the thick mucus layer and the impaired mucociliary clearance (Schobert and Jahn, 2010) generate a markedly hypoxic niche, which reaches zero DO after *Pseudomonas* infection (Worlitzsch et al., 2002). However, it has been described that *Pseudomonas* growth in the CF lung requires aerobic respiration (Alvarez-Ortega and Harwood, 2007), so we can safely assume that these bacteria present a hybrid metabolism. The most complex profile is observed in thick biofilms in aerated environments, where the surface is oxygenated, but the DO decreases gradually with biofilm depth. In this case, all the different stages of adaptation that we described could potentially be encountered in different layers. Both with and without substrates for denitrification, layers below the zero-DO level could still hold active cells. While this article was in preparation, a study (Schiessl et al., 2019) was published that demonstrated this effect. When *P. aeruginosa* biofilms are studied with GFP, only a single metabolically active layer appears (Borriello et al., 2004); however, by using a new method based on stable isotope labeling, Schiessl *et al*. showed a second activity layer in the zero-DO area, even in the absence of nitrate (Schiessl et al., 2019). This layer was present below an intermediate low-activity adaptation area, as shown in our AnaeroTrans experiments.

E. coli shows a significantly different behavior (**Fig. A5:7B**). Under aerobic conditions, cytochrome bo' is the active terminal oxidase, which exhibits a high efficiency (Bettenbrock et al., 2014). The transcriptional regulator Fnr exhibits activity as soon as the oxygen availability decreases (**Fig. A5:6B**), including regulation of its own expression via a negative feedback loop (Supporting Information **Fig. A5:S7**). Among the expected actions of Fnr in this range is the repression of cytochrome bo', which is replaced by cytochrome bd-I. This last cytochrome exhibits significantly less energetic efficiency but presents a very low K_m (Bettenbrock et al., 2014). Consequently, in this range, both *E. coli* strains, namely, the commensal K-12 and enterohemorrhagic O157:H7, show increased doubling times (**Fig. A5:3B**) and a significant decrease in the oxygen consumption rate (**Fig. A5:3A**), reaching a value that remains stable during most of the transition. Although many of the Fnr-regulated genes already exhibit an effect at this stage (Rolfe et al., 2012), the ArcBA system is described to be most important for the regulation of anaerobic metabolism in the early to mid-microaerobic range, whereas Fnr becomes more important in the late microaerobic range and under strict anaerobiosis (Tseng et al., 1996). Among other actions, in this range ArcBA participates in the repression of cytochrome bo', and it is responsible for the microaerobic activation of cytochrome bd-I. The ArcBA system can also activate the initial steps of mixed-acid fermentation, the formate pathway (Becker et al., 1997; Shalel-Levanon et al., 2005). Although more experiments will be needed to fully understand the sequence of events during the microaerobic adaptation of *E. coli*, there are evidences of an important adaptation event occurring at approximately 8% O_2 in our system, where Fnr activity becomes highly noticeable (**Fig.**

A5:6A), and coinciding with a first peak in the number of dead cells (**Fig. A5:3C**; Supporting Information Fig. S2C). It is at less than 2% O_2, however, that Fnr becomes essential (**Fig. A5:6A**), most likely coinciding with the full Fnr-dependent activation of fermentative pathways. It is not until this point that *E. coli* stops consuming oxygen (**Fig. A5:3A**). The aerobic respiration is deactivated via the repression of cytochrome bd-I expression by Fnr, which only occurs under very low oxygen availability (Tseng et al., 1996). *E. coli* exhibits increased doubling times and stress effects at this stage, and the final adaptation occurs only when *E. coli* has been exposed for some time to strict anaerobic conditions (**Fig. A5:3B**; **Fig. A5:3C**).

In *E. coli*, the RNR network presents a pattern of regulation opposite to that of *Pseudomonas*: instead of keeping the aerobic machinery active and conditionally expressing the anaerobic machinery, in *E. coli*, the class III RNR exhibits basal expression, while classes Ia and Ib are repressed under reduced oxygen availability (**Fig. A5:4B**). This repression is Fnr-dependent and becomes noticeable in the early microaerobic range (**Fig. A5:6D**), although no Fnr boxes have been identified in the corresponding promoters (Boston and Atlung, 2003). The class Ib RNR was poorly expressed during all the process (data not shown).

In the lower intestine, both commensal and pathogenic *E. coli* strains encounter a largely hypoxic niche. Although traditionally this environment has been considered to be anaerobic (Backhed et al., 2005), EPR imaging shows the presence of oxygen in the gut (He et al., 1999), exhibiting a gradually decreasing gradient throughout the gastrointestinal tract and reaching below 0.5 ppm DO in the colon. These conditions remarkably reproduce the late microaerobic conditions in our experiments, where *E. coli* can still perform respiration. Jones *et al*. demonstrated that both the anaerobic and microaerobic machinery are required for gut colonization (Jones et al., 2007) and proposed that successful colonizers are adapted to low levels of oxygen and can use both metabolisms sequentially or simultaneously, which is consistent with the AnaeroTrans results. The influence of anaerobic respiration versus fermentation was considered to be beyond of the scope of this study, but future experiments using minimal media with different substrates can help ascertain the role of each option in *E. coli* metabolism and pathogenesis.

Our results represent not only the first description of the RNR profile under different oxygen availability conditions but also provide a global image of how different facultative anaerobes behave between aerobiosis and anaerobiosis, as well as a proof of concept for a system designed to studying this microaerobic range. The use of the gas-phase oxygen concentration as the state variable necessarily implies that differences in system architecture, which alter the oxygen transference rate, change the exact values at which specific events occur, although the transition profiles as a whole would remain comparable. Nevertheless, the results obtained via an independent technique (**Fig. A5:4F**) demonstrate that even under a completely different architecture, the figures remain remarkably similar.

To the best of our knowledge, the only published system that successfully describes the state of oxygen availability in the microaerobic range is the AU scale (Bettenbrock et al., 2014), which emphasizes

reproducibility between laboratories. However, this approach requires a demanding setup, is based on the determination of acetate levels by HPLC, and can only be applied to *E. coli* grown under specific conditions (Bettenbrock et al., 2014). In comparison, AnaeroTrans does not require the control of gas compositions, does not rely on external measurements, and can be applied to virtually all facultative anaerobes with a wide variety of conditions and media. If comparing exact oxygen concentration values is essential, multiplexing with a gene that is already known to exhibit gradual induction, such as *nrdD* in *P. aeruginosa*, could standardize results between laboratories. Future experiments may explore this possibility, as well as the use of AnaeroTrans to reproduce specific environments (such as the cystic fibrosis mucus) or the applications of this method in general transcriptomics.

Experimental procedures

Bacterial strains, plasmids and growth conditions

Bacterial strains and plasmids are listed in Supporting Information Table S1. *Escherichia coli* and *Pseudomonas aeruginosa* were routinely grown in Luria-Bertani broth (LB). Anaerobic cultures of *P. aeruginosa* were grown in LB supplemented with 10 g l^{-1} KNO_3 (LBN). All routine anaerobic cultures were grown in screw-cap tubes (Hungate tubes) purged with N_2 (99.999% purity). When needed, gentamicin was added to the *P. aeruginosa* cultures at a final concentration of 100 µg ml^{-1}.

Bioreactor setup and continuous culture techniques

The setup that we used for AnaeroTrans experiments is illustrated in **Fig. A5:1A**, a chemostat-type stirred-tank bioreactor. The culture was grown in a three-neck round-bottom flask with a fixed volume of 275 ml of liquid and 55 ml of gas. The necks were sealed with turn-over flange rubber stoppers, and in and out connections were drilled through the stoppers and sealed with silicone rubber. The culture flask was partially submerged in a water bath sitting on a stirrer hotplate.

The inflow tube (carrying fresh culture medium) and the outflow tube (carrying grown culture to a waste bottle containing bleach) were made of nontoxic Norprene food tubing (Masterflex, Cole-Parmer) with an internal diameter of 800 µM to reduce the void volume. The tubes passed through the same peristaltic pump. The flow rates that we used for this study ranged between 18 ml h^{-1} and 360 ml h^{-1}, equivalent to dilution rates between 0.065 h^{-1} and 1.309 h^{-1}. The gas tubes were made of a Tygon E-Lab low-gas-permeability formulation. The gas inflow was connected to either a compressed-air supply or a nitrogen supply and crossed through a hot water bath set to obtain a stable gas temperature of 35 ºC. The inflow gas was filtered through a 0.22-µM filter before entering the culture flask. The gas outflow was collected in a waste solution containing bleach. Unless otherwise stated, the flow rate for both air and nitrogen was 180 ml min^{-1}.

The oxygen concentration in the gas phase in the culture flask was monitored using an Oxymicro fiber-optic sensor system (World Precision Instrument) connected to a micro-optode oxygen sensor in a fixed-needle housing (PreSens). For the initial setup, a temperature probe was introduced in the water bath of the culture flask. During the experiments, the oxygen measurements were obtained by assuming a constant gas temperature of 35 ºC. Micro-optode sensors were calibrated using temperature-compensated measurements of air saturated with water vapor (100% air saturation point, assumed to contain 20.95% O_2) and the nitrogen phase of a Hungate tube containing an oxygen-free 10 g l^{-1} solution of sodium dithionite (0% O_2 point).

In a standard AnaeroTrans experiment, the system starts with the culture flask filled with 275 ml of fresh medium. The airflow is set at 180 ml $min^{-1,}$ and the dilution rate is set at 0.065 h^{-1}. When the air and culture have reached the desired temperatures and the system is stable, the medium is inoculated with a 1:100 volume of an overnight culture of the desired strain through a preplaced needle. Culture samples are taken from the outflow, and the OD_{600} is measured to monitor bacterial growth. When an OD_{600} of 0.50 ± 0.05 is reached, the dilution rate is gradually increased until the biomass of the culture is stable (steady state). Then, the first sample (aerobic) is obtained (see RNA techniques for sampling protocols), the gas flow is stopped, and the gas connections in the culture chamber are closed. Bacterial growth is monitored as the culture gradually consumes all available oxygen, and other samples are obtained at the required times. To purge the remaining oxygen, the gas circuit is connected to a nitrogen supply and connected with the culture at the desired moment. The final anaerobic sample is obtained after 1 h of nitrogen flow, unless otherwise stated.

Alternative setups were used in this study when required (see main text). First, to measure the oxygen concentration in the liquid phase, a continuous-flow micro-optode housing was used, and the measurement was compensated by temperature, placing the probe in contact with the flow chamber. Continuous-flow micro-optodes were calibrated using temperature-compensated measurements of water saturated with air (100% air saturation point, 8.25 mg l^{-1} at 25 ºC and 1 atm) and a 10 g l^{-1} solution of sodium dithionite (0% O_2 point). Second, to eliminate in-place the oxygen in the inlet medium, the fresh medium was obtained from a sealed bottle (with "in" and "out" gas connections drilled into the bottle cap) placed in a stirrer hotplate, and the in-gas nitrogen was separated after the filter in two streams: one connected to the culture flask and the other to the inlet culture medium bottle. The nitrogen flow rate was increased to 400 ml min^{-1} and first only connected to the medium bottle, 1 hour before opening the second connection and starting the nitrogen purge of the culture.

Estimation of bacterial fitness

As a simple method to estimate the fitness of the culture, doubling times were determined from the bioreactor data. Considering the culture flask to be a stirred tank bioreactor with perfect mixing and operating in a steady state, the specific growth rate of the culture (μ) is equal to the dilution rate (D) as in (1):

$$\mu = D = \frac{flow\ rate}{culture\ volume} = \frac{F}{V} \qquad (1)$$

The doubling time (τ) can be calculated as a function of the dilution rate (2):

$$\tau = \frac{\ln 2}{\mu} = \frac{\ln 2}{D} \qquad (2)$$

Estimated doubling times were calculated at time points when the biomass was deemed stable enough to safely assume a steady state. We chose only time points were OD_{600} presented less than 5% variation for the previous 20 minutes and for 2 or more samples.

The oxygen consumption rate was also represented in control charts to illustrate changes in oxygen metabolism throughout the experiment. Unless otherwise stated, the O_2 consumption rates are 20-minute averages of variations in O_2 concentration expressed in $\Delta(\%O_2)$ h^{-1}.

RNA techniques

Samples for RNA extraction were obtained at an OD_{600} of 0.50 ± 0.05. Two milliliters of the bioreactor outflow or control aerobic or anaerobic cultures were sampled, treated with RNAprotect Bacteria Reagent (QIAGEN), and extracted using the RNeasy Mini Kit (QIAGEN) according to the manufacturer's instructions. Samples from the bioreactor were eluted directly onto RNAprotect to avoid variations due to air exposure. DNase I (Turbo DNA-free, Applied Biosystems) was used to remove DNA contamination. The absence of DNA was verified by PCR. First-strand cDNA synthesis was performed using Maxima reverse transcriptase (ThermoFisher Scientific) with 250 ng (*P. aeruginosa* samples) or 500 ng (*E. coli* samples) of total RNA and random hexamer primers (ThermoFisher Scientific) according to the manufacturer's instructions.

Quantitative real-time PCR (qRT-PCR) was conducted using PowerUP Sybr Green Master Mix (ThermoFisher Scientific) in a StepOnePlus real-time PCR system (Applied Biosystems) according to the manufacturer's instructions. All the qRT-PCR reactions used specific gene primers, as detailed in Supporting Information Table S2. The glyceraldehyde-3-phosphate dehydrogenase A gene *gapA* was used as an internal standard.

Fluorescence microscopy and LIVE/DEAD assay

Samples for microscopy were obtained at an OD_{600} of 0.50 ± 0.05. Ten milliliters of the bioreactor outflow or control aerobic or anaerobic cultures were sampled. For anaerobic pulse samples (see Supporting Information **Fig. A5:S2A-2B**), five milliliters of an aerobic culture at an OD_{600} of 0.50 were transferred to an anaerobic Hungate tube and incubated for 2 h before sampling. Sample cells were harvested by centrifugation and stained using the LIVE/DEAD BacLight Viability Kit (ThermoFisher Scientific) according to the manufacturer's instructions. Fluorescent bacteria were visualized using a Nikon ECLIPSE Ti-S/L 100 inverted fluorescence microscope (Nikon) using a 100× 1.30 oil objective and a Nikon DS-Qi2 camera. Ten to fifteen representative images were obtained for each sample and were used to count the percentage of green/red cells. NIS-Elements microscope imaging software (Nikon) was used for image analysis.

Gene reporter assay in a controlled atmosphere

To verify the AnaeroTrans-derived gene expression data by an independent technique, we used green fluorescent protein (GFP)-based gene-reporter assays conducted in atmospheres with controlled oxygen concentration using a Spark multimode microplate reader (TECAN) coupled to an N_2 supply (99.999% purity) to control the oxygen concentration. This method used the family of plasmids derived from pETS130-GFP (see Supporting Information Table S1), which encode transcriptional fusions of the promoters of all *nrd* operons with GFP (Sjoberg and Torrents, 2011; Crespo et al., 2015). To evaluate the expression of these operons under different oxygenation conditions, a full experiment was conducted for each desired oxygen concentration using strains containing each transcriptional fusion, as well as one with a promoterless GFP plasmid to evaluate the fluorescence level of a blank reaction.

The cultures were performed in 96-well black fluorescence plates. Two hundred microliters of the cultures of each strain in LB (*E. coli*) or LBN (*P. aeruginosa*) supplemented with gentamycin 100 µg ml^{-1} were inoculated with an aerobic overnight culture of the corresponding strain to a final OD_{600} of 0.05. Six replicates per strain were included. The plate was placed inside a humidity cassette (TECAN) to keep the system humid and avoid evaporation.

The culture was initially incubated at 37 ºC and 21% v/v O_2 for 2 h and 30 min with orbital shaking. The culture was ventilated for 10 s every 5 minutes in automatic ventilation steps where shaking was stopped and the lid of the humidity cassette was lifted. After this incubation, the OD_{600} (initial OD) and GFP fluorescence intensity (initial GFP) were determined. Then, the oxygen concentration was changed to the desired concentration, and the culture was incubated for an additional period of 5 h to allow adaptation to the new oxygenation conditions using the same ventilation settings. After the adaptation period, a short incubation with high oxygen levels was conducted (20 min at 21% O_2, ventilating for 10 s per minute, with orbital shaking) to oxidize the GFP that was produced under anaerobiosis (Tsien, 1998). The final OD_{600} (final OD) and GFP fluorescence intensity (final GFP) were then determined.

The absorbance for each well was calculated by removing the average absorbance of blank wells (including only LB/LBN). The normalized fluorescence for each well was calculated by first dividing the fluorescence intensity of the well in relative fluorescence units by the absorbance of the well (RFU/OD_{600}) and subtracting the RFU/OD_{600} of promoterless GFP. Finally, the gene expression was presented as an induction factor, dividing the final normalized fluorescence of each well by the average initial normalized fluorescence of the corresponding strain.

References

Alexeeva, S., Hellingwerf, K.J., and Teixeira de Mattos, M.J. (2002) Quantitative assessment of oxygen availability: perceived aerobiosis and its effect on flux distribution in the respiratory chain of *Escherichia coli*. *J Bacteriol* **184**: 1402-1406.

Alvarez-Ortega, C., and Harwood, C.S. (2007) Responses of *Pseudomonas aeruginosa* to low oxygen indicate that growth in the cystic fibrosis lung is by aerobic respiration. *Mol Microbiol* **65**: 153-165.

Arai, H. (2011) Regulation and Function of Versatile Aerobic and Anaerobic Respiratory Metabolism in *Pseudomonas aeruginosa*. *Front Microbiol* **2**: 103.

Arai, H., Kodama, T., and Igarashi, Y. (1997) Cascade regulation of the two CRP/FNR-related transcriptional regulators (ANR and DNR) and the denitrification enzymes in *Pseudomonas aeruginosa*. *Mol Microbiol* **25**: 1141-1148.

Arai, H., Kawakami, T., Osamura, T., Hirai, T., Sakai, Y., and Ishii, M. (2014) Enzymatic characterization and in vivo function of five terminal oxidases in *Pseudomonas aeruginosa*. *J Bacteriol* **196**: 4206-4215.

Backhed, F., Ley, R.E., Sonnenburg, J.L., Peterson, D.A., and Gordon, J.I. (2005) Host-bacterial mutualism in the human intestine. *Science* **307**: 1915-1920.

Baughn, A.D., and Malamy, M.H. (2004) The strict anaerobe *Bacteroides fragilis* grows in and benefits from nanomolar concentrations of oxygen. *Nature* **427**: 441-444.

Becker, S., Holighaus, G., Gabrielczyk, T., and Unden, G. (1996) O2 as the regulatory signal for FNR-dependent gene regulation in *Escherichia coli*. *J Bacteriol* **178**: 4515-4521.

Becker, S., Vlad, D., Schuster, S., Pfeiffer, P., and Unden, G. (1997) Regulatory O2 tensions for the synthesis of fermentation products in Escherichia coli and relation to aerobic respiration. *Arch Microbiol* **168**: 290-296.

Bettenbrock, K., Bai, H., Ederer, M., Green, J., Hellingwerf, K.J., Holcombe, M. et al. (2014) Towards a systems level understanding of the oxygen response of *Escherichia coli*. *Adv Microb Physiol* **64**: 65-114.

Borriello, G., Werner, E., Roe, F., Kim, A.M., Ehrlich, G.D., and Stewart, P.S. (2004) Oxygen limitation contributes to antibiotic tolerance of Pseudomonas aeruginosa in biofilms. *Antimicrob Agents Chemother* **48**: 2659-2664.

Boston, T., and Atlung, T. (2003) FNR-mediated oxygen-responsive regulation of the *nrdDG* operon of *Escherichia coli*. *J Bacteriol* **185**: 5310-5313.

Cendra Mdel, M., Juarez, A., and Torrents, E. (2012) Biofilm modifies expression of ribonucleotide reductase genes in *Escherichia coli*. *PLoS One* **7**: e46350.

Chen, F., Xia, Q., and Ju, L.K. (2006) Competition between oxygen and nitrate respirations in continuous culture of Pseudomonas aeruginosa performing aerobic denitrification. *Biotechnol Bioeng* **93**: 1069-1078.

Crespo, A., Pedraz, L., and Torrents, E. (2015) Function of the *Pseudomonas aeruginosa* NrdR Transcription Factor: Global Transcriptomic Analysis and Its Role on Ribonucleotide Reductase Gene Expression. *PLoS One* **10**: e0123571.

Crespo, A., Pedraz, L., Astola, J., and Torrents, E. (2016) *Pseudomonas aeruginosa* Exhibits Deficient Biofilm Formation in the Absence of Class II and III Ribonucleotide Reductases Due to Hindered Anaerobic Growth. *Front Microbiol* **7**: 688.

Crespo, A., Gavalda, J., Julian, E., and Torrents, E. (2017) A single point mutation in class III ribonucleotide reductase promoter renders *Pseudomonas aeruginosa* PAO1 inefficient for anaerobic growth and infection. *Sci Rep* **7**: 13350.

de Beer, D., Stoodley, P., Roe, F., and Lewandowski, Z. (1994) Effects of biofilm structures on oxygen distribution and mass transport. *Biotechnol Bioeng* **43**: 1131-1138.

Dietrich, L.E., Okegbe, C., Price-Whelan, A., Sakhtah, H., Hunter, R.C., and Newman, D.K. (2013) Bacterial community morphogenesis is intimately linked to the intracellular redox state. *J Bacteriol* **195**: 1371-1380.

Filiatrault, M.J., Wagner, V.E., Bushnell, D., Haidaris, C.G., Iglewski, B.H., and Passador, L. (2005) Effect of anaerobiosis and nitrate on gene expression in *Pseudomonas aeruginosa*. *Infect Immun* **73**: 3764-3772.

Galimand, M., Gamper, M., Zimmermann, A., and Haas, D. (1991) Positive FNR-like control of anaerobic arginine degradation and nitrate respiration in *Pseudomonas aeruginosa*. *J Bacteriol* **173**: 1598-1606.

Garriga, X., Eliasson, R., Torrents, E., Jordan, A., Barbe, J., Gibert, I., and Reichard, P. (1996) *nrdD* and *nrdG* genes are essential for strict anaerobic growth of *Escherichia coli*. *Biochem Biophys Res Commun* **229**: 189-192.

Georgellis, D., Kwon, O., and Lin, E.C. (2001) Quinones as the redox signal for the arc two-component system of bacteria. *Science* **292**: 2314-2316.

Govan, J.R., and Deretic, V. (1996) Microbial pathogenesis in cystic fibrosis: mucoid *Pseudomonas aeruginosa* and *Burkholderia cepacia*. *Microbiol Rev* **60**: 539-574.

Grinberg, I., Shteinberg, T., Gorovitz, B., Aharonowitz, Y., Cohen, G., and Borovok, I. (2006) The Streptomyces NrdR transcriptional regulator is a Zn ribbon/ATP cone protein that binds to the promoter regions of class Ia and class II ribonucleotide reductase operons. *J Bacteriol* **188**: 7635-7644.

Guest, J.R. (1992) Oxygen-regulated gene expression in *Escherichia coli*. The 1992 Marjory Stephenson Prize Lecture. *J Gen Microbiol* **138**: 2253-2263.

He, G., Shankar, R.A., Chzhan, M., Samouilov, A., Kuppusamy, P., and Zweier, J.L. (1999) Noninvasive measurement of anatomic structure and intraluminal oxygenation in the gastrointestinal tract of living mice with spatial and spectral EPR imaging. *Proc Natl Acad Sci U S A* **96**: 4586-4591.

Hofer, A., Crona, M., Logan, D.T., and Sjoberg, B.M. (2012) DNA building blocks: keeping control of manufacture. *Crit Rev Biochem Mol Biol* **47**: 50-63.

Hong, C.S., Kuroda, A., Ikeda, T., Takiguchi, N., Ohtake, H., and Kato, J. (2004) The aerotaxis transducer gene *aer*, but not *aer*-2, is transcriptionally regulated by the anaerobic regulator ANR in *Pseudomonas aeruginosa*. *J Biosci Bioeng* **97**: 184-190.

Jones, S.A., Chowdhury, F.Z., Fabich, A.J., Anderson, A., Schreiner, D.M., House, A.L. et al. (2007) Respiration of *Escherichia coli* in the mouse intestine. *Infect Immun* **75**: 4891-4899.

Lyczak, J.B., Cannon, C.L., and Pier, G.B. (2002) Lung infections associated with cystic fibrosis. *Clin Microbiol Rev* **15**: 194-222.

Malpica, R., Franco, B., Rodriguez, C., Kwon, O., and Georgellis, D. (2004) Identification of a quinone-sensitive redox switch in the ArcB sensor kinase. *Proc Natl Acad Sci U S A* **101**: 13318-13323.

Martin, J.E., and Imlay, J.A. (2011) The alternative aerobic ribonucleotide reductase of *Escherichia coli*, NrdEF, is a manganese-dependent enzyme that enables cell replication during periods of iron starvation. *Mol Microbiol* **80**: 319-334.

McKethan, B.L., and Spiro, S. (2013) Cooperative and allosterically controlled nucleotide binding regulates the DNA binding activity of NrdR. *Mol Microbiol* **90**: 278-289.

Mettert, E.L., and Kiley, P.J. (2007) Contributions of [4Fe-4S]-FNR and integration host factor to fnr transcriptional regulation. *J Bacteriol* **189**: 3036-3043.

Monje-Casas, F., Jurado, J., Prieto-Alamo, M.J., Holmgren, A., and Pueyo, C. (2001) Expression analysis of the *nrdHIEF* operon from *Escherichia coli*. Conditions that trigger the transcript level in vivo. *J Biol Chem* **276**: 18031-18037.

Murphy, T.F., Brauer, A.L., Eschberger, K., Lobbins, P., Grove, L., Cai, X., and Sethi, S. (2008) *Pseudomonas aeruginosa* in chronic obstructive pulmonary disease. *Am J Respir Crit Care Med* **177**: 853-860.

Partridge, J.D., Sanguinetti, G., Dibden, D.P., Roberts, R.E., Poole, R.K., and Green, J. (2007) Transition of *Escherichia coli* from aerobic to micro-aerobic conditions involves fast and slow reacting regulatory components. *J Biol Chem* **282**: 11230-11237.

Poole, A.M., Logan, D.T., and Sjoberg, B.M. (2002) The evolution of the ribonucleotide reductases: much ado about oxygen. *J Mol Evol* **55**: 180-196.

Rani, S.A., Pitts, B., Beyenal, H., Veluchamy, R.A., Lewandowski, Z., Davison, W.M. et al. (2007) Spatial patterns of DNA replication, protein synthesis, and oxygen concentration within bacterial biofilms reveal diverse physiological states. *J Bacteriol* **189**: 4223-4233.

Roca, I., Ballana, E., Panosa, A., Torrents, E., and Gibert, I. (2008) Fumarate and nitrate reduction (FNR) dependent activation of the *Escherichia coli* anaerobic ribonucleotide reductase *nrdDG* promoter. *Int Microbiol* **11**: 49-56.

Rolfe, M.D., Ocone, A., Stapleton, M.R., Hall, S., Trotter, E.W., Poole, R.K. et al. (2012) Systems analysis of transcription factor activities in environments with stable and dynamic oxygen concentrations. *Open Biol* **2**: 120091.

Sabra, W., Kim, E.J., and Zeng, A.P. (2002) Physiological responses of *Pseudomonas aeruginosa* PAO1 to oxidative stress in controlled microaerobic and aerobic cultures. *Microbiology* **148**: 3195-3202.

Sawers, R.G. (1991) Identification and molecular characterization of a transcriptional regulator from *Pseudomonas aeruginosa* PAO1 exhibiting structural and functional similarity to the FNR protein of *Escherichia coli*. *Mol Microbiol* **5**: 1469-1481.

Schiessl, K.T., Hu, F., Jo, J., Nazia, S.Z., Wang, B., Price-Whelan, A. et al. (2019) Phenazine production promotes antibiotic tolerance and metabolic heterogeneity in Pseudomonas aeruginosa biofilms. *Nat Commun* **10**: 762.

Schobert, M., and Jahn, D. (2010) Anaerobic physiology of *Pseudomonas aeruginosa* in the cystic fibrosis lung. *Int J Med Microbiol* **300**: 549-556.

Shalel-Levanon, S., San, K.Y., and Bennett, G.N. (2005) Effect of ArcA and FNR on the expression of genes related to the oxygen regulation and the glycolysis pathway in *Escherichia coli* under microaerobic growth conditions. *Biotechnol Bioeng* **92**: 147-159.

Sjoberg, B.M., and Torrents, E. (2011) Shift in ribonucleotide reductase gene expression in *Pseudomonas aeruginosa* during infection. *Infect Immun* **79**: 2663-2669.

Stewart, P.S. (2003) Diffusion in biofilms. *J Bacteriol* **185**: 1485-1491.

Stewart, P.S., and Franklin, M.J. (2008) Physiological heterogeneity in biofilms. *Nat Rev Microbiol* **6**: 199-210.

Tata, M., Wolfinger, M.T., Amman, F., Roschanski, N., Dotsch, A., Sonnleitner, E. et al. (2016) RNASeq Based Transcriptional Profiling of *Pseudomonas aeruginosa* PA14 after Short- and Long-Term Anoxic Cultivation in Synthetic Cystic Fibrosis Sputum Medium. *PLoS One* **11**: e0147811.

Tenaillon, O., Skurnik, D., Picard, B., and Denamur, E. (2010) The population genetics of commensal *Escherichia coli*. *Nat Rev Microbiol* **8**: 207-217.

Torrents, E. (2014) Ribonucleotide reductases: essential enzymes for bacterial life. *Front Cell Infect Microbiol* **4**: 52.

Torrents, E., Grinberg, I., Gorovitz-Harris, B., Lundstrom, H., Borovok, I., Aharonowitz, Y. et al. (2007) NrdR controls differential expression of the Escherichia coli ribonucleotide reductase genes. *J Bacteriol* **189**: 5012-5021.

Trunk, K., Benkert, B., Quack, N., Munch, R., Scheer, M., Garbe, J. et al. (2010) Anaerobic adaptation in *Pseudomonas aeruginosa*: definition of the Anr and Dnr regulons. *Environ Microbiol* **12**: 1719-1733.

Tseng, C.P., Albrecht, J., and Gunsalus, R.P. (1996) Effect of microaerophilic cell growth conditions on expression of the aerobic (*cyoABCDE* and *cydAB*) and anaerobic (*narGHJI*, *frdABCD*, and *dmsABC*) respiratory pathway genes in *Escherichia coli*. *J Bacteriol* **178**: 1094-1098.

Tsien, R.Y. (1998) The green fluorescent protein. *Annu Rev Biochem* **67**: 509-544.

Tuggle, C.K., and Fuchs, J.A. (1986) Regulation of the operon encoding ribonucleotide reductase in *Escherichia coli*: evidence for both positive and negative control. *EMBO J* **5**: 1077-1085.

Unden, G., Becker, S., Bongaerts, J., Schirawski, J., and Six, S. (1994) Oxygen regulated gene expression in facultatively anaerobic bacteria. *Antonie Van Leeuwenhoek* **66**: 3-22.

Unden, G., Becker, S., Bongaerts, J., Holighaus, G., Schirawski, J., and Six, S. (1995) O2-sensing and O2-dependent gene regulation in facultatively anaerobic bacteria. *Arch Microbiol* **164**: 81-90.

Worlitzsch, D., Tarran, R., Ulrich, M., Schwab, U., Cekici, A., Meyer, K.C. et al. (2002) Effects of reduced mucus oxygen concentration in airway *Pseudomonas* infections of cystic fibrosis patients. *J Clin Invest* **109**: 317-325.

Xu, K.D., Stewart, P.S., Xia, F., Huang, C.T., and McFeters, G.A. (1998) Spatial physiological heterogeneity in *Pseudomonas aeruginosa* biofilm is determined by oxygen availability. *Appl Environ Microbiol* **64**: 4035-4039.

Yoon, M.Y., Lee, K.M., Park, Y., and Yoon, S.S. (2011) Contribution of cell elongation to the biofilm formation of *Pseudomonas aeruginosa* during anaerobic respiration. *PLoS One* **6**: e16105.

Zumft, W.G. (1997) Cell biology and molecular basis of denitrification. *Microbiol Mol Biol Rev* **61**: 533-616.

A5 Supporting information

Gradual adaptation of facultative anaerobic pathogens to microaerobic and anaerobic conditions

Supporting Information Fig. A5:S1. Oxygen concentration in the liquid phase under AnaeroTrans conditions.

Control charts of AnaeroTrans experiments with *P. aeruginosa* PAO1 (**A**) or *E. coli* K-12 *substr*. MG1655 (**B**) at an air flow rate of 180 ml min^{-1}. Biomass (OD_{600}) is represented in orange, dissolved oxygen (DO) is represented in blue (mg l^{-1}) and oxygen consumption rate (mg l^{-1} h^{-1}) is represented in green.

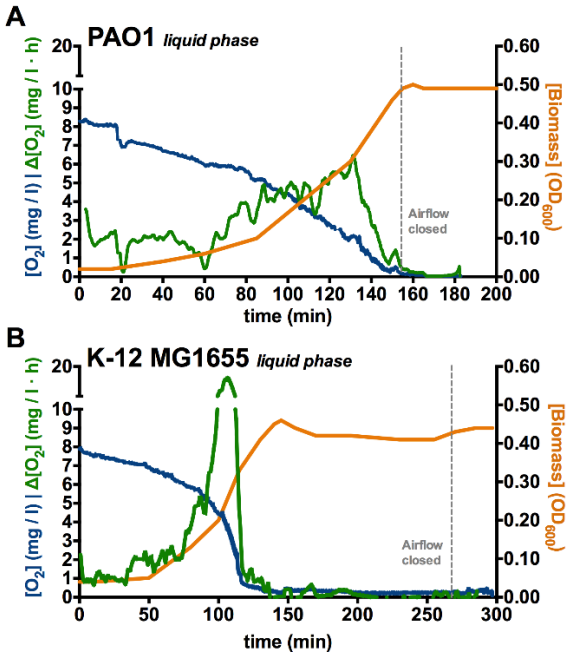

Supporting Information Fig. A5:S2. Fluorescence microscopy images of AnaeroTrans samples and controls.

A-B, Fluorescence microscopy images of LIVE/DEAD viability staining in *P. aeruginosa* PAO1 (**A**) or *E. coli* K-12 *substr*. MG1655 (**B**). Control samples are labeled in black and were obtained from *in vitro* aerobic cultures ("Aero."), anaerobic cultures in Hungate tubes ("Anaero.") or anaerobic pulse studies, which were injected in a Hungate tube and incubated for two hours before sampling ("Anaero. pulse"). All K-12 samples were grown in LB medium. All PAO1 samples were grown in LBN medium (LB + KNO_3) except for the "Aero. LB" control. Three images per sample (from a total group of ten to fifteen per sample) are displayed. The percentage of red "dead" cells in the complete set is provided in the *average ± standard deviation* format. The scale bar represents 10 µM. **C**, percentage of dead cells depending on the concentration of oxygen in the gas phase of standard AnaeroTrans experiments (see Fig. A5:2A and Fig. A5:3A).

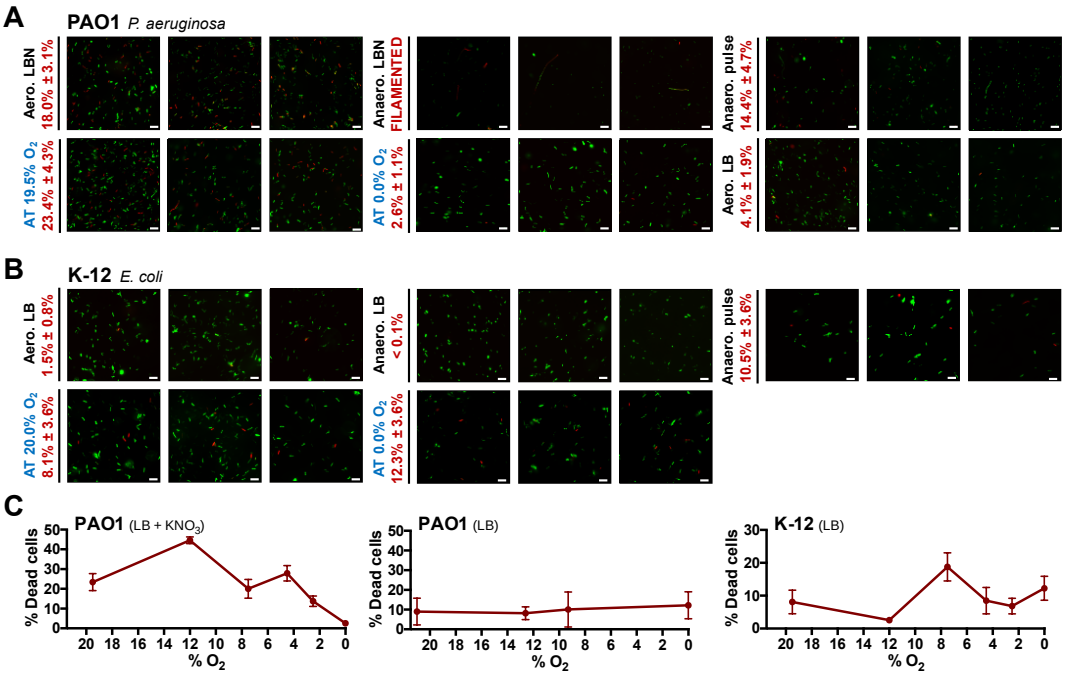

Supporting Information Fig. A5:S3. Additional AnaeroTrans control charts

A, C, D, E, Control charts of additional AnaeroTrans experiments, representative of two repetitions per strain, for *P. aeruginosa* PAO1 grown in LB medium instead of LBN (**A**), PAO1 isogenic mutant strains Δ*nrdR* (**C**), Δ*anr* and Δ*dnr* (**D**), and *E. coli* K-12 *substr*. MG1655 isogenic mutant strain Δ*fnr* (**E**). Biomass (OD_{600}) is represented in orange, oxygen concentration (O_2% v/v) in blue, and oxygen consumption rate (ΔO_2 h^{-1}) in green. Sampling points are indicated by red bars. **B,** estimated doubling time of *P. aeruginosa* PAO1 grown in LB medium (black), compared to values obtained in LBN medium (green). Doubling time is represented in minutes, depending on the oxygen concentration in the gas phase (% O_2 v/v).

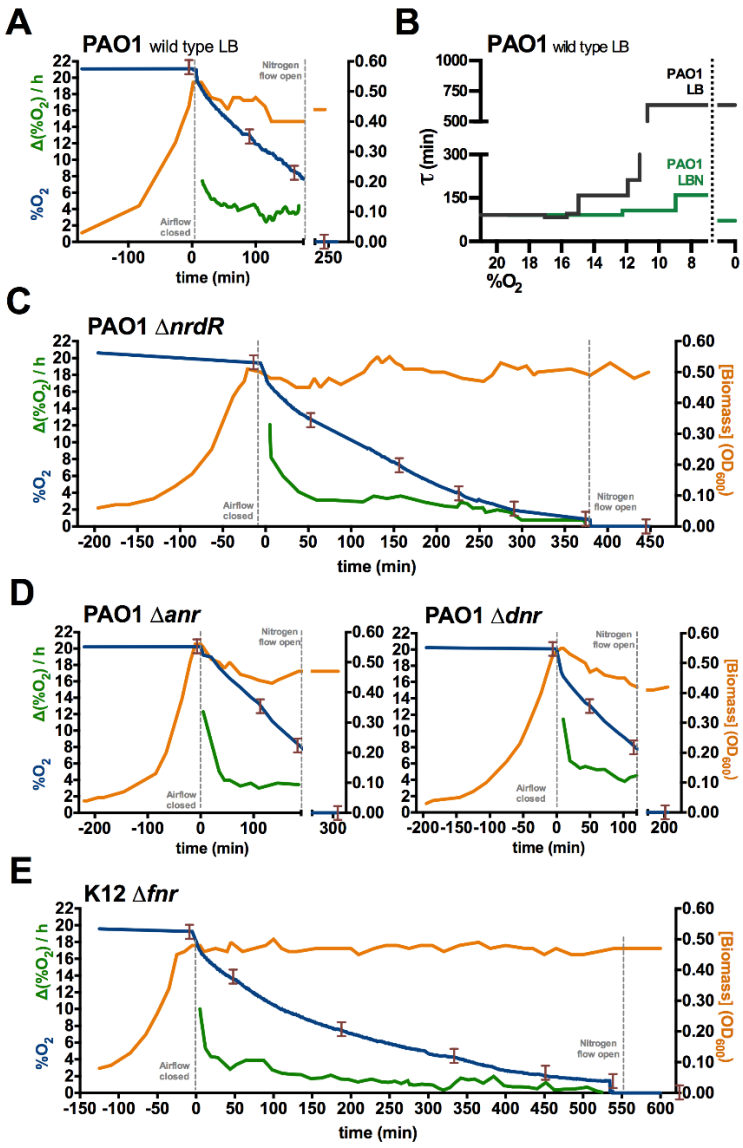

Supporting Information Fig. A5:S4. Effect of nitrogen purging and long anaerobic incubation in AnaeroTrans.

AnaeroTrans experiments conducted using in-place nitrogen-purged inlet media. Samples were obtained after reaching asymptotical oxygen concentration values (Anaero), immediately after eliminating the remaining oxygen in the gas-phase with nitrogen (N_2), and after one and five hours of incubation with nitrogen bubbling (N_2 + 1 h / 5 h). The experiments were conducted with *P. aeruginosa* PAO1 (left) and *E. coli* K-12 *substr*. MG1655 (right). Fold-change is determined compared to the first aerobic sample of each experiment. Error bars represent positive standard deviation.

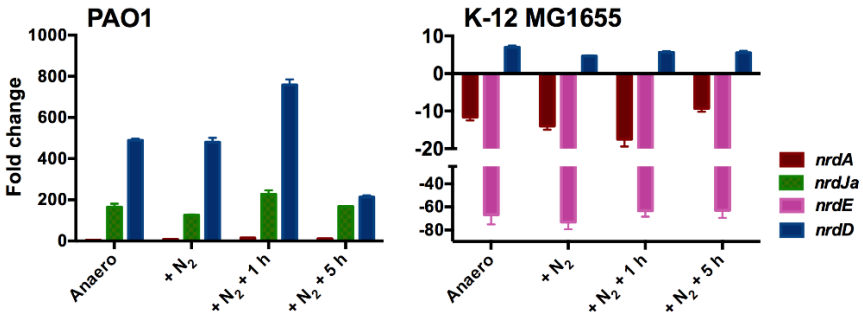

Supporting Information Fig. A5:S5. Reproducibility of AnaeroTrans gene expression profiles.

Examples of replicates for the gene expression profiles shown in Figure 4, obtained from independent AnaeroTrans experiments and qRT-PCR quantifications. Fold-change (each sample compared to the first aerobic measurement) of *nrd* genes of *P. aeruginosa* PAO1 (**A**), *E. coli* K-12 *substr* MG1655 (**B**) and *E. coli* O157:H7 (**C**). Error bars represent standard deviation.

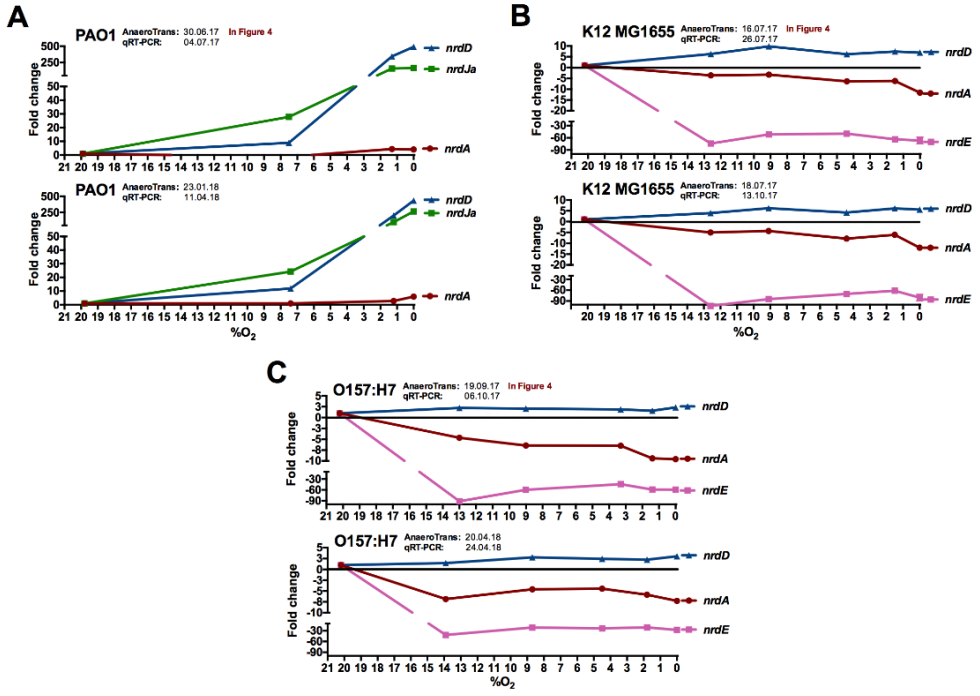

Supporting Information Fig. A5:S6. Aerobic expression level of the studied genes.

Fold-change of all studied genes compared to *gapA* in *P. aeruginosa* PAO1 (**A**), and *E. coli* K-12 *substr.* MG1655 (**B**) measured under aerobic conditions. Error bars represent standard deviation.

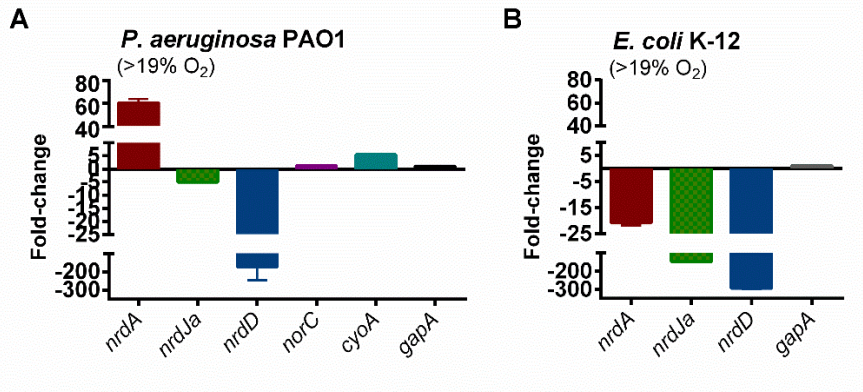

Supporting Information Fig. A5:S7. Expression of the anaerobiosis regulators throughout the oxygen gradients.

Fold-change (each sample compared to the first aerobic measurement) of genes encoding the master regulators of anaerobiosis of *P. aeruginosa* PAO1 (**A**) and *E. coli* K-12 *substr*. MG1655 (**B**). Along with the *anr* and *dnr* genes in PAO1, we included the closely related *narL* gene of the NarXL two-component system. Likewise, we included *arcA* of the ArcBA two-component system of K-12. Error bars represent standard deviation.

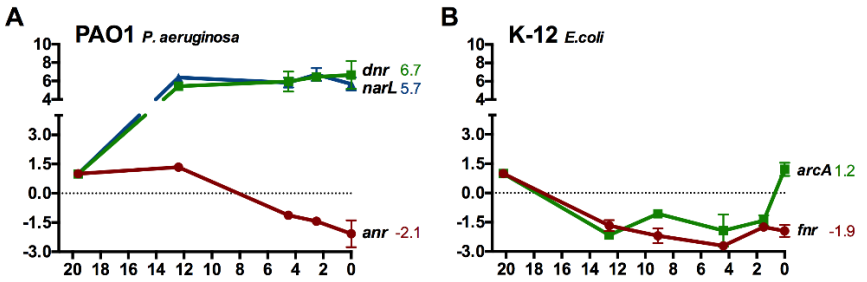

Supporting Information Table A5:S1. Strains and plasmids used in this study

Strains and plasmids are listed with simplified, self-explanatory names (referred to as…), which are commonly used in the text. For strains, a detailed genotype is also provided.

Item	Referred to as	(Strain) Genotype	Description	Source
Strains				
PAO1	PAO1 (WT)	Wild-type (ATCC® 15692 / CECT 4122)	Wild-type *P. aeruginosa* lab strain	ATCC
PW1967	PAO1 Δ*dnr*	*P. aeruginosa* PAO1 *dnr*::IS*lacZ*/hah; Tc^R	PAO1 isogenic *dnr* deletion mutant	(1)
PW3874	PAO1 Δ*anr*	*P. aeruginosa* PAO1 *anr*::IS*lacZ*/hah; Tc^R	PAO1 isogenic *anr* deletion mutant	(1)
PW7854	PAO1 Δ*nrdR*	*P. aeruginosa* PAO1 *nrdR*::IS*lacZ*/hah; Tc^R	PAO1 isogenic *nrdR* deletion mutant	(1)
PAET1	PAET1	Wild-type	CF strain isolated from chronic patient	(2)
K-12	K12 MG1655	$F^- \lambda^- ilvG^-$ *rfb*-50 *rph*-1 (ATCC 700926)	Wild-type *E. coli* lab strain	Laboratory stock
B6914-MS1	O157:H7	Serotype O157:H7 (ATCC® 43888 / CDC B6914-MS1)	O157:H7 EPEC, does not produce Shiga-like toxin I/II	ATCC
JW1328	K12 Δ*fnr*	F^-, Δ(*araD-araB*)567, Δ*lacZ*4787(::*rrnB*-3) λ^- Δ*fnr*-771::kan *rph*-1, Δ(*rhaD-rhaB*)568 *hsdR*514	K12 isogenic *fnr* deletion mutant	(3)
Plasmids				
pETS130-GFP	pETS130		Broad host range, promoterless GFP; Gm^R	(4)
pETS134	pETS-P*nrdA*		pETS130 derivative carrying *nrdA* promoter	(4)
pETS180	pETS-P*nrdJ*		pETS130 derivative carrying *nrdJa* promoter	(5)
pETS136	pETS-P*nrdD*		pETS130 derivative carrying *nrdD* promoter	(4)

1. Jacobs MA, Alwood A, Thaipisuttikul I, Spencer D, Haugen E, Ernst S, et al. Comprehensive transposon mutant library of *Pseudomonas aeruginosa*. Proceedings of the National Academy of Sciences of the United States of America. 2003;100(24):14339-44.

2. Crespo A, Gavalda J, Julian E, Torrents E. A single point mutation in class III ribonucleotide reductase promoter renders *Pseudomonas aeruginosa* PAO1 inefficient for anaerobic growth and infection. Scientific reports. 2017;7(1):13350.

3. Baba T, Ara T, Hasegawa M, Takai Y, Okumura Y, Baba M, et al. Construction of Escherichia coli K-12 in-frame, single-gene knockout mutants: the Keio collection. Molecular systems biology. 2006;2:2006 0008.

4. Sjoberg BM, Torrents E. Shift in ribonucleotide reductase gene expression in *Pseudomonas aeruginosa* during infection. Infection and immunity. 2011;79(7):2663-9.

5. Crespo A, Pedraz L, Torrents E. Function of the *Pseudomonas aeruginosa* NrdR Transcription Factor: Global Transcriptomic Analysis and Its Role on Ribonucleotide Reductase Gene Expression. PloS one. 2015;10(4):e0123571.

Supporting Information Table A5:S2. PCR primers used in this study

Number	Name	Sequence (5'-3')	Application
1	qRT_PAO-norC_fw	AGGGCTTCAACACCTTCCTC	qRT-PCR; *P. aeruginosa* control genes
2	qRT_PAO-norC_rv	CCTCGCTGAGATGGAACTGC	qRT-PCR; *P. aeruginosa* control genes
3	qRT_PAO-norC-rt	TCAACCCTCCTTGTTCGGC	qRT-PCR; *P. aeruginosa* control genes; technical test
4	qRT_PAO-cyoA_fw	CCAGATCACCTCGGATTCGG	qRT-PCR; *P. aeruginosa* control genes
5	qRT_PAO-cyoA_rv	TCAGGTGCAGCTTGGTCATC	qRT-PCR; *P. aeruginosa* control genes
6	qRT_PAO-cyoA-rt	GAAGCCCTGCTCGGAGG	qRT-PCR; *P. aeruginosa* control genes; technical test
7	qRT_PAO-nrdA_fw	ACCTGGAGAAACTGGGCAAG	qRT-PCR; *P. aeruginosa* RNR genes
8	qRT_PAO-nrdA_rv	TGTGGATGAAGTAGCGGTCG	qRT-PCR; *P. aeruginosa* RNR genes
9	qRT_PAO-nrdJ_fw	CGAATTCATCCGCGCCAAG	qRT-PCR; *P. aeruginosa* RNR genes
10	qRT_PAO-nrdJ_rv	TCCACCGCCTGCATGAAC	qRT-PCR; *P. aeruginosa* RNR genes
11	qRT_PAO-nrdD_fw	TTGCTGAACGAAGGCCTGAA	qRT-PCR; *P. aeruginosa* RNR genes
12	qRT_PAO-nrdD_rv	TGCCGAGGAAGTTGACCATC	qRT-PCR; *P. aeruginosa* RNR genes
13	qRT_PAO-gapA_fw	CCTCCCATCGGATCGTCTC	qRT-PCR; *P. aeruginosa* RNR genes
14	qRT_PAO-gapA_rv	GGTCATCAGGCCGTGCTC	qRT-PCR; *P. aeruginosa* RNR genes
15	qRT_PAO-anr_fw	GGAAGACATGGATTCGCTGG	qRT-PCR; *P. aeruginosa* anaerobic reg. genes
16	qRT_PAO-anr_rv	GCAAAGACCGAGCCGAAAG	qRT-PCR; *P. aeruginosa* anaerobic reg. genes
17	qRT_PAO-dnr_fw	CGCACGCCTTCTACTACCTG	qRT-PCR; *P. aeruginosa* anaerobic reg. genes
18	qRT_PAO-dnr_rv	GTGTTGCGTTCGTTGGTCAC	qRT-PCR; *P. aeruginosa* anaerobic reg. genes
19	qRT_PAO-narL_fw	CATGAACGGCCTGGACACC	qRT-PCR; *P. aeruginosa* anaerobic reg. genes
20	qRT_PAO-narL_rv	GACCACGTCGCCCTTGTC	qRT-PCR; *P. aeruginosa* anaerobic reg. genes
21	qRT_PAO-aer_fw	CGTCAAGAACCGCTGCAAG	qRT-PCR; *P. aeruginosa* anaerobic reg. genes
22	qRT_PAO-aer_rv	TTGACCCGCACCGACTC	qRT-PCR; *P. aeruginosa* anaerobic reg. genes
23	qRT_ECO-nrdA_fw	GTGTGAAAGCCGTTGAGCTG	qRT-PCR; *E. coli* RNR genes
24	qRT_ECO-nrdA_rv	ACGGGCTATGGGTATTGCAG	qRT-PCR; *E. coli* RNR genes
25	qRT_ECO-nrdE_fw	CCCGATATTCTGCGTTTTCTCG	qRT-PCR; *E. coli* RNR genes
26	qRT_ECO-nrdE_rv	ATATCCGGGATCACCACGC	qRT-PCR; *E. coli* RNR genes
27	qRT_ECO-nrdD_fw	ATGGTCGTAACAACCTCGGC	qRT-PCR; *E. coli* RNR genes
28	qRT_ECO-nrdD_rv	ACCAGACGTTCATCCAGCAG	qRT-PCR; *E. coli* RNR genes
29	qRT_ECO-gapA_fw	TCCGGCTAACCTGAAATGGG	qRT-PCR; *E. coli* RNR genes
30	qRT_ECO-gapA_rv	GCGGTGATGTGTTTACGAGC	qRT-PCR; *E. coli* RNR genes
31	qRT_ECO-arcA_fw	TGTTGCGTTGATGTTCCTGAC	qRT-PCR; *E. coli* anaerobic reg. genes
32	qRT_ECO-arcA_rv	CGGGTTGAACGGTTTGGTG	qRT-PCR; *E. coli* anaerobic reg. genes
33	qRT_ECO-fnr_fw	ATTGCCAGGATTGCAGCATC	qRT-PCR; *E. coli* anaerobic reg. genes
34	qRT_ECO-fnr_rv	ATAGGCTTCTTCCGCTCAATG	qRT-PCR; *E. coli* anaerobic reg. genes

Discussion

The articles presented in the "Results" section addressed different aspects of the regulation of ribonucleotide reductases (RNRs) expression in *Escherichia coli* and *Pseudomonas aeruginosa*. These two species are facultative anaerobic pathogens, and thus require complex regulatory machinery to adapt their metabolism to different oxygenation conditions, different nutrient sources, host defense mechanisms, etc. The adaptation of the RNR network is no exception. In this section, we divided the discussion of the results into three blocks corresponding to three global aspects of the RNR regulation. The first one corresponds to the AlgZR two-component system, specific of *P. aeruginosa*, and strongly related to surface colonization, biofilm formation and chronification, being the main regulator of the mucoid phenotype. Block two corresponds to NrdR, the master regulator of ribonucleotide reduction, the molecular mechanism of which is addressed for the first time in this work. Finally, block three corresponds to microaerobic and anaerobic regulation, with a special focus on the oxygen gradients formed in the biofilm structure and the aerobic-anaerobic transition, which is crucial for infection in facultative anaerobic pathogens.

The discussion presented here addresses only the most important results and the reasoning behind the general conclusions of this thesis; consult the discussion section of each article for more detail.

The AlgZR two-component system and its effects on the RNR network

Article 1, titled "*Regulation of ribonucleotide synthesis by the Pseudomonas aeruginosa AlgR two-component system*"[185] is focused on the effects the AlgZR two-component systems presents on the RNR network in *P. aeruginosa*.

Although this system is mainly associated to alginate production[189, 190], it has also been associated to many other pathways, mostly related to biofilm formation and chronic infection[10], including type IV pili formation, rhamnolipid biosynthesis, type III secretion, and several aspects of anaerobic metabolism. Two studies aimed toward studying the global AlgR regulon through high throughput techniques, one published in 2004 by *Lizewski et al.*[52] using DNA microarray analysis and a second one published in 2015 by *Kong et al*.[57] using ChIP-seq, indicated that RNR gene transcription might also be regulated by AlgR.

For that reason, our first step was to confirm if there were indeed elements of the RNR network controlled by AlgZR. While class II RNR genes *nrdJa* and *nrdJb* had been detected as putative AlgR-regulated genes[52], the association to class Ia RNR was due to the detection of a ChIP-seq read mapping to the intergenic region between class Ia RNR operon *nrdAB* and the neighboring gene PA1157[57]. As seen in **Figure A1:1**, we demonstrated that both class I and class II RNR operons were regulated by AlgR, and not PA1157. As expected, class III RNR was demonstrated to not be regulated by AlgR under the conditions studied.

To identify the location of the AlgR-boxes, we designed an optimized bioinformatical search: AlgR regulated genes include *weak* and *strong* binders[10], and we used several consensus sequences to address both, as detailed in **Figure A1:2** and **Supplementary Fig A1:S1**. Using the bioinformatical search to identify candidates, and then both GFP-based gene reporter assays and EMSAs to confirm them, we established that the AlgR regulation of RNR operon occurred via its binding to one single AlgR-box in P*nrdA*, located in position -545 (facing *backward*, that is, the consensus sequence as commonly defined fits in a 3'-5' orientation relative to the sense strand of *nrdAB*), and two AlgR-boxes in P*nrdJ,* located in positions -299 and -128. All positions are measured from the center of the binding site, and relative to the ATG codons of *nrdAB* and *nrdJab*. The location of the P*nrdA* AlgR-box is less anomalous than it looks at first glance: it is the combined results of the *nrdA* messenger RNA having a well-described long 5' untranslated region[90] and AlgR boxes being commonly placed a long distance upstream of the transcription start site, so that it has been hypothesized that AlgR might interact with the base promoter through DNA bending[10]; furthermore, although most AlgR-regulated genes, as happens for other members of the AgrA family, present more than one binding site[10], other AlgR regulated genes controlled by a single box have been described (*rhlA*, *rhlI*, *hcnA*), and AlgR-boxes have been described in either orientation (see **Supplementary Figure A1:S3**). The DNA bending effect was demonstrated using Atomic Force Microscopy (AFM) imaging of the DNA-protein complexes (**Figure A1:4**), in which constitutes, to the best of our knowledge, the first demonstration of this long-hypothesized phenomenon.

As a member of a two-component system, AlgR is phosphorylated by the membrane-bound kinase AlgZ (FimS), which responds to a still unknown environmental signal[49, 56]. As described in the Introduction to Article 1, AlgR commonly appears in the cell as low levels of a phosphorylatable protein, but during the mucoid phenotype switches to much higher levels of non-phosphorylated AlgR[10]. To explore if RNR genes are regulated by phosphorylated or non-phosphorylated AlgR and address the biological role of this regulation, we used a series of GFP-based gene reporter assays in different models of *P. aeruginosa* growth (planktonic culture, surface colonization, and static biofilm formation), including complementation of the Δ*algR* mutant strain with a non-phosphorylatable AlgR variant named AlgR D54N[190], as well as with wild-type AlgR.

The interpretation of the planktonic culture results (**Figures A1:1** and **A1:3**), surface colonization results (**Figure A1:5**), and static biofilm results (**Figure A1:6**) considers the difference between phosphorylated and non-phosphorylated AlgR, as well as the effect of individual AlgR boxes, analyzed via a series of point mutations. In summary, the P*nrdA* AlgR-box was demonstrated to be responsible for the activation of class Ia RNR, as well as being especially sensitive to phosphorylated AlgR; the same effect is observed for P*nrdJ* AlgR-box2. In **Figure A1:7** we associated this positive regulation to a very well-known but previously unexplained effect, the induction of RNR expression via oxidative stress[8, 137, 186]. On the other hand, P*nrdJ* AlgR-box1 was demonstrated to be responsible for class II RNR repression and associated with the specific repression of this RNR class observed in the mucoid phenotype. A

detailed discussion of these results and a model of how these new regulation events fit in the AlgZR regulon and the life cycle of *P. aeruginosa* can be found in the Discussion for Article 1 and **Figure A1:8**.

NrdR, a master regulator of ribonucleotide reductases

The next two articles are focused on the transcription factor NrdR, the bacteria-specific global repressor of the RNR network. **Article 2**, titled "Function of the *Pseudomonas aeruginosa NrdR transcription factor: global transcriptomic analysis and its role on ribonucleotide reductase gene expression*"[187] mainly addresses the general role of NrdR in *P. aeruginosa*, as it had already been described for *E. coli* or *S. coelicolor*. **Article 3**, titled "*Mechanism of action of NrdR, a global regulator of ribonucleotide reduction*" is a comprehensive study of the molecular mechanism of action of NrdR conducted in both *E. coli* and *P. aeruginosa*.

The first characterization of NrdR in *S. coelicolor*[128, 172] described this protein as composed by a Zn-finger DNA binding domain (an atypical rubredoxin-like Zn-ribbon module) and a nucleotide-binding ATP-cone domain, similar to the overall activity allosteric site present in most class I and class III RNRs[178, 180]. These findings served to *hypothesize* NrdR to be a nucleotide-sensitive transcription factor controlling the expression of ribonucleotide reductases. Later, the description of the NrdR-box and the global search for *nrdR* and NrdR-boxes in all domains of life[9] served to demonstrate that NrdR was encoded by almost all bacterial species, while being completely absent in *Eukarya* and *Archaea*, and to understand that all RNR classes encoded by a particular bacterial species are regulated by NrdR (thus implying its function to be universal). It also became noticeable that NrdR-boxes appear as pairs separated by an integer number of turns in the DNA helix, which was interpreted as this transcription factor requiring protein-protein interactions for its mechanism, and that these pairs overlap the basal promoter of the RNR operons (thus portraying NrdR a repressor).

All these claims have been since then tested and verified in different bacterial species, such as *S. coelicolor*[128, 172, 178], *Escherichia coli*[133], *Salmonella typhimurium*[181], *Chlamydia trachomatis*[182], *Streptococcus pyogenes*[183], and *Bacillus subtilis*[184]. Our first efforts were aimed towards extending this knowledge to *P. aeruginosa*.

In this species, *nrdR* is encoded in a *nrdR-ribD* operon (**Figure A2:1**), and, as expected, acts as a repressor of all three RNR classes (classes Ia, II and III), which we characterized at a transcription level by gene reporter assays and qRT-PCR, but also at a functional level measuring dNTP concentrations in the cells (**Figure A2:3**). This repression can be attributed to the same NrdR-boxes predicted by *Rodionov et al.*[9] (**Supplementary Figure A2:S3**) in 2005. Surprisingly, the expression of the *P. aeruginosa nrdR*, although detectable under all conditions tested, is induced under anaerobiosis (**Figure A2:1**). We identified that this activation was caused by the NarXL system, a two-component system mostly associated with the activation of denitrification during anaerobic growth in *P. aeruginosa*[36], but also known to take part in many aspects of the adaptation of this species to anaerobic conditions. NarL

activates the transcription of *nrdR* via its binding to two binding sites located in positions -37 and -15 in the P*nrdR* promoter (measured from the center of the binding site, and relative to the ATG of *nrdR*) (**Figure A2:2**). Although the effect of NarL on *nrdR* transcription in the absence of substrates for denitrification was never tested, as the anaerobic regulation mediated by NarXL occurs via the phosphorylation of NarL upon detection of nitrate[36] we can assume that *nrdR* transcription is activated anaerobically by phosphorylated NarL.

Another remarkable peculiarity of the NrdR regulon in *P. aeruginosa* can be observed in **Figure A2:3**: while all RNR classes are sensitive to NrdR repression, the anaerobically active class II and class III RNRs are repressed the most (in relative terms) under aerobic conditions, while its repression becomes mostly unnoticeable under anaerobiosis. Differences in the way NrdR represses distinct RNR classes can be attributed to variable NrdR-box placement, as well as to the possible interaction between NrdR and other transcription factors. This include Dnr, which activates class II RNR transcription under anaerobic conditions (**Figure A4:3**, see Article 4[188]), AlgR, which can activate or repress class II RNR transcription depending on environmental conditions (**Figure A1:8**, see Article 1[185]), or Anr, which is responsible for the anaerobic activation of class III RNR[191]. However, it remains puzzling to explain a potential biological role for this differential repression mechanism, detailed in **Figure A2:7**. It could be assumed that, as *nrdR* expression is induced anaerobically but class II and class III RNRs are less sensitive to its effects, repressing class Ia could be its main role under this condition. However, it must be noticed that class Ia RNR in *P. aeruginosa* does not suffer a significant anaerobic repression (**Figure A5:4**, see Article 5).

In *P. aeruginosa*, NrdR is also responsible for the transcriptional activation of the DNA topoisomerase I gene *topA*, which we proved using GFP-based gene reporter assays, as well as functionally by detecting differences in DNA topology in the *nrdR* mutant strain (**Figure A2:4**). This was first suggested in the original description of the NrdR-box[9], when one single NrdR box was identified in promoter P*topA*, in position -75 (measured from the center of the binding site, relative to the ATG of *topA*). Beyond the importance of this particular regulatory event, this finding is relevant as a demonstration that NrdR can regulate other genes via a completely different mechanism to the established one.

A global search for NrdR-boxes conducted in promoter-enriched DNA queries of the genomes of *E. coli* and *P. aeruginosa* revealed a large number of potential NrdR binding sites, with a total of 113 hits and 33 hits, respectively (**Figure A3:1**, **Supplementary Tables A3:S2** and **A3:S3**). However, given the large number of sequences analyzed, it can be assumed that most of these hits may be false positives. To distinguish which of these hits may correspond to real NrdR-regulated operons, the NrdR-box search results were correlated with general transcriptomics data exploring the comparison of *nrdR* mutant strains with its isogenic wild-type strains, obtained by DNA microarray analysis and RNA-seq. These data (*P. aeruginosa* DNA microarray, **Figure A2:5**, **Table A2: 2**, **Supplementary Figures A2:S4** and **A2:S5**, **Supplementary Tables A2:S2** and **A2:S3**; *P. aeruginosa* RNA-seq, **Supplementary Tables A3:S4** and

A3:S5; *E. coli* DNA microarray[192], **Supplementary Tables A3:S6** and **A3:S7**) also produce a significant number of differentially expressed genes, of which we can assume most may be false positive or the result of indirect effect. However, the correlation data (**Figure A3:1**) reveals a surprising result: out of all genes in *P. aeruginosa* PAO1 (5570 genes) and *E. coli* K-12 *substr.* MG1655 (4705 genes), only the ribonucleotide reductase genes are simultaneously differentially expressed in a *nrdR* mutant strain (by DNA microarray analysis or RNA-seq) and exhibit potential NrdR-boxes in their promoter regions. This result should not be understood as that NrdR only regulates RNR genes, but as a demonstration that the mechanism we know, in which NrdR represses gene expression under any physiological conditions via its binding to pairs of NrdR-boxes, is limited to ribonucleotide reductases. This last interpretation is further supported by the NrdR-mediated activation of *topA* described above (**Figure A2:4**, see Article 2).

To study the molecular mechanism of action of NrdR, one of the main challenges to overcome is the obtention of a recombinant NrdR protein with enough purity and activity to use in *in vitro* experiments, as mentioned by different studies addressing NrdR oligomerization and functionality[133, 172, 177, 182]. To overcome this issue, we designed a series of NrdR fusion proteins (**Figure A3:2**, **Supplementary Figure A3:S1**), which take advantage of the stabilization and solubilization effects of the SUMO tag[193, 194], together with different tag to assist purification, and use SUMO or TEV proteases[194, 195] to eliminate this added elements and recover untagged NrdR with only a small N-terminal linker peptide.

Using these proteins, we conducted a series of experiments (Size-Exclusion Chromatography and SEC-MALS) (**Figure A3:3**, **Table A3:1**, **Supplementary Figures A3:3** and **A3:4**, **Supplementary Table A3:S8**) aimed toward exploring the oligomerization state of NrdR depending on the nucleotide co-factor bound to it. The ATP-cone domain present in ribonucleotide reductase enzymes controls the overall enzymatic activity by affecting the quaternary structure of the protein complex[118, 180], and, thus, a similar mechanism can be expected for this domain in NrdR. Later experiments were focused on explaining the physiological role of these oligomeric forms using EMSA experiments to study their DNA-binding capabilities and *in vitro* transcription to study their functional effect in the repression of RNA transcription (**Figures A3:4** and **A3:5**, **Supplementary Figures A3:S5** and **A3:S6**). In summary, the results obtained demonstrated that NrdR from both *E. coli* and *P. aeruginosa*, given the broad shape of its SEC peaks, the range of absolute molar masses determined by MALS, and its polydispersity indexes, does not exist as stable protein complexes with defined stoichiometry, but rather as a dynamic populations of nucleotide-dependent oligomeric forms, which agrees with previous observations[172, 177]. When dATP is bound to NrdR, controlled protein-protein interactions occur and the most represented NrdR oligomeric form detected is the hexamer, which presents maximum activity in both DNA-binding and RNR repression. On the other hand, when ATP is bound to NrdR, intensive oligomerization occurs, and oligomeric forms such as 10-mers, 12-mers and 14-mers are detected, which are functionally inactive. A detailed discussion of these results and a model of the NrdR mechanism of action can be found in **Figure A3:7** and the Discussion for Article 3.

The technique used for *in vitro* transcription experiments was developed for this work. We called it Regulated *in Vitro* Transcription Assay (ReViTA), and it is based on the pReViTA plasmid (**Supplementary Figure A3:S6**), which is used as template for the transcription reactions. This plasmid features two genes whose transcription remains completely independent due to the action of strong, synthetic transcription terminators. The expression of one of these genes is regulated by the desired transcription factor (here, NrdR), while the other gene presents constitutive transcription. Both genes (TEST and CTRL, respectively) are transcribed *in vitro* in the same reaction, and the resulting mRNAs are quantified by qRT-PCR absolute quantitation. TEST copy numbers of each sample are then divided by the CTRL copy numbers as a normalization procedure. Normalized TEST copies can then be used to compare between conditions and study the effect of the transcription factor. This technique was born as an improvement of the *in vitro* transcription experiments conducted by *Case et al.*[182] to study NrdR, and allowed us to demonstrate the nucleotide-dependent RNR repression activity of this protein, but can also be applied to the study of other transcription factors.

Anaerobic regulation of the RNR network

The final two articles are focused on different aspects of anaerobic regulation in facultative anaerobes and their effects on the RNR network. **Article 4**, titled "*Pseudomonas aeruginosa exhibits biofilm formation in the absence of class II and class III ribonucleotide reductases due to hindered anaerobic growth*" addresses the importance of the aerobically active class II and class III RNRs in *P. aeruginosa* during anaerobic growth and biofilm formation, and the regulatory mechanisms responsible for their induction during these conditions. **Article 5**, titled "*Gradual adaptation of facultative anaerobic pathogens to microaerobic and anaerobic conditions*" is focused on the development of a new technique to study the effects that oxygen concentration gradients have on gene expression and its application for reproducing the aerobic-anaerobic transition of *E. coli* and *P. aeruginosa*, as well as the gradual adaptation the ribonucleotide reductase network suffers throughout this transition.

As expected, in *P. aeruginosa*, class II and class III RNRs are of great importance for biofilm formation in both static and continuous-flow biofilm models, as demonstrated by the fact that mutating these RNRs caused a severe reduction in biofilm thickness and biomass (**Figure A4:1**) and alterations in cell morphology throughout the different layers of the biofilm (**Figure A4:2**). The effect is more significant when biofilms are initiated under anaerobic conditions; however, even when the initial conditions are anaerobic, biofilms still contain oxygen gradients, where inner areas are hypoxic or anoxic[5] as described by the reaction-diffusion theory[25].

Class II and class III RNRs are also induced under anaerobic conditions and during biofilm formation (**Table A4:1**). The planktonic-anaerobic versus biofilm comparison demonstrates that class II RNR is further induced in the biofilm by factors not related to anaerobiosis: this effect could be caused by AlgR, whose effect on class II RNR transcription was demonstrated to be independent of the anaerobic

induction (**Figure A1:1**, **Supplementary Figure A1:S4**, see Article 1), but could also be caused by other regulatory elements that are important in the biofilm and have not yet been described to regulate the RNR network, such as quorum sensing systems.

Using GFP-based gene reporter assays, quantitative western blot, and point mutations, we demonstrated that the anaerobic induction of class II RNR is controlled by the anaerobic regulator Dnr, via its binding to a single binding site located at position -21 relative to the ATG of *nrdJa* (**Figures A3:3**, **A3:4**, and **A3:5**). At the moment, we did not explain the anaerobic induction of class III RNR, as we failed to detect any cis element in the P*nrdD* promoter corresponding to anaerobic regulator Anr, Dnr, or NarL. However, a later study in our laboratory, conducted by *Crespo et al*.[191], demonstrated that class III RNR transcription in *P. aeruginosa* is indeed regulated by Anr, but the common laboratory strain *P. aeruginosa* PAO1 harbors a mutation in the corresponding binding site, which renders the strain less effective for anaerobic growth. As discussed later, this mutation is responsible for the delayed activation of class III RNR in PAO1 (**Figure A5:4**, see Article 5).

Both class II and class III RNRs are enzymatically active under anaerobic conditions. However, class II RNRs require 5'deoxyadenosylcobalamin, a derivative of vitamin B_{12}, and the synthesis of this vitamin in *Pseudomonas* occurs only under aerobic conditions[196]. This causes class II RNR to be unable to sustain anaerobic growth of *P. aeruginosa* unless vitamin B_{12} is supplied to the culture (**Supplementary Table A4:S3**). However, in a biofilm, where the surface remains aerobic while inner layers are microaerobic or anaerobic, vitamin B_{12} can be synthesized near the surface and diffuse toward the bottom layers, potentially reaching areas were oxygen has already been depleted. Class II RNR can sustain growth in this area, while class III RNR will be required at even further depth. This model is summarized in **Figure A4:6**.

To further study the gradual adaptation of the ribonucleotide reductase network in this oxygen gradients, isolating this phenomenon from any other effects occurring in the biofilm, we developed a new continuous culture technique named *AnaeroTrans*. This technique takes advantage of a chemostat-like bioreactor designed for this work (**Figure A5:1**), in which a bacterial culture can be kept at a steady state in a gas-tight environment with controlled oxygenation. During an AnaeroTrans experiment, the culture is allowed to grow to the desired growth phase while air bubbling is applied. When the culture has reached a steady state at the desired growth phase, the air bubbling is stopped, and oxygen concentration starts to decrease due to the aerobic respiration performed by the culture itself.

The fact that the changes in oxygenation are driven by self-consumption presents three remarkable advantages compared to systems were the user controls the composition of the gas phase: first, it causes the oxygen consumption profile of the culture to be by itself a valuable source of information. Second, it grants reproducibility, as the same culture in the same experimental setup will always consume oxygen at the same rate, and thus the effects observed at a gene expression level will not

depend on external factors. Second, as the composition of the gas-phase only varies as a result of the slow changes introduced by the culture, and not due to quick changes introduced by the operator, which may not yet take time to be reflected in the physiological state of the culture, it allows for the use of gas-phase oxygen concentration as the state variable to define oxygen availability to the cells. The lack of such a variable is one of the major challenges to overcome in the study of the microaerobic range[17, 197].

The study of the oxygen consumption profiles and bacterial fitness throughout the aerobic-anaerobic transition in *P. aeruginosa* (**Figure A5:2**) and *E. coli* (**Figure A5:3**) provides valuable information concerning the general physiological changes undergone. In summary, *P. aeruginosa* suffers a smooth transition, displaying a gradual decrease in its oxygen consumption rate and no significant reduction of fitness during the first half of the microaerobic range (early microaerobic range, 21% O_2 – 12 % O_2). A significant decrease in fitness is noted during the mid-microaerobic range (12% O_2 – 5 % O_2), which is later recovered for lower oxygen concentration and anaerobiosis. On the other hand, *E. coli* suffers a gradual decrease in growth speed and fitness during the aerobic-anaerobic transition, which is only recovered after a long adaptation period under anaerobic conditions. A strong stepwise adaptation is observed, in which the fully aerobic machinery abruptly transitions to microaerobic systems, causing a reduced oxygen consumption rate that is kept for all the microaerobic range. The underlying changes producing these effects in *P. aeruginosa* and *E. coli* are explained by changes in the most important elements composing the transition: microaerobic adaptation of the aerobic respiration, exemplified by changes in terminal oxidases, anaerobic metabolism (anaerobic respiration or mixed-acid fermentation pathways) and the differential activation of the anaerobic regulators (**Figure A5:6**). A detailed discussion of these results and a model of the aerobic-anaerobic transition in these two facultative anaerobic pathogens can be found in **Figure A5:7** and the Discussion for Article 5.

Concerning the RNR network, *P. aeruginosa* and *E. coli* display remarkably opposite behaviors during the aerobic-anaerobic transition (**Figure A5:4**). *P. aeruginosa* maintains a very low base level of expression of class II and class III RNRs. In the early microaerobic range, a first, moderate induction of these classes occurs; at this level becomes very noticeable the point mutation in the Anr binding box that *P. aeruginosa* PAO1 harbors, as this strain will suffer a delayed activation of class III RNR, which is counterbalanced by a surprising compensatory activation of class II RNR. The exact mechanism behind this adaptation has not been demonstrated, but a decrease in the dNTP pool, followed by NrdR derepression, may explain it (**Figure A3:7**). In the late microaerobic range, *P. aeruginosa* suffers another event of induction of class II and class III RNR expression, reaching anaerobiosis levels. On the other hand, *E. coli* presents a significantly high basal expression level of its anaerobically active class III RNR; thus, the only adaptation the RNR network displays during the aerobic-anaerobic transition is a gradual repression of class Ia and class Ib RNRs (**Figure A5:4**).

A significant information that can be extracted from the results presented in Article 5 is that hybrid metabolism occurs during the aerobic-anaerobic transition for both *E. coli* and *P. aeruginosa*. While this phenomenon has already been described in both species[82, 198], it is still very common among many authors to think of the aerobic-anaerobic transition as a clean switch. Examining the AnaeroTrans data as a whole, it becomes evident that, during most of the microaerobic range, the anaerobic metabolism is already induced, and the anaerobic regulators are already active or even essential, while aerobic respiration is still occurring.

Finally, it is important to remark the effect that the *nrdR* mutation had on the aerobic-anaerobic transition of *P. aeruginosa* (**Figure A5:5**). While the anaerobic induction of class II and class III RNR still occurred, as these are processes independent of NrdR, the gradual pattern of adaptation disappeared completely. This indicates that the native system of gradual activation requires a continuous level of competition with NrdR repression to occur and may provide an explanation for the anaerobic activation of *nrdR* transcription (**Figure A2:2**).

Conclusions

1. The AlgZR two-component system regulates the transcription of class I and class II RNRs in *P. aeruginosa* during planktonic culture, surface colonization and biofilm formation. Class III RNR is not affected by this system.

2. The regulation the AlgZR system of *P. aeruginosa* exerts on class I RNR occurs via the binding of the transcription factor AlgR in a single binding site (AlgR-box) located in the position --545 in promoter P*nrdA,* relative to the ATG of the first gene in the operon. On the other hand, the regulation this system exerts on class II RNR occurs via the binding of the transcription factor AlgR in two AlgR-boxes, namely AlgR-box1 and AlgR-box2, located in positions -299 and -128 in promoter P*nrdJ*, respectively.

3. AlgR is responsible for the well-known activation of class I and class II RNR in *P. aeruginosa* under oxidative stress via its binding to the AlgR-box located in promoter P*nrdA* and AlgR-box2 in promoter P*nrdJ.*

4. AlgR is responsible for the repression of class II RNR in mucoid biofilms of *P. aeruginosa* via its binding to AlgR-box1 in promoter P*nrdJ,* most likely in benefit of class III RNR, which remains unrepressed.

5. The binding of AlgR in the RNR promoters and the promoter region controlling *algD* transcription causes a DNA bending effect detectable by Atomic Force Microscopy, as has been commonly hypothesized for AlgR-regulated operons.

6. As previously described for other species, such as *E. coli* or *S. coelicolor*, the NrdR transcription factor acts as a repressor of all RNR classes encoded by *P. aeruginosa*. This regulation occurs via its binding to the NrdR-boxes predicted by *Rodionov et al* in 2005.

7. The degree of repression exerted by NrdR on the different RNR classes of *P. aeruginosa* is subject to variation, so that the anaerobically active class II and class III RNRs are less repressed by NrdR under anaerobic conditions. This difference is most likely a result of differences in NrdR-box placement and interactions between NrdR and other transcription factors.

8. NrdR acts as an activator of *topA* transcription via its binding to a single NrdR-box, located in position -68 relative to the ATG of the first gene in the operon. The effect of this activation is only noticeable, at both transcriptional and functional levels, during the exponential growth phase.

9. *nrdR* transcription in *P. aeruginosa* increases under anaerobic conditions. This activation is caused by the NarXL system, via the binding of (presumably phosphorylated) NarL to two binding sites located in positions -37 and -15 in promoter P*nrdR*, relative to the ATG of *nrdR*.

10. Numerous putative NrdR-boxes can be identified in the regions upstream of coding genes in *E. coli* and *P. aeruginosa*, with a total of 113 hits and 33 hits, respectively. However, the identification of this binding sites only coincides with genes that are differentially expressed in *nrdR* mutant strains (compared to their isogenic wild-type strains) for the RNR operons.

11. Numerous genes are found to be differentially expressed (DEGs) in *nrdR* mutant strains of *E. coli* and *P. aeruginosa*, compared to their isogenic wild-type strains, using general transcriptomics techniques, such as RNA-seq (47 DEGs in *P. aeruginosa*) and DNA microarrays (111 DEGs in *P. aeruginosa*, 57 in *E. coli*). However, these DEGs only coincide with the identification of putative NrdR-boxes in the case of RNR operons.

12. Stable and pure recombinant NrdR proteins from *E. coli* and *P. aeruginosa* can be obtained with a two-step purification procedure when this transcription factor is initially expressed as fusion proteins including solubilization tags and protease digestion sites (SUMO, TEV) and adding nucleotide co-factors during the purification procedure when necessary.

13. NrdR exists as a dynamic population of nucleotide-dependent oligomeric forms with no fixed stoichiometry in both *P. aeruginosa* and *E. coli*.

14. Binding of dATP to NrdR causes controlled protein-protein interaction leading to the formation of medium-order oligomeric forms, where the hexamer is the most represented. Longer incubation of the protein *in vitro* with dATP does not cause a significant shift in the composition of its oligomer population. The hexameric form of NrdR is active both at the DNA-binding level and at a function level, as determined by EMSA and *in vitro* transcription (ReViTA), respectively.

15. Binding of ATP to NrdR causes intense oligomerization, leading to the formation of high-order oligomeric forms, in which up to 14-mer have been detected. These forms display no activity at both the DNA-binding levels and at a functional level, as determined by EMSA and *in vitro* transcription (ReViTA), respectively.

16. Alteration of *nrdR* expression in *P. aeruginosa*, both via deletion or overexpression, negatively affects bacterial fitness, decreasing growth speed and viable counts. This effect correlates with an increase of *Galleria mellonella* larvae survival when infected with the corresponding *P. aeruginosa* strains, although the same effect was not reproduced in *Drosophila melanogaster* infection tests.

17. The simultaneous *in vitro* transcription of two genes, encoded in the same plasmid and expressed as different mRNAs, and arranged so that the transcription of one gene is controlled by a transcription factor of interest while the other gene is expressed constitutively, can be used to characterize *in vitro* the functional effects of the transcription factor chosen. The resultant technique was called ReViTA (Regulated *in Vitro* Transcription Assay).

18. Class II and class III RNRs in *P. aeruginosa* play are essential for anaerobic growth and play an important role during biofilm formation in both static and continuous-flow models.

19. The transcription of class II and class III RNRs in *P. aeruginosa* is induced during anaerobic growth and in the biofilm. This last effect can be attributed to the microaerobic and anaerobic conditions that appear in certain areas of the biofilm structure.

20. Class II RNR transcription in *P. aeruginosa* is induced anaerobically by the master anaerobic regulator Dnr via its biding to a single binding site located at position -21 relative to the ATG of *nrdJa*.

21. The activation of class II RNR transcription in *P. aeruginosa* by the anaerobic master regulator Dnr and by the AlgZR two-component systems are independent, and thus are additive.

22. A chemostat-like bioreactor in which steady-state bacterial cultures are exposed to changing oxygenation conditions driven by the oxygen consumption of the culture itself can be effectively used to reproduce the effects of the aerobic-anaerobic transition on the culture.

23. The oxygen availability detected by the cells of a bacterial culture in steady-state where changes in oxygenation are only driven by the oxygen consumption of the culture can be monitored using the concentration of oxygen in the gas phase above the culture as the state variable.

24. *P. aeruginosa* suffers a smooth adaptation profile throughout the aerobic-anaerobic transition, displaying a gradual decrease in its oxygen consumption rate and no negative effects on bacterial fitness during the first half of the microaerobic range (early microaerobic range). A significant decrease in fitness is noted during the mid-microaerobic range (12% O_2 – 5 % O_2), which is later recovered under lower oxygen concentrations and anaerobiosis.

25. *E. coli* suffers a gradual decrease in growth speed and fitness during the aerobic-anaerobic transition, which is only recovered after long adaptation to anaerobic conditions. A strong stepwise adaptation is observed, in which the fully aerobic machinery abruptly transitions to microaerobic systems, causing a reduced oxygen consumption rate that is kept for all the microaerobic range.

26. A previously described single point mutation in the Anr box controlling anaerobic induction of class III RNR in *P. aeruginosa* PAO1 causes a delayed activation of this RNR during the aerobic-anaerobic transition. The peak in class III RNR expression that is observed in the early microaerobic range (21% O_2 to 12% O_2) in strains without the mutation does not occur until the late microaerobic range (5% O_2 to O% O_2). This causes a significant reduction in the growth speed of *P. aeruginosa* PAO1 during the mid-microaerobic range, compared to other strains of *P. aeruginosa.*

27. The RNR network of *P. aeruginosa* displays a coordinated and gradual shift in gene expression during the aerobic-anaerobic transition: classes II and III RNR are activated as a result of two consecutive events during the microaerobic range (early microaerobic range and late microaerobic range), while class Ia RNR expression remains unchanged. On the other hand, RNR in *E. coli* display the opposite pattern of regulation, where the aerobically active class Ia and Ib are gradually repressed during the aerobic-anaerobic transition.

28. An *nrdR* mutant strain of *P. aeruginosa* does not lose the microaerobic and anaerobic induction of their class II and class III RNRs; however, in the absence of NrdR-repression, the gradual pattern of microaerobic induction observed in the wild-type strain disappears.

29. In the aerobic-anaerobic transition of *P. aeruginosa*, the anaerobic master regulator Anr becomes essential during the early microaerobic range, while Dnr only becomes essential in the late microaerobic range. On the other hand, the master anaerobic regulator Fnr in *E. coli* becomes essential in the late microaerobic range (below 2% O2), but the effects of its mutations on bacterial fitness are noticeable since the start of the aerobic-anaerobic transition.

30. Both *E. coli* and *P. aeruginosa* display hybrid metabolism during the aerobic-anaerobic transition, as evidenced by the fact that, for significant stretches of the microaerobic range, anaerobic regulators such as Fnr or Anr are active or even essential, while aerobic respiration is still occurring.

References

1. Jonna VR, Crona M, Rofougaran R, Lundin D, Johansson S, Brannstrom K, et al. Diversity in Overall Activity Regulation of Ribonucleotide Reductase. The Journal of biological chemistry. 2015;290(28):17339-48.

2. Puri P, Goel A, Bochynska A, Poolman B. Regulation of acetate kinase isozymes and its importance for mixed-acid fermentation in Lactococcus lactis. Journal of bacteriology. 2014;196(7):1386-93.

3. Arai H, Kawakami T, Osamura T, Hirai T, Sakai Y, Ishii M. Enzymatic characterization and in vivo function of five terminal oxidases in *Pseudomonas aeruginosa*. Journal of bacteriology. 2014;196(24):4206-15.

4. Nordlund P, Reichard P. Ribonucleotide reductases. Annu Rev Biochem. 2006;75:681-706.

5. Stewart PS, Franklin MJ. Physiological heterogeneity in biofilms. Nature reviews Microbiology. 2008;6(3):199-210.

6. Stubbe J. Ribonucleotide reductases: the link between an RNA and a DNA world? Curr Opin Struct Biol. 2000;10(6):731-6.

7. Arai H. Regulation and Function of Versatile Aerobic and Anaerobic Respiratory Metabolism in *Pseudomonas aeruginosa*. Frontiers in microbiology. 2011;2:103.

8. Torrents E. Ribonucleotide reductases: essential enzymes for bacterial life. Frontiers in cellular and infection microbiology. 2014;4:52.

9. Rodionov DA, Gelfand MS. Identification of a bacterial regulatory system for ribonucleotide reductases by phylogenetic profiling. Trends Genet. 2005;21(7):385-9.

10. Okkotsu Y, Little AS, Schurr MJ. The Pseudomonas aeruginosa AlgZR two-component system coordinates multiple phenotypes. Frontiers in cellular and infection microbiology. 2014;4:82.

11. Unden G, Becker S, Bongaerts J, Schirawski J, Six S. Oxygen regulated gene expression in facultatively anaerobic bacteria. Antonie van Leeuwenhoek. 1994;66(1-3):3-22.

12. Unden G, Becker S, Bongaerts J, Holighaus G, Schirawski J, Six S. O2-sensing and O2-dependent gene regulation in facultatively anaerobic bacteria. Archives of microbiology. 1995;164(2):81-90.

13. Haddock BA, Jones CW. Bacterial respiration. Bacteriological reviews. 1977;41(1):47-99.

14. Patel MS, Nemeria NS, Furey W, Jordan F. The pyruvate dehydrogenase complexes: structure-based function and regulation. The Journal of biological chemistry. 2014;289(24):16615-23.

15. Akram M. Citric acid cycle and role of its intermediates in metabolism. Cell biochemistry and biophysics. 2014;68(3):475-8.

16. Anraku Y. Bacterial electron transport chains. Annu Rev Biochem. 1988;57:101-32.

17. Bettenbrock K, Bai H, Ederer M, Green J, Hellingwerf KJ, Holcombe M, et al. Towards a systems level understanding of the oxygen response of *Escherichia coli*. Adv Microb Physiol. 2014;64:65-114.

18. Jurtshuk P, Jr., Mueller TJ, Acord WC. Bacterial terminal oxidases. CRC critical reviews in microbiology. 1975;3(4):399-468.

19. Trotter EW, Rolfe MD, Hounslow AM, Craven CJ, Williamson MP, Sanguinetti G, et al. Reprogramming of Escherichia coli K-12 metabolism during the initial phase of transition from an anaerobic to a micro-aerobic environment. PloS one. 2011;6(9):e25501.

20. Becker S, Vlad D, Schuster S, Pfeiffer P, Unden G. Regulatory O2 tensions for the synthesis of fermentation products in Escherichia coli and relation to aerobic respiration. Archives of microbiology. 1997;168(4):290-6.

21. Henkel SG, Ter Beek A, Steinsiek S, Stagge S, Bettenbrock K, de Mattos MJ, et al. Basic regulatory principles of Escherichia coli's electron transport chain for varying oxygen conditions. PloS one. 2014;9(9):e107640.

22. Fuchs G, El Said Mohamed M, Altenschmidt U, Koch J, Lack A, Brackmann R, et al. Biochemistry of anaerobic biodegradation of aromatic compounds. In: Ratledge C, editor. Biochemistry of microbial degradation. Dordrecht: Springer Netherlands; 1994. p. 513-53.

23. Costerton JW, Stewart PS, Greenberg EP. Bacterial biofilms: a common cause of persistent infections. Science. 1999;284(5418):1318-22.

24. Xu KD, Stewart PS, Xia F, Huang CT, McFeters GA. Spatial physiological heterogeneity in *Pseudomonas aeruginosa* biofilm is determined by oxygen availability. Appl Environ Microbiol. 1998;64(10):4035-9.

25. Stewart PS. Diffusion in biofilms. Journal of bacteriology. 2003;185(5):1485-91.

26. Dietrich LE, Okegbe C, Price-Whelan A, Sakhtah H, Hunter RC, Newman DK. Bacterial community morphogenesis is intimately linked to the intracellular redox state. Journal of bacteriology. 2013;195(7):1371-80.

27. Borriello G, Werner E, Roe F, Kim AM, Ehrlich GD, Stewart PS. Oxygen limitation contributes to antibiotic tolerance of Pseudomonas aeruginosa in biofilms. Antimicrob Agents Chemother. 2004;48(7):2659-64.

28. Lenz AP, Williamson KS, Pitts B, Stewart PS, Franklin MJ. Localized gene expression in *Pseudomonas aeruginosa* biofilms. Appl Environ Microbiol. 2008;74(14):4463-71.

29. Rani SA, Pitts B, Beyenal H, Veluchamy RA, Lewandowski Z, Davison WM, et al. Spatial patterns of DNA replication, protein synthesis, and oxygen concentration within bacterial biofilms reveal diverse physiological states. Journal of bacteriology. 2007;189(11):4223-33.

30. Soeren Molin B. Pseudomonas: Model Organism, Pathogen, Cell Factory. The Quarterly Review of Biology. 2009;84(2):204-5.

31. Govan JR, Deretic V. Microbial pathogenesis in cystic fibrosis: mucoid *Pseudomonas aeruginosa* and *Burkholderia cepacia*. Microbiol Rev. 1996;60(3):539-74.

32. Lyczak JB, Cannon CL, Pier GB. Lung infections associated with cystic fibrosis. Clinical microbiology reviews. 2002;15(2):194-222.

33. Murphy TF, Brauer AL, Eschberger K, Lobbins P, Grove L, Cai X, et al. *Pseudomonas aeruginosa* in chronic obstructive pulmonary disease. Am J Respir Crit Care Med. 2008;177(8):853-60.

34. Stover CK, Pham XQ, Erwin AL, Mizoguchi SD, Warrener P, Hickey MJ, et al. Complete genome sequence of *Pseudomonas aeruginosa* PAO1, an opportunistic pathogen. Nature. 2000;406(6799):959-64.

35. Galan-Vasquez E, Luna B, Martinez-Antonio A. The Regulatory Network of Pseudomonas aeruginosa. Microbial informatics and experimentation. 2011;1(1):3.

36. Schreiber K, Krieger R, Benkert B, Eschbach M, Arai H, Schobert M, et al. The anaerobic regulatory network required for *Pseudomonas aeruginosa* nitrate respiration. Journal of bacteriology. 2007;189(11):4310-4.

37. Yoon MY, Lee KM, Park Y, Yoon SS. Contribution of cell elongation to the biofilm formation of *Pseudomonas aeruginosa* during anaerobic respiration. PloS one. 2011;6(1):e16105.

38. Filiatrault MJ, Picardo KF, Ngai H, Passador L, Iglewski BH. Identification of *Pseudomonas aeruginosa* genes involved in virulence and anaerobic growth. Infection and immunity. 2006;74(7):4237-45.

39. Driscoll JA, Brody SL, Kollef MH. The epidemiology, pathogenesis and treatment of Pseudomonas aeruginosa infections. Drugs. 2007;67(3):351-68.

40. Sousa AM, Pereira MO. Pseudomonas aeruginosa Diversification during Infection Development in Cystic Fibrosis Lungs-A Review. Pathogens (Basel, Switzerland). 2014;3(3):680-703.

41. Pier GB, Grout M, Zaidi TS, Olsen JC, Johnson LG, Yankaskas JR, et al. Role of mutant CFTR in hypersusceptibility of cystic fibrosis patients to lung infections. Science. 1996;271(5245):64-7.

42. Rodrigue A, Quentin Y, Lazdunski A, Mejean V, Foglino M. Two-component systems in Pseudomonas aeruginosa: why so many? Trends in microbiology. 2000;8(11):498-504.

43. Vallis AJ, Yahr TL, Barbieri JT, Frank DW. Regulation of ExoS production and secretion by Pseudomonas aeruginosa in response to tissue culture conditions. Infection and immunity. 1999;67(2):914-20.

44. O'Malley YQ, Reszka KJ, Rasmussen GT, Abdalla MY, Denning GM, Britigan BE. The Pseudomonas secretory product pyocyanin inhibits catalase activity in human lung epithelial cells. American journal of physiology Lung cellular and molecular physiology. 2003;285(5):L1077-86.

45. Mensa J, Barberan J, Soriano A, Llinares P, Marco F, Canton R, et al. Antibiotic selection in the treatment of acute invasive infections by Pseudomonas aeruginosa: Guidelines by the Spanish Society of Chemotherapy. Revista espanola de quimioterapia : publicacion oficial de la Sociedad Espanola de Quimioterapia. 2018;31(1):78-100.

46. Sole M, Fabrega A, Cobos-Trigueros N, Zamorano L, Ferrer-Navarro M, Balleste-Delpierre C, et al. In vivo evolution of resistance of Pseudomonas aeruginosa strains isolated from patients admitted to an intensive care unit: mechanisms of resistance and antimicrobial exposure. The Journal of antimicrobial chemotherapy. 2015;70(11):3004-13.

47. Hentzer M, Teitzel GM, Balzer GJ, Heydorn A, Molin S, Givskov M, et al. Alginate overproduction affects Pseudomonas aeruginosa biofilm structure and function. Journal of bacteriology. 2001;183(18):5395-401.

48. Leid JG, Willson CJ, Shirtliff ME, Hassett DJ, Parsek MR, Jeffers AK. The exopolysaccharide alginate protects Pseudomonas aeruginosa biofilm bacteria from IFN-gamma-mediated macrophage killing. Journal of immunology (Baltimore, Md : 1950). 2005;175(11):7512-8.

49. Deretic V, Dikshit R, Konyecsni WM, Chakrabarty AM, Misra TK. The algR gene, which regulates mucoidy in Pseudomonas aeruginosa, belongs to a class of environmentally responsive genes. Journal of bacteriology. 1989;171(3):1278-83.

50. Martin DW, Schurr MJ, Mudd MH, Govan JR, Holloway BW, Deretic V. Mechanism of conversion to mucoidy in Pseudomonas aeruginosa infecting cystic fibrosis patients. Proceedings of the National Academy of Sciences of the United States of America. 1993;90(18):8377-81.

51. Mohr CD, Hibler NS, Deretic V. AlgR, a response regulator controlling mucoidy in Pseudomonas aeruginosa, binds to the FUS sites of the algD promoter located unusually far upstream from the mRNA start site. Journal of bacteriology. 1991;173(16):5136-43.

52. Lizewski SE, Schurr JR, Jackson DW, Frisk A, Carterson AJ, Schurr MJ. Identification of AlgR-regulated genes in Pseudomonas aeruginosa by use of microarray analysis. Journal of bacteriology. 2004;186(17):5672-84.

53. Damron FH, Goldberg JB. Proteolytic regulation of alginate overproduction in Pseudomonas aeruginosa. Molecular microbiology. 2012;84(4):595-607.

54. Hogardt M, Hoboth C, Schmoldt S, Henke C, Bader L, Heesemann J. Stage-specific adaptation of hypermutable Pseudomonas aeruginosa isolates during chronic pulmonary infection in patients with cystic fibrosis. The Journal of infectious diseases. 2007;195(1):70-80.

55. Mena A, Smith EE, Burns JL, Speert DP, Moskowitz SM, Perez JL, et al. Genetic adaptation of Pseudomonas aeruginosa to the airways of cystic fibrosis patients is catalyzed by hypermutation. Journal of bacteriology. 2008;190(24):7910-7.

56. Lizewski SE, Lundberg DS, Schurr MJ. The transcriptional regulator AlgR is essential for Pseudomonas aeruginosa pathogenesis. Infection and immunity. 2002;70(11):6083-93.

57. Kong W, Zhao J, Kang H, Zhu M, Zhou T, Deng X, et al. ChIP-seq reveals the global regulator AlgR mediating cyclic di-GMP synthesis in Pseudomonas aeruginosa. Nucleic acids research. 2015;43(17):8268-82.

58. Arai H, Kodama T, Igarashi Y. Cascade regulation of the two CRP/FNR-related transcriptional regulators (ANR and DNR) and the denitrification enzymes in *Pseudomonas aeruginosa*. Molecular microbiology. 1997;25(6):1141-8.

59. Trunk K, Benkert B, Quack N, Munch R, Scheer M, Garbe J, et al. Anaerobic adaptation in *Pseudomonas aeruginosa*: definition of the Anr and Dnr regulons. Environmental microbiology. 2010;12(6):1719-33.

60. Sabra W, Kim EJ, Zeng AP. Physiological responses of *Pseudomonas aeruginosa* PAO1 to oxidative stress in controlled microaerobic and aerobic cultures. Microbiology. 2002;148(Pt 10):3195-202.

61. Williams HD, Zlosnik JE, Ryall B. Oxygen, cyanide and energy generation in the cystic fibrosis pathogen Pseudomonas aeruginosa. Adv Microb Physiol. 2007;52:1-71.

62. Eschbach M, Schreiber K, Trunk K, Buer J, Jahn D, Schobert M. Long-term anaerobic survival of the opportunistic pathogen *Pseudomonas aeruginosa* via pyruvate fermentation. Journal of bacteriology. 2004;186(14):4596-604.

63. Zumft WG. Cell biology and molecular basis of denitrification. Microbiol Mol Biol Rev. 1997;61(4):533-616.

64. Schobert M, Jahn D. Anaerobic physiology of *Pseudomonas aeruginosa* in the cystic fibrosis lung. International journal of medical microbiology : IJMM. 2010;300(8):549-56.

65. Galimand M, Gamper M, Zimmermann A, Haas D. Positive FNR-like control of anaerobic arginine degradation and nitrate respiration in *Pseudomonas aeruginosa*. Journal of bacteriology. 1991;173(5):1598-606.

66. Sawers RG. Identification and molecular characterization of a transcriptional regulator from *Pseudomonas aeruginosa* PAO1 exhibiting structural and functional similarity to the FNR protein of *Escherichia coli*. Molecular microbiology. 1991;5(6):1469-81.

67. Yoon SS, Karabulut AC, Lipscomb JD, Hennigan RF, Lymar SV, Groce SL, et al. Two-pronged survival strategy for the major cystic fibrosis pathogen, Pseudomonas aeruginosa, lacking the capacity to degrade nitric oxide during anaerobic respiration. Embo j. 2007;26(15):3662-72.

68. Arai H, Kodama T, Igarashi Y. Effect of nitrogen oxides on expression of the nir and nor genes for denitrification in Pseudomonas aeruginosa. FEMS microbiology letters. 1999;170(1):19-24.

69. Tenaillon O, Skurnik D, Picard B, Denamur E. The population genetics of commensal *Escherichia coli*. Nature reviews Microbiology. 2010;8(3):207-17.

70. Partridge JD, Scott C, Tang Y, Poole RK, Green J. *Escherichia coli* transcriptome dynamics during the transition from anaerobic to aerobic conditions. The Journal of biological chemistry. 2006;281(38):27806-15.

71. Unden G, Schirawski J. The oxygen-responsive transcriptional regulator FNR of *Escherichia coli*: the search for signals and reactions. Molecular microbiology. 1997;25(2):205-10.

72. Kaper JB, Nataro JP, Mobley HL. Pathogenic Escherichia coli. Nature reviews Microbiology. 2004;2(2):123-40.

73. Friesen JD. Escherichia coli and Salmonella typhimurium: Cellular and Molecular Biology. Science. 1988;240(4859):1678-81.

74. Nataro JP, Kaper JB. Diarrheagenic Escherichia coli. Clinical microbiology reviews. 1998;11(1):142-201.

75. Russo TA, Johnson JR. Proposal for a new inclusive designation for extraintestinal pathogenic isolates of Escherichia coli: ExPEC. The Journal of infectious diseases. 2000;181(5):1753-4.

76. Backhed F, Ley RE, Sonnenburg JL, Peterson DA, Gordon JI. Host-bacterial mutualism in the human intestine. Science. 2005;307(5717):1915-20.

77. Jones SA, Chowdhury FZ, Fabich AJ, Anderson A, Schreiner DM, House AL, et al. Respiration of *Escherichia coli* in the mouse intestine. Infection and immunity. 2007;75(10):4891-9.

78. He G, Shankar RA, Chzhan M, Samouilov A, Kuppusamy P, Zweier JL. Noninvasive measurement of anatomic structure and intraluminal oxygenation in the gastrointestinal tract of living mice with spatial and spectral EPR imaging. Proceedings of the National Academy of Sciences of the United States of America. 1999;96(8):4586-91.

79. Dreux N, del Mar Cendra M, Massier S, Darfeuille-Michaud A, Barnich N, Torrents E. Ribonucleotide reductase NrdR as a novel regulator for motility and chemotaxis during adherent-invasive *Escherichia coli* infection. Infection and immunity. 2015;83(4):1305-17.

80. Partridge JD, Sanguinetti G, Dibden DP, Roberts RE, Poole RK, Green J. Transition of *Escherichia coli* from aerobic to micro-aerobic conditions involves fast and slow reacting regulatory components. The Journal of biological chemistry. 2007;282(15):11230-7.

81. Poole RK, Cook GM. Redundancy of aerobic respiratory chains in bacteria? Routes, reasons and regulation. Adv Microb Physiol. 2000;43:165-224.

82. Rolfe MD, Ocone A, Stapleton MR, Hall S, Trotter EW, Poole RK, et al. Systems analysis of transcription factor activities in environments with stable and dynamic oxygen concentrations. Open biology. 2012;2(7):120091.

83. Green J, Scott C, Guest JR. Functional versatility in the CRP-FNR superfamily of transcription factors: FNR and FLP. Adv Microb Physiol. 2001;44:1-34.

84. Bekker M, Alexeeva S, Laan W, Sawers G, Teixeira de Mattos J, Hellingwerf K. The ArcBA two-component system of *Escherichia coli* is regulated by the redox state of both the ubiquinone and the menaquinone pool. Journal of bacteriology. 2010;192(3):746-54.

85. Myers KS, Yan H, Ong IM, Chung D, Liang K, Tran F, et al. Genome-scale analysis of *Escherichia coli* FNR reveals complex features of transcription factor binding. PLoS Genet. 2013;9(6):e1003565.

86. Lindahl T. Instability and decay of the primary structure of DNA. Nature. 1993;362(6422):709-15.

87. Crick F. Central dogma of molecular biology. Nature. 1970;227(5258):561-3.

88. Thieffry D, Sarkar S. Forty years under the central dogma. Trends in Biochemical Sciences. 1998;23(8):312-6.

89. Reichard P, Rutberg L. Formation of deoxycytidine 5'-phosphate from cytidine 5'-phosphate with enzymes from Escherichia coli. Biochim Biophys Acta. 1960;37:554-5.

90. Torrents E, Shanin M, Sjöberg B-M. The ribonucleotide reductase family - genetics and genomics. Ribonucleotide reductases. Hauppauge, NY: Nova Science Publishers; 2008. p. 17-77.

91. Gandhi VV, Samuels DC. A review comparing deoxyribonucleoside triphosphate (dNTP) concentrations in the mitochondrial and cytoplasmic compartments of normal and transformed cells. Nucleosides, nucleotides & nucleic acids. 2011;30(5):317-39.

92. Reichard P, Ehrenberg A. Ribonucleotide Reductase-- a Radical Enzyme. Science. 1983;221(4610):514-9.

93. Eklund H, Uhlin U, Farnegardh M, Logan DT, Nordlund P. Structure and function of the radical enzyme ribonucleotide reductase. Prog Biophys Mol Biol. 2001;77(3):177-268.

94. Ehrenberg A. Free radical transfer, fluctuating structure and reaction cycle of ribonucleotide reductase. Bio Systems. 2001;62(1-3):9-12.

95. Holmgren A. Hydrogen donor system for Escherichia coli ribonucleoside-diphosphate reductase dependent upon glutathione. Proceedings of the National Academy of Sciences of the United States of America. 1976;73(7):2275-9.

96. Holmgren A, Sengupta R. The use of thiols by ribonucleotide reductase. Free Radic Biol Med. 2010;49(11):1617-28.

97. Lillig CH, Berndt C, Holmgren A. Glutaredoxin systems. Biochim Biophys Acta. 2008;1780(11):1304-17.

98. Torrents E, Aloy P, Gibert I, Rodriguez-Trelles F. Ribonucleotide reductases: divergent evolution of an ancient enzyme. J Mol Evol. 2002;55(2):138-52.

99. Jordan A, Reichard P. Ribonucleotide reductases. Annu Rev Biochem. 1998;67:71-98.

100. Blakley RL, Barker HA. Cobamide stimulation of the reduction of ribotides to deoxyribotides in Lactobacillus leichmannii. Biochemical and biophysical research communications. 1964;16(5):391-7.

101. Fontecave M, Eliasson R, Reichard P. Enzymatic regulation of the radical content of the small subunit of Escherichia coli ribonucleotide reductase involving reduction of its redox centers. The Journal of biological chemistry. 1989;264(16):9164-70.

102. Reichard P. The anaerobic ribonucleotide reductase from Escherichia coli. The Journal of biological chemistry. 1993;268(12):8383-6.

103. Jordan A, Pontis E, Atta M, Krook M, Gibert I, Barbé J, et al. A second class I ribonucleotide reductase in Enterobacteriaceae: characterization of the Salmonella typhimurium enzyme. Proceedings of the National Academy of Sciences. 1994;91(26):12892-6.

104. Hogbom M, Stenmark P, Voevodskaya N, McClarty G, Graslund A, Nordlund P. The radical site in chlamydial ribonucleotide reductase defines a new R2 subclass. Science. 2004;305(5681):245-8.

105. Nordlund P, Eklund H. Structure and function of the Escherichia coli ribonucleotide reductase protein R2. Journal of molecular biology. 1993;232(1):123-64.

106. Uhlin U, Eklund H. Structure of ribonucleotide reductase protein R1. Nature. 1994;370(6490):533-9.

107. Ekberg M, Sahlin M, Eriksson M, Sjoberg BM. Two conserved tyrosine residues in protein R1 participate in an intermolecular electron transfer in ribonucleotide reductase. The Journal of biological chemistry. 1996;271(34):20655-9.

108. Zimanyi CM, Ando N, Brignole EJ, Asturias FJ, Stubbe J, Drennan CL. Tangled up in knots: structures of inactivated forms of E. coli class Ia ribonucleotide reductase. Structure. 2012;20(8):1374-83.

109. Jordan A, Aslund F, Pontis E, Reichard P, Holmgren A. Characterization of Escherichia coli NrdH. A glutaredoxin-like protein with a thioredoxin-like activity profile. The Journal of biological chemistry. 1997;272(29):18044-50.

110. Cotruvo JA, Stubbe J. Class I ribonucleotide reductases: metallocofactor assembly and repair in vitro and in vivo. Annu Rev Biochem. 2011;80:733-67.

111. Cotruvo JA, Jr., Stubbe J. An active dimanganese(III)-tyrosyl radical cofactor in Escherichia coli class Ib ribonucleotide reductase. Biochemistry. 2010;49(6):1297-309.

112. Stubbe J. Di-iron-tyrosyl radical ribonucleotide reductases. Current opinion in chemical biology. 2003;7(2):183-8.

113. Jiang W, Yun D, Saleh L, Barr EW, Xing G, Hoffart LM, et al. A manganese(IV)/iron(III) cofactor in Chlamydia trachomatis ribonucleotide reductase. Science. 2007;316(5828):1188-91.

114. Roshick C, Iliffe-Lee ER, McClarty G. Cloning and characterization of ribonucleotide reductase from Chlamydia trachomatis. The Journal of biological chemistry. 2000;275(48):38111-9.

115. Sintchak MD, Arjara G, Kellogg BA, Stubbe J, Drennan CL. The crystal structure of class II ribonucleotide reductase reveals how an allosterically regulated monomer mimics a dimer. Nature structural biology. 2002;9(4):293-300.

116. Lawrence CC, Gerfen GJ, Samano V, Nitsche R, Robins MJ, Retey J, et al. Binding of Cob(II)alamin to the adenosylcobalamin-dependent ribonucleotide reductase from Lactobacillus leichmannii. Identification of dimethylbenzimidazole as the axial ligand. The Journal of biological chemistry. 1999;274(11):7039-42.

117. Eliasson R, Pontis E, Jordan A, Reichard P. Allosteric control of three B12-dependent (class II) ribonucleotide reductases. Implications for the evolution of ribonucleotide reduction. The Journal of biological chemistry. 1999;274(11):7182-9.

118. Reichard P. Ribonucleotide reductases: the evolution of allosteric regulation. Arch Biochem Biophys. 2002;397(2):149-55.

119. Logan DT, Andersson J, Sjoberg BM, Nordlund P. A glycyl radical site in the crystal structure of a class III ribonucleotide reductase. Science. 1999;283(5407):1499-504.

120. Ollagnier S, Mulliez E, Gaillard J, Eliasson R, Fontecave M, Reichard P. The anaerobic Escherichia coli ribonucleotide reductase. Subunit structure and iron sulfur center. The Journal of biological chemistry. 1996;271(16):9410-6.

121. Ollagnier S, Mulliez E, Schmidt PP, Eliasson R, Gaillard J, Deronzier C, et al. Activation of the anaerobic ribonucleotide reductase from Escherichia coli. The essential role of the iron-sulfur center for S-adenosylmethionine reduction. The Journal of biological chemistry. 1997;272(39):24216-23.

122. King DS, Reichard P. Mass spectrometric determination of the radical scission site in the anaerobic ribonucleotide reductase of Escherichia coli. Biochemical and biophysical research communications. 1995;206(2):731-5.

123. Torrents E, Eliasson R, Wolpher H, Graslund A, Reichard P. The anaerobic ribonucleotide reductase from Lactococcus lactis. Interactions between the two proteins NrdD and NrdG. The Journal of biological chemistry. 2001;276(36):33488-94.

124. Andersson J, Westman M, Sahlin M, Sjoberg BM. Cysteines involved in radical generation and catalysis of class III anaerobic ribonucleotide reductase. A protein engineering study of bacteriophage T4 NrdD. The Journal of biological chemistry. 2000;275(26):19449-55.

125. Torrents E, Trevisiol C, Rotte C, Hellman U, Martin W, Reichard P. Euglena gracilis ribonucleotide reductase: the eukaryote class II enzyme and the possible antiquity of eukaryote B12 dependence. The Journal of biological chemistry. 2006;281(9):5604-11.

126. Martin JE, Imlay JA. The alternative aerobic ribonucleotide reductase of Escherichia coli, NrdEF, is a manganese-dependent enzyme that enables cell replication during periods of iron starvation. Molecular microbiology. 2011;80(2):319-34.

127. Lundin D, Gribaldo S, Torrents E, Sjoberg BM, Poole AM. Ribonucleotide reduction - horizontal transfer of a required function spans all three domains. BMC evolutionary biology. 2010;10:383.

128. Borovok I, Gorovitz B, Yanku M, Schreiber R, Gust B, Chater K, et al. Alternative oxygen-dependent and oxygen-independent ribonucleotide reductases in Streptomyces: cross-regulation and physiological role in response to oxygen limitation. Molecular microbiology. 2004;54(4):1022-35.

129. Lundin D, Torrents E, Poole AM, Sjoberg BM. RNRdb, a curated database of the universal enzyme family ribonucleotide reductase, reveals a high level of misannotation in sequences deposited to Genbank. BMC genomics. 2009;10:589.

130. Blattner FR, Plunkett G, 3rd, Bloch CA, Perna NT, Burland V, Riley M, et al. The complete genome sequence of Escherichia coli K-12. Science. 1997;277(5331):1453-62.

131. Garriga X, Eliasson R, Torrents E, Jordan A, Barbe J, Gibert I, et al. *nrdD* and *nrdG* genes are essential for strict anaerobic growth of *Escherichia coli*. Biochemical and biophysical research communications. 1996;229(1):189-92.

132. Jordan A, Aragall E, Gibert I, Barbe J. Promoter identification and expression analysis of Salmonella typhimurium and Escherichia coli nrdEF operons

encoding one of two class I ribonucleotide reductases present in both bacteria. Molecular microbiology. 1996;19(4):777-90.

133. Torrents E, Grinberg I, Gorovitz-Harris B, Lundstrom H, Borovok I, Aharonowitz Y, et al. NrdR controls differential expression of the Escherichia coli ribonucleotide reductase genes. Journal of bacteriology. 2007;189(14):5012-21.

134. Jang S, Imlay JA. Micromolar intracellular hydrogen peroxide disrupts metabolism by damaging iron-sulfur enzymes. The Journal of biological chemistry. 2007;282(2):929-37.

135. Park S, You X, Imlay JA. Substantial DNA damage from submicromolar intracellular hydrogen peroxide detected in Hpx- mutants of Escherichia coli. Proceedings of the National Academy of Sciences of the United States of America. 2005;102(26):9317-22.

136. Cendra Mdel M, Juarez A, Torrents E. Biofilm modifies expression of ribonucleotide reductase genes in *Escherichia coli*. PloS one. 2012;7(9):e46350.

137. Monje-Casas F, Jurado J, Prieto-Alamo MJ, Holmgren A, Pueyo C. Expression analysis of the *nrdHIEF* operon from *Escherichia coli*. Conditions that trigger the transcript level in vivo. The Journal of biological chemistry. 2001;276(21):18031-7.

138. Jordan A, Torrents E, Sala I, Hellman U, Gibert I, Reichard P. Ribonucleotide reduction in Pseudomonas species: simultaneous presence of active enzymes from different classes. Journal of bacteriology. 1999;181(13):3974-80.

139. Torrents E, Westman M, Sahlin M, Sjoberg BM. Ribonucleotide reductase modularity: Atypical duplication of the ATP-cone domain in Pseudomonas aeruginosa. The Journal of biological chemistry. 2006;281(35):25287-96.

140. Johansson R, Jonna VR, Kumar R, Nayeri N, Lundin D, Sjoberg BM, et al. Structural Mechanism of Allosteric Activity Regulation in a Ribonucleotide Reductase with Double ATP Cones. Structure. 2016;24(6):906-17.

141. Torrents E, Poplawski A, Sjoberg BM. Two proteins mediate class II ribonucleotide reductase activity in Pseudomonas aeruginosa: expression and transcriptional analysis of the aerobic enzymes. The Journal of biological chemistry. 2005;280(17):16571-8.

142. Crona M, Hofer A, Astorga-Wells J, Sjoberg BM, Tholander F. Biochemical Characterization of the Split Class II Ribonucleotide Reductase from Pseudomonas aeruginosa. PloS one. 2015;10(7):e0134293.

143. Mathews CK. DNA precursor metabolism and genomic stability. Faseb j. 2006;20(9):1300-14.

144. Wheeler LJ, Rajagopal I, Mathews CK. Stimulation of mutagenesis by proportional deoxyribonucleoside triphosphate accumulation in Escherichia coli. DNA repair. 2005;4(12):1450-6.

145. Herrick J, Sclavi B. Ribonucleotide reductase and the regulation of DNA replication: an old story and an ancient heritage. Molecular microbiology. 2007;63(1):22-34.

146. Hakansson P, Hofer A, Thelander L. Regulation of mammalian ribonucleotide reduction and dNTP pools after DNA damage and in resting cells. The Journal of biological chemistry. 2006;281(12):7834-41.

147. Thelander L. Ribonucleotide reductase and mitochondrial DNA synthesis. Nature genetics. 2007;39(6):703-4.

148. Brown NC, Reichard P. Role of effector binding in allosteric control of ribonucleoside diphosphate reductase. Journal of molecular biology. 1969;46(1):39-55.

149. Larsson KM, Jordan A, Eliasson R, Reichard P, Logan DT, Nordlund P. Structural mechanism of allosteric substrate specificity regulation in a ribonucleotide reductase. Nature structural & molecular biology. 2004;11(11):1142-9.

150. Larsson KM, Andersson J, Sjoberg BM, Nordlund P, Logan DT. Structural basis for allosteric substrate specificity regulation in anaerobic ribonucleotide reductases. Structure. 2001;9(8):739-50.

151. Ormo M, Sjoberg BM. An ultrafiltration assay for nucleotide binding to ribonucleotide reductase. Analytical biochemistry. 1990;189(1):138-41.

152. Eriksson M, Uhlin U, Ramaswamy S, Ekberg M, Regnstrom K, Sjoberg BM, et al. Binding of allosteric effectors to ribonucleotide reductase protein R1: reduction of active-site cysteines promotes substrate binding. Structure. 1997;5(8):1077-92.

153. Rofougaran R, Vodnala M, Hofer A. Enzymatically active mammalian ribonucleotide reductase exists primarily as an alpha6beta2 octamer. The Journal of biological chemistry. 2006;281(38):27705-11.

154. Ingemarson R, Thelander L. A kinetic study on the influence of nucleoside triphosphate effectors on subunit interaction in mouse ribonucleotide reductase. Biochemistry. 1996;35(26):8603-9.

155. Zhao X, Chabes A, Domkin V, Thelander L, Rothstein R. The ribonucleotide reductase inhibitor Sml1 is a new target of the Mec1/Rad53 kinase cascade during growth and in response to DNA damage. Embo j. 2001;20(13):3544-53.

156. Davies BW, Kohanski MA, Simmons LA, Winkler JA, Collins JJ, Walker GC. Hydroxyurea induces hydroxyl radical-mediated cell death in Escherichia coli. Molecular cell. 2009;36(5):845-60.

157. Jacobson BA, Fuchs JA. Multiple cis-acting sites positively regulate Escherichia coli nrd expression. Molecular microbiology. 1998;28(6):1315-22.

158. Tuggle CK, Fuchs JA. Regulation of the operon encoding ribonucleotide reductase in Escherichia coli: evidence for both positive and negative control. Embo j. 1986;5(5):1077-85.

159. Sun L, Jacobson BA, Dien BS, Srienc F, Fuchs JA. Cell cycle regulation of the Escherichia coli nrd operon: requirement for a cis-acting upstream AT-rich sequence. Journal of bacteriology. 1994;176(8):2415-26.

160. Augustin LB, Jacobson BA, Fuchs JA. Escherichia coli Fis and DnaA proteins bind specifically to the nrd promoter region and affect expression of an nrd-lac fusion. Journal of bacteriology. 1994;176(2):378-87.

161. Han JS, Kwon HS, Yim JB, Hwang DS. Effect of IciA protein on the expression of the nrd gene encoding ribonucleoside diphosphate reductase in E. coli. Molecular & general genetics : MGG. 1998;259(6):610-4.

162. Lee YS, Kim H, Hwang DS. Transcriptional activation of the dnaA gene encoding the initiator for oriC replication by IciA protein, an inhibitor of in vitro oriC replication in Escherichia coli. Molecular microbiology. 1996;19(2):389-96.

163. Zheng D, Constantinidou C, Hobman JL, Minchin SD. Identification of the CRP regulon using in vitro and in vivo transcriptional profiling. Nucleic acids research. 2004;32(19):5874-93.

164. Cendra Mdel M, Juarez A, Madrid C, Torrents E. H-NS is a novel transcriptional modulator of the ribonucleotide reductase genes in Escherichia coli. Journal of bacteriology. 2013;195(18):4255-63.

165. Borovok I, Gorovitz B, Schreiber R, Aharonowitz Y, Cohen G. Coenzyme B12 controls transcription of the Streptomyces class Ia ribonucleotide reductase nrdABS operon via a riboswitch mechanism. Journal of bacteriology. 2006;188(7):2512-20.

166. Vassinova N, Kozyrev D. A method for direct cloning of fur-regulated genes: identification of seven new fur-regulated loci in Escherichia coli. Microbiology. 2000;146 Pt 12:3171-82.

167. Sjöberg B-M, Torrents E. Shift in Ribonucleotide Reductase Gene Expression in Pseudomonas aeruginosa during Infection. Infection and immunity. 2011;79(7):2663-9.

168. Filiatrault MJ, Wagner VE, Bushnell D, Haidaris CG, Iglewski BH, Passador L. Effect of anaerobiosis and nitrate on gene expression in *Pseudomonas aeruginosa*. Infection and immunity. 2005;73(6):3764-72.

169. Tolla DA, Savageau MA. Regulation of aerobic-to-anaerobic transitions by the FNR cycle in Escherichia coli. Journal of molecular biology. 2010;397(4):893-905.

170. Boston T, Atlung T. FNR-mediated oxygen-responsive regulation of the *nrdDG* operon of *Escherichia coli*. Journal of bacteriology. 2003;185(17):5310-3.

171. Roca I, Ballana E, Panosa A, Torrents E, Gibert I. Fumarate and nitrate reduction (FNR) dependent activation of the *Escherichia coli* anaerobic ribonucleotide reductase *nrdDG* promoter. International microbiology : the official journal of the Spanish Society for Microbiology. 2008;11(1):49-56.

172. Grinberg I, Shteinberg T, Gorovitz B, Aharonowitz Y, Cohen G, Borovok I. The Streptomyces NrdR transcriptional regulator is a Zn ribbon/ATP cone protein that binds to the promoter regions of class Ia and class II ribonucleotide reductase operons. Journal of bacteriology. 2006;188(21):7635-44.

173. Borovok I, Kreisberg-Zakarin R, Yanko M, Schreiber R, Myslovati M, Aslund F, et al. Streptomyces spp. contain class Ia and class II ribonucleotide reductases: expression analysis of the genes in vegetative growth. Microbiology. 2002;148(Pt 2):391-404.

174. Masalha M, Borovok I, Schreiber R, Aharonowitz Y, Cohen G. Analysis of transcription of the Staphylococcus aureus aerobic class Ib and

anaerobic class III ribonucleotide reductase genes in response to oxygen. Journal of bacteriology. 2001;183(24):7260-72.

175. Alkema WB, Lenhard B, Wasserman WW. Regulog analysis: detection of conserved regulatory networks across bacteria: application to Staphylococcus aureus. Genome research. 2004;14(7):1362-73.

176. Tatusov RL, Galperin MY, Natale DA, Koonin EV. The COG database: a tool for genome-scale analysis of protein functions and evolution. Nucleic acids research. 2000;28(1):33-6.

177. McKethan BL, Spiro S. Cooperative and allosterically controlled nucleotide binding regulates the DNA binding activity of NrdR. Molecular microbiology. 2013;90(2):278-89.

178. Grinberg I, Shteinberg T, Hassan AQ, Aharonowitz Y, Borovok I, Cohen G. Functional analysis of the Streptomyces coelicolor NrdR ATP-cone domain: role in nucleotide binding, oligomerization, and DNA interactions. Journal of bacteriology. 2009;191(4):1169-79.

179. Naveen V, Hsiao CD. NrdR Transcription Regulation: Global Proteome Analysis and Its Role in Escherichia coli Viability and Virulence. PloS one. 2016;11(6):e0157165.

180. Aravind L, Wolf YI, Koonin EV. The ATP-cone: an evolutionarily mobile, ATP-binding regulatory domain. J Mol Microbiol Biotechnol. 2000;2(2):191-4.

181. Panosa A, Roca I, Gibert I. Ribonucleotide reductases of Salmonella typhimurium: transcriptional regulation and differential role in pathogenesis. PloS one. 2010;5(6):e11328.

182. Case ED, Akers JC, Tan M. CT406 encodes a chlamydial ortholog of NrdR, a repressor of ribonucleotide reductase. Journal of bacteriology. 2011;193(17):4396-404.

183. Zhang Y, Okada R, Isaka M, Tatsuno I, Isobe K, Hasegawa T. Analysis of the roles of NrdR and DnaB from Streptococcus pyogenes in response to host defense. APMIS. 2015;123(3):252-9.

184. Castro-Cerritos KV, Yasbin RE, Robleto EA, Pedraza-Reyes M. Role of Ribonucleotide Reductase in Bacillus subtilis Stress-Associated Mutagenesis. Journal of bacteriology. 2017;199(4).

185. Crespo A, Pedraz L, Van Der Hofstadt M, Gomila G, Torrents E. Regulation of ribonucleotide synthesis by the *Pseudomonas aeruginosa* two-component system AlgR in response to oxidative stress. Scientific reports. 2017;7(1):17892.

186. Gon S, Beckwith J. Ribonucleotide reductases: influence of environment on synthesis and activity. Antioxidants & redox signaling. 2006;8(5-6):773-80.

187. Crespo A, Pedraz L, Torrents E. Function of the *Pseudomonas aeruginosa* NrdR Transcription Factor: Global Transcriptomic Analysis and Its Role on Ribonucleotide Reductase Gene Expression. PloS one. 2015;10(4):e0123571.

188. Crespo A, Pedraz L, Astola J, Torrents E. *Pseudomonas aeruginosa* Exhibits Deficient Biofilm Formation in the Absence of Class II and III Ribonucleotide Reductases Due to Hindered Anaerobic Growth. Frontiers in microbiology. 2016;7:688.

189. Darzins A, Chakrabarty AM. Cloning of genes controlling alginate biosynthesis from a mucoid cystic fibrosis isolate of Pseudomonas aeruginosa. Journal of bacteriology. 1984;159(1):9-18.

190. Whitchurch CB, Erova TE, Emery JA, Sargent JL, Harris JM, Semmler AB, et al. Phosphorylation of the Pseudomonas aeruginosa response regulator AlgR is essential for type IV fimbria-mediated twitching motility. Journal of bacteriology. 2002;184(16):4544-54.

191. Crespo A, Gavalda J, Julian E, Torrents E. A single point mutation in class III ribonucleotide reductase promoter renders *Pseudomonas aeruginosa* PAO1 inefficient for anaerobic growth and infection. Scientific reports. 2017;7(1):13350.

192. Cendra MdM. Estudi de l'expressió i funció de les Ribonucleotidil Reductases d'Escherichia coli. 2013.

193. Hay RT. SUMO: A History of Modification. Molecular cell. 2005;18(1):1-12.

194. Kuo D, Nie M, Courey AJ. SUMO as a solubility tag and in vivo cleavage of SUMO fusion proteins with Ulp1. Methods in molecular biology (Clifton, NJ). 2014;1177:71-80.

195. Goulas T, Cuppari A, Garcia-Castellanos R, Snipas S, Glockshuber R, Arolas JL, et al. The pCri System: a vector collection for recombinant protein expression and purification. PloS one. 2014;9(11):e112643.

196. Lee KM, Go J, Yoon MY, Park Y, Kim SC, Yong DE, et al. Vitamin B12-mediated restoration of defective anaerobic growth leads to reduced

biofilm formation in *Pseudomonas aeruginosa*. Infection and immunity. 2012;80(5):1639-49.

197. Alexeeva S, Hellingwerf KJ, Teixeira de Mattos MJ. Quantitative assessment of oxygen availability: perceived aerobiosis and its effect on flux distribution in the respiratory chain of *Escherichia coli*. Journal of bacteriology. 2002;184(5):1402-6.

198. Chen F, Xia Q, Ju LK. Competition between oxygen and nitrate respirations in continuous culture of Pseudomonas aeruginosa performing aerobic denitrification. Biotechnol Bioeng. 2006;93(6):1069-78.

Annexes

Annex 1: Report on the status and impact factor of the articles presented

I hereby declare that the status of the articles presented in this thesis, as of its date of submission, is as follows:

- Article 1, titled "Regulation of ribonucleotide synthesis by the *Pseudomonas aeruginosa* AlgR two-component system", is **published**. It was published in *Scientific Reports* in December 2017. The impact factor of *Scientific reports* in 2017 was **4.122**. The article presented in this thesis constitutes an accurate reproduction of the published article, which can be found with DOI 10.1038/s41598-017-17917-7. Mr. Lucas Pedraz is the **first author** of this article, a position he shares with Dr. Anna Crespo.
- Article 2, titled "Function of the *Pseudomonas aeruginosa* NrdR transcription factor: global transcriptomic analysis and its role on ribonucleotide reductase gene expression" is **published**. It was published in *PLoS ONE* in April 2015. The impact factor of *PLoS ONE* in 2015 was **3.057**. The article presented in this thesis constitutes an accurate reproduction of the published article, which can be found with DOI 10.1371/journal.pone.0123571. Mr. Lucas Pedraz is the **second author** of this article.
- Article 3, titled "Mechanism of action of NrdR, a global regulator of ribonucleotide reduction" is **in preparation**. The article presented in this thesis is a veracious representation of the state of the research Mr. Lucas Pedraz is conducting on this topic, as of September 2019. Mr. Lucas Pedraz is the **first author** of this article, and shares with me the role of **corresponding author**.
- Article 4, titled "*Pseudomonas aeruginosa* exhibits deficient biofilm formation in the absence of class II and class III ribonucleotide reductases due to hindered anaerobic growth" is **published**. It was published in *Frontiers in Microbiology* in May 2016. The impact factor of *Frontiers in Microbiology* in 2016 was **4.165**. The article presented in this thesis is an accurate representation of the published article, which can be found with DOI 10.3389/fmicb.2016.00688. Mr. Lucas Pedraz is the **second author** of this article.
- Article 5, titled "Gradual adaptation of facultative anaerobic pathogens to microaerobic and anaerobic conditions" is **sent for publication**. It was sent to *Environmental microbiology* in August 2019. The impact factor of *Environmental microbiology* in 2018, the latest available, was **5.147**. The article presented in this thesis constitutes an accurate reproduction of the version sent for publication (ID: EMI-2019-1258). Mr. Lucas Pedraz is the **first author** of this article, and shares with me the role of **corresponding author**.
- Article 6, titled "Optimal environmental and culture conditions allow the *in vitro* coexistence of *Pseudomonas aeruginosa* and *Staphylococcus aureus* in stable biofilms" is **sent for publication**. It was sent to *Scientific Reports* in August 2019. The impact factor of *Scientific Reports* in 2018, the latest available, was **4.011**. The article presented in this thesis constitutes an accurate reproduction of the version sent for publication (ID: SREP-19-24791A).

Barcelona, 26 September 2019

Thesis Director
Dr. Eduard Torrents

Annex 2: Report on the participation in the articles presented

I hereby declare that the participation of Mr. Lucas Pedraz in the articles presented in this thesis is as follows:

- Article 1. The two first authors (Lucas Pedraz and Anna Crespo), as stated in the published article, contributed equally to this work. Mr. Pedraz actively contributed to this study and was involved in the experimental work illustrated in figures 1, 2, 3, 4, 5 and 6, as well as in all supplementary figures and tables. He also contributed in the designing of the model illustrated in figure 8. Overall, he was involved in experiment design, experimental work, data analysis, and writing of the manuscript.
- Article 2. Lucas Pedraz contributed actively to this study and was involved in the experimental work illustrated in figures 2, 5, 7, S1, S2, S3, S4, and tables 1 and 2. Overall, Mr. Pedraz was involved in experimental work, data analysis, and writing of the manuscript. This manuscript in its published form was also included in the doctoral thesis presented by Dr. Anna Crespo in 2017. However, due to the implication of Mr. Lucas Pedraz in this article and its connections with article 3, I consider adequate to include it also as a part of this thesis.
- Article 3. Lucas Pedraz is the first author of this article, and shares with me the role of corresponding author. Mr. Pedraz actively contributed to the design of this study and all the experimental work presented, though SEC-MALS experiments and the purification of the $NrdR_2$ proteins were conducted in collaboration with Dr. Maria Solà group (IBMB-CSIC). Other than that, Mr. Pedraz is solely responsible for this work, including the writing of the manuscript as presented here.
- Article 4. Lucas Pedraz contributed actively to this study and was involved in the experimental work illustrated in figures 3, 4, 5 and table 1, as well as in the designing of the model illustrated in figure 6. Overall, Mr. Pedraz was involved in experimental work, data analysis, and writing of the manuscript. This manuscript in its published form was also included as a part of the doctoral thesis presented by Dr. Anna Crespo in 2017. However, due to the implication of Mr. Lucas Pedraz in this article and its connections with article 5, I consider adequate to include it also as a part of this thesis.
- Article 5. Lucas Pedraz is the first author of this articles, and shares with me the role of corresponding author. Mr. Pedraz actively contributed to the design of this study and all the experimental work presented. Confocal microscopy experiments and LIVE/DEAD counting were done by Lucas Pedraz and Nuria Blanco. Other than that, Mr. Pedraz is solely responsible for this work, including the writing of the manuscript.
- Article 6. This article is presented as an annex, as the role played in it by Mr. Lucas Pedraz was not as significant as for the other articles presented. Nevertheless, Mr. Lucas Pedraz participated in the part of the experimental design related to measuring oxygen consumption, and actively contributed to the work illustrated in figures 5, 7, and S3.

Other than the aforementioned cases, these articles have not been used as part of other doctoral theses.

Lucas Pedraz is the first author in 3 of the articles presented. I want to remark that, due to the high performance of Mr. Pedraz as a researcher, he is also corresponding author in two of these articles, which were submitted for publication recently.

Barcelona, 26 September 2019

Thesis Director

Dr. Eduard Torrents

Annex 3: Article 6

Optimal environmental and culture conditions allow the in vitro coexistence of *Pseudomonas aeruginosa* and *Staphylococcus aureus* in stable biofilms

Sent for publication to *Scientific Reports* (Q1, IF_{2018} = 4.011)

August 2019

María del Mar Cendra [1], Nuria Blanco[1], Lucas Pedraz[1], and Eduard Torrents[1*]

[1] Bacterial Infections: Antimicrobial Therapies, Institute for Bioengineering of Catalonia (IBEC), The Barcelona Institute of Science and Technology, Barcelona, Spain.

*: Corresponding author: Eduard Torrents (etorrents@ibecbarcelona.eu)

Abstract

The coexistence between species that occurs in some infections remains hard to achieve *in vitro* since bacterial fitness differences eventually lead to a single organism dominating the mixed culture. *Pseudomonas aeruginosa* and *Staphylococcus aureus* are major pathogens found growing together in biofilms in disease-affected lungs or wounds.

Herein, we tested and analyzed different culture media, additives and environmental conditions to support *P. aeruginosa* and *S. aureus* coexistence *in vitro.* We have unraveled the potential of DMEM to support the growth of these two organisms in mature cocultured biofilms (three days old) in an environment that dampens the pH rise. Our conditions use equal initial inoculation ratios of both strains and allow the stable formation of separate *S. aureus* microcolonies that grow embedded in a *P. aeruginosa* biofilm, as well as *S. aureus* biofilm overgrowth when bovine serum albumin is added to the system. Remarkably, we also found that *S. aureus* survival is strictly dependent on a well-characterized phenomenon of oxygen stratification present in the coculture biofilm. An analysis of differential tolerance to gentamicin and ciprofloxacin treatment, depending on whether *P. aeruginosa* and *S. aureus* were growing in mono- or coculture biofilms, was used to validate our *in vitro* coculture conditions.

Introduction

Most chronic infections occur due to the inherent capacity of some bacterial pathogens to grow in biofilms[1]. Although they have been historically investigated as monoculture events, some infection-associated biofilms are currently recognized to be mainly polymicrobial and involve synergistic interactions that often worsen the disease outcome[2,3].

Polymicrobial biofilms can develop greater antimicrobial resistance than single-species biofilms[4]. The way bacteria are distributed and interact with each other or with the host fluctuates depending on the environment[5,6]. For instance, *Pseudomonas aeruginosa*, in addition to forming large mushroom-shaped biofilm structures *in vitro*, can behave differently and form different bacterial arrangements *in vivo*. Clusters or aggregates perfectly arranged and determined by the different bacteria that are able to grow concurrently are more likely to occur during the establishment and persistence of the infection. Therefore, there is an intrinsic effect of the surrounding environment on the way microbes behave and establish their connections[3].

Regarding human pathogenesis, cystic fibrosis (CF) is a model example of how bacterial interactions within biofilms can modulate the outcome of the disease, thus playing a critical role in the patient's wellbeing[7]. CF is a lethal genetic disease characterized by the production of abnormal secretions in different organs[8]. Lungs especially are affected by CF. In the lung, a thick and dense mucus builds up over the pulmonary epithelium, converting it into the perfect niche for bacterial colonization and growth[9,10]. CF-affected lungs contain changing gradients of oxygen, nutrients and pH, which together provide a heterogeneous environment that favors the coexistence and proliferation of a wide range of microbial species and, consequently, exacerbating the progression of the disease[9]. *P. aeruginosa* and *Staphylococcus aureus* are two major pathogens commonly isolated from CF-affected airways and sputum. Although *S. aureus* usually colonizes the lung epithelium during childhood and *P. aeruginosa* is more likely to be acquired in the transition to adult life, both microorganisms have been detected coexisting and synergistically contributing to the disease severity[11,12]. A similar scenario is found in infected wounds, where both bacterial species can often be found infecting simultaneously[13]. Despite the knowledge that both organisms can grow in unison *in vivo,* it remains difficult to mimic the conditions that sustain this close relationship *in vitro.*

The discovery of the culture conditions able to maintain mixed *P. aeruginosa* and *S. aureus* simultaneous growth *in vitro* has become a scientific hotspot, and several studies can be found in the bibliography addressing the interactions of these microorganisms. In their attempt to elucidate the principles of the coexistence of these species, some studies have used a higher inoculation ratio of *S. aureus vs P. aeruginosa* to establish the mixed biofilm or introduced the latter once the *S. aureus* biofilm has been established[14]. Equal inoculation ratios of both microorganisms have also been tested; however, coexistence under these conditions did not last longer than 24 h or only information related

to the mixed biofilm biomass (not from each organism independently within the cocultured biofilm) can be found in the literature[15-17]. Some researchers used *P. aeruginosa* supernatant to evaluate its impact on the coculture system[18-20], while other studies were based on wound models[21,22].

Our study focused on deciphering the optimal coculture conditions and environmental requisites that would allow the simultaneous and stable growth of *P. aeruginosa* and *S. aureus* in mixed biofilms over time. We reasoned that the achievement of a stable *in vitro* coculture biofilm, able to grow with balanced populations of both organisms and to remain for an extended period of time, would be useful to understand the pathophysiology associated with the interaction of these two-species and for generating optimized chemotherapies to treat such biofilm-related diseases. Therefore, we developed a combination of coculture conditions that enable the stable formation of *P. aeruginosa* and *S. aureus* mixed biofilms on different abiotic surfaces. The coculture biofilms were formed using equal initial bacterial inoculation ratios and grew stably for up to three days of testing in an environmental background that dampens the pH rise. Furthermore, we provide evidence that *S. aureus* survival during coculture biofilm growth with *P. aeruginosa* is strictly dependent on oxygen diffusion. To validate the combination of the coculture conditions and environmental prerequisites identified, we treated the mixed biofilms with known antibiotics to confirm differences in antibiotic tolerance depending on whether the strains were growing in mono- or coculture biofilms.

Results

Testing and analyzing P. aeruginosa and S. aureus balanced population co-growth in different culture media.

The culturing conditions able to block the antagonistic relationship between *P. aeruginosa* and *S. aureus in vitro* have yet to be discovered. As shown in **Fig. A6:1a** - LB, when both bacterial strains are grown together in Luria-Bertani (LB) medium, *P. aeruginosa* tends to dominate the culture and compromise *S. aureus* survival in the system (at 28 h). As our goal was to achieve balanced and stable *P. aeruginosa* and *S. aureus* mixed growth, selection of the bacterial strains to use was thought to be crucial to accomplish our objective. In this study, we used the *P. aeruginosa* PA14 strain together with the *S. aureus* Newman strain. This pair of microorganisms has been used in other polymicrobial studies[15,18,23,24]; hence, we considered them suitable for use in our study.

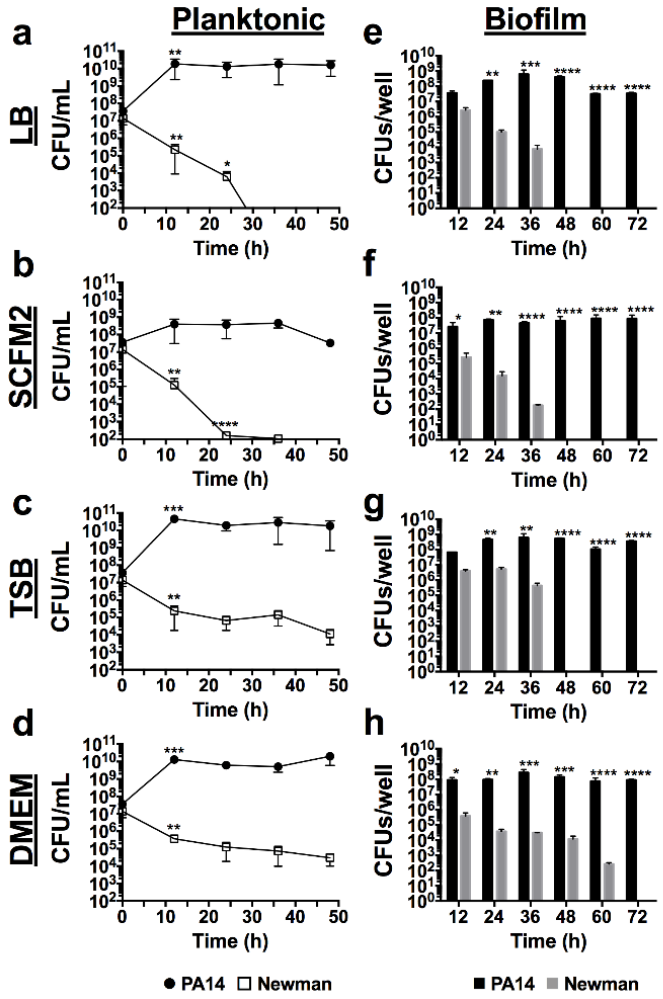

Figure A6:1. Time-course planktonic and biofilm growth *of P. aeruginosa* PA14 and *S. aureus* Newman in LB, SCFM2, TSB and DMEM. (a) $\log_{10}$ CFUs/mL of each bacterial strain during planktonic growth in coculture at the time of initial inoculation and after 12, 24, 36 and 48 h of incubation at 37ºC with shaking. (b) $\log_{10}$ CFUs/well of PA14 and Newman strains during coculture biofilm growth on 96-well polystyrene plates over 72 h of static incubation at 37ºC. Three independent experiments were performed for both experiments, and error bars indicate the standard error of the mean from the representative triplicate. Statistical significance between $\log_{10}$ CFUs/mL and between $\log_{10}$ CFUs/well at the different time points is indicated with an asterisk (*p<0.05; ** p<0.01; *** p<0.001; and **** p<0.0001).

LB, tryptic soy broth (TSB), Dulbecco's modified Eagle's medium (DMEM) and synthetic cystic fibrosis sputum medium 2 (SCFM2) were tested as a base to develop a medium that maintains the coexistence and growth of both organisms over time. Thus, mixed cultures of PA14 and Newman strains and the respective CFUs were analyzed after 0, 12, 24, 36 and 48 h of incubation. For PA14-Newman planktonic cultures grown in LB and SCFM2, a significant decrease in *S. aureus* Newman CFUs/mL (p<0.05) was detected during the initial 24 h of incubation with no CFUs counted after 24-36 h post-initial inoculation (**Fig. A6:1a, b** - LB and SCFM2). In contrast, TSB and DMEM maintained *S. aureus* Newman survival at ~10^5 CFUs/mL over the 48 h with no significant changes detected after 12 h (p>0.05; Fig. 1c, d - TSB and DMEM). PA14 growth was stable and maintained at ~10^{10}-10^{11} CFUs/mL in the different media tested except for SCFM2, in which the strain reached maximal growth at ~10^9 CFUs/mL (**Fig. A6:1** - planktonic).

Since *P. aeruginosa* and *S. aureus* are commonly found in chronic infections promoted by biofilm formation[11], this type of growth was examined next. Coculture biofilm growth was assessed in independent 96-well polystyrene microtiter plates after 12, 24, 36, 48, 60 and 72 h (**Fig. A6:1** - biofilm). Mixed biofilms grown in LB and SCFM2 showed similar patterns for PA14 and Newman strains in planktonic growth. However, while *Pseudomonas* maintained a constant number of biofilm-forming CFUs during the 72 h checked, the presence of Newman in the mixed biofilm progressively decreased, and by 48 h no *S. aureus* CFUs were detected in the cocultured biofilm (**Fig. A6:1e, f** - LB and SCFM2). Similar to the results obtained in the planktonic experiments, coculture growth in TSB or DMEM enhanced *S. aureus* survival in the mixed biofilm. However, while TSB supported Newman growth at ~10^6 CFUs/well for 36 h of incubation, *S. aureus* survival dropped by 48 h, with no countable CFUs detected from that time onward (**Fig. A6:1g** - TSB). In contrast, DMEM promoted constant Newman growth (~10^5-10^4 CFUs/well) in the mixed biofilm during the initial 48 h analyzed, with a slight decrease to ~10^2 CFUs/well after 60 h of incubation; no countable CFUs were detected only after 72 h (**Fig. A6:1h** - DMEM). Although significantly increased viability of *S. aureus* was detected when coculture biofilm was growing in DMEM, percentage numbers of the organism within the mixed biofilm did not vary among the media used (**Supplementary Table A6:S1**). PA14 levels within the mixed biofilm were similar among the four media tested, with ~10^7-10^8 CFUs counted per well during the 72 h of the course of the experiment (**Fig. A6:1** - biofilm).

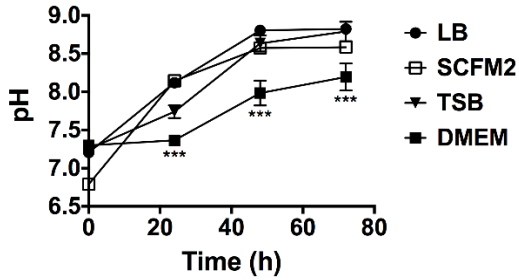

Figure A6:2. pH evolution during coculture biofilm growth in different culture media. The plot shows the pH measurements of the different supernatant phases of *P. aeruginosa* PA14 and *S. aureus* Newman coculture biofilms grown in LB, TSB, SCFM2 and DMEM. Measurements were performed at the time of initial inoculation (0 h) and after 24, 48 and 72 h of incubation at 37ºC. Statistical significance of the pH measured in DMEM at different time points compared to the pH measured in the other media at the same time points is denoted with asterisks (**** p*<0.001).

The physiochemical environment where microbes grow can influence the bacterial distribution in the community[3]. Furthermore, pH homeostasis is critical to maintaining the integrity of all living cells[25,26]. Therefore, we next thought it important to examine the pH change during the coculture biofilm growth in the different media tested. The pH was evaluated at the initial establishment of the biofilms in microtiter plates at 37ºC and after 24, 48 and 72 h. Differences in pH changes were found depending on if biofilms were grown in monoculture (Supplementary **Fig. A6:S1**) or coculture (**Fig. A6:2**). As shown in Figure A6:2, the pH rapidly increased when biofilms were grown in LB, SCFM2 or TSB, reaching pH ~8.7-8.8 by 48 h of incubation when growing in coculture. However, in DMEM, the pH was reduced and measured ~0.5-1 lower, (p<0.001) compared to that of the other media during the 72 h tested. This rapid increase of pH was not observed when both organisms were grown in monoculture biofilms (**Supplementary Fig. A6:S1**). In that case, pH tended to be maintained or acidified (especially for *S. aureus* monoculture biofilms), during the 72 h examined.

Taken together, these results indicate that DMEM has the highest potential to maintain *S. aureus* survival over time when grown together with *P. aeruginosa.*

Optimizing P. aeruginosa and S. aureus coculture conditions.

Several conditions have been described to influence *P. aeruginosa* and *S. aureus* fitness. Accordingly, we next looked for molecules or additives to supplement the DMEM with the aim of increasing Newman survival in the mixed biofilm. Therefore, nicotinamide adenine dinucleotide phosphate (NADPH; 0.2 mM), adenosine monophosphate (AMP; 10 mM), bovine serum albumin (BSA; 5% w/v) and L-arginine (L-arg; 0.4% w/v) were chosen to be tested for the ability to compromise *P. aeruginosa*

pathogenesis (AMP, BSA and L-arg), influence *S. aureus* fitness (BSA) and combat oxidative stress (NADPH)[16,21,27-29].

To evaluate the effect of the different additives, mixed biofilms were grown in independent microtiter plates in DMEM supplemented with NADPH, BSA, AMP or L-arg (**Fig. A6:3** and **Supplementary Table A6:S2**) for 72 h at 37ºC, and the respective biofilm-forming CFUs were counted on selective agar plates. Generally, no major differences were detected in PA14 growth (CFU/well) within the coculture biofilm with any of the additives used compared to nonsupplemented DMEM (**Fig. A6:1h** - DMEM). Furthermore, *P. aeruginosa* CFUs/well were ~10^7-10^8 at all time-points and conditions checked (**Fig. A6:3**). A different scenario was observed with the *S. aureus* strain. Although all additives tended to maintain stable *S. aureus* Newman levels of ~10^6-10^7 CFUs/well during the initial 24 h (**Fig. A6:3**), the NADPH- or AMP-supplemented medium (**Figs A6:3a, c**) did not enhance *S. aureus* growth after 36-48 h of incubation compared to nonsupplemented medium and by 60 h, no Newman CFUs were counted within the mixed biofilm in these two incubatory conditions. In contrast, coculture incubation in DMEM+BSA or DMEM+L-arg promoted sustained *S.* aureus CFU numbers of ~10^5-10^6 during the initial 48 h of the experiment, and these numbers decreased only after 60 h of incubation. Significantly, while in the presence of BSA, *S. aureus* CFUs were ~10^4 CFUs/well after 72 h of incubation; the L-arg condition showed a gradual decrease in the viability of the cocci, with ~10^2 CFUs/well counted at the end of the experiment (**Figs A6:3b, d**). Remarkably, all additives increased the *S. aureus* cell percentage within the mixed biofilm if compared to that calculated in coculture biofilms grown in unsupplemented DMEM (**Supplementary Table A6:S1**), with percentages calculated ~12 – 25 % of the total mixed biofilm (**Supplementary Table A6:S2**).

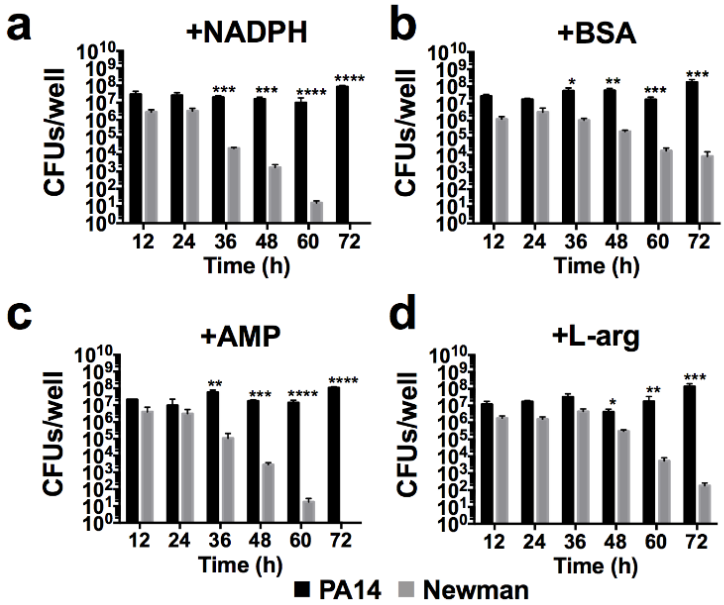

Figure A6:3. Effect of NADPH, BSA, AMP and L-arg on extending *S. aureus* survival during coculture biofilm growth with *P. aeruginosa*. Coculture biofilms were grown *in vitro* on 96-well polystyrene plates for 72 h in static conditions at 37ºC. The different graphs show biofilm cells of *P. aeruginosa* and *S. aureus* $\log_{10}$ CFUs/well during biofilm growth in DMEM supplemented with NADPH at 0.2 mM (a), BSA at 5% w/v (b), AMP at 10 mM (c) and L-arg at 0.4% w/v (d) after 12, 24, 36, 48, 60 and 72 h. Conditions were tested in triplicate, and bars represent the mean of three independent experiments. The standard error of the mean is included in the plots. Significant differences between PA14 and Newman CFUs/well at the different incubation times are indicated by asterisks (*p<0.05; ** p<0.01; *** p<0.001; and **** p<0.0001).

Oxygen diffusion within PA14-Newman mixed biofilms plays a key role in maintaining balanced bacterial populations.

The next step was to evaluate other environmental parameters that could influence the coculture biofilm during *in vitro* growth. Since oxygen competition between *P. aeruginosa* and *S. aureus* has been described to compromise the viability of the latter in a CF model[15], this parameter was next assessed in our system.

We next aimed to identify the position inside the well where PA14-Newman biofilm growth occurred and to detect possible differences when compared to monoculture biofilm growth. Crystal violet staining of 48 h-old biofilms confirmed that the bacterial biofilm growth was limited to the air-liquid interphase (ALI) area of the microplate well (**Fig. A6:4a**). These results indicate that the CFU values determined in **Figure A6:3** come from cocultured biofilms formed in the ALI area of the microtiter plate. OD_{570} measurements revealed that PA14 forms a larger monoculture than the *S. aureus* strain. Interestingly, no additive effect was observed in the PA14 biofilm during coculture biofilm growth with *S. aureus* (**Supplementary Fig. A6:S2**).

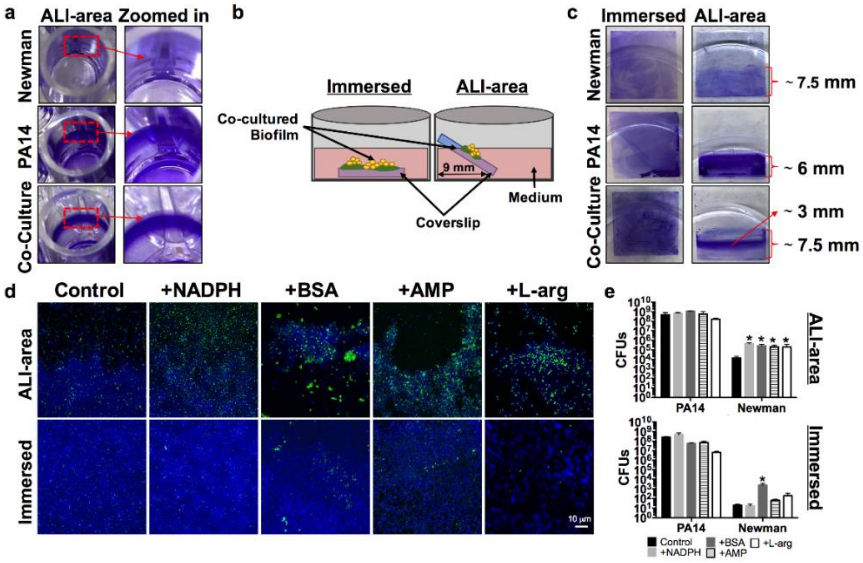

Figure A6:4. Balanced *P. aeruginosa* PA14 and *S. aureus* Newman populations growing in a coculture biofilm is dependent on the air availability. Total PA14 and Newman biomass grown in monoculture or coculture biofilms and stained with crystal violet. (a) Pictures show the biofilm growth of monoculture and coculture biofilms in the air-liquid interphase area (ALI area) of a 96-well plate. A zoomed image highlighting a region of interest of each biofilm is included in the figure. (b) Schematic representation of the coverslip position within the well during incubation of the PA14-Newman coculture biofilm immersed in the medium or in the ALI area. (c) Biofilm biomass staining of PA14 and Newman mono- and coculture biofilm growth over a coverslip immersed or in the ALI area. The length of the stained area in the coverslip is included on the plot. (d, e) PA14-Newman coculture biofilms grown in the ALI area or immersed in DMEM (control) and DMEM + NADPH, BSA, AMP and L-arg. (d) Confocal images of the mixed biofilms at the different time points were taken at 63X magnification, PA14 is shown in blue (DAPI) and Newman in green (CF^{TM}-488A). A representative image of each biofilm from three independent experiments. (e) Plots show the different log_{10} value of PA14 and Newman CFUs covering each coverslip after 3 days of incubation. The results show the mean of three independent experiments with the corresponding standard error of the mean. Statistical significance (p<0.05) compared to the relative bacterial control condition is indicated by an asterisk (*) over each bar.

To further investigate the role of oxygen during coculture biofilm formation, we changed the *in vitro* microplate model to use coverslips. Thus, to analyze the immersed biofilm growth, the coverslip was placed in the bottom of the well of a 6-well plate and completely submerged in the medium. To assess the biofilm growing in the ALI area, the coverslip was positioned to line the well wall (see schematic representation in **Fig. A6:4b**). Crystal violet staining of 48 h-old biofilms revealed no significant differences between immersed biofilms, with similar intense violet staining detected between the mono- and cocultured biofilms (**Fig. A6:4c**). However, clear differences were observed between biofilms grown in the ALI area. While the PA14 monoculture biofilm showed more intense violet staining than the Newman monoculture biofilm, greater biofilm coverage of the coverslip was observed with the *S. aureus* strain (**Fig. A6:4c**). Measurement of the stained biofilms revealed that the Newman monoculture biofilm covered ~7.5 mm of the coverslip, in contrast to the ~6 mm covered by the PA14 monoculture biofilm. An intensive violet-stained band of ~3 mm was detected in the middle of a greater coverage area of ~7.5 mm when both organisms were grown in unison (**Fig. A6:4c**).

Coculture viability was next analyzed to assess the coexistence of both organisms within the mixed biofilm depending on the proximity to the medium surface during growth. Since increased coculture biofilm was obtained in the presence of NADPH, BSA, AMP and L-arg in 96-well plates (**Fig. A6:3**), these additives were also included in the experiment. After three days of incubation, a greater presence of *S. aureus* was observed by confocal microscopy when biofilms were grown in the ALI area compared to when they were grown completely immersed in the medium (**Fig. A6:4d**). Increased growth of *S. aureus* in the ALI area was also confirmed by CFU counting (**Fig. A6:4e**). In the nonsupplemented DMEM (control) and DMEM+NADPH conditions, the *S. aureus* strain appeared to be dispersed over the glass, whereas in DMEM+BSA, DMEM+AMP and DMEM +L-arg, the strain emerged embedded in aggregates within the PA14 biofilm **(Fig. A6:4d** - ALI area). In the validation of the results obtained in **Figure A6:3**,

significantly increased numbers of the Newman strain were counted in the mixed biofilms incubated in DMEM including the different additives (**Fig. A6:4d**). A different scenario was observed when biofilms were grown immersed in the medium, wherein PA14 completely covered the different coverslips, and the Newman strain was barely detected (**Fig. A6:4d** - Immersed). Only Newman CFUs counted in the mixed biofilm grown in DMEM+BSA showed a significant increase relative to the control condition (p<0.05), although the levels were drastically reduced compared to those counted in the ALI area (**Fig. A6:4e**). Interestingly, the addition of L-arg to the system resulted in a more dispersed PA14 biofilm formation compared to that visualized with the other additives (**Fig. A6:4d** - L-arg).

Overall, these results confirm that although different additives increase *S. aureus* survival during mixed biofilm growth with *P. aeruginosa*, biofilm formation in the ALI area is fundamental to achieving this enhanced survival of *S. aureus*.

A gradient of dissolved oxygen in the coculture biofilm system explains the differential bacterial growth

Different oxygen concentrations across the culture system may explain differential bacterial growth within the coculture biofilm. To validate this hypothesis, the dissolved oxygen concentration during biofilm incubation was measured in different areas of interest using an oxygen microsensor system (**Fig. A6:5**, **Supplementary Fig. A6:S3**). Thus, the oxygen consumption rates in the area immediately above the immersed biofilm (ALI area) and in the medium surface (top position) were measured and analyzed over time (**Fig. A6:5a**). Additionally, a spatial oxygen profile was also measured in the medium immediately after the bottom area became depleted of oxygen (**Fig. A6:5b**). The microsensor measurements reflected a gradual decrease in the oxygen content from ~5.5 (~80% of the dissolved oxygen) to ~0 mg/L in the initial ~80 min when the PA14-Newman combined biofilm was growing completely immersed in the medium (**Fig. A6:5a**, green line). However, sensor placement in the ALI area (Fig. 5a, red line) confirmed a maintained oxygen concentration of ~5.5 mg/L during these initial 80 min. Progressive oxygen consumption was detected after that time point, reaching ~1 mg/L (~20% of the dissolved oxygen) by ~110 min from the initial incubation. Interestingly, the oxygen concentration was sustained at ~1 mg/L for approximately ~50 additional minutes before decreasing to ~0.5 mg/L (~6% of the dissolved oxygen). The oxygen levels were then maintained at ~0.5 mg/L without reaching complete depletion. A different result was obtained when the sensor was placed close to the medium surface (top position; **Fig. A6:5a** - blue line). In this position, and comparable to the ALI area, a sustained concentration of ~5.5 mg/L was measured during the initial 80 min of incubation. However, in this case, a linear oxygen decrease occurred immediately after that time point, reaching 0 mg/L after ~125 min (**Fig. A6:5a**). Analysis of the oxygen stratification at different depths revealed that most of the medium in which the coculture biofilm was growing was oxygen-free. This area showed 0 mg/mL oxygen and accounted for the initial ~3 mm of the medium depth. Only the area closest to the

surface, the first ~1 mm, revealed oxygen content and showed a progressive increase that reached ~6.5 mg/L (~95% of the dissolved oxygen) at the medium surface (**Fig. A6:5b**).

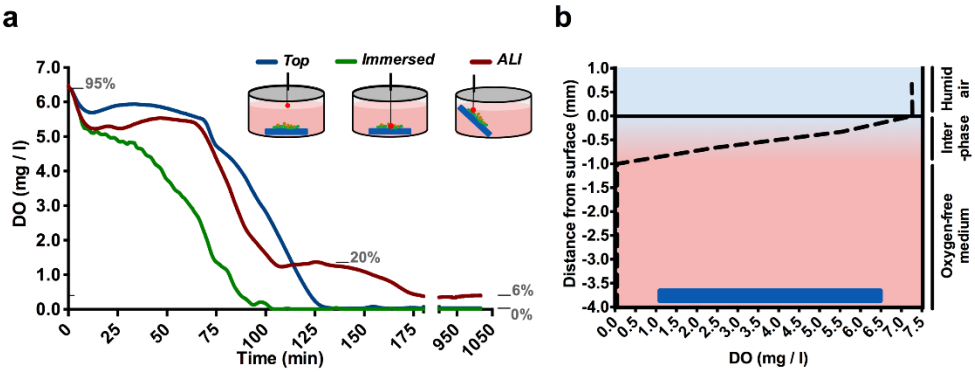

Figure A6:5. Differences in oxygen concentration depending on the position in the well where PA14 and Newman are cocultured and growing. Dissolved oxygen concentration (DO) was determined in the different areas of interest in the PA14 and Newman *in vitro* coculture biofilm model. (a) Plot shows the DO (mg/L; ppm) given by the optical fiber microsensor, depending on the position placed in the coculture system: top, immersed and in the ALI area. A schematic showing the approximate position of each measurement is included in the plot. The equivalence of significant DO values to the percentage of dissolved oxygen saturation (gray numbers) is provided as a reference. (b) DO at different depths of the culture well after the immersed area reached a DO of 0 mg/L (approximately 85 min of incubation). An interpretation of the oxygenation states across the different layers is provided on the right: **1**, humid air (the oxygen value is a result of the saturation of the sensor); **2**, oxygenated interphase; and **3**, anaerobic culture.

These results may suggest that, given the proximity to the surface, the ALI area would not reach oxygen depletion and would be able to maintain some oxygen content even though it would be a low percentage of the dissolved oxygen.

DMEM supports P. aeruginosa and S. aureus balanced coculture biofilm growth and stabilization over time.

To reinforce the potential of our developed DMEM culture conditions in forming and preserving *P. aeruginosa-S. aureus* mixed biofilms, we established a continuous-flow biofilm. Continuous-flow biofilms are the closest approximation known for the growth of biofilms with similar physical, chemical and biological heterogeneity as those naturally formed *in vivo*[30].

After three days of continuous flow, we confirmed that only DMEM was able to sustain stable growth of both populations in the biofilm. Mixed biofilms grown in TSB (**Fig. A6:6a**) or TSB supplemented with BSA (**Fig. A6:6b**) did not show any growth or increase in *S. aureus* survival within the coculture system compared to those in DMEM (**Figs A6:6c, d, f**). Biomass evaluation using the COMSTAT 2 software determined that when the experiment was performed in TSB, *P. aeruginosa* accounted for ~90% of the

coculture biofilm, while *S. aureus* accounted for only ~10% of the system. The addition of BSA to TSB barely increased *S. aureus* growth, and its presence in the coculture biofilm was calculated to be ~15% in this incubatory condition (**Fig. A6:6f**). However, coculture biofilms grown in DMEM or DMEM+BSA revealed an increased presence of *S. aureus* when they were visualized with a confocal microscope (**Figs A6:6c, d**). In general, we observed that both strains did not grow mixed together but independently and well distributed in the flow-cell channel. Interestingly, while microcolonies of *S. aureus* were detected growing embedded in the PA14 biofilm in unsupplemented DMEM (**Fig. A6:6c**), a thick and compact layer of *S. aureus* was visualized covering the *P. aeruginosa* biofilm when BSA was added to the flow system (**Fig. A6:6d**). COMSTAT 2 software revealed that this dense layer of Newman biofilm had an average thickness of ~12.50 μm, whereas the *P. aeruginosa* biofilm growing the beneath *S. aureus* was ~6.73 μm thick.

The orthogonal views, 3D representations and evaluation of the different regions of interest (ROIs) of the coculture biofilms were next analyzed to assess how bacterial populations were distributed within the mixed biofilm system. Our experimental approach confirmed the presence of *S. aureus* microcolonies growing in clusters within PA14 biofilms during growth with DMEM (**Fig. A6:6c**). Two schematic drawings are presented in **Fig. A6:6e** to clearly show how bacterial populations are distributed within the coculture biofilm during growth in DMEM and DMEM+BSA. Enumeration of these microcolonies revealed an average growth of approximately 65-90 of cells per bacterial aggregate, with a maximum count of approximately ~150 of Newman cells (**Supplementary Fig. A6:S4**). These image analyses also verified that *S. aureus* biofilm growth occurred on top of the *P. aeruginosa* biofilm, which was particularly evident during incubation with DMEM+BSA (**Fig. A6:6d, e**). These results are in agreement with those presented in **Figure A6:4**. Therefore, both bacterial species maintain separate growth and distribution in coculture biofilms. Biomass evaluation revealed balanced growth of both bacterial populations of ~35% and ~65% for Newman and PA14, respectively, during incubation in DMEM (**Fig. A6:6e**). However, and confirming the confocal microscopy observations, a greater percentage of the *S. aureus* Newman population was measured in DMEM+BSA, accounting for ~70% of the total coculture system (**Fig. A6:6f**).

The continuous-flow biofilm confirmed that DMEM favors the coexistence of *P. aeruginosa* and *S. aureus* in mixed biofilms. Furthermore, we also detected how the addition of BSA changed the architecture of the biofilm by increasing *S. aureus* proliferation and identified different spatial distributions of the strains in the biofilm.

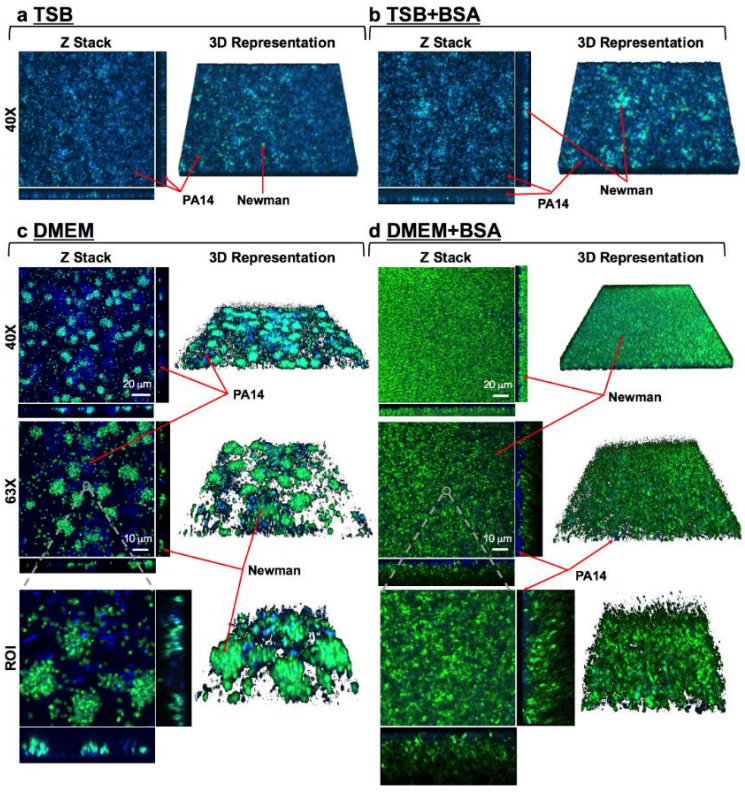

TSB		TSB+BSA		DMEM		DMEM+BSA	
PA14	Newman	PA14	Newman	PA14	Newman	PA14	Newman
90%	10%	85%	15%	65%	35%	30%	70%

Figure A6:6. Balanced and stable *P. aeruginosa* PA14 and *S. aureus* Newman strain populations within a three-day-old mixed biofilm grown in continuous flow. PA14 and Newman were grown simultaneously in a continuous-flow biofilm in TSB (a), TSB+BSA (b), DMEM (c) and DMEM+BSA (d) for three days. At the indicated time point, the biomass growing over the different channels was stained with DAPI (blue, PA14) and CF^{TM}-488A (green, Newman) and visualized using confocal microscopy. The figure shows the composite of the sum of the slices (Z Stack), with the respective orthogonal views, and the 3D representation of each mixed biofilm formed using both ImageJ and ZEN software. Mixed biofilms were tested in triplicate, and a representative image from those taken at magnifications of 40X and 63X is shown. A region of interest (ROI), including the different microscope projections and representations, is also presented in the figure. Red arrows indicate PA14 and Newman strains within the mixed biofilm. (e) Schematic representations of the cocultured biofilm depending on growth in DMEM or DMEM+BSA from the previous confocal microscope Z-stacks and orthogonal views. *P. aeruginosa* is represented in blue, and *S. aureus* is represented in green. (f) Table shows the percentage of blue *Pseudomonas* and green *Staphylococcus* present in the different cocultured biofilms calculated from the different microscope stacks using the COMSTAT 2 software.

Oxygen stratification within the coculture biofilm is a key modulator of PA14 and Newman coexistence.

We next wanted to verify the existence of an oxygen-stratified environment in the continuous-flow biofilm that may influence *S. aureus* survival and stable growth alongside *P. aeruginosa*. Oxygen diffusion within the biofilm was evaluated with the assumption that fresh and oxygenated medium was added continuously in the system (~6.5 mg/mL oxygen measured with the oxygen microsensor).

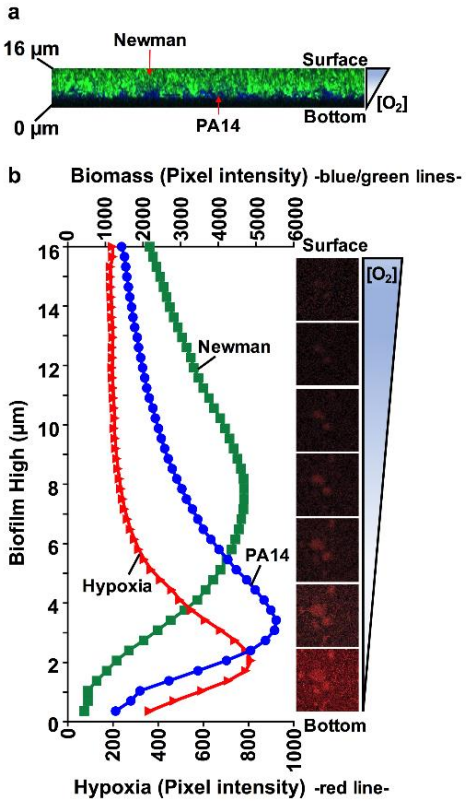

Figure A6:7. Oxygen stratification within the cocultured biofilm determines the spatial distribution of *P. aeruginosa* and *S. aureus* and their coexistence. (a) XZ-orthogonal view of a *P. aeruginosa* and *S. aureus* coculture biofilm grown in DMEM+BSA (see Fig. 6d). The image shows the separate position of Newman and PA14 within the ~16 µm-biofilm and the possible oxygen gradient present in the system. (b) Graph shows the average pixel intensities of PA14 (blue) and Newman (Green) biomasses (plotted on the left Y-axis) compared to the oxygen-related red intensity (plotted on the right Y-axis) along the different thicknesses (µm) of a 3-day-old co-cultured biofilm in flow. Pixel intensity averages were calculated from ten different images using ImageJ software. Included in the figure, is a sequential set of micrographs showing the red fluorescence emission given by the hypoxia probe through the different biofilm layers, indicating the oxygen stratification present along the thickness of the continuous-flow cocultured biofilm. Intense red emission relates to the hypoxic environment through the different biofilm depths (µm), from the bottom to the surface, additionally indicated with a schematic of the oxygen gradient present in the system.

Orthogonal views of the coculture biofilm grown in the flow-cell channel confirmed the clear distribution of the *S. aureus* biofilm on top of *P. aeruginosa* in the area closest to the medium surface (**Fig. A6:7a**). Consequently, we next wanted to validate the presence of an oxygen gradient that could be crucial for Newman survival in the mixed biofilm, and a key modulator of the bacterial distribution detected. To probe different oxygen concentrations within the coculture system, the continuous-flow biofilm was analyzed using the Hypoxia Probe dye. The key attribute of this dye is that its fluorescence is quenched by oxygen, so the lower the oxygen concentration is, the greater the red fluorescence signal emitted by the stained cells, thus allowing the detection of an anaerobic environment. Red-light emission (hypoxia) through the different layers of the coculture biofilm confirmed the bright fluorescence during the initial ~4 μm of biofilm thickness that gradually decreased across the bacterial community. Red fluorescence was barely detected in the more superficial biofilm layers, thus confirming aerobic conditions in that area (**Fig. A6:7b**). Additionally, pixel intensity analysis of the hypoxic region (red) corroborated that red emission peaked around the initial ~2 μm of the biofilm depth. Furthermore, the PA14-Newman biomass was also quantified in this continuous-flow biofilm. *P. aeruginosa* PA14 (blue) displayed a maximum peak intensity at ~3 μm of the biofilm depth, corresponding to the more anaerobic region of the biofilm, with fluorescence extending to a thickness of ~10 μm. *S. aureus* Newman (green) clearly showed a pixel intensity curve shifted to higher and more oxygenic biofilm layers (**Fig. A6:7b**). Green intensity measurements confirmed that *S. aureus* was barely detectable in the initial ~3 μm of the mixed biofilm (coinciding with the anoxic part of the biofilm); the intensity increased, achieving a maximum and extended peak at ~6-9 μm of depth, with fluorescence emission extending to ~14–10 μm of the biofilm thickness.

Taken together, these results demonstrate that the coculture biofilm formed in continuous flow also displays oxygen stratification across the different biofilm layers. *P. aeruginosa* growth occurred across the deepest layers of the biofilm, where less oxygen content was detected, while *S. aureus* biofilm growth was quantified closer to the biofilm surface, corresponding to the most oxygenated area.

Antibiotic resistance of P. aeruginosa and S. aureus is critically increased during coculture biofilm growth.

Biofilm-associated infections have historically been treated as single-species events. Nevertheless, some of these infections are now known to be composed of multiple combinations of bacteria, involving complex interactions that can influence their fitness and antibiotic tolerance[2,4]. The demonstration of altered antibiotic susceptibilities of PA14 and Newman when grown in coculture biofilms was thought to be necessary to validate the combination of coculture conditions and environmental prerequisites identified in this study. Hence, 72 h-old PA14 and Newman mono- and coculture biofilms were treated with ciprofloxacin (Cpx) and gentamicin (Gm). The respective biofilm-forming CFUs were subsequently counted on selective agar. The antibiotics and concentrations used were chosen according to their reported minimal inhibitory concentrations (MICs) and their usage in

treating both bacterial infections[4,31]. The experiment was performed in a 96-well microtiter plate and included BSA since it was the additive that showed the greatest potential for maintaining the stable growth of both bacterial populations *in vitro*.

Bacterial CFUs that remained viable within the mono- and the coculture biofilms after the antibiotic treatment were enumerated (**Supplementary Table A6:S3**), and the percentages of viable CFUs that persisted in each biofilm after the different treatments, compared to each untreated biofilm, were subsequently calculated (**Fig. A6:8**). Crystal violet staining of control wells confirmed that the mature biofilm grew in the ALI area of the well (data not shown). A similar behavioral pattern was observed in both organisms after the respective antibiotic treatments; however, *S. aureus* revealed a much greater benefit of growing in coculture than *P. aeruginosa,* since its viability during both treatments increased exponentially when grown in coculture with *P. aeruginosa*. Compared to the monoculture biofilm treatment, the growth of *P. aeruginosa* in coculture increased in the presence of 0.5 and 1 μg/mL doses of Gm by ~5- and ~4-fold, respectively (**Fig. A6:8a** - graph PA14%), and ~5- and ~57.5-fold in the presence of Cpx at the same concentrations as Gm (**Fig. A6:8b** - graph PA14%). Interestingly, *P. aeruginosa* exhibited greater tolerance to Gm than to Cpx, since none of the Gm concentrations used were sufficient to completely clear this bacterium from any of the cultured biofilms. Cpx at ≥1 and ≥4 μg/mL cleared PA14 from the mono- and coculture biofilms, respectively (**Figs A6:8a**, b-graph PA14%). The percentage calculations revealed that growing *S. aureus* in coculture enhanced its capacity to grow in the presence of Gm >835-fold, at a concentration of 0.5 μg/mL, and >505-fold at 1 μg/mL (**Fig. A6:8a** - graph Newman%). A similar pattern was detected for Cpx treatment; within a coculture biofilm with *P. aeruginosa,* the viability of *Staphylococcus* increased ~42-fold when the antibiotic was used at 0.5 μg/mL and ~7-fold when it was used at 1 μg/mL (**Fig. A6:8b** - graph Newman%). Only doses ≥2 μg/mL of either Gm or Cpx cleared *S. aureus* from the mixed biofilm. In contrast, treatments with 0.5 μg/mL Gm and 1 μg/mL Cpx were sufficient to clear *S. aureus* from a 72 h-old monoculture biofilm. When these high concentrations were used, the viability of the *S. aureus* strain was drastically reduced.

Comparisons between the percentages of the viable *P. aeruginosa* and *S. aureus* CFUs in the coculture biofilm after the antibiotic treatments to those calculated in the monoculture biofilms revealed significance in all cases (p<0.001). These results confirm the increased antibiotic tolerance of *P. aeruginosa* PA14 and *S. aureus* Newman strains when grown in a mixed biofilm rather than in a monoculture biofilm, thus validating the coculture conditions established in this study.

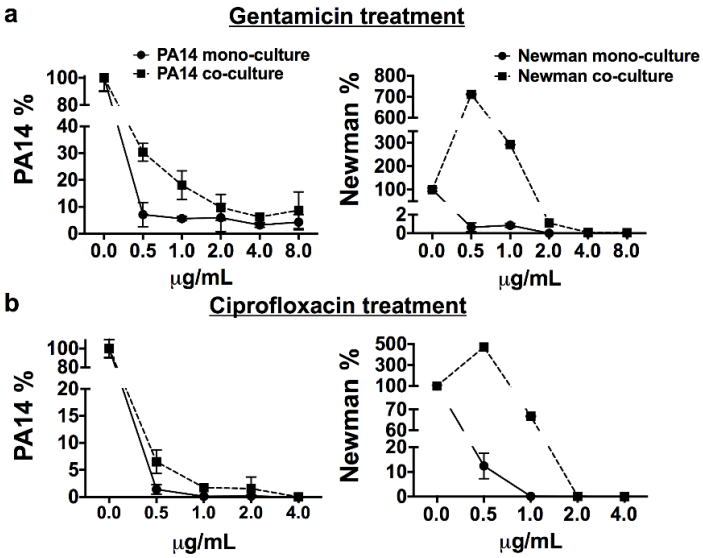

Figure A6:8. *P. aeruginosa* PA14 and *S. aureus* Newman coculture biofilms induce enhanced tolerance to antibiotic treatment compared to monoculture biofilms. After 72 h, matured mono- and cocultured PA14 and Newman biofilms grown in microtiter plates were treated with 0.5, 1.0, 2.0, 4.0 and 8.0 μg/mL gentamicin (a) and 0.5, 1.0, 2.0, and 4.0 μg/mL ciprofloxacin (b) for 15 h. Symbols in the plots represent the remaining percentage of CFUs of each strain in the biofilm after different antibiotic treatments compared to the relative untreated biofilm. Each graph shows the percentages of PA14 and Newman CFUs compared according to whether the biofilms were grown in mono- or coculture. Percentages were calculated according to the bacterial CFUs counted on selective agar plates after different antimicrobial treatments (Supplementary Table S3). Analysis of the statistical significance between the calculated percentages of bacterial CFUs that remained in the cocultured biofilm (after each antibiotic treatment) and those calculated in the monocultured biofilms revealed significance with $p<0.0001$ in all cases.

Discussion

Biofilm-associated infections are currently a critical worldwide threat[32-34]. The increasing emergence of antimicrobial-resistant bacteria and the knowledge that some of these infections are polymicrobial challenge the antimicrobial chemotherapy to administrate and aggravates the disease outcome[2,35,36]. *P. aeruginosa* and *S. aureus* are two major pathogens commonly found growing together in intricate biofilms in disease-affected lungs[11] or wounds[13]. Herein, we have unraveled the potential of DMEM to sustain a *P. aeruginosa* PA14 and *S. aureus* Newman combined biofilm for up to three days *in vitro* and identified BSA as a valuable and critical additive that significantly increases *S. aureus* survival and growth in the coculture system. Remarkably, we also demonstrated the importance of continuous oxygen diffusion in limiting *S. aureus* survival and keeping the growth of both bacterial populations balanced, highly influencing their distribution in the coculture biofilm. Furthermore, using our developed coculture conditions, we confirmed that the antimicrobial susceptibilities of *P. aeruginosa* and *S. aureus* differ depending on whether they are growing in monoculture or coculture in biofilms.

Among the different media evaluated (LB, TSB and SCFM2), DMEM was the greatest at controlling *S. aureus* survival during simultaneous growth (planktonic and biofilm) with *P. aeruginosa*. DMEM is a rich culture medium used in routine cell culture experiments, which contains numerous amino acids, vitamins, and inorganic salts, among other components[37]. Remarkably, the D-glucose concentration in this medium is ~17.5 mM, which is greater than the usual 0.2% (~11.1 mM) added to LB or TSB medium in routinely used biofilm formation protocols[38-40], or the 3 mM present in the SCFM2 medium[41]. In healthy people, glucose concentration in the airway surface liquid (ASL) is ~0.4 mM, 12 times lower than blood glucose[42,43]. However, lung inflammation, caused by diseases such as CF or chronic airway inflammation, increases glucose flux through the epithelial cell membrane, raising ~10-12 times the glucose concentration in the ASL. Different studies have described how increased glucose levels in ASL promote bacterial lung infection[42,44,45]. Furthermore, diabetes-affected people have wound healing issues and increased risk of infection due to an impaired host defence[46]. Glucose is not the preferred carbon source of *P. aeruginosa*[47] but is the preferred carbon source of *S. aureus,* which exhibits preferential uptake of this sugar, especially during infection[48]. Therefore, it is plausible to hypothesize that *S. aureus* could benefit from the high glucose concentration in DMEM and grow without competition for the substrate. Additionally, a differential planktonic growth pattern was detected in *S. aureus* Newman depending on whether the bacterium was grown in DMEM or TSB (**Supplementary Fig. A6:S5**). In DMEM, *S. aureus* grew rapidly and achieved late-exponential/stationary phase, with growth maintained during the course of the experiment. However, in TSB, the strain exhibited the usual bacterial growth curve with lag, exponential and stationary phases. This result indicates increased efficiency of *S. aureus* growth in DMEM, especially during the initial stage of growth, which we hypothesize could be beneficial during simultaneous biofilm growth with *P. aeruginosa* to rapidly form a microcolony after initial attachment, thus providing defense against *Pseudomonas*[49]. *S.*

aureus growth in firmly packed microcolonies during coculture biofilm growth with *P. aeruginosa* PAO1 has been previously seen by Yang and coworkers[50]. In our study, this microcolony formation may also be facilitated by the increased concentration of NaCl present in the DMEM formulation (~120 mM), which is >3-fold higher than in LB, TSB or SCFM2 and has been seen to stimulate biofilm aggregation and growth[51,52]. The concentration of glutamine present in DMEM (~2.5 mM) may also affect the coexistence of both microorganisms by diminishing the specific competition for this amino acid, as a nitrogen and energy source, which has been recently reported to occur early during coculture[53].

Significantly, DMEM contains HEPES (4-(2-hydroxyethyl)-1-piperazineethanesulfonic acid; ~15 mM), which is considered a "good buffer" for its limited effect on biochemical reactions and for being chemically and enzymatically stable, among other properties[54]. The buffering properties of HEPES were evident in the growing coculture biofilms, and the pH rise was dampened compared to that measured in the other media (**Fig. A6:2**). pH homeostasis is critical to maintaining the integrity of cytoplasmic proteins in all living cells, and their optimal pH fluctuates in a narrow range of 7.4-7.8[25,26]. Although SCFM2 contains 3-morpholinopropanesulfonic acid, it failed to maintain the pH levels in the coculture. This synthetic CF medium was developed based on CF sputum that contained high concentrations of *P. aeruginosa*[41], which may explain why SCFM2 did not support *S. aureus* viability in the system. Additionally, a factor increasing the perturbation of *P. aeruginosa* and *S. aureus* coexistence in this fluctuating pH environment is the production of different proteases by *P. aeruginosa* in an alkaline environment of pH ~8. In particular, the *P. aeruginosa* staphylolytic protease LasA possesses optimal activity at approximately pH 8.5[55-57].

DMEM supplementation with BSA and L-arginine increased *S. aureus* viability throughout the 72 h of coculture biofilm growth with *P. aeruginosa*. Although coculturing the biofilm in DMEM+L-arg increased the Newman biofilm-forming CFUs, confocal microscopy revealed an altered coculture biofilm architecture, with disaggregated clumps covering the coverslip (**Fig. A6:4d**), which is consistent with the phenotype promoted by L-arginine that has been seen in other biofilm communities[58-60]. Thus, we conclude that among the additives tested, BSA possesses the greatest potential to increase *S. aureus* viability and maintain the population balance in a well-engineered coculture biofilm with *P. aeruginosa.* Subsequent experiments in flow-cell biofilms corroborated the effect of BSA in increasing *S. aureus* survival and growth during mixed biofilm formation with *P. aeruginosa* (**Fig. A6:6d**). Although albumin has been described to diminish *P. aeruginosa* killing of *S. aureus* in wounds by binding and sequestering *Pseudomonas* quorum sensing molecules[21], which is also likely what occurred in our model, we also believe albumin has a direct effect on *S. aureus* viability, although further experiments are needed to confirm this hypothesis. Albumin is the main plasma protein and a carrier of numerous molecules, such as metals and other ions, bilirubin, amino acids, fatty acids, enzymes, and hormones[61]. With an unknown mechanism, it is known that the presence of this protein in the culture medium enhances *S. aureus* growth exponentially, possibly by scavenging traces of protein-bound nutrients[62-64]. Therefore, we suggest that albumin could play a direct role in inducing prompt microcolony

formation by increasing the proliferation rate of *S. aureus* in a hostile environment with *P. aeruginosa.* Furthermore, although expression of different virulence factors of *Pseudomonas* has detected increased during coculture growth with *S. aureus* (e.g. LasA protease or pyocyanin production)[53], some staphylococcal factors (e.g. the Panton-Valentin leukocidin protein) have been also observed during these coculture conditions, which may be playing a role also in competing with the *Pseudomonas*[65].

Remarkably, in this study, we demonstrate an important role for oxygen in achieving continuous and stable coculture biofilms of *P. aeruginosa* and *S. aureus*. We also observed a differential distribution of the bacterial populations depending on the oxygen content in the surrounding environment. Lungs are not entirely aerobic, especially those affected by CF, in which the thick mucus present in the airways generates diverse oxygen content between pulmonary regions, thus enhancing the heterogeneity of microbes able to proliferate and persist at the same site[66-68]. Oxygen diffusion also mediates the different spatial distribution of bacteria in wounds; hence, *P. aeruginosa* has been found deeper in the tissue than *S. aureus,* which grows predominantly at the wound surface[13]. *Pseudomonas* is able to grow in anaerobic conditions in the presence of nitrates, which are included in the DMEM formulation. *S. aureus* encodes a set of genes required for growth either aerobically or anaerobically[69,70]; however, aerobic respiration is preferred by *S. aureus* during monoculture growth. Despite these metabolic preferences, during simultaneous growth with *P. aeruginosa*, oxygen competition between organisms drives *S. aureus* to shift to fermentative metabolism. This metabolic shift is also triggered by the expression of siderophores, phenazines and other exoproducts (i.e., 2-heptyl-4-hydroxyquinoline N-oxide (HQNO) production) by *Pseudomonas* that compromise *S. aureus* viability[15,71]. In our model, increased *S. aureus* Newman survival was detected when the coculture biofilms were grown in the ALI area, either in a 96-well plate or over coverslips, rather than during complete medium immersion. Furthermore, we confirmed the existence of an oxygen gradient across the medium depth during biofilm growth, with a continuous micro-oxygenated phase at the medium surface (corresponding to the ALI area). Therefore, we hypothesize that persistent oxygen diffusion at the ALI area of the coculture system increases *S*. *aureus* survival within the mixed biofilm by diminishing the oxygen competition between the organisms and the subsequent production of *P. aeruginosa* molecules that eventually kill *S. aureus.*

The public health concern about biofilm-associated diseases is linked to the altered antimicrobial susceptibilities that these communities present[36]. Unoptimized therapies and variations in the antibiotic concentration across the biofilm layers promote the development of resistance since bacteria are usually exposed to subinhibitory concentrations of the antimicrobial[4]. Exacerbating the problem is the fact that these biofilms tend to be composed of multiple species, with different fitness values and high levels of cooperative and synergistic interactions that are often detrimental to the host[2,4]. For instance, the simple addition of *P. aeruginosa* supernatant to *S. aureus* Newman biofilms has been seen to be sufficient to increase the tolerance of *S. aureus* to a wide range of antibiotics, such as vancomycin, tobramycin and oxacillin[18]. Furthermore, it has been seen that continuous exposure of

S. aureus to *P. aeruginosa* HQNO promotes the formation of antibiotic-resistant small colony variants of the bacterium, enhancing its resistance to aminoglycosides[23]. *P. aeruginosa* and *S. aureus* showed enhanced tolerance to gentamicin and ciprofloxacin antibiotics when they were grown in coculture biofilms (**Fig. A6:8**). Hence, we believe that the use of the conditions revealed in this study allows the stable formation of *P. aeruginosa* PA14 and *S. aureus* Newman coculture biofilms involving the intricate and interspecific relations responsible for influencing the antimicrobial tolerance of each strain.

In summary, in this study, we elucidated the potential of DMEM for *P. aeruginosa* and *S. aureus in vitro* coculture. Additionally, we have discovered that supplementing DMEM with BSA and providing continuous oxygen diffusion allows the formation of a mature mixed biofilm with stable populations of *P. aeruginosa* and *S. aureus.* This study provides useful insights about the establishment of a *P. aeruginosa* and *S. aureus* combined biofilm *in vitro*, which we believe would be of help for the study of phenotypes derived from this clinically challenging bacterial cooperation as well as for optimizing the antimicrobial therapy used to treat these infections.

Methods

Bacterial strains and growth conditions.

Pseudomonas aeruginosa PA14 wild type[72] and *Staphylococcus aureus* Newman (ATCC 13420) were used throughout this study, although *S. aureus* ATCC 12600 and ATCC 29213 were also initially tested. Overnight cultures (O/N) were performed aerobically at 37ºC in Luria-Bertani medium (LB; Scharlab, S.L., Barcelona, Spain) and in tryptic soy broth (TSB; Scharlab, S.L.) for the PA14 and Newman strains, respectively.

P. aeruginosa PA14 and S. aureus Newman coculture medium conditions.

LB, TSB, synthetic cystic fibrosis sputum medium 2 (SCFM2), prepared as previously described[41], and Dulbecco's modified Eagle's medium/nutrient mixture F-12 (DMEM; Thermo Fisher Scientific, Waltham, Massachussetts) were tested. When required, reduced nicotinamide adenine dinucleotide phosphate (NADPH; 0.2 mM), adenosine monophosphate (AMP; 10 mM), bovine serum albumin (BSA; 5% w/v) and L-arginine (0.4% w/v) were added to the medium. O/N cultures of PA14 and Newman strains were washed twice with 1X phosphate-buffered saline (PBS, pH=7.4). To prepare the initial mixed bacterial suspension, each strain was inoculated at a final optical density λ=550 nm (OD_{550}) of 0.05 for planktonic experiments, and an OD_{550} of 0.10 for biofilm experiments.

Planktonic coculture growth.

Mixed bacterial suspensions in a final volume of 20 mL were incubated aerobically at 37ºC with vigorous shaking (200 rpm). At given time points, each planktonic culture was serially diluted in 1X PBS and plated on LB agar (Scharlab, S.L.) to count *P. aeruginosa* CFUs, and tryptic soy agar (TSA; Scharlab, S.L.) supplemented with 7.5% (w/v) NaCl to selectively count *S. aureus* CFUs[73].

Coculture biofilm growth under static conditions.

Static *P. aeruginosa* PA14-*S. aureus* Newman mixed biofilm growth was tested on (i) plastic and (ii) glass surfaces:

i) **Plastic surface:** 200 µl of each mixed bacterial suspension was inoculated in triplicate in 96-well polystyrene plates with a flat bottom (Corning; Sigma-Aldrich, San Luis, Missouri) and incubated at 37ºC without shaking. At different time points, the planktonic phase was removed, and each well was washed three times with 1X PBS. The biofilm phase formed over the wall of each well was removed using a pipette tip, and the triplicates were mixed together. For CFU quantification, each biofilm cell suspension was placed in an ultrasonic bath (USC100T, VWR) for 5 min and subsequently vortexed for 30 seconds, to help dispersing the biofilm. Bacterial suspensions were then serially diluted in 1X PBS and plated on selective agar as described for planktonic growth. Separately, the biofilm mass formed inside the well was stained with 0.1% (w/v) crystal violet, and the biomass (OD_{570}) was determined as previously described[74].

ii) **Glass surface:** 18x18 mm coverslips (Menzel-Gläser, Thermo Fisher Scientific) were placed in a 6-well polystyrene plate with lid (Dd biolab, Barcelona, Spain), and each well was filled with 3 mL of the PA14-Newman bacterial suspension. The coverslip was positioned completely immersed in the bacterial suspension or only half immersed. The half immersion, with the air-liquid interphase (ALI) area, was achieved by placing the coverslip at a ~45º angle against the wall of the well (see **Fig. A6:4b**). Unattached cells were removed after three hours of incubation, and 3 mL of fresh medium was subsequently added again. This procedure was repeated every 12 h during the course of the experiment. At the given time points, the coverslip, covered with the established mixed biofilm, was gently washed with PBS. To determine bacterial

CFUs, biofilm-forming cells were scraped off the coverslip, and serial dilutions were plated on selective agar plates as described above. In addition, the biomass of the PBS-washed coverslip was stained with crystal violet or with different dyes for confocal microscopy as described below.

pH measurements

The pH of the supernatant phase of each PA14 and Newman monoculture and coculture biofilm was measured using a GLP 21 pH meter (Crison®, Hospitalet de Llobregat, Barcelona). For this experiment, biofilms were grown in a volume of 3 mL in 6-well polystyrene plates. pH measurements were taken in triplicate for each culture medium and time point, directly in the microplate well where the biofilm was growing.

Confocal laser scanning microscopy and image analysis.

To differentially stain *P. aeruginosa* PA14 and *S. aureus* Newman, a Bacterial Viability and Gram Stain kit (Biotium, Fremont, California) was used following the manufacturer's instructions. This kit uses the cell membrane differences between gram-negative and gram-positive bacteria to differentially stain each species. Briefly, the kit combines DAPI to stain the bacterial DNA blue with CF™-488A-wheat germ agglutinin (WGA) to bind, specifically, the N-acetylglucosamine present in the peptidoglycan of the cell wall in gram-positive bacteria. Consequently, *P. aeruginosa* PA14 will be stained blue, and *S. aureus* Newman will be stained green. To detect bacterial cells growing in different oxygen concentrations, we used the phosphorescent light-emitting iridium complex Hypoxia Probe (Organogenix; Bionova científica, Barcelona, Spain) according to the manufacturer's instructions.

Stained bacteria were imaged using a Zeiss LSM 800 confocal laser scanning microscope (CSLM, Zeiss, Oberkochen, Germany), and images were analyzed with ImageJ and ZEN (Zeiss software).

Assessment of the oxygen concentration in the coculture system.

The coculture biofilm was established as described above but using lids for the 6-well plates with small holes drilled in the desired locations. After the addition of fresh medium, the plate was transferred to equipment for oxygen measurement described in Supplementary **Fig. A6:S3**. The dissolved oxygen was measured using an Oxymicro Fiber-Optic Sensor System (World Precision Instruments) connected to a micro-optode oxygen sensor in a syringe-type housing (PreSens, Regensburg, Germany); the needle of the housing crossed the lid of the plate, and the optical fiber was placed using the plunger at the desired location. All measurements were compensated with temperature using a temperature probe placed directly above the culture plate.

Micro-optodes were calibrated using temperature-compensated measurements of water saturated with air (100% air saturation, 8.25 mg/L at 25ºC and 1 atm) and a 10 g/L solution of sodium dithionite (0% O_2).

Coculture biofilm incubated in a continuous-flow system.

The *P. aeruginosa* and *S. aureus* mixed bacterial suspension (each strain at OD_{550}=0.10) was inoculated in a three-channel flow-cell (DTU Systems biology, Technical University of Denmark). Media was pumped at a constant flow rate of 42 µl per minute and channel using an Ismatec ISM 943 pump (Ismatec, Wertheim, Germany), as previously described[75]. After 3 days of growth, biofilms were stained with the Bacterial Viability and Gram Stain kit or with the Hypoxia Probe and observed by confocal microscopy. Images were generated, and biomass was calculated using ImageJ and COMSTAT 2 software[75]. Percentage of *S. aureus* in the coculture biofilm was calculated taking the pixels given by *S. aureus*-CF™-488A (channel 0) from the pixels given by the total DAPI staining (channel 1). *P. aeruginosa* percentage in the coculture biofilm was subsequently obtained by subtracting the percentage of *S. aureus* coverage from the total biofilm (100%).

Antimicrobial treatments

P. aeruginosa PA14 and *S. aureus* Newman 72 h coculture biofilms in 96-well polystyrene plates were treated with gentamicin sulfate (Panreac AppliChem, Castellar del Vallès, Spain) at concentrations of 0.5, 1, 2, 4 and 8 μg/mL and with ciprofloxacin hydrochloride (Cayman Chemical, Ann Arbor, Michigan) at 0.5, 1, 2 and 4 μg/mL. After 15 h of incubation with antibiotics, biofilms were washed with 1X PBS and scraped off each well. Serial dilutions were then plated on selective agar plates.

Statistics

Differences in bacterial CFUs/mL and CFUs/well between time points or strains were analyzed using one-way ANOVA with Dunnett's multiple comparison test using GraphPad Prism 6.0 software. To compare the significance between the percentages of bacterial CFUs that remained in the coculture biofilm after gentamicin and ciprofloxacin treatment compared to those calculated in the monoculture biofilms, we used the χ^2 test[76].

References

1 Bjarnsholt, T., Ciofu, O., Molin, S., Givskov, M. & Hoiby, N. Applying insights from biofilm biology to drug development - can a new approach be developed? *Nat Rev Drug Discov* **12**, 791-808, doi:10.1038/nrd4000 (2013).

2 Murray, J. L., Connell, J. L., Stacy, A., Turner, K. H. & Whiteley, M. Mechanisms of synergy in polymicrobial infections. *J Microbiol* **52**, 188-199, doi:10.1007/s12275-014-4067-3 (2014).

3 Stacy, A., McNally, L., Darch, S. E., Brown, S. P. & Whiteley, M. The biogeography of polymicrobial infection. *Nat Rev Microbiol* **14**, 93-105, doi:10.1038/nrmicro.2015.8 (2016).

4 Algburi, A., Comito, N., Kashtanov, D., Dicks, L. M. & Chikindas, M. L. Control of Biofilm Formation: Antibiotics and Beyond. *Appl Environ Microbiol* **83**, doi:10.1128/AEM.02508-16 (2017).

5 Baas Becking, L. G. M., Canfield, D. E., Sherwood, D. & Stuip, M. *Baas Becking's: geobiology, or, introduction to environmental science*. (Wiley Blackwell, 2016).

6 Fuhrman, J. A. Microbial community structure and its functional implications. *Nature* **459**, 193-199, doi:10.1038/nature08058 (2009).

7 Goss, C. H. & Burns, J. L. Exacerbations in cystic fibrosis. 1: Epidemiology and pathogenesis. *Thorax* **62**, 360-367, doi:10.1136/thx.2006.060889 (2007).

8 Kreda, S. M., Davis, C. W. & Rose, M. C. CFTR, mucins, and mucus obstruction in cystic fibrosis. *Cold Spring Harb Perspect Med* **2**, a009589, doi:10.1101/cshperspect.a009589 (2012).

9 Yang, L., Jelsbak, L. & Molin, S. Microbial ecology and adaptation in cystic fibrosis airways. *Environ Microbiol* **13**, 1682-1689, doi:10.1111/j.1462-2920.2011.02459.x (2011).

10 Puchelle, E., Bajolet, O. & Abely, M. Airway mucus in cystic fibrosis. *Paediatr Respir Rev* **3**, 115-119 (2002).

11 Hauser, A. R., Jain, M., Bar-Meir, M. & McColley, S. A. Clinical significance of microbial infection and adaptation in cystic fibrosis. *Clin Microbiol Rev* **24**, 29-70, doi:10.1128/CMR.00036-10 (2011).

12 Hotterbeekx, A., Kumar-Singh, S., Goossens, H. & Malhotra-Kumar, S. *In vivo* and *In vitro* Interactions between *Pseudomonas aeruginosa* and *Staphylococcus* spp. *Front Cell Infect Microbiol* **7**, 106, doi:10.3389/fcimb.2017.00106 (2017).

13 Fazli, M. *et al.* Nonrandom distribution of *Pseudomonas aeruginosa* and *Staphylococcus aureus* in chronic wounds. *J Clin Microbiol* **47**, 4084-4089, doi:10.1128/JCM.01395-09 (2009).

14 Woods, P. W., Haynes, Z. M., Mina, E. G. & Marques, C. N. H. Maintenance of *S. aureus* in Co-culture With *P. aeruginosa* While Growing as Biofilms. *Front Microbiol* **9**, 3291, doi:10.3389/fmicb.2018.03291 (2018).

15 Filkins, L. M. *et al.* Coculture of *Staphylococcus aureus* with *Pseudomonas aeruginosa* Drives *S. aureus* towards Fermentative Metabolism and Reduced Viability in a Cystic Fibrosis Model. *J Bacteriol* **197**, 2252-2264, doi:10.1128/JB.00059-15 (2015).

16 Limoli, D. H. *et al. Pseudomonas aeruginosa* Alginate Overproduction Promotes Coexistence with *Staphylococcus aureus* in a Model of Cystic Fibrosis Respiratory Infection. *MBio* **8**, doi:10.1128/mBio.00186-17 (2017).

17 Wijesinghe, G. *et al.* Influence of Laboratory Culture Media on in vitro Growth, Adhesion, and Biofilm Formation of *Pseudomonas aeruginosa* and *Staphylococcus aureus*. *Med Princ Pract* **28**, 28-35, doi:10.1159/000494757 (2019).

18 Orazi, G. & O'Toole, G. A. *Pseudomonas aeruginosa* Alters *Staphylococcus aureus* Sensitivity to Vancomycin in a Biofilm Model of Cystic Fibrosis Infection. *MBio* **8**, doi:10.1128/mBio.00873-17 (2017).

19 Alves, P. M. *et al.* Interaction between *Staphylococcus aureus* and *Pseudomonas aeruginosa* is beneficial for colonisation and pathogenicity in a mixed biofilm. *Pathog Dis* **76**, doi:10.1093/femspd/fty003 (2018).

20 Orazi, G., Ruoff, K. L. & O'Toole, G. A. *Pseudomonas aeruginosa* Increases the Sensitivity of Biofilm-Grown *Staphylococcus aureus* to Membrane-Targeting Antiseptics and Antibiotics. *MBio* **10**, doi:10.1128/mBio.01501-19 (2019).

21 Smith, A. C. *et al.* Albumin Inhibits *Pseudomonas aeruginosa* Quorum Sensing and Alters Polymicrobial Interactions. *Infect Immun* **85**, doi:10.1128/IAI.00116-17 (2017).

22 DeLeon, S. *et al.* Synergistic interactions of *Pseudomonas aeruginosa* and *Staphylococcus aureus* in an in vitro wound model. *Infect Immun* **82**, 4718-4728, doi:10.1128/IAI.02198-14 (2014).

23 Hoffman, L. R. *et al.* Selection for *Staphylococcus aureus* small-colony variants due to growth in the presence of *Pseudomonas aeruginosa*. *Proc Natl Acad Sci U S A* **103**, 19890-19895, doi:10.1073/pnas.0606756104 (2006).

24 Baldan, R. *et al.* Adaptation of *Pseudomonas aeruginosa* in Cystic Fibrosis airways influences virulence of *Staphylococcus aureus in vitro* and murine models of co-infection. *PLoS One* **9**, e89614, doi:10.1371/journal.pone.0089614 (2014).

25 Padan, E., Bibi, E., Ito, M. & Krulwich, T. A. Alkaline pH homeostasis in bacteria: new insights. *Biochim Biophys Acta* **1717**, 67-88, doi:10.1016/j.bbamem.2005.09.010 (2005).

26 Krulwich, T. A., Sachs, G. & Padan, E. Molecular aspects of bacterial pH sensing and homeostasis. *Nat Rev Microbiol* **9**, 330-343, doi:10.1038/nrmicro2549 (2011).

27 Zhu, Y. *et al. Staphylococcus aureus* biofilm metabolism and the influence of arginine on polysaccharide intercellular adhesin synthesis, biofilm formation, and pathogenesis. *Infect Immun* **75**, 4219-4226, doi:10.1128/IAI.00509-07 (2007).

28 Sheng, L. *et al.* Interkingdom adenosine signal reduces *Pseudomonas aeruginosa* pathogenicity. *Microb Biotechnol* **5**, 560-572, doi:10.1111/j.1751-7915.2012.00338.x (2012).

29 Deng, X. *et al.* Steady-state hydrogen peroxide induces glycolysis in *Staphylococcus aureus* and *Pseudomonas aeruginosa*. *J Bacteriol* **196**, 2499-2513, doi:10.1128/JB.01538-14 (2014).

30 Stewart, P. S. & Franklin, M. J. Physiological heterogeneity in biofilms. *Nat Rev Microbiol* **6**, 199-210, doi:10.1038/nrmicro1838 (2008).

31 Amirkia, V. D. & Qiubao, P. The Antimicrobial Index: a comprehensive literature-based antimicrobial database and reference work. *Bioinformation* **5**, 365-366 (2011).

32 Parsek, M. R. & Singh, P. K. Bacterial biofilms: an emerging link to disease pathogenesis. *Annu Rev Microbiol* **57**, 677-701, doi:10.1146/annurev.micro.57.030502.090720 (2003).

33 Malyshkin, A. P. Chronic infections: causes and possible approach to treatment. *Research Journal of Infectious Diseases* **2**, doi:10.7243/2052-5958-2-3 (2014).

34 Sadekuzzaman, M., Yang, S., Mizan, M. F. R. & Ha, S. D. Current and Recent Advanced Strategies for Combating Biofilms. *Comprehensive Reviews in Food Science and Food Safety* **14**, 491-509, doi:doi:10.1111/1541-4337.12144 (2015).

35 Wolcott, R., Costerton, J. W., Raoult, D. & Cutler, S. J. The polymicrobial nature of biofilm infection. *Clin Microbiol Infect* **19**, 107-112, doi:10.1111/j.1469-0691.2012.04001.x (2013).

36 Del Pozo, J. L. Biofilm-related disease. *Expert Rev Anti Infect Ther* **16**, 51-65, doi:10.1080/14787210.2018.1417036 (2018).

37 Dulbecco, R. & Freeman, G. Plaque production by the polyoma virus. *Virology* **8**, 396-397 (1959).

38 Sambrook, J. *Molecular cloning : a laboratory manual*. (Third edition. Cold Spring Harbor, N.Y. : Cold Spring Harbor Laboratory Press, [2001] ©2001, 2001).

39 Mc, C. N. Laboratory tests in the diagnosis of brucellosis. *Am J Public Health Nations Health* **39**, 866-869 (1949).

40 O'Toole, G. A. Microtiter dish biofilm formation assay. *J Vis Exp*, doi:10.3791/2437 (2011).

41 Turner, K. H., Wessel, A. K., Palmer, G. C., Murray, J. L. & Whiteley, M. Essential genome of *Pseudomonas aeruginosa* in cystic fibrosis sputum. *Proc Natl Acad Sci U S A* **112**, 4110-4115, doi:10.1073/pnas.1419677112 (2015).

42 Mallia, P. *et al.* Role of airway glucose in bacterial infections in patients with chronic obstructive pulmonary disease. *J Allergy Clin Immunol* **142**, 815-823 e816, doi:10.1016/j.jaci.2017.10.017 (2018).

43 Baker, E. H. & Baines, D. L. Airway Glucose Homeostasis: A New Target in the Prevention and Treatment of Pulmonary Infection. *Chest* **153**, 507-514, doi:10.1016/j.chest.2017.05.031 (2018).

44 Brennan, A. L. *et al.* Airway glucose concentrations and effect on growth of respiratory pathogens in cystic fibrosis. *J Cyst Fibros* **6**, 101-109, doi:10.1016/j.jcf.2006.03.009 (2007).

45 Pezzulo, A. A. *et al.* Glucose depletion in the airway surface liquid is essential for sterility of the airways. *PLoS One* **6**, e16166, doi:10.1371/journal.pone.0016166 (2011).

46 Abu-Ashour, W., Twells, L. K., Valcour, J. E. & Gamble, J. M. Diabetes and the occurrence of infection in primary care: a matched cohort study. *BMC Infect Dis* **18**, 67, doi:10.1186/s12879-018-2975-2 (2018).

47 Rojo, F. Carbon catabolite repression in *Pseudomonas* : optimizing metabolic versatility and interactions with the environment. *FEMS Microbiol Rev* **34**, 658-684, doi:10.1111/j.1574-6976.2010.00218.x (2010).

48 Vitko, N. P., Grosser, M. R., Khatri, D., Lance, T. R. & Richardson, A. R. Expanded Glucose Import Capability Affords *Staphylococcus aureus* Optimized Glycolytic Flux during Infection. *MBio* **7**, doi:10.1128/mBio.00296-16 (2016).

49 Lister, J. L. & Horswill, A. R. *Staphylococcus aureus* biofilms: recent developments in biofilm dispersal. *Front Cell Infect Microbiol* **4**, 178, doi:10.3389/fcimb.2014.00178 (2014).

50 Yang, L. *et al.* Pattern differentiation in co-culture biofilms formed by *Staphylococcus aureus* and *Pseudomonas aeruginosa*. *FEMS Immunol Med Microbiol* **62**, 339-347, doi:10.1111/j.1574-695X.2011.00820.x (2011).

51 Lim, Y., Jana, M., Luong, T. T. & Lee, C. Y. Control of glucose- and NaCl-induced biofilm formation by *rbf* in *Staphylococcus aureus*. *J Bacteriol* **186**, 722-729 (2004).

52 Rode, T. M., Langsrud, S., Holck, A. & Moretro, T. Different patterns of biofilm formation in *Staphylococcus aureus* under food-related stress conditions. *Int J Food Microbiol* **116**, 372-383, doi:10.1016/j.ijfoodmicro.2007.02.017 (2007).

53 Tognon, M., Kohler, T., Luscher, A. & van Delden, C. Transcriptional profiling of *Pseudomonas aeruginosa* and *Staphylococcus aureus* during in vitro co-culture. *BMC Genomics* **20**, 30, doi:10.1186/s12864-018-5398-y (2019).

54 Good, N. E. *et al.* Hydrogen ion buffers for biological research. *Biochemistry* **5**, 467-477 (1966).

55 Harjai, K. *et al.* Effect of pH on production of virulence factors by biofilm cells of *Pseudomonas aeruginosa*. *Folia Microbiol (Praha)* **50**, 99-102 (2005).

56 Kessler, E., Safrin, M., Olson, J. C. & Ohman, D. E. Secreted LasA of *Pseudomonas aeruginosa* is a staphylolytic protease. *J Biol Chem* **268**, 7503-7508 (1993).

57 Duan, K. & Surette, M. G. Environmental regulation of *Pseudomonas aeruginosa* PAO1 Las and Rhl quorum-sensing systems. *J Bacteriol* **189**, 4827-4836, doi:10.1128/JB.00043-07 (2007).

58 Kolderman, E. *et al.* L-arginine destabilizes oral multi-species biofilm communities developed in human saliva. *PLoS One* **10**, e0121835, doi:10.1371/journal.pone.0121835 (2015).

59 Borriello, G., Richards, L., Ehrlich, G. D. & Stewart, P. S. Arginine or nitrate enhances antibiotic susceptibility of *Pseudomonas aeruginosa* in biofilms. *Antimicrob Agents Chemother* **50**, 382-384, doi:10.1128/AAC.50.1.382-384.2006 (2006).

60 Jakubovics, N. S. *et al.* Critical roles of arginine in growth and biofilm development by *Streptococcus gordonii*. *Mol Microbiol* **97**, 281-300, doi:10.1111/mmi.13023 (2015).

61 Peters, T., Jr. Serum albumin. *Adv Protein Chem* **37**, 161-245 (1985).

62 Cheng, A. G., Missiakas, D. & Schneewind, O. The giant protein Ebh is a determinant of *Staphylococcus aureus* cell size and complement resistance. *J Bacteriol* **196**, 971-981, doi:10.1128/JB.01366-13 (2014).

63 de Chateau, M., Holst, E. & Bjorck, L. Protein PAB, an albumin-binding bacterial surface protein promoting growth and virulence. *J Biol Chem* **271**, 26609-26615 (1996).

64 Dekio, S. & Jidoi, J. Effect of serum albumin on growth of *Staphylococcus aureus* in synthetic tissue culture medium. *J Dermatol* **10**, 505-508 (1983).

65 Miller, C. L. *et al.* Global transcriptome responses including small RNAs during mixed-species interactions with methicillin-resistant *Staphylococcus aureus* and *Pseudomonas aeruginosa*. *Microbiologyopen* **6**, doi:10.1002/mbo3.427 (2017).

66 Lambiase, A., Catania, M. R. & Rossano, F. Anaerobic bacteria infection in cystic fibrosis airway disease. *New Microbiol* **33**, 185-194 (2010).

67 Worlitzsch, D. *et al.* Effects of reduced mucus oxygen concentration in airway *Pseudomonas* infections of cystic fibrosis patients. *J Clin Invest* **109**, 317-325, doi:10.1172/JCI13870 (2002).

68 Filkins, L. M. & O'Toole, G. A. Cystic Fibrosis Lung Infections: Polymicrobial, Complex, and Hard to Treat. *PLoS Pathog* **11**, e1005258, doi:10.1371/journal.ppat.1005258 (2015).

69 Fuchs, S., Pane-Farre, J., Kohler, C., Hecker, M. & Engelmann, S. Anaerobic gene expression in *Staphylococcus aureus*. *J Bacteriol* **189**, 4275-4289, doi:10.1128/JB.00081-07 (2007).

70 Crespo, A., Gavalda, J., Julian, E. & Torrents, E. A single point mutation in class III ribonucleotide reductase promoter renders *Pseudomonas aeruginosa* PAO1 inefficient for anaerobic growth and infection. *Sci Rep* **7**, 13350, doi:10.1038/s41598-017-14051-2 (2017).

71 Voggu, L. *et al.* Microevolution of cytochrome bd oxidase in Staphylococci and its implication in resistance to respiratory toxins released by *Pseudomonas*. *J Bacteriol* **188**, 8079-8086, doi:10.1128/JB.00858-06 (2006).

72 He, J. *et al.* The broad host range pathogen *Pseudomonas aeruginosa* strain PA14 carries two pathogenicity islands harboring plant and animal virulence genes. *Proc Natl Acad Sci U S A* **101**, 2530-2535 (2004).

73 Chapman, G. H. The significance of sodium chloride in studies of staphylococci. *J Bacteriol* **50**, 201-203 (1945).

74 Cendra Mdel, M., Juarez, A. & Torrents, E. Biofilm modifies expression of ribonucleotide reductase genes in *Escherichia coli*. *PLoS One* **7**, e46350, doi:10.1371/journal.pone.0046350 (2012).

75 Crespo, A., Blanco-Cabra, N. & Torrents, E. Aerobic Vitamin B12 Biosynthesis Is Essential for *Pseudomonas aeruginosa* Class II Ribonucleotide Reductase Activity During Planktonic and Biofilm Growth. *Front Microbiol* **9**, 986, doi:10.3389/fmicb.2018.00986 (2018).

76 Pearson, K. On the criterion that a given system of deviations from the probable in the case of a correlated system of variables is such that it can be reasonably supposed tohave arisen from random sampling. *Philosophical Magazine* **302**, 157-175 (1900).

Author Contributions

MC and ET designed the study. MC, NB-C and LP performed the experiments. All authors analyzed the data. MC and ET wrote the paper. All authors revised and approved the final version of the paper.

A6 Supporting information

Optimal environmental and culture conditions allow the in vitro coexistence of *Pseudomonas aeruginosa and Staphylococcus aureus* in stable biofilms

Supplementary Fig. A6:S1. pH evolution during monoculture biofilm growth of *P. aeruginosa* and *S. aureus.*

pH was measured at 0, 24, 48 and 72 h monoculture biofilm growth in LB, SCFM2, TSB and DMEM medium.

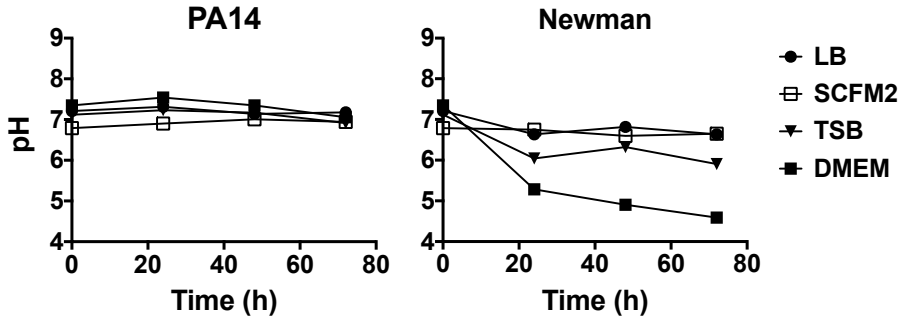

Supplementary Fig. A6.S2. Cristal violet biomass staining of Newman and PA14 mono- and co-cultured biofilms formed with DMEM medium on a 96-well plate.

The average OD_{570} of 5 wells with the respective error bars indicating the standard error of the mean is shown in the plot. PBS was added as a control.

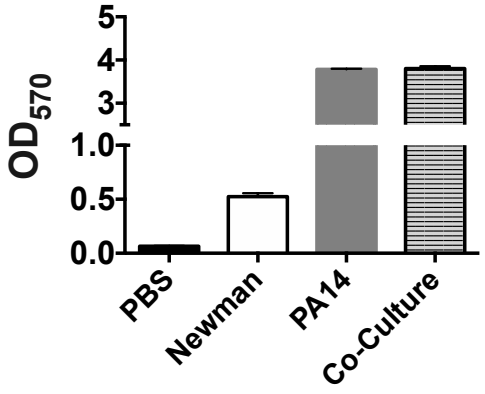

Supplementary Fig. A6:S3. Schematic representation showing how was the oxygen concentration measured in the different static co-cultured biofilms.

The experiment is set up in a bacterial incubator (1) at 37 ºC. The culture grows in a 6-well cell culture plate (2) sitting on an EPS box full of moist paper towel (3) to keep the system humid. The height of the plate is regulated by a scissor lifting platform (4). The oxygen saturation in the system is measured through an OxyMicro device (5). The temperature cable (6) connects a temperature probe inside the incubator (7). An optical fiber cord (8) is connected to a syringe-type micro-optode (9) ending in a needle (10). The needle crosses the lid (11) of the culture plate through small holes and the measuring end of the optical fiber (12) is immersed in the culture medium (13). The OxyMicro processor is connected (14) to power and a laptop. The coverslip for cell growth can be placed leaning on a wall for air-liquid interphase measurements (15) or fully immersed (16). In (a) is shown the complete setting up of the experiment while in (b) are detailed the positions where the oxygen was measured during the co-culture biofilm growth. 6-well plates were purchased sterile, but when required, the system was additionally sterilized using UV light to ensure sterile conditions.

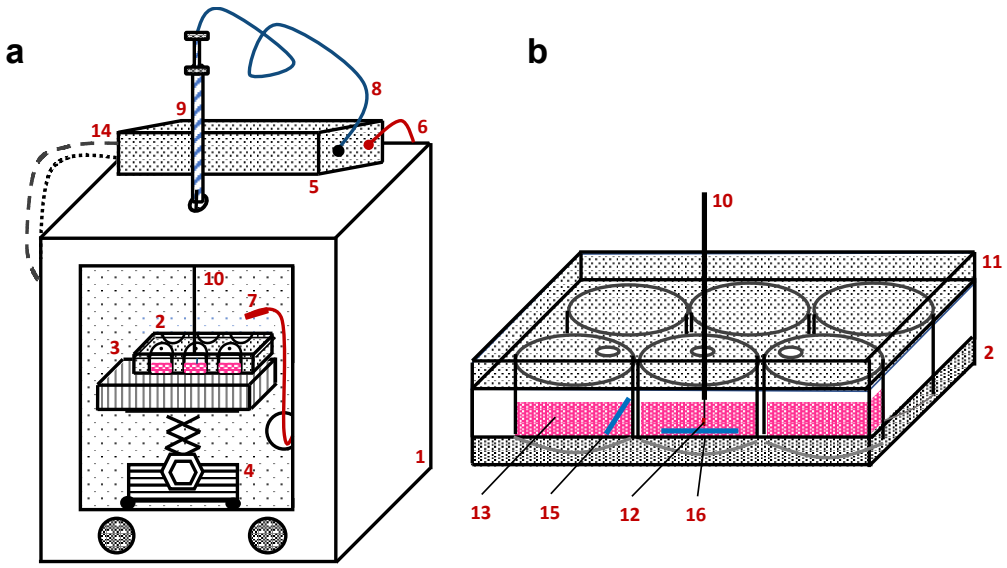

Supplementary Fig. A6:S4. Average population of *S. aureus* Newman microcolonies in a 3-days old continuous flow co-cultured biofilm with *P. aeruginosa* PA14.

(a) Confocal microscopy micrographs of different Newman's microcolonies grown embedded of *P. aeruginosa* biofilm. Both strains were growing together in continuous flow of DMEM medium for three days. The corresponding average number of Newman cells counted per microcolony is shown in (b).

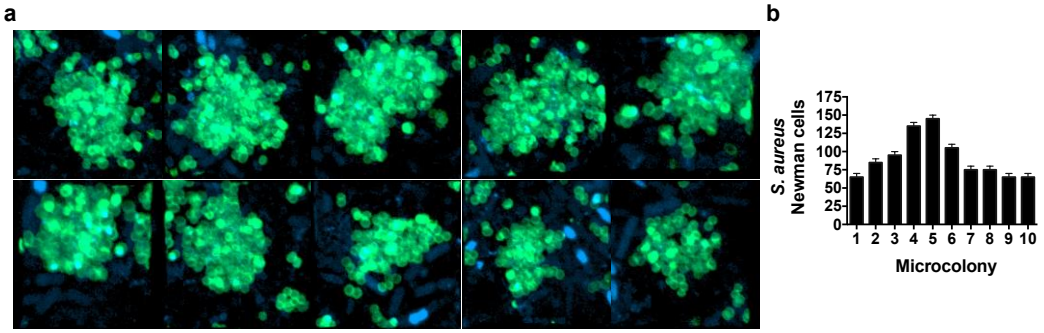

Supplementary Fig. A6:S5. Planktonic *S. aureus* mono-bacterial growth in DMEM and TSB.

O/N cultures were washed in 1X PBS, adjusted to initial OD_{550} = 0.05 in DMEM and TSB and inoculated in triplicate in a 96-well polystyrene plate. OD_{550} was subsequently measured every 15 min for 450 min (7.5 hours).

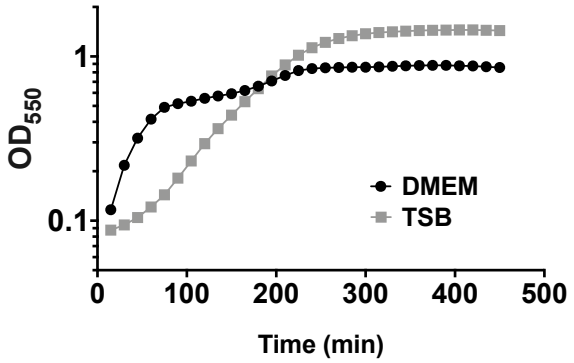

Supplementary Table A6:S1. *P. aeruginosa* PA14 and *S. aureus* Newman cells percentage within the mixed biofilm grown in different media.

	Time (h)	PA14 %	Newman %
LB	12	92.95 %	7.04%
	24	99.96 %	0.03 %
	36	99.99 %	0.001 %
	48	100 %	0.00025 %
	60	100 %	0 %
	72	100 %	0 %
TSB	12	94.41 %	5.58 %
	24	98.85 %	1.14 %
	36	99.92 %	0.07 %
	48	100 %	0.00001%
	60	100 %	0 %
	72	100 %	0 %
DMEM	12	99.57 %	0.42 %
	24	99.96 %	0.039 %
	36	99.98 %	0.011 %
	48	99.99 %	0.008 %
	60	99.99 %	0.0003%
	72	100 %	0 %
SCFM2	12	99.00 %	0.99 %
	24	99.97 %	0.022 %
	36	99.99 %	0.0004 %
	48	99.99 %	0.0004%
	60	100 %	0 %
	72	100 %	0 %

Supplementary Table A6:S2. *P. aeruginosa* PA14 and *S. aureus* Newman cells percentage within the mixed biofilm grown in DMEM supplemented with NADPH, BSA, AMP and L-arg at different timepoints.

	Time (h)	PA14 %	Newman %
DMEM+NADPH	12	84.16 %	15.84 %
	24	75.33 %	24.66 %
	36	99.81 %	0.18 %
	48	99.98 %	0.016 %
	60	99.99 %	0.0001 %
	72	100 %	0 %
DMEM+BSA	12	95.56 %	4.43 %
	24	84.61 %	15.38 %
	36	98.13 %	1.86 %
	48	99.59 %	0.41 %
	60	99.89 %	0.10 %
	72	99.99 %	0.005 %
DMEM+AMP	12	91.38 %	8.61 %
	24	88.99 %	11.00 %
	36	99.89 %	0.109 %
	48	99.98 %	0.01 %
	60	99.99 %	0.0001 %
	72	100 %	0 %
DMEM+L-arg	12	86.92 %	13.07 %
	24	91.54 %	8.46 %
	36	87.64 %	12.35 %
	48	93.21 %	6.79 %
	60	99.97 %	0.029 %
	72	99.99 %	0.00013 %

Supplementary Table A6:S3. *P. aeruginosa* PA14 and *S. aureus* Newman remaining biofilm forming CFUs after gentamicin (Gm) and ciprofloxacin (Cpx) treatment of 48 h old mono- and co-cultured biofilms.

Antibiotic	µg/mL	CFU's mean	SD
Untreated			
PA14 mono-culture	0.00	$3.81x10^8$	$2.23x10^7$
PA14 co-culture	0.00	$2.80x10^8$	$2.83x10^7$
Newman mono-culture	0.00	$1.68x10^8$	$1.87x10^7$
Newman co-culture	0.00	$2.25x10^8$	$2.48x10^5$
Gm treatment			
PA14 mono-culture	0.50	$2.71x10^7$	$1.26x10^7$
	1.00	$2.14x10^7$	$2.23x10^6$
	2.00	$2.28x10^7$	$1.45x10^6$
	4.00	$1.23x10^7$	$2.42x10^6$
	8.00	$1.64x10^7$	$1.97x10^6$
PA14 co-culture	0.50	$8.50x10^7$	$9.05x10^7$
	1.00	$5.06x10^7$	$4.30x10^7$
	2.00	$2.74x10^7$	$1.35x10^7$
	4.00	$1.75x10^7$	$2.12x10^6$
	8.00	$2.44x10^7$	$1.92x10^6$
Newman mono-culture	0.50	$1.08x10^6$	$1.30x10^6$
	1.00	$1.43x10^6$	$6.08x10^5$
	2.00	$1.84x10^4$	$2.26x10^3$
	4.00	$2.60x10^3$	$5.66x10^2$
	8.00	$1.05x10^3$	$2.12x10^2$
Newman co-culture	0.50	$1.60x10^7$	$5.66x10^6$
	1.00	$6.58x10^6$	$2.01x10^6$
	2.00	$2.51x10^4$	$1.27x10^3$
	4.00	$2.05x10^3$	$7.78x10^2$
	8.00	$1.41x10^3$	$1.68x10^2$
Cpx treatment			
PA14 mono-culture	0.50	$5.30x10^6$	$2.40x10^6$
	1.00	$4.05x10^5$	$2.19x10^5$
	2.00	$5.90x10^5$	$1.80x10^5$
	4.00	$2.65x10^4$	$1.91x10^4$
PA14 co-culture	0.50	$1.83x10^7$	$1.17x10^7$
	1.00	$4.90x10^6$	$1.56x10^6$
	2.00	$4.33x10^6$	$5.98x10^5$
	4.00	$3.50x10^4$	$7.07x10^3$
Newman mono-culture	0.50	$2.08x10^7$	$1.44x10^7$
	1.00	$2.51x10^5$	$2.25x10^5$
	2.00	$1.16x10^5$	$1.77x10^4$
	4.00	$1.41x10^3$	$2.66x10^2$
Newman co-culture	0.50	$1.06x10^7$	$1.97x10^6$
	1.00	$1.50x10^6$	$7.07x10^5$
	2.00	$3.05x10^3$	$3.68x10^2$
	4.00	$4.10x10^2$	$5.73x10^1$

Annex 4: Resumen de los contenidos (castellano)

Las bacterias anaeróbicas facultativas pueden crecer en presencia o ausencia de oxígeno. Para ello, llevan a cabo, cuando hay oxígeno disponible un catabolismo basado en la respiración aeróbica, un proceso por el cual la energía acumulada en moléculas orgánicas es liberada mediante su oxidación gradual y almacenada en forma de ATP o GTP obtenidos por fosforilación a nivel de sustrato, y en el cual el oxígeno es utilizado como aceptor final de electrones en el proceso. En cambio, cuando no hay oxígeno disponible, estos organismos adaptan su metabolismo a una forma anaeróbica, bien sea respiración anaeróbica (un proceso análogo al descrito anteriormente pero que utiliza aceptores finales de electrones alternativos, con un potencial redox inferior al del oxígeno) o fermentación (en la cual se produce una oxidación parcial de las moléculas orgánicas en ausencia de aceptores finales para una cadena de transporte de electrones).

Numerosas especies significativas por su importancia clínica son anaeróbicas facultativas, dado que muchos ambientes en el cuerpo presentan condiciones hipóxicas o anóxicas. También se dan ambientes microaeróbicos o anaeróbicos en los biofilms formados en infecciones crónicas. No obstante, la vida anaeróbica facultativa supone también un coste superior en cuanto a la complejidad de su regulación genética. Una de las vías metabólicas que requerirá de dicha regulación es la reducción de ribonucleótidos.

La reducción de ribonucleótidos es el proceso por el cual los ribonucleótidos (NTPs) se transforman en desoxirribonucleótidos (dNTP), formando así los precursores básicos necesarios para la síntesis y la reparación del ADN. Esta reacción es catalizada por una familia de enzimas altamente sofisticadas, las ribonucleótido reductasas (RNR). Todas las RNR son metaloproteínas que emplean un mismo mecanismo catalítico basado en radicales libres. No obstante, dependiendo del mecanismo específico que emplean para la generación de dicho radical, el tipo de cofactores que requieren o las diferencias estructurales que presentan, se divide a las RNR en tres clases (clase I, clase II y clase III). Dichas clases también presentan diferentes relaciones con el oxígeno: la clase I es dependiente de oxígeno, la clase II es independiente de oxígeno, y la clase III es sensible a oxígeno. Los organismos eucarióticos utilizan exclusivamente ribonucleótido reductasas de clase I, pero las bacterias pueden codificar todas las clases en cualquier combinación posible, lo que les confiere una importante herramienta para adaptarse a diferentes condiciones ambientales. En patógenos anaeróbicos facultativos las ribonucleótido reductasas deben ser finamente reguladas para responder a distintas concentraciones de oxígeno, cambios en la velocidad de crecimiento, mecanismos de defensa del anfitrión, etc.

Este trabajo se ha enfocado en los patógenos anaeróbicos facultativos y las estrategias que usan para regular y equilibrar la reducción de ribonucleótidos bajo diversos estímulos ambientales y condiciones variables de oxigenación, así como durante la infección y la formación de biofilm. Para

ello, hemos trabajado con dos especies ampliamente conocidas: *Pseudomonas aeruginosa* y *Escherichia coli*.

Pseudomonas aeruginosa es un bacilo Gram-negativo, perteneciente a la clase γ-Proteobacteria, que se encuentra frecuentemente como organismo de vida libre en suelos y aguas, pero también puede causar infecciones en un amplio espectro de hospedadores, incluyendo plantas y animales. En humanos, es considerado fundamentalmente un patógeno oportunista, conocido especialmente por sus infecciones pulmonares crónicas en grupos de riesgo, tales como los pacientes de Fibrosis Quística (FQ) o Enfermedad Pulmonar Obstructiva Crónica (EPOC). *P. aeruginosa* es también ampliamente conocida como una bacteria extremadamente adaptativa: su genoma, de 6.3 millones de pares de bases, codifica para más de 690 factores de transcripción, en una compleja red regulatoria en la que se han descrito más de mil interacciones. Como otra manifestación de su adaptabilidad, a pesar de no poder usar metabolismo fermentativo para un crecimiento anaeróbico efectivo, esta bacteria es capaz de crecer en condiciones anaeróbicas estrictas usando respiración anaeróbica de nitratos o nitritos.

Escherichia coli, por otra parte, es otro bacilo Gram-negativo anaeróbico facultativo, pero presenta tanto un ciclo de vida como un metabolismo anaeróbico ampliamente diferentes de los expuestos para *Pseudomonas*. *E. coli* es encontrada habitualmente como comensal en el intestino de la mayor parte de animales de sangre caliente; aún así, algunas cepas de *E. coli son capaces de causar graves infecciones intraintestinales* o extraintestinales. Es capaz de crecer anaeróbicamente tanto por respiración anaeróbica (de un amplio rango de sustratos) como por fermentación ácido-mixta.

El trabajo presentado en esta tesis está agrupado en cinco artículos. El primero de ellos, titulado "*Regulation of deoribonucleotide synthesis by the Pseudomonas aeruginosa AlgR two-component system"* (Regulación de la síntesis de desoxirribonucleótidos por parte del sistema de dos componentes AlgR en *Pseudomonas aeruginosa*) se centra en un sistema regulatorio concreto de *P. aeruginosa*, el sistema de dos componentes AlgZR, fuertemente asociado a la síntesis de alginato, y encargado de coordinar múltiples vías relacionadas con la formación de biofilm, la infección y la cronificación. Varios trabajos de transcriptómica general, basados tanto en microarrays de ADN como en ChIP-seq, habían relacionado previamente al sistema de dos componentes AlgZR con la red de las ribonucleótido reductasas.

En el Artículo 1, por lo tanto, realizamos una caracterización exhaustiva de la acción que el sistema AlgZR ejerce sobre la red de las RNR. Comenzamos realizando una búsqueda bioinformática optimizada para la detección de sitios de unión AlgR tanto débiles como fuertes, encontrando que las RNR de clases Ia y II incluyen sitios de unión predichos para este factor transcripcional. Posteriormente, *in vitro*, caracterizamos los sitios de unión AlgR mediante EMSA y AFM; *in vivo*, por otra parte, exploramos los efectos de la regulación de las RNR de clases Ia y II por parte de AlgR en tres modelos de crecimiento distintos (cultivo planctónico, colonización de superficies y formación de biofilm).

La siguiente parte de esta tesis se centra en el factor de transcripción NrdR, el regulador global específico de la red de las RNR. Este regulador fue descubierto en *Streptomyces coelicolor* en el año 2004, y desde entonces se ha caracterizado su acción en múltiples especies bacterianas. Hoy en día, se sabe que este regulador está presente en prácticamente todas las especies bacterianas, mientras que se encuentra completamente ausente en los dominios *Eukarya* y *Archaea*. En bacterias, NrdR actúa como un represor global de todas las clases de ribonucleótido reductasas. Sin embargo, el mecanismo molecular y el significado biológico de este regulador son aún desconocidos.

En el Artículo 2, titulado "*Function of the Pseudomonas aeruginosa NrdR transcripotion factor: global transcriptomic análisis and its role on ribonucleotide reductase gene expresión*" (Función del factor transcripcional NrdR de *Pseudomonas aeruginosa*: análisis transcriptómico global y su papel en la expresión génica de la ribonucleótido reductasa) nos centramos en extender el conocimiento existente sobre el factor transcripcional NrdR a una nueva especie bacteria, *P. aeruginosa*. Caracterizamos el operón en el que se transcribe este gen y las características de su expresión. Identificamos que está positivamente regulado por el sistema de dos componentes NarXL bajo condiciones anaeróbicas que permitan la denitrificación. Demostramos también que, como era esperable, NrdR actúa como un represor de las tres clases de ribonucléotido reductasas codificadas por *P. aeruginosa* (RNR de clase Ia, II y III). No obstante, sorprendentemente NrdR actúa también como un activador transcripcional de *topA*, el gen de la topoisomerasa I de ADN. Igualmente, en este artículo estudiamos el efecto diferencial que NrdR ejerce sobre las distintas clases de RNR en *P. aeruginosa*: en condiciones aeróbicas, las clases de RNR activas en anaerobiosis (clases II y III) se ven más fuertemente afectadas, en términos relativos, por la represión por parte de NrdR que la RNR de clase Ia; en cambio, en condiciones anaeróbicas las clases II y III se hacen prácticamente insensibles a la represión. En el artículo 2 también realizamos una primera caracterización del regulón NrdR en *P. aeruginosa* mediante un microarray de ADN, y un estudio de los efectos que la alteración de la expresión de *nrdR* tiene sobre la virulencia de *P. aeruginosa*, utilizando *Drosophila melanogaster* como modelo de infección.

Posteriormente, nos centramos en descubrir el mecanismo molecular de NrdR. Este es el tema en el que se centra el Artículo 3, titulado "Mechanism of action of NrdR, a global regulator of ribonucleotide reduction" (Mecanismo de acción de NrdR, un regulador global de la reducción de ribonucleótidos).

En este artículo, realizamos un estudio exhaustivo de este factor transcripcional en *E. coli* y *P. aeruginosa*. En primer lugar, hacemos una caracterización completa del regulón NrdR utilizando datos de transcriptómica en ambas especies (tanto microarrays de DNA como RNA-seq) y correlacionado estos datos con una búsqueda bioinformática optimizada a nivel global de cajas de unión NrdR (NrdR-box).

Uno de los mayores retos para el estudio de NrdR es que obtener éste como proteína recombinante, dado que es inestable y poco soluble, y tiende a precipitar durante el proceso de purificación o los ciclos de congelación/descongelación. Por ello, el siguiente paso que realizamos es el diseño, expresión y purificación de una serie de proteínas de fusión encaminadas a mejorar la estabilidad de NrdR y

facilitar su purificación por cromatografía de afinidad. Estas proteínas emplean el residuo solubilizante SUMO-tag, así como varias etiquetas para purificación proteica, y hacen uso de proteasas (SUMO proteasa o TEV proteasa) que permitirán recuperar la proteína NrdR nativa, con tan solo un pequeño adaptador N-terminal imposible de eliminar.

Utilizando estas proteínas, hacemos una caracterización completa de la oligomerización dependiente de nucleótidos de la proteína NrdR y su importancia cara a la regulación de las ribonucleótido reductasas a nivel funcional. Para dicha caracterización funcional, en este trabajo diseñamos una nueva técnica de biología molecular basada en la transcripción *in vitro*, denominada ReViTA (Regulated *in Vitro* Transcription Assay). Globalmente, en este artículo trazamos un primer modelo de el mecanismo molecular del factor transcripcional NrdR.

La última parte de esta tesis está centrada en los efectos de la regulación del metabolismo anaeróbico sobre la red de las RNR, especialmente en gradientes de oxígeno, como los que se encuentran en las estructuras de los biofilms.

El Artículo 4, titulado "*Pseudomonas aeruginosa exhibits deficient biofilm formation in the absence of class II and class III ribonucleotide reductases due to hindered anaerobic growth"* (*Pseudomonas* aeruginosa muestra una formación de biofilm deficiente en ausencia de las ribonucleótido reductasas de clases II y III debido a un defecto en el crecimiento anaeróbico) está centrado en el paper que las distintas clases de RNR desempeñan en el biofilm de *P. aeruginosa*. Determinamos que las RNR de clase II y III son esenciales para el crecimiento anaeróbico de esta bacteria, e, igualmente, que la RNR de clase II únicamente puede sostener el crecimiento anaeróbico por sí sola cuando se suplemente al cultivo bacteriano con una fuente de vitamina B_{12}. Igualmente, comprobamos que la formación de biofilm se reduce significativamente en ausencia de las RNR de clase II y III, dado que la formación de biofilms maduros implica el establecimiento de áreas microaeróbicas y anaeróbicas. Consecuentemente, las RNR de clase II y III ven su expresión inducida en cultivos anaeróbicos y durante la formación de biofilm. Empleando tanto cultivos planctónicos como biofilms caracterizamos en detalle la inducción anaeróbica de la clase II, que está orquestada por el regulador anaeróbico general Dnr.

Finalmente, el Artículo 5, titulado "*Gradual adaptation of facultative anaerobic pathogens to microaerobic and anaerobic conditions"* (Adaptación gradual de patógenos anaeróbicos facultativos a condiciones microaeróbicas y anaeróbicas) se centra en el desarrollo de una técnica para la caracterización de la expresión génica bacteriana en la transición aerobiosis-anaerobiosis y su aplicación al estudio de la adaptación gradual de *E. coli* y *P. aeruginosa* en gradientes de concentración de oxígeno, haciendo especial énfasis en la adaptación de la red de las RNRs.

La técnica desarrollada se denomina *AnaeroTrans*, y se basa en el uso de un biorreactor tipo quimiostato, desarrollado específicamente para este trabajo, que permite mantener un cultivo bacteriano en estado estacionario en un entorno aislado y exponerlo a distintas concentraciones de

oxígeno utilizando como único sistema para la variación de las condiciones de oxigenación el consumo propio del cultivo por respiración aeróbica. Este sistema permite caracterizar condiciones de disponibilidad de oxígeno a nivel celular mediante una variable de estado reproducible (la concentración de oxígeno en fase gas de un cultivo en estado estacionario para la biomasa y donde la única variación en la oxigenación es producida por el cultivo en sí mismo).

Empleando esta técnica, caracterizamos el comportamiento general de *E. coli* y *P. aeruginosa* en la transición aerobiosis-anaerobiosis, analizando la evolución de su tasa de oxígeno, velocidad de crecimiento y *fitness*. Caracterizamos igualmente en detalle la adaptación gradual de la red de las RNR en dichas condiciones, así como el papel que llevan a cabo los reguladores anaeróbicos generales en su modulación. Finalmente, podemos dividir la transición aerobiosis-anaerobiosis en una serie de etapas reproducibles y elaborar un modelo de la adaptación gradual que se produce en ellas.

Annex 5: Conclusiones generales (castellano)

1. El sistema de dos componentes AlgZR regula la transcripción de las RNR de clases I y II de *P. aeruginosa* en cultivo planctónico, durante la colonización de superficies (formación de colonias) y la formación de biofilm. La RNR de clase III no se ve afectada por este sistema.

2. La regulación que el sistema de dos componentes AlgZR de *P. aeruginosa* ejerce sobre la RNR de clase I se produce mediante la unión del factor de transcripción AlgR a una única secuencia (denominada AlgR-box) en la posición -545 del promotor P*nrdA* (respecto al ATG del primer gen en el operón). Por otra parte, la regulación que este sistema ejerce sobre la RNR de clase II se produce mediante la unión de AlgR a dos secuencias (denominadas AlgR-box1 y AlgR-box2), que se encuentran, respectivamente, en las posiciones -299 y -128 del promotor P*nrdJ*.

3. AlgR es responsable de la activación de las RNR de clases I y II en *P. aeruginosa* bajo estrés oxidativo, un fenómeno ya ampliamente descrito. Este factor transcripcional ejerce dicha activación mediante su unión en la AlgR-box del promotor P*nrdA* y la AlgR-box2 del promotor P*nrdJ*.

4. AlgR es responsable de la represión de la RNR de clase II en *P. aeruginosa* en biofilms mucoides. Este factor transcripcional ejerce dicha activación mediante su unión a la AlgR-box1 del promotor P*nrdJ*. Muy probablemente esta represión se produce para que prevalezca la RNR de clase III, que no es reprimida.

5. La unión de AlgR a las regiones promotoras de los operones RNR, así como a la región promotora que controla la transcripción de *algD*, produce un efecto de curvatura en el DNA detectable mediante Microscopía de Fuerza Atómica (AFM). Este proceso ha sido planteado a menudo como hipótesis para diversos operones regulados por AlgR.

6. Tal y como ha sido previamente descrito para otras especies, como es el caso de *E. coli* o *S. coelicolor*, el factor de transcripción NrdR actúa como represor de todas las clases de RNR codificadas por *P. aeruginosa*. Esta regulación ocurre mediante su unión a las secuencias NrdR-box, predichas por *Rodionov et al.* en 2005.

7. El grado de represión ejercido por NrdR sobre las distintas clases de RNR de *P. aeruginosa* es variable, tal que las RNR de clases II y III, activas en anaerobiosis, sufren una menor represión por parte de NrdR bajo condiciones anaeróbicas. Esta diferencia es, con total probabilidad, resultado de diferencias en la localización de las secuencias de unión e interacciones de NrdR con otros factores transcripcionales.

8. NrdR actúa como activador de la transcripción de *topA* mediante su unión a una única caja de unión NrdR-box en la posición -68 (respecto al ATG de *topA*). El efecto de esta activación es

únicamente visible (a nivel tanto transcripcional como funcional) durante la fase de crecimiento exponencial.

9. La transcripción de *nrdR* en *P. aeruginosa* aumenta bajo condiciones anaeróbicas. Esta activación es causada por el sistema NarXL, mediante la unión de NarL (probablemente fosforilado) a dos secuencias en las posiciones -37 y -15 del promotor P*nrdR* (respecto al ATG de *nrdR*).

10. Un gran número de posibles NrdR-boxes fueron identificadas en las secuencias inmediatamente aguas arriba de las secuencias codificantes en el genoma de *E. coli* y *P. aeruginosa* (un total de 113 resultados y 33 resultados, respectivamente). No obstante, tan sólo aquellas presentes en los operones de las ribonucleótido reductasas coinciden con genes diferencialmente expresados en una cepa mutante *nrdR*, comparada con su correspondiente cepa isogénica salvaje.

11. Un gran número de posibles genes diferencialmente expresados en cepas mutantes *nrdR* (comparadas con sus correspondientes cepas isogénicas salvajes) fueron identificados tanto en *E. coli* como en *P. aeruginosa*. Se emplearon técnicas de transcriptómica general, como RNA-seq (47 genes diferencialmente expresados identificados en *P. aeruginosa*) y microarrays de ADN (111 genes diferencialmente expresados identificados en *P. aeruginosa*, y 57 en *E. coli*). No obstante, tan sólo los genes presentes en los operones de las ribonucleótido reductasas coinciden con la presencia de posibles cajas de unión NrdR-boxes.

12. Se pueden obtener proteínas NrdR recombinantes de *E. coli* y *P. aeruginosa* en una forma estable y pura mediante un protocolo de purificación de dos pasos, si éstas son expresadas desde un comienzo como proteínas de fusión que incluyan dominios de solubilización y sitios de digestión de proteasas (SUMO, TEV), así como añadiendo nucleótidos, cuando sea necesario, como cofactores durante el proceso de purificación.

13. La proteína NrdR existe como una población dinámica de formas oligoméricas dependientes de cofactores nucleotídicos y sin estequiometría fija, tanto en el caso de *P. aeruginosa* como el de *E. coli*.

14. La unión de dATP a NrdR provoca interacciones proteína-proteína controladas que llevan a la formación de oligómeros de tamaño medio, de entre los cuales el hexámero es el más representado. Un tiempo superior de incubación *in vitro* con dATP no causa una variación significativa en la composición de la población de oligómeros. La forma hexamérica de NrdR es activa tanto a nivel de unión a ADN como a nivel funcional, según ha sido determinado mediante EMSA y transcripción *in vitro* (ReViTA), respectivamente.

15. La unión de ATP a NrdR provoca oligomerización intensiva, lo que lleva a la formación de oligómeros de gran tamaño, entre los cuales se han detectado formas con hasta 14 unidades NrdR. Estas formas no muestran actividad ni a nivel de unión a DNA ni a nivel funciona, según ha sido determinado mediante EMSA y transcripción *in vitro* (ReViTA), respectivamente.

16. Una alteración de la expresión de *nrdR* en *P. aeruginosa*, bien sea por deleción o sobreexpresión, presenta un efecto negativo sobre el *fitness* bacteriano, reduciendo tanto la velocidad de crecimiento como el conteo de viables. Este efecto se correlaciona con un aumento en la supervivencia de las larvas de *Galleria mellonella* infectadas con las cepas de *P. aeruginosa* correspondientes, aunque dicho efecto no se ha logrado reproducir en infecciones en *Drosophila melanogaster*.

17. La transcripción *in vitro* simultánea de dos genes codificados en un mismo plásmido, tal que éstos sean expresados como ARN mensajeros diferentes y su expresión sea, para el primer gen, controlable por un factor de transcripción determinado, y, para el segundo gen, constitutiva, puede usarse para la caracterización *in vitro* del efecto del factor transcripcional elegido a nivel funcional. La técnica resultante fue denominada ReViTA (Regulated *in Vitro* Transcription Assay).

18. Las RNR de clases II y III desempeñan un papel esencial en el crecimiento anaeróbico de *P. aeruginosa*, así como durante la formación de biofilm en modelos tanto estático como de flujo continuo.

19. La transcripción de las RNR de clases II y III en *P. aeruginosa* se ve inducida durante el crecimiento anaeróbico y la formación de biofilm. Este último efecto se puede atribuir a la presencia de condiciones microaeróbicas y anaeróbicas en ciertas áreas de la estructura del biofilm.

20. La transcripción de la RNR de clase II en *P. aeruginosa* se ve inducida anaeróbicamente por el regulador general anaeróbico Dnr, mediante su unión a una única secuencia en posición -21 (respecto al ATG del gen *nrdJa*).

21. La inducción de la transcripción de la RNR de clase II en *P. aeruginosa* realizada por el regulador anaeróbico Dnr y la realizada por el sistema de dos componentes AlgZR son independientes, y, como tal, aditivas.

22. Un biorreactor de tipo quimiostato en el que un cultivo en estado estacionario es expuesto a cambios en la oxigenación inducidos únicamente por el consumo de oxígeno del propio cultivo puede utilizarse como sistema para reproducir los efectos de la transición aerobiosis-anaerobiosis sobre dicho cultivo. El método resultante fue denominado *AnaeroTrans*.

23. La disponibilidad celular de oxígeno, tal y como es percibida por células bacterianas en un cultivo en estado estacionario que únicamente sufre cambios en la oxigenación inducidos por su propio consumo de oxígeno, puede controlarse utilizando la concentración de oxígeno en la fase gas sobre el cultivo como variable de estado.

24. *P. aeruginosa* experimenta un perfil de adaptación suave durante la transición aerobiosis-anaerobiosis. Su tasa de consumo de oxígeno se reduce gradualmente. Esta especie no muestra efectos negativos sobre su *fitness* durante la primera mitad del rango microaeróbico (*early microaerobic range*). Se produce una reducción significativa en el *fitness* bacteriano durante el rango microaeróbico medio (*mid-microaerobic range,* 12% O_2 – 5% O_2), aunque éste se recupera posteriormente, bajo concentraciones de oxígeno inferiores o anaerobiosis estricta.

25. *E. coli* experimenta una reducción gradual de su velocidad de crecimiento y *fitness* durante la transición aerobiosis-anaerobiosis, del cual únicamente se recupera tras un periodo largo de adaptación bajo condiciones anaeróbicas. En esta especie se da una adaptación fuertemente escalonada, bajo la cual la maquinaria metabólica aeróbica sufre una brusca transición a los sistemas de microaerobiosis, provocando una tasa de consumo de oxígeno reducida que se mantendrá durante todo el rango microaeróbico.

26. Una única mutación puntual en el sitio de unión del regulador anaeróbico Anr en el promotor de la RNR de clase III en *P. aeruginosa* (previamente descrita) provoca una activación tardía de esta ribonucleótido reductasa durante la transición aerobiosis-anaerobiosis. Así, el pico en la expresión de la RNR de clase III que se observa en el rango microaeróbico inicial (*early microaerobic range,* 21% O_2 – 12% O_2) en cepas que no presentan dicha mutación, no ocurre en *P. aeruginosa* PAO1 hasta el rango microaeróbico tardío (*late microaerobic range*, 5% O_2 – 0% O_2). Esto produce una reducción significativa en la velocidad de crecimiento de esta cepa durante el rango microaeróbico medio en comparación con otras cepas de *P. aeruginosa*.

27. La red de las RNR presenta una respuesta coordinada y gradual en la adaptación de su expresión génica durante la transición aerobiosis-anaerobiosis: las RNR de clases II y III se activan como resultado de dos eventos consecutivos durante el rango microaeróbico, mientras que la expresión de la RNR de clase Ia no sufre cambios. Por otra parte, las RNR de *E. coli* presentan el patrón de regulación contrario, en tanto son las RNR de clases Ia y Ib, activas bajo condiciones aeróbicas, las que son gradualmente reprimidas durante la transición aerobiosis-anaerobiosis.

28. Una cepa de *P. aeruginosa* mutante *nrdR* no pierde la inducción de sus RNR de clase II y clase III bajo condiciones microaeróbicas y anaeróbicas; no obstante, el patrón gradual de inducción de su expresión desaparece por completo.

29. Durante la transición aerobiosis-anaerobiosis en *P. aeruginosa*, el regulador anaeróbico principal Anr se vuelve esencial durante el rango microaeróbico inicial (*early microaerobic range*), mientras que Dnr solo se hace esencial en el rango tardío. En *E. coli*, por otra parte, el regulador anaeróbico general Fnr sólo se hace esencial por debajo de 2% de oxígeno, pero el efecto de su mutación supone una pérdida apreciable de *fitness* desde prácticamente el comienzo del rango microaeróbico.

30. Tanto *E. coli* como *P. aeruginosa* presentan metabolismo híbrido durante la transición aerobiosis-anaerobiosis, como es demostrado por el hecho de que, durante una gran parte del rango microaeróbico, reguladores anaeróbicos como Fnr o Anr se encuentren activos o incluso sean esenciales, mientras la respiración aeróbica aún se está produciendo.